ALT
INTERNATIONAL CONFERENCE
Advanced Laser Technologies

Jointly with the 22nd Asia-Pacific Conference on
Fundamental Problems of Opto- and Microelectronics

APCOM 2024

BOOK OF ABSTRACTS

THE 31ST INTERNATIONAL CONFERENCE ON ADVANCED LASER TECHNOLOGIES

ALT

VLADIVOSTOK•RUSSIA '24
23-27 September

Abstracts of the 31th International Conference on Advanced Laser Technologies – 2024. – 333 с.

The book contains abstracts of ALT'24 conference reports devoted to fundamental and applied aspects of innovative laser technologies: laser-matter interaction, biomedical photonics, laser systems and materials, laser diagnostics and spectroscopy, nonlinear and terahertz photonics, photonics in quantum technologies, advanced optical materials and metamaterials, agricultural and biophysical photonics. The book contains abstracts of plenary, invited, oral and poster presentations. The official language of the conference is English.

ALT Conference Books of Abstracts are available on the website: https://altconference.org/proceedings

TABLE OF CONTENTS

PLENARY SPEAKERS

Modification of diamond by laser radiation:
from ablation to single NV-centers formation

Vitali Kononenko

A.M. Prokhorov General Physics Institute of RAS

vitali.kononenko@nsc.gpi.ru

Diamond is a unique material, the use of which is quite desirable in the different technological advances, from constructive elements operating in hot and aggressive media to the platform for quantum communication and computing. The downside is the extreme hardness of diamond crystal. While the problem of diamond synthesis has been largely solved and (poly)monocrystalline substrates are commercially available, the existing diamond processing techniques are still unable to meet the many application requirements and are in a thorough development process. Here, the fundamental aspects of the laser-diamond interaction are reviewed, focusing on the irreversible structural transformations that affect the physical and optical properties of the crystals.

Experiments with harmonics of the Ti-sapphire laser (100 fs, 266-800 nm) and many other pico- and nanosecond pulsed sources have revealed a number of different laser-stimulated processes developing on the diamond surface. This diversity is due to two fundamental properties of diamond: the ability to graphitize, which completely changes the coordination geometry of the carbon bonds, and the ability to chemically react with ambient gases. Modern pulsed lasers enable both scenarios: (1) heating of the crystal lattice up to ~2000 C with single pulse graphitization and ablation (~10 nm/pulse), and (2) nonlinear photoexcitation of the binding electrons with quite slow surface etching – "nanoablation" ($<10^{-2}$ nm/pulse). Special attention will be paid to the accumulative regime of the laser effect, when the laser fluence is lower than the single pulse ablation threshold and the graphitization develops with a certain delay – after multi-pulse laser treatment. Both accumulative graphitization and nanoablation are atomic-scale processes that pave the way for photolytic formation of structural defects in diamond.

Effective and controllable generation of color centers is a key problem in diamond-based quantum technologies. To date, several vacancy-based defects have been demonstrated to be created as a result of laser treatment of diamond. The most well-known of these is the nitrogen-vacancy complex (NV center), the formation mechanisms of which are discussed in both the accumulation and nanoablation regime. Luminescence measurements confirm that during long irradiation, e.g. with 266 nm femtosecond pulses, the NV concentration gradually increased and can increase tenfold (Fig. 1). The correlation between the coloration of the diamond and the nanoablation of its surface is demonstrated. Taken together, the results presented here indicate that laser preablation irradiation is a promising tool to precisely control the number of generated vacancies in the lattice and thus the probability of formation of a single NV center at the desired location of a crystal.
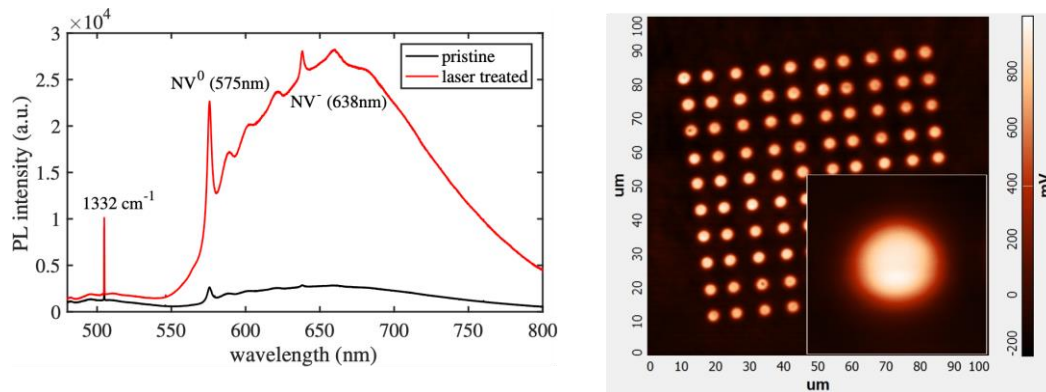
Figure 1. PL spectra of irradiated and original diamond (left) and PL image of 10×10 array with a period of 8 μm and magnified image of individual pixel in the insert (right). The irradiation was made with a third harmonic of Ti-sapphire laser (100 fs, 266 nm, 0.4 J/cm^2, 0.5 million pulses).

Quantum technologies: state of the art and prospects

Sergei Kulik

Lomonosov Moscow State University

sergei.kulik@physics.msu.ru

The report examines the current state and prospects of the interdisciplinary field of knowledge – Quantum information processing or Quantum technologies. The emphasis is on the basic physical principles underlying three subtechnologies developed in the world and, especially, in the Russian Federation, which will potentially lead or have already led to the creation of quantum simulators, quantum communication systems and highly sensitive sensors in the near future.

In the field of quantum computing devices, these are technologies that use neutral atoms and ions in traps, superconducting systems, impurity structures and linear-optical systems as working physical systems.

In the field of quantum communication, this is the creation of a global network based on fiber-optic, atmospheric and space channels.

In the field of quantum sensorics, these are three groups of sensors: quantum clocks/gravimeters; electric and magnetic field sensors and quantum metrology/photometry.

The main problems of physical and technical implementation of certain units/elements of quantum simulators and quantum communication systems are considered separately.

Laser nanotechnologies for perovskite photonics and optoelectronics

Sergey Makarov[1,2]

1- ITMO University, 49 Kronverksky pr., 197101, St. Petersburg, Russia
2- Qingdao Innovation and Development Center, Harbin Engineering University, Qingdao 266000, Shandong, China

s.makarov@metalab.ifmo.ru

Recently, nanostructured halide perovskites [1] have attracted enormous attention due to their exceptional optical and electrical properties being useful various optoelectronic devices [2] as shown in Fig.1. As a result, this family of materials can provide a prospective platform for modern nanophotonics and meta-optics [3,4], allowing us to overcome many obstacles associated with the use of conventional semiconductor materials. Here, we review the recent progress on laser ablation for application in halide perovskite nanophotonics starting from single-particle light-emitting nanoantennas [5,6] and nano/micro-lasers [7] to the large-scale designs working for surface coloration, anti-reflection, optical information encoding [8]. Moreover, we discuss high potential of the femtosecond laser ablation for improvement of perovskite solar cells [9,10], creation of microscale light-emitting devices [11] and photodetectors.
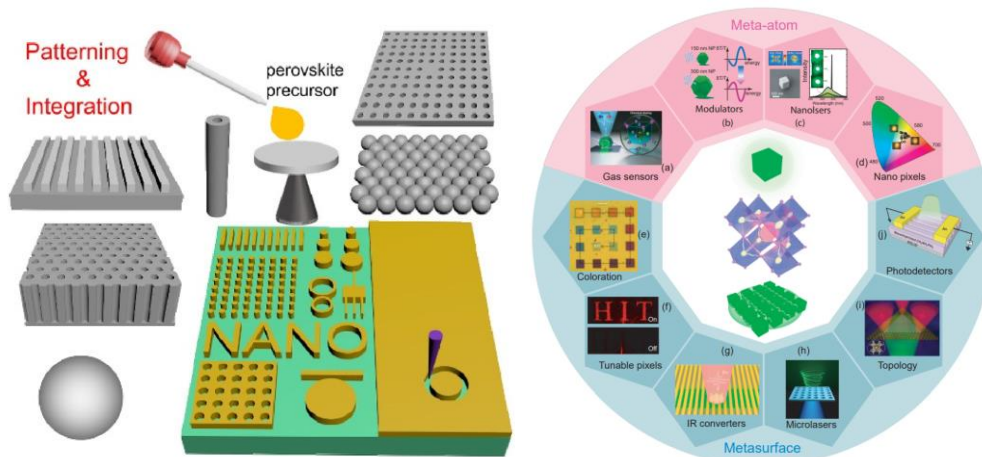
Figure 1. Schematic illustrations of methods for patterning and integration (left side) as well as applications of perovskite nanostructures in nanophotonics and optoelectronics (right side).

[1] C. Soci, G. Adamo, D. Cortecchia, et al, Roadmap on perovskite nanophotonics, Optical Materials: X, 17, 100214 (2023).
[2] A. Berestennikov, P. Voroshilov, S. Makarov, Y. Kivshar, Active meta-optics and nanophotonics with halide perovskites, Applied Physics Reviews, vol. 6, pp. 3 (2019).
[3] P. Tonkaev, I. Sinev, M. Rybin, S. Makarov, Y. Kivshar, Multifunctional and transformative metaphotonics with emerging materials, Chemical Reviews, vol. 122(19), pp. 15414-15449 (2022).
[4] E. Tiguntseva, G. Zograf, P., Komissarenko, et al, Light-emitting halide perovskite nanoantennas, Nano Letters 18(2), pp.1185-1190 (2018).
[5] E. Tiguntseva, D. Baranov, A. Pushkarev, et al, Tunable hybrid Fano resonances in halide perovskite nanoparticles, Nano Letters, vol.18(9), pp.5522-5529 (2018).
[6] A. Zhizhchenko, S. Syubaev, A. Berestennikov, Single-mode lasing from imprinted halide-perovskite microdisks, ACS Nano, vol.13(4), pp.4140-4147 (2019).
[7] A. Zhizhchenko, P. Tonkaev, D. Gets, et al, Light-emitting nanophotonic designs enabled by ultrafast laser processing of halide perovskites, Small, p.2000410 (2020).
[8] A. Furasova, E. Calabró, E. Lamanna, et al, Resonant silicon nanoparticles for enhanced light harvesting in halide perovskite solar cells, Advanced Optical Materials, vol.6(21), pp.1800576 (2018).
[9] A. Furasova, M. Krassas, M. Tountas, et al, Photovoltaic parameters improvement via size control of monodisperse Mie-resonant nanoparticles in perovskite solar cells, Chemical Engineering Journal, pp.152771 (2024).
[10] A. Marunchenko, V. Kondratiev, A. Pushkarev, et al, Mixed Ionic-Electronic Conduction Enables Halide-Perovskite Electroluminescent Photodetector, Laser & Photonics Reviews, vol.17(9), pp.2300141 (2023).
[11] A. Marunchenko, M. Baranov, E. Ushakova, et al, Single-Walled Carbon Nanotube Thin Film for Flexible and Highly Responsive Perovskite Photodetector, Advanced Functional Materials, vol.32(12), pp.2109834 (2022).

Fiber lasers in modern medical technologies

Vladimir Minaev

IRE-Polus Ltd, Fryazino, Moscow Region, Russia

vminaev@ntoire-polus.ru

The first fiber laser (FL) was created by E. Snitzer (Polaroid) in 1961 [1] and at 1989 their output power reached 120 mW. In 1990 V. Gapontsev and I. Samartsev presented FL with an output power of 2 W [2]. The following year, they presented a 3.9 W FL and proved the possibility of creating FL with an output power of more than 100 W [3]. Thus, prerequisites were created for expanding the field of FL use, including in medicine. In the early 2000s, NTO "IRE-Polyus" developed and registered medical devices with FL with wavelengths $\lambda = 1.55; 1.06; 1.94\ \mu m$ and two independently controlled radiations $\lambda = 0.97 + 1.55\ \mu m$ [4].

The developed medical devices with FL, as well as with diode lasers, were revolutionary differs from devices based on traditional lasers:

- Making the optical part of the apparatus in the form of an integrated fiber device increases their reliability, reduces the impact of the environment and mechanical effects on them, simplifies and reduces the cost of use. They do not require regular maintenance.

- They are distinguished by high efficiency, small dimensions, weight and consumption.

- Possibility to output in thin working fiber. It is simple to output several independently controlled radiations with different wavelengths into the working fiber.

Active work with leading Russian doctors, begun in the early 2000s, made it possible to develop and register more than 10 medical technologies, many of which have no analogues based on other methods of action.

Developed by D. Gapontsev and V. Kancharia (IPG-Photonics) lasers based on thulium FL with $\lambda \approx 1.9\ \mu m$ and output power of more than 100 W allowed N. Fried and K. Murray [5] to show their effectiveness in urology for lithotripsy and BPH surgery. Based on these results, the IRE-Polyus Ltd has developed, registered and continues to improve devices of the "UroLase" ("FiberLase U") family, superior in characteristics to analogues with solid-state lasers. Urological devices with thulium FL from IPG are popular all over the world. With varying degrees of success, Russian and world manufacturers are trying to repeat them.

Now, the set of working wavelengths available in fiber lasers has been expanded, in particular:

- Visible laser family with wavelengths $\lambda \approx 0.54, 0.56, 0.59, 0.62$ and $0.66\ \mu m$ with output power ≥ 10 W [6].

- Raman laser with a wavelength of $\lambda \approx 1.68\ \mu m$, corresponding to the minimum absorption in hemoglobin, with an output power of ≥ 10 W [7].

- Optical parametric generators with pumping from FL and a wavelength of $\lambda \approx 3\ \mu m$, corresponding to the maximum absorption in water with an output power of up to 25 W [8].

All this created a groundwork for the development of new medical devices and technologies.

[1] E. Snitzer, Optical Maser Action of Nd^{+3} in Barium Crown Glass, Phis. Rev. Lett., 7, No 12, pp.444–446, 1961.
[2] V. Gapontsev and I. Samartsev, High-Power Fiber Laser, Conference edition. Advanced Solid-State Lasers (Formerly Tunable Solid-State Lasers), March 5–7, 1990, Salt Lake City, Utah, p.127.
[3] V. Gapontsev and I. Samartsev, High-Power Fiber Laser, OSA Proceedings on Advanced Solid-State Lasers, 1991, 6 p.258.
[4] V. Gapontsev, V. Minaev, V. Savin, I. Samartsev, Medical instruments based on high-power diode and fibre lasers, Quantum Electronics (2002), 32(11), pp.1003-1006.
[5] N. Fred and K. Murray, High-Power Thulium Fiber Laser ablation of the Canine Prostate, Proc. of SPIE, v.5686.
[6] A. Surin, T. Borisenko, Yu. Stirmanov, et al, A line of high-power continuous-wave VLM lasers with radiation power from 1.5 to 20 W in the range of 513-730 nm, Laser-Inform No 11-12, (2018).
[7] K.M. Zhilin, V. Minaev, I. Samartsev, Ya. Tezadov, Raman Laser at 1,68 μm for Medical Applications, 5th International Symposium on High-Power Fiber Lasers and their Applications, at ICLO 2010 June 28th – July 1st, 2010, St.Petersburg, Russia.
[8] I.A. Larionov, A.S. Gulyashko, D.A. Alekseev, et al, High-efficient DFG of fiber lasers radiation in the spectral region of 3um for soft tissue ablation. 6th International Symposium on Lasers in Medicine and Biophotonics, at ICLO 2020. November 1st-5th.

Optical fiber-based technologies & applications

Perry Shum

Southern Univ of Science & Technology

shum@ieee.org

Optical fiber-based devices have been widely deployed in recent years. There are many advantages of using fiber as a sensor. These include electrically-passive operation, light weight, immunity to radio frequency interference and electromagnetic interference, high sensitivity, compact size, corrosion resistance, easily multiplexing and potentially low cost.

Several novel fiber-based sensors and technologies developed are presented here, including fiber Bragg grating (FBG) based sensors, photonic crystal fiber (PCF) based sensors, specialty fiber-based sensors and distributed fiber sensing systems. FBGs as instinctive sensors, are ingeniously designed as two-dimensional (2D) tilt sensors, displacement sensors, accelerometers and corrosion sensors here; PCF based evanescent field absorption sensor, PCF induced Mach-Zehnder interferometer and Fabry-Perot refractometer for temperature and refractive index sensing are presented; based on localized surface Plasmon resonant (LSPR) effect, nano-sized fiber tip with gold nanoparticles are demonstrated for live cell index bio-sensing applications.

[1] J. Hu, et al, A novel high-fidelity Raman spectral preprocessing scheme to enhance biomedical applications and chemical resolution visualization, Light: Science and Applications, 2024.

[2] J. Li, et al, SNR enhancement of quasi-distributed weak acoustic signal detection by elastomers and MMF integrated Φ-OTDR, Optics Express, 2023.

[3] Z. Liang, et al, Strong bulk photovoltaic effect in engineered edge-embedded van der Waals structures, NATURE COMMUNICATIONS, 2023.

[4] B. Li, et al, Resolution enhancement for interrogating fiber Bragg grating sensor network using dilated U-Net, OPTICS LETTERS, 2023.

[5] Y. Wang, et al, Multifunctional Electronic Textiles by Direct 3D Printing of Stretchable Conductive Fibers, Advanced Electronic Materials, 2023.

[6] X. Yu, et al, A generative adversarial network with multi-scale convolution and dilated convolution res-network for OCT retinal image despeckling, Biomedical Signal Processing and Control, 2023.

[7] H. Dang, et al, Deconvolutional suppression of resolution degradation in coherent optical spectrum analyzer, Journal of Lightwave Technology, 2023.

[8] X. Shen, et al, Fast and Storage-Optimized Compressed domain vibration detection and classification for Distributed acoustic sensing, Journal of Lightwave Technology, 2023.

[9] P.P. Shum, et al, Highly sensitive microfiber ultrasound sensor for photoacoustic imaging, OPTO-ELECTRONIC ADVANCES, 2023.

[10] Z. Zhou, et al, Poincaré Beam for Magnetic Field Sensing, Journal of Lightwave Technology, 2023.

Mid-Infrared quantum-cascade lasers

Grigorii Sokolovskii

Ioffe Institute, St. Petersburg, Russia

gs@mail.ioffe.ru

The report will present an overview of the global state of research and development of the mid-infrared quantum cascade lasers, as well as discussion of the original research results at the Ioffe Institute. Among these, it is worth noting the demonstration of the output power of laser generation of more than 22 W at a wavelength around 4.5 μm with pulse duration 100 ns and repetition rate 11 kHz and a record-high power exceeding 21 W achieved from QCLs of 8 μm spectral range with pulse duration 100 ns and repetition rate 11 kHz, the dynamic characteristics of the mid-infrared quantum cascade lasers, as well as the characteristics of quantum cascade detectors for 7-9 μm range fabricated from the structure of the record-high power quantum-cascade laser with measured sensitivity of 20 mA/W, which is superior to that of similar detectors with a specially optimized structure.

SiC nanostructures and their optoelectronic device applications

Weiyou Yang

Ningbo University of Technology, China

Silicon carbide (SiC) is recognized as one of most important candidates of third generation semiconductors, owing to its superior properties such as outstanding mechanical properties, excellent chemical inertness, high thermal stability as well as high thermal conductivity, which allow the SiC materials to be serviced under high-temperature/high-voltage/high-power harsh environments. Here, we share our recent works on the controlled growth of SiC low-dimensional nanostructures, and their potential applications in optoelectronic devices, such as field emission cathodes, pressure sensors, photoelectric detection and energy storage.

In situ fabricated perovskite quantum dots for photonic applications

Haizheng Zhong

School of Materials Science & Engineering, Beijing Institute of Technology, China

hzzhong@bit.edu.cn

Perovskite quantum dots (PQDs) are now emerging as functional materials for many photonic applications due to their superior optical properties and easy fabrication. In 2015, we report ligand-assisted reprecipitation (LARP) of brightly luminescent and color tunable perovskite quantum dots. In 2016, we reported the *in-situ* fabrication of PQDs in polymeric films with high transparency, superior photoluminescence emission and additional processing benefits for down-shifting applications. The potential use of *in-situ* fabricated PQDs as color converters in LCD backlights was successfully demonstrated, showing bright potential in display technology. Very recently, we developed the *in-situ* fabricated PQDs patterns for Micro LED and other down conversion applications. In addition, we also demonstrate the use of *in-situ* fabricated perovskite quantum dots for other applications including UV enhanced silicon photodetectors, photovoltaics, quantum dots based hyperspectrometer, CW laser etc. In all, the *in-situ* fabricated PQDs provide promising functional materials for many photonic and optoelectronic applications.
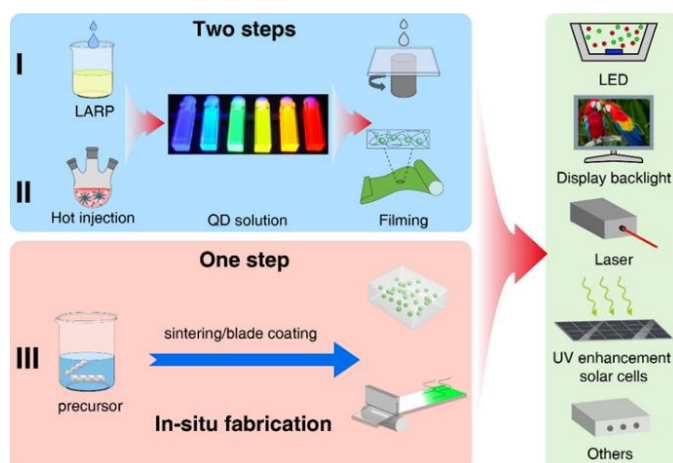

Figure 1. *In-situ* fabrication and *ex-situ* fabrication of perovskite quantum dots for photonic applications.

LASER-MATTER INTERACTION

Laser synthesis of boron nanoparticles for BNCT

K.O. Aiyyzhy[1*], E.V. Barmina[1]

1- Prokhorov General Physics Institute of the Russian Academy of Sciences, Vavilova str. 38, 119991 Moscow, Russia

* aiyyzhy@phystech.edu

Boron neutron capture therapy (BNCT) is one of the most appealing radiotherapy modalities, whose efficiency can be further improved by the employment of boron nanoparticles (NPs) [1,2]. But the fabrication of biologically friendly, water-dispersible NPs with high boron content and favorable physicochemical characteristics still presents a great challenge. In this work, we study the synthesis of elemental boron NPs using pulsed laser fragmentation in the liquid of commercial boron powders (grade A, grade B and boron enriched with the ^{10}B isotope). A solid-state Nd:YAG laser with a wavelength of 1064 nm, a pulse duration of 10 ns, a pulse repetition rate of 10 kHz, and a pulse energy of 1 mJ was used as a source of laser radiation in all our experiments. Deionized water and isopropanol were used as the working liquid. Laser fragmentation in deionized water is accompanied by the formation of boric acid [3], while laser fragmentation in isopropanol leads to the formation of carbon-containing NPs due to the partial decomposition of isopropanol during its optical breakdown [4]. Nevertheless, decomposition products of liquid and large NPs fractions were replaced to pure isopropanol by centrifugation of boron NPs colloid.

Analysis of X-ray diffraction patterns shows that micropowders of boron grade A and boron enriched with the ^{10}B isotope are amorphous, grade B is crystalline. The isotopic composition measured on a secondary ion mass spectrometer of micropowders of boron grade A, boron enriched with the isotope ^{10}B, and boron grade B shows a ^{10}B content of 19.2%, 85.1% and 17.5%, respectively. Laser fragmentation of boron micropowders leads to the formation of spherical NPs. The size distributions obtained using a disk centrifuge CPS 24000 were in the range of 5-100 nm for NPs grade A and 10-40 nm for NPs grade B. The size distribution for boron NPs enriched with the ^{10}B isotope obtained using dynamic light scattering was in the range 10-100 nm. Transmission electron microscopy studies confirm the data obtained using disk centrifuge and dynamic light scattering. Elemental analysis (EDX) shows high purity of boron NPs grade A and boron NPs enriched with the ^{10}B isotope (boron content 99.1%), while boron NPs grade B contains boron in an amount of 91.5%. The obtained B NPs were functionalized with polyethylene glycol polymer to improve colloidal stability and biocompatibility. Using the obtained B NPs in BNCT led to a dramatical enhancement in cancer cell death [5].
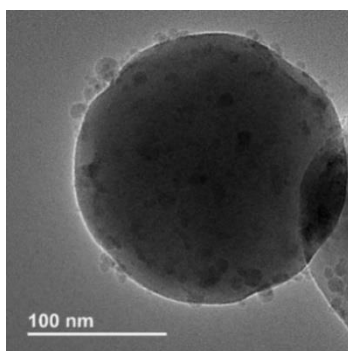
Fig. 1. TEM image of boron nanoparticles after laser fragmentation by 10 ns laser pulses in isopropanol. Fragmentation time was 40 min.

[1] R.F. Barth, A.H. Soloway, R.G. Fairchild, Boron neutron capture therapy for cancer, Scientific American, 263, 100 (1990).

[2] V. Torresan, et al, Biocompatible iron–boron nanoparticles designed for neutron capture therapy guided by magnetic resonance imaging, Advanced Healthcare Materials, 10, 2001632 (2021).

[3] A.I. Pastukhov, et al, Laser-ablative aqueous synthesis and characterization of elemental boron nanoparticles for biomedical applications, Scientific Reports, 12, 9129 (2022).

[4] K.O Aiyyzhy, E.V. Barmina, V.V. Voronov, G.A. Shafeev, G.G. Novikov, O.V. Uvarov, Laser ablation and fragmentation of Boron in liquids, Optics & Laser Technology, 155, 108393 (2022).

[5] I.N. Zavestovskaya, et al, Laser-Synthesized Elemental Boron Nanoparticles for Efficient Boron Neutron Capture Therapy, International Journal of Molecular Sciences, 24, 17088 (2023).

Evolution from high-spatial-frequency laser-induced periodic surface structures to laser-induced periodic surface structures on surface of Ti and stainless steel target by sub-nanosecond laser ablation in air

D.A. Antipov[1*], E.V. Barmina[1], I.O. Bruslavskiy[1,2]

1- Prokhorov General Physics Institute of the Russian Academy of Sciences, Vavilova str. 38, 119991 Moscow, Russia
2- National Research Nuclear University MEPhI (Moscow Engineering Physics Institute), 31, Kashirskoye highway, 115409 Moscow, Russia

* antipov.dima.99@mail.ru

In this presentation, we introduce the latest research on the creation of laser-induced periodic surface structures (LSPL) and high-spatial-frequency laser-induced periodic surface structures (HSFL) on solid surfaces by their sub-nanosecond laser ablation in air. The laser formation of periodic nanostructures (NS) model is based on the theory of wave processes in materials. We found that thermocapillary instability in the melted layer on the surface leads to HSFL synthesis. Accompanying formation of self-organized NS on HSFL and LSFL is studied in relation to laser parameters and target material [1,2]. This report showcases the transformation of surface morphology from HSFL to LSFL formed through laser ablation in air varying laser parameters. In our experiments we used two types of lasers. The first was Nd:YAG laser with wavelength of 1064 nm, pulse duration of 30 ps and repetition rate of 1 kHz. The second laser beam was Yb:fiber fs-laser with wavelength of 1030 nm, pulse duration of 6 ps and repetition rate of 1 kHz. As targets were used Ti and stainless steel. Images from field emission scanning microscopy (Mira TESCAN) show that number pulses and fluence of incident laser irradiation affect to target's morphology as transfer from HSFl to LSFl. In special laser conditions such NS can co-exist as in melt bath of co-rectangle periodic structures with period from 10 to 1000 nm scale.

Presented experimental data was used as base for theoretical calculations of HSFL formation as wave mechanism [3,4].

Laser nanotechnologies discussed in this context have diverse applications, such as significantly boosting external applied field strength, altering antifriction properties, and creating structured surfaces with unique optical properties like ultra-black absorbance.

Additionally, the presentation will cover recent progress in understanding the mechanisms behind these structure formations, address current limitations, and explore emerging possibilities and future prospects.

[1] J. Reif, Dynamics and Processes on Laser-Irradiated Surfaces, Nanomaterials, 13, 379, (2023).
[2] J. Bonse and S. Gräf, Maxwell meets, Laser & Photonics Reviews, 14(10), 2000215, (2020).
[3] N.A. Kirichenko, E.V. Barmina, G.A. Shafeev, Theoretical and Experimental Investigation of the Formation of High Spatial Frequency Periodic Structures on Metal Surfaces Irradiated by Ultrashort Laser Pulses, Physics of Wave Phenomena, 26(4), 264–273, (2018).
[4] S. Kuleshov and V.D. Kobtsev, Distribution of aluminum clusters and their ignition in air during dispersion of aluminum nanoparticles in a shock wave, Combustion, Explosion, and Shock Waves, vol. 56(5), pp. 566-575, (2020).

Laser-induced thermo-mechanical effect in regenerative medicine

O.I. Baum

Institute of Photon Technologies of the Kurchatov Complex of Crystallography and Photonics,
National Research Center "Kurchatov Institute"

baumolga@gmail.com

Our scientific group is developing new laser technologies for structure modification, shape correction and tissue reconstruction in otolaryngology, orthopedics and ophthalmology. The thermo-mechanical effect can be useful in correction of refraction [1,2], treatment of glaucoma [3,4] and laser reshaping of rib cartilage for larynx stenosis surgery [5,6].

Based on our previous research, we have recently focused on studying laser effects in regenerative medicine. It has been shown that laser-induced thermo-mechanical effect can be used to trigger targeted cellular regeneration in avascular biological tissues.

[1] O. Baum, A. Yuzhakov, A. Bolshunov, et al, New laser technologies in ophthalmology for normalisation of intraocular pressure and correction of refraction, Quantum electronics, 47(9), p.860, 2017.

[2] O.I. Baum, A.I. Omelchenko, E.M. Kasianenko, V.Ya. Panchenko, R.V. Skidanov, N.L. Kazanskiy, E.N. Sobol', A.V. Bolshunov, S.E. Avetisov, Control of laser-beam spatial distribution for correcting the shape and refraction of eye cornea, Quantum Electronics, 2020, Vol. 50, № 1, pp.87-93.

[3] O. Baum, S. Wachsmann-Hogiu, T. Milner, E. Sobol, Laser-assisted formation of micropores and nanobubbles in sclera promote stable normalization of intraocular pressure, Laser Physics Letters, 14 (6), p.065601, 2017.

[4] O.I. Baum, V.Y. Zaitsev, A.V. Yuzhakov, A.P. Sviridov, M.L. Novikova, A.L. Matveyev, L.A. Matveev, A.A. Sovetsky, E.N. Sobol, Interplay of temperature, thermal-stresses and strains in laser-assisted modification of collagenous tissues: Speckle-contrast and OCT-based studies, J Biophotonics, 2019.

[5] O. Baum, Y. Soshnikova, E. Sobol, Laser reshaping of costal cartilage for transplantation, Lasers in surgery and medicine, 43 (6), pp.511-515 (2011).

[6] O.I. Baum, Yu.M. Alexandrovskaya, V.M. Svistushkin, S.V. Starostina, E.N. Sobol, New clinical application of laser correction of cartilage shape for implantation in otolaryngology, 2019, Laser Phys. Lett., 16, 035603.

Laser swelling at femtosecond nanostructuring of material

A. Afanasiev, N. Sapogova, M. Sveshnikova, A. Pikulin, <u>N. Bityurin</u>[*]

Institute of Applied Physics Russian Academy of Science, Nizhniy Novgorod

* bit@appl.sci-nnov.ru

Investigation of the effect of a pair of femtosecond laser pulses, one of the fundamental frequency (FF) and the other of the second harmonic (SH) of a Ti:sapphire laser, on polymer surfaces coated with a layer of colloidal polystyrene microparticles 1 μm in diameter, when the sum frequency is in the bandgap of the material, reveals that the maximum depth of the ablation craters is achieved when the SH pulse comes 133–200 fs before the FF [1]. Further investigation studying the volume change of the irradiated areas rather than the crater depth shows that decrease in volume (effective ablation) occurs only when the SH comes first. In opposite case one observes the increase in volume that is effective swelling despite the presence of a crater (see Fig. 1).
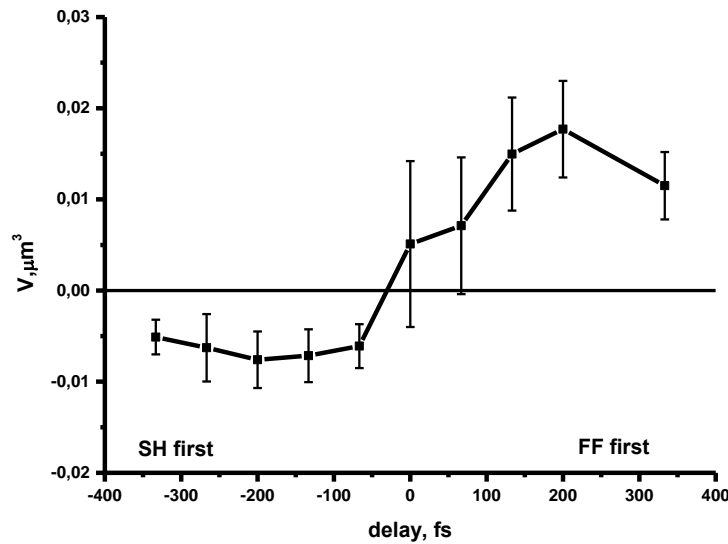
Fig. 1. Change in the volume of material under the sphere as a result of irradiation by a pair of different-colored laser pulses depending on the delay between them. Negative delay – the second harmonic pulse comes first.

This phenomenon is addressed by the hydrodynamic model for laser swelling [2] where the evolution of surface layers of a glassy material heated by a laser pulse above the glass transition temperature and cooled by heat diffusion is considered as the flow of a stretchable viscous fluid. The strong dependence of viscosity on temperature and pressure leads to the appearance of a hump with reduced density. New solutions of the model have been received and the results are compared to the above experimental data.

[1] A. Afanasiev, I. Ilyakov, B. Shishkin, N. Bityurin, Nanopatterning of the dielectric surface by a pair of femtosecond laser pulses of different color through a monolayer of microspheres, Optics Express, 31(8), 12423-12432 (2023).
[2] N. Bityurin and N. Sapogova, Hydrodynamic model for laser swelling, Preprint ArXiv 2409.06370 (2024).

Liquid-assisted laser texturing: a game-change technology toward advanced Si optoelectronics

Yu. Borodaenko[1*], S. Gurbatov[1], A. Shevlyagin[1], A. Kuchmizhak[1,2]

1- Institute of Automation and Control Processes, Far Eastern Branch, Russian Academy of Sciences,
5 Radio Str., Vladivostok, Russia
2- Pacific Quantum Center, Far Eastern Federal University, Vladivostok, Russia

* borodaenko_yu@mail.ru

Nanotextured silicon has emerged as paramount material in optoelectronics, significantly improving the performance of Si-based photodetectors and solar cell devices through optimization of light absorption and charge carrier transport characteristics [1]. Simple non-lithographic methods such as direct femtosecond laser patterning of silicon allows to create diverse self-organized surface morphologies spanning from periodic nanogratings (referred to as laser-induced periodic surface structures; LIPSS) [2] to random spiky structures. Nanostructures could improve photodetector devices [3], while their fabrication can be potentially upscaled at low cost through common CMOS technology. Here, using liquid-assisted fs-laser nanopatterning of silicon with nanogratings we demonstrated fabrication of advanced Si photodetectors (PD) with polarization-sensitive response (Figure 1). Moreover, laser-induced defect generation was also found to enhance the detector photoresponse at near-IR wavelengths (i.e. Si within transparency), while subsequent over-coating of its active areas with calcium disilicide allowed to construct hybrid devices for efficient photothermal-thermoelectric conversion with competitive performance [4,5].
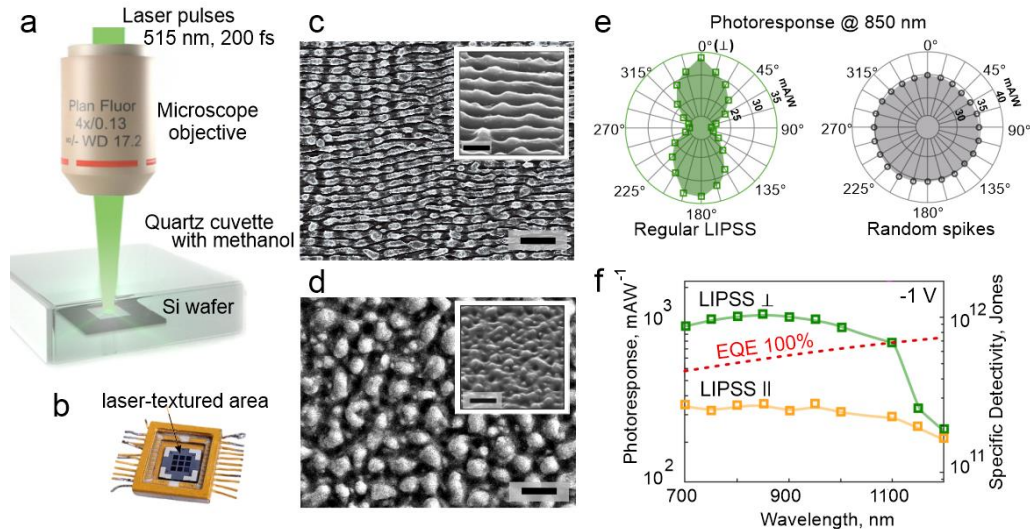
Fig. 1. (a) Schematically illustrated procedure of fs-laser nanotexturing of Si p-n junction in methanol. (b) Optical photograph of the fabricated p-n Si PD. SEM images (top view) of the (c) LIPSS and (d) spikes produced over Si surface. Insets: enlarged and tilted view of the corresponding morphologies. Scale bars on main and inset images correspond to 1 and 0.5 μm, respectively. (e) Photoresponse as a function of polarization angle Θ of the incident 850-nm wavelength laser beam measured for Si PDs patterned with (e) LIPSS and (f) spike structures (the polarization is set perpendicular to the LIPSS nanotrenches at $\Theta_\perp$=0°/180°). (f) Comparative photoresponse spectra of the Si PD patterned with LIPSS measured for cross-polarized pump radiation ($\Theta_\perp$ and Θ_{II} nanotrenches) at -1 V bias voltage conditions, the red dashed line indicates the response of an ideal photodetector with 100% external quantum efficiency.

[1] D. Zielke, D. Sylla, T. Neubert, R. Brendel, J. Schmidt, IEEE Journal of Photovoltaics 3, 656 (2012).
[2] Y. Borodaenko, S. Syubaev, S. Gurbatov, A. Zhizhchenko, A. Porfirev, S. Khonina, E. Mitsai, A.V. Gerasimenko, A. Shevlyagin, E. Modin, A. Kuchmizhak, ACS Applied Materials & Interfaces 13, 54551 (2021).
[3] Y. Borodaenko, D. Pavlov, A. Cherepakhin, E. Mitsai, S. Gurbatov, S. Syubaev, A. Shevlyagin, A. Kuchmizhak, Liquid-Assisted Laser Nanotexturing of Silicon: Onset of Hydrodynamic Processes Regulated by LIPSS. Advanced Materials Technologies, 9(8), 2301567 (2024).
[4] S. Huang, Q. Wu, Z. Jia, X. Jin, X. Fu, H. Huang, X. Zhang, J. Yao, J. Xu, Black silicon photodetector with excellent comprehensive properties by rapid thermal annealing and hydrogenated surface passivation, Advanced Optical Materials, 8, 1901808 (2020).
[5] H. Cansizoglu, et al, Dramatically enhanced efficiency in ultra-fast silicon MSM photodiodes via light trapping structures, IEEE Photonics Technology Letters, 31, 1619-1622 (2019).

Lead halide perovskite micro-optics fabrication by femtosecond laser ablation

A. Cherepakhin[1*], A. Zhizhchenko[1,2], A. Porfirev[3], A. Pushkarev[4], S. Makarov[4], A. Kuchmizhak[1]

1- Institute of Automation and Control Processes, Far Eastern Branch of RAS, Vladivostok 690061, Russia
2- Far Eastern Federal University, Vladivostok 690061, Russia
3- Image Processing Systems Institute of the RAS-Branch of FSRC "Crystallography & Photonics" of the RAS, Samara 443001, Russia
4- ITMO University, St. Petersburg, Russia, 197101

* cherepakhinab@yandex.ru

In this work, by applying method of direct imprinting using single-pulse fs-laser projection lithography we demonstrate fabrication of optical-quality micro-scale Fresnel zone plates (FZP) for generation of focused laser beam, as well as binary fork-shaped gratings (FSGs) and binary spiral micro-axicons which allow generation of vortex beams in reflection mode on a surface of chemically synthesized $CsPbBr_3$ perovskite microcrystals. The achieved ultra-smooth ablation of perovskite microcrystals was explained by ultrafast laser-induced thermalization rate as well as extremely low conductivity of the $CsPbBr_3$ material. These findings highlight the potential of $CsPbBr_3$ microcrystals to be a promising material for the realization of intricate 2D micro-optical elements and holograms, directly imprinted using non-destructive and practically relevant laser technologies.
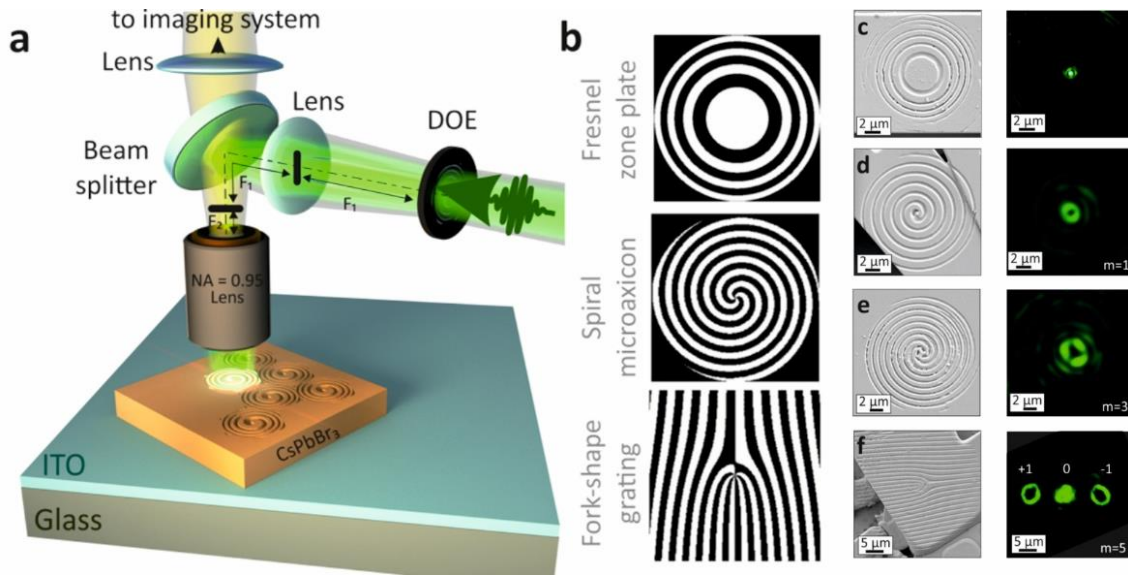
Figure 1. (a) Schematic illustration of the setup for fs-laser projection lithography. (b) Design of the amplitude masks used to generate intensity patterns for laser printing of the FZP, spiral microaxicons and fork-shaped gratings. (c) Top-view SEM images of the $CsPbBr_3$ microcrystal surface imprinted with various micro-optical elements including FZP, binary spiral axicons (b,c) and binary fork-shape grating (d) of the as well as corresponding focal-plane intensity distributions at 515 nm excitation wavelength showing focusing performance of the imprinted 2D perovskite micro-optics.

The excellent performance of the imprinted micro-optics demonstrates the suitability of fs-laser projection lithography for the direct fabrication of various functional elements and devices. The lateral resolution of fs-laser ablation at 515 nm on $CsPbBr_3$ can achieve 250-300 nm. This high resolution is generally attributed to the material's extremely low thermal conductivity, two orders of magnitude lower than that of silicon and its exceptionally fast thermalization rate upon laser exposure. The sub-picosecond timescale of $CsPbBr_3$ thermalization, facilitated by Auger recombination of photo-excited carriers effectively minimizes the heat-affected zone.

Laser centrifugal atomization

Yu. Chivel

MerPhotonics, 42100 Saint-Etienne, France

yuri.chivel@gmail.com

The highest quality spherical powders are produced by centrifugal atomization. On an industrial scale, the PREP (plasma rotating electrode process) method is used, in which the melting of the end of a rotating cylinder is carried out by a plasmatron. The method has significant disadvantages – high energy costs, the inability to obtain powders smaller than 30 microns. The new method – laser centrifugal atomization (LCA) and systems for its implementation have developed, which allow us to overcome these shortcomings. In new method, the end of a rotating hollow cylinder with a wall thickness of 4 mm is melted by a system of several lasers, whose focal spots with a diameter of, for example 2 mm are located evenly around the perimeter of the cylinder. When the cylinder rotates, a pulse-periodic mode of action is implemented for each point of the end.

When exposed in a pulse-periodic mode, the average power density of laser radiation is determined during long-term heating $t \gg r^2 / 4 \cdot a$ (r – radius of focal spot, a – thermal diffusivity) according to the relation:

$$A \cdot q_b = \lambda \cdot T_b / r \; - \; \text{for boiling}; \quad A \cdot q_m = \lambda \cdot T_m / r \; - \; \text{for melting},$$

$V = \pi \cdot D \cdot n$ – velocity of focus spot, A – absorptivity, n – rotation frequency, D – diameter of cylinder.

Calculations of the processes of melting and evaporation of the end of a rotating hollow cylinder with a diameter of 5 cm at a speed of 170 rp/s were carried out under the influence of 4 lasers with a power of 10 to 40 kW.

Atomization of the melt is carried out in an atmosphere of inert gas. And atomization of an erosion plume or erosion plasma is carried out under conditions of vacuum or reduced pressure.

The results of calculations show that the productivity of obtaining powders from the melt (size 30-200 microns) will be up to 500 kg/h with an efficiency of 0.41 kWh/kg, and nanoparticles from the vapor plume or plasma – up to 150 kg/h with an efficiency of 0.87 kWh/kg.

Since the plume of vapor (plasma) is deflected by centrifugal force, the restrictions on the power of laser radiation associated with shielding the target are removed.

Laser-driven formation of chiral and achiral plasmonic nanostructures for biosensing applications

D.R. Dadadzhanov[1,2*], **N.S. Petrov**[2], **A.V. Palekhova**[2], **I.A. Gladskikh**[2],
T.A. Vartanyan[2], **G. Markovich**[1]

*1- School of Chemistry, Raymond and Beverly Sackler Faculty of Exact Sciences, Tel Aviv University,
Tel Aviv 6997801, Israel*
*2- International Research and Education Centre for Physics of Nanostructures, ITMO University,
49 Kronverksky Pr., St. Petersburg 197101, Russian Federation*

* daler.dadadzhanov@gmail.com

In this work we utilized pulsed and continuous wave laser to prepare achiral and chiral nanoparticles made of silver. The second harmonic of pulsed Nd:YAG laser was applied for formation of silver nanoparticles in water solution. A straightforward physical technique has been introduced to produce stable oligomers of silver nanoparticles. These nanoparticles are initially generated through pulsed laser ablation of a metal target submerged in a liquid. The formation of silver nanoparticle oligomers occurs in an aqueous solution after extended centrifugation at 18,000 g, followed by ultrasonication of the original colloidal solution containing spherical nanoparticles produced by laser ablation. The plasmon resonance in these oligomers shifts by 140 nm to the longer-wavelength region compared to the plasmon resonance of the spherical nanoparticles. Thanks to their capability to shift plasmon resonance into the long-wavelength spectral region without relying on conventional chemical synthesis methods, surfactant-free silver nanoparticle oligomers hold significant promise for diverse applications in biomedical imaging, targeted drug delivery, and photothermal therapy.

Another approach to utilizing laser radiation involved the application of continuous visible lasers (405 nm and 532 nm) on isotropic silver nanoparticles, which were produced by depositing metal vapors onto a dielectric substrate. The transformation from achiral silver nanostructures, consisting of nanoparticles with inhomogeneous sizes and shapes, to chiral structures using continuous wave laser with circularly polarized states was explored. We propose that chirality induction relies on disrupting the equilibrium between two "enantiomers" through laser heating of resonant and non-resonant silver nanoparticles, subsequently prompting reshaping.

Hardness increases of titanium samples by laser treatment under compressed graphite powder

X. Egorova[*], **A. Shamova, A. Sidorova, D. Polyakov, D. Sinev**

Institute Laser Technology, University ITMO, Kronverksky avenue 49, St. Petersburg, 197101, Russia

* x_egorova@itmo.ru

Laser processing of metal parts by varying the parameters of laser radiation allows obtaining specific surface layer properties such as increased hardness, wear and corrosion resistance and resistance. In addition, laser processing provides precise and controlled modification of metal surfaces, allowing to obtain the required characteristics with high accuracy and reproducibility of results in short processing time [1,2]. Thus, further study of laser machining of metal parts has great potential to develop more efficient and sustainable manufacturing processes. But to identify the potential of laser machining to improve the functional properties of the formed surfaces and ensure high productivity of the method, it is necessary to investigate and search for new approaches of machining realization.

This study presents the results of an experimental and analytical investigation into the optimization of laser treatment parameters to regulate the mechanical characteristics of the surface layer of metal samples. The treatment was conducted under an additional compressed layer of graphite powder, which resulted in the formation of a solid coating on the surface with hardness of 2500 HV [3,4]. However, when attempting to scale the layer for real production tools, a few problems were encountered, specifically in providing uniformity distributions of mechanical properties on the surface. Thermal imaging measurements of temperature on the back samples surface performed during laser processing suggested a significant influence of thermal processes on structural changes in the material. Within the framework of the extended approach [5], analytical 3D modeling of the accumulative heating of a titanium plate coated with a graphite layer was carried out under multipulse nanosecond laser irradiation in scanning mode. Comparison of experimental data with modeling results allowed us to evaluate the influence of accumulated heat on the inhomogeneity in the distribution of mechanical properties of samples after laser processing. The obtained results can demonstrate the potential for improving the operational characteristics of products in mechanical engineering or metalworking.

[1] G. Hou and A. Li, Effect of surface micro-hardness change in multistep machining on friction and wear characteristics of titanium alloy, Applied Sciences, vol. 11 (16), pp. 7471, (2021).
[2] M. Rajabi, R. Miresmaeili, M. Aliofkhazraei, Hardness and wear behavior of surface mechanical attrition treated titanium, Materials Research Express, vol. 6 (6), pp. 065003, (2019).
[3] X.A. Egorova, K.A. Rozanov, A.I. Kiian, et al, Features of Additive Laser Processing for the Surface Layer Hardness Increase on Titanium Samples, Photonics Russia, vol 17(1), pp. 16-24, (2023).
[4] X.A. Egorova, K.A. Rozanov, A.D. Sidorova, et al, Hardness enhancement by laser modification of titanium under an auxiliary graphite layer, Appl. Phys. A, 129, 855 (2023).
[5] D. Polyakov, G. Shandybina, A. Shamova, Analytical 3D modeling of accumulative heating under multipulse laser irradiation of inorganic materials and biological tissues, Thermal Science and Engineering Progress, vol. 31, pp. 101284, (2022).

The progress of rl-SNMS machine development in Yekaterinburg: what already has been done and what has to be done soon?

V.M. Gadelshin[1,2]

1- Ural Federal University, Institute of Physics and Technology, Mira st. 19, 620002 Yekaterinburg, Russia
2- Institute of Industrial Ecology UB RAS, Sofia Kovalevskaya st. 20, 620990 Yekaterinburg, Russia

gadelshinvm@mail.ru

Resonantly (laser) ionized Sputtered Neutral Mass Spectrometry (rl-SNMS) is the most advanced version of the secondary ion mass spectrometry (SIMS) – a method for studying the chemical composition and its distribution over the surface and in the volume of a sample material. Due to the use of the laser resonance ionization, it is possible to address neutral particles, which are sputtered in a standard SIMS in the ratio of ~100:1 to secondary ions [1]. As a consequence, for certain chemical elements the matrix effects become negligible, and a higher sensitivity to rare-earth and transuranium elements on an ultra-trace, even femtogram level can be achieved [2]. Moreover, in a combination with time-of-flight (TOF) mass analyzer, the laser resonance ionization allows to handle the purified ion beam of a desired nuclide almost without isobaric interferences.

In the talk the basic principles of the method and an overview of recent rl-SNMS applications are going to be given. Currently, a new rl-SNMS machine is being developed in Yekaterinburg in the frame of a joint laboratory between the Ural Federal University and the Institute of Industrial Ecology UB RAS. The used laser system is based on tunable Ti:Sapphire lasers of the Johannes Gutenberg University Mainz design [3] pumped by a commercial pulsed Nd:YAG laser with a repetition rate of 10 kHz (Photonics Industries DM60-532). In comparison with other known projects, the status of the rl-SNMS machine in Yekaterinburg as well as the upcoming research program will be presented.

[1] A. Wucher. Laser post-ionisation – fundamentals, in TOF-SIMS: Materials Analysis by Mass Spectrometry, 2nd ed. – Charlton, United Kingdom: IM Publications Open LLP. – 2013. – pp. 217–246.
[2] H. Bosco, et al, New horizons in microparticle forensics: Actinide imaging and detection of 238 Pu and 242m Am in hot particles, Science Advances, vol. 7(44). – 2021. – p. eabj1175.
[3] M. Franzmann, H. Bosco, C. Walther, K. Wendt, A new resonant Laser-SNMS system for environmental ultra-trace analysis: Installation and optimization, International Journal of Mass spectrometry, vol. 423. – 2017. – pp. 27–32.

Modeling of short-pulse laser interactions with monolithic and porous silicon targets with an atomistic–continuum approach

M. Grigoryeva[1,2*], **D. Ivanov**[1], **S. Lukashenko**[3], **A. Fronya**[1,2], **I. Zavestovskaya**[1,4]

1- P.N. Lebedev Physical Institute of the Russian Academy of Sciences, 53 Leninskiy Prospekt, Moscow 199991, Russian Federation
2- National Research Nuclear University MEPhI (Moscow Engineering Physics Institute), 31 Kashirskoe shosse, Moscow 115409, Russian Federation
3- Institute for Analytical Instrumentation of the Russian Academy of Sciences, 26 Rizhsky Prospect, St. Petersburg 190103, Russian Federation
4- National Research Center "Kurchatov Institute", 1 Academician Kurchatov Square, Moscow 123182, Russian Federation

* grigorevams@lebedev.ru

The acquisition of reliable knowledge about the mechanism of short laser pulse interactions with semiconductor materials is an important step for high-tech technologies towards the development of new electronic devices, the functionalization of material surfaces with predesigned optical properties, and the manufacturing of nanorobots (such as nanoparticles) for bio-medical applications [1-4].

The laser-induced nanostructuring of semiconductors, however, is a complex phenomenon with several interplaying processes occurring on a wide spatial and temporal scale. In this work, we apply the atomistic–continuum approach for modeling the interaction of an fs-laser pulse with a semiconductor target, using monolithic crystalline silicon (c-Si) and porous silicon (p-Si) [5]. This model addresses the kinetics of non-equilibrium laser-induced phase transitions with atomic resolution via molecular dynamics, whereas the effect of the laser-generated free carriers (electron–hole pairs) is accounted for via the dynamics of their density and temperature.

The combined model was applied to study the microscopic mechanism of phase transitions during the laser-induced melting and ablation of monolithic crystalline (c-Si) and porous Si targets in a vacuum. The melting thresholds for the monolithic and porous targets were found to be 0.32 J/cm^2 and 0.29 J/cm^2, respectively. The limited heat conduction mechanism and the absence of internal stress accumulation were found to be involved in the processes responsible for the lowering of the melting threshold in the porous target. The results of this modeling were validated by comparing the melting thresholds obtained in the simulations to the experimental values. A difference in the mechanisms of ablation of the c-Si and porous Si targets was considered. Based on the simulation results, a prediction regarding the mechanism of the laser-assisted production of Si nanoparticles with the desired properties is drawn.

[1] K. Busch, G. von Freymann, S. Linden, S.F. Mingaleev, L. Tkeshelashvili, M. Wegener, Periodic nanostructures for photonics, Physics Reports, vol. 444, pp. 101–202, (2007).
[2] D.S Zhang, B. Goekce, S. Barcikowski, Laser Synthesis and Processing of Colloids: Fundamentals and Applications, Chemical Reviews, vol. 117, pp. 3990–4103, (2017).
[3] A.V. Kabashin, P. Delaporte, A. Pereira, D. Grojo, R. Torres, T. Sarnet and M. Sentis, Nanofabrication with Pulsed Lasers, Nanoscale Research Letters, vol. 5, pp. 454-463, (2010).
[4] A.V. Kabashin, A. Singh, M.T. Swihart, I.N. Zavestovskaya, P.N. Prasad, Laser Processed Nanosilicon: A Multifunctional Nanomaterial for Energy and Health Care, ACS Nano, vol. 13, pp. 9841–9867, (2019).
[5] V.P. Lipp, B. Rethfeld, M.E. Garcia, D.S. Ivanov, Atomistic-Continuum Modeling of Short Laser Pulse Melting of Si Targets, Physical Reviev B, vol. 90, pp. 245306, (2014).

High-power laser interaction with transparent solid-solid interface: applications to laser damage of optical coatings

V. Gruzdev[1]

1- Department of Physics and Astronomy, University of New Mexico,
210 Yale Boulevard NE, Albuquerque, NM, 87106, USA

vgruzdev@unm.edu

Interactions of high-power laser pulses with interfaces between two transparent solids involves some effects that are characteristic of the system and are not met in case of bulk solids or surfaces (i.e., solid-gas interfaces). The special features arise from a fundamental fact [1] that nonlinear absorption and associated excitation of electronic sub-systems of the two solids happen at different rates and result in different levels of energy deposition and free-carrier density. Gradients of the free-carrier density across the interface can reach huge values and stimulate ultrafast diffusion through the interface. The diffusion results in charge separation within a layer of few-nanometers thick and build-up of a quasi-static electric field around the interface. The quasi-static field can stimulate numerous effects, e.g., dynamic Shottky effects, Stark shift of energy levels of interface defects, or band-gap reduction due to the Franz-Keldysh effect. Localization of those effects in space substantially depends on screening capabilities of electron sub-systems of the two materials that make the interface. Formation of large temperature gradients can also take place at the interface due to different values of heat-transfer coefficients of the two materials. Relevant effects include thermo-mechanical stresses and possible thermo-voltaic effects at the interface if heating is combined with separation of laser-generated free carriers.

In this talk, we overview those laser-interface interactions and estimate their contributions in case of an interface between two transparent materials characteristic of multilayer optical coatings. To be specific, we consider material parameters of fused silica SiO_2 and hafnia HfO_2 as those materials are the most frequently utilized in optical coatings [2,3]. Of particular interest is application of the laser-interface interaction models to interpret some experimental data from the field of laser damage of high-quality optical coatings. Optical coatings suffer from reduced thresholds of laser damage in spite of tremendous improvement of their quality [2,3]. Traditional approaches attribute the reduced damage thresholds to various defects that inevitably appear during deposition process [2-5]. However, formation of flat-bottom damage sites [2,5] and anomalously high damage thresholds of Rugate high reflectors with cosine variations of refractive index [2,4] cannot be interpreted based on the concept of defect-induced local damage. In particular, the Rugate multilayer reflectors demonstrated increase of absorption by 200%-300% accompanied by increase of damage threshold almost by one order of magnitude compared to similar multilayers of the traditional design [2,4]. Considering 5.6-eV band gap of hafnia and 9-eV band gap of fused silica, we first simulated nonlinear absorption and free-carrier generation. Difference between the free-carrier densities delivered a huge gradient of free-electron density of the order of 10^{28} 1/cm^4 at the interface. Free-electron dynamics was treated based on equation for ambipolar diffusion that incorporated generation of quasi-static electric field due to charge separation. Estimations of the quasi-dc field magnitude delivered values of the order of $10^6 – 10^7$ V/m. The field was sufficient enough to stimulate band-gap reduction by as much as 1-2 eV. Estimations of diffusion time for the free-electron transfer across the interface delivered values between 1 and 10 fs depending on material and laser-pulse parameters. In this connection, we consider applications of this model to the case of ultrashort laser pulses bearing in mind that flat-bottom damage sites were also observed for ultrashort pulses [5].

Based on obtained results, we discuss approaches to control the laser-interface interactions and some of the recently proposed modifications of coating design [6] to address the interface effects.

[1] V. Gruzdev, JOSA B, under review (2024).
[2] C. J. Stolz, in Laser-Induced Damage in Optical Materials, D. Ristau, Ed. (CRC Press, New York), Chapter 14, pp. 385-409 (2014).
[3] J. Zhang, et al, Opt. Eng. 57 (12) (2018), 127909.
[4] S. Dong, et al, Prog. Surf. Sci. 97, 100663 (2022).
[5] N. Talisa, et al, Opt. Lett. vol. 45, p. 2672 (2020).
[6] M. Zhu, N. Xu, B. Roshanzadeh, et al, Nanolaminate-based design for UV laser mirror coatings, Light Sci Appl 9, 20 (2020).

Interaction of optical, soft X-ray, and hard X-ray lasers with solids

N. Inogamov[1,2]

1- L.D. Landau Institute for Theoretical Physics of Russian Academy of Sciences, 142432 Chernogolovka, prospekt Akademika Semenova, 1A, RF
2- N.L. Dukhov Automatics Research Institute (VNIIA) ROSATOM, 127055 Moscow, ulitsa Sushchevskaya, 22, RF

nailinogamov@gmail.com

This report is about the results of the recent papers [1-4]. The paper [1] is devoted to analysis of an action of ultrashort (20 fs, femtoseconds) laser pulse of hard (9 keV) X-ray on a LiF dielectric. Hard photons have a very long attenuation length d_{att} in all materials (metals, dielectrics, semiconductors) except heavy metals with many-electron shells. This dramatically differentiates fs optical breakdown of dielectrics or fs surface ablation (metals, dielectrics) by optical lasers from the laser-matter interaction in the case with a fs hard X-ray laser with a well collimated beam (spot down to small fractions of a micron) and a huge d_{att}. If optical breakdown is used to study polymorphic phase transitions [5-7], the mass of the region in which such a transition has taken place is limited to extremely small values from $\sim 10^{14}$ to 10^{13} g [5,6]. In the case of the X-ray impact we are considering, this mass is three orders of magnitude larger. If we compare optical ablation and X-ray action, the mechanism of induced substance transport is fundamentally changed. In the process of optical ablation of the surface, the metal enters the vapor-plasma state and flies away (ablation - substance entrainment). Whereas in our situation, the removal into air/vacuum is small. The main displacement is cavity formation by indentation. E.g., when processing highly toxic beryllium (Be), this peculiarity is essential because only a small fraction of Be is atomized into the laboratory volume.

In [2], the propagation of a double-jump elastic - fracture laser-induced shock in diamond is considered. Understanding the behavior of matter at extreme pressures of the order of a megabar (Mbar) is essential to gain in-sight into various physical phenomena at macroscales – the formation of planets, young stars, and the cores of super-Earths, and at microscales – damage to ceramic materials and high-pressure plastic transformation and phase transitions in solids.

In [3], the melting/crystallization of titanium (Ti) by a multi-megabar shock is described. Such a shock is generated by a fs optical laser pulse (Ti:Sapp). The problem has applications in LSP (laser shock peening) – there is a refinement of large crystallites (tens of microns) to nanosize.

In [4] the coefficients of electron-phonon interaction and thermal conductivity in gold with strongly excited electron subsystem were determined.

[1] S. Makarov, et al, Damage threshold of LiF crystal irradiated by femtosecond hard XFEL pulse sequence, Opt. Express, 31, 26383-26397, (2023).
[2] S. Makarov, et al, Direct imaging of shock wave splitting in diamond at Mbar pressure, Matter and Radiation at Extremes, 8, 066601, (2023).
[3] V. Zhakhovsky, et al, Shock-induced melting and crystallization in titanium irradiated by ultrashort laser pulse, Physics of Fluids, 35(4), 096104, (2023).
[4] N. Inogamov, et al, Determination of the most important parameters of metal irradiated by ultrashort laser pulse (in Russian), Zhurnal Exp. Teor. Fiziki, 165, 165-190, (2024).
[5] S. Juodkazis, et al, Laser-Induced Microexplosion Confined in the Bulk of a Sapphire Crystal: Evidence of Multimegabar Pressures, Phys. Rev. Lett., 96, 166101, (2006).
[6] L. Smillie, et al, Exotic silicon phases synthesized through ultrashort laser-induced microexplosion: Characterization with Raman microspectroscopy, Phys. Rev. Mater., 4(9), 093803 (2020).
[7] E. Mareev, F. Potemkin, Dynamics of ultrafast phase transitions in MgF_2 triggered by laser-induced THz coherent phonons, Sci. Rep., 12, 6621 (2022).

Merging of defect modes in one-dimensional photonic crystals with two defect layers

A.O. Kamenev[1,2*], **A.A. Malinchenko**[1], **N.A. Vanyushkin**[1], **I.M. Efimov**[1],
S.S. Golik[1,2], **V.G. Chigrinov**[3], **A.H. Gevorgyan**[1]

1- Far Eastern Federal University, Institute of High Technologies and Advanced Materials, 690922 Vladivostok, Russia
2- Institute of Automation and Control Processes, Far East Branch, Russian Academy of Sciences, 690041 Vladivostok, Russia
3- Foshan University, School of Physics and Optoelectronic Engineering, 528011 Foshan, China

* kamenev.ao@dvfu.ru

With the development of optics and photonics, research into the possibilities of photonic crystals (PCs) is becoming increasingly popular. A well-known property of such structures is their ability to control the light passing through them due to the so-called photonic bandgap (PBG). In one-dimensional (1D) PCs, defect modes (DMs) represent resonant peaks in the transmission spectra. The number of DMs within the PBG is determined by the number of defect layers (DLs) in the structure of the PC and their optical thicknesses. The parameters of the DL directly influence the position of the DMs in the spectra, which is the basis for the operation of 1D PC-based sensors. Over the past few decades, many different optical sensors based on 1D PCs with DLs have been developed for a wide range of applications. Additionally, many papers have been published on the optimization of 1D PCs and their properties [1-3]. However, the application potential of PCs with several defects in the structure is not well investigated. In particular, no paper presents a condition for the merging of two DMs appearing in such structures. That is why we have studied this question in more detail. Here we have derived the condition for the merging of two DMs in 1D PCs with two DLs. This condition is demonstrated by formula 1:

$$\Delta\varphi = \frac{1}{2} i \cdot \ln \left[\frac{r_{II}\tilde{r}_{II}^*}{r_{III}\tilde{r}_{I}^*} \frac{2 - |r_{II}|^2 \pm 2\sqrt{1 - |r_{II}|^2}}{|r_{II}|^4} \right] - \pi q_2, \tag{1}$$

where $\Delta\varphi = \varphi_1 - \varphi_2$ is the phase difference, r is the reflection coefficients for each of the three PCs in the structure, $\tilde{r}$ is the reflection coefficient for each of the three PCs when the wave is incident from the right, i.e., from the DL side, $q_2 \in Z$, $\varphi_{1,2} = \frac{2\pi}{\lambda} n_{d1,2} d_{d1,2}$ are the changes of phase of the wave at a single passage through the first and second DLs in the structure, n_{d1} and n_{d2} are the refractive indices of two DLs, d_{d1} and d_{d2} are their thicknesses. Using this formula, we have found such PC parameters at which the DMs merge and a large localization of the electromagnetic field in the DLs and at the wavelength of the merging of two DMs in the 1D PC with two DLs is observed.

[1] I.M. Efimov, et al, Sensor with enhanced performance based on photonic crystal with a defect layer, Computer Optics, vol. 47, pp. 572–79, (2023).

[2] I.M. Efimov, N.A. Vanyushkin, A.H. Gevorgyan, Peculiarities of the Electromagnetic Field Distribution Inside a 1D Photonic Crystal with a Defect Layer, Bulletin of the Russian Academy of Sciences: Physics, vol. 86, pp. 60–65, (2022).

[3] A.O. Kamenev, et al, On the sensitivity of defect modes outside the first photonic bandgap in optical sensors based on defected 1D photonic crystals, Physica Scripta, vol. 99(4), pp. 045521, (2024).

Investigation of microrelief formation features under multi-pulse nanosecond laser irradiation of metal surface under increased pulse repetition rate

<u>Yu. Karlagina</u>[1*], V. Veiko[1], D. Polyakov[1], G. Romanova[1]

1- Institute of Laser Technologies, ITMO University, 14-16 Birzhevaya Line, Saint Petersburg, Russia, 199034

* jujukarlagina@itmo.ru

This study investigates the influence of laser pulse repetition rate (in the kilohertz range) on the characteristics of the microrelief formed on the surface of a metal during its laser nanosecond ablation.

Previously, it was assumed that during laser ablation of metal surfaces with short pulses (from units to hundreds of nanoseconds), the main role in the formation of microrelief (depressions or craters, holes, etc.) is played by such parameters of laser radiation as pulse duration, pulse energy density, and irradiation multiplicity (number of pulses). However, with the growing popularity of industrial fiber laser systems, which have high average power and a wide-range adjustable pulse repetition rate, the issue of high-frequency microprocessing for various applications, such as creating functional coatings, forming microchannels, wetting gradients, etc., has become particularly relevant.

The purpose of this study is to investigate the role of heat accumulation during multi-pulse laser processing with a scanning beam in near-threshold ablation regimes, developed ablation regimes (above the ablation threshold), and under conditions of formation of radiation-absorbing plasma by using different energy density Q. In the experiments, the same effective exposure time t to the surface area was ensured at a variable frequency f in the range from 1.6 kHz to 100 kHz. A theoretical calculation was carried out to investigate the influence of the laser pulse repetition rate on the cumulative heating of titanium using a thermal model of laser ablation.
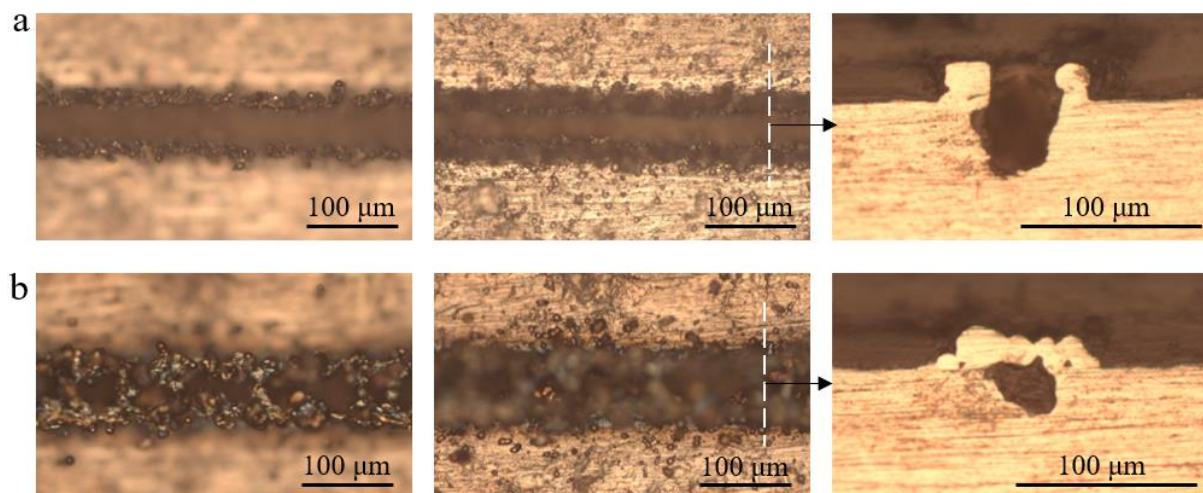
Fig. 1. Optical microscopy – Two limiting cases a) f_1=1.6 kHz and b) f_2=45 kHz (Q=const, t=const) demonstrating the significant role of heat accumulation effects in the target on the formation of microrelief during multi-pulse laser processing.

Regularities and ranges of effective laser ablation regimes were established to control the dynamics of melting by varying the pulse repetition rate, and the mechanisms of surface microgeometry formation were described.

Laser-assisted synthesis of materials for electrochemical applications

E. Khairullina[1,2*], **A. Levshakova**[1], **M. Kaneva**[1,3], **M. Panov**[1,4], **A. Manshina**[1]

1- St. Petersburg University, 7/9 Universitetskaya Emb., St. Petersburg 199034, Russia
2- School of Physics and Engineering, ITMO University, Lomonosova, 9, Saint-Petersburg, 191002, Russia
3- Ioffe Institute, St. Petersburg 194021, Russia
4- St. Petersburg State Chemical Pharmaceutical University Faculty of Pharmaceutical Technology, Professor Popov Str., 14, Lit. A, St. Petersburg 197022, Russia

* e.khayrullina@spbu.ru

Materials for electrochemical applications, including sensors, batteries and supercapacitors, are a rapidly evolving field with a constant search for innovative synthesis methods to improve performance, durability and efficiency. The development of novel materials with properties optimised for supercapacitors and sensors can be achieved by harnessing the precision and controlled energy input offered by laser technology.

In this work, we explore various laser-assisted techniques for the fabrication of materials for electrochemical applications, with a particular interest in non-enzymatic electrochemical sensors. Special attention is given to flexible sensors, which are rapidly becoming a dynamic group due to their mechanical adaptability. The prospects for using flexible electrochemical sensors in wearable electronics are particularly significant, as they can provide continuous real-time monitoring. A major focus has been the study of laser-induced processes for the reduction of transition metals ions at the substrate-precursor interface, leading to the formation of conductive metallic structures. These structures have been used as working electrodes in sensor systems, demonstrating their potential for electrochemical detection of a broad spectrum of target substances.

The effects of laser parameters on the structural, morphological and electrochemical properties of the synthesised materials were investigated. The use of laser synthesis offers significant advantages over conventional methods, particularly in terms of synthesis localisation. This facilitates the creation of electrodes with specific geometries on substrates of any shape.

Development of an activation station for irradiation of photocatalytic coatings based on titanium oxides

V. Khmelevsky[1*], Yu. Karlagina[1], N. Afanasyev[1], E. Prokofiev[1], G. Romanova[1]

1- ITMO University, Russia, Saint-Petersburg, Birzhevaya street 14-16

* hotlinevalery@yandex.ru

A critical task in medicine and laboratory settings is surface sterilization to prevent bacterial contamination. One of the most effective methods for combating bacterial contamination is UV sterilization, whose efficiency can be increased by using it in combination with semiconductor coatings [1,2]. This method triggers photocatalysis in the semiconductor, leading to the generation of reactive oxygen species and subsequent bacterial destruction [3,4]. This study investigates the photocatalytic activity of oxide films formed on titanium samples during laser surface oxidation, utilizing a developed activation station (AS).

Tasks performed during the work:

1. Design and assemble the activation station. This includes calculating the electrical circuit parameters and determining the overall station specifications.
2. Evaluate the stability of the AS under normal and specified operating conditions.
3. Investigate the photocatalytic activity and physicochemical properties of laser-induced oxide coatings created on the surface of titanium samples.

Brief description of the results obtained:

We developed and built an AS for irradiating laser-induced oxide coatings. We created test samples with oxide films on their surfaces using laser thermochemical processing. We investigated the photocatalytic activity of the created semiconductor coatings using the AS. We studied the relationship between the photocatalytic yield efficiency and the laser radiation dose for samples irradiated using the AS at a wavelength of 400 nm. Samples created with the highest laser irradiation dose exhibited the greatest photocatalytic activity. We investigated the surface morphology of laser-induced oxide coatings and the dependence of photocatalytic yield efficiency on the physicochemical properties of these coatings.

[1] W. Ahmed, Z. Zhai, C. Gao, Adaptive antibacterial biomaterial surfaces and their applications, Materials Today Bio. – V. 2. – P. 100017, (2019).
[2] N. Zrelovs, et al, Sorting out the superbugs: Potential of sortase A inhibitors among other antimicrobial strategies to tackle the problem of antibiotic resistance, Antibiotics. – V. 10. – №. 2. – P. 164, (2021).
[3] J. Wang, et al, Oxygen-vacancy-enhanced singlet oxygen production for selective photocatalytic oxidation, ChemSusChem. – V. 13. – №. 13. – P. 3488-3494, (2020).
[4] Y. Karlagina, et al, Laser-induced antibacterial coating on the surface of an individual titanium membrane designed by a neural network, Optical and Quantum Electronics, – V. 55. – №. 9. – P. 775, (2023).

Ultrafast hot electron diffusion in nickel one-dimensional plasmonic crystals

M.A. Kiryanov[*], I.A. Novikov, A.Y. Frolov. T.V. Dolgova. A.A. Fedyanin

Faculty of Physics, Lomonosov Moscow State University, Moscow, 119991 Russia

* *kiryanovma@my.msu.ru*

One of the promising fields of nanophotonics is studying plasmonic crystal optical response on external stimulus such as a femtosecond laser radiation. An ultrashort "pump" pulse heats electron gas of metals and modifies dielectric permittivity. The induced changes can be observed by measuring reflectance or transmittance of a "probe" pulse. Plasmonic crystals reflectance or transmittance spectra are sensitive to dielectric permittivity changes near a resonance, therefore they can be used to significantly enhance thermooptical response. Evolution of a plasmonic crystal optical response is described by hot electron dynamics inside a metal. In case of a nanostructured surface electric field localization of "pump" and "probe" pulses inside plasmonic crystal may be spatially inhomogeneous, which allows detection of hot electron diffusion along surface.

In this work, ultrafast differential reflectance of reference nickel plate and three nickel one-dimensional plasmonic crystals with the sinusoidal surface shape, the same spatial period, and different corrugation depths were measured by femtosecond spectroscopy "pump-probe" technique. Differential reflectance time traces at resonant wavelength of plasmonic crystals showed considerably slower dynamics compared to reference plate and literature: both rise and relaxation of differential reflectance took longer time. The lag became more pronounced with corrugation depth increase. The effect is associated with inhomogeneous absorbing of pump pulse by nickel concentrated at the bottoms of the plasmonic crystal, consequent transfer of hot electrons along sides of the plasmonic crystal up to the tops and detection of entire surface temperature by resonant probe pulse. To confirm this interpretation combined two-temperature and electromagnetic calculation were done.

Synthesis, properties and applications of innovative nanoformulations for binary technologies of medical treatment

S. Klimentov[1]*, **A. Popov[1]**, **G. Tikhonowski[1]**, **M. Savinov[1]**, **D. Tzelikov[1]**,
I. Zavestovskaya[2], **A. Kabashin[1,3]**

1- National Research Nuclear University (MEPhI), Moscow, Russia
2- Russian Nuclear Center "Kurchatov Institute", Moscow, Russia
3- Laboratoire LP3, Aix-Marseille University, CNRS, Marseille, France

* smklimentov@mephi.ru

Synthesis and characterization of new nanoparticles (NPs) and nanoformulations (NFs) are traditionally the focus of research and technology innovations, including new approaches to medical diagnostics and treatment. This sustained interest is due to the broad variety of nanostructures properties based not only on their size and chemical composition, but also on morphology and subtle nuances related to their fabrication techniques. In this regard, laser ablation in liquids looks most versatile and adaptive in terms of wide range of allowed materials and fine control of physical and chemical characteristics of the resulting nanomaterials. This especially applies to ablation induced by ultrashort laser pulses, femtosecond and short picosecond, demonstrating non-thermal decomposition of the source material, avoiding this way the stage of melting. Colloidal solutions obtained this way are featured by exceptional purity and, in many cases, colloidal stability without using of ligands, which makes them an extremely promising choice for variety of biomedical applications.

We report here the results of an extensive research on laser ablative fabrication, characterization and applications of multimodal nanosensitizers i.e. NPs and more complex NFs, which can serve as contrast agents for diagnostics and local therapies under external physical stimuli, including x-ray radiation, neutron and proton beams, and CW laser radiation [1-3]. The first group of single element nanomaterials is based on heavy metals like gold and bismuth, the second includes boron-based and other materials featured by large interaction cross section with the corresponding particle beams, the third embraces a number of synthesized two element nanomaterials (nitrides and borides) demonstrating an excellent absorptivity of laser light in the biological tissue transparency window due to their plasmonic properties. We also present our recent results on fabrication and study of more complex composite multimodal nanomaterials [4], produced via multi-step laser assisted technologies, every particular component of which is activated by the different external physical factors or by combination of those. Significant number of the reported nanomaterials exhibits the potential for use in theranostic applications via combination of diagnostic and therapeutic modalities.

[1] A.I. Pastukhov, I.B. Belyaev, J.C. Bulmahn, I.V. Zelepukin, A.A. Popov, I.N. Zavestovskaya, S.M. Klimentov, S.M. Deyev, P.N. Prasad, A.V. Kabashin, Laser-ablative aqueous synthesis and characterization of elemental boron nanoparticles for biomedical applications, Scientific Reports, Vol. 12, p. 9129, (2022).
[2] A.A. Popov, G.V. Tikhonowski, P.V. Shakhov, E.A. Popova-Kuznetsova, G.I. Tselikov, R.I. Romanov, A.M. Markeev, S.M. Klimentov, A.V. Kabashin, Synthesis of Titanium Nitride Nanoparticles by Pulsed Laser Ablation in Different Aqueous and Organic Solutions, Nanomaterials, Vol. 12, p. 1672, (2022).
[3] V.A. Oleshchenko, A.Yu. Kharin, A.F. Alykova, O.V. Karpukhin, N.V. Karpov, A.A. Popov, V.V. Bezotosnyi, S.M. Klimentov, I.N. Zavestovskaya, A.V. Kabashin, V.Yu. Timoshenko, Localized infrared radiation-induced hyperthermia sensitized by laser-ablated silicon nanoparticles for phototherapy applications, Applied Surface Science, Vol. 516, p. 30, (2020).
[4] O.Yu. Griaznova, I.B. Belyaev, A.S. Sogomonyan, I.V. Zelepukin, G.V. Tikhonowski, A.A. Popov, A.S. Komlev, P.I. Nikitin, D.A. Gorin, A.V. Kabashin, S.M. Deyev, Laser Synthesized Core-Satellite Fe-Au Nanoparticles for Multimodal In Vivo Imaging and In Vitro Photothermal Therapy, Pharmaceuticals, Vol. 14, p. 994, (2022).

Oriented carbon chain – new route for thin-films photonics devices

A. Kucherik[1*], V. Samyshkin[1], A. Abramov[1],
A. Lelekova[1], S. Arakelian[1], A. Povolotskiy[2], A. Osipov[1]

1- Department of Physics and Applied Mathematics, Stoletov Vladimir State University, 600000 Gorkii street, Vladimir, Russia
2- Institute of Chemistry, St. Petersburg State University,198504, Ulianovskaya str. 5, St. Petersburg, Russia

* kucherik@vlsu.ru

Carbon has established itself as one of the most promising materials for a number of nanotechnology applications. The variety of allotropic forms of carbon allows the creation of a wide range of nanostructures that possess unique optical and electronic properties. Over the past decade, many research papers have been dedicated to the synthesis and fabrication of sp-hybridized carbon structures. The nanoscience community pays special attention to one-dimensional sp-carbon due to its unusual band structure, leading to its ability to emit and absorb visible light.

The control of the chain length and types of interatomic bonds in linear chains is essential for controlling the electric resistance and photoluminescence of fabricated films. In our works, we developed the method of the synthesis and fabrication of linear carbon chains via the laser fragmentation of colloidal systems [1,2], resulting in the stabilization of linear sp-chains by gold anchors attached to their ends [3].

This study demonstrates the synthesis of linear carbon structures through laser irradiation of colloidal systems containing carbon nanoparticles. The use of nanosecond laser pulses allows for partial particle fragmentation, disrupting bonds between layers and leading to the formation of linear structures from graphene layers. Under laser irradiation, sp-fragments of linear chains form, experience kinks, and bond to create sp^2- and sp^3-bonds. During ablation in a liquid medium, linear chains become more resistant due to viscous forces, as observed in the Raman spectra. We investigated the optical properties of extremely thin carbon chains.

We show that the gold clusters also act as a source of electron doping thus changing the intensity of photoluminescence from quadratic dependence on the pumping intensity without gold to linear with gold. We also observe that the excitation of the film at the gold plasmon frequency causes the blue shift of photoluminescence and estimate on the basis of this effect the minimum length of the carbyne chains [4]. The high degree of alignment of the gold-terminated carbyne chains results in strongly anisotropic light absorption characterized by a distinctive cosine dependence on the angle between the carbyne molecule and polarization plane of the excitation.

[1] V. Samyshkin, A. Lelekova, A. Osipov, D. Bukharov, I. Skryabin, S. Arakelian, A. Kucherik, S. Kutrovskaya, Photosensitive free-standing ultra-thin carbyne-gold films, Opt. Quantum Electron., 51, 394, (2019).
[2] A.O. Kucherik, S.M. Arakelian, S.V. Garnov, S.V. Kutrovskaya, D.S. Nogtev, A.V. Osipov, K.S. Khor'kov, Two-stage laser-induced synthesis of linear carbon chains, Quantum Electron., 46, 627, (2016).
[3] S. Kutrovskaya, A. Osipov, S. Baryshev, A. Zasedatelev, V. Samyshkin, S. Demirchyan, O. Pulci, D. Grassano, L. Gontrani, R. Hartmann, et al, Excitonic Fine Structure in Emission of Linear Carbon Chains, Nano Lett., 20, 6502−6509, (2020).
[4] A. Kucherik, A. Osipov, V. Samyshkin, R.R. Hartmann, A. Povolotskiy, M.E. Portnoi, Polarization-sensitive photoluminescence from aligned carbon chains terminated by gold clusters, PRL, 132, 056902, (2024).

Femtosecond laser printing of structural colors for information encryption and anti-counterfeit labeling

<u>V. Lapidas</u>[1*], A. Zhizhchenko[1], S. Shevlyagina[1], A. Cherepakhin[1], A. Kuchmizhak[1,2]

1- Institute of Automation and Control Processes, Far Eastern Branch, Russian Academy of Sciences, 5 Radio Str., Vladivostok, Russia
2- Pacific Quantum Center, Far Eastern Federal University, Vladivostok, Russia

* vslapidas@gmail.com

Structural colors, as a result of light interaction with nanoscale structures, offer a promising alternative to pigments, as they are non-fading and resistant to UV and heat. However, achieving precise control over color tones and saturation at the submicron level currently requires expensive and limited lithographic techniques for creating pixelated nanostructures. To address this, researchers have explored direct laser-based approaches for cost-effective fabrication of structural color. One method involves using focused laser beams to induce dewetting of gold films deposited on Fabry-Perot filters, forming plasmonic nanoparticles [1]. However, this approach suffers from a lack of control over the color, as the nanoparticles are formed randomly, and their size depends on the initial gold film thickness. Our work presents an alternative method that overcomes these limitations. Here, instead of random dewetting, we utilized unique and highly controllable thermomechanical behavior of fs-laser-irradiated thin noble metal film to demonstrate template-free high-resolution color printing at a superior lateral resolution up to 50000 dots per inch (dpi). Diverse ablative and ablation-free scenarios of surface nanotexturing can be simultaneously realized on the top noble-metal film of the MIM sandwich allowing wide tunability of the color tone and saturation. Ability to produce properly arranged subwavelength arrays of isolated hollow nano-bumps supporting reach plasmonic behavior was also utilized to demonstrate the security labeling with facile optical readout [2].
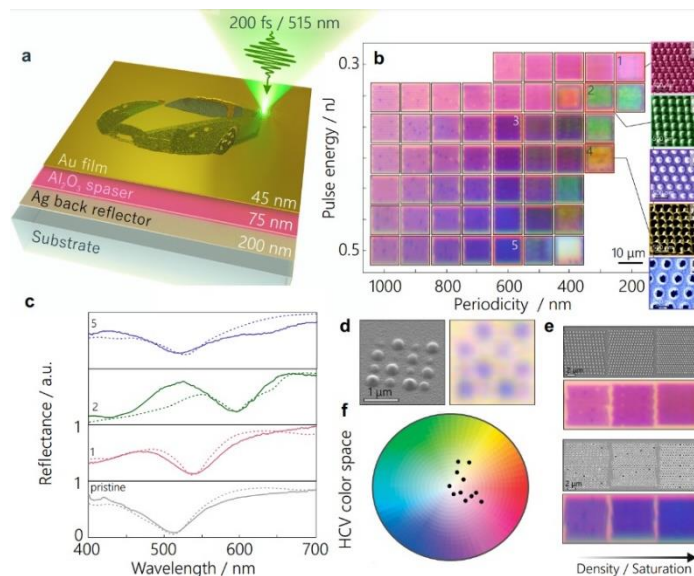
Figure 1. Direct laser printing of structural colors. (a) Schematic of the proposed fs-laser printing of high-resolution structural color images of the surface of top Au layer coating 75-nm thick Al_2O_3 spacer and 200-nm thick Ag reflecting mirror. (b) Color palette illustrated by a series of bright-field optical images of the laser-patterned pixels (10×10 μm^2) fabricated by varying the incident pulse energy and nanostructure periodicity. Insets provide top-view SEM images of representative surface morphologies marked by numbers. (c) Measured (solid curves) and calculated (dashed curves) reflectance spectra of the representative nanotextured surfaces as well as pristine sandwich structure. (d) Correlated SEM and bright-field optical images showing optical appearance of isolated nanobumps of variable size printed at 500 nm periodicity. (e) Tuning the color saturation by increasing the density of nanobumps (top panels) and nanoholes (bottom panels) as illustrated by correlated SEM and optical images. (f) Reflectance spectra of the color palette pixels represented as coordinates in the HCV color space.

[1] A.S. Roberts, S.M. Novikov, Y. Yang, Y. Chen, S. Boroviks, J. Beermann, S.I. Bozhevolnyi, Laser writing of bright colors on near-percolation plasmonic reflector arrays, ACS Nano, Vol. 13, pp. 71-77, (2018).
[2] V. Lapidas, A. Zhizhchenko, E. Pustovalov, D. Storozhenko, A. Kuchmizhak, Direct laser printing of high-resolution physically unclonable function anti-counterfeit labels, Applied Physics Letters, Vol. 120, p. 261104, (2022).

Highly efficient laser-induced synthesis of sensor-active materials on flexible surfaces from deep eutectic solvents

<u>A. Levshakova</u>[1*], E. Khairullina[1], R. Ninayan[1], A. Manshina[1]

1- Institute of Chemistry, Saint Petersburg University, SPbU, 7/9 Universitetskaya nab., St. Petersburg 199034, Russia

* sashkeens@gmail.com

In recent years, the fabrication of sensor-active materials has received a lot of attention from the scientific community and has been used in various fields such as health monitoring, environment, biotechnology and space applications [1]. Flexible sensors are of particular interest as they can be integrated on irregularly shaped surfaces or surfaces subject to bending. Various additive manufacturing methods have been used to develop such materials, including laser-induced liquid phase deposition (LID), which is a highly efficient and cost-effective method for laser synthesis of sensor-active materials on dielectric surfaces [2]. In this method, the laser beam is focused on the phase boundary of the metal solution-substrate and the reduction of metal ions occurs, resulting in the deposition of metal nanostructures on the substrate.

Previous work from our group has shown that deep eutectic solvents (DES) can be used as a deposition medium for the synthesis of copper structures on glass surfaces using laser irradiation [3]. DES are a promising replacement for molecular organic solvents and ionic liquids. The use of DES in laser-induced synthesis has led to a more than 200-fold increase in process speed compared to aqueous systems [4].

In this work, DES LID on the surfaces of the flexible polymers PEN, PI and PET is presented. In addition, despite significant progress in the field of laser synthesis, the problem of high consumption of reagents and human labour in the process of optimising experimental parameters is still unresolved. The laser response is most influenced by parameters such as laser power and scanning speed. Therefore, in the present work it has been proposed to carry out the optimisation of LID conditions from DES on the surfaces of different polymers (PEN, PET, PI) using the Nelder-Mead method (fig. 1). The proposed approach can be used for highly efficient, fast and cost-effective synthesis of flexible metal electrodes for enzyme-free sensor detection.
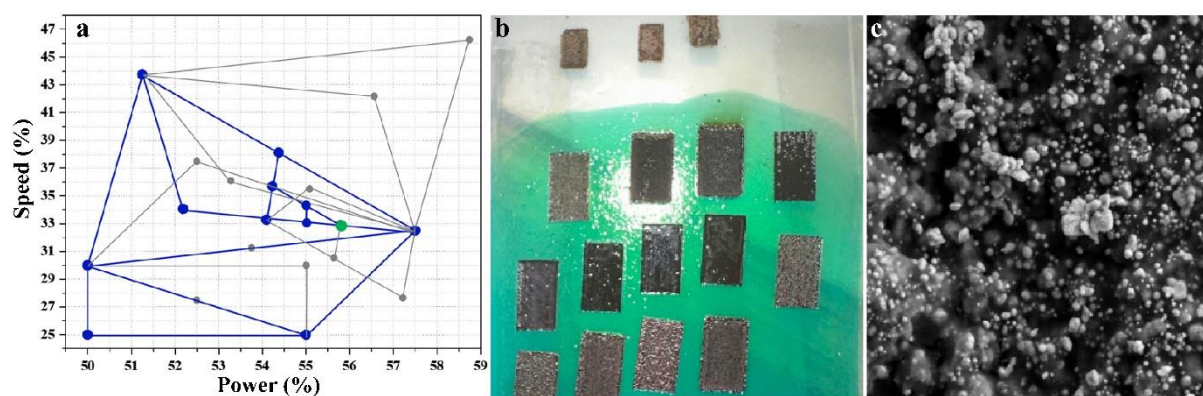
Figure 1. a) Diagram of the Nelder-Mead method for laser synthesis of copper structures on the PET surface, b) Electrode photographs, c) SEM images of electrodes.

[1] Y. Liu, et al, Micro/Nano Electrode Array Sensors: Advances in Fabrication and Emerging Applications in Bioanalysis, Front Chem. Vol. 8, (2020).
[2] E. Khairullina, et al, Rapid and effective method of laser metallization of dielectric materials using deep eutectic solvents with copper acetate, J Mater Sci. Vol. 58, № 22, P. 9322–9336, (2023).
[3] A.S. Levshakova, et al, Modification of nickel micropatterns for sensor-active applications from deep eutectic solvents, Opt Quantum Electron. Vol. 55, № 3, P. 267, (2023).
[4] R. Ninayan, et al, Water-induced changes in choline chloride-carboxylic acid deep eutectic solvents properties, Colloids Surf A Physicochem Eng Asp., Vol. 679, P. 132543, (2023).

Non-Markovian behavior of exciton-polaritonic Bose-Einstein condensates

N.V. Kuznetsova[1], D.V. Makarov[1*], N.A. Asriyan[2], A.A. Elistratov[2], Yu.E. Lozovik[3,4]

1- V.I. Il'ichev Pacific Oceanological Institute FEB RAS, Baltiyskaya Str. 43, Vladivostok, 690041, Russia
2- N.L. Dukhov All-Russia Research Institute of Automatics, Sushchevskaya Str. 22, Moscow, 127055, Russia
3- Institute of Spectroscopy RAS, Fizicheskaya Str. 5, Troitsk, 142190, Russia
4- Moscow Institute of Electronics and Mathematics, National Research University Higher School of Economics, Bol. Trekhsvyatitel'sky per. 1-3/12, build. 8, Moscow, 101000, Russia

* makarov@poi.dvo.ru

Exciton-polaritons are quasiparticles being coupled states of semiconductor excitons and cavity photons. Contemporary technologies of cavity fabrication allow for exciton-polariton lifetimes of hundred picoseconds that makes them experimentally observable. Owing to strong interaction of excitons, exciton-polaritons can form a Bose-Einstein condensate (BEC). Exciton-polaritonic BEC is an intrinsically open quantum system, where strong particle loss is compensated by external incoherent laser pumping. The pumping leads to stimulated relaxation of reservoir excitons into the condensate and the onset of a quasistationary state.

In the present work dynamics of exciton-polaritons is considered for temperatures of few ten kelvins, when coupling of BEC to the excitonic reservoir is essentially non-Markovian [1]. The non-Markovian stochastic Gross-Pitaevskii equation is developed to describe temporal evolution of the condensate wave function [2,3]. It is shown that variation of temperature results in phase transitions according to the BKT scenario. Also, it is found that these phase transitions are highly suppressed in the case of exciton-polaritonic condensates forming a lattice.

[1] D.V. Makarov, A.A. Elistratov, Yu.E. Lozovik, Non-Markovian effects in dynamics of exciton-polariton Bose condensates, Physics Letters A, vol. 384, 126942, (2020).
[2] A.A. Alliluev, D.V. Makarov, N.A. Asriyan, A.A. Elistratov, Yu.E. Lozovik, Formation of exciton-polaritonic BEC in the non-Markovian regime, Physics Letters A, vol. 453, 128492, (2022).
[3] A.A. Alliluev, D.V. Makarov, N.A. Asriyan, A.A. Elistratov, Yu.E. Lozovik, Non-Markovian stochastic Gross-Pitaevskii equation for the exciton-polariton Bose-Einstein condensate, J. Low Temper. Phys. Vol. 214, pp. 331-343, (2024).

Magnetically induced exceptional points in helically structured 1D photonic crystals

A.A. Malinchenko[1*], **A.O. Kamenev**[1,2], **N.A. Vanyushkin**[1], **I.M. Efimov**[1], **S.S. Golik**[1],
V.G. Chigrinov[3], **A.H. Gevorgyan**[1,2]

*1- Far Eastern Federal University, Institute of High Technologies and Advanced Materials, 10 Ajax Bay,
Russky Island, Vladivostok 690922, Russia*
*2- Institute of Automation and Control Processes, Far East Branch, Russian Academy of Sciences, 690041
Vladivostok, Russia*
3- Foshan University, School of Physics and Optoelectronic Engineering, 528011 Foshan, China

* malinchenko.aa@dvfu.ru

In the past years, the research on exceptional points has been growing enormously especially in optics and photonics [1,2]. In photonics exceptional points have been connected to a plethora of interesting effects and suggested applications, including ultrasensitive sensors, loss-induced revival of lasing, orbital-angular momentum micro-lasers, chiral perfect absorbers, coherent perfect transmitters, single-mode lasing, electromagnetically induced transparency, optical amplifiers, and optical filters with sharp transmission peaks, ideal unidirectional transmitter, etc. The research exceptional points is still a vital field with important open problems. One of the main tasks is the tunability of exceptional points, but by changing the applied external fields rather than changing exactly the structure of the system itself. Since, once the necessary nanostructures are created, as a rule, their parameters are difficult to change so the possibility of controllability is practically lost. Thus, creating systems with externally field-tunable exceptional points is a highly demanding task [3]. Here we investigated the linear nonreciprocal and tunable in helically structured 1D photonic crystals in external magnetic field when the parameter of magneto-optical activity g is constant and is independent of wavelength. We will demonstrate the existence of this effect and its tunability. We will investigate some new and interesting features of this effect, too.

[1] A.H. Castro Neto, F. Guinea, N.M.R. Peres, K.S. Novoselov, A.K. Geim, The electronic properties of graphene, Rev. Mod. Phys. 81, 109 (2009).
[2] M.-A. Miri and A. Alù, Exceptional points in optics and photonics, Science 363, eaar7709 (2019).
[3] A.H. Gevorgyan, Exceptional points and lines and Dirac points and lines in magnetoactive cholesteric liquid crystals, J. Mol. Liq., 390, 123180 (2023).

Laser pump – X-ray probe diagnostics of nanosecond dynamics in LiNbO₃

E.I. Mareev[1*], **A.G. Kulikov**[1,2], **F.S. Pilyak**[1,2], **N.M. Asharchuk**[1], **N.N. Obydennov**[1,3], **Y.V. Pisarevsky**[1,2], **A.E. Blagov**[1], **F.V. Potemkin**[3]

1- Kurchatov Complex for Crystallography and Photonics of NRC "Kurchatov institute", Leninskiy pr-kt 59, Moscow, Russia
2- Kurchatov Complex for Synchrotron and Neutron Investigations of NRC "Kurchatov institute", Pl. akademika Kurchatova 1, Moscow, Russia
3- Faculty of Physics, M.V. Lomonosov Moscow State University, Leninskie Gory bld. 1/2, 119991 Moscow, Russia

* mareev.evgeniy@physics.msu.ru

Synchronization of laser and X-ray sources plays a critical role in conducting time-resolved measurements to explore ultrafast processes, including phenomena like photo-induced piezoelectric effect, phase transitions, and lattice dynamics in semiconductors and dielectrics such as LiNbO₃. By combining optical diagnostics and optical pump – X-ray probe diagnostics using a universal approach that leverages a field-programmable gate array (FPGA), we achieved precise synchronization between nanosecond laser and synchrotron X-ray sources in KISI-Kurchatov. This synchronization method offers exceptional advantages, including high flexibility, rapid response times, and minimal jitter, enabling the synchronization of systems with varying repetition rates. We demonstrated the successful synchronization of MHz systems with a time resolution of 250 ps. Using this approach we demonstrated an unusual time-delayed variations in X-ray diffraction parameters in LiNbO₃ and LiNbO₃:Fe crystals after nanosecond laser impact, see Fig.1. The crystals' response to optical impact led to a reversible shift in center of mass and a decrease in integral intensity of the diffraction rocking curve (DRC), recovering in ~35 nanoseconds after the impact. The dynamics of lattice deformation suggest the formation and subsequent decay of an electrically charged layer near the surface due to directed migration of photoelectrons caused by the bulk photovoltaic effect. The decrease in the integral intensity of the DRCs seems to stem from a propagating strain wave generated by a piezoelectric deformation. In the case of the nominally undoped crystal, time-delayed processes occur within a similar timeframe but with notably smaller amplitudes.
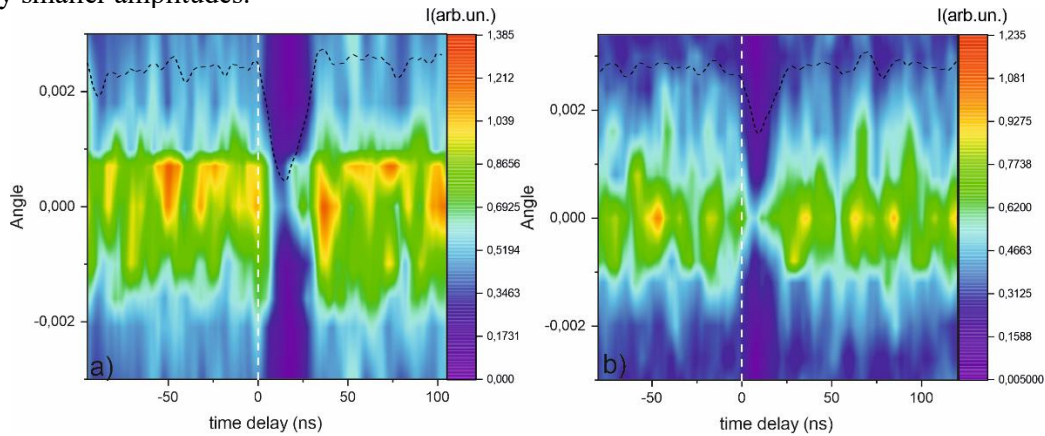
Fig.1. Dynamics of diffraction rocking curve (DRC) of a LiNbO₃:Fe (a) and pure crystal exposed to a laser pulse (τ_p = 4 ns, Ep = 2.0 mJ) over a time range of 150 ns, obtained for the 0012 reflection. The dotted lines indicate the dynamics of the DRC integral.

[1] M.V. Kovalchuk, E.I. Mareev, A.G. Kulikov, F.S. Pilyak, N.N. Obydennov, F.V. Potemkin, Yu.V. Pisarevsky, N.V. Marchenkov, A.E. Blagov, Subnanosecond x-ray diffraction technique for the study of photoinduced polarization-dependent processes on the KISI-Kurchatov, Crystallography Reports, 69, 165–172 (2024).
[2] N. Marchenkov, E. Mareev, A. Kulikov, F. Pilyak, E. Ibragimov, Y. Pisarevskii, F. Potemkin, Hybrid approach for multiscale and multimodal time-resolved diagnosis of ultrafast processes in materials via tailored synchronization of laser and x-ray sources at MHz repetition rates, Optics, 5(1), 1–10 (2024).

The blue color of the sky before sunrise

V.E. Ogluzdin

Prokhorov General Physics Institute of the Russian Academy of Sciences, Russia

ogluzdin@kapella.gpi.ru

On a cloudless summer morning before sunrise, the blue-blue firmament illuminates the earth's surface. The photons that an observer registers on the earth's surface cannot be photons emitted by the sun (the sun is still below the horizon). After leaving the sun, the photons head towards the earth without interacting with each other (laminar motion). Moving in a straight line from beyond the horizon, photons in the upper layers of the atmosphere meet oxygen and nitrogen atoms. Photons, whose energy is equal to the energy of the electronic inter-level transitions of nitrogen and oxygen atoms, are absorbed in the upper layers of the atmosphere, while the electrons of the atoms move from the ground level to the excited ones. The same thing happens with electrons in the case when the energy of photons is different from the energy of inter-level transitions. In this case, the electrons move to excited levels due to the annihilation of pairs of solar photons with the formation of short-lived axions. The annihilation of two quanta (photons) in the field of the atomic nucleus can lead to the birth of the axion $- A^0$:

$$h\nu + h\nu = A^0 = h\nu_{ij} + h\nu_{0j} \qquad (1)$$

During the decay of axions, part of the photons, whose frequency $- h\nu_{0j}$ is equal to the Bohr frequency of electron transitions, is absorbed by oxygen and nitrogen atoms. The second part of the photons, whose frequency is indicated by the value $- h\nu_{ij}$, is scattered into an angle of 4π steradian. In the morning hours before sunrise, some of these new photons reach the earth's surface. This radiation is recorded by an observer on the surface of the earth. The absence of harsh solar ultraviolet radiation on the earth's surface in the morning hours indicates their absorption in the atmosphere. The proposed interpretation differs from the traditional one, according to which solar radiation interacts with inhomogeneities of air, which includes oxygen and nitrogen atoms. Elastic light scattering occurs on these inhomogeneities of the air. The sky is blue because, when sunlight passes through the atmosphere, the blue color is more likely to dissipate than red. That is, the blue color of the sky is the photons of sunlight scattered in the atmosphere. This interpretation does not answer the questions: what is the reason for the warming up of the atmosphere in the morning? How does energy transfer to the atmosphere occur with elastic light scattering, if the wavelength of radiation does not change with elastic Rayleigh scattering?

[1] V.E. Ogluzdin, Engineering Physics, No. 2. 18, 2024.

Features of the "Radiation shaking" process in complex environments when exposed to highly intense radiation with a wide energy spectrum

M.Kh. Ashurov[1], I. Nuritdinov[1], B.L. Oksengendler[2*], S.H. Suleymanov[2],
S.T. Boyboboeva[1], N.N. Nikiforova[2], F.A. Iskandarova[3]

1- Institute of Nuclear Physics AN RUz. Tashkent, village Ulugbek, Khurasan street, Uzbekistan
2- Institute of Materials Science AN RUz. Tashkent, Bodomzor yili 2B, Uzbekistan
3- Nanotechnology Development Center at NUU, Tashkent, Universitetskaya str. 4, Uzbekistan

* oksengendlerbl@yandex.ru

Among the many interesting concepts introduced into radiation physics over the past 150 years, universal concepts have always played a special role, and among them radiation shaking [1-5]. In modern radiation physics of a solid body and radiation physics of condensed matter, the role of radiation shaking has increased even more, but also become more complicated; this work is devoted to this problem, concerning multicomponent media (characterized by a set of "size and dimensions", combined dimensions including fractals, hierarchy of structures – such a set of properties of the medium ensures the applicability of the results to Living and Inanimate Nature [4-8]). Our mathematical model has shown that the greatest efficiency of radiation shaking (from shock waves of various origins) is manifested when the time of passage of the shock wave through a metastable object is less than the inverse frequency of the coordinate of the decay reaction. The properties of the breadth of the energy spectrum and the high intensity of radiation provide a high probability of combined excitation of a metastable center considered as a hierarchical structure. The proposed analysis is applied to the cases of radiation exposure to synchrotron, lasers, a large solar Furnace, electron emission accelerators [8,9].

[1] V.L. Indenbom, A new hypothesis on the mechanism of radiation-stimulated processes, JTF Letters, vol.5, pp.489-492 (1979).
[2] P.K. Khabibullaev, B.L. Oksengendler, Yu.V. Pakharukov, The mechanism of radiation shaking in structurally disordered substances, Fizika Tverdogo Tela, vol.28, pp.3132-3133, (1986).
[3] P.K. Khabibullaev, B.L. Oksengendler, Yu.V. Pakharukov, A new hypothesis of radiation resistance of disordered semiconductors, JTF Letters, vol.12, pp.132-1322, (1986).
[4] I.P. Chernov, Ordering the crystal structure by ionizing radiation (the effect of low doses of ionizing radiation), Izv.TPU, vol.303, pp.74, (2000).
[5] I. Nuritdinov, M.Tu. Tashmetov, U.O. Khodzhaev, et al, Influence of electron irradiation on the crystal structure, surface microrelief and bandganp width of the triple crystals of iron doped monoselenide of thallium and indium, Eur. Phys. Tech. J, vol.20, pp.23-32, (2023).
[6] M.Kh. Ashurov, I. Nuritdinov, S.T. Boyboboeva, Spectral–luminescence characteristics of crystals and nanoceramics based BaF_2: Ce, Book of abstracts of III International Conference on Nanophotonics, Metamaterials and Photovoltaic (ICNMP-2023), Samarkand, Uzbekistan, pp.38-39, (2023).
[7] M.Kh. Ashurov, I. Nuritdinov, S.T. Boyboboeva, The multiplicity of cerium centers in optical nanoceramics based on BaF_2-CeF_3. Optics and spectroscopy, vol.131, pp.341-345, (2023).
[8] B.L. Oksengendler, A.Kh. Ashirmetov, F.A. Iskandarova, et al, Interaction of Radiation with Hierarchical Structures, J. Surf. Invest.: X-ray, Synchrotron and Neutron Techniques, vol.17, pp.31–42, (2023).
[9] B.L. Oksengendler, A.Kh. Ashirmetov, N.N. Turaeva, et al, The features of Auger destruction in quasi-one-dimensional objects of inorganic and organic nature, Nuclear Instruments and Methods in Physics Research, pp.66-75, (2022).

Formation, stabilization and orientation of linear carbon chains using arc discharge and laser radiation

A. Osipov[*], **V. Samyshkin, A. Kucherik, A. Abramov**

Vladimir State University, Russia

* *osipov@vlsu.ru*

We present a method of synthesis of sp-carbon allotropes or carbynes. Linear chains of carbon atoms are obtained from graphite placed in a joint field of laser plasma and arc discharge. The combined action of laser and arc discharge allows to create conditions for the formation of a variety of carbon allotropes, whose structural composition is governed by the interplay of external fields. The stabilization of the obtained structures realizes in water by attaching them to gold nanoparticles (NPs) by means of the laser ablation process. Resulting nanoobjects represent pairs of NPs connected by multiple straight carbon chains of several nanometer lengths. If NPs at the opposite ends of a chain differ in size, the structure acquires a dipole moment due to the difference in work functions of the two NPs. We take advantage of the dipole polarisation of carbon chains for ordering them by the external electric field. We deposit them on a glass substrate by the sputtering method in the presence of static electric fields of magnitudes up to 10^5 V/m. The formation of one-dimensional carbyne quasi-crystals deposited on a substrate is evidenced by high-resolution TEM and X-ray diffraction measurements. The original kinetic model describing the dynamics of ballistically flowing nano-dipoles reproduces the experimental diagram of orientation of the deposited chains. The method may be employed in the mass production of sp- and sp^2-hybridized carbon for the needs of possible applications in micro and nanoelectronics, biosensing.

We have developed an experimental setup based on a combined effect of an electric arc discharge and laser irradiation on a fluid containing carbon and Au NPs. By optimization of the setup we have found a regime allowing for predominant synthesis of sp- or sp^2-carbon nanostructures. The combined effect of an electric arc discharge and laser field offers a powerful tool for the synthesis of sp-carbon in liquid media, as confirmed by our Raman spectroscopy data. It is important to note that the presence of stabilizing metal nanoparticles is strongly essential stabilization of linear carbon formation. We have successfully deposited the synthesised polyyne chains on a gold platinum grid. High resolution TEM images confirm formations of a multitude of linear carbon chains attached to gold nanoparticles.

Influence of non-equilibrium heating of gold nanospheres on the dynamics of ultrafast optical response of a multiresonant metasurface

G.S. Ostanin[1*], M.A. Kiryanov[1], D.A. Safiullin[1], T.V. Dolgova[1], M. Inoue[2], A.A. Fedyanin[1]

1- Faculty of Physics, Lomonosov Moscow State University, Moscow, 119991 Russia
2- Department of Electrical and Electronic Information Engineering, Toyohashi University of Technology 1-1
Tempaku-cho, Toyohashi, Aichi, 441-8580 Japan

* ostanings@my.msu.ru

The study of optical effects in hybrid nanoscale metasurfaces represents a significant field of nanophotonics. Hybrid metal-dielectric metasurfaces combine the unique properties of metals and dielectrics, and various resonances can be exited at a metal-dielectric interface. For example, periodic array of nanoparticles can support surface lattice resonances (SLR). Another rapidly developing field is ultrafast all-optical control. "Pump-probe" femtosecond spectroscopy technique can achieve sufficient temporal resolution to detect non-equilibrium electron gas heating [1]. Moreover, there are number of studies that describes electron gas relaxation processes. The intersection of these two scientific areas is ultrafast plasmonics [2], which unites nanoscale structures with subpicosecond processes.

In this work the gold dielectric permittivity time dependencies based on evolution of the electron energy distribution following a femtosecond laser pulse were calculated on the basis of the two-temperature model [3] the Boltzmann kinetic equation and interband theory. The maximum change in the electron gas temperature is 1500 K and the final change in the lattice temperature is 60 K, which is in agreement with theoretical estimates. The calculations were used to describe anomalous temporal behavior of the 2D periodic array of gold nanospheres coated with a layer of bismuth-substituted iron-yttrium garnet, which was experimentally studied earlier [4].

[1] F. Caruso and D. Novko, Adv. Phys. X, vol 7, 2095925, (2022).
[2] T. Stoll, et al, Eur. Phys. J. B, vol. 87, 1-19, (2014).
[3] S.I. Anisimov, et al, Sov. Phys. JETP, vol. 66, 375-377, (1974).
[4] M.A. Kiryanov, et al, JETP Lett., vol. 117, 196-201, (2023).

Multifunctional superhydrophobic platform for control of water microdroplets by non-uniform electrostatic field

G. Pavliuk[1*], A. Zhizhchenko[2], O. Vitrik[2]

1- Far Eastern Federal University, Ajax Bay, 10, Russky Island, Vladivostok, Russia, 690922
2- Institute of Automation and Control Processes (IACP) FEB RAS, Vladivostok, Russia, 690041

* georgii.23542@gmail.com

Platforms for manipulating liquid microdroplets (PMD) are required in microfluidic systems [1,2] in particular in laboratories on a chip, as well as advanced sensors and other devices [3,4]. The implementation of a sequence of controlled biochemical, biological and analytical reactions on such platforms is achieved by controlled selective movement and coalescence of droplets or their groups on the working surface of PMD. In this work, we report a new approach to the control of liquid microdroplets based on non-uniform electrostatic fields. This field, created near the selected droplet, leads to its polarization. That is, the droplet acquires a pronounced dipole moment. Since the field is non-uniform, the polarized droplet begins to accelerate in the direction of the field gradient (Fig. 1a). To increase the mobility of the droplet, the latter is placed on a superhydrophobic surface (Fig. 1b).
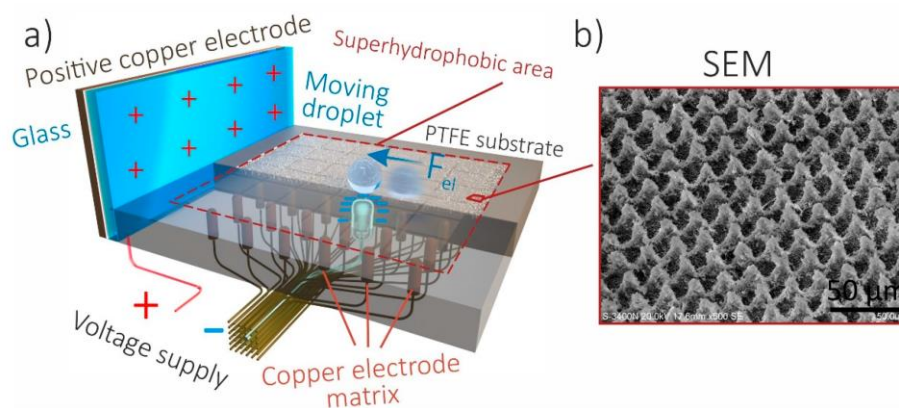
Fig. 1. (a) Schematic of the platform for micromanipulation of liquid droplets and its mechanism of action.
(b) SEM image of the topography of a superhydrophobic surface.

The developed PMD has demonstrated the ability to move droplets along predefined trajectories in the volume range from 0.2 μL to 200 μL. In the most demanded from a practical point of view range of volumes $3 \div 15$ μL, the speed of movement is $17 \div 75$ mm/s. The developed platform also provides the possibility of controlled coalescence of droplets, controlled chemical reactions for their contents, including analytical ones. We believe that the presented liquid droplet micromanipulation platform has great potential in chemical and biological analysis and can become a useful tool for various microfluidics applications.

[1] D. Mark, S. Haeberle, G. Roth, et al, Microfluidic lab-on-a-chip platforms: requirements, characteristics and applications, Microfluidics based microsystems, 305-376, (2010).
[2] E.K. Sackmann, A.L. Fulton, D.J. Beebe, The present and future role of microfluidics in biomedical research, Nature, 507(7491), 181-189, (2014).
[3] D. Baigl, Photo-actuation of liquids for light-driven microfluidics: state of the art and perspectives, Lab on a Chip, 12(19), 3637-3653, (2012).
[4] L. Ma, J. Wang, J. He, et al, Biotemplated Fabrication of a Multifunctional Superwettable Shape Memory Film for Wearable Sensing Electronics and Smart Liquid Droplet Manipulation, ACS Applied Materials & Interfaces, 13(26), 31285-31297, (2021).

Laser field enhancement near defects in close-packed colloidal monolayers of dielectric spherical microlenses

M. Sveshnikova, A. Pikulin[*], N. Bityurin

Institute of Applied Physics, 46 Ulyanov Str., 603950 Nizhny Novgorod, Russia

* pikulin@ipfran.ru

Colloidal lithography (CL) is a cost-effective technique capable of producing surface structures of various kinds. This technique employs the particle monolayers that are deposited from the colloidal solution on a material surface. There almost perfect particle arrangement can be obtained due to the self-organization. Particularly, the near-field CL relies on the irradiation of the spherical particles by the laser beam [1]. The dielectric microspheres act as near-field microlenses that generate localized photonic jets, which provide local material modification.

Typically, each sphere provides its own photonic jet thus resulting in a hexagonal periodical pattern on the surface. However, more complex patterns may be required for applications. By combining the near-field colloidal lithography and the multiple-beam interference of the incident laser light one can obtain more complex patterns of the jets [2]. Another way is to produce patterns of spheres themselves. For instance, tri-block Janus particles self-organize in a Kagome lattice [3]. Alternatively, patterns can be produced from ordinary polystyrene (PS) microspheres on the substrate where the surface wettability is selectively modified by UV radiation [4].

Despite the physical approach that results in a non-regular placement of the spheres, calculation of the field enhancement near different types of defects in the periodical monolayer of spheres proves to be important. In this work, we model the field enhancement near the spheres at the edge of the close-packed domain. The calculation shows the greater field enhancement beneath the edge spheres than others.

Another often seen defect is the vacancy, i.e. the missing sphere. Calculation shows the field enhancement maximum under the vacancy. This maximum is of similar strength compared to those under the spheres (see Fig. 1).
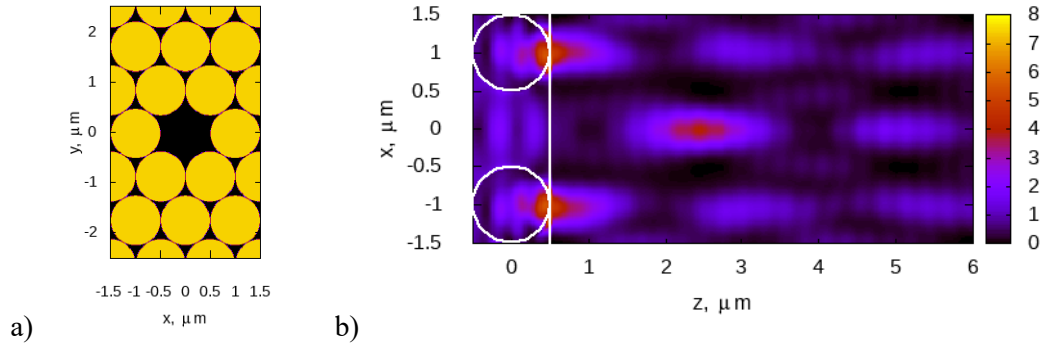
Fig. 1. a) Vacancy defect within the monolayer of dielectric spheres; b) enhancement of the electric field square under the vacancy and the surrounding spheres.

Formation of the field maximum under the vacancy is explained by the superposition of the contributions from the spheres surrounding the vacancy. This is an important result that can explain the material modification under the vacancy.

[1] L. Chen, Y. Zhou, Y. Li, M. Hong, Microsphere enhanced optical imaging and patterning: From physics to applications, Appl. Phys. Rev. 6, 021304, (2019).
[2] N. Mitin and A. Pikulin, Interference surface patterning using colloidal particle lens arrays, Opt. Lett. 45, 6134, (2020).
[3] Q. Chen, S.C. Bae, S. Granick, Directed self-assembly of a colloidal kagome lattice, Nature 469, 381, (2011).
[4] V. Bredikhin and N. Bityurin, 2D mesoscale colloidal crystal patterns on polymer substrates, Mater. Res. Express 5, 055306, (2018).

Processes accompanying ablation of thin-film and bulk chalcogenide glass As$_2$Se$_3$ under multipulse femtosecond laser irradiation

A. Shamova[*], **D. Polyakov**, **G. Shandybina**

ITMO University, 49 Kronverksky Ave, Saint Petersburg, Russia, 197101

* alex.shamova94@gmail.com

Femtosecond laser processing opens up new prospects for chalcogenide glasses for use in optoelectronics and photonics due to a wide change in their structural properties [1]. From the point of view of near- and mid-infrared optics, the most promising materials are glassy arsenic chalcogenides, in particular arsenic selenide As$_2$Se$_3$. At high laser radiation intensities the presence of the toxic element (arsenic) requires a thorough study of damage mechanisms. Currently, a complete picture of glassy arsenic chalcogenides ablation under femtosecond laser irradiation, as well as the accompanying modification processes through the formation of surface periodic nano- and microstructures, has not been developed [1-3], which complicates the industrial implementation of femtosecond laser technology.

The report presents the results of an experimental and theoretical study of ablation processes in thin-film and bulk arsenic selenide As$_2$Se$_3$ under the influence of femtosecond laser pulses in the visible and near-IR ranges depending on pulse energy, number, and repetition rate. The morphological features of irradiated samples and the chemical composition of laser ablation products were studied using digital optical microscopy and Raman spectroscopy.

The experimental results are compared with the results of numerical modeling of the spatiotemporal distribution of As$_2$Se$_3$ film optical properties performed within the framework of n-TTM model [4]. A mechanism has been proposed for the formation of previously unobserved microstructures on As$_2$Se$_3$ thin film surface with a period on the order of the wavelength, oriented parallel to the polarization vector.

Theoretical estimates of accumulative heating of the bulk chalcogenide glass As$_2$Se$_3$ surface allowed us to propose that in the megahertz range of femtosecond pulse repetition rates, redox processes develop in the vapor phase, which contributes to the formation of amorphous selenium and toxic arsenolite crystals (As$_2$O$_3$) in the deposition products.

The results are important for the creation of elements based on chalcogenide glasses for use in high-power laser systems.

[1] S.V. Zabotnov, P.K. Kashkarov, A.V. Kolobov, S.A. Kozyukhin, Structural Transformations and Formation of Microstructures and Nanostructures in Thin Films of Chalcogenide Vitreous Semiconductors, Nanobiotechnology Reports, vol. 18, pp. 829-841, (2023).
[2] Q. Li, D. Qi, X. Wang, X. Shen, R. Wang, K. Tanaka, Femto-and nano-second laser-induced damages in chalcogenide glasses, Japanese Journal of Applied Physics, vol. 58, pp. 080911, (2019).
[3] K.T. Paula, N.S. Dutta, J.M. Almeida, L.K. Nolasco, M.B. Andrade, C.B. Arnold, C.R. Mendonça, Femtosecond laser induced damage threshold incubation and oxidation in As$_2$S$_3$ and As$_2$Se$_3$ thin films, Applied Surface Science, vol. 654, pp. 159449, (2024).
[4] D.S. Polyakov, G.D. Shandybina, A.A. Shamova, Ultrafast changes of optical properties of semiconductors at wavelength near the edge of interband absorption after excitation by femtosecond laser pulse, Optik, vol. 256, pp. 168751, (2022).

Duality of Au-dopant forms in laser hyperdoping of Si surface

V. Pryakhina[1*], S. Kudryashov[1,2], I. Gordeev[3], M. Kovalev[1,2], S. Starikov[4], A. Akhmatkhanov[1]

1- Ural Federal University, Ekaterinburg, Russia
2- Lebedev Physical Institute, Moscow, Russia
3- Joint Institute for High Temperatures of RAS, Moscow, Russia
4- Interdisciplinary Centre for Advanced Materials Simulation, Ruhr-University, Germany

* viktoria.pryahina@urfu.ru

The hyperdoping technology, material saturation with dopants at the concentration higher than the equilibrium solubility level, extends the spectral response of silicon to near- and mid-infrared range and increase impurity absorption [1]. Laser hyperdoping can be naturally combined with laser annealing which restores doped layer crystallinity, while preserving the non-equilibrium dopant state. Chemically-inert gold is a promising doping candidate for Si-based near-infrared photo-detectors, exhibiting both donor and acceptor states, high trapping efficiency with low carrier lifetime and poor transport characteristics. Tuning laser processing parameters could facilitate obtaining dopant concentrations, doped layer thicknesses and doping/annealing conditions for specific applications.

In this work, Au-dopant distribution and chemical state in the Si surface layer, hyperdoped from the pre-deposited Au film and annealed by non-ablative nanosecond laser treatment, were studied by cross-sectional X-ray photoelectron spectroscopy and scanning electron microscopy imaging.

Au-coated initially undoped Si(100) wafers had been irradiated in the ambient atmosphere by 100-ns laser pulses at 1064-nm wavelength using a MiniMarker-2 M20 marking system (LTC, Russia) equipped with Yb fiber laser (IPG Photonics, IRE-Polus, Russia). The used fluence of 8 J/cm^2 was lower, than the ablation threshold of gold, but close to the one of silicon.

Partial ablation of the gold film on the wafer surface, gold nanocrystallites precipitated on the Si nanograins inside the recrystallized layer and small gold clusters sedimented in the hyperdoped layer Si over the gold diffusion length ($\sim 1~\mu m$) were observed. The hyperdoping process crystallization characteristics studied at the atomic level by the molecular dynamics simulation were in good agreement with those experimental results. The laser-hyperdoped Si samples with removed residual gold have shown lower transmittance in the intra-gap spectral range ($> 1.1~\mu m$) comparing to the highly transmissive Si wafer which implies the impurity absorption.

These findings shed the light on ambiguity of previously reported electrical characteristics of gold-hyperdoped Si and pave the way toward controllable fabrication of Au-Si based optoelectronic devices.

[1] M. Kovalev, et al, Au-hyperdoped Si nanolayer: laser processing techniques and corresponding material properties, *Materials*, vol. 16, pp. 4439, (2023).

Hand-held device "Laser brush" for creating art objects: new functional and technological capabilities

V. Veiko[1], V. Romanov[1*], A. Morozova[1], D. Galiev[2]

1- ITMO University, Saint-Petersburg, Russia
2- LLC "Laser Center", Saint-Petersburg, Russia

* vvromanov@itmo.ru

Currently, new technologies for modifying a shape and a color of a material are increasingly used to create art objects. Laser processing is a promising technology in this field, as it allows one to influence a material surface in a completely new way to create an art object on it. For example, due to the laser formation of an oxide film on a metal surface, it is possible to create color images without using paints. The use of an optical system and numerical control of such devices allows one to create high-resolution images (about 500 dpi). However, to create a hand-made art object, it is necessary to have an opportunity for actor to control the movement of the laser beam in the creative process. Focusing on this aspect, a hand-held device "Laser brush" was developed [1].

For the convenience of using the "Laser brush", the device design is implemented on the basis of a continuous fiber laser source. The collimator of such a laser source is enough small in size, because it does not have additional optical components that are present in the collimators of pulsed fiber laser sources. It is worth noting that the formation of oxide films on the surface of titanium by continuous laser radiation has been under-explored.

The report presents the results of testing the convenience of working with the "Laser brush" device. Based on the data obtained, a new device design has been developed. Additionally, software has been developed to teach color management skills before working with a "Laser brush" device. The technological possibilities of erasing and rewriting colors after repeated laser processing, applicable to a continuous laser source, are demonstrated. Previously, these capabilities were presented only for a pulse source [2]. Focusing on a comparative analysis of the functional and technological opportunities of a hand-held device and a stationary laser complex, a new method for creating color images is proposed. This method involves the sharing of devices, which allows you to create expressive art objects.

[1] V.P. Veiko, et al, Production of laser art miniatures using localized oxidation of metals, J. Opt. Technol. – 2020. – №. 87. – P. 633-637.
[2] V.P. Veiko, et al, Laser paintbrush as a tool for modern art, Optica. – 2021. – Vol. 8. – №. 5. – P. 577-585.

Laser control of wettability metals and glass surfaces: new applications

<u>G.V. Romanova</u>[1], V.P. Veiko[1], I.A. Filatov[1], A.G. Bondarenko[1], E.A. Davydova[1]

1- ITMO University, Saint-Petersburg, Russia

Laser methods have been developed to control the wettability of the surface of metals and glasses for various applications: the creation of microfluidic systems, protection against biofouling in an aquatic environment, reducing corrosion resistance, etc.

The phenomenon of wetting plays an important role in the life of many plants and animals, helping them both to obtain moisture and to protect themselves from its excess. By recreating biomimetic structures on the surface of parts and devices, we can give them similar surface properties. By controlling the wettability of the surface of metals and glasses, we can influence other functional properties: the superhydrophilic surface of metal implants promotes the adhesion of proteins at the initial stages of osseointegration [1], and increasing hydrophobicity on the surface of metal products, creating so-called "slippery" coatings, gives the surface antibacterial properties [2]. The hydrophobic properties of the surface of steel and aluminum lead to a reduction in their biofouling in an aquatic environment by reducing the adhesion of microorganisms [3] and contribute to protection against corrosion in an air environment with high humidity [4].

In this work, we propose to use laser irradiation as a means of controlling the wettability of metal and glass surfaces. Unlike traditional chemical and mechanical methods, laser processing provides locality (the ability to create local areas with different contact angles), environmental friendliness (the ability to change contact angles without the use of additional materials) and a non-contact approach. We are studying the effect of laser-induced topography on surface wettability with the goal of minimizing biofouling on steel surfaces in aqueous environments and increasing the corrosion resistance of steel in high-humidity air environments. The formation of a stable hydrophobic wetting gradient on the steel surface is shown, which promotes the movement of droplets at a speed of 33 mm/s over a distance of 12 mm. The technology for laser recording of microfluidic systems on quartz glass for biochemical applications is also demonstrated.

[1] A. Cunha, O.F. Zouani, L. Plawinski, A.M. Botelho do Rego, A. Almeida, R. Vilar, M. Durrieu, Human mesenchymal stem cell behavior on femtosecond laser-textured Ti-6Al-4V surfaces, Nanomedicine, 10, №5, 725-739, (2015).
[2] E. Fadeeva, B. Chichkov, Biomimetic Liquid-Repellent Surfaces by Ultrafast Laser Processing, Applied Sciences, 8, №9, 1424, (2018).
[3] Y. Yu, Y. Wei, B. Li, H. Gao, T. Liu, X. Luan, R. Qiu, Y. Ouyang, Bioinspired metal-organic framework-based liquid-infused surface (MOF-LIS) with corrosion and biofouling prohibition properties, Surfaces and Interfaces, 34, 102363, (2022).
[4] A.O. Ijaola, P.K. Farayibi, E. Asmatulu, Superhydrophobic coatings for steel pipeline protection in oil and gas industries: A comprehensive review, Journal of Natural Gas Science and Engineering, 83, 103544, (2020).

Numerical analysis of anomalous optical transmittance dynamics in Au-Bi:YIG metasurface

D.A. Safiullin[1*], M.A. Kiryanov[1], G.S. Ostanin[1], T.V. Dolgova[1], M. Inoue[2], A.A. Fedyanin[1]

1- Faculty of Physics, Lomonosov Moscow State University, Moscow, 119991 Russia
2- Department of Electrical and Electronic Information Engineering, Toyohashi University of Technology 1-1
Tempaku-cho, Toyohashi, Aichi, 441-8580 Japan

* safiullinda@my.msu.ru

One of the important directions of nanophotonics is the study of optical effects in nanoscale hybrid metasurfaces allowing to control light by external influences. Using the hybrid metal-dielectric metasurfaces allows one to excite various electromagnetic resonances. The dynamics of ultrafast processes near the studied resonances can be investigated by "pump-probe" technique. One such process is the ultrafast heating of metal by an ultrashort laser pulse of high peak power, as a result of which the metal dielectric permittivity changes.

In this work, the differential transmittance ($\Delta T/T$) spectra of the hybrid metasurface were numerically studied. The sample is a 2D periodic array of gold nanospheres coated with a layer of bismuth-substitute iron-yttrium garnet. The $\Delta T/T$ spectra were obtained previously by "pump-probe" technique at different delay times for different pump beam energy densities and p- and s-polarizations of the probe [1]. It supports various electromagnetic resonances in the visible spectral range, e.g., the quasi-waveguide mode (QWG) and surface lattice resonances (SLR). However, the time dependencies in the vicinity of the QWG mode show anomalous dynamics [1]. This, unlike SLR, is not described by the classical two-temperature model (TTM) [2].

The consideration of $\Delta T/T$ time dependences for only one wavelength does not allow us to correctly describe and explain the nature of the obtained anomalous effects. So, it is necessary to analyse the spectral window in which the studied resonance is located by Lorentzian approximation:

$$\frac{\Delta T}{T} = \frac{A(t)}{1 + \left(\frac{\omega(\lambda) - \omega_0(t)}{\Delta\Omega}\right)^2} = A(t) \times L(\lambda, t).$$

The approximation makes it possible to obtain time dependences of the amplitude A, characteristic width $\Delta\Omega$ and spectral position ω_0 of the resonance. A modified TTM is used to describe the amplitude, which takes into account the linear contribution of metal temperature to the change in dielectric permittivity [3]. As a result of the fitting, we obtained that at the beginning under the action of the laser pulse electron-electron thermalization occurs with characteristic time $\tau_{ee} \approx 100$ fs. Further electrons transfer energy to the lattice, due to which electron-phonon relaxation occurs with characteristic time $\tau_{ep} \approx 2.5$ fs. With increasing pump beam energy density, τ_{ee} decreases and τ_{ep} increases.

It was found that the spectral position of the QWG mode shifts to the blue region. The scale of this mode shift is commensurate with the characteristic width. It is assumed that the shift of the resonance is related to the change of the sample geometry caused by the thermal expansion of gold nanospheres with the following excitation of breathing vibrational modes [4]. The period of these oscillations can be estimated as $T \approx 40$ ps, with the oscillation period increasing with increasing pump beam energy density.

By determining the time dependences of the lorentzian parameters, we were able to distinguish two processes with different timescales manifesting in amplitude A(t) and spectral shape $L(\lambda,t)$. Thus, the anomalous dynamics of the differential transmittance in the vicinity of the QWG mode consists of the linear dependence of the resonance amplitude on temperature and the spectral shift of the resonance. Taking these two processes into account allows us to analytically describe the time dependence of $\Delta T/T$ in the vicinity of the QWG mode.

[1] M.A. Kiryanov, et al, JETP Lett., vol. 117, 196-201, (2023).
[2] S.I. Anisimov, et al, Sov. Phys. JETP, vol. 66, 375-377, (1974).
[3] T. Stoll, et al, Eur. Phys. J. B, vol. 87, 1-19, (2014).
[4] G.V. Hartland, et al, Chem. Rev., vol. 111, 3858-3887, (2011).

Pressure generation mechanisms in picosecond laser – metal interaction

<u>A.A. Samokhin</u>[1*], D.S. Ivanov[2], V.I. Priklonskii[3], P.A. Pivovarov[1]

1- Prokhorov General Physics Institute of the Russian Academy of Sciences, st. Vavilova 38, Moscow, 119991 Russian Federation
2- P.N. Lebedev Physical Institute of Russian Acad. Sci., Leninskiy Pr. 53, 119991 Moscow, Russian Federation
3- Faculty of Physics Lomonosov Moscow State University, 1 Leninskie Gory, bldg. 2, Moscow, 119234 Russian Federation

* asam40@mail.ru

Studying the behavior of the recoil pressure generated in a metal under pulsed laser irradiation is necessary to clarify the possible manifestations of the critical parameters of a substance under nonequilibrium conditions. In [1], during MD modeling of picosecond laser ablation of aluminum against the background of a characteristic thermoacoustic pressure pulse, additional peaks were also observed during irradiation (peak1) and after its completion (peak2), associated with the movement of the melting front and subsurface cavitation, respectively. In the considered exposure mode, no noticeable effect of the subcritical evaporation process on the recoil pressure was observed.
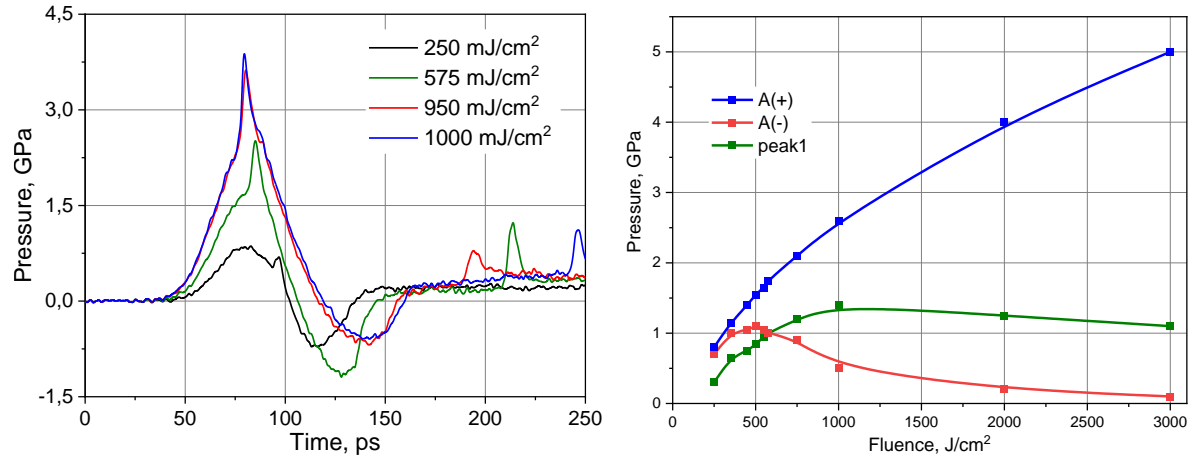
Fig.1: **(a)** Pressure curves with additional peaks (peak1 and delayed peak2). **(b)** Fluence dependencies of thermoacoustic positive (A(+)) and negative (A(-)) amplitudes together with peak1.

Fig.1(a) shows several pressure curves and the dependence of their amplitudes on the irradiation energy density. The difference in the behavior of positive and negative amplitudes (fig.1(b)) is due to the nonlinear effects of the thermoacoustic response, which is consistent with the continuum modeling performed in the present study. The role of the thermoacoustic mechanism in the formation of recoil pressure can also be significantly influenced by an increase in the radiation absorption length in the metal, which, apparently, was observed during nanosecond irradiation of mercury in [2], but has not yet been sufficiently studied.

[1] D.S. Ivanov and A.A. Samokhin, Pressure recoil behavior in picosecond laser metal interaction: MD simulation, Abstract book of International Conference on Advanced Laser Technologies (ALT), (2023).
[2] A.A. Samokhin, E.V. Shashkov, N.S. Vorobiev, A.E. Zubko, On acoustical registration of irradiated surface displacement during nanosecond laser-metal interaction and metal–nonmetal transition effect, Appl. Surf. Sci., 502, 144261, (2020).

Features of the Bragg diffraction on the regular domain structures with inclined walls in MgO:LiNbO₃

E. Savchenkov[1*], A. Dubikov[1], D. Belskaya[1], S. Shandarov[1], M. Chuvakova[2], A. Akhmathanov[2], V. Shur[2]

1- Tomsk State University of Control Systems and Radioelectronics, Tomsk, Russia
2- Ural Federal University, Ekaterinburg, Russia

* rossler@mail.ru

Controlling the parameters of laser beams in the temporal and spatial regions on the base of Bragg diffraction of light waves in ferroelectric crystals on regular domain structures (RDS) formed in them is the important task for different applications [1–5]. The RDS in MgO:LiNbO₃ crystals have domain walls characterized by an inclination to the polar axis at the angle $\pm\alpha = 0.2°$ and more [6,7]. The features of the distribution of light intensity in Bragg maxima, which are to correspond to various spatial harmonics in disturbances of the optical properties of a 5%MgO:LiNbO₃ crystal created by RDS with inclined walls, have been studied in [6] for a cylindrical probing Gaussian beam with a radius of $r_0 \approx 0.16$ mm. In this report the results of experimental studies and theoretical analysis of Bragg diffraction of light on RDS with inclined domain walls in a 5%MgO:LiNbO₃ sample for an elliptical probing laser beam with a waist of $2z_0 \approx 25$ µm at different positions of its center along the polar axis Z are presented.

The examined RDS having a spatial period $\Lambda = 8.79$ µm has been formed in a 5%MgO:LiNbO₃ crystal with dimensions of $40\times2\times1$ mm³ along the *X*, *Y* and *Z* axes, respectively. The domain walls RDS of the *Y*-type in this sample described earlier in [6] had an inclination to the polar Z-axis at the angle $\alpha = \pm0.31°$. The sample was placed on a turntable, which allowed to specify the Bragg angle in the *XY* plane to observe diffraction in the first order. The probing Gaussian beam of a He-Ne laser with an extraordinary polarization, wavelength $\lambda = 632.8$ nm, power 22.5 mW and aperture $r_0 = 0.7$ mm was focused on the input face of the crystal $y = 0$ by a cylindrical lens with a focal length of 95 mm in the form of a narrow elliptical Gaussian light spot with an aperture of 2200×25 µm² along the *X* and *Z* axes, respectively. The dependence of diffraction efficiency $\eta(z)$ on the position of the probing beam shifted along the Z axis by a micrometer system at spacing of 25 µm. It has been found that $\eta(z)$ is characterized by nonmonotonic behavior and reached the minimum value $\eta = 0.02$ for $z = 0.45$ mm as well as two maxima: $\eta = 0.11$ for $z = 0.19$ mm and $\eta = 0.15$ for $z = 0.80$ mm.

The approach developed earlier in [6] for a probing Gaussian beam with a narrow angular spectrum was used in the theoretical analysis of the diffraction efficiency and intensity distribution in diffraction maxima for elliptical probing Gaussian beam under study. The integral expressions to be allowed to describe both the dependences of $\eta(z)$ and the intensity distribution of $I_{dm}(z)$ in the Bragg diffraction maxima corresponding to spatial harmonics with number *m* in the distribution of optical disturbances created by RDS with different parameters of domain walls have been obtained. Numerical calculations have demonstrated satisfactory agreement between the theoretical dependences for $\eta(z)$ and $I_{dm}(z)$ and the relevant experimental data.

[1] M. Yamada, et al, Electric-field induced cylindrical lens, switching and deflection devices composed of the inverted domains in LiNbO₃ crystals, Appl. Phys. Lett., V. 69, P. 3659 (1996).
[2] J. Abernethey, et al, Demonstration and optical characteristics of electro-optic Bragg modulators in periodically poled lithium niobate in the near-infrared, Appl. Phys. Lett., V. 81, No 14, P. 2514, (2002).
[3] I. Mhaouech, et al, Low drive voltage electro-optic Bragg deflector using a periodically poled lithium niobate planar waveguide, Opt. Lett., V. 41, No 18, P. 4174, (2016).
[4] H. Gnewuch, et al, Nanosecond response of bulk-optical Bragg-diffraction modulator based on periodically poled LiNbO₃, IEEE Photon. Technol. Lett., V. 10, No 12, P. 1730, (1998).
[5] M. Yamada, Electrically induced Bragg-diffraction grating composed of periodically inverted domains in lithium niobate crystals and its application devices, Rev. Sci. Instrum., V. 71, No 11, P. 4010, (2000).
[6] E. Savchenkov, et al, Diffraction of Light on a Regular Domain Structure with Inclined Walls in MgO:LiNbO₃, JETP Letters, V. 110, No. 3, P. 178, (2019).
[7] M. Schröder, Conductive domain walls in ferroelectric bulk single crystals. Diss., Dresden, Technische Universität Dresden. (2014).

Plasmonic laser-synthesized transition metal nitrides nanoparticles as novel prospective biomedical agents

M.S. Savinov[1*], **A.A. Popov**[1], **G.V. Tikhonowski** [1], **I.V. Zelepukin**[1,2], **A.I. Pastukhov**[3], **S.M. Klimentov**[1], **A.V. Kabashin**[3]

1- MEPhI, Institute of Engineering Physics for Biomedicine (PhysBio), Moscow, Russia
2- Shemyakin-Ovchinnikov Institute of Bioorganic Chemistry of Russian Academy of Sciences, Moscow, Russia
3- Aix-Marseille University, CNRS, LP3, Marseille, France

* MSSavinov@mephi.ru

Today, cancer treatment is still facing significant challenges, as traditional methods are often associated with severe side effects and limited localization of therapeutic effects. To overcome this problem, alternative approaches that minimize side effects and improve diagnostic resolution are being developed, although their clinical application is still very limited. Recent advances in nanotechnology, particularly plasmonic nanomaterials such as gold (Au) and silver (Ag) nanoparticles (NPs), offer prospects for innovative non-invasive cancer theranostics techniques such as photoacoustic imaging (PAI) and targeted photothermal therapy (PTT). In these procedures, NPs serve as both contrast agents and efficient sensitizers of external radiation destroying cancer cells by localized overheating (hyperthermia). However, since spherical Au NPs have plasmonic peak around 520-540 nm, which is far from the transparency window of biological tissues (650-950 nm), complex architectures, including Au core-shells, nanorods, or nanocages, have to be used to solve the plasmonic mismatch problem. The use of nanomaterials based on group IV transition metal nitrides (TMN) such as TiN, ZrN, and HfN is considered as another solution to this challenge. This type of nanomaterials is currently being actively discussed as alternative plasmonic structures due to the broad plasmonic peak located in the window of relative tissue transparency, along with their low cost and high availability.

However, the synthesis of TMN-based NPs suitable for biological use faces problems, as in the case of chemical approaches, related to surface contamination and possible subsequent toxic effects. On the other hand, the use of "dry" methods such as the arc plasma process leads to the formation of aggregated, hardly water-dispersible structures, which typically form very unstable colloids. So, femtosecond (fs) pulsed laser ablation in liquids (PLAL) is often used as an alternative laser-based technology in the synthesis of many nanomaterials for biological applications. This technique, remarkable for its high throughput and simplicity, allows to obtain stable colloidal solutions of clean NPs with controllable physicochemical properties.

Here, we demonstrate our recent results on the fabrication of TMN-based NPs synthesized by PLAL technique, followed by surface modification of the formed NPs, and evaluate the prospects for their applications in bioimaging, PTT, proton therapy, and computed tomography.

The mechanisms of laser-induced rGO/polymer composite formation

M. Fatkullin, D. Cheshev, G. Murastov, A. Averkiev, E. Dogadina, E. Abyzova, I. Petrov, R.D. Rodriguez, E. Sheremet[*]

* esheremet@tpu.ru

Laser processing is a remarkably convenient technique for inducing graphene-based conductive substrates on polymers and even organic matter. However, such structures are fragile, with limited applicability. Laser-induced reduced graphene oxide (rGO)/polymer composites are very robust conductive patterns formed by a mechanism of the integration of rGO to polymer substrate. It involved both photothermal and photochemical processes. Graphene oxide (GO) under laser irradiation is transformed into rGO, that in turn heats up the polymer substrate. The process depends on laser wavelength, power, pulse width and other irradiation parameters as well as the polymer nature. Here we explore the mechanisms of GO reduction and show the photochemical nature of the process for visible wavelengths of light. Further we look into the power dependence of rGO integration into the polymer substrate for eight different thermoplastic polymers and make conclusions about the effect of the substrate thermal properties and structure on the optimal integration parameters [1]. These studies while being fundamental have great potential for the robust flexible electronics based on laser processing.
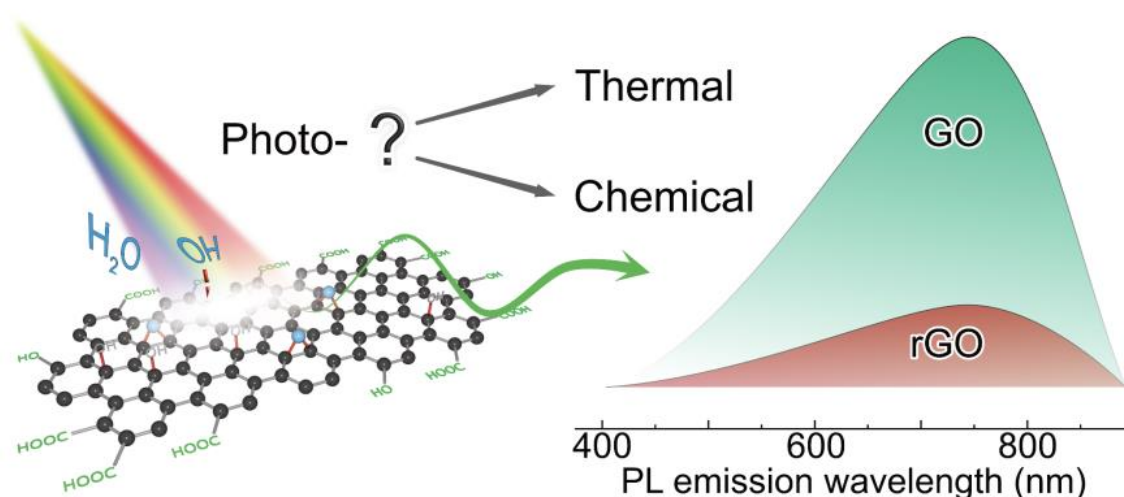
[1] E. Abyzova, I. Petrov, I. Bril', D. Cheshev, A. Ivanov, M. Khomenko, A. Averkiev, M. Fatkullin, D. Kogolev, E. Bolbasov, A. Matkovic, J.-J. Chen, R.D. Rodriguez, E. Sheremet, Universal Approach to Integrating Reduced Graphene Oxide into Polymer Electronics, Polymers 2023, 15 (24), 4622.

Irreversible aggregation of Au nanoparticles in aqueous colloids resulting in formation of chain-like structures during solvent evaporation

A.V. Simakin[1*], **A.O. Dikovskaya[1]**, **I.V. Baimler[1]**, **S.V. Gudkov[1]**

1- Prokhorov General Physics Institute of the Russian Academy of Sciences, 38 Vavilova Street, 119991 Moscow, Russia

* avsimakin@gmail.com

According to DLVO model, nanoparticles in a colloidal solution have a layer of adsorbed environmental components on their surface, which affects their properties and characteristics [1]. If particles are not fully coated during the synthesis process, aggregation may occur. Gold nanoparticles, known for their stability, have a significant electrical charge and a layer of gold hydroxide on their surface [2]. As the nanoparticles approach each other, the dipole-dipole potential becomes more significant, leading to an increasing force of attraction and aggregation [3]. However, this approach does not provide a general explanation for the irreversible formation of aggregates. Although many aspects of aggregation have been studied, the fundamental physico-chemical mechanisms underlying reversible and irreversible aggregation of metal nanoparticles in liquids remain poorly understood.
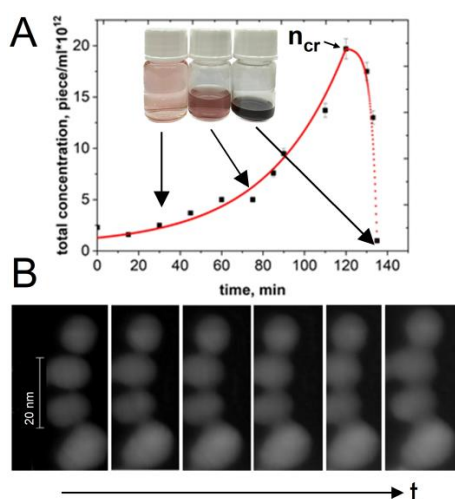
Fig. 1. (A) Dependence of the concentration of Au NPs on evaporation time,
(B) TEM images of the formation of chain-like aggregates of Au NPs.

This work demonstrates the existence of a critical concentration limit for the stability of aqueous colloidal solutions of gold nanoparticles without use of surfactants (Fig.1A). It was shown that as the volume of the solvent in the solution decreases, the size and concentration of the nanoparticles change in a non-monotonic manner. When the concentration of nanoparticles in a solution containing gold nanoparticles with a diameter of approximately 15 nanometers reaches approximately 10^{13} NPs/mL, intense aggregation occurs, forming elongated aggregates of nanoparticles (Fig.1B). This was confirmed using transmission electron microscopy and optical absorption spectroscopy. The nanoparticle aggregation process has been shown to be irreversible, and the zeta potential of the colloid does not change during this process.

[1] T. Kim, C.H. Lee, S.W. Joo, K. Lee, Kinetics of gold nanoparticle aggregation: experiments and modeling, Journal of colloid and interface science, 318(2), 238-243, (2008).

[2] G. Palazzo, G. Valenza, M. Dell'Aglio, A. De Giacomo, On the stability of gold nanoparticles synthesized by laser ablation in liquids, Journal of colloid and interface science, 489, 47-56, (2017).

[3] H. Zhang and D. Wang, Controlling the growth of charged-nanoparticle chains through interparticle electrostatic repulsion, Angewandte Chemie, 120(21), 4048-4051, (2008).

Nonlinear absorption and photoluminescence of direct and charge-transfer excitons in CdTe/CdSe nanotetrapods

A.M. Smirnov[1,2*], **V.N. Mantsevich**[1], **E.A. Shirshin**[1], **R.B. Vasiliev**[3]

1- Faculty of Physics, Lomonosov Moscow State University, Leninskie Gory 1-2, Moscow 119991, Russia
2- Kotelnikov Institute of Radioengineering and Electronics of RAS, Mokhovaya 11-7, Moscow 125009, Russia
3- Faculty of Materials Science, Lomonosov Moscow State University, Leninskie Gory 1-73, Moscow 119991 Russia

* alsmir1988@mail.ru

The photoluminescence (PL) peculiarities and the excited state absorption of the tetrapod-shaped CdTe/CdSe nanocrystals (Fig.1a) are studied in the single-photon excitation regime [1]. Tetrapod-shaped type II heterostructured nanocrystals composed by different materials are among the most intriguing low dimensional semiconductor nanostructures with anisotropic shape [2]. From a fundamental point of view, heterostructured nanotetrapods allow more efficient long-range induced separation of photoexcited electrons and holes.

We demonstrate the pump intensity dependent giant blue shift ($\approx$129 meV) of the indirect transition (charge-transfer – CT) emission band (Fig.1b) caused by the exciton's space filling effect and the modification of energy level structure by the induced internal electric field in both domains. The PL lines of the CdTe and CdSe domains, originating from direct electron-hole transitions were observed in addition to the tunable PL across the indirect gap (Fig.1b). Differential transmission spectra reveal the superposition of the exciton's transitions bleaching originating from different structural domains of the CdTe/CdSe nanocrystals, which confirms the observed separated excitonic emission bands in the PL spectra. The observed features of the PL and differential transmission spectra allow to determine and to analyze possible exciton's relaxation channels in the CdTe/CdSe nanocrystals (Fig.1c). The first-principles calculations reveal that the ground states of both electrons and holes are localized in the CdSe domain, but the charge carrier spatial separation is still present, as holes are localized at the interface [3]. This picture is proven by the time-resolved PL measurements from the sub-picoseconds to tens of nanoseconds range, which demonstrate the presence of a picosecond time scale corresponding to the indirect excitons being much smaller than the previously observed value.
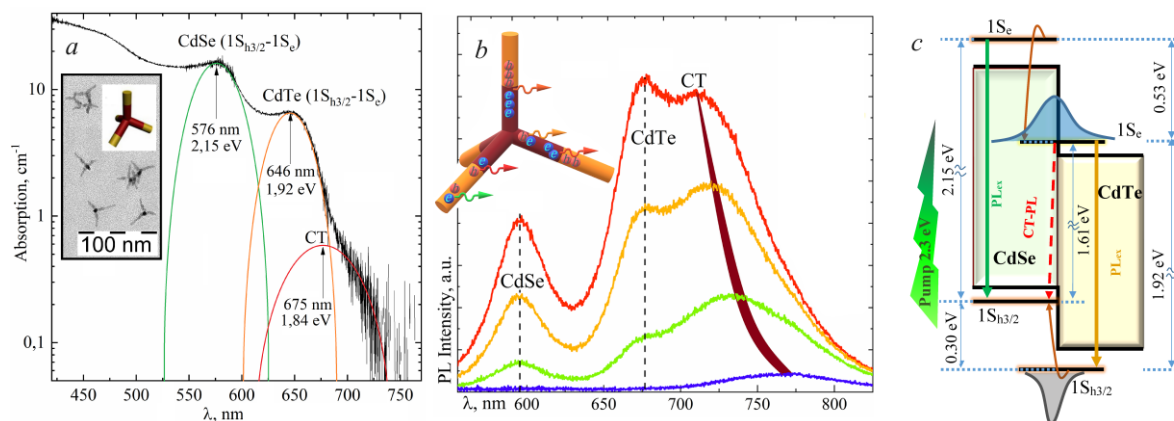
Fig. 1. a) The linear absorption spectrum of the tetrapod-shaped CdTe/CdSe nanocrystals. Gaussian bands corresponding to the CdSe and CdTe excitonic absorption bands (green and yellow lines) and charge-transfer (CT) band (red line). The inset shows transmission electron microscopy (TEM) image of the nanotetrapods and its sketch: red color demonstrates the core and the arms; yellow color shows the tips. b) PL spectra of the CdTe/CdSe nanotetrapod's colloidal solution for different pump intensities. c) Energy scheme of the CdTe/CdSe heterostructure. The scheme shows the band gap and the ground state energy levels for holes and electrons and schematically demonstrates the spatial localization of the electron and hole wave functions. Vertical (direct excitons) and inclined (indirect excitons) lines with arrows show main transitions, which contribute to the PL spectrum.

[1] A.D. Golinskaya, A.M. Smirnov, M.V. Kozlova, E.V. Zharkova, R.B. Vasiliev, V.N. Mantsevich, V.S. Dneprovskii, Tunable blue-shift of the charge-transfer photoluminescence in tetrapod-shaped CdTe/CdSe nanocrystals, Results in Physics, 27, 104488, (2021).
[2] R.B. Vasiliev, D.N. Dirin, M.S. Sokolikova, V.V. Roddatis, A.L. Vasiliev, A.G. Vitukhnovsky, A.M. Gaskov, Facet-selective growth and optical properties of CdTe/CdSe tetrapod-shaped nanocrystal heterostructures. J. Mater. Res., 26, 1621–1616, (2011).
[3] A.M. Smirnov, M.O. Nestoklon, E.A. Shirshin, K.V. Ezhova, A.V. Gayer, R.B. Vasiliev, V.S. Dneprovskii, V.N. Mantsevich, Charge Carrier Localization Impact on the Spectral–Temporal Photoluminescence Separation in Type II CdTe/CdSe Nano-Heterostructures, J. Phys. Chem. C, V.127, № 23, pp. 11119-11127, (2023).

Spherical microlasers with carbon dots and organic dyes

A.A. Starovoytov[1], E.O. Soloveva[1], K. Kurassova[1], K.V. Bogdanov[1], I.A. Arefina[1],
N.N. Shevchenko[2], A.A. Mitusova[3], T.A. Vartanyan[1], D.R. Dadadzhanov[1], N.A. Toropov[1,4*]

*1- International Research and Education Center for Physics of Nanostructures, ITMO University, 49
Kronverksky Pr., St. Petersburg 197101, Russia*
*2- Institute of Macromolecular Compounds, Russian Academy of Sciences, Bolshoy pr. 31 St. Petersburg
199004, Russia*
3- Pavlov First Saint Petersburg State Medical University, L'va Tolstogo str. 6-8, St. Petersburg 197022, Russia
4- Optoelectronics Research Centre, University of Southampton, Southampton SO17 1BJ, UK

* nikita.a.toropov@gmail.com

Microlasers based on whispering gallery modes (WGMs) have attracted attention in recent years as biosensors due to their biocompatibility, compact size, high Q-factor and narrow spectral width of resonance lines [1,2]. These properties make sensors based on such microlasers extremely sensitive to the slightest changes in the refractive index of the environment [3]. Popular fluorescent dopants for the development of WGM emitting cavities are quantum dots, but their application may be limited due to potential toxicity caused by the presence of heavy metals in their composition. The counterparts of quantum dots – carbon dots (CDs) – are much more biocompatible and non-toxic, which makes them safe for use in biological systems [4].

In this work, we propose a low-cost methodology to fabricate carbon-dot-doped WGM-based spherical microresonators (preliminary tested with rhodamine molecules) to develop a biocompatible sensor that is suitable for *in vivo* cell tagging and tracking applications. The sensing properties were tested by depositing bovine serum albumin (BSA), a protein commonly used as a reference protein to study interactions with drugs and nanoparticles, onto CDs-doped spheres. The effect of polystyrene microresonators on THP-1 and B16 cell lines survival was also investigated.

For the sensing experiments, 4 µL of aqueous bovine serum albumin solution was added to the tested sample of PS microresonators and left to dry out under room conditions. A concentration series of experiments was performed with 10^{-12}, 10^{-15}, 10^{-16}, 10^{-18} M BSA to determine the limit of detection. The mode shift in the emission spectra is caused by the change in the refractive index of the surrounding medium, so-called reactive sensing. A sufficiently large frequency shift is observed even at a concentration of 10^{-15} M; it is about 1.5 nm and becomes smaller with decreasing BSA concentration. A reproducible character of frequency shifts was demonstrated on the normalized emission spectra, however, at 10^{-18} M it becomes spectrally unresolvable for the used sensor. Thus, the detection limit was 10^{-16} M and the dynamic range was at least four orders of concentration.

In order to study the biocompatibility of PS microresonators, experiments were performed to introduce CDs-doped microspheres into THP-1 cells. The transmitted light image obtained by laser scanning confocal microscope shows that added polystyrene spheres doped with CDs accumulate on the cell damage. In addition, cell survival tests were performed when CDs and PS microspheres doped with CDs were added to cells. THP-1 and B16 cell lines were selected for the survival tests. The obtained dependence of the percentage of cell survival on the concentration of the additive shows that in most cases the percentage of survival is higher when the CDs are embedded in PS microspheres.

[1] N. Toropov, G. Cabello, M.P. Serrano, R.R. Gutha, M. Rafti, F. Vollmer, Review of biosensing with whispering-gallery mode lasers, Light Sci. Appl., 10, 42, (2021).
[2] M.C. Houghton, S.V. Kashanian, T.L. Derrien, K. Masuda, F. Vollmer, Whispering-Gallery Mode Optoplasmonic Microcavities: From Advanced Single-Molecule Sensors and Microlasers to Applications in Synthetic Biology, ACS Photonics, 11, 892–903, (2024).
[3] A. Capocefalo, S. Gentilini, L. Barolo, P. Baiocco, C. Conti, N. Ghofraniha, Biosensing with free space whispering gallery mode microlasers, Photonics Research, 11(5), 732-741, (2023).
[4] H.H. Jing, F. Bardakci, S. Akgöl, K. Kusat, M. Adnan, M.J. Alam, R. Gupta, S. Sahreen, Y. Chen, S.C.B. Gopinath, S. Sasidharan, Green Carbon Dots: Synthesis, Characterization, Properties and Biomedical Applications, J. Funct. Biomater., 14, 27, (2023).
[5] A. Döring, E. Ushakova, A.L. Rogach, Chiral carbon dots: Synthesis, optical properties, and emerging applications, Light Sci. Appl., 11, 75, (2022).

Formation of a weld joint using laser radiation with different pulse shapes

E. Surmenko[1*], **P. Ustinov**[1], **T. Sokolova**[1], **D. Bessonov**[1]

1- Yuri Gagarin State Technical University of Saratov, 77 Polytechnicheskaya st., 410054, Saratov, Russia

* surmenko@yandex.ru

The temporal shape of the laser pulse has a significant effect on the dynamics of surface heating during laser welding [1]. Modern laser technological set-ups allow varying the pulse shape in a wide range.

The aim of the study is to determine the optimal conditions for laser welding of thin sheet metal plates by changing the shape of the laser radiation pulse. The paper describes the sequence of study stages, including determining the optimal pulse duration, its energy, shape and repetition rate.

The weld was modeled on plates of 29NK material (Kovar, ASTM F15, UNS K94610, Fe-29Ni-17Co). Laser processing was carried out on the LRS-50 installation (LLC EDB "Bulat"): Nd:YAG-laser, pulse duration 0.2-20 ms, pulse repetition rate 0.5-100 Hz. The obtained weld spots and joints were examined with microscopes. The elemental composition of the joint and its changes under various welding modes were determined by the LIBS-method. The following welding modes were studied in various parameter combinations: pulse repetition rate 1 and 5 Hz, pulse duration 5 ms, 10 ms and 15 ms, pulse shapes 1 – triangular with amplitude increase, 2 – triangular with amplitude decrease, 3 – rectangular (Fig. 1). The energy input was changed by the voltage supplied to the pump lamp, from 200 to 240 V. To compare the obtained data, the value of the "speed" of change in the joint width with a change in energy input V (μm/V) was introduced.
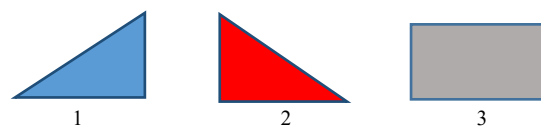
Fig. 1. Laser welding pulse shapes.

It was found out that, for both repetition rates 1 Hz and 5 Hz, the following distribution is characteristic.

Pulse 1: the joint width steadily increases with increasing of pulse duration at all pump voltage; the speed of increase in the joint width with increasing pump energy increases with increasing pulse duration (the longer the pulse, the faster the heating).

Pulse 2: the joint width also steadily increases at all pump voltages with increasing of pulse duration, but the speed of increase in the joint width with increasing pump energy decreases with increasing pulse duration (the longer the pulse, the slower the heating). Pulse 3: the joint width steadily increases with increasing pump. The maximum speed of joint width growth with increasing energy input is observed at a pulse duration of 5 ms, and then decreases with increasing pulse duration to 15 ms.

Rectangular pulse 3: the joint width steadily increases with increasing pump voltage, remaining less than with Pulse 1. The speed of joint width increase, when increasing pumping energy, increases within the measurement accuracy, remaining less than with Pulse 1 (about 80%).

LIBS-study of the joint centerline composition was performed for pulses 1 and 2 with different combinations of repetition rates and durations. It was found out that the depletion and enrichment trends for the same elements are almost similar in different modes. But Ti demonstrated different behavior with different pulse shapes.

[1] L.Ya. Min'ko, A.N. Chumakov, Yu.L. Chivel, Effect of the laser pulse shape on the formation of plasma near absorbing targets, Quantum Electronics, 11:11, pp. 2241–2245, (1984).

Laser-induced alloying and crystallization of multielement nanostructures in liquids

N. Tarasenka[1,2], V. Kornev[1], <u>N. Tarasenko</u>[1*]

1- B.I. Stepanov Institute of Physics, National Academy of Sciences of Belarus,
68-2 Nezalezhnasti Ave., 220072 Minsk, Belarus
2- Nanotechnology and Integrated Bio-Engineering Centre, Ulster University, Belfast, UK

* n.tarasenko@ifanbel.bas-net.by

Multielement nanostructures, such as perovskites and high entropy alloys have a wide range of applications in different fields, including catalysis, magnetism, biomedical science, photovoltaics, etc. However, preparation of such nanostructures with attaining a composition control poses a persistent challenge. Pulsed laser irradiation (PLI) in liquid can be an effective technique for alloying and crystallization of multielement nanostructures, as laser irradiation can induce targeted changes in the structural and physical properties of nanoparticles (NPs), that makes laser-induced modification of NPs a relevant topic in the last decades [1,2]. By varying laser pulse duration, wavelength and fluence, a precise control of NPs inner structure and surface composition can be achieved.

For multielement nanomaterials synthesis, PLI can be used in different ways: for example, laser irradiation of the colloidal mixtures, laser ablation of preliminary prepared multielement targets or laser processing of the deposited multicomponent thin films under liquid layer in a surface scanning mode, that results in a fabrication of multielemental nanostructured films on a substrate (Fig. 1). In this study, we have applied PLI of multimetallic CuZnFeMo colloids and PbZrTi layers deposited on the silicon substrate aiming synthesis of nanostructures with nearly equiatomic element composition in the first case and polycrystalline $Pb(Zr_{0.5}Ti_{0.5})O_3$ ferroelectric films in the second case. As a laser source, the unfocused beams of the second and forth harmonic (wavelength 532 and 266 nm, respectively) of the Nd:YAG laser (LOTIS TII, LS2134D) were used for laser-induced modification. The laser operated at repetition rate 10 Hz and pulse duration 10 ns. The phase composition, morphology, structure and optical properties of the prepared nanostructures were investigated. The results demonstrated that crystalline $Pb(Zr_{0.5}Ti_{0.5})O_3$ films were formed on Si substrates during 532 nm laser irradiation of deposited seeded three-phasic colloidal precursors. In the conditions created, the formation of multielemental phases proceeds via generation of thermal energy by photoexcitation, followed by co-melting, and re-solidification processes at high cooling rates under optimized laser processing parameters. The results obtained demonstrated that PLI of colloidal NPs provides unique possibilities not only for a change of the NPs morphology, but also for the synthesis of compound and alloyed NPs with a control over their phase composition.
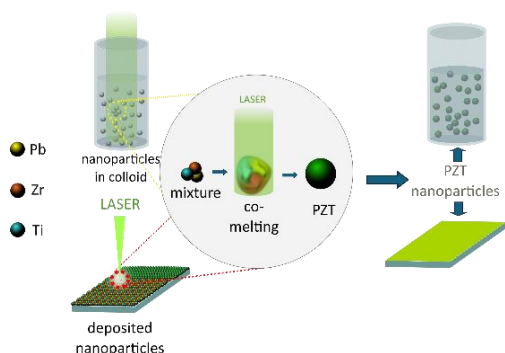
Fig. 1. A principal scheme of laser assisted synthesis and modification experiments used for PZT perovskite nanomaterials preparation performed with colloids and thin films.

[1] D. Zhang, B. Gökce, S. Barcikowski, Laser Synthesis and Processing of Colloids: Fundamentals and Applications, Chem. Rev., vol. 117, pp. 3990-4103, (2017).
[2] N.N. Tarasenka, N.V. Tarasenko, V.V. Pankov, Preparation of Germanium-Tin Alloy Nanoparticles by Laser-Assisted Techniques in Liquid, Intern. J. of Nanoscience, vol. 18, p. 1940049, (2019).

Broadband radiation detector based on laser-induced graphene embedded in polyimide

A. Telegin[1*], Yu. Sukhorukov, R.G. Zonov[2], K. Mikheev[2], G. Mikheev[2]

1- M.N. Mikheev Institute of Metal Physics, UB of RAS, 620108, Yekaterinburg, Russia
2- Udmurt Federal Research Center, UB of RAS, 426067, Izhevsk, Russia

* telegin@imp.uran.ru

The unique physicochemical properties of graphene offer broad possibilities for its use across all technical sectors. For instance, the zero bandgap in graphene's energy spectrum suggests it for creating an electromagnetic radiation detector working from ultraviolet to the submillimeter range. However, graphene has low light absorption and, consequently, low optical efficiency. In study [1], a high-speed and cost-effective method of synthesis of graphene through the pyrolysis of a polyimide film subjected to laser treatment by continuous CO_2 laser was considered. The formation of a porous graphene structure (LIG) significantly increased light absorption and led to reveal ultrafast photoinduced effects in visible range [1]. However, the spectral and low-frequency characteristics of the LIG are less studied.

In this work, the bolometric characteristics of the newly synthesized LIG samples (Fig.1a,b) are studied under exposure to visible and infrared light. It is shown that the thermal resistance coefficient of LIG is $\beta \sim 0.05\%$/deg at ambient conditions and increases to $\sim 0.15\%$/deg upon cooling. The sensitivity of the LIG detector at a wavelength of 532 nm is $\sim 0.08\%$/W at frequencies up to 10 kHz (Fig.1c), which is an only order of magnitude lower than the literature data for the best graphene structures. The spectral dependences of the ΔV are measured up to 21 µm due to technical limitations of the setup.
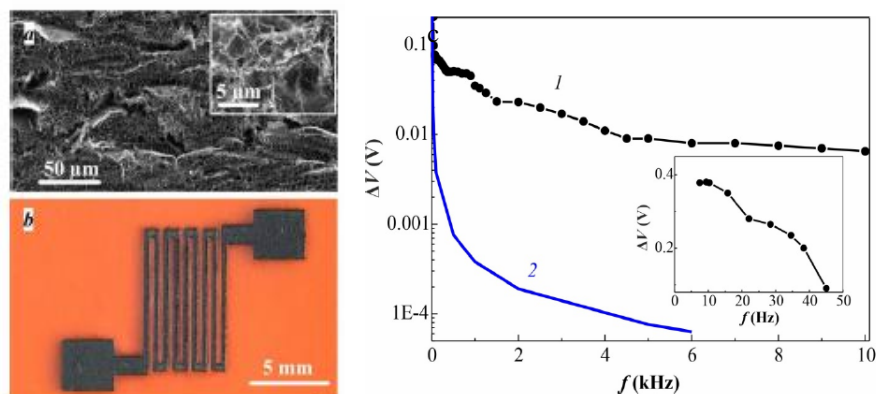
Fig.1 a) Images of a fragment of the LIG sample, b) the LIG detector on a polyimide substrate, c) Frequency dependence of the photoresponse ΔV of the LIG (1) and the ideal bolometer (2).

The frequency dependence of the LIG is formed by the contribution of several processes [2]. The first, thermal (bolometric), is associated with the heating of LIG due to the light absorption. The second is weakly dependent on the frequency of the emitter and is related to the photoinduced change in mobility and concentration of charge carriers due to trapping at defects. The spectral behavior is well described by Wien's law, except for features related to the generation of photoelectrons in the varieties of 2D graphene layers of porous graphene and light absorption in the optical scheme.

Therefore, the simple synthesis technology and wide spectral, time and frequency ranges of LIG can be considered for creating broadband bolometric type electromagnetic radiation detectors.

[1] K.G. Mikheev, et al, Laser-induced graphene on a polyimide film: observation of the photon drag effect, Technical Physics Letters, vol.46, pp. 458–461, (2020).
[2] Yu.P. Sukhorukov, et al, Laser-induced graphene based visible and near-infrared radiation detector, Optical materials, vol.133, p. 112957, (2022).

Nanosecond laser ablation in a free expansion and in confined modes of erosion laser plasma: physical aspects and applications

D.S. Polyakov[1*], V.P. Veiko, A. Ramos-Velazques

1- ITMO University, Saint-Petersburg, Russia

* *polyakovdmitry1988@gmail.com*

Nanosecond laser ablation is a complex physical process whose various aspects are used for numerous applications. In the simplest case of ablation in the ambient gas atmosphere (free expansion mode) the process consists of the following main stages: absorption of laser radiation and heating material up to evaporation point, transport of evaporated atoms through Knudsen layer, gas-dynamic expansion of vapor/plasma accompanied with possible additional absorption in the plume, mixing of the vapor with ambient gas accompanied with gas phase chemical reactions, condensation inside the plume (formation of nanoparticles and nanoclusters), deposition of condensed species back to the surface. The transition from the ablation in free expansion mode to the ablation in the confined mode (i.e. when the ablation proceeds in thin gap between the ablated material and transparent substrate) may significantly change the parameters of vapor/plasma plume, dynamics of its expansion and related phenomena. Despite that such ablation mode is widely used for several important applications such as CLIµPA [1,2] and LIBT/LIRT [3,4] the physics of the process is steel poorly understood.

In this talk we would like to present the results the of gas-dynamic simulation of nanosecond laser ablation of metals in confined mode with different gap sizes (from several microns up to several hundreds of microns) and in free expansion mode. Fig. 1 demonstrate the example of calculations of vapor density distribution inside the gap, that illustrate spreading of vapor in the radial directions. The results of the simulations are compared with experimental results on laser induced backward transfer of metals on glass substrate. Based on the results of such comparison the general physical picture and features of nanosecond laser ablation in confined mode will be revealed. It will be demonstrated that nanosecond laser ablation in confined mode can be used as a new method of polychromic marking of glasses. Possibilities and limitations of this method will be discussed.
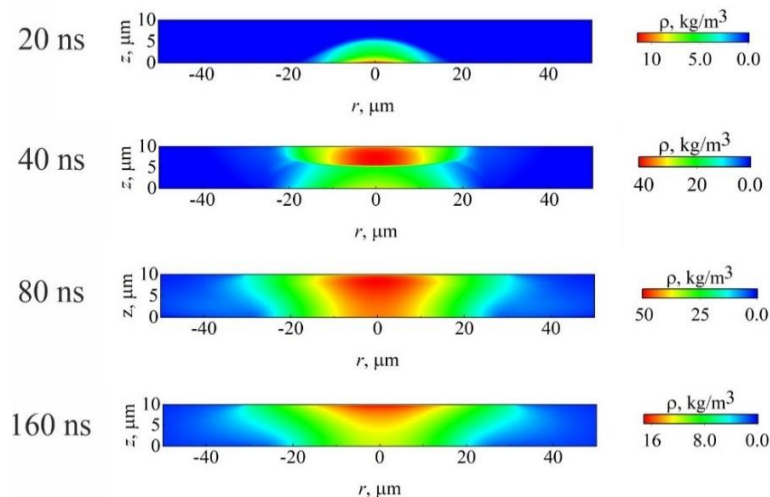
Fig. 1. Calculated vapour density distribution inside the gap during nanosecond laser ablation of titanium.

[1] V.P. Veiko, S.A. Volkov, R.A. Zakoldaev, M.M. Sergeev, Laser-induced microplasma as a tool for microstructuring transparent media, Quantum Electronics, 2017, Vol. 47, No. 9, pp. 842-848.
[2] V.A. Shkuratova, G.K. Kostyuk, M.M. Sergeev, R.A. Zakoldaev, E. Yakovlev, O.S. Medvedev, Rapid fabrication of spiral phase plate on fused silica by laser-induced microplasma, Applied Physics B: Lasers and Optics, 2020, Vol. 126, No. 4, pp. 1-6.
[3] A. Ramos-Velazquez, J. Amiaga, D. Pankin, G. Odintsova, R. Zakoldaev, V. Veiko, Laser-induced micro-scale polychrome marking of glass materials, Materials Letters, 2023, Vol. 343, pp. 134372.
[4] J. Macdonald, H. de Fossard, N. Gabbani, et al, Material ejection dynamics in direct-writing of low resistivity tracks by laser-induced reverse transfer, Appl.Surf.Sci., 2021, Vol. 536, pp. 147924.

Does a custom-designed metasurface outperform a self-assembled nanoparticle array in chemiluminescence enhancement?

D.R. Dadadzanov[1], N.B. Leonov[1], N.S. Petrov[1], A.V. Palekhova[1], D.V. Kononov[1], N.A. Virts[1,2], A.S. Bukatin[3,4], N.A. Filatov[1,4], <u>T.A. Vartanyan</u>[1*]

1- IR&EC PhysNano, ITMO University, St. Petersburg, Russia
2- Novosibirsk State University, 630090 Novosibirsk, Russia
3- Institute for Analytical Instrumentation of the Russian Academy of Sciences, Saint-Petersburg, Russia
4- Alferov University, St. Petersburg, Russia

* Tigran.Vartanyan@mail.ru

Chemiluminescence (CL) detection is an analytical method characterized by high sensitivity, wide linear range, easy operation, and simple instruments. Despite these advantages, CL of diluted and limited in volume analytes is weak and needs amplification. We attacked this problem with a promising approach akin to metal-enhanced fluorescence. Metal-enhanced chemiluminescence has already been demonstrated in several studies [1,2]. The idea behind this method is based on the notion that the radiative transition yield of the excited state formed as a result of photochemical reaction is low due to unfavorable competition with non-radiative transitions that occur much faster than the radiative transitions do. Thus, the natural way to enhance CL intensity is to speed up the radiative transitions via coupling of chemiluminescent species to a faster radiator. According to previous studies [3-5] localized surface plasmons in metal nanoparticles may serve for this purpose very well, although there remain doubts about the role played by the concurrent catalytic processes induced on metal surfaces.

Fig.1. The photo on the left panel shows a microfluidic chip comprising 7 individual channels with self-organized granular silver films deposited at their bottoms. The graphs on the right panel prove the considerable overlap between the CL spectrum of luminol and the plasmon band of silver nanoparticles survived all steps of the microfluidic chip preparation.

We are developing a microfluidic platform for well-controlled mixing of chemiluminescent species like luminol and lucigenin with oxidizes like hydrogen peroxide and other reactive oxygen species in the presence of metal nanoparticles possessing localized surface plasmon resonance. Silver nanoparticles arrays are arranged on the bottoms of the microfluidic channels in such a way that CL takes place under the influence of nearby silver nanoparticles. Both self-organized nanoparticle arrays fabricated via physical vapor deposition and specially designed periodic arrays of identical cylindrical nanoparticles are considered and compared for their efficiency as CL enhancer.

[1] M.H. Chowdhury, S.N. Malyn, K. Aslan, J.R. Lakowicz, C.D. Geddes, First Observation of Surface Plasmon-Coupled Chemiluminescence (SPCC), Chem. Phys. Lett., vol. 435, pp. 114–118 (2007).
[2] K. Aslan and C.D. Geddes, Metal-enhanced chemiluminescence: advanced chemiluminescence concepts for the 21st century, Chem. Soc. Rev., vol. 38, pp. 2556–2564, (2009).
[3] D.R. Dadadzhanov, I.A. Gladskikh, M.A. Baranov, T.A. Vartanyan, A. Karabchevsky, Self-organized plasmonic metasurfaces: The role of the Purcell effect in metal-enhanced chemiluminescence (MEC), Sen. & Act.: B. Chemical, vol. 333, p. 129453 (2021).
[4] N.A. Virts, D.R. Dadadzhanov, A.S. Yablokov, D.V. Shershnev, T.A. Vartanyan, Chemiluminescent hydrogen peroxide sensor based on luminol and a colloidal solution of metal nanoparticles, Opt. and Spectr., vol. 131, pp. 1531-1534 (2023).
[5] D.A. Gorbenko, P.V. Filatov, D.R. Dadadzhanov, K.K. Kirichek, M.Yu. Berezovskaya, T.A. Vartanyan, Chemiluminescent detection of nucleic acids induced by peroxidase-like targeted DNAnanomachines (PxDm) mixed with plasmonic nanoparticles, Proc. SPIE, vol. 12663, p. 1266307 (2023).

Liquid-phase laser synthesis of magnetic nanoparticles from thin Co films

I. Dzhun[1], V. Nesterov[2,3*], Ya. Mineev[2], D. Shuleiko[2], D. Presnov[1,2], E. Konstantinova[2], N. Chechenin[1,2], S. Zabotnov[2]

1- Lomonosov Moscow State University, Skobeltsyn Institute of Nuclear Physics, 1/2 Leninskie Gory, Moscow, 119991, Russia
2- Lomonosov Moscow State University, Faculty of Physics, 1/2 Leninskie Gory, Moscow, 119991, Russia
3- Moscow Institute of Physics and Technology, 9 Institutsky lane, Dolgoprudny, 141701, Russia

* nesterovvy@my.msu.ru

Today, magnetic nanoparticles (MNPs) are widely used in biomedicine, catalysis, data storage, environmental remediation and sensorics. Cobalt oxides are of interest due to their relatively high magnetic moment, spinel structure, unique properties and low cost [1]. Pulsed laser ablation in liquid (PLAL) is a universal, efficient and "green" method for producing chemically pure cobalt oxide MNPs in a one-step process, without the use of chemical reagents. The advantages of the PLAL method are the ability to control the size and composition of MNPs by varying the laser radiation parameters and the choice of buffer liquid.

Using PLAL targets of thin films of varying thicknesses instead of a bulk target for MNPs production potentially adds an additional possibility to control MNPs sizes. In our work, we studied PLAL generation of colloidal MNPs in distilled water from thin (5–500 nm) Co films magnetron sputtered. These films were irradiated by a Nd:YAG laser EKSPLA PL 2143A (1064 nm, 34 ps).

The MNPs obtained are predominantly spherical agglomerates at ablation target thicknesses of more than 35 nm (Fig. 1a); for smaller target thicknesses, PLAL additionally results in formation of flakes and coagulants of various shapes (Fig. 1b). The dependence of the average hydrodynamic size of MNPs obtained from dynamic light scattering data on the film thickness is non monotonic (Fig. 1c). The corresponding size distributions are characterized by the following standard deviations: ~40% for 500–35 nm films and ~20% for the thinner films [2]. The ablation threshold value and ablation craters profile were found to be dependent on the thickness of the Co film. Thus, the ablation threshold for thicknesses of 5–35 nm ranges from 0.6 to 1.5 mJ/mm^2 and the ablation craters are typical for the phase explosion. The ablation threshold for thicknesses of 35–500 nm lies in the range of 1.5–3 mJ/mm^2 and in these cases typical for spallative ablation craters occur. These peculiarities are connected to changing the ablation mechanism near the skin layer depth that was estimated as 38 nm.
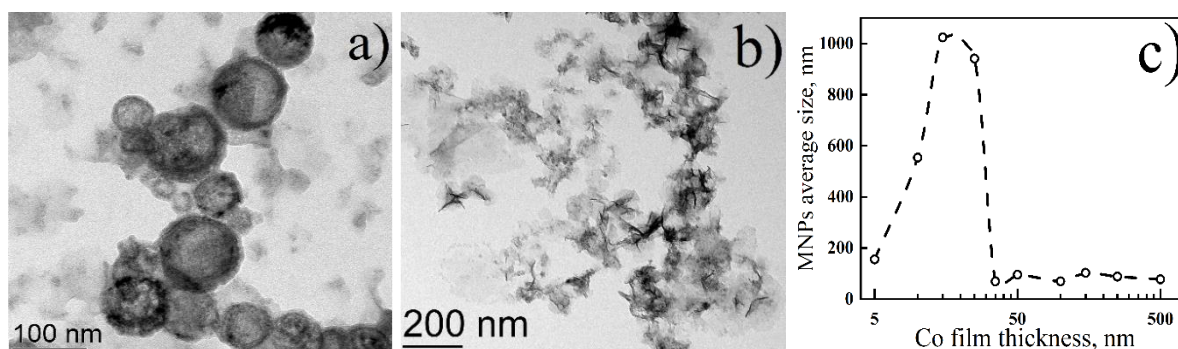
Fig. 1. Transmission electron microscopy images of MNPs obtained by laser ablation of Co films with thicknesses of 500 nm (a) and 15 nm (b) and the dependence of the average size of MNPs on the thickness of the Co film (c).

The produced colloids of MNPs demonstrated magnetic response. Electron paramagnetic resonance spectra for MNPs are characterized by absorption peaks at a resonance field value of ~3700 Oe at 9.65 GHz pumping frequency, which is close to the typical value for cobalt oxide Co_3O_4 and indirectly indicates its presence in the MNPs obtained. The Raman spectra of all formed MNPs also nearly correspond to ones for the mineral guite (Co_3O_4).

[1] E.N. Ghaem, D. Dorranian, A.H. Sari, External magnetic field effects on the characteristics of cobalt nanoparticles prepared by pulsed laser ablation, Opt. Quant. Electron., 53, 36 (2021).
[2] I.O. Dzhun, V.Yu. Nesterov, D.V. Shuleiko, et al, Magnetic Nanoparticles Produced by Pulsed Laser Ablation of Thin Cobalt Films in Water, Bull. RAS: Phys., 88, 540-548 (2024).

Investigation of physical mechanisms of laser cleaning applicable for cleaning rolled metal from mill scale

D.V. Zhurba[1,2*]**, V.M. Zhurba**[2]**, V.P. Veiko**[1]

1- ITMO University, Russia, Saint Petersburg, Sablinskaya Street, 14
2- NPP VOLO LLC, Russia, Saint Petersburg, 17th line V.O., 4-6

* zhurba.danila306@ya.ru

A cleaning of rolled metal from scale is a very important for industry and at the same time very complicated and ambitious aim. The most demanded and, at the same time, the most difficult task here is the removal of oxide layers from the surface of hot-rolled carbon steels (mill scale). Well known methods such as mechanical, chemical and evaporative laser cleaning of rolling scale is an insufficiently efficient and low-productivity processes [1]. A new approach to realize this process by means of the mechanisms of scale destruction due to phase change of the surface layers with appearance of the wustit phase with its small adhesion to the main metal followed by thermal stresses has been suggested. This approach was realized be means of continuous laser radiation of fiber laser [2].

The possibility of destruction of mill scale due to thermochemical reactions in the scale and subsequent thermomechanical destruction has been identified and substantiated. The search and optimization of laser exposure modes has been carried out to increase the cleaning efficiency. For a more complete description of the laser cleaning process, attention is paid to the structure of rolled scale and the features of its formation and probable phase transformations under the action of laser heating are described (fig).
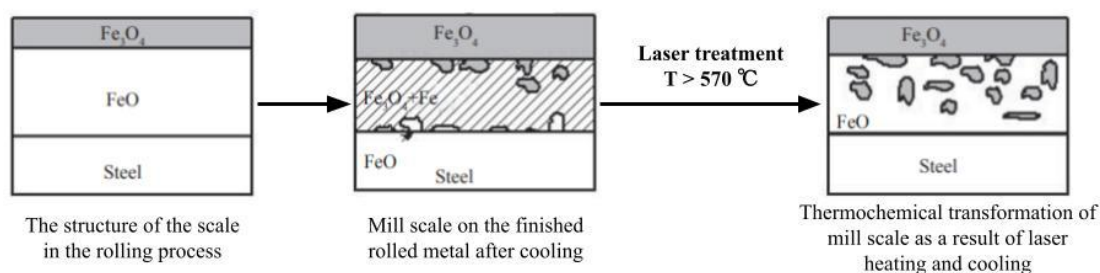
Fig. The formation of rolling scale and its transformation during laser heating and subsequent cooling.

The field of modes of exposure to continuous laser radiation, which leads to thermomechanical destruction of scale, without the contribution of evaporation, is investigated. The studied range of exposure durations is $10^{-5} - 10^{-4}$ s. The studied range of power densities is $50 - 1000$ kW/cm^2. A method of two-stage roughing and finishing laser cleaning is proposed, which allows to increase the productivity and quality of cleaning.

[1] J.M. Deschênes and A. Fraser, Empirical Study of Laser Cleaning of Rust, Paint, and Mill Scale from Steel Surface. In: J. Lee, S. Wagstaff, G. Lambotte, A. Allanore, F. Tesfaye (eds), Materials Processing Fundamentals. The Minerals, Metals & Materials Series. Springer, Cham (2020).
[2] D.V. Zhurba, V.M. Zhurba, A.E. Puisha, Laser cleaning of surfaces of structures of pipeline transportation of hydrocarbons, Drilling and oil, № S2. pp. 61-67, (2023).

BIOMEDICAL PHOTONICS

Two-dimensional metalenses for creation of portable biosensors of single molecules

A. Barulin[1,2*], S. Novikov[1], A. Chernov[1,3]

1- Center for Photonics and 2D Materials, Moscow Institute of Physics and Technology, Dolgoprudny 141700, Russia
2- Department of Biophysics, Institute of Quantum Biophysics, Sungkyunkwan University, Suwon, 16419, Republic of Korea
3- Russian Quantum Center, Moscow 121205, Russia

* alexbarulin73@gmail.com

Dielectric metalenses can focus light with the spatial resolution of the diffraction limit with sufficient control over the numerical aperture, size, and chromatic aberration correction. Due to micrometer-size thickness, this nanophotonic structure appears a compact planar analogue of refractive optical elements. Metalenses find their applications in multi-functional and miniaturized high aperture optical devices for visualizing biological objects, however, detection of single-molecule fluorescence, which is a key element in molecular biology and medicine, requires the use of high-quality and costly optical and optoelectronic components with high collection efficiency of fluorescence photons. We present a metalens made of nanofins of amorphous silicon, which has high numerical aperture and focusing power [1]. This metalens is capable of detecting single fluorescent Alexa647 molecules using fluorescence correlation spectroscopy, and is also capable of determining the size of fluorescent nanoparticles with nanometer accuracy. The demonstrated optical device greatly reduces the size of the refractive lens and practically does not lose the efficiency of collecting photons at the same values of the numerical aperture. The proposed nanophotonic platform will make it possible to create compact and portable fluorescent biosensors for medicine and point-of-care diagnostics and for screening environmental pollution.

[1] A. Barulin, et al, Dual-wavelength metalens enables Epi-fluorescence detection from single molecules, Nature Communications 15, 26 (2024).

New generation of nanostructures with laser-controllable biological and luminescence properties

<u>G. Bikbaeva</u>[1*], A. Pilip[2], A. Egorova[3], I. Kolesnikov[4], D. Pankin[4], V. Medvedev[1], K. Laptinskii[5,6], A. Vervald[6], T. Dolenko[6], A. Manshina[1]

1- Institute of Chemistry, St. Petersburg State University, St. Petersburg 198504, Russia
2- St. Petersburg Federal Research Center of the Russian Academy of Sciences (SPC RAS), Scientific Research Centre for Ecological Safety of the Russian Academy of Sciences, St. Petersburg 197110, Russia
3- St. Petersburg State Technological Institute (Technical University), St. Petersburg 190013, Russia
4- Center for Optical and Laser Materials Research, St. Petersburg State University, St. Petersburg 198504, Russia
5- Faculty of Physics, M.V. Lomonosov Moscow State University, Moscow 119991, Russia
6- Skobeltsyn Institute of Nuclear Physics, M.V. Lomonosov Moscow State University (SINP MSU), Moscow 119991, Russia

* BikbaevaGI@yandex.ru

Design of hybrid nanostructures by combination of different components is a promising strategy to obtain advanced functional materials [1]. For example, incorporation of photoswitchable fragment as component of hybrid nanomaterial provides opportunity of its remote control by laser irradiation. By now hybrid nanostructures with photoswitchable-enhanced functional properties have been demonstrated as optical logic elements, optoelectronic devices, drug delivery, etc [2].

Here we present unique hybrid nanostructures based on photo-switchable and bioactive phosphonate molecules and luminescent carriers (oxide nanoparticles doped with rare earth ions $LaVO_4:Eu^{3+}$, carbon quantum dots). The study of the obtained hybrids with luminescent spectroscopy, IR spectroscopy and IPC–micro analysis of neurotoxins revealed a pronounced effect of laser radiation on the optical and biological properties of new objects. Hybrids demonstrate not only properties of initial components – luminescence and photo-switchable butyrylcholinesterase inhibition, but also strong effect of carrier nature on bioactivity, and photo-switchable effect on luminescence properties [3]. Thus, the presented hybrid nanomaterials were found to demonstrate a remarkable combination of all-in-one properties important for photopharmacology: (i) bioactivity toward butyrylcholinesterase inhibition, (ii) strong change of inhibition degree as a result of laser irradiation, luminescence as an indicator of (iii) bioactivity state, and of (iv) spatial localization on the surface of a sample. The functionality of the hybrids has been demonstrated both *in vitro* and *in vivo* on various biological test objects.

[1] F. Cardano, M. Frasconi, S. Giordani, Photo-Responsive Graphene and Carbon Nanotubes to Control and Tackle Biological Systems, Front. Chem. 6, (2018).
[2] X. Zhang, L. Hou, P. Samorì, Coupling carbon nanomaterials with photochromic molecules for the generation of optically responsive materials, Nat. Commun. 7, 11118 (2016).
[3] G. Bikbaeva, et al, All-in-One Photoactivated Inhibition of Butyrylcholinesterase Combined with Luminescence as an Activation and Localization Indicator: Carbon Quantum Dots@Phosphonate Hybrids, Nanomaterials 13, 2409 (2023).

Detecting the Raman signature responsible for the life activity of regenerating worm *A. Viride* using Raman and two-photon fluorescence lifetime imaging spectroscopy

P.M. Badgujar[1], P.-Y. Huang[1], A.V. Karmenyan[1], V.V. Nikolaev[2],
Y.V. Kistenev[2], J.-H. Chen[3], C.-L. Cheng[1*]

1- Department of Physics, National Dong Hwa University, Hualien 97401, Taiwan
2- Department of Physics, Tomsk State University, Tomsk, 634050, Russia
3- Department of Life Sciences, National Taiwan University, Taipei, Taiwan

* clcheng@gms.ndhu.edu.tw

In regenerative organisms, regeneration arises with the help of repatterning co-existing tissues after a wound or trauma has occurred in a regenerative organism. Understanding these mechanisms is crucial as critical metabolic functions are involved during the process of regeneration. With the emerging field of regenerative medicine, understanding the "molecular signature" of what determines and triggers the process of regeneration is of utmost importance. In this study, we uncover the molecular signature responsible for the process of regeneration; in one of the simpler and advanced freshwater regenerative annelid, *Aeolosoma Viride* (*Annelida, Aeolosomatidae*). *A. viride* is tasked with building entire body segments out of their single starting cell at their amputated region and undergoing epimorphic regeneration; therefore these annelids are the most suitable for the study of regeneration [1]. In this work, we carefully address the participation of primary and secondary Carotenoids in the life activity of the regenerating anterior region of *A. viride*. At the site of regeneration, primary antioxidant carotenoids were detected with the Raman spectral band of zeaxanthin at 1525-1527 cm^{-1}, 1159 cm^{-1}, and 1005-1008 cm^{-1}. The secondary role of carotenoids in the process of cell signaling was confirmed with the upregulation of the *Cu/Zn superoxide* (SOD1) gene at the regenerated area at the cell patterning state. The intracellular participation and distribution of the proliferated blastemal cells in the anterior regeneration segments were monitored by applying a phasor approach to the TP-FLIM label-free without any specific staining. The application of micro Raman spectroscopy with the combination of Two-photon fluorescence lifetime imaging can be a good technique in the study of regenerative medicine. Furthermore, we demonstrated that a high amount of reactive oxygen species is produced at the wound healing state and the blastema budding state during the anterior regeneration process. In the field of regenerative medicine; the approach of the Raman spectroscopic technique in combination with the TP-FLIM could be an advancement in the regenerative studies.
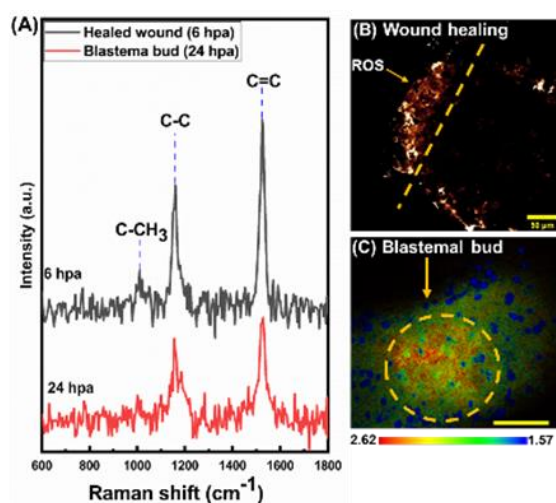
Fig. 1. (A) The Raman spectroscopic signature at wound healing (6 hpa) and budding blastema cells at 24 (hpa). (B) Detection of Reactive Oxygen Species at the wound healing at the anterior regenerated segment. (C) Two-Photon Fluorescence Lifetime Imaging label-free direct screening of the Blastema bud at 24 hpa.

[1] C.-P. Chen, S.K.-W. Fok, Y.-W. Hsieh, et al, General characterization of regeneration in Aeolosoma viride (Annelida, Aeolosomatidae). Invertebr Biol. 139:e12277 (2020).

Cancer cells' response to chemotherapeutic treatment in the presence of collagen: monitoring with fluorescence and phosphorescence lifetime imaging techniques

I. Druzhkova[1*], E. Nikonova[2,3], A. Komarova[1,4], A. Mozherov[1], N. Ignatova[1], I. Koryakina[5],
M. Zyuzin[5], V. Baigildin[6], Yu. Shakirova[6], U. Lisitsa[1], E. Shirshin[2,3], V. Shcheslavskiy[1], S. Tunik[6],
M. Shirmanova[1]

1- Institute of Experimental Oncology and Biomedical Technologies, Privolzhsky Research Medical University
2- Lomonosov Moscow State University, Faculty of Physics, Moscow, Russian Federation
3- Sechenov First Moscow State Medical University of the Ministry of Health of the Russian Federation
(Sechenov University), Moscow, Russian Federation
4- Institute of Biology and Biomedicine, Lobachevsky State University of Nizhny Novgorod
5- School of Physics and Engineering, ITMO University, 9 Lomonosova St., St. Petersburg 191002, Russia
6- Saint-Petersburg State University, Institute of Chemistry, St. Petersburg, Russia

* danirin@yandex.ru

The extracellular matrix (ECM), in which collagen is the most abundant protein, impacts many aspects of tumor physiology, including cellular metabolism, intracellular pH (pHi) as well as efficacy of chemotherapy [1]. Meanwhile, the role of collagen in differential cell response to treatment within heterogeneous tumor environment remains poorly investigated.

In this study, we compared effectiveness of chemotherapeutic drugs against cancer cells in vitro in the models with and without collagen. The effects of the drugs on cellular metabolism and intracellular pH (pHi) were investigated. For this, a combination of optical methods was used: Second Harmonic Generation (SHG) imaging of collagen, multiphoton fluorescence microscopy to visualize distribution of doxorubicine (DOX), fluorescence lifetime imaging (FLIM) of redox cofactor NAD(P)H [2], and phosphorescence lifetime imaging (PLIM) of pHi sensor. The pHi was followed using the new pH-sensitive probe BC-Ga-Ir [3].

We explored distribution of DOX in the presence of collagen with different structures in 3D collagen-based models and monitored metabolic changes in urinary bladder cancer cells using FLIM. Also, we monitored simultaneously the changes in pHi and metabolism in living colorectal cancer cells growing in collagen in vitro upon treatment with FOLFOX.

It was found that viability of different cancer cell types was better in the presence of collagen. Collagen slowed down the diffusion of DOX and thus decreased the cellular drug uptake. Besides nuclei, DOX also targeted mitochondria leading to inhibition of oxidative phosphorylation, which was more pronounced in the cells growing in the absence of collagen [4]. It was found that FOLFOX treatment caused an early temporal intracellular acidification (reduction of pHi) followed by a shift to more alkaline values. Notably, cancer cells changed cellular metabolism to a more oxidative state after treatment, but in the absence of collagen the changes were more pronounced [5].

Taken together, our data illustrate that tumor collagen contributes to heterogeneous and sub-optimal response to investigated chemotherapeutic drugs and highlight the challenges in improving drug delivery and efficacy.

[1] M. Najafi, et al, Extracellular matrix (ECM) stiffness and degradation as cancer drivers, Journal of cellular biochemistry 120, 2782-2790 (2019).
[2] M. Shirmanova, et al, Exploring Tumor Metabolism with Time-Resolved Fluorescence Methods: From Single Cells to a Whole Tumor, Chapter 3 in Multimodal Optical Diagnostics of Cancer, pp. 133–155 (2020).
[3] J.R. Shakirova, et al, Intracellular pH Sensor Based on Heteroleptic Bis-Cyclometalated Iridium (III) Complex Embedded into Block-Copolymer Nanospecies: Application in Phosphorescence Lifetime Imaging Microscopy. Advanced Functional Materials 33, 2212390 (2023).
[4] I. Druzhkova, et al, Effect of Collagen Matrix on Doxorubicin Distribution and Cancer Cells' Response to Treatment in 3D Tumor Model, Cancers (Basel), Nov 8;14(22):5487 (2022).
[5] I. Druzhkova, et al, Monitoring the Intracellular pH and Metabolic State of Cancer Cells in Response to Chemotherapy Using a Combination of Phosphorescence Lifetime Imaging Microscopy and Fluorescence Lifetime Imaging Microscopy, Int J Mol Sci. Dec 19; 25(1):49 (2023).

Marker-free diagnostics for assessing pancreas and islet quality

P. Ermakova[1*], E. Vasilchikova[1], A. Kashirina[1], A. Bogomolova[1], N. Naraliev[1], D. Kuchin[1,2], L. Lugovaya[1], E. Zagaynova[1,3], V. Zagainov[1,4], A. Kashina[1]

1- Privolzhsky research medical university, Russia
2- Nizhny Novgorod Regional Clinical Hospital named after Semashko, Russia
3- Lopukhin federal research and clinical center of physical-chemical medicine, Russia
4- Nizhny Novgorod Regional Oncology Dispensary, Nizhny Novgorod, Russia

* bardina-polina@mail.ru

Insulin-deficient conditions present a significant global public health challenge. Cellular stress and dysfunction precede the gradual loss of cell mass in conditions such as type 1 and type 2 diabetes, or pancreatitis. Cell dysfunction arises from altered glucose metabolism as part of a conserved pro-survival signaling mechanism. In healthy cells, elevated glucose levels lead to increased adenosine triphosphate (ATP) production through oxidative phosphorylation (OxPhos), which in turn influences insulin secretion via membrane channels. In contrast, stressed cells exhibit increased glycolysis unrelated to OxPhos, resembling the Warburg effect seen in cancer cells.

Conventional methods like PCR, immunohistochemistry, and transcriptomic studies are typically used to study cell metabolism but may offer incomplete or conflicting insights into islets. Therefore, a single method for fast, non-staining assessment of islet quality in both whole tissues and post-isolation is lacking. Metabolic Fluorescence Lifetime Imaging Microscopy (FLIM) has emerged as a potent tool for non-invasive, label-free diagnostics of pancreatic islet quality.

To make FLIM more clinically applicable, new criteria must be established to evaluate islet quality and metabolism across various insulin-deficient conditions. FLIM can be used to assess islet quality in whole tissues affected by insulin deficiency diseases or to monitor islet status pre- and post-transplantation. This study utilized FLIM and intracellular metabolite NAD(P)H to develop a non-invasive, label-free method for assessing isolated islet cell and pancreatic islet quality.

Fluorescence lifetimes and the relative proportions of free and bound NAD(P)H forms were analyzed using advanced FLIM systems. The FLIM parameters of islet cells from pathological and normal pancreases differed, with an increased glycolytic phenotype observed in pancreases with type 1 and type 2 diabetes/chronic pancreatitis. Metabolic FLIM imaging proved effective in evaluating isolated islet cell metabolism and viability.

FLIM data showed an increase in bound NAD(P)H levels and a predominance of oxidative phosphorylation over glycolysis upon glucose stimulation, which correlated with elevated insulin production in isolated cells. This confirmed the functional activity and viability of isolated islets. Non-contrast FLIM diagnostics can aid in establishing new criteria for identifying islet cell quality and metabolism, offering a swift technique for assessing islet viability in transplantation settings.

Overall, FLIM is a valuable tool for assessing islet quality in both whole tissues and during isolation, enhancing its utility in transplantation technologies.

Fluorescent sensing of metal ions in biological environment with carbon dots

L.I. Fatkhutdinova[1*], E.N. Gerasimova[1], I.I. Vazhenin[1], P. Ginzburg[2,3], M.V. Zyuzin[1]

1- School of Physics, ITMO University, Lomonosova str. 9, 191002 St. Petersburg, Russia
2- Triangle Regional Research and Development Center, Kfar Qara' 3007500, Israel
3- Light-Matter Interaction Centre, Tel Aviv University, Tel Aviv, 69978, Israel

* landysh.fatkhutdinova@gmail.com

Microelements play critical roles in numerous physiological functions by circulating in the bloodstream [1]. Ferrous ions (Fe^{2+}), integral to hemoglobin, facilitate oxygen transportation within the body [2]. Additionally, they are vital for hematopoiesis, molecule conveyance, and nutrient dispersion. A deficiency in these ions can result in anemia, while an excess leads to hemochromatosis and potential organ impairments [3,4]. Elevated levels may trigger oxidative damage and ischemic harm. Cobalt (Co^{2+}) is another essential element found in the water-soluble Cobalamin (Vitamin B-12) complex, crucial for metabolic processes [4]. It aids in lowering homocysteine levels, protecting cardiovascular health, and supporting blood cell generation, along with maintaining healthy nervous system function. Vitamin B-12 deficiency can cause anemia, while excess amounts may lead to asthma, rhinitis, and cardiomyopathy [5]. Detection of metal ions like Fe^{2+} and Co^{2+} is essential for health monitoring and sustaining bodily functions.

Spectroscopic methods are gaining attention for swiftly detecting metal ions, offering a viable option compared to other complex techniques [6]. Optically-responsive nanomaterials like quantum dots, plasmonic nanoparticles, and carbon dots show promise in effectively sensing biological molecules. Carbon dots, with their low photobleaching and high water solubility, are particularly notable for detecting various metal ions such as Pd^{2+}, Hg^{2+}, and Fe^{2+} [7-9]. Monitoring their fluorescence intensity and lifetime aids in understanding their response to metal ions, crucial for ion sensing applications.

Thus, the optical sensing capabilities of synthesized meta-phenylenediamine CDs were examined by combining them with various metal ions to enhance specificity [10]. The CDs, derived from phenylenediamine, were chosen for their remarkable sensitivity and attraction to metal ions at incredibly low concentrations, as demonstrated in earlier studies. We show that the CDs exhibit a strong sensitivity towards Fe^{2+}, Fe^{3+}, and Co^{2+}. Additionally, the fundamental processes behind this selective sensing are studied. Further tests are carried out in blood serum to validate the concept. Leveraging these unique properties, these CDs could potentially pave the way for a detection system for Fe^{2+}, Fe^{3+}, and Co^{2+}, thereby making significant contributions to advancements in medical diagnostics and environmental monitoring.

[1] M. Brancaccio, C. Mennitti, A. Cesaro, F. Fimiani, M. Vano, B. Gargiulo, M. Caiazza, F. Amodio, I. Coto, G. D'Alicandro, C. Mazzaccara, B. Lombardo, R. Pero, D. Terracciano, G. Limongelli, P. Calabro, V. D'Argenio, G. Frisso, O. Scudiero, The biological role of vitamins in athletes' muscle, heart and microbiota, Int. J. Environ. Res. Public Health, vol. 19(3), p. 1249, 2022.

[2] N. Abbaspour, R. Hurrell, R. Kelishadi, Review on iron and its importance for human health, J. Res. Med. Sci., vol 19(2), pp. 164–174, 2014.

[3] A. Babuponnusami and K. Muthukumar, A review on fenton and improvements to the fenton process for wastewater treatment, J. Environ. Chem. Eng., vol. 2(1), pp. 557–572, 2014.

[4] Z. Abdi, S. Balaghi, S. Sologubenko, M.-G. Willinger, M. Vandichel, J.-R. Shen, S. Allakhverdiev, G. Patzke, M. Najafpour, Understanding the dynamics of molecular water oxidation catalysts with liquid-phase transmission electron microscopy: the case of Vitamin B_{12}, ACS Sustainable Chem. Eng., vol. 9(28), pp. 9494–9505, 2021.

[5] M. Umar, N. Jahangir, M. Faisal Khan, Z. Saeed, F. Sultan, A. Sultan, Cobalt cardiomyopathy in hip arthroplasty, Arthroplast. Today, vol. 5(3), pp. 371–375, 2019.

[6] M.D. Shirsat and T. Hianik, Electrochemical detection of heavy metal ions based on nanocomposite materials, J. Compos. Sci., vol. 7(11), p. 473, 2023.

[7] V. Sharma, A. Saini, S. Mobin, Multicolour fluorescent carbon nanoparticle probes for live cell imaging and dual palladium and mercury sensors, J. Mater. Chem. B, vol. 4(14), pp. 2466–2476, 2016.

[8] G. Ren, Q. Zhang, S. Li, S. Fu, F. Chai, C. Wang, F. Qu, One pot synthesis of highly fluorescent N doped C-dots and used as fluorescent probe detection for Hg^{2+} and Ag^+ in aqueous solution, Sens. Actuators B: Chem., vol. 243, pp. 244–253, 2017.

[9] X. Sun, J. Zhang, X. Wang, J. Zhao, W. Pan, G. Yu, Y. Qu, J. Wang, Colorimetric and fluorimetric dual mode detection of Fe^{2+} in aqueous solution based on a carbon dots/phenanthroline system, Arab. J. Chem., vol. 13(4), pp. 5075–5083, 2020.

[10] M. Batool, H. Junaid, S. Tabassum, F. Kanwal, K. Abid, Z. Fatima, A. Shah, Metal ion detection by carbon dots — a review, Crit. Rev. Anal. Chem., vol. 52(4), pp. 756–767, 2022.

Peculiarities of generation of silver nanoparticles created for giving antibacterial properties to polymers in different fluids

D.E. Fominov[1*], Yu.Yu. Karlagina[1], Y.S. Andreev[1], G.V. Romanova[1]

1- ITMO University, Russian Federation, 197101, St. Petersburg, Kronverksky pr. 49, lit. A.

* denis_fominov@niuitmo.ru

Surgical sutures are the main method of joining tissues after surgery or wounds. However, this method is prone to inflammation due to bacterial contamination. The most common way to prevent such infections is to modify the suture material with antibiotic drugs. However, given the increasing number of antibiotic-resistant bacteria [1,2], as well as undesirable side effects such as toxic effects, the need for repeated use [3], and allergic reactions, there is a need to search for alternative suture materials. One of the promising approaches is the use of suture material with antibacterial properties by enriching it with nanosilver. Our concept is to create a resorbable suture material with a bactericidal effect using colloidal silver obtained by laser ablation in liquid, the antibacterial activity of which has been proved [4].

The realization of this idea includes three main steps: 1. Development of a method for generating nanoparticles in liquid; 2. Investigation of bactericidal properties of the material used for suture material; 3. Development of the technology of creating resorbable suture material. The purpose of this work is to study the result of the process of obtaining colloidal silver in distilled water and physiological solution by laser ablation. In order to achieve this goal, the following tasks should be solved: 1. To synthesize silver nanoparticles solution by laser ablation method in distilled water; 2. To synthesize silver nanoparticles solution by laser ablation method in physiological solution; 3. Analyze the properties of the obtained colloids depending on the parameters of the laser beam and ablation medium; 4. To carry out comparative analysis.

The experiments were made using the Minimarker-2 laser complex equipped with an ytterbium fiber laser with a wavelength of 1064 nm. Silver plates (99.9% purity, sample 999) were used as a material. Before ablation, the material was mechanically polished using a mini-drill and polishing pastes, and cleaned in an ultrasonic bath in deionized water. Distilled water and 0.9% aqueous NaCl solution were used as ablation media. Characterization of the obtained nanoparticle solutions was carried out by dynamic light scattering and scanning electron microscopy methods with preliminary application of colloid on silicon plates.

Experiments were carried out to optimize the parameters of laser radiation for the generation of silver nanoparticles by pulsed laser ablation in liquid. The influence of laser beam parameters (power, pulse duration) and ablation medium (distilled water and physiological solution) on colloid characteristics was investigated. According to the results of colloid analysis, it was found that the used mode provides generation of silver nanoparticles with the size of 50-250 nm. The present study is an important part that determines the possibility of further research within the purpose of the whole project.

[1] D.M. Syukri, et al, Antibacterial functionalization of nylon monofilament surgical sutures through in situ deposition of biogenic silver nanoparticles, Surface and Coatings Technology 413 (2021): 127090.

[2] D.M. Syukri, et al, Antibacterial-coated silk surgical sutures by ex situ deposition of silver nanoparticles synthesized with Eucalyptus camaldulensis eradicates infections, Journal of Microbiological Methods 174 (2020): 105955.

[3] B.O. Kabeshev, D.N. Boncevich, A.Y. Vasilkov, Antibacterial suture material, Surgery. Eastern Europe 3 (2012): 294-296.

[4] C.G. Anjali Das, et al, Antibacterial activity of silver nanoparticles (biosynthesis): A short review on recent advances, Biocatalysis and Agricultural Biotechnology 27 (2020): 101593.

Skin optical clearing *in vivo*: application for photodynamic therapy

V.D. Genin[1,2*], D.K. Tuchina[1,2], A.B. Bucharskaya[2,3], E.A. Genina[1,2], N.A. Navolokin[3], D.A. Mudrak[3], G.N. Maslyakova[3], V.V. Tuchin[1,2,4]

1- Department of Optics and Biophotonics, Saratov State University, Astrakhanskaya St., 83, 410012 Saratov, Russia
2- Laboratory of Laser Molecular Imaging and Machine Learning, Tomsk State University, 36 Lenin Ave., 634050 Tomsk, Russia
3- Department of Pathological Anatomy, Saratov State Medical University, Bolshaya Kazachaya St., 112, 410012 Saratov, Russia
4- Institute of Precision Mechanics and Control Problems of the Russian Academy of Sciences, Federal Research Center "Saratov Scientific Center of the RAS", Rabochaya St., 24, 410028 Saratov, Russia

* versetty2005@yandex.ru

A promising method for increasing the selectivity of laser treatment of tumors is the combination of photodynamic therapy (PDT) using a photosensitizer, coupled with the technique of optical clearing (OC) of biotissues. A photosensitizer delivered to the tumor helps to provide locally photosensitivity of the tumor, as the use of an optical clearing agent (OCA) reduces the damage of healthy tissues located on the path of laser beam and increases light penetration to deep tumors. The mechanism of OCA action is to match the refractive indices of the tissue structural components and interstitial fluid to reduce tissue scattering.

The aim of the study was to investigate diffuse reflectance spectra changes in the healthy skin *in vivo* under action of OC and tumor region after the PDT with and without OC in rats with transplanted cholangiocarcinoma of the PC-1 line.

Diffuse reflectance spectra were measured using fiber-optical spectrometers in the spectral range of 400-2100 nm. The measured skin reflection spectra were used to determine the effective optical density of the skin.

The values of the characteristic diffusion time, effective diffusion coefficient and effective skin permeability coefficient of volunteers *in vivo* for 70% glycerol solution as an OCA were obtained.

For PDT, Photosens solution in saline with a concentration of 2 mg/ml was used as a photosensitizer. A mixture of 70% glycerol, 5% DMSO, 25% water was used as the OCA.

When the tumor volume reached 3 ± 0.3 cm^3, the rats were intratumorally injected with Photosens solution at a dose of 0.4 ± 0.05 ml. Then rats were divided into two groups. The rats in the first group (PDT group) were exposed to PDT only: 10-30 min after Photosens injection, the tumors were irradiated percutaneously with a 662 nm laser at a power density of 0.5 W/cm^2 for 15 min. The rats in the second group (PDT+OC group) were exposed to OC before the same PDT exposition: OCA was applied to the surface of the skin over the tumor and treated with a therapeutic sonophoresis device for 5 min with the following parameters: 1.2 W, 1 MHz, and 50% duty cycle. Sonophoresis was used as an enhancer of the OCA diffusion into the skin. The temperature of local heating of the tumor was monitored using a thermal imager. During the procedures, the temperature on the surface of the skin above the tumor did not exceed 40°C. Diffuse reflectance spectra were measured at different stages of the experiment and analyzed.

An innovative approach to phototherapy of model cancer in rats: skin optical clearing and combined PDT/PTT

E.A. Genina[1,2*], **V.D. Genin**[1,2], **A.B. Bucharskaya**[3], **N.A. Navolokin**[3], **D.A. Mudrak**[3], **G.N. Maslyakova**[3], **B.N. Khlebtsov**[4], **N.G. Khlebtsov**[4], **V. Tuchin**[1,2,5]

1- Institution of Physics, Saratov State University, 83, Astrakhanskaya St., Saratov, 410012 Russia
2- Laboratory of Laser Molecular Imaging and Machine Learning, National Research Tomsk State University, 36, Lenin Ave., Tomsk, 634050 Russia
3- Department of Faculty Surgery and Oncology, Saratov State Medical University, 112, Bolshaya Kazachya St., Saratov, 410012 Russia
4- Institute of Biochemistry and Physiology of Plants and Microorganisms of the Russian Academy of Sciences, FRC "Saratov Science Center of the RAS", 13, Entuziastov Ave., Saratov, 410049 Russia
5- Institute of Precision Mechanics and Control, FRC "Saratov Scientific Centre of the RAS", 24, Rabochaya St., Saratov, 410028 Russia

* eagenina@yandex.ru

In this study Wistar rats with transplanted cholangiocarcinoma PC-1 were used. For photodynamic therapy (PDT), photosensityzers indocyanine green (ICG-PDT) or Photosence® (PS-PDT) were chosen. A solution of ICG in polyethylene glycol (MW=300 Da) had a maximum absorption wavelength of about 790 nm; and PS dissolved in saline had a maximum absorption wavelength of about 670 nm. Gold nanorods (GNRs) with an aspect ratio of 4:1 were used for photothermal therapy (PTT). A plasmon resonance of GNRs was observed in the spectral range of 800-820 nm. All components were injected intratumorally. For ICG-PDT/PTT and PS-PDT, laser irradiation was used for 15 min with a wavelength of 808 nm at a power density of 2.3 W/cm^2 or with a wavelength of 660 nm at a power density of ~0.5 W/cm^2, respectively. Optical clearing agent (aqueous solution of 70% glycerol and 5% DMSO) was applied topically to the skin above the tumor before the therapy. Skin heating was monitored using an IR visualizer. Diffuse reflectance spectra were registered before and after the procedures in the spectral range of 400-900 nm.

The withdrawal of animals and sampling of tumor tissues for histological examination was performed 72 hours after combination therapy. Morphological studies of tumor tissue were performed on tumor sections stained by standard methods and with immunohistochemical staining for the proliferation marker Ki-67 and the apoptosis marker Bax.
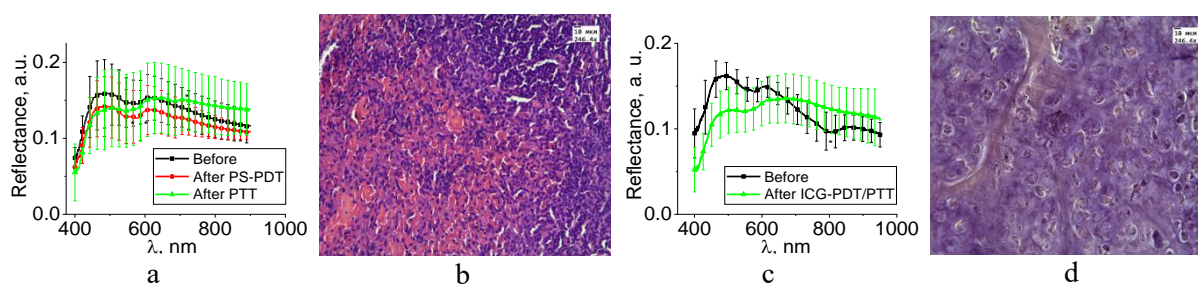
Fig. 1. Diffuse reflectance spectra of the surface of rat skin above the tumor before and after laser exposure and the morphological picture of cholangiocarcinoma 72 hours after combined exposure to PS-PDT/PTT a), b) and ICG-PDT/PTT c), d), respectively. Magnification of histological images is 246.4.

A significant rise in tumor heating temperature, up to 60±4.1º C, was observed during combined PDT/PTT. Heating caused significant changes in the spectral range of hemoglobin absorption (Fig. 1). After 72 hours, pronounced damage to tumor tissue was noted in rats. In a morphological study after PDT therapy, necrosis fields occupied from 30 to 50% of the section area; with single PTT and combined PDT/PTT, necrosis occupied up to 80% of the tumor section area. Intact tumor cells were observed only at the periphery of the tumor. An immunohistochemical study revealed a significant decrease in the expression of the proliferation marker Ki-67 and an increase in the expression of the apoptosis marker Bax in intact tumor cells.

Where does photonics meet acoustics and nanostructured materials for biomedical applications?

D.A. Gorin

Skolkovo Institute of Science and Technology, Moscow, Russia

d.gorin@skoltech.ru

This report will review the combination of photonic and acoustic tools and nano- and microstructured materials that can be used for visualization of pathological tissue and organs, navigation of drug delivery carriers and remote-controlled release of encapsulated bioactive substances, and last but not least, the application of optical sensors for early diagnosis and evaluation treatment efficiency. There are many biological objects that can be used as markers of various pathological states including cancer. These comprise, but are not limited to, proteins, exosomes, and circulation tumor cells. Exosomes are a very promising marker for early cancer diagnosis and even for evaluating treatment efficiency. An exosome is a small vesical at 100 nm size produced by a cell. The exosomes can be sent by both normal and pathological cells. It can be used for early diagnosis of neuro, cardio, and onco-diseases. The combination of a photonic integrated circuits (PIC), a microfluidic devices (MF) and a surface modification improves not only the sensitivity but also the specificity of exosomes' detection [1].

The application of photonic and acoustic tools can be used for visualization, navigation of multifunctional carriers and remote-controlled release of bioactive substances. These particles will combine the ability to deploy drugs in a controllable manner with physical triggering, multimodal detection, and visualization as well as sensing of important biological markers. It is required to apply a new bottom-up method as layer by layer assembly [2] and freezing induced loading [3] and their combination [4]. It can be allowed us to vary the volume fraction of components and their chemical composition led to the control of the optical and thermal properties of multifunctional carriers [5]. Raman spectroscopy is perspective method for *in situ* monitoring of freezing induced loading method [6]. Physical targeting of carriers was realized by the magnetic field gradient [4], optical tweezers approach [7]. Acoustics has a good perspective for the same purpose. The carrier sensitivity to external influences such as laser irradiation, ultrasound (US) treatment can be changed by variation of volume fraction and chemical composition of inorganic nanoparticles and/or organic dyes in the carrier shells. The same approach is applied for drug delivery carriers imaging by MRI, fluorescence imaging (FI), USI and optoacoustics (OA) [4,8]. Additionally, there are some trends of modern biophotonics: 1) combination of OA, US and FI [9]; 2) transfer to mid-IR [10]; 3) preparation of multimodal contrast agents, that can be provided the contrast by some clinical methods including OA, FI, MRI, USI etc. [8]; 4) using minimally invasive OA [11,12] by developing PIC based US transducers [13] using biomimetic approach for preparation a sensitive part (membrane) of such type of sensors [14,15]; 5) using optical clearing approach [16]. In lecture will be presented also the results of *in vivo* optoacoustic applications and besides both optoacoustic mesoscopy and tomography. Particular attention will be devoted to the implementation of near and mid-IR for OA microscopy and endoscopy and the prospects for its application for *in vitro* and *in vivo* studies, for example, for the analysis of histological sections, as well as for determining the type of atherosclerotic plaques, respectively. Thus, the combination of photonic and acoustic tools with nanostructured materials has a good perspective for application in biology and medicine.

[1] A. Kuzin, et al, Applied Physics Letters, 2023, 123, 193702.
[2] M.V. Novoselova, et al, J. Biophotonics, 12 (4), 2019, e201800265.
[3] S.V. German, et al, Scientific Reports, 8, 2018, 17763.
[4] M.V. Novoselova, et al, Colloids and Surfaces B, 2021, 111576.
[5] R. E. Noskov, et al, Adv. Mater. 2021, 2008484.
[6] S.V. German, et al, Langmuir, 2021, 37,4, 1365.
[7] E.S. Vavaev, et al, ACS Applied Nano Materials, 2022 5 (2), 2994-3006.
[8] E.A. Maksimova, et al, Laser & Photonics Reviews, 2023, 2300137.
[9] M.D. Mokrousov, et al, Biomedical Optics Express, 12(6), 2021, 3181.
[10] M.A. Pleitez, et al, Nat. Biotechnol., 38(3), 2020, 293.
[11] H. Guo, et al, J. Biophotonics, 13(12), 2020, 1–20.
[12] N. Kaydanov, et al, ACS Photonics, 8, 11, 2021, 3346–3356.
[13] W.J. Westerveld, et al, Nature Photonics, 15, 202, 341.
[14] J. Cvjetinovic, et al, Scientific Reports, 13, 2023, 5518.
[15] J. Cvjetinovic, et al, Applied Physics Letters, 2023, 123 (18), 184101.
[16] M.V. Novoselova, et al, Photoacoustics, 2020, 100186.

Recognition of malignant cutaneous melanoma by multimodal analysis of optical biopsy data

I. Matveeva[1]

1- Samara National Research University, Moskovskoye shosse 34, Samara, 443086, Russia

m-irene-a@yandex.ru

The International Agency for Research on Cancer (IARC) estimates that approximately 325,000 new cases of malignant melanoma (MM) were diagnosed worldwide in 2020 and 57,000 people died from the disease. Moreover, researchers predict that the number of new cases of MM per year will increase by more than 50% from 2020 to 2040 [1]. Externally, MM may be similar to a pigmented nevus (PN). Therefore, the quality of diagnosing MM by visual examination largely depends on the level of qualifications and professional experience of the doctor and is 40-80% accurate [2]. The most complete clinical picture is provided by taking a biopsy, which involves taking a sample of the neoplasm and its further histological examination by a specialist pathologist [3]. Due to the "aggressive" behavior and high risks of metastasis due to external influence, such a procedure is usually not used [4]. Optical methods are recognized as promising tools for studying skin tissue. Such methods include dermatoscopy [5], Raman spectroscopy [6,7], hyperspectral imaging [8], etc. However, at the moment, optical biopsy methods do not exceed the accuracy of the "gold standard" of diagnosis, that is, histological examination. One of the ways to overcome the limited accuracy values is the combined use of several optical methods [9]. The previous research showed an increase in the classification accuracy of MM and PN by joint analysis of Raman spectra and dermoscopic images [5]. The aim of this research is to develop a method for identifying MM based on multimodal joint analysis of Raman scattering data, dermatoscopic images, and hyperspectral images. An *in vivo* study of skin neoplasms was carried out at the Samara Regional Clinical Oncology Center. Experimental skin Raman spectra were recorded using a portable setup that includes a laser source with a central wavelength of 785 nm. The spectra were recorded with a spectral resolution of 0.2 nm in the range from 837 to 920 nm, which corresponds to 792-1874 cm^{-1} [6]. Dermatoscopic images of skin neoplasms were obtained using a digital dermatoscope [5]. To record hyperspectral images, an acoustooptical hyperspectral camera was used, which makes it possible to obtain an image of the area under study at an arbitrarily set wavelength in the range of 440-750 nm with a spectral resolution of 2.5 nm and the spatial resolution of 0.14 mm [8]. Machine learning methods, in particular, logistic regression and convolutional neural networks, were used for analysis of the registered data. The classification model for MM and PN has shown an increase in accuracy compared to the analysis of Raman spectra, dermatoscopic images, or hyperspectral images alone. As a result, a comprehensive multimodal approach for the detection of MM, which takes into account both specific spectral characteristics of neoplasms and spatial inhomogeneities in the distribution of optical density, has been proposed. The studied approaches to the analysis of optical biopsy data can potentially be integrated into the software for automated screening diagnostics of skin.

[1] J. Ferlay, M. Colombet, I. Soerjomataram, D.M. Parkin, M. Piñeros, A. Znaor, F. Bray, Cancer statistics for the year 2020: An overview, International journal of cancer, vol. 149(4), pp. 778-789, 2021.

[2] H.A. Haenssle, C. Fink, R. Schneiderbauer, F. Toberer, T. Buhl, A. Blum, A. Kalloo, A.B.H. Hassen, L. Thomas, A. Enk, L. Uhlmann, Man against machine: diagnostic performance of a deep learning convolutional neural network for dermoscopic melanoma recognition in comparison to 58 dermatologists, Annals of oncology, vol. 29(8), pp. 1836-1842, 2018.

[3] G.V. Long, S.M. Swetter, A.M. Menzies, J.E. Gershenwald, R.A. Scolyer, Cutaneous melanoma, The Lancet, vol. 402(10400), pp. 485-502, 2023.

[4] R.J. Friedman, D.S. Rigel, A.W. Kopf, Early detection of malignant melanoma: the role of physician examination and self-examination of the skin., CA: a cancer journal for clinicians, vol. 35(3), pp. 130-151, 1985.

[5] I.A. Matveeva, A.I. Komlev, O.I. Kaganov, A.A. Moryatov, V.P. Zakharov, Multidimensional Analysis of Dermoscopic Images and Spectral Information for the Diagnosis of Skin Tumors, Journal of Biomedical Photonics & Engineering, vol. 10(1), pp. 010307, 2024.

[6] I.A. Bratchenko, L.A. Bratchenko, A.A. Moryatov, Y.A. Khristoforova, D.N. Artemyev, O.O. Myakinin, A.E. Orlov, S.V. Kozlov, V.P. Zakharov, In vivo diagnosis of skin cancer with a portable Raman spectroscopic device, Experimental Dermatology, vol. 30(5), pp. 652-663, 2021.

[7] I. Matveeva, I. Bratchenko, Y. Khristoforova, L. Bratchenko, A. Moryatov, S. Kozlov, O. Kaganov, V. Zakharov, Multivariate curve resolution alternating least squares analysis of in vivo skin Raman spectra, Sensors, vol. 22(24), pp. 9588, 2022.

[8] B.V. Grechkin, V.O. Vinokurov, Y.A. Khristoforova, I.A. Matveeva, VGG convolutional neural network classification of hyperspectral images of skin neoplasms, Journal of Biomedical Photonics & Engineering, vol. 9(4), pp. 040304, 2023.

[9] L. Rey-Barroso, S. Peña-Gutiérrez, C. Yáñez, F.J. Burgos-Fernández, M. Vilaseca, S. Royo, Optical technologies for the improvement of skin cancer diagnosis: a review, Sensors, vol. 21(1), pp. 252, 2021.

Photothermal and dissolution properties of germanium nanoparticles for biomedical applications

A. Kanavin[1,2*], **A. Fronya**[1,2], **D. Donchenko**[2], **E. Mavreshko**[1,2], **I. Tupitsyn**[1], **M. Grigoryeva**[1,2], **I. Zavestovskaya**[1,3]

1- P.N. Lebedev Physical Institute of the Russian Academy of Sciences, 53 Leninskiy Prospekt, Moscow 199991, Russian Federation
2- National Research Nuclear University MEPhI (Moscow Engineering Physics Institute), 31 Kashirskoe shosse, Moscow 115409, Russian Federation
3- National Research Center "Kurchatov Institute", 1 Academician Kurchatov Square, Moscow 123182, Russian Federation

* kanavinap@lebedev.ru

Currently, medicine is actively developing the direction of creating biodegradable nano-sized devices that can act inside the human body as temporary diagnostic and therapeutic platforms [1]. For this purpose, biodegradable materials are being sought. From the point of view of medical applications, it is essential to be able to control the time and rate of dissolution of the material in order to ensure maximum diagnostic and therapeutic effect. One of candidate for such application is the semiconductor element germanium [1,2].

In the presented work, experiments were carried out on the synthesis of germanium nanoparticles and the study of the dynamics of dissolution of such particles in liquids. Germanium nanoparticles were synthesized by nanosecond laser ablation of single-crystalline germanium target in a liquid. The distilled water and isopropanol were used as liquid for ablation. Over the course of a month the dissolution of germanium nanoparticles in liquids was studied. The results showed that germanium nanoparticles are completely soluble in distilled water. And it happens within the first day after synthesis.

Also, the experiment on heating a solution of germanium nanoparticles with laser radiation at a wavelength of 937-938 nm was carried out. Experiments have shown that the addition of germanium nanoparticles allows one to increase the maximum heating temperature. Experimental data made it possible to estimate the dynamics of heating and cooling of the nanoparticle solution. Heating of a germanium nanoparticles solution by 11°C and 14°C, with a laser radiation power of 1.81 W and 2.52 W, respectively, was demonstrated. The heating time for the solution was 10 minutes, on average.

[1] R. Li, L. Wang, L. Yin, Materials and Devices for Biodegradable and Soft Biomedical Electronics. Materials 2018, 11, 2108.
[2] A.S. Almuslem, A.N. Hanna, T. Yapici, N. Wehbe, E.M. Diallo, A.T. Kutbee, R.R. Bahabry, M.M. Hussain, Water soluble nano-scale transient material germanium oxide for zero toxic waste based environmentally benign nano-manufacturing, Appl. Phys. Lett. 2017; 110 (7): 074103.

Erythrocyte-ghost integrated gold nanostars for synergistic therapy in hypoxic tumors

A.V. Karmenyan[1*], W.G. Pearl[1], R. Selvam[1], H.Y. Lee[2], T.E. Hsu[1], E.V. Perevedentseva[3], H.H. Chang[2], S.Y. Wu[1], C.L. Cheng[1]

1- Department of Physics, National Dong Hwa University, Hualien 97401, Taiwan
2- Department of Molecular Biology and Human Genetics, Tzu-Chi University, Hualien 97004, Taiwan
3- P.N. Lebedev Physics Institute of Russian Academy of Sciences, Moscow, 119991, Russia

* artashes@gms.ndhu.edu.tw

Modern lasers provide wide variety of radiation parameters. This makes it possible to select conditions for their multifunctional use for diagnostics and combined treatment. In the present work gold nanostars (AuNSt) are tested as promising agents for dual photo-based therapies, combining photodynamic therapy (PDT) and photothermal therapy (PTT) to tackle a cancer. In cases where tumors exhibit low oxygen levels, making them resistant to conventional therapies, PDT utilizes light to generate reactive oxygen species (ROS), inducing oxidative damage to cancer cells, while PTT leverages light to produce heat, destroying the tumor microenvironment. In this study, AuNSt with a plasmon absorption peak at 800 nm were synthesized [1] and loaded onto erythrocyte ghosts. Containing residual hemoglobin erythrocyte ghosts were utilized as oxygen supplements and carriers to overcome the hypoxic environment of tumors. The AuNSt facilitated enhanced ROS production and exhibited photothermal conversion efficiency under near-infrared (NIR) irradiation. Application of AuNSt@Ghost in various cell lines under normoxic and hypoxic conditions, exposed to NIR irradiation, demonstrated a significant synergistic antitumor effect. This biomimetic approach shows promise in theranostics, offering a viable strategy for treating cancers with improved efficacy and reduced systemic toxicity.
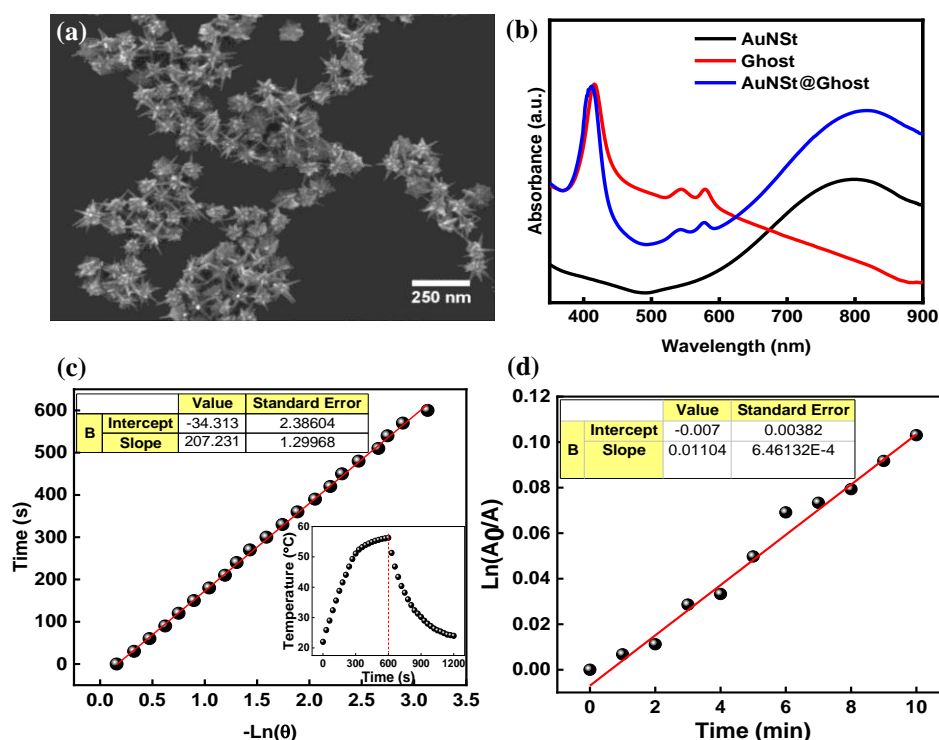
Fig. 1. (a) SEM image of AuNSt; (b) UV-Vis absorption spectra of AuNSt, Ghost, and AuNSt@Ghost; (c) Linear-time data showing the negative natural logarithm of the temperature driving force obtained during the cooling stage of AuNSt. Inset: Heating-cooling cycle of AuNSt solution; and (d) The rate constant for the AuNSt sample, measured by 2'7'-dichlorofluorescein absorbance changes at 410 nm caused by ROS generated from AuNSt under 808 nm laser irradiation.

[1] W.G. Pearl, E.V. Perevedentseva, A.V. Karmenyan, V.A. Khanadeev, S.Y. Wu, Y.R. Ma, N.G. Khlebtsov, C.L. Cheng, Multifunctional plasmonic gold nanostars for cancer diagnostic and therapeutic applications, J Biophotonics, e202100264 (2021).

Application of laser-synthesized boron nanoparticles for boron neutron capture therapy

A. Kasatova[1,2*], K. Kuzmina[2], I. Zelepukin[3], K. Aiyyzhy[4], E. Barmina[1,4], A. Popov[5], I. Razumov[6],
E. Zavjalov[6], M. Grigoryeva[1], S. Klimentov[1,5], V. Ryabov[1], S. Deyev[3,5], A. Kabashin[7],
S. Taskaev[1,2], I. Zavestovskaya[1,8]

1- P.N. Lebedev Physical Institute of the Russian Academy of Sciences, Moscow 119991, Russia
2- Budker Institute of Nuclear Physics of the Siberian Branch of the Russian Academy of Sciences, Novosibirsk 630090, Russia
3- Shemyakin-Ovchinnikov Institute of Bioorganic Chemistry of the Russian Academy of Sciences, Moscow 117997, Russia
4- A.M. Prokhorov General Physics Institute of the Russian Academy of Sciences, Moscow 119991, Russia
5- National Research Nuclear University MEPhI, Moscow 115409, Russia
6- Institute of Cytology and Genetics of the Siberian Branch of the Russian Academy of Sciences, Novosibirsk 630090, Russia
7- Aix-Marseille University, CNRS, LP3, Marseille13288, France
8- National Research Center "Kurchatov Institute", 1 Academician Kurchatov Square, Moscow 123182, Russia

* a.i.kasatova@inp.nsk.su

Boron neutron capture therapy (BNCT) is a binary form of radiation therapy based on the selective destruction of cells of malignant tumors. The basic principle of BNCT is in the high ability of the non-radioactive ^{10}B nucleus to absorb a thermal neutron, resulting in the reaction $^{10}B(n,\alpha)^7Li$, the products of which have a high deceleration rate and a short path length, thus the released energy of 2.79 MeV is limited by the size of one cell [1].

An important aspect of the successful implementation of BNCT in clinical practice is the development of targeted boron delivery drugs [2]. We investigated elemental boron nanoparticles (BNPs) fabricated using the methods of pulsed laser ablation in liquids as potential boron-containing agents for BNCT. Depending on the conditions (nanosecond and femtosecond pulses) of laser-ablative synthesis, the NPs were amorphous (a-BNPs) or partially crystallized (pc-BNPs) with a mean size of 20 nm or 50 nm, respectively, both coated with polyethylene glycol to improve their colloidal stability [3,4].

In *in vitro* experiments human tumor cell lines U87 (glioblastoma) and SW-620 (colorectal adenocarcinoma) were used. MTT-test and clonogenic assay did not show any cytotoxicity effects of BNPs up to ^{10}B concentrations of 100 μg/mL. The cells were preliminarily incubated with BNPs at a ^{10}B concentration of 40 μg/mL and were then irradiated with a thermal neutron beam at the accelerator-based neutron source at the Budker Institute of Nuclear Physics [5] for 30 min, providing the equivalent calculated dose of 8 Gy-Eq. Colony forming capacity of SW-620 cells dropped down to 12.6% for BNCT group previously incubated with a-BNPs and 1.6% for pc-BNPs BNCT group. Colony-forming capacity for U87 cells dropped down to 17%. The data is confirmed by MTT results.

For future BNCT *in vivo*, the boron biodistribution study was performed. Intratumoral administration of BNPs in immunodeficient SCID mice with subcutaneous U87 tumors demonstrated highest accumulation of boron in the tumor of 56 μg/g and 82 μg/g at 30 and 90 min after BNPs administration, respectively. The concentration of boron in the blood and in the surrounding normal tissue (skin and muscle) was statistically significantly lower, close to background values. Therefore, laser ablation of elemental boron powders and targets leads to the formation of spherical nanoparticles with a size of 20-50 nm. This technique provides the achieved boron content in the tumor, and the tumor/blood, tumor/ normal tissue boron concentration ratios is sufficient for successful BNCT in the case of boron enrichment with the therapeutically suitable isotope boron-10.

[1] M.A. Dymova, S.Y. Taskaev, V.A. Richter, E.V. Kuligina, Boron neutron capture therapy: Current status and future perspectives, Cancer Commun., vol. 40, pp. 406–421, 2020.
[2] R.F. Barth, P. Mi, W. Yang, Boron delivery agents for neutron capture therapy of cancer, Cancer Commun., vol. 38, pp. 35, 2018.
[3] A. Kabashin, P. Delaporte, A. Pereira, D. Grojo, R. Torres, T. Sarnet, M. Sentis, Nanofabrication with pulsed lasers, Nanoscale Res. Lett., vol. 5, pp. 454–463, 2010.
[4] K.O. Aiyyzhy, E.V. Barmina, V.V. Voronov, G.A. Shafeev, G.G. Novikov, O.V. Uvarov, Laser ablation and fragmentation of Boron in liquids, Opt. Laser Technol., vol. 155, 2022.
[5] S. Taskaev, E. Berendeev, M. Bikchurina, T. Bykov, D. Kasatov, I. Kolesnikov, A. Koshkarev, A. Makarov, G. Ostreinov, V. Porosev, S. Savinov, I. Shchudlo, E. Sokolova, I. Sorokin, T. Sycheva, G. Verkhovod, Neutron Source Based on Vacuum Insulated Tandem Accelerator and Lithium Target, Biology, vol. 10, 350, 2021.

Gold and graphene oxide coated tilted fiber Bragg grating biosensor design for clinical decisions

P.B. Prathap[1], K. Saara[2*]

1- Department of Electronics and Communication Engineering, Malnad College of Engineering, Hassan-573202
2- Department of Electronics and Communication Engineering, School of Engineering, Dayananda Sagar University, Bangalore-560114

* saara-ece@dsu.edu.in, saarakhamar@gmail.com

Abstract: Fiber Bragg Grating (FBG) sensors excel in clinical decision-making due to their superior sensitivity and resolution. This study proposes a gold and graphene oxide-coated Tilted FBG (TFBG) biosensor with a grating angle of 9 degrees. The gold coating enhances reflectivity and sensitivity, while the graphene oxide (GO) coating improves plasmonic attraction and antibody/antigen absorption. The GO coating increases the refractive index, causing significant spectral shifts for biosensing. Simulated results demonstrate the sensor's potential for protein analysis and immunological assessments, supporting accurate therapeutic decisions.

I. INTRODUCTION

The growing worldwide population and pressure on healthcare infrastructures and human expertise have prompted business to automate and improve diagnosis and pharmaceutical solutions. Hardware advancements, especially sensor technology, have made diagnostics faster and more scalable. Rising health issues require more accurate and reliable sensors for early detection and diagnosis. This can minimize mortality and prevent complications if discovered and treated early. Highly sensitive sensors are needed for biomechanical, physiological, non-invasive surgery, and biosensing [1-3].

II. RESULTS AND DISCUSSION

Performance characterization is based on wavelength shift in response to changes in the surrounding refractive index to assess biosensor resilience. Increasing target molecule absorption on the coating surface raises the density and refractive index (η_3), causing coupling wavelength shifts and amplitude reductions. The proposed biosensor design was evaluated for wavelength shift, transmission power vs. wavelength (λ), and zero-crossing point shift.

Simulated spectral outputs for different surrounding indices (η_3=1.50 and 1.56) show increased density and refractive index on the coating surface. Results indicate that an exceedingly high refractive index saturates the transmission spectra (dB), with spectral output at η=1.50 resembling that at η=1.6. High saturation or density due to excessive molecular absorption at the cladding mode or coating surface can result in zero internal reflection, making the fiber core act as a normal dielectric hollow cylinder. Additional simulations for surrounding indices (η_3=1.45, η_3=1.50, η_3=1.56, η_3=1.60, and η_3=1.65) are shown in Fig. 1 (a-c).
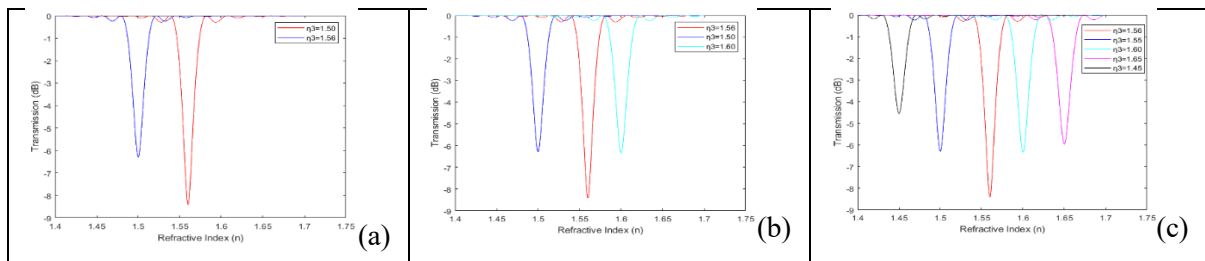
Fig. 1. (a-c) Transmission spectrum with different refractive indices.

[1] A.G. Leal-Junior, C.A.R. Diaz, L.M. Avellar, M.J. Pontes, C. Marques, A. Frizera, Polymer optical Fiber sensors in healthcare applications: A comprehensive review, Sensors, 19(14), 3156, (2019).
[2] S. Korganbayev, M. De Landro, A. Wolf, D. Tosi, P. Saccomandi, Tilted Fiber Bragg Grating Measurements during Laser Ablation of Hepatic Tissues: Quasi-Distributed Temperature Reconstruction and Cladding Mode Resonances Analysis, in IEEE Sensors Journal, 22(16), 15999-16007, (2022).
[3] D. Lo Presti, et al, Fiber Bragg Gratings for Medical Applications and Future Challenges: A Review, in IEEE Access, 8, 156863-156888, (2020).

Recent advances in dual-wavelength fluorescence imaging with chlorin-based photosensitizers

A. Khilov[1*], D. Kurakina[1], A. Malygina[2], E. Sergeeva[1], A. Mironycheva[1,2], V. Perekatova[1], I. Shlivko[2], S. Gamayunov[1,3], I. Turchin[1], M. Kirillin[1]

1- A.V. Gaponov-Grekhov Institute of Applied Physics of the Russian Academy of Sciences, 46 Ul'yanov Street, Nizhny Novgorod, 603950, Russia
2- Privolzhsky Research Medical University, 10/1 Minin and Pozharsky Sq., Nizhny Novgorod, 603005, Russia
3- Nizhny Novgorod Regional Oncological Hospital, Delovaya 11/1, Nizhny Novgorod, 603126, Russia

* alhil@inbox.ru

Photodynamic therapy (PDT) is a modern rapidly developing treatment technique based on photoactivation of a photosensitizer (PS), which is accumulated primarily in abnormal cells after its administration prior to the procedure. Photodynamic reaction is launched by consecutive therapeutic light exposure, which produces singlet oxygen inducing abnormal cells death. This treatment technique has shown its efficiency against a number of tumor and non-tumor pathologies [1]. Moreover, PDT efficiency can be enhanced by its repetition or combination with other treatment modalities or corrections in PDT regimen, which includes variations of delivered light dose and PS concentration, thus implementing the trending principles of personalized medicine. A number of imaging techniques are reported for non-invasive monitoring of PDT, while the most promising tools for real-time PDT control are optical imaging methods.

Since most of PSs possess fluorescence properties, it is reasonable to merge therapy and fluorescence diagnostics, thus implementing theranostics principles. Fluorescence imaging (FI) allows for normal/pathology differentiation and imaging-guided surgery [2] as well as for the assessment of PDT efficiency upon decrease in PS fluorescence, known as PS photobleaching [3].

The employment of PS with two or more peaks in absorption spectrum (chlorin e6, PPIX and others) allows for the choice of PDT regimen [4] and, consequently, of therapeutic impact depth. Dual-wavelength fluorophore excitation also allows for the estimation of fluorophore localization based on ratiometric approach [5,6]. Ratiometric approach requires a priori knowledge of optical properties of surrounding tissues, thus, dual-wavelength FI combined with diffuse reflectance spectroscopy, which allows for non-invasive estimation of optical properties based on registered diffuse reflectance spectrum, may further enhance the efficiency of reported technique.

We present the results of *in vivo* dual-wavelength FI of actinic keratosis and basal cell carcinoma PDT procedures with chlorin-based PS performed in clinical environment. It is shown that dual-wavelength ratiometric FI not only provides with the estimations of therapeutic impact depth, but also reveals prognostic factors for long-term prognosis of target tissue response to PDT.

[1] J.P. Celli, B.Q. Spring, I. Rizvi, C.L. Evans, K.S. Samkoe, S. Verma, B.W. Pogue, T. Hasan, Imaging and photodynamic therapy: mechanisms, monitoring, and optimization, Chemical reviews 110, 2795-2838 (2010).
[2] J. He, L. Yang, W. Yi, W. Fan, Y. Wen, X. Miao, L. Xiong, Combination of fluorescence-guided surgery with photodynamic therapy for the treatment of cancer, Molecular imaging 16, 1536012117722911 (2017).
[3] A. Johansson, F. Faber, G. Kniebühler, H. Stepp, R. Sroka, R. Egensperger, W. Beyer, F.W. Kreth, Protoporphyrin IX fluorescence and photobleaching during interstitial photodynamic therapy of malignant gliomas for early treatment prognosis, Lasers in surgery and medicine 45, 225-234 (2013).
[4] M. Kirillin, D. Kurakina, A. Khilov, A. Orlova, M. Shakhova, N. Orlinskaya, E. Sergeeva, Red and blue light in antitumor photodynamic therapy with chlorin-based photosensitizers: a comparative animal study assisted by optical imaging modalities, Biomedical Optics Express 12, 872-892 (2021).
[5] A.V. Khilov, E.A. Sergeeva, D. Kurakina, I.V. Turchin, M.Y. Kirillin, Analytical model of fluorescence intensity for the estimation of fluorophore localisation in biotissue with dual-wavelength fluorescence imaging, Quantum Electronics 51, 95 (2021).
[6] M. Kirillin, A. Khilov, D. Kurakina, A. Orlova, V. Perekatova, V. Shishkova, A. Malygina, A. Mironycheva, I. Shlivko, S. Gamayunov, Dual-Wavelength Fluorescence Monitoring of Photodynamic Therapy: From Analytical Models to Clinical Studies, Cancers 13, 5807 (2021).

Novel analytical and numerical models for spectral and fluorescence optical modalities

M.Yu. Kirillin[1*], D.A. Kurakina[1], A.A. Getmanskaya[1,2], A.V. Khilov[1],
V.V. Perekatova[1], V.A. Shishkova[1], M.G. Kalashnikov[1,2], I.V. Turchin[1], E.A. Sergeeva[1]

1- A.V. Gaponov-Grekhov Institute of Applied Physics RAS, Nizhny Novgorod, Russia
2- N.I. Lobachevsky State University of Nizhny Novgorod, Nizhny Novgorod, Russia

* kirillin@ipfran.ru

Improvement of modern optical biomedical diagnostic modalities require development of novel refined models of light transport in biotissues. Among modalities aimed functional diagnostics, spectral and fluorescence optical modalities could be distinguished. Spectral modalities provide high sensitivity to variations in concentrations of different chromophores owing to their unique shapes of absorption spectra [1,2], while fluorescence modalities exhibit high sensitivity to the presence of particular fluorophores featuring unique excitation and emission spectra [3]. Moreover, spectral approach could be extended to fluorescence techniques to obtain additional information, for example, about fluorophore localization [3].

The choice of a model for light transport in biotissue is governed by two basic factors: accuracy of the model and calculation speed that determines the time requires to get the desired solution using the chosen model. The last aspect plays a crucial role in the recent decade, when the machine learning approaches became widely employed, and the construction of a training set could require considerable time. Traditionally, analytical models were implemented into reconstruction algorithms of optical diagnostics modalities owing to their speed. However, this speed comes at the expense of accuracy, since the radiative transfer equation in general form has no general analytic solution, while different approximation has limited applicability. Modern development in computational technologies resulted in active employment of numerical models of light transport that have higher versatility as compared to analytical approaches. Numerical approaches usually include finite-difference solutions of light transport equation or Monte Carlo technique [1].

In this paper application of different analytical models and Monte Carlo technique for forward and inverse problems in diffuse optical spectroscopy (DOS) and fluorescence imaging (FI) are reviewed. In DOS studies the novel refined analytical model [4] is compared to the results of Monte Carlo simulations providing the estimations of the range of parameters where analytical model could be employed without loss in accuracy, while for other sets of parameters Monte-Carlo generated look-up tables could be generated.

In FI models of light transport in biological tissues could help in quantification of the location of a fluorescing object within biotissue. The most of the drugs for photodynamic therapy exhibit fluorescence, which make fluorescence imaging a convenient tool for procedure monitoring. Moreover, other drug that are delivered through intravenous injection could be monitored using FI, if drug and fluorescent marker are combined in a nanoconstruct [5]. In this paper the results of Monte Carlo simulations of signal formation in dual-wavelength FI are reported together with simulations of FI in complex and anatomical geometries. The models for FI are based on a dual-step approach consisting in simulating of absorption map of exciting radiation followed by simulation of fluorescence emission propagation, while the distributed fluorescence source is built based on the simulated excitation absorption map.

[1] D. Kurakina, V. Perekatova, E. Sergeeva, A. Kostyuk, I. Turchin, M. Kirillin, Probing depth in diffuse reflectance spectroscopy of biotissues: a Monte Carlo study, Laser Physics Letters, vol. 19, p. 035602 (2022).
[2] I. Turchin, et al, Multimodal optical monitoring of auto and allografts of skin on a burn wound, Biomedicines, vol. 11, p. 351 (2023).
[3] M. Kirillin, et al, Dual-wavelength fluorescence monitoring of photodynamic therapy: from analytical models to clinical studies, Cancers, 13(22), 5807 (2021).
[4] E. Sergeeva, D. Kurakina, I. Turchin, M. Kirillin, A refined analytical model for reconstruction problems in diffuse reflectance spectroscopy, Journal of Innovative Optical Health Sciences, 2342002 (2023).
[5] I. Turchin, et al, Combined Fluorescence and Optoacoustic Imaging for Monitoring Treatments against CT26 Tumors with Photoactivatable Liposomes, Cancers, 14 (1), 197 (2022).

IR and terahertz spectroscopy and machine learning for medical and ecological applications

Yu. Kistenev[*], **V. Prishepa, V. Skiba**[1]**, V. Nikolaev, G. Rasponin, D. Makashev, A. Borisov**

LMIML Laboratory, Tomsk State University, Tomsk, Russia

* yuk@iao.ru

IR and THz spectra are associated with "molecular fingerprints" because these spectral ranges contain useful information about vibration, rotation, intramolecular and intermolecular modes of large number of molecules [1]. This information allows conducting a sample qualitative and quantitative analysis. Terahertz time domain spectroscopy (THz-TDS) is based on measurement of electric field of transmitted through the sample femtosecond terahertz pulses 0,3]. THz-TDS has a spectral resolution of several GHz that is enough for solid or dried liquid samples analysis. THz high-resolution absorption spectroscopy has spectral resolution of several kHz that enough for gas mixture analysis. Symmetric molecules have no strong absorption lines in THz range, polar possess absorption in both spectral ranges. Therefore, spectral analysis of a sample by a THz spectrometer is complementary to IR spectrometry. But combination of THz and IR spectra means that data are presented in high dimension feature space. In this case, data are highly correlated. It makes inefficient data analysis using conventional methods like Multivariate Curve Resolution [4], Univariate Calibration 0. Machine learning methods are becoming the best tool to solve the discussed tasks.

Several applications of THz and IR spectroscopy combined with machine learning methods will be presented.

[1] O. Cherkasova, M. Konnikova, Yu. Kistenev, V. Vaks, J.-L. Coutaz, A. Shkurinov, Terahertz spectroscopy of biological molecules in solid, liquid, and gaseous states, In Molecular and Laser Spectroscopy; Gupta, V.P. Elsevier, Ch. 13, pp. 433-478 (2022) (Advances and Applications: V.3).

[2] M. Walther, et al, Collective vibrational modes in biological molecules investigated by terahertz time-domain spectroscopy, Biopolymers: Original Research on Biomolecules, V. 67 (4-5), 310-313 (2002).

[3] O. Smolyanskaya, N. Chernomyrdin, A. Konovko, K. Zaytsev, I. Ozheredov, O. Cherkasova, M. Nazarov, J.-P. Guillet, S. Kozlov, Y. Kistenev, et al, Terahertz biophotonics as a tool for studies of dielectric and spectral properties of biological tissues and liquids, Prog. Quantum Electron., 62, 1–77 (2018).

[4] A. de Juan and R. Tauler, Multivariate Curve Resolution: 50 years addressing the mixture analysis problem – A review, Analytica Chimica Acta, V. 1145, 59-78 (2021).

[5] P. Kościelniak and M. Wieczorek, Univariate analytical calibration methods and procedures. A review, Analytica Chimica Acta, V. 944, 14-28 (2016).

Development of the analysis of experimental data in laser diffractometry of erythrocytes

M.S. Lebedeva[1*], E.G. Tsybrov[2], S.Yu. Nikitin[1]

1- Faculty of Physics, Lomonosov Moscow State University, Moscow, Russia
2- Faculty of Computational Mathematics and Cybernetics, Lomonosov Moscow State University, Moscow, Russia

* 2mary.lebedeva@gmail.com

Laser diffractometry is known to be one of the methods of studying ensembles of red blood cells. The purpose of our work is to create a set of algorithms that would allow us to analyze real diffraction patterns with high accuracy and to obtain central moments of the distribution of red blood cells by size-shape and deformability. At present, a number of algorithms that take into account the degree of uniformity of the blood sample under study and the area of analysis of the diffraction pattern has been developed in our laboratory. The numerical experiment shows a high accuracy of such algorithms, however, in practice, the final result of the diffraction pattern analysis is influenced by many parameters, ranging from the method of preparing a suspension of cells to the resolution of the diffraction pattern registration system.

In this work we compare the experimental results obtained using the algorithms we developed with the results calculated directly by processing microscopic images of red blood cells to understand which of the parameters play a key role in the analysis. We selected the following parameters of cell ensembles for the analysis: the relative widths of the size distribution (RDWR) and deformability distribution (RDWD) of erythrocytes. These values are introduced by analogy with the RDW parameter of a standard blood test and they are dimensionless.

As an example, the result of processing experimental data for a blood sample from a healthy donor is shown below.
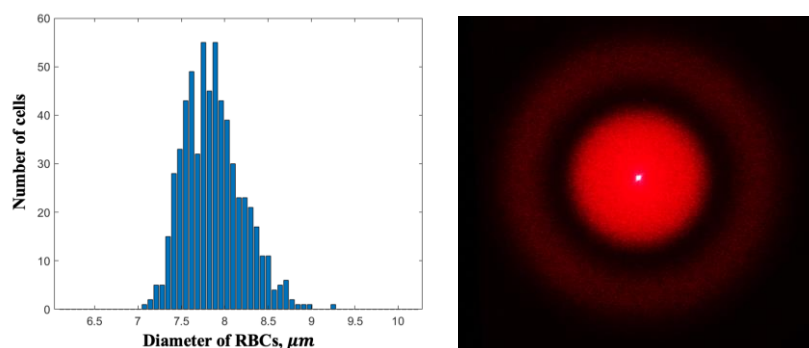
Fig.1. On the left there is a graph of red blood cells size distribution obtained by processing images of cells from a microscope. One of the diffraction patterns for this donor is shown on the right.

The calculated values of RDWR were 0.0428 and 0.0874 for microscopy and diffractometry, respectively. This can be explained by the fact that laser diffractometry takes into account a large number of variations in values than microscopic analysis. Currently, there is a reason to believe that RDWR value is 3-6% for a healthy donor.

At the moment, the key factors affecting the accuracy of the results obtained by laser diffractometry include the method of preparing a blood sample, the degree of uniformity of the studied ensemble of cells, the area of analysis of the diffraction pattern, the noise level and the resolution of the diffraction pattern registration system.

The main goals for our further work are to accumulate the experimental data on healthy donors and patients with socially significant diseases (for example, diabetes mellitus, cardiovascular diseases), to search for correlations between the parameters of the red blood cell ensemble and these diseases, as well as to continue the process of verification of data processing algorithms developed by us.

Effect of optical clearing agents on microcirculation studied *in vivo* with digital capillaroscopy and laser speckle contrast imaging

**A. Lugovtsov[1], P. Ermolinskiy[1], P. Moldon[1], D. Umerenkov[1], M. Maksimov[1],
P. Timoshina[2], P. Li[3], V. Tuchin[2], A. Priezzhev[1]**

1- Lomonosov Moscow State University, 1-2 Leninskiye Gory, Moscow, Russia, 119991
2- Chernyshevsky Saratov State University, 83 Astrakhanskaya str., Saratov, Russia, 410012
3- Huazhong University of Science and Technology, Luoyu Road, 1037, Wuhan, China

* anlug@biomedphotonics.ru

The optical clearing agents (OCA) are used to increase the depth of light penetration into the biological tissues and, as a result, to improve the visualization of blood capillaries in the skin and blood microcirculation assessment with speckle contract imaging technique [1]. Digital capillaroscopy is a method widely used for visualisation of human capillaries *in vivo*, in particular, of nail bed capillaries to identify disorders of the circulatory system at the early stages and monitoring the effectiveness of treatment [2]. The application of these methods can be enhanced by using the OCA [3]. When applied to a tissue surface, OCA penetrate inside the tissue and reduce the contribution of multiple light scattering to image formation. The mechanism of their operation is based on a decrease in the relative refractive index of optical inhomogeneities after diffuse penetration into the tissue. However, OCA penetrate to the bloodstream through the walls of capillaries in the deep layers of biological tissues. Most of OCA are osmotically active and can change the microrheological properties of red blood cells (RBC), which determine blood viscosity, that in turn can locally alter the diagnosed blood flow, introducing errors in capillary blood flow measurements using digital capillaroscopy. In this work, we examined the efficiency of 15 different OCAs for increasing the light penetration depth and improving the visualization of human nail bed capillaries. The effect of optical clearing (OC) was assessed using the OCT method on the nail bed area of volunteers' finger after the application of OCAs. The effect of OCAs on RBC aggregation and deformability properties was measured *in vitro* by diffuse light scattering method implemented in RheoScan device (RheoMediTech Inc., Seoul, Republic of Korea) [2]. For performing the experiments, the OCAs including fructose 50%, polyethylene glycol 300, polypropylene glycol 400, omnipaque, visipaque, accupack, glycerol, cedar oil, mineral oil, oleic acid, and various combinations of these agents were used. The effect of 4 most efficient OCAs (cedar oil, oleic acid, glycerin (98.2%), Visipaque-270) on capillary blood flow was studied by digital capillaroscopy technique.

Imaging of the nail bed capillaries showed that all OPAs except Visipaque-270 demonstrated improved image quality of the nail bed capillaries. The most effective OCA is glycerol. We demonstrated that the parameters obtained by capillaroscopy (capillary blood flow velocity and average capillary filling) of the nail bed depend on the OCA used to visualize the capillaries. We believe that the mechanism for the observed differences is most likely that OCA penetrate to capillaries and change the properties of the vessel walls and RBC. Thus, it was shown that the aggregation and deformability properties of RBC dramatically changed when blood was incubated with OCAs [3].

The obtained results demonstrate the capabilities of OC to improve the visualization of capillary blood flow and necessity to correct the parameters measured using digital capillaroscopy. These results can also be used to optimize and improve the speckle contrast imaging of the celebral blood flow. This work was supported by the Russian Science Foundation (Grant No. 23-45-00027).

[1] E. Genina, A. Bashkatov, Y. Sinichkin, I. Yanina, V. Tuchin, Optical clearing of biological tissues: Prospects of application in medical diagnostics and phototherapy. Journal of Biomedical Science and Engineering, vol. 1, pp. 22-58, (2015).
[2] A. Lugovtsov, Y. Gurfinkel, P. Ermolinskiy, A. Maslyanitsina, L. Dyachuk, A. Priezzhev, Optical assessment of alterations of microrheologic and microcirculation parameters in cardiovascular diseases, Biomedical Optics Express. vol. 10, pp. 3974-3986, (2019).
[3] P.A. Moldon, et al, Influence of optical clearing agents on the scattering properties of human nail bed and blood microrheological properties: in vivo and in vitro study, Journal of Biophotonics, pp. e202300524, (2024).

The impact of interferon-alpha on RBC-endothelium interaction assessed with optical tweezers

M. Maksimov[1*], P. Ermolinskiy[1], D. Umerenkov[1],
O. Scheglovitova[2], A. Lugovtsov[1], A. Priezzhev[1]

1- Faculty of Physics, Lomonosov Moscow State University, 1-2 Leninskiye Gory, Moscow, Russia, 119991
2- The Gamaleya National Center, 18 Gamaleya St., Moscow, Russia, 123098

* madoway@yandex.ru

Physiological functions of red blood cells (RBCs) include oxygen and carbon dioxide transport, immune response, blood coagulation and regulation of blood rheology. The inner surface of human vessels is covered with endothelial cells, which serve as a semipermeable barrier between the blood and the tissues. Endothelial cells release signaling molecules, which can change the properties of other cells, RBCs included. Thus, RBCs can interact with endothelium not only through adhesion to these cells, but also via biochemical signals. One of such signaling biomolecules is nitric oxide (NO), which is known to increase RBC deformability and decrease RBC aggregation [1].

Interferon alpha-2b (IFN-α) is an approved antiviral drug against hepatitis C and B. Lately it was used to treat patients with COVID-19 [2]. It is known that IFN-α impacts endothelial cells, decreasing their permeability and reducing NO production [3,4]. While endothelium is badly damaged in some cases of COVID-19, it is of interest, whether IFN-α alters RBC-endothelium interaction, either direct (adhesion) or indirect (NO production).

The main aim of this study was to investigate *in vitro* RBC-endothelium interaction and endothelial impact on RBC aggregation at different concentrations of IFN-α (0, 10, 30, 100, 300, 1000 units/ml). To achieve these, optical tweezers trapping technique was applied to measure forces of interaction between single RBCs as well as between RBC and the monolayer of endothelial cells.

The human umbilical vein endothelial cells (HUVEC) were incubated with corresponding concentrations of IFN-α for approximately 24 hours. Lithium heparin anticoagulant was used for blood drawing. The studied samples represented microcuvettes with endothelial monolayer at the bottom, filled with blood plasma containing small number of RBCs (with the hematocrit of approximately 0.05%). Laser tweezers provide the ability to trap and manipulate single cells, allowing to measure their interaction forces in the pN range. In this work, homemade dual-beam laser tweezers setup with two traps based on Nd:YAG laser (1064 nm) was used [5].

Our results demonstrate statistically significant decrease in RBC aggregation in the presence of endothelium and IFN-α. The degree of the effect is higher if IFN-α was added to the plasma without preliminary incubation. On the contrary, samples with endothelium incubated with IFN-α for 24 hours, but lacking IFN-α in the plasma during the measurements, showed weaker tendencies in decreasing RBC aggregation. The force of RBC-endothelium adhesion was in the range of 1-2 pN in almost all of the experiments and demonstrated weak tendencies to decreasing with the increase in IFN-α concentration. These results may witness in favor of short-time IFN-α effect on the RBC-endothelium system. Further investigation of RBC-endothelium-IFN-α interplay may spread light on the underlying mechanisms and provide clues for new therapeutic targets.

[1] A. Muravyov, et al, Comparative efficiency of three gasotransmitters (nitric oxide, hydrogen sulfide and carbon monoxide): analysis on the model of red blood cell microrheological responses, Journal of Cellular Biotechnology, Vol. 7, №1, pp. 1-9, (2021).
[2] R. Pereda, et al, Therapeutic effectiveness of interferon alpha 2b treatment for COVID-19 patient recovery, Journal of Interferon & Cytokine Research, Vol. 40, № 12, pp. 578–588, (2020).
[3] A. Minagar, et al, Interferon (IFN)-ß1a and IFN-ß1b block IFN-?-induced disintegration of endothelial junction integrity and barrier, Endothelium Vol. 10, № 6, pp. 299-307, (2003).
[4] J. Jones Buie, J. Oates, Role of interferon alpha in endothelial dysfunction: insights into endothelial nitric oxide synthase–related mechanisms, Am J Med Sci, Vol. 348, № 2, pp. 168–175, (2014).
[5] A. Lugovtsov, et al, Optical assessment of alterations of microrheologic and microcirculation parameters in cardiovascular diseases, Biomed Opt Express, Vol. 10, № 8, pp. 3974-3986, (2019).

Optimizing photothermal therapy for melanoma: the role of peptide-coated gold nanorods and laser irradiation parameters

L. Mikhailova[1*], E. Vysotina[1], M. Zyuzin[1]

1- School of Physics and Engineering, ITMO University, St. Petersburg 191002, Russian Federation

* lidia.mikhailova@metalab.ifmo.ru

Melanoma is a type of skin cancer characterised by the uncontrolled growth of melanocytes, which are cells that produce the pigment melanin. It is one of the most aggressive forms of skin cancer, and its incidence is increasing worldwide [1]. Current treatments for melanoma include surgery, chemotherapy, and immunotherapy; however, these treatments often have significant side effects and may not be effective for all patients [2,3]. Targeted therapy is a promising approach for the treatment of melanoma. This approach uses affine molecules specifically designed to target and destroy cancer cells [4]. These molecules can be used to modify nanoparticles or complexes bringing therapeutic properties. Gold nanorods (Au NRs) are a type of agent for targeted therapy that is effective for treating various types of cancer because of their ability to heat under laser irradiation, which can provoke cell death [5]. Since melanoma metastasises very rapidly and aggressively, targeted photothermal therapy is an excellent treatment option. It allows targeted agents to be delivered to tumour sites and effectively affect them.

This study presents a novel approach to melanoma therapy using gold nanorods (Au NRs) modified with two distinct melanoma-targeted peptides and evaluated under femtosecond (FS) and nanosecond (NS) pulsed laser irradiation regimes. The Au NRs were coated with Ac-12, which closely mimics the α-melanocyte-stimulating hormone (αMSH) sequence, and GKR, which targets melanocortin receptors (MC1R) and includes additional linkers for enhanced conjugation. The peptide-coated Au NRs were extensively characterised and tested *in vitro* and *in vivo* for their targeting ability, heating efficiency, and therapeutic efficacy.

Au NRs were synthesised and coated with Ac-12 or GKR peptides using a ligand exchange procedure. Cellular uptake, melanogenesis, and cell viability studies were conducted using B16-F10 melanoma cells. *In vivo* studies used C57BL/6 mice injected with B16-F10 cells to model melanoma. Photoacoustic imaging was used to assess tumour targeting, and histological analysis was performed to determine the safety of Au NRs. Photothermal therapy (PTT) was performed using FS (1030 nm, 1400 mW/cm^2) and NS (1064 nm, 1400 mW/cm^2) laser irradiation for 3 min.

In vitro studies showed that both Au@Ac-12 and Au@GKR effectively targeted and internalised into melanoma cells, causing concentration-dependent receptor-mediated melanogenesis. FS laser irradiation resulted in a more distinct temperature distribution profile and induced more intense tumour ablation than NS laser irradiation. *In vivo* photoacoustic imaging revealed that Au@Ac-12, with its higher affinity to MC1R, accumulated in tumours at a higher rate than Au@GKR. FS laser irradiation led to a significant decrease in tumour volume, particularly when applied shortly after Au NR injection. Histological analysis confirmed the safety of intravenously and intratumorally injected Au NRs, with no inflammatory reactions or cytotoxicity effects observed in the major organs.

This study demonstrates the potential of targeted melanoma therapy using peptide-coated Au NRs and differential laser irradiation. The Ac-12 peptide, with its higher affinity to MC1R, and the FS laser irradiation regime, with its enhanced heating capabilities, showed the most promising results in terms of tumour targeting and destruction.

[1] Five-Year Survival Rates | SEER Training, (n.d.). https://training.seer.cancer.gov/melanoma/intro/survival.html (accessed May 7, 2024).

[2] B. Katta, C. Vijayakumar, S. Dutta, The Incidence and Severity of Patient-Reported Side Effects of Chemotherapy in Routine Clinical Care: A Prospective Observational Study, Cureus, vol. 15,4 e38301, (2023).

[3] H. Majeed, V. Gupta, Adverse Effects of Radiation Therapy, StatPearls Publishing; 2024 Jan-. Available from: https://www.ncbi.nlm.nih.gov/books/NBK563259/.

[4] B. Yin, W. Ho, X. Xia, A Multilayered Mesoporous Gold Nanoarchitecture for Ultraeffective Near-Infrared Light-Controlled Chemo/Photothermal Therapy for Cancer Guided by SERS Imaging, Small, 19, 6, (2023).

[5] H. Kong, J. Han, M. Yang, Two-dimensional peptide nanosheets functionalized with gold nanorods for photothermal therapy of tumors, Journal of Materials Chemistry B, 11, 3445-3452, (2023).

Laser-assisted microbiology: engineering of microbial systems with laser bioprinting

N.V. Minaev[1*], V.S. Zhigarkov[1], V.S. Cheptsov[1,2], V.I. Yusupov[1]

1- Institute of Photon Technologies of Kurchatov Complex Crystallography and Photonics, NRC "Kurchatov Institute", Pionerskaya St. 2, 108840 Moscow, Troitsk, Russia
2- Soil Science Faculty, Lomonosov Moscow State University, Leninskie Gory bld.12, 119991 Moscow, Russia

* minaevn@gmail.com

The technologies of laser-induced forward transfer of living cells objects (cells aggregates – spheroids [1,2], microorganisms [3–5]) are widely used in biomedicine and microbiology for printing prototype of biological tissue [1,2], isolating of microorganisms [4], separation of symbiotic microorganisms [6], giving the cells of living microorganisms unusual properties [7].

As a result of our research, it was shown that it is possible to select a spatial transfer mode [8], when the impact of negative factors on living systems is minimal. Among such negative factors are: metal nanoparticles formed during the destruction of the absorbing donor coating [9,10], shock and acoustic waves [11,12], temperature surges [13], exposure of transmitted laser radiation [14], high dynamic loads [14] and the influence of the external environment [8].

The influence of some negative factors can be avoided by switching to other principles of laser printing and hardware implementation. For example, the use of infrared radiation with a wavelength of ~3 microns [15,16] allows laser printing with a donor plate without a metal absorbing layers and, thus, getting rid of the negative influence of nanoparticles. The availability of the laser printing method for practical problems of microbiology has significantly increased due to recent advances in the field of laser technology, incl. affordable hardware emerging that developed and manufactured in Russia. We have developed prototypes of various types of laser bioprinting systems, with the help of which we have demonstrated the high efficiency and usefulness of the presented method for microbiological problems. Currently, a mobile laser bioprinting system is being developed, which is unpretentious and relatively small in size, which will allow long-awaited experiments to be carried out in an "on-site" mode on the territory of specialized microbiology institutions.

Among the latest achievements [7] obtained using the Laser Engineering of Microbial Systems (LEMS) method, the following result can be highlighted. It has been shown that LIMS does not cause significant damage to the plasmalemma of cells, but for a short time leads to a significant increase in the permeability of cell membranes. This phenomenon requires further study and is of great interest from a practical point of view, for example, for the use of LEMS for introducing various molecules into cells.

[1] A. Antoshin, et al, LIFT of cell spheroids: Proof of concept, Bioprinting, Vol. 34, pp. e00297 (2023).
[2] E.D. Minaeva, et al, Laser Bioprinting with Cell Spheroids: Accurate and Gentle. Micromachines, Vol. 14, pp. 1152 (2023).
[3] V. Cheptsov, V. Zhigarkov, I. Maximova, N. Minaev, V. Yusupov, Laser-assisted bioprinting of microorganisms with hydrogel microdroplets: peculiarities of Ascomycota and Basidiomycota yeast transfer, World J. Microbiol. Biotechnol., Vol. 39, pp. 29 (2023).
[4] M.V. Gorlenko, et al, Laser microsampling of soil microbial community, J. Biol. Eng., Vol. 12, pp. 27 (2018).
[5] V.I. Yusupov et al, Laser engineering of microbial systems, Laser Phys. Lett., Vol. 15, pp. 065604 (2018).
[6] T.V. Kochetkova, et al, Tepidiforma bonchosmolovskayae gen. nov., sp. nov., a moderately thermophilic Chloroflexi bacterium from a Chukotka hot spring (Arctic, Russia), representing a novel class, Tepidiformia, which includes the previously uncultivated lineage OLB14, Int. J. Syst. Evol. Microbiol, Vol. 70, pp. 1192–1202 (2020).
[7] E.V. Grosfeld, V.S. Zhigarkov, A.I. Alexandrov, N.V. Minaev, V.I. Yusupov, Theoretical and Experimental Assay of Shock Experienced by Yeast Cells during Laser Bioprinting, Int. J. Mol. Sci., Vol. 23, pp. 001016 (2022).
[8] V. Yusupov, et al, Laser-induced Forward Transfer Hydrogel Printing: A Defined Route for Highly Controlled Process, Int. J. Bioprinting, Vol. 6, pp. 1–16 (2020).
[9] V. Zhigarkov, I. Volchkov, V. Yusupov, B. Chichkov, Metal Nanoparticles in Laser Bioprinting, Nanomaterials, Vol. 11, 2584 (2021).
[10] V.S. Zhigarkov, I.S. Volchkov, V.I. Yusupov, On the Shape of Metal Nanoparticles in Laser Printing With Gel Microdroplets, IEEE Photonics Technol. Lett., Vol. 34, pp. 227–230 (2022).
[11] E. Mareev, N. Minaev, V. Zhigarkov, V. Yusupov, Evolution of Shock-Induced Pressure in Laser Bioprinting, Photonics, Vol. 8, pp. 374 (2021).
[12] V.S. Zhigarkov and V.I. Yusupov, Impulse pressure in laser printing with gel microdroplets, Opt. Laser Technol., Vol. 137, pp. 106806 (2021).
[13] V.P. Zarubin, V.S. Zhigarkov, V.I. Yusupov, A.A. Karabutov, Physical processes affecting the survival of microbiological systems in laser printing of gel droplets, Quantum Electron., Vol. 49, pp. 1068–1073 (2019).
[14] V.I. Yusupov, et al, Laser-induced transfer of gel microdroplets for cell printing, Quantum Electron., Vol. 47, pp. 1158–1165 (2017).
[15] A.V. Pushkin, N.V. Minaev, F.V. Potemkin, V.S. Cheptsov, V.I. Yusupov, Bioprinting with 3-μm laser pulses, Opt. Laser Technol., Vol. 172, pp. 110482 (2024).
[16] V. Cheptsov, et al, Laser bioprinting without donor plate, Laser Phys. Lett., Vol. 19, pp. 085602 (2022).

Colloidal stability of gold nanoparticles conjugates with lysozyme under the influence of both environmental acidity and temperature factors

E. Molkova[*], **V. Pustovoy, R. Sarimov, S. Gudkov, A. Simakin, E. Nagaev, T. Matveeva**

Prokhorov General Physics Institute of the Russian Academy of Sciences, 38 Vavilova Str. Moscow, Russia

* bronkos627@gmail.com

Upon entering the biological environment, any nanoscale systems instantly bind proteins that form a "protein crown" [1]. The protein corona is formed due to the thermodynamics of the aqueous environment and is mediated by Coulomb and van der Waals forces, hydrogen bonds and hydrophobic interactions [2]. The stability of such agglomerates can be influenced by a large number of factors. The absence of reliable knowledge about the effect of the resulting protein corona on further interactions of nanoparticles with the environment is a serious problem [3]. In our previous work, we considered the factor of the influence of the acidity of the medium on aggregation – disaggregation [4]. Since not one factor affects any process, but several, the next step in studying the colloidal stability of the nanosystem "lysozyme + gold nanoparticles" is to investigate the influence of the acidity of the medium coupled with temperature exposure. The measurements were carried out in the pH range from 2 to 12 and at a temperature from 25 to 80°C. The choice of the upper temperature limit is determined by the melting point of the protein lysozyme. Optical research methods were chosen as the fastest and most convenient for studying the states of a colloidal solution.

[1] R. Cai and C. Chen, The Crown and the Scepter: Roles of the Protein Corona in Nanomedicine, Advanced Materials, 1805740, (2018).

[2] T. Kopac, Protein corona, understanding the nanoparticle–protein interactions and future perspectives: A critical review, International Journal of Biological Macromolecules, 169, 290–301, (2021).

[3] J. Gebauer, M. Malissek, S. Simon, S. Knauer, M. Maskos, R. Stauber, L. Treuel, Impact of the Nanoparticle–Protein Corona on Colloidal Stability and Protein Structure. Langmuir, 28(25), 9673–9679, (2012).

[4] E. Molkova, V. Pustovoy, E. Stepanova, I. Gorudko, M. Astashev, A. Simakin, R. Sarimov, S. Gudkov, pH-Dependent HEWL-AuNPs Interactions: Optical Study, Molecules, 29, 82, (2024).

Laser-induced agonist release for blood platelets activation control

E. Starodubtseva[1], T. Karogodina[2], A. Moskalensky[1*]

1- Novosibirsk State University, Pirogova str. 2, Novosibirsk, 630090, Russia
2- N.N. Vorozhtsov Novosibirsk Institute of Organic Chemistry SB RAS, 9 Lavrentiev Avenue, Novosibirsk, 630090, Russia

* a.mosk@nsu.ru

Blood platelets are involved in many physiological processes: apart from their main hemostatic function, they participate in immune and inflammatory responses, release growth factors and regulate angiogenesis. The assessment of platelet activation at the single-cell level is a promising approach for the research of platelet function in physiological and pathological conditions. We have previously developed a technique to trigger the activation by optical pulse, which enables detailed *in vitro* study of the early stage of this process [1]. The technique relies on the special UV-sensitive analogue of adenosine diphosphate (ADP), common platelet activation agonist.

By this work we extend the method of optical activation of platelets by several means. First, instead of uniform illumination of the sample, we used laser beam focused on a small spot within the observation area. Since the photorelease of ADP is caused by localized stimulus, the spatial spreading of activation between platelets can be measured. Second, we used other activation agonists along with ADP, such as UV-sensitive analogs of epinephrine. It allows us to study the complex interplay between chemical stimuli. Third, in order to mimic the physiological conditions, we used nitric oxide (NO) donors which are also light-controllable. NO is constantly produced in blood vessels and is known to inhibit platelet activation. In our system, NO release is induced by visible light, which allow independent control of activation and inhibition pathways.

The obtained results can be used for the development of novel *in vitro* platelet activation assays. They also could lead to fundamental understanding of platelet function and reaction to complex stimuli. The study was supported by the Russian Science Foundation, project # 23-75-10049.

[1] D.V. Spiryova, A.Yu. Vorobev, V.V. Klimontov, E.A. Koroleva, A.E. Moskalensky, Optical uncaging of ADP reveals the early calcium dynamics in single, freely moving platelets, Biomed. Opt. Express 11, 3319-3330 (2020).

In scattered light of cell proliferation: cell growth and attachment monitoring

M. Naumenko[1], A. Moskalensky[1*]

1- Novosibirsk State University, 1, Pirogova Str., Novosibirsk, 630090, Russia

* a.mosk@nsu.ru

Studying cell growth, division, and adhesion advances scientific knowledge across a wide range of disciplines, including cancer formation research and anticancer drug development [1]. Despite the existence of a diverse array of techniques and assays (e.g. automatic cell counting, XCelligence electric impedance measurements) the need for development of cost-effective, non-invasive, and easy-to-perform methods for tracing cell proliferation remains high. This work is focused on development and validation of a device that monitors adherent and suspension cell cultures via laser light scattering measurements.

Firstly, we modified the device created in our laboratory before to trace the changes of cells cultured in suspension [2]. Originally, the optical part of the device comprises a 850 nm, 3 mW dot laser module along with the BPW34 photodiodes arranged in a row to align with the width of a standard T25 biological cell flask. In order to enable measurements of adherent cell layer formation we extended the optical scheme of the device with the second laser of 660 nm, 5 mW directed along the bottom of the flask. We validated the device using various cell models, e.g. *E.coli* bacterial suspension culture and HEK293 adherent cell culture. We determined the dynamic range of the device using serially diluted suspension cell cultures. Also, we implemented complementary assays to verify our method.

Since the adherent cell layer is heterogeneous and consists of cells of different adhesion strength that is correlated with cell potential to metastasize [3], we are performing another modification to use the total internal reflection mode. For this purpose, we use the laser module with the wavelength of 980 nm and special optics to make the radiation 'trapped' in the flask bottom. The interaction of the evanescent wave with adherent cells leads to enhanced intensity of the scattered light.

The reproducibility and accuracy of the measurements was testified with experimental results. Therefore, we developed a novel optical device to control cell proliferation and attachment under the standard biological conditions. The device allows continuous measurements of cell system proliferation and perturbations in a cost-effective non-invasive manner and could be widely applicable in various fields of cell research including the studies of cancer.

[1] E. Sazonova, M. Chesnokov, B. Zhivotovsky, et al, Drug toxicity assessment: cell proliferation versus cell death, Cell Death Discov. 8, 417 (2022).
[2] D. Litunenko and A. Moskalensky, Wireless monitoring of cell cultures based on light scattering: a novel optical scheme and portable prototype, J. Biophotonics, 17(1):e202300234 (2024).
[3] E. Vargas-Accarino, C. Herrera-Montávez, Y. Cajal, S. Ramón, T. Aasen, Spontaneous Cell Detachment and Reattachment in Cancer Cell Lines: An In Vitro Model of Metastasis and Malignancy, Int J Mol Sci., 22(9):4929 (2021).

The diagnostic capabilities of the optical spectroscopy of blood serum after freezing

P. Nurgalieva[1*], **B. Yakimov**[1,2], **E. Tokar**[3], **O. Parashchuk**[1], **M. Varentsov**[4], **S. Aripshev**[4], **D. Paraschuk**[1], **I. Bratchenko**[5], **N. Sorokin**[4], **O. Cherkasova**[6,7], **A. Kamalov**[4], **E. Shirshin**[1,2**]

1- Faculty of Physics, M.V. Lomonosov Moscow State University, 1-2 Leninskie Gory, Moscow, Russia
2- Laboratory of Clinical Biophotonics, Sechenov First Moscow State Medical University, Moscow, Russia
3- LLC "Medeum", Moscow, Russia
4- Department of Urology, Medical Research and Education Center, Lomonosov Moscow State University, Moscow, Russia
5- Department of Laser and Biotechnical Systems, Samara University, Samara, Russia
6- Institute of Automation and Electrometry, Siberian Branch, Russian Academy of Sciences, Novosibirsk, Russia
7- National Research Centre "Kurchatov Institute", Moscow, Russia

* nurgalieva.pk17@physics.msu.ru, ** shirshin@lid.phys.msu.ru

The non-invasive and rapid measurement capabilities of optical spectroscopy make it an attractive choice for biomedical applications. In a variety of clinical settings, fluorescence and Raman spectroscopy of blood serum have great potential as diagnostic tools [1-3]. The first step of blood serum optical spectroscopy and biochemistry analysis is a pre-analytical stage, namely, sample preparation step. The pre-analytical stage is of high importance, as it may affect the subsequent results. In case of blood serum optical spectroscopy, the pre-analytical stage includes blood collection into serum separation tube by venipuncture, tube centrifugation for serum preparation and freeze-thaw cycle. The freeze-thaw cycle is not essential, but it is commonly employed because it can simplify the research process and facilitate its translation in clinical settings. Although many studies have demonstrated the potential of blood serum optical spectroscopy in biomedical diagnostics, there is still a lack of reports on the optical properties of fresh frozen blood serum. This gap poses a challenge for the practical use of optical spectroscopy of blood serum in real clinical settings.

The objective of this study was to examine the impact of freezing on the optical properties and diagnostic potential of blood serum. In this work, we assessed the effect of blood serum storage at -20°C for 24 hours on its optical spectroscopy signal, namely on autofluorescence, regular Raman spectroscopy and surface-enhanced Raman spectroscopy (SERS) signal.

[1] A.V. Gayer, et al, Multifarious analytical capabilities of the UV/Vis protein fluorescence in blood plasma, Spectrochimica Acta Part A: Molecular and Biomolecular Spectroscopy, 286, 122028-122036, (2023).
[2] J.L. Pichardo-Molina, et al, Raman spectroscopy and multivariate analysis of serum samples from breast cancer patients, Lasers in medical science, 22, 229-236, (2007).
[3] S.Z. Al-Sammarraie, et al, Human blood plasma SERS analysis using silver nanoparticles for cardiovascular diseases detection, Journal of Biomedical Photonics & Engineering, 10(1), 4-12, (2024).

Spectral characterization of transparency mechanisms in cardiac muscle

M. Pinheiro[1], M. Carvalho[1,2], V. Tuchin[3,4,5], L. Oliveira[1,6*]

1- Institute for Systems and Computer Engineering, Technology and Science (INESC TEC), Campus da FEUP, Rua Dr. Roberto Frias, 4200-465 Porto, Portugal
2- Department of Electrical and Computer Engineering, Faculty of Engineering of Porto University (FEUP), Rua Dr. Roberto Frias, 4200-465 Porto, Portugal
3- Institute of Physics and Science Medical Center, Saratov State University, 83 Astrakhanskaya str., Saratov 410012, Russian Federation
4- Laboratory of Laser Diagnostics of Technical and Living Systems, Institute of Precision Mechanics and Control of the FRC "Saratov Scientific Centre of the Russian Academy of Sciences", 24 Rabochaya, Saratov 410028, Russian Federation
5- Laboratory of Laser Molecular Imaging and Machine Learning, Tomsk State University, Tomsk 634050, Russian Federation
6- Physics Department, School of Engineering, Polytechnic of Porto, Rua Dr. António Bernardino de Almeida nº 431, 4249-015 Porto, Portugal

* lmo@isep.ipp.pt

The evaluation of the diffusion properties of drugs, chemicals and other agents in biological tissues has a great interest in various fields, such as diagnostic and treatment applications, pharmacology, and cosmetology. These properties are also fundamental for the characterization of the mechanisms that lead to transient transparency effects in tissues that are induced by optical clearing agents (OCAs) and therefore are of great importance for laser treatments of heart pathologies. Different optical methods have been used to evaluate the diffusion properties of various OCAs in different tissues [1]. With the purpose of characterizing the two fundamental optical clearing mechanisms in cardiac muscle, kinetic thickness and spectroscopy measurements were performed from tissue samples to evaluate the diffusion times and the diffusion coefficients of water and glycerol in this tissue, as well as the efficiency of transport of laser beams through cardiac muscle.

[1] V. Tuchin, D. Zhu, E. Genina, Handbook of Tissue Optical Clearing (CRC Press), (2022).

Optoacoustic angiography and diffuse optical spectroscopy to study tumor vascularization and oxygenation dynamics

A. Orlova[1*]**, A. Glyavina**[1,2]**, K. Akhmedzhanova**[1,2]**, A. Kurnikov**[1]**, D. Khochenkov**[3]**,
Yu. Khochenkova[3]**, A. Maslennikova**[1,2]**, A. Korobov**[1,4]**, I.V. Turchin**[1]**, P.V. Subochev**[1]

1- A.V. Gaponov-Grekhov Institute of Applied Physics RAS, 46 Ulyanov Street, Nizhny Novgorod, Russia
2- Lobachevsky State University of Nizhny Novgorod, 23 Gagarin Avenue, Nizhny Novgorod, Russia
3- N.N. Blokhin National Medical Research Center of Oncology, 23 Kashirskoye Highway, Moscow, Russia
4- Skolkovo Institute of Science and Technology, 30 Bolshoy Boulevard, Moscow, Russia

* ag.orlova@mail.ru

The study of tumor angiogenesis and the oxygen state is crucial for understanding the role of the circulatory system in the mechanisms of neoplasm growth and its response to therapy [1]. In this study, we utilized complementary optoacoustic (OA) imaging and diffuse optical spectroscopy (DOS) to compare the characteristics of vascular networks in different tumor models and assess their response to antiangiogenic and radiation therapies. OA imaging [2] provides label-free optical-contrast angiography with ultrasonic resolution at optical penetration depths. DOS relies on the detection of multiply scattered diffuse light that has passed through a biological tissue, allowing for the reconstruction of the concentrations of key tissue chromophores, such as oxy- and deoxyhemoglobin [3].

For OA we used a raster-scan system equipped with a pulsed laser (532 nm; 1 ns; 2 kHz) and a wideband PVDF detector, achieving a lateral spatial resolution of less than 50 μm. For DOS we utilized a fiber-optic-based system in a reflectance geometry, featuring a broadband LED as the light source and a spectrometer for detection.

As a first step of the work, we compared vascularity across tumor models of human renal cell carcinoma SN-12C, human colon carcinoma HCT-116, and Colo320. OA and DOS studies were conducted when the average tumor volume reached 700 mm³. Next, the study on the effects of the antiangiogenic therapy was performed on Colo320, with axitinib administered to animals at a dose of 50 mg/kg, five days per week for four weeks. Finally, the investigation of tumor responses to radiation therapy was conducted on murine colon carcinoma CT26, with assessments before and at intervals of 1-3 days following irradiation at single doses of 6, 12, and 18 Gy.

OA revealed the highest values of vessel size and fraction in Colo320 tumors. DOS indicated an increased content of deoxyhemoglobin, leading to reduced blood oxygen saturation level in Colo320 compared to other tumor models [4]. Axitinib treatment resulted in a gradual reduction in vessel segment sizes by more than two times compared to the control. This reduction was accompanied by a transient increase in blood oxygen saturation level.

Experiments evaluating the response of tumors to irradiation showed a decrease in density and an increase in fragmentation of small vessels, while large vessels exhibited the opposite reaction. The duration of the vascular response increased with higher radiation doses. Radiation-induced reoxygenation was detected only at high doses, occurring despite the incomplete recovery of vascular damage [5].

The combination of OA and DOS methods for *in vivo* analysis of vessel structure and oxygenation in experimental tumors has been demonstrated. This approach can be used to identify the features of blood vessel structure and their influence on tumor oxygenation, as well as to monitor the vascular response to treatment.

[1] J. Brown and W. Wilson, Exploiting tumour hypoxia in cancer treatment, Nat. Rev. Cancer, 4, pp. 437-447, (2004).
[2] L. Wang and S. Hu, Photoacoustic tomography: in vivo imaging from organelles to organs, Science, 335, pp. 1458-1462, (2012).
[3] T. Durduran, R. Choe, W. Baker, A. Yodh, Diffuse Optics for Tissue Monitoring and Tomography, Rep Prog Phys., 73, p. 076701, (2010).
[4] K. Akhmedzhanova, A. Kurnikov, D. Khochenkov, Yu. Khochenkova, A. Glyavina, V. Kazakov, A. Yudintsev, A. Maslennikova, I. Turchin, P. Subochev, A. Orlova, In vivo monitoring of vascularization and oxygenation of tumor xenografts using optoacoustic microscopy and diffuse optical spectroscopy, BOE, 13, pp. 5695-5708, (2022).
[5] A. Orlova, K. Pavlova, A. Kurnikov, A. Maslennikova, M. Myagcheva, E. Zakharov, D. Skamnitskiy, V. Perekatova, A. Khilov, A. Kovalchuk, A. Moiseev, I. Turchin, D. Razansky, P. Subochev, Noninvasive optoacoustic microangiography reveals dose and size dependency of radiation-induced deep tumor vasculature remodeling, Neoplasia, 26, p. 100778, (2022).

Monte Carlo-based semi-analytical approximation for diffuse reflectance spectroscopy

V. Perekatova[1*], M. Kirillin[1], A. Khilov[1], E. Sergeeva[1], D. Kurakina[1], I. Turchin[1]

1- A.V. Gaponov-Grekhov Institute of Applied Physics of the Russian Academy of Sciences, 46 Ul'yanov Street, Nizhny Novgorod, 603950, Russia

* valeriya1000@yandex.ru

A number of applied studies require quantitative characterization of concentrations of biological chromophores within studied tissue. Diffuse reflectance spectroscopy (DRS) is recognized as a go-to technique for non-invasive reconstruction of concentrations of various tissue chromophores [1] from absorption and scattering spectra of a tissue reconstructed from measured diffuse reflectance spectrum.

The diversity of absorption and scattering spectra of various chromophores presented in tissues makes the reconstruction problem multiparametric and causes the necessity of the most accurate possible solution of direct problem of light transport in tissue.

The simplest approach to the reconstruction of optical properties from diffuse reflectance spectrum uses the solution of Radiative Transfer Equation (RTE) for an infinite medium and diffusion approximation [2]. A more precise analytical model reported by Farrell et al [3] is also based on diffusion approximation of RTE and accounts for semi-infinite refraction-mismatched boundary. However, this model is not applicable at for source-detector distances (SDD) less than a few transport lengths of the tissue. A refined model of diffuse reflectance recently proposed by Sergeeva et al [4] is also based on diffusion approximation of RTE, however, it accounts for the detection fiber diagram.

An alternative way to obtain analytical expressions for diffuse reflectance is to approximate in silico or experimental data with analytical functions. Monte Carlo look-up table for a single SDD value of 0.25 mm and variations of absorption from 0.1 to 5 mm^{-1} and scattering from 0 to 5 mm^{-1} was reported in [5], while in look-up [6] tables were created from diffuse reflectance spectra obtained on calibrated phantoms for SDD values of 0.75, 2.00, 3.00, and 4.00 mm with interpolation for reduced scattering values between 0.4 and 1.2 mm^{-1} and absorption values between 0 and 0.8 mm^{-1}.

We report on a novel semi-analytical fit (SAF) of Monte Carlo simulated diffuse reflectance spectra for SDDs in the range of 0.3 – 9.9 mm and wide range of reduced scattering and absorption coefficients values that covers the physiological range for human skin and most of soft tissues. The comparison of presented model and analytical models based on diffuse approximations reveals the areas of the models' applicability. In this study we also demonstrate a comparison of the accuracy of reconstructing chromophore concentrations from DR spectra simulated for generic tissue using different analytical models and SAF.

[1] R. Nachabé, B.H. Hendriks, M. van der Voort, A.E. Desjardins, H.J. Sterenborg, Estimation of biological chromophores using diffuse optical spectroscopy: benefit of extending the UV-VIS wavelength range to include 1000 to 1600 nm, Biomedical optics express 1, 1432-1442 (2010).

[2] M.S. Patterson, B. Chance, B.C. Wilson, Time resolved reflectance and transmittance for the noninvasive measurement of tissue optical properties, Applied optics 28, 2331-2336 (1989).

[3] T.J. Farrell, M.S. Patterson, B. Wilson, A diffusion theory model of spatially resolved, steady-state diffuse reflectance for the noninvasive determination of tissue optical properties in vivo, Medical physics 19, 879-888 (1992).

[4] E. Sergeeva, D. Kurakina, I. Turchin, M. Kirillin, A refined analytical model for reconstruction problems in diffuse reflectance spectroscopy, Journal of Innovative Optical Health Sciences, 2342002 (2024).

[5] R. Hennessy, S.L. Lim, M.K. Markey, J.W. Tunnell, Monte Carlo lookup table-based inverse model for extracting optical properties from tissue-simulating phantoms using diffuse reflectance spectroscopy, Journal of biomedical optics 18, 037003-037003 (2013).

[6] G. Greening, A. Mundo, N. Rajaram, T.J. Muldoon, Sampling depth of a diffuse reflectance spectroscopy probe for in-vivo physiological quantification of murine subcutaneous tumor allografts, Journal of biomedical optics 23, 085006-085006 (2018).

Spectroscopic studies of cyanobacteria and its potential for renewable energetics

E. Perevedentseva[1*], **N. Melnik**[1], **I. Elanskaya**[2], **E. Muronets**[2], **S. Savinov**[1], **D. Korshunov**[3], **V. Ilyin**[3], **E. Demikhov**[3]

1- P.N. Lebedev Physical Institute of Rus. Acad. Sci. 119991 Moscow, Russia
2- Faculty of Biology, Moscow State University, 119991 Moscow, Russia
3- Institute of Biomedical Problems of Rus. Acad. Sci. 123007 Moscow, Russia

* perevedencevaev@lebedev.ru

Identification of cyanobacteria and analysis of their distribution and role in ecological societies, study of the composition of various strains and metabolic processes in them are important tasks [1] for both scientific and applied research. Modern spectroscopic methods are a promising tool for solving relevant problems [2,3].

In the present research Raman spectroscopy and absorption (UV-visible) spectroscopy were used to investigate the cyanobacterium *Synechocystis* sp. PCC6803, as a model of oxygenic photosynthetic organisms, and its mutants with disruption of individual components of the photosynthetic or respiratory electron transport chains of (such as phycobiliproteins allophycocyanin and C-phycocyanin, flavodiironproteins, quinoloxidase, cytochrome *c* oxidase, etc.).

Combining UV-visible spectroscopy and Raman spectroscopy allows to analyse the structure of the cyanobacterial light-harvesting antennae [4] via observing phycobiliproteins (in particular, C-phycocyanin and allophycocyanin), structural components of the phycobilisomes, and considering carotenoids as component of compensatory mechanism of for overcoming the deficiency of phycobiliproteins acting like an additional internal antenna of photosystems, as an antioxidant (quencher of triplet chlorophyll and singlet oxygen) and as a photoprotector (protect the photosynthetic apparatus from excess excitation energy at high light intensity) [5]. Raman spectroscopy was applied for study of Photosystem II in dark-adapted cells and structural changes in the cell under following illumination with white light.

As cyanobacteria are recently considered quite promising for various biotechnological applications [1,6] the spectroscopic analysis can be used for monitoring of cyanobacteria in biotechnological production of substances or energy. In particular, using Raman for estimation of state of biomass and advantages of cyanobacteria use in the biomass for renewable energy generation are discussed.

[1] M.M. Allaf and H. Peerhossaini, Cyanobacteria: Model Microorganisms and Beyond, Microorganisms. 10(4), 696, (2022).
[2] I. Tanniche, E. Collakova, C. Denbow, R.S. Senger, Characterizing metabolic stress-induced phenotypes of Synechocystis PCC6803 with Raman spectroscopy, PeerJ, 8, e8535, (2020).
[3] I. Tanniche, E. Collakova, C. Denbow, R.S. Senger, Characterizing glucose, illumination, and nitrogen-deprivation phenotypes of Synechocystis PCC6803 with Raman spectroscopy, PeerJ, 8, e8585, (2020).
[4] E. Perevedentseva, N. Melnik, E. Muronets, A. Averyushkin, A. Karmenyan, I. Elanskaya, Raman spectroscopy with near IR excitation for study of structural components of cyanobacterial phycobilisomes, J Luminescence, 265, 120224, (2024).
[5] F. Pagels, V. Vasconcelos, A.C. Guedes, Carotenoids from Cyanobacteria: Biotechnological Potential and Optimization Strategies, Biomolecules 11(5), 735, (2021).
[6] K.B. Singh, Kaushalendra, S. Verma, R. Lalnunpuii, J.P. Rajan, Current Issues and Developments in Cyanobacteria-Derived Biofuel as a Potential Source of Energy for Sustainable Future, Sustainability 15(13), 10439, (2023).

Drug-free inhibition of cancer cells by visible optical radiation

V. Plavskii[*]**, A. Svechko, O. Dudinova, L. Plavskaya, A. Tretyakova, A. Mikulich, R. Nahorny, T. Ananich, A. Sobchuk, S. Yakimchuk, I. Leusenka**

B.I. Stepanov Institute of Physics of the National Academy of Sciences of Belarus, Minsk, Belarus

* v.plavskii@ifanbel.bas-net.by

A quarter of a century after establishment of inhibitory effect of blue light on growth of cancer cells, their migration and invasion, many aspects of the mechanism of photophysical and photochemical processes underlying the effect of this physical factor have been quite well studied. However, the most pressing and controversial question remains about molecules that are acceptors of optical radiation, localized in cells and capable of influencing metabolic processes after light absorption [1]. Important information about possible participation of a particular endogenous compound in the implementation of the photobiomodulation effect can be obtained from a comparison of its absorption spectrum and the spectrum of action of optical radiation on cells. In this regard, we studied the spectral-dependent light-induced changes in metabolic activity of HeLa cells, as well as the dependence of the level of ROS formation in cells when exposed to radiation from LED sources peaking at $\lambda_{max} = 395, 405, 415, 445$ and 465 nm, in the energy dose range of $1.5–15.0$ J/cm^2.

It has been shown that the observed spectral-dependent light-induced inhibition of the metabolic activity of cancer cells and the light-induced formation of ROS is due to the changing contribution of endogenous porphyrins and flavins to the total absorption of the influencing radiation when its wavelength changes within the blue spectral region. In this case, the contribution of each endogenous photosensitizer is determined by its concentration, molar absorption coefficient, ROS generation efficacy, spatial localization in the cell near photosensitive molecules and ROS quenchers (interceptors), which have a decisive influence on the efficacy of sensitized processes.

Despite the significantly lower concentration of endogenous porphyrins compared to flavins, tetrapyrrole photosensitizers (protoporphyrin IX, coproporphyrin III, uroporphyrin III, Zn-protoporphyrin IX, Zn-coproporphyrin III) play a decisive role in the generation of ROS and inhibition of the metabolic activity of cancer cells during exposure to blue light, which is confirmed by the higher efficacy of the above processes when exposed to radiation with $\lambda_{max} = 405$ nm (corresponding to the maximum of the Soret band of endogenous porphyrins and the local minimum of the absorption band of flavins) in comparison with $\lambda_{max} = 445$ nm (corresponding to the long-wavelength maximum of the absorption spectrum of flavins and minimal absorption of porphyrins).

Using specific quenchers (interceptors) of ROS, it was shown, for the first time, that immediately after the cessation of irradiation, the decisive role in light-induced damage to cancer cells is played by singlet oxygen, formed due to the excitation of endogenous photosensitizers, and, to a lesser extent, by hydrogen peroxide. When monitoring the light-induced decrease in the metabolic activity of cells one day after their irradiation, it was found that the decisive role in this process belongs to hydrogen peroxide. It is concluded that the change in the contribution of various types of ROS to the effects of photobiomodulation over time after the cessation of light exposure on cells is explained by a wave of massive secondary production of ROS, and above all, hydrogen peroxide, which, according to literature data, during sensitized processes is recorded in cells several hours later after completion of irradiation.

The effect of blue light on cancer cells is not limited to damage to cellular structures, which ultimately leads to cell death (apoptosis and necrosis). A significant influence on the light-induced decrease in metabolic activity is exerted by changes in cell cycle parameters monitored by flow cytometry: a decrease in the relative number of cells in the G0/G1 stages, an increase in the relative number of cells in the G2/M stages, and their slight increase in the S stage. Moreover, for all studied indicators at the same energy doses, more significant changes are induced by exposure to light with $\lambda_{max} = 405$ nm compared to $\lambda_{max} = 445$ nm.

[1] V.Y. Plavskii, A.N. Sobchuk, A.V. Mikulich, O.N. Dudinova, L.G. Plavskaya, A.I. Tretyakova, R.K. Nahorny, T.S. Ananich, A.D. Svechko, S.V. Yakimchuk, I.A. Leusenka, Identification by methods of steady-state and kinetic spectrofluorimetry of endogenous porphyrins and flavins sensitizing the formation of reactive oxygen species in cancer cells, Photochem Photobiol, 2024 Jan 23.

The role of endogenous porphyrin photosensitizers in the inhibitory effect of blue light on cancer cells

V. Plavskii[*], **O. Dudinova, L. Plavskaya, A. Sobchuk, A. Mikulich, A. Tretyakova, R. Nahorny, T. Ananich, A. Svechko, S. Yakimchuk, I. Leusenka**

B.I. Stepanov Institute of Physics of the National Academy of Sciences of Belarus, Minsk, Belarus

* v.plavskii@ifanbel.bas-net.by

The ability of optical radiation in blue spectral region ($\lambda = 400$–485 nm) of low intensity (0.5–100 mW/cm^2) to inhibit the growth of cancer cells is currently practically beyond doubt. It is characteristic that in studies in which, *in vitro*, the effect of light of the same spectral and energy parameters on cancer and non-transformed cells was compared, the presence of pronounced differences in their response to the influence of the specified physical factor was noted. However, the reasons for the increased sensitivity of cancer cells to the action of blue light remain unclear. In our opinion, a complicating factor in resolving this issue is the lack of complete understanding of the mechanisms of photophysical and photochemical processes that determine the effects of photobiomodulation initiated by exposure to blue light. The question of the primary acceptor molecules responsible for the regulatory action of this physical factor remains the least studied and most debated [1]. The studies carried out in this work showed the important role of endogenous porphyrins (free-base and their zinc complexes) in the generation of reactive oxygen species in cells (and, above all, singlet oxygen), which are capable of influencing, by changing the redox state of cells upon absorption of blue light, the metabolic processes occurring in them. It has been shown that the decisive role of porphyrins in the effects of cell sensitization occurs despite higher, at least two orders of magnitude, concentrations of flavins (riboflavin, FMN, FAD) in cells.

The manifestation of the sensitizing properties of porphyrins in cells is facilitated by: a) higher efficacy of formation of singlet oxygen sensitized by them and higher values of their molar extinction coefficients compared to flavins; b) localization of porphyrins in mitochondria, while a significant proportion of flavins are localized in the cytosol; c) binding of flavins to proteins that perform a protective function against flavin-sensitized damage to cellular structures; d) pronounced antioxidant properties of flavins, which contributes to the quenching of ROS generated by them during photoexcitation.

The leading role of porphyrins, and not flavins, in the photobiological processes that determine cell metabolism when exposed to blue light is confirmed by a higher rate of inhibition of cell metabolic activity and higher levels of ROS formation, recorded using the chemiluminescence assay, when a cell suspension is exposed to radiation with $\lambda = 405$ nm compared to $\lambda = 445$ nm. In this case, radiation with a wavelength of $\lambda = 405$ nm corresponds to the maximum of the absorption spectrum of protoporphyrin IX and the local minimum of the absorption spectrum of flavins, and radiation with $\lambda = 445$ nm corresponds to the maximum of the absorption spectrum of flavins and the region of local minimum of the absorption spectrum of porphyrins.

For the first time, it has been shown that one of the reasons for the increased sensitivity of cancer cells compared to normal cells to the blue light is the higher concentration of endogenous porphyrin sensitizers, which is confirmed by fluorescent analysis methods. The determining role of porphyrins in the difference in the reactions of cancer and normal cells to the blue light on their suspension is also evidenced by higher levels of ROS formation and a higher rate of light-induced inhibition of the metabolic activity of HeLa cancer cells compared to normal BGM cells.

In addition to differences in the concentrations of endogenous porphyrin sensitizers in cancer and normal cells, the reason for the specificity of their reactions to exposure to blue light may lie in the fact that cancer and normal cells differ in their cellular response to the effects of ROS; and cancer cells may be more prone to apoptosis as a result of an imbalance in the intracellular antioxidant system caused by excess ROS production.

[1] V.Y. Plavskii, L.G. Plavskaya, O.N. Dudinova, A.I. Tretyakova, A.V. Mikulich, A.N. Sobchuk, R.K. Nahorny, T.S. Ananich, A.D. Svechko, S.V. Yakimchuk, I.A. Leusenko, Endogenous photoacceptors sensitizing photobiological reactions in somatic cells, J. Appl. Spectrosc, Vol. 90, pp. 334–345, (2023).

Multimodal OCT detection of uterine tissue pathologies

__A.A. Plekhanov__[1*], M.M. Loginova[1], E.A. Avetisyan[2], A.A. Shepeleva[2], A.A. Sovetsky[3],
A.A. Moiseev[3], M.M. Karabut[1], S.V. Gamayunov[2], G.V. Gelikonov[3], G.O. Grechkanev[1],
M.A. Sirotkina[1], V.Y. Zaitsev[3], N.D. Gladkova[1]

1- Privolzhsky Research Medical University, Nizhny Novgorod, Russia
2- Nizhny Novgorod Regional Oncologic Hospital, Nizhny Novgorod, Russia
3- Institute of Applied Physics of the Russian Academy of Sciences, Nizhny Novgorod, Russia

* strike_gor@mail.ru

Pathologies of the uterine tissue are widespread and lead to serious consequences from impaired reproductive function of a woman to cancer burden [1]. However, the most of them pathologies are considered to have a favorable prognosis with the possibility of preserving reproductive function by implementation of timely primary diagnosis and optimal treatment tactics during the early stage of disease. The most clinically significant pathologies of uterine tissue are associated with changes in the endometrium [2]. A generally accepted and reliable diagnosis of endometrial pathologies involves highly traumatic procedures of blind collecting material (pipelle biopsy / dilation and curettage) for realization of histological examination [3]. Recently, the endometrial biopsy under hysteroscopy is increasingly being chosen to reduce trauma and increase the targeting of pathologies diagnosis. Nevertheless, the ambiguity of visual hysteroscopic assessment and the incorrect selection of a suspicious endometrial area for subsequent histological examination often leads to a false pathological diagnosis and underestimating endometrial cancer [4]. Therefore, there is a need for a new diagnostic tool for highly accurate and minimally invasive morphological assessment of endometrial tissue.

Our study is aimed at identifying the capabilities of the Multimodal Optical Coherence Tomography (MM OCT) in diagnosing pathologies of uterine tissue. Recent pilot studies by colleagues have shown the promise of identifying qualitative differences between various endometrial pathologies using structural OCT [5,6]. Our research is focused to differentiation of the morphological structures of uterine tissue under normal conditions (endometrium and myometrium) and pathologies (endometrial hyperplasia, adenomyosis and cancer) by studying the characteristic polarization (by cross-polarization OCT [7]) and elastic (by compression OCT-elastography [8]) tissue properties. Cross-polarization OCT imaging of *ex vivo* uterine tissue samples made it possible to differentiate normal endometrium from myometrium and identify foci of adenomyosis by calculating the original attenuation coefficient (described earlier [9]). Compression OCT-elastography made it possible to differentiate sites of endometrial hyperplasia and cancer by decreasing and increasing of absolute stiffness values, respectively [10]. The obtained results indicate the potential for detecting uterine tissue pathologies using MM OCT and the relevance of further development of the technology for non-traumatic diagnosis/treatment monitor of uterine disease and targeted endometrial biopsy.

[1] R.L. Siegel, K.D. Miller, N.S. Wagle, et al, Cancer statistics, 2023. CA: a cancer journal for clinicians, 73(1), 17–48, (2023).
[2] A.R. Murphy, H. Campo, J.J. Kim. Strategies for modelling endometrial diseases, Nature reviews. Endocrinology, 18(12), 727-743, (2022).
[3] S.G. Vitale, G. Buzzaccarini, G. Riemma, et al, Endometrial biopsy: Indications, techniques and recommendations. An evidence-based guideline for clinical practice, Journal of gynecology obstetrics and human reproduction, 52(6), 102588, (2023).
[4] G. Garuti, P.F. Sagrada, A. Frigoli, et al, Hysteroscopic biopsy compared with endometrial curettage to assess the preoperative rate of atypical hyperplasia underestimating endometrial carcinoma, Archives of gynecology and obstetrics, 308(3), 971–979, (2023).
[5] T.S.M. Law, F. Wu, H. Xu, et al, Endometrium imaging using real-time rotational optical coherence tomography imaging system: A pilot, prospective and ex-vivo study, Medicine, 98(44), e17738, (2019).
[6] B. Ding, T. Jinyuan, K. Tao, et al, A pilot and ex-vivo study of examination of endometrium tissue by catheter based optical coherence tomography. BMC medical imaging, 22(1), 162, (2022).
[7] K.S. Yashin, E.B. Kiseleva, E.V. Gubarkova, et al, Cross-Polarization Optical Coherence Tomography for Brain Tumor Imaging, Frontiers in oncology, 9, 201, (2019).
[8] A.A. Plekhanov, M.A. Sirotkina, A.A. Sovetsky, et al, Histological validation of in vivo assessment of cancer tissue inhomogeneity and automated morphological segmentation enabled by Optical Coherence Elastography, Scientific reports, 10(1), 11781, (2020).
[9] A. Moiseev, E. Sherstnev, E. Kiseleva, et al, Depth-resolved method for attenuation coefficient calculation from optical coherence tomography data for improved biological structure visualization, Journal of biophotonics, 16(12), e202100392, (2023).
[10] G.O. Grechkanev, A.A. Plekhanov, M.M. Loginova, et al, First experience of using multimodal optical coherence tomography for diagnostics of hyperplastic processes in the endometrium, Russian bulletin of obstetrician-gynecologist, 23(5), 66-72, (2023).

Spectroscopic study of methylene blue to the leucomethylene blue transition *in vitro* and *in vivo*

D.V. Pominova[1,2*], **A.V. Ryabova**[1,2], **I.V. Markova**[2], **A.S. Skobeltsin**[1,2], **I.D. Romanishkin**[1]

1- Prokhorov General Physics Institute of Russian Academy of Sciences, Moscow, Russia
2- National Research Nuclear University MEPhI (Moscow Engineering Physics Institute), Moscow, Russia

* pominovadv@gmail.com

Methylene blue (MB) is second-generation FDA-approved photosensitizer [1]. Photodynamic therapy with MB is reported to be effective [2], but the results are promising not for all tumor types. This may be related to the different bioavailability of MB in target tissues due to the transition of MB to the colorless leucoform, which reduces its photodynamic activity. In addition to this, the reduction of MB into the leucomethylene blue (LMB) can play a role in various redox processes occurring in the body and affect metabolism. For example, MB can interact with the mitochondrial electronic circuit, donating electrons to complexes I and III and/or providing partial restoration of the Krebs cycle [3], which not only determines its neuroprotective properties [4], but can also be used to increase the effectiveness of antitumor therapy. The interaction of MB with coenzymes, such as NADH is important in this aspect. A high ratio of NADH/NAD$^+$ has been reported to be a key feature of malignant cells [5]. When interacting with NADH, MB is reduced to the leucoform, and NADH is oxidized to NAD$^+$, providing also metabolic changes: increase of pyruvate:lactate ratio and reactivation of electron transport chain [3]. Under the influence of molecular oxygen and reactive oxygen species, LMB can be oxidized back to MB.

The purpose of this work was to study the MB to LMB transition under the influence of various factors, such as coenzymes, oxygen and reactive oxygen species, as well as under the influence of laser radiation using spectroscopic methods.

Absorption and fluorescence spectra, as well as fluorescence lifetimes of MB in solutions during interaction with coenzymes and products of biochemical reactions (NADH, FADH, lactate, pyruvate, glutathione) under normal oxygen conditions and hypoxia were studied. Then studies were carried out on cell cultures with different metabolism (glycolysis and oxidative phosphorylation) and finally verified *in vivo* on small laboratory animals. A model was proposed that describes the transition of MB-LMB in various tissues depending on their metabolism, redox state, of the microenvironment, oxygen supply and MB concentration. The proposed model will allow optimizing MB concentrations for effective photodynamic therapy or for its use as an antioxidant and neuroprotector.

[1] G. Alimu, et al, Liposomes loaded with dual clinical photosensitizers for enhanced photodynamic therapy of cervical cancer, RSC Adv., 13, 3459–3467 (2023).
[2] A. Taldaev, et al, Methylene blue in anticancer photodynamic therapy: systematic review of preclinical studies, Front. Pharmacol., 14, 1264961 (2023).
[3] T. Komlódi and L. Tretter, Methylene blue stimulates substrate-level phosphorylation catalysed by succinyl–CoA ligase in the citric acid cycle, Neuropharmacology, 123, 287–298 (2017).
[4] E. Poteet, et al, Neuroprotective Actions of Methylene Blue and Its Derivatives, PLoS ONE, 7, e48279 (2012).
[5] A. Chiarugi, C. Dölle, R. Felici, M. Ziegler, The NAD metabolome — a key determinant of cancer cell biology, Nat Rev Cancer, 12, 741–752 (2012).

Correlation of pathologic alterations of microrheologic and microcirculation parameters measured by laser-optical techniques

A.V. Priezzhev[*], **A.E. Lugovtsov, P.E. Ermolinskiy, D.A. Umerenkov, Yu.I. Gurfinkel**

Lomonosov Moscow State University, 1-2 Leninskiye Gory, Moscow, Russia, 119991

* avp@biomedphotonics.ru

The goal of this work was to assess the correlation of pathologic alterations of red blood cells (RBC) deformability, i.e. the dependance of their elongation on shear stress, and aggregation properties, i.e. hydrodynamic strength of RBC aggregates, characteristic time of RBC aggregates formation, aggregation index, forces of pair aggregation of RBC, aggregation rate and degree of platelets, measured *in vitro* in blood samples drawn from patients suffering from socially important diseases and from healthy donors (control group) with alterations of the microcirculation parameters measured in these individuals *in vivo. In vitro* measurements were performed using the techniques of diffuse light scattering, turbidimetry, laser diffractometry, laser trapping and manipulation [1]. Digital capillaroscopy was used *in vivo* to visualize the capillaries and quantitatively evaluate the capillary blood flow in the nailfold vessels [2].

It was shown that in the groups of patients suffering from type 2 diabetes mellitus (DM) and cardio-vascular diseases (CVD), the ability of RBC to deform is slightly reduced while the aggregation rate and forces of the cells interaction are significantly increased relative to those in the control group [3]. The degree and rate of platelets aggregation in patients suffering from DM and CVD are increased compared to the control group. The blood microcirculation in nailfold capillaries is impaired as well. The calculated correlation matrices have shown that the alterations of the parameters measured *in vivo* and *in vitro* for patients with different stages of these diseases are interrelated [4]. Good agreement between the results obtained with different techniques, and their applicability for the diagnostics of abnormalities of rheological properties of blood were demonstrated.

[1] A. Lugovtsov, Y. Gurfinkel, P. Ermolinskiy, A. Maslyanitsina, L. Dyachuk, A. Priezzhev, Optical assessment of alterations of microrheologic and microcirculation parameters in cardiovascular diseases, Biomedical Optics Express, vol. 10, pp. 3974-3986 (2019).
[2] P. Ermolinskiy, Yu. Gurfinkel, E. Sovetnikov, A. Lugovtsov, A. Priezzhev, Correlation between the capillary blood flow characteristics and endothelium function in healthy volunteers and patients suffering from coronary heart disease and atrial fibrillation: A pilot study, Life. 13(10) (2043).
[3] A. Maslianitsyna, P. Ermolinskiy, A. Lugovtsov, A. Pigurenko, M. Sasonko, Yu. Gurfinkel, A. Priezzhev, Multimodal diagnostics of microrheologic alterations in blood of coronary heart disease and diabetic patients, Diagnostics 11, 76 (2021).
[4] I. Kadanova, A. Neznanov, A. Lugovtsov, Yu. Gurfinkel, A. Pigurkenko, L. Dyachuk, A. Priezzhev. Relationship between capillary blood flow parameters measured in vivo and blood microrheological parameters measured in vitro in arterial hypertension and coronary heart disease, Regional Blood Circulation and Microcirculation, 20(1), pp. 17-24 (2021). (in Russian).

Thermal modulation of the electrophysiological properties of neurons and HEK 293 cells using diamond heater-thermometer

A. Romshin[1*], N. Aseyev[2], O. Idzhilova[2], A. Koryagina[2], V. Zeeb[1,3], I. Vlasov[1], P. Balaban[2]

1- Prokhorov General Physics Institute of the Russian Academy of Sciences, Moscow, Russia
2- Institute of Higher Nervous Activity and Neurophysiology of the Russian Academy of Sciences, Moscow, Russia
3- Institute of Theoretical and Experimental Biophysics of the Russian Academy of Sciences, Moscow, Russia

* alex_31r@mail.ru

Pulsed infrared radiation and thermoplasmonics, which enable fast and targeted control of temperature at the microscale, have recently opened a novel chapter in the study of the electrophysiological properties of living cells. It has been demonstrated that local heating at cellular scale elicits depolarizing capacitive currents across the phospholipid membrane [1,2], sufficient for triggering trains of action potentials in neurons [3]. However, the mismatch in spatial and temporal scale between applied heat and electric response of the cell remain the exact mechanisms by which local temperature affects membrane potential incompletely understood.

The present study explores the impact of local heat on the electrophysiological properties of living cells at the subcellular level using the diamond heater-thermometer (DHT) [4], which integrates the functions of a thermometer and a heater within a single microparticle covering less than 3% of the cell surface. Experimentally, the DHT demonstrated the ability to control local temperatures with an accuracy of less than 0.2°C in the vicinity of the cell. Millisecond heat pulses evoked reversible changes in membrane potential and elicited capacitive currents in primary cultured neurons and HEK 293 cells. A typical voltage shift for local temperatures from 25 to 70°C was ~1 mV. Contrary to expectations, at local temperatures around 50°C, an abrupt increase in cellular response by an order of magnitude was observed allowing the cell to be effectively and reproducibly clamped by temperature. Henceforth, even lower temperatures (<35°C) elicited depolarizations up to 10 mV in primary neurons, sufficient to trigger action potentials (AP) at rates up to 40 Hz. Such an irreversible transition to so-called temperature-clamp mode (TCM) was attributed to heat-induced phase changes in the phospholipid membrane at the point where DHT touches the cell. In addition, the effects of high temperatures beyond the physiological range on cellular electrophysiology were assessed, with a focus on action potential formation. These findings enhance our understanding of how local heat influences cellular functions and provide valuable insights into the thermal modulation of cell activity.

[1] M. Shapiro, K. Homma, S. Villarreal, C.-P. Richter, F. Bezanilla, Infrared light excites cells by changing their electrical capacitance, Nature Communications, vol. 3, pp. 736, (2012).
[2] H. Beier, G. Tolstykh, J. Musick, R. Thomas, B. Ibey, Plasma membrane nanoporation as a possible mechanism behind infrared excitation of cells, Journal of neural engineering, vol. 11(6), pp. 066006, (2014).
[3] J. Carvalho-de-Souza, J. Treger, B. Dang, S. Kent, D. Pepperberg, F. Bezanilla, Photosensitivity of neurons enabled by cell-targeted gold nanoparticles, Neuron, vol. 86(1), pp. 207-217, (2015).
[4] A. Romshin, V. Zeeb, E. Glushkov, A. Radenovic, A. Sinogeikin, I. Vlasov, Nanoscale thermal control of a single living cell enabled by diamond heater-thermometer, Scientific Reports, vol. 13, pp. 8546, (2023).

Effect of methylene blue on the NADH metabolic index of tumor cells before and after PDT

A.V. Ryabova[1,2*], **D.V. Pominova**[1,2], **I.V. Markova**[2], **I.D. Romanishkin**[1], **V.B. Loschenov**[1,2]

1- Prokhorov General Physics Institute of the Russian Academy of Sciences, 119991 Russia, Moscow, Vavilova st. 38
2- National research nuclear university MEPHI, 115409 Russia, Moscow, Kashirskoye sh. 31

* *nastya.ryabova@gmail.com*

Hypoxia plays an important role in the interaction of cancer cells, stroma and immune cells and contributes to tumor resistance to treatment [1]. Strategies to overcome hypoxia include oxygen delivery or *in situ* generation, reduction of oxygen consumption by the tumor, normalization of the tumor vasculature [2]. Our previous studies showed that MB leads to increased tumor oxygenation in a mouse model of Lewis lung carcinoma [3]. The effect of the methylene blue (MB) photosensitizer on the tumor cells' metabolism is due to, among other things, interaction with NADH, while MB is reduced to the leuco form, and NADH is oxidized to NAD+, providing an increase in the ratios of pyruvate:lactate and reactivation of the electron transport chain [4].

This paper presents studies of the effect of PDT with MB and the combination of MB/chlorin e6 photosensitizers in terms of metabolic changes in tumor cells. The studies were performed on HeLa tumor cell culture *in vitro* and on murine Ehrlich adenocarcinoma *in vivo*. PDT on HeLa cells *in vitro* included 1 hour incubation of cells with 5 mg/kg of chlorin e6 and 1-20 mg/kg of MB and their combination; 660 nm, 30-100 mW/cm^2. *In vivo* PDT with 5 mg/kg of chlorin e6, 10 mg/kg of MB and their combination; 660 nm, 60 J/cm^2. Control animals were animals with and without MB/chlorin e6, without irradiation. Using confocal microscopy, mitochondrial stress and generation of reactive oxygen species in cells in response to laser irradiation with MB were studied. The changes in cellular metabolism in response to PDT were assessed by analyzing the fluorescence life-time imaging microscopy (FLIM) of NADH.

Oxidative stress from chlorin e6 incubation in combination with 1-20 mg/kg MB or for 10-20 mg/kg MB without chlorin e6 leads to an elongation of the NADH fluorescence distribution on the FLIM phasor diagram along the NADH metabolic trajectory 0.4-2.5 ns.

After PDT with MB, NADH fluorescence lifetime becomes shorter (closer to anaerobic glycolysis). After PDT with MB and chlorin e6, however, it shifts towards longer lifetimes (closer to oxidative phosphorylation). With a large dose of PDT (strong oxidative stress), the NADH fluorescence distribution on the phasor diagram becomes rounded; dead cells a day after PDT also retain a rounded distribution of the NADH fluorescence cloud on the phasor. The obtained data will make it possible to optimize hypoxic tumor treatment, increasing the sensitivity of cancer and immune cells triggering the process of immunogenic cell death.

[1] V. Petrova, M. Annicchiarico-Petruzzelli, G. Melino, et al, The hypoxic tumour microenvironment. Oncogenesis, **7**(10), 1-13 (2018).
[2] Z. Shen, Q. Ma, X. Zhou, et al, Strategies to improve photodynamic therapy efficacy by relieving the tumor hypoxia environment. NPG Asia Mater, 13(39), 1-19 (2021).
[3] D. Pominova, A. Ryabova, A. Skobeltsin, I. Markova, K. Linkov, I. Romanishkin, The use of methylene blue to control the tumor oxygenation level, Photodiagnosis and Photodynamic Therapy, 46, 104047:1-8 (2024).
[4] T. Komlódi and L.Tretter, Methylene blue stimulates substrate-level phosphorylation catalysed by succinyl-CoA ligase in the citric acid cycle, Neuropharmacology, 123, 287-298, (2017).

Separate reconstruction of absorption and scattering coefficients spectra from the diffuse reflectance spectroscopy data based on the refined analytical model

E. Sergeeva[1], A. Kostyuk[1], D. Kurakina[1], A. Khilov[1], M. Kirillin[1]

1- A.V. Gaponov-Grekhov Institute of Applied Physics RAS; 46 Ulyanov st., Nizhny Novgorod 603950 Russia

* sergeeva_ea@ipfran.ru

Despite its technical simplicity and decades of practical implementation in experimental biophotonics, diffuse reflectance spectroscopy (DRS) is still an in-demand technique for fast noninvasive quantification of biological chromophores and tracking dynamical changes in their concentrations in various biotissues including studies of brain hemodynamics and superficial biotissues. Systems equipped with multiple detectors such as hyperspectral cameras or multifiber setups are aimed at mapping the chromophores distribution from the absorption coefficient spectra reconstructed from the measured spectra of diffuse reflectance at various source-detector distances (SDDs). There are numerous approaches to solve the DRS inverse task: from approximate analytical models involving calibrated reflectors measurements and up to machine learning algorithms based on numerical solutions of a forward task in a realistic geometry. For large volumes of processed data a time-saving recovery algorithm based on an adequate analytical model is preferrable. The most common approach to recover the chromophores content from DRS data is to fit the reflectance spectra or the ratio of spectra measured at one or several SDDs by the analytically calculated reflectance where the absorption spectrum is assumed as a weighted sum of partial spectra of a priori known chromophores, and the reduced scattering spectrum is fitted by a given function with a small number of parameters [1]. However, in some cases the basic set of chromophores may be incomplete so the composed guess spectrum does not reflect the features of real absorption spectrum. Besides, in biotissues with spatially non-uniform distribution of chromophores such as skin the sensitivity of a wideband DRS system to different layers varies for different parts of the wavelength range, which violates the assumption of constant partial weights of basic chromophores.

We propose an algorithm for separate, condition-free reconstruction of absorption and reduced scattering spectra of biotissue from DRS data for small SDDs (below 5 mm) based on the refined analytical model [2]. The algorithm has been verified by Monte Carlo simulated data mimicking wideband DRS spectra measured from uniform and two-layered skin structures that emulate dermis and epidermis-dermis geometry, respectively. Further the algorithm has been tested in the model and *in vivo* experiments in volunteers performed with the custom-made DRS system operating in the wavelength range of 450-1000 nm [3]. We discuss the accuracy of the algorithm in separate reconstruction of absorption and scattering spectra of a liquid phantom of biotissue which optical properties and preliminary evaluated from the spectrophotometry measurements. We demonstrate examples of determination of optical properties of skin in different locations *in vivo* and discuss the ability and limitations to recover the chromophore composition.

[1] S.L. Jacques, Optical properties of biological tissues: a review, Phys. Med. Biol., vol.58, pp. R37-R61 (2013).

[2] E. Sergeeva. D. Kurakina, I. Turchin, M. Kirillin, A refined analytical model for reconstruction problems in diffuse reflectance spectroscopy, Journal of Innovative Optical Health Sciences, 2342002 (2023).

[3] V. Perekatova, A. Kostyuk, M. Kirillin, E. Sergeeva, D. Kurakina, O. Shemagina, A. Orlova, A. Khilov, I. Turchin, VIS-NIR diffuse reflectance spectroscopy system with Self-calibrating fiber-optic probe: study of perturbation resistance, Diagnostics (Basel), vol.13, pp. 457 (1–20) (2023).

Advances in wideband (0.3-30 MHz) laser optoacoustic diagnostics

P. Subochev

Laboratory of ultrasound and optoacoustic diagnostics, Institute of Applied Physics RAS

pavel@ipfran.ru

Biomedical optoacoustic diagnostics combine the molecular specificity of optical methods with the depth and spatial resolution of ultrasound [1]. The angiographic capabilities of optoacoustic diagnostics – the ability to visualize blood vessels of various calibers – largely depend on the sensitivity and bandwidth of the ultrasound antennas used [2]. Recent advances in the development of wideband (0.3-30 MHz) highly sensitive (10 Pa) piezopolymer (PVDF-TrFE) ultrasound antennas [3] allow for superior quality angiographic imaging in both clinical and preclinical research. The presentation will cover biomedical applications related to the diagnosis and treatment of vascular abnormalities, focusing on the technological capabilities of high-resolution real-time optoacoustic imaging systems. The potential of noninvasive optoacoustic microangiography in revealing deep vascular remodeling of experimental tumors during radiation therapy [4], as well as the capabilities of clinical scanning optoacoustic angiography in diagnosing angiopathies [5], will be demonstrated. Challenges, limitations, and research directions will also be discussed, illustrating the potential of piezopolymer ultrasound detectors in clinical biomedical optoacoustic imaging of the future.
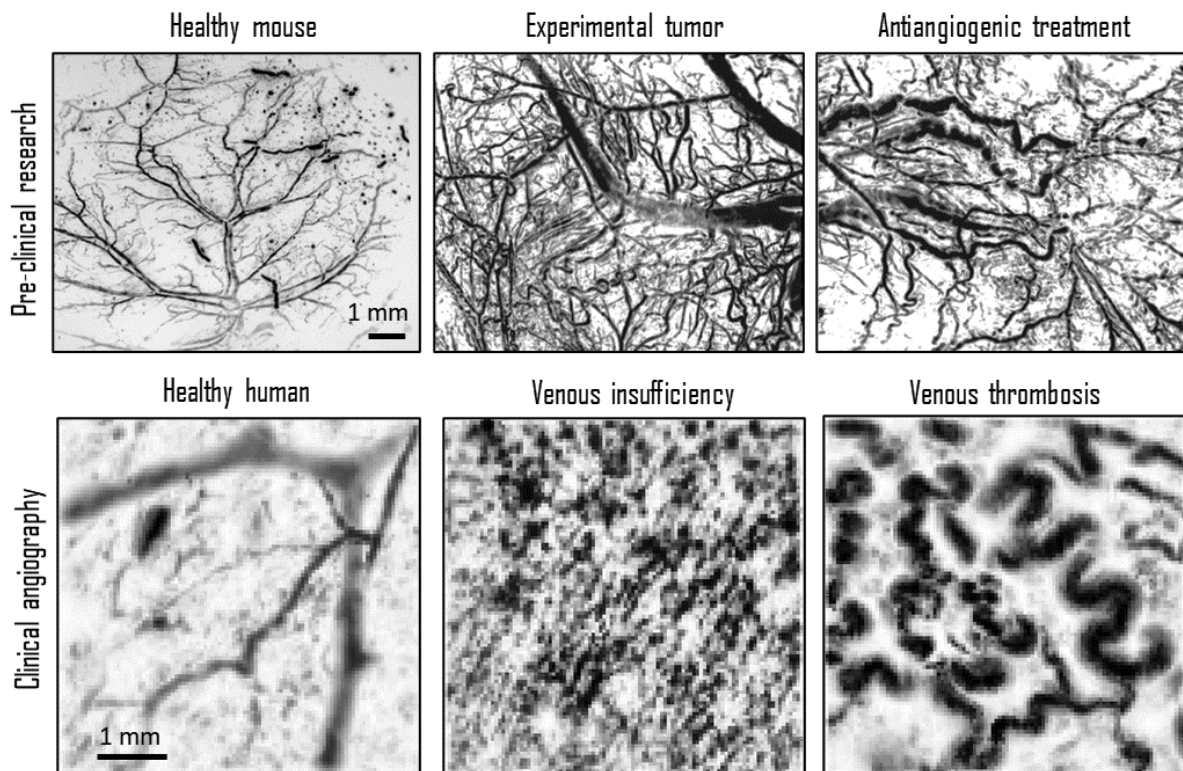

Figure 1: Laser optoacoustic angiography in clinical and preclinical research.

[1] L.V. Wang and S. Hu, Photoacoustic tomography: in vivo imaging from organelles to organs, Science, 335(6075), (2012).

[2] T.D. Khokhlova, I.M. Pelivanov, V.V. Kozhushko, A.N. Zharinov, V.S. Solomatin, A.A. Karabutov, Optoacoustic imaging of absorbing objects in a turbid medium: ultimate sensitivity and application to breast cancer diagnostics, Applied optics, 46(2), (2007).

[3] Y.H. Liu, A. Kurnikov, W. Li, P. Subochev, D. Razansky, Highly sensitive miniature needle PVDF-TrFE ultrasound sensor for optoacoustic microscopy, Advanced Photonics Nexus, 2(5), (2023).

[4] A. Orlova, K. Pavlova, A. Kurnikov, A. Maslennikova, M. Myagcheva, E. Zakharov, ... I. Turchin, P. Subochev, Noninvasive optoacoustic microangiography reveals dose and size dependency of radiation-induced deep tumor vasculature remodeling, Neoplasia, 26, 100778, (2022).

[5] S. Nemirova, A. Orlova, A. Kurnikov, Y. Litvinova, V. Kazakov, I. Ayvazyan, P. Subochev, Scanning optoacoustic angiography for assessing structural and functional alterations in superficial vasculature of patients with post-thrombotic syndrome: A pilot study, Photoacoustics, 100616, (2024).

Diagnostics of bacteria using Fabry-Perot interference in silicon nanostructures of various morphologies

<u>M. Wang</u>[1*], K.A. Gonchar[1], P.A. Rachishena[1], D.A. Nazarovskaia[1], P.A. Domnin[2], I.I. Tsiniaikin[1], S.A. Ermolaeva[2], L.A. Osminkina[1]

1- Lomonosov Moscow State University, Faculty of Physics, Leninskie gory 1, 119991, Moscow, Russia
2- National Research Center for Epidemiology and Microbiology N. F. Gamaleya Gamaleyi St., 18, 123098, Moscow, Russia

* van.m17@physics.msu.ru

The most common optical sensors are based on the effects of light interference in thin layers of silicon nanostructures, such as porous silicon (PS) [1] or silicon nanowires (SNF) [2].

In this work three different nanostructures were studied: (i) porous silicon film (e-pSi) obtained by electrochemical (EC) etching of crystalline silicon substrate; (ii) sacrificial-etched porous silicon film (se-pSi) obtained by double electrochemical (EC) etching of a crystalline silicon substrate with the first e-pSi layer dissolved in NaOH solution; (iii) porous silicon nanowire layer (pSiNWs) obtained by metal-assisted chemical etching (MACE) of crystalline silicon substrate.

SEM micrographs of the obtained silicon nanostructures with various morphologies after adsorption of *E. coli*. Bacteria are presented in Figure 1.
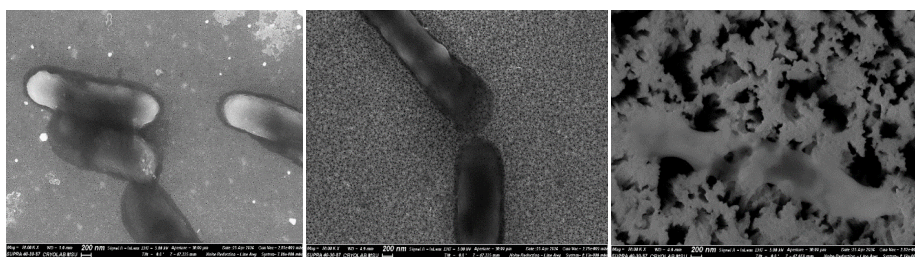
Fig. 1. SEM micrographs of silicon nanostructures with various morphologies after adsorption of *E. coli*.

IR reflectance spectra of the samples were measured without and with *E. Coli* at a concentration of 106 CFU/ml. Then, the change in the effective optical thickness of the nanostructures ($EOT = 2{\times}L{\times}n_{eff}$) was determined using fast Fourier transform, and the adsorption efficiency of the bacteria was measured.

As a result, this work showed the possibility of diagnosing bacteria using Fabry-Perot interference in silicon nanostructures.

[1] A. Jane, R. Dronov, A. Hodges, N.H. Voelcker, Porous silicon biosensors on the advance, Trends in biotech., vol. 27(4), pp. 230-239, (2009).
[2] K.A. Gonchar, S.N. Agafilushkina, D.V. Moiseev, I.V. Bozhev, A.A. Manykin, E.A. Kropotkina, A.S. Gambaryan, L.A. Osminkina, H1N1 influenza virus interaction with a porous layer of silicon nanowires, Mater. Res. Express, vol. 7, pp. 035002, (2020).

Optical clearing as a new approach to increasing the efficiency of laser thermolysis of adipose tissue

I.Yu. Yanina[1,2]*, D.K. Tuchina[1,2], P.A. Timoshina[1,2], E.A. Genina[1,2], V.V. Tuchin[1,2]

1- Saratov State University (National Research University), Institute of Physics, 83 Astrakhanskaya str., Saratov 410012, Russia
2- Tomsk State University (National Research University), Laboratory of laser molecular imaging and machine learning, 36 Lenin's av., Tomsk 634050, Russia

* irina-yanina@list.ru

The technique based on the combination of photochemical and photothermal effects induces adipose tissue optical clearing (OC) on the cell level [1-6]. In this technique, to control the optical scattering properties of the adipose tissue laser radiation is used. Depending on the intensity of laser radiation, the biological response of the cell may lead to reversible or irreversible injury of the cell membrane, which results in the creation of new pores or enlargement of the already existing ones, through which efficient exchange between the cell content and the environment takes place. For adipocytes, the presence of pores promotes lipolysis, as a result of which the intercellular space is filled with the contents of the cells and their decay products (triglycerides, fatty acids, water and glycerol) [2,7]. The appearance in the intercellular space of such an immersion fluid contributes to the process of OC of adipose tissue [8]. However, application of this technique can be accompanied by necrosis of irradiated adipocytes. Thus, it is necessary to reduce the side effects of OC procedure.

The possibility of temperature monitoring within adipose tissue in a wide temperature range, from room to human body temperatures and above by using of thermosensitive luminescent upconversion nanoparticles (UCNPs) [NaYF$_4$:Yb^{3+}, Er^{3+}] [9]. The increase of luminescent intensity at high temperatures can be explained by OC associated with the phase transition of lipids. Application of optical clearing agents (OCAs) leads to a significant increase of detected intensity of laser-induced luminescence from the UCNPs. The obtained results confirm a high sensitivity of the luminescent UCNPs to the temperature variations within tissues and show a strong potential for providing of the controlled adipose tissue thermolysis. Also at immersion OC, a more reliable temperature measurement technique in tissues can be proposed by using luminescence from laser induced UCNPs.

The paper focuses on the technology of OC of abdominal fat tissue *ex vivo* using different complex hyperosmotic OCAs (dimethyl sulfoxide, diatrizoic acid, metrizoic acid, sucrose, and fructose solutions) and tissue permeability enhancers (fractional laser microablation and sonophoresis with various modes and their combinations). Kinetics and efficacy of the OC was evaluated using spatially resolved back reflectance measurements. Tissue morphology modification was monitored using the histological studies. Maximal clearing effect (83.5%) was observed for the samples subjected to the fructose-ethanol solution action during 90 min with gentle modes of fractional laser microablation and sonophoresis.

[1] V.V. Tuchin, I.Y. Yanina, G.V. Simonenko, Destructive fat tissue engineering using photodynamic and selective photothermal effects, Proc. of SPIE, 7179, 71790C-1–11 (2009).
[2] V.A. Doubrovskii, I.Yu. Yanina, V.V. Tuchin, Kinetics of Changes in the Coefficient of transmission of the adipose tissue in vitro as a result of photodynamic action, Biophysics 57 (1), 94–97 (2012).
[3] I.Yu. Yanina, N.A. Trunina, V.V. Tuchin, Photoinduced cell morphology alterations quantified within adipose tissues by spectral optical coherence tomography, J. Biomed. Opt. 18(11), 111407 (2013).
[4] C. Ma, C. Jian, L. Guo, et al, Adipose Tissue Targeting Ultra-Small Hybrid Nanoparticles for Synergistic Photodynamic Therapy and Browning Induction in Obesity Treatment, Small, 2308962 (2023).
[5] R. Chen, S. Huang, T. Lin, et al, Photoacoustic molecular imaging-escorted adipose photodynamic–browning synergy for fighting obesity with virus-like complexes, Nature Nanotechnology, 16(4), 455-465 (2021).
[6] R. Shrestha, P. Gurung, J. Lim, T.B. Thapa Magar, C.W. Kim, H.Y. Lee, Y.W. Kim, Anti-Obesity Effect of Chlorin e6-Mediated Photodynamic Therapy on Mice with High-Fat-Diet-Induced Obesity, Pharmaceuticals, 16(7), 1053 (2023).
[7] V.A. Dubrovskii, B.A. Dvorkin, I.Yu. Yanina, V.V. Tuchin, Photoaction upon adipose tissue cells in vitro, Cell and Tissue Biology. 5(5), 520–529 (2011).
[8] B. Alberts, D. Bray, J. Lewis, M. Raff, K. Roberts, J.D. Watson, Molecular biology of the cell. 2nded. Vol. 1. - New York, London: Garland Publishing. Inc., (1989).
[9] I.Yu. Yanina, E.K. Volkova, D.K. Tuchina, Ju.G. Konyukhova, V.I. Kochubey, V.V. Tuchin, Controlling of upconversion nanoparticle luminescence at heating and optical clearing of adipose tissue, Proc SPIE 10417-5, 1–7 (2017).

Optical coherence elastography for quantitative visualization of diffusion processes in biotissues

V.Y. Zaitsev[1*], A.A. Sovetsky[1], E.M. Kasianenko[1,2], A.L. Matveyev[1], A.A. Zykov[1],
Y.M. Alexandrovskaya[3]

1- A.V. Gaponov-Grekhov Institute of Applied Physics of the Russian Academy of Sciences, Nizhny Novgorod, Russia
2- National Research Center Kurchatov Institute, Moscow, Russia
3- Terra Quantum GmbH, Munich, Germany

* vyuzai@ipfran.ru

In this report we present an emerging application of Optical Coherence Tomography (OCT) based on mapping of strains induced by diffusion of osmotically active solutions into the depth of various biotissues as well as artificial tissue-like materials such a polyacrilamide gels. In recent years, processing of sequences of phase-sensitive OCT scans demonstrated high efficiency for imaging of mechanically produced strains in tissues for realization of Compression Optical Coherence Elastography (C-OCE) [1]. However, a similar principle can be applied for imaging strains of diverse origins (e.g. thermally-induced ones, drying-induced strains, etc.)

A new direction is OCE application for studying diffusion of various solutions which are often osmotically active, so that their penetration in tissues is accompanied by the development of osmotic strains [2,3]. OCE makes it possible to quantitatively monitor in real time the development of osmotically induced slow deformations (on time intervals from seconds to tens of minutes). Such observation may give new information about penetration in tissues of various drugs or osmotically-active solutions often used as optical clearing agents, such as solutions of glycerol. It was found that for many solutions, their diffusion in the tissue bulk is accompanied by the development of peculiar sign-alternating spatial patterns of strain. Depth positions of the visualized positive and negative strain extrema clearly demonstrate proportionality to the square root of the elapsed time, which is typical of diffusion processes. Monitoring of the extremum's position makes it possible to estimate the diffusion coefficient. It was demonstrated that the analysis of dynamics of osmotically-induced deformations can be used to diagnose difference in the cross-linking degree of polyacrylamide gels [3], whereas observations of magnitude and rate of osmotic strains caused by penetration of glycerol in cartilage samples was found to be dependent on the degree of degradation of proteoglycans in cartilage [4]. Application of a similar technique was demonstrated for observing tissue deformations caused by the development of crosslinks under the action of crosslinkers.

The reported results further extent the area of OCE applications beyond the most widely discussed [1] diagnostics of tissue types/states based on differences in their elastic properties.

[1] V.Y. Zaitsev, A.L. Matveyev, L.A. Matveev, A.A. Sovetsky, M.S. Hepburn, A. Mowla, B.F. Kennedy, Strain and elasticity imaging in compression optical coherence elastography: The two-decade perspective and recent advances, Journal of Biophotonics, 14(2), e202000257 (2021).
[2] Y. Alexandrovskaya, O. Baum, A. Sovetsky, A. Matveev, L. Matveev, E. Sobol, V. Zaitsev, Optical Coherence Elastography as a Tool for Studying Deformations in Biomaterials: Spatially-Resolved Osmotic Strain Dynamics in Cartilaginous Samples, Materials, V. 15, 904. (2022).
[3] Y.M. Alexandrovskaya, E.M. Kasianenko, A.A. Sovetsky, A.L. Matveyev, V.Y. Zaitsev, Spatio-Temporal Dynamics of Diffusion-Associated Deformations of Biological Tissues and Polyacrylamide Gels Observed with Optical Coherence Elastography, Materials, V. 16, 2036 (2023).
[4] Y.M. Alexandrovskaya, E.M. Kasianenko, A.A. Sovetsky, A.L. Matveyev, D.A. Atyakshin, O.I. Patsap, M.A. Ignatiuk, A.V. Volodkin, V.Y. Zaitsev, Optical coherence elastography with osmotically induced strains: Preliminary demonstration for express detection of cartilage degradation, Journal of Biophotonics, 1–15 (2024).

Enhanced spectral domain optical coherence tomography using a linear wavenumber spectrometer

Y. Cai[1], J. Zhang[2*]

1- School of Optoelectronic Engineering, Guilin University of Electronic Technology, China
2- School of Life and Environmental Sciences, Guilin University of Electronic Technology, China

* junzhang8819@gmail.com

In spectral-domain optical coherence tomography (SDOCT), conventional spectrometers, which use a grating and a line-scan camera, inherently suffer from nonlinear wavenumber responses. This nonlinearity reduces the sensitivity and axial resolution of OCT signals, necessitating post-processing to remap spectral interferograms into wavenumber functions. However, this approach is limited due to the uneven frequency spacing between the camera's pixels, which restricts the imaging range.

To address these challenges, we present a novel linear-wavenumber spectrometer design. Our design, employing a dual-prism and reflector arrangement, is cost-effective, straightforward, and significantly enhances the linearity of spectral dispersion in wavenumbers, a critical factor for SDOCT. We utilize iterative calculations through a global stochastic gradient descent method to effectively linearize higher-order dispersion. Compared to conventional designs, our method achieves a substantial improvement in wavenumber linearity for an 80 nm bandwidth at an 850 nm wavelength.

To verify this wavenumber linearity, we developed an accurate calibration method that uses the interference phase to determine the wavenumber of each pixel in the detection spectrum. Additionally, our new structure eliminates the need for resampling, enabling depth imaging at the Nyquist sampling limit. This advancement marks a significant improvement in spectrometer design for SDOCT, offering enhanced performance and resolution without the complexities and limitations of traditional systems.

Resonant dielectric nanoparticles for all-optical nanoscale heating and temperature sensing in cells

M.V. Zyuzin[1*], **E.N. Gerasimova**[1]

1- School of Physics and Engineering, ITMO University, 191002 St. Petersburg, Russia

* mikhail.zyuzin@metalab.ifmo.ru

Abstract: This study presents two innovative methods for accurate temperature monitoring during medical treatments, which could significantly reduce the risk of cell and tissue damage from overheating. We focus on optically-detected magnetic resonance (ODMR) and a unique thermally sensitive Stokes shift in Raman response for real-time monitoring during the delivery of bioactive compounds and photothermal therapy.

Maintaining the right temperature is crucial for controlling cellular functions and processes [1]. Uncontrolled temperature increases during therapies like photothermal treatment can disrupt cell metabolism, growth, and survival [2,3]. To mitigate these risks, our study utilizes nanostructured materials, enabling precise temperature control at the cellular level.

Our first investigated method uses the optically detected magnetic resonance (ODMR) of nanodiamonds with nitrogen-vacancy centers (NV-centers) [4]. These centers change frequency with temperature variations, allowing for precise monitoring when combined with drug carriers. By integrating gold nanoparticles (Au NPs) as heating agents and NV-centers as nanothermometers within one carrier, we have developed a system for controlled photoinduced drug delivery with built-in temperature regulation, and photothermal therapy *in vivo*. Our research shows that the placement of Au NPs and their concentration within delivery carriers' impact on required laser power density for carrier rupture, however, the temperature of carrier decomposition remains the same [5].

The second method involves thermally sensitive shifts in Raman response [6]. We explored the potential of optically resonant dielectric nanoparticles, particularly α-Fe_2O_3 NPs (NPs), and silicon (Si)/silicon-gold (Si-Au) NPs, as temperature sensors. Similarly to previous study, the α-Fe_2O_3, which heat up under light, have been incorporated into drug carriers, enabling synchronized drug release and temperature measurement. This approach allows us to precisely track and control the temperature at which these carriers release their payload inside cells [7].

Additionally, we investigated the use of Si and Si-Au nanoparticles in optical hyperthermia of cells. To apply Si NPs as optical heaters, they should possess a narrow size distribution to meet the critical coupling conditions. Typically produced by laser ablation, Si NPs often suffer from polydispersity. To address this, we combined plasmonic (Au) and dielectric (Si) nanostructures in a single platform, creating hybrid nanomaterials with enhanced optical heating capabilities and real-time temperature monitoring inside cells. Our results showed that these hybrid Si-Au NPs were more effective for optical hyperthermia in biological media [8].

In summary, our findings suggest that accurate temperature measurement at the cellular level can enhance the effectiveness and safety of modern medical treatments. Further research, especially *in vivo* studies, is needed to fully develop and validate these methods.

[1] M. Quintanilla, M. Henriksen-Lacey, C. Renero-Lecuna, L.M. Liz-Marzán, Challenges for optical nanothermometry in biological environments, Chem Soc Rev, vol. 51, no. 11, pp. 4223–4242, 2022.
[2] J. Zhou, B. del Rosal, D. Jaque, S. Uchiyama, D. Jin, Advances and challenges for fluorescence nanothermometry, Nature Methods, vol. 17, no. 10, pp. 967–980, 2020.
[3] C. Bradac, et al, Optical Nanoscale Thermometry: From Fundamental Mechanisms to Emerging Practical Applications, Adv Opt Mater, vol. 8, no. 15, p. 2000183, 2020.
[4] G. Kucsko, et al, Nanometre-scale thermometry in a living cell, Nature, vol. 500, no. 7460, pp. 54–58, 2013.
[5] E.N. Gerasimova, et al, Real-Time Temperature Monitoring of Photoinduced Cargo Release inside Living Cells Using Hybrid Capsules Decorated with Gold Nanoparticles and Fluorescent Nanodiamonds, ACS Appl Mater Interfaces, vol. 13, no. 31, pp. 36737–36746, 2021.
[6] G.P. Zograf, M.I. Petrov, S.V. Makarov, Y.S. Kivshar, All-dielectric thermonanophotonics, Advances in Optics and Photonics, vol. 13, no. 3, pp. 643–702, 2021.
[7] G.P. Zograf, et al, All-Optical Nanoscale Heating and Thermometry with Resonant Dielectric Nanoparticles for Controllable Drug Release in Living Cells, Laser Photon Rev, vol. 14, no. 3, p. 1900082, 2020.
[8] E.N. Gerasimova, et al, Single-Step Fabrication of Resonant Silicon-Gold Hybrid Nanoparticles for Efficient Optical Heating and Nanothermometry in Cells, ACS Appl Nano Mater, vol. 6, no. 20, pp. 18848–18857, 2023.

LASER SYSTEMS AND MATERIALS (INCLUDING OPTICAL FIBERS)

Optically pumped rare gas laser (OPRGL)

Yu.A. Adamenkov, M.A. Gorbunov, E.V. Kabak,
A.A. Kalacheva, V.A. Shaidullina, A.V. Yuriev

FSUE "RFNC-VNIIEF", 607190, Sarov, Mira prosp, 37

oefimova@otd13.vniief.ru

Optical pumped rare gas Laser (OPRGL) on metastable atoms of inert gases is new promising optical generator in which high quantum efficiency is combined with good optical quality of the output beam. The optical medium of the laser consists of a mixture of rare gases containing a buffer gas (usually helium) and a gas on the atoms of which generation occurs – Ne, Ar, Kr or Xe. The content of generating gas in the mixture ranges from 1 to 5%. Since receiving the first generation on inert gas atoms (Kr) in 2012 [1], studies of the active medium [2,3] have been carried out aimed at optimizing laser parameters, such as increasing the generation output and the efficiency of using optical pumping.

This paper presents the results of experiments on the study of a laser on a mixture of inert gases with optical pumping (OPRGL). Dependence of generation power on repetition frequency of discharge pulses and on gas mixture flow rate for medium 2% Ar + 98% He is presented. The results of generation study experiments for 2% Ar + 98% Ne medium are presented.

Pulse-periodic discharge was used to create active medium. During the experiments, the following parameters were varied: pressure and flow rate of the gas medium, transmission coefficient of the mirrors of the optical resonator, repetition rate of electric discharge pulses. The maximum generation power obtained in the experiments was 4.5 watts. Some experiments were carried out with neon acted as a buffer gas for argon instead of helium.

[1] J. Han and M.C. Heaven, Gain and lasing of optically pumped metastable rare gas atoms, Optics Letters. – 2012. – Vol. 37, No. 11, pp. 2157-2159.

[2] P. Sun, D. Zuo, P.A. Mikheyev, J. Han, M.C. Heaven, Time-dependent simulations of a CW pumped, pulsed DC discharge Ar metastable laser system, Opt. Express, 27, 22289 (2019).

[3] П.А. Михеев, Лазеры на метастабильных атомах инертных газов с оптической накачкой, «Квантовая электроника» – 2015, 45, № 2.

Multimode-diode-pumped watt-level bismuth-doped fiber lasers and amplifiers

S.V. Alyshev[1*], **M.A. Melkumov**[1], **S.V. Firstov**[1]

1- Prokhorov General Physics Institute of the Russian Academy of Sciences, Dianov Fiber Optics Research Center, 38 Vavilov str., 119333 Moscow, Russia

* sergevlad@gmail.com

Bismuth-doped laser-active fibers have come a long way since the first Bi-doped fiber laser was reported in 2005 [1]. The unique properties of these media allowed researchers to demonstrated lasers and optical amplifiers operating in a broad range starting from around 1270 nm and going up to 1775 nm. The next logical step in the development of the Bi-Doped Fiber Lasers and Amplifiers (BDFLs, BDFAs) would be the scaling up the output power, which goes hand in hand with the utilization of more powerful pump sources. This would necessitate the usage of multimode high aperture diodes, which only can be used if pumping into the cladding of a fiber is possible. The realization of cladding pumped Bi-doped devices is met with difficulties stemming from the fact that that the addition of Bi into the core leads not only to the creation of Bismuth-related active centers (BACs) but also to the increase of the background loss, which grows faster than linearly with the increase of the total Bi concentration. Thus, doping with Bi beyond a certain limit is counterproductive, and results in very inefficient devices. On the other hand, this meant that cladding absorption of pump radiation at wavelengths suitable for pumping in the metastable level, which had been utilised for core-pumped devices, would unlikely be at an acceptable level.

Those difficulties notwithstanding, the solution was found, which entailed the utilization of pumping into a higher-laying pump layer. This approach provides two advantages. First, the pump wavelengths conveniently fall into the 800-nm range, where high-power multimode diodes are commercially available. Secondly, the BACs' absorption at these wavelengths is much higher. These two factors allowed us to develop cladding pumped amplifiers, which at very least have performance on par with their core-pumped counterparts, while having slight improvements on noise performance due to the possibility of achieving higher inversion levels [2]. On the lasers side, it was also possible to achieve lasing, albeit, with very small efficiency. After optimization of inner cladding geometry, the efficiency of the lasers reached a level of 3 to 5% with the output power of 260 mW [3].

At the conference we are going to present our further improvements on the matter, which allowed us to reach 0.8 W (and more) of output power.

[1] E. Dianov, V. Dvoyrin, V. Mashinsky, A. Umnikov, M. Yashkov, A. Gur'yanov, CW bismuth fibre laser, Quantum Electron. 35(1), 1083-1084 (2005).

[2] A. Vakhrushev, A. Khegai, S. Alyshev, K. Riumkin, A. Kharakhordin, E. Firstova, A. Umnikov, A. Lobanov, F. Afanasiev, A. Guryanov, M. Melkumov, S. Firstov, Cladding pumped bismuth-doped fiber amplifiers operating in O-, E-, and S-telecom bands, Opt. Lett. 48, 1339-1342 (2023).

[3] A. Vakhrushev, Y. Ososkov, S. Alyshev, A. Khegai, A. Umnikov, F. Afanasiev, K. Riumkin, E. Firstova, A. Guryanov, M. Melkumov, S. Firstov, Output Power Saturation Effect in Cladding-Pumped Bismuth-Doped Fiber Lasers, Journal of Lightwave Technology, 41(2), 709-715, (2023).

Factors affecting the radiation resistance of optical fibers exposed to ionizing radiation

I. Azanova[1*], **Yu. Sharonova**[1], **E. Lunegova**[1], **D. Khisamov**[1]

1- Open Joint-stock company "Perm Scientific-Industrial Instrument Making Company"

* azanova@pnppk.ru

Silica-based optical fibers (OF) are widely applied in various industries for telecommunication, monitoring systems and fiber-based sensors. There are severe and harsh environments, which associated with ionizing radiation. When optical fibers are under ionizing radiation it causes generation of optically active point defects – radiation color centers (RCC), which absorb light at different wavelengths. The phenomenon of the optical absorption caused by colour centers is known as radiation induced attenuation (RIA).

When using optical fibers in fiber-based systems, a certain budget for optical losses is included. This budget is determined by the optical power of the light-source and the dynamic range of the photodetector so that the total optical losses in the system do not exceed this budget over the entire operating temperature range. The loss budget includes losses at welded splices and connections, optical attenuation along the length of the optical fiber, an increase in optical attenuation caused by increased or decreased temperatures and mechanical deformations. RIA is also a part of this budget, so there is necessarily a total limit on RIA. RIA depends not only on the total ionizing dose, dose rate, type of radiation, but also on such operational factors as temperature, an operating wavelength, injected optical power level, level of stress-strain state of the optical fiber. The purpose of this work is to show the influence of operational factors on RIA levels.

Operating wavelength. The most common types of OF are germanium-doped (GeO_2) or pure-silica core (PSC) (SiO_2) fibers. For both types of fibers, the most disadvantageous wavelength for application in radiation environments is 850 nm, as opposed to the wavelength of 1550 nm, where RIA levels are minimal. It should be noted that the wavelength of 1550 nm has minimum losses at the hall range from 200 to 1700 nm [1,2].

Temperature and injected optical power. The RIA of optical fibers is determined by the operation temperature as well as by the injected optical power level. For same injected optical power 0.1 µW at same operating wavelength the difference in RIA levels for temperatures +25°C and -60°C can reach more than 10 dB/km. At the same time, by increasing the optical power level to 1-5 mW, this difference could be significantly reduced [3].

Dose rate through the example of anisotropic OF "Panda". To use OF in space it has to work at the dose rate about 10-5 Gy/s. Furthermore, to cut the time tests are usually carried at a significantly higher dose rate at about 100 Gy/s. However, for some applications there is a need to know under real irradiation conditions at average dose rates [4]. The tests results of RIA levels in the anisotropic OF "Panda" with SiO_2 core have been obtained at the dose rate from 0.05 to 350 Gy/s. So, the RIA predictably increases with increasing the dose rate, but it should be noted that, starting with the dose rate of 10 rad/s, no correlation is observed.

Thus, the conscious choice of the operating wavelength, environment temperature and injected optical power allows us to reduce the RIA levels during exploitation.

[1] S. Girard, et al, Radiation effects on silica-based optical fibers: Recent advances and future challenges, IEEE Transactions on Nuclear Science, vol. 60, pp. 2015-2036, (2013).
[2] P. Kashaykin, A. Tomashuk, V. Khopin, et al, Gamma Radiation Induced Attenuation in Ge-doped Fibers in Near IR Range: Influence of Irradiation Temperature and Doping Level, GeY-center, OSA Advanced Photonics Congress, (2018).
[3] A. Paveau, G. Cros, S. Masson, R. Mangeret, S. Marioujouls, J.J. Bonnefois, Robustness of Astrix Fiber Optic Gyros in space radiative environment, CEAS Space Journal, №11, pp. 219-227. (2018).
[4] E. Friebele, M. Gingerich, D. Griscom, Survivability of optical fibers in space, Optical materials reliability and testing: Benign and adverse environments, International Society for Optics and Photonics, vol. 1791, pp. 177-189, (1993).

Fiber optic magnetometer on SPUN fiber

A. Chuvyzgalov[1]*, D. Gilev[1], V. Maksimenko[1], K. Ovchinnikov[1], V. Krishtop[1]

1- Perm National Research Polytechnic University. 614990, Perm region, Perm

* chuvyzgalov_anton@mail.ru

The paper presents the possibility of using a Sagnac optical circuit with a 3×3 divider as an optical magnetometer, as well as interference interactions in a 3×3 fiber-optic divider in the optical circuit of a magnetometer on SPUN fiber. The field applied to the sensitive region of the SPUN fiber circuit makes it possible to control the Sagnac phase, and, therefore, knowing the Sagnac phase, one can judge the magnitude of the applied magnetic field. This design of the magnetometer makes it possible not to use Faraday mirrors, which makes it possible to use the magnetometer under more severe conditions.

Cr^{2+} - Fe^{2+} ions interaction in ZnSe based solid solutions

M.E. Doroshenko[1*], H. Jelinkova[2]

1- Prokhorov General Physics Institute of the Russian Academy of Sciences, 119991, Vavilov Str. 38, Moscow, Russia
2- Czech Technical University, Břehová 7, 115 19 Prague, Czech Republic

* dorosh@lst.gpi.ru

ZnSe crystals doped with divalent chromium and iron ions are actively used for the development of widely tunable mid-IR lasers. Recently, noticeable progress in the maximal output power and efficiency of these lasers was achieved. An output power in excess of 10 W with an efficiency of over 40% and a pulsed energy of over 1 J were demonstrated for ZnSe:Fe^{2+} [1,2]. The main disadvantage of Fe^{2+}-based lasers is the need for relatively complex pump sources operating around 3 μm. One of the alternatives to the development of new simple and efficient pump sources might be the utilization of Cr^{2+} co-doping of known Fe^{2+} doped matrices, and the pumping of chromium ions by a number of commercially available pump sources within the 1500-2300 nm range together with fast nonradiative transfer of excitation energy to iron ions. The possibility of quite efficient Cr^{2+}→Fe^{2+} energy transfer in ZnSe crystal was discussed earlier, but strong competition with Fe^{2+} ion fluorescence quenching by Cr^{2+} ions [3] has not yet permitted the lasing of Fe^{2+} ions in this particular crystal. However, such lasing has already been demonstrated for ZnSe-based solid solutions of Zn$_{1-x}$Mn$_x$Se and Zn$_{1-x}$Mg$_x$Se type co-doped with Cr^{2+} and Fe^{2+} ions [4].

The possible formation of Cr^{2+} and Fe^{2+} clusters and the influence of such clustering on the TM ion spectroscopic properties have been previously discussed. Similar Cr^{2+}-Fe^{2+} clusters will be shown to form in this study. Their strong influence on both Cr^{2+} ions spectroscopic properties and, consequently, the Cr^{2+}→Fe^{2+} energy transfer process will be presented. As an example, Fig.1 illustrates the position of the Cr^{2+} ions absorption maximum across a wide temperature range for Cr^{2+}-only-doped and Cr^{2+},Fe^{2+}-co-doped Zn$_{1-x}$Mn$_x$Se solid solutions. A striking difference in the position and temperature behaviour of the Cr^{2+} ions in co-doped sample (upper graph in Fig.1b) can be easily observed. The process of Cr^{2+}-Fe^{2+} ions cluster formation, depending on TM ion concentrations, spectroscopic properties, and their influence on Cr^{2+}→Fe^{2+} energy transfer and Fe^{2+} ions fluorescence quenching, will be presented and discussed.
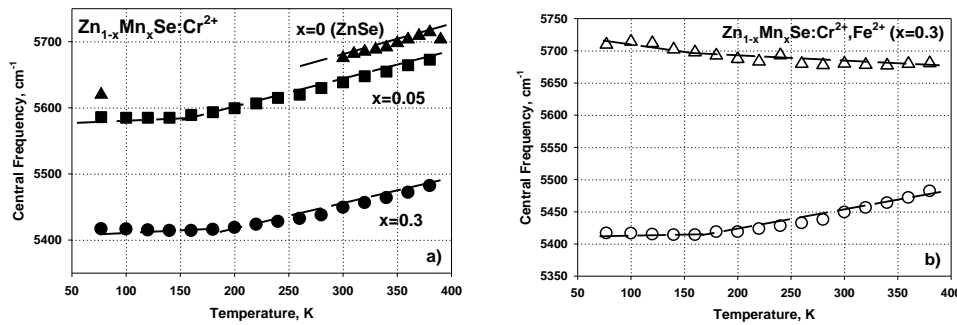

Fig.1. Position of Cr^{2+} ions absorption maximum at different temperatures in Zn$_{1-x}$Mn$_x$Se crystal doped only with Cr^{2+} ions (a) and in Cr^{2+},Fe^{2+} co-doped crystal (b).

[1] S.B. Mirov, et al, Frontiers of Mid-IR Lasers Based on Transition Metal Doped Chalcogenides, in IEEE Journal of Selected Topics in Quantum Electronics, vol. 24, no. 5, pp. 1-29, Sept.-Oct. 2018, Art no. 1601829.
[2] K.N. Firsov, et al, Laser on single-crystal ZnSe:Fe^{2+} with high pulse radiation energy at room temperature, Laser Phys. Lett. 13 015002 (2016).
[3] V. Fedorov, et al, Energy transfer in iron-chromium co-doped ZnSe middle-infrared laser crystals, Opt. Mater. Express 9, 2340-2347 (2019).
[4] A. Říha, et al, Diode-pumped Cr-doped ZnMnSe and ZnMgSe lasers, Proc. SPIE 10603, Photonics, Devices, and Systems VII, 1060312 (1 December 2017).

Stimulated emission in HgCdTe heterostructures with quantum wells in 3 – 5 µm spectral window

**A. Dubinov[1*], K. Kudryavtsev[1], M. Fadeev[1], V. Utochkin[1], A. Razova[1],
A. Yantser[1], K. Mazhukina[1], D. Shengurov[1], N. Gusev[1], N. Mikhailov[2],
S. Dvoretskii[2], V. Rumyantsev[1], S. Morozov[1]**

1- Institute of Microstructure Physics RAS, Nizhny Novgorod, 603087, Russia
2- Institute of Semiconductor Physics RAS, Novosibirsk, 630090, Russia

* sanya@ipmras.ru

Hg(Cd)Te/CdHgTe heterostructures with narrow quantum wells (QWs) are one of the promising materials for lasers in the mid-infrared range. The quasi-hyperbolic dispersion law of charge carriers provides a noticeable suppression of non-radiative Auger processes in such structures. Previously, stimulated emission (SE) was obtained in HgCdTe QWs in the wavelength range from 2 to 31 µm [1,2].

In this work, we focus on the range of 3–5 µm, a window of atmospheric transparency containing a large number of absorption lines of trace atmospheric gases. We study losses in waveguide HgCdTe heterostructures and balance the number of QW in the active region to achieve the best performance of a laser structure [3]. We show that non-threshold Auger processes may have a greater contribution to the overall recombination rate than expected before and then work out the optimal structure design by analysing the photoluminescence intensity dependence on temperature [4]. The results allowed us to achieve stimulated emission in the vicinity of 3.55 µm approaching room temperature operation (290 K).

Using laser or explosive lithography and ion etching methods microdisk, microring and stripe-shaped optical cavities were formed from Hg(Cd)Te/CdHgTe QWs heterostructures. Etching was carried out with argon ions. Photoresist and metal masks (Al or Cr/V/Ni) were compared to figure out the best mask type. Finally, we demonstrate laser action under optical pumping in the temperature range attainable by Peltier cooling. However, in all mesa structures the maximum operating temperature T_{max} decreases by an average of 30–40 K compared to T_{max} of the original unprocessed structures. The T_{max} drop is attributed to increase in the optical losses, which are negligible in the macroscopic samples providing SE. In addition, surface recombination and defects appearing after ion etching process are also believed to make an impact. However, laser emission in best mesastructures persists up to 230 K and the integral power of optical pumping for a 50 µm microdisk is estimated to be about 1 W, which is achievable for commercial semiconductor diode lasers. Thus, the results of the work pave the way to optically pumped converters operating in 3–5 µm spectral window under thermoelectric cooling.

[1] S.V. Morozov, V.V. Rumyantsev, M.S. Zholudev, et al, Coherent Emission in the Vicinity of 10 THz due to Auger-Suppressed Recombination of Dirac Fermions in HgCdTe Quantum Wells. ACS photonics 8 (12), 3526 (2021).
[2] A.A. Andronov, Yu.N. Nozdrin, A.V. Okomel'kov, A.A. Babenko, V.S. Varavin, D.G. Ikusov, R.N. Smirnov, Stimulated radiation of optically pumped $Cd_xHg_{1−x}$Te-based heterostructures at room temperature. Semiconductors 42 (2), 179 (2008).
[3] M.A. Fadeev, A.A. Dubinov, A.A. Razova, et al, Balancing the Number of Quantum Wells in HgCdTe/CdHgTe Heterostructures for Mid-Infrared Lasing. Nanomaterials 12 (24) (2022).
[4] K.E. Kudryavtsev, A.A. Yantser, M.A. Fadeev, et al, Quantifying non-threshold Auger-recombination processes in mid-wavelength infrared range HgCdTe quantum wells. Applied Physics Letters 123 (18) (2023).

Comb generation in fiber laser with integrated ring microcavity

Yu. Gladush[1*], A. Mkrtchyan[1], A. Netrusova[1], M. Mishevsky[1],
Z. Ali, N. Dmitriev, S. Minkov, I. Bilenko[2], A. Nasibulin[1]

1- Skolkovo institute of science and technology, Moscow, Russia
2- Russian quantum center, Moscow, Russia

* y.gladush@skoltech.ru

Optical combs generator, a device that provide a wide spectrum consisting of narrow equidistant lines, finds many applications, including optical clocks, coherent communications, optical coherence tomography, dual comb spectroscopy, etc. Traditional source of the comb is a mode-locked laser, for which a distance between comb lines (FSR) is defined by length of the resonator and usually reaches tens of MHz. Another approach for comb generation is based on the integrated microring resonators with high quality factor exceeding 10^6 [1]. Here the microring is pumped by CW light in one of the resonances which leads to the comb formation due to four wave mixing mechanism. This type of comb usually provides FSR from 50 GHz to 1 THz, but suffers from low CW to comb conversion efficiency, requires expensive sweeping laser and suffers from low stability.

One of the solutions to overcome these limitations suggests integrating microcavity into the fiber laser resonator. By merging the properties of fiber laser and microcavity it was demonstrated 150 nm wide soliton combs with 75% pump to comb efficiency [2]. In these work authors used four-port ring resonator inside fiber laser ring cavity. Emission from the fiber laser propagated through one buss waveguide to the microcavity and returned from another drop-port waveguide.

We suggest significant simplification of the scheme by utilizing the two-port integrated chip with microcavity working as a reflecting mirror in fiber laser resonator (see Fig. 1a). Here laser resonator is formed by the gold mirror on one side and microring resonator on the other. In the microring directly propagating comb give rise to the counter propagating comb due to Rayleigh scattering, which goes back into the laser cavity forming an optical feedback. With this approach we show robust self-starting soliton comb generation with spectral width more than 400 nm, which greatly exceeds erbium amplification window (see Fig. 1b).
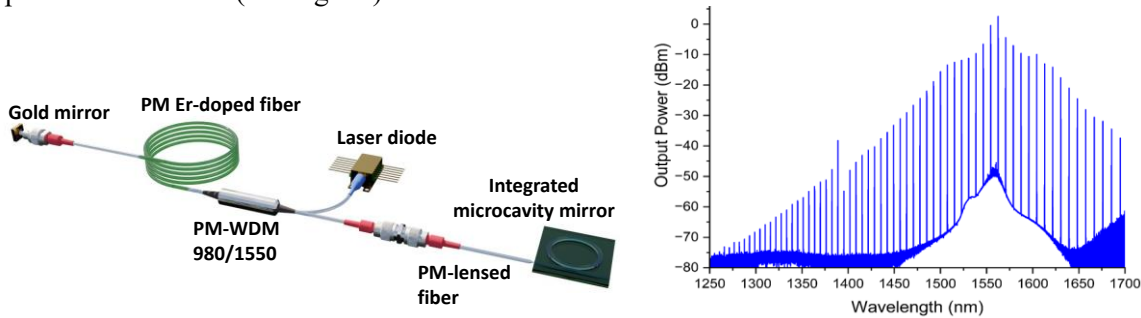

Fig. 1. (a) Scheme of the fiber laser with microring cavity (not in scale); (b) Spectrum of the optical comb on the output of laser.

[1] T.J. Kippenberg, R. Holzwarth, S.A. Diddams, Microresonator-Based Optical Frequency Combs, Science 80., 332, 6029, 555–559, (2012).
[2] H. Bao, et al, Laser cavity-soliton microcombs, Nat. Photonics 136, 13, 6, pp. 384–389, (2019).

Gas fiber lasers: recent advances and prospects

A.V. Gladyshev

Prokhorov General Physics Institute of the Russian Academy of Sciences, Dianov Fiber Optics Research Center, 38 Vavilov st., Moscow, Russia, 119991

alexglad@fo.gpi.ru

In recent years, gas fiber lasers (GFLs) have shown rapid progress. An active medium of such lasers is based on gas-filled hollow-core fibers (HCFs), thus providing wide opportunities in generating laser radiation at various wavelengths. Moreover, the GFLs open up the possibility of achieving high peak and/or average powers that exceed the damage threshold of any solid-core fibers.

Depending on the gas that fills the HCF, the GFLs can be divided into two types: 1) the Raman GFLs, which implement stimulated Raman scattering to transfer the pump power to longer wavelengths, and 2) the GFLs based on population inversion.

The Raman GFLs have demonstrated great potential for high-power operation with average output power now as high as 110 W [1]. Moreover, the Raman GFLs enabled a convenient way of generating ultrashort pulses in the mid-IR [2] and allowed mid-IR supercontinuum generation in HCFs [3].

The population inversion GFLs appeared to be convenient for continuous-wave operation. This type of GFLs have demonstrated the output powers as high as 8 W at the wavelength of 3.1 μm [4].

The vast majority of the population inversion GFLs demonstrated so far required *optical* pumping by other laser sources (Fig. 1a). Strictly speaking, such GFL scheme presents not a generator, but only an optical *converter* of the pump radiation. The progress in *generating* of laser radiation inside a HCF has been achieved very recently by demonstrating the first GFLs pumped by a 2.45-GHz microwave *gas discharge* (Fig. 1b) [5,6].

These results open up new opportunities for laser generation at various wavelengths from ultraviolet to mid-infrared that are hardly accessible by other methods.
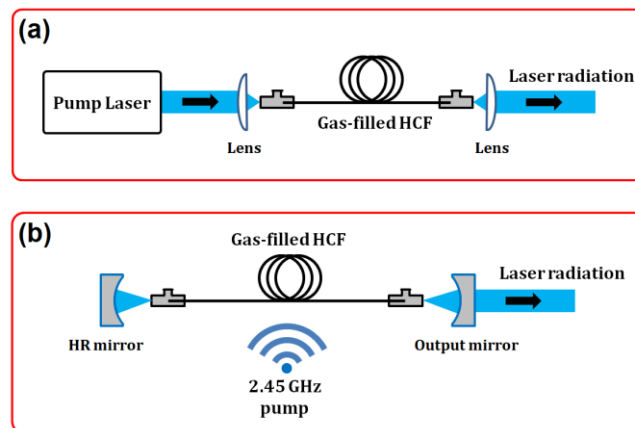

Fig. 1. The schemes of gas lasers based on hollow-core fibers (HCF):
(a) Commonly used optical converter of the pump laser radiation.
(b) Recently demonstrated optical generator.

[1] Y. Cui, et al, A 110 W fiber gas Raman laser at 1153 nm, High Power Laser Science and Engineering, vol. 11, p. e10, (2023).
[2] A. Gladyshev, et al, Mid-infrared 10-μJ-level subpicosecond pulse generation via stimulated Raman scattering in a gas-filled revolver fiber, Opt. Mater. Express, vol. 10, pp. 3081–3089, (2020).
[3] A. Gladyshev, et al, Mid-Infrared Lasers and Supercontinuum Sources Based on Stimulated Raman Scattering in Gas-Filled Hollow-Core Fibers, IEEE J. Sel. Top. Quantum Electron., vol. 30(6), Art no. 1400207, (2024).
[4] W Huang, et al, Fiber laser source of 8 W at 3.1 μm based on acetylene-filled hollow-core silica fibers, Opt. Lett., vol. 47(9), pp. 2354-2357, (2022).
[5] A. Gladyshev, et al, Gas-Discharge Fiber Laser with Microwave Pumping, Bull. Lebedev Phys. Inst., vol. 50, pp. 403–408, (2023).
[6] A. Gladyshev, et al, Gas-Discharge He-Xe Fiber Laser, IEEE J. Sel. Top. Quantum Electron., vol. 30(6), Art no. 0900107, (2024).

Research progress of Bi-doped silica-based fibers for wide-band amplifier and laser application in SIOM

M. Guo[1], **J. Tian**[1,2], **X. Li**[1,3], **F. Wang**[1], **Y. Wang**[1], **C. Yu**[1,3,4*], **L. Hu**[1,3,4*]

1- Advanced Laser and Optoelectronic Functional Materials Department, Special Glasses and Fibers Research Center, Shanghai Institute of Optics and Fine Mechanics, Chinese Academy of Sciences, Shanghai 201800, China
2- School of Physical Sciences, University of Science and Technology of China, Hefei 230026, China
3- Center of Materials Science and Optoelectronics Engineering, University of Chinese Academy of Sciences, Beijing 100049, China
4- Hangzhou Institute for Advanced Study, University of Chinese Academy of Sciences, Hangzhou 310024, China

* sdycllcy@163.com, * hulili@siom.ac.cn

In order to meet the growing demand of communication capacity, bismuth-activated glass fibers with broadband near-infrared luminescence (1000–1800 nm) covering the second communication window are considered promising candidates for a new generation of wide-band amplifiers and tunable lasers. Significant progress has been made in the development of Bi-doped silica-based fibers (BDF) abroad. Nowadays, the Bi-doped fiber amplifiers and lasers have been systematically studied aboard, and thus to hatch series of products.

Since 2021, some breakthroughs of Bi-doped fiber amplifiers and lasers have been made in SIOM [1-5]. We achieved the optical amplification in the O, E, S and U band based on the homemade BDFs. Based on the highly phosphorous and bismuth co-doped silica fiber (BPDF), a maximum gain of 38.3 dB at 1330 nm was obtained in the double pass setup for a signal power of -30 dBm and pump one of 785 mW at 1240 nm. For the E+S-band amplification, a gain coefficient as high as 1.57 dB/m and a maximum gain of 39.3 dB were achieved using only 25 m lowly germanium and bismuth co-doped silica fiber (BGDF). For the highly germanium and bismuth co-doped silica-based fiber (Hi-BGDF), we proposed that germanium oxygen vacancy defects play a pivotal role in promoting the formation of the bismuth near-infrared active luminescence centers BAC-Ge [6]. According to the above mechanism, we built a U-band fiber amplifier based on the home-made Hi-BGDF. A maximum gain of 31.8 dB at 1750 nm was measured when the pump power was 936 mW at 1550 nm. More importantly, a gain coefficient as high as 0.48 dB/m at 1750 nm with a maximum gain above 23 dB was obtained based on another Hi-BGDF with higher absorption coefficient.

In addition, we achieved laser output based on above BDFs. Furthermore, a single-frequency fiber laser (SFFL) operating at 1440 nm based on BGDF has been obtained for the first time. A maximum slope efficiency of 16.4% and output power of 133 mW at 1313 nm were achieved with 96 m BPDF in a linear cavity structure. For the SFFL at 1440 nm, the maximum single-longitudinal-mode laser output power of about 6 mW was obtained with an OSNR of more than 75 dB. Based on the Hi-BGDF, the output power of 48 mW at 1720 nm was achieved with an OSNR of 60 dB in a linear cavity structure.

[1] M. Guo, J. Tian, F. Wang, et al, Amplification in E band based on highly phosphorus and bismuth co-doped silica fiber, Chinese Journal of Luminescence, vol.4, pp. 478-481, (2022).
[2] J. Tian, M. Guo, F. Wang, et al, High gain E-band amplification based on the low loss Bi/P co-doped silica fiber, Chinese optics Letters, vol.20, pp. 100602, (2022).
[3] J. Tian, M. Guo, F. Wang, et al, High gain optical amplification and lasing performance of the Bi/P co-doped silica fiber in the O-band, Chinese optics Letters, vol.21, pp. 050601, (2023).
[4] M. Guo, J. Tian, F. Wang, et al, E+S-band amplification based on the homemade germanium and bismuth co-doped silica fiber, Chinese Journal of lasers, vol. 50, pp. 0616002, (2023).
[5] M. Guo, J. Tian, F. Wang, et al, Domestic high germanium bismuth-doped silica-based fiber for high gain U-band amplification, Chinese Journal of lasers, vol. 50, pp. 2416006, (2023).
[6] X, Li, M, Guo, C, Shao, et al, Broadband L+ near-infrared luminescence in bismuth/germanium co-doped silica glass prepared by the sol–gel method, Journal of Materials Chemistry C, vol.11, pp. 16152–16158, (2023).

Enhanced stability in WGM microresonator coupling using reinforced tapered fiber

__K.N. Min'kov__[1,2*], D.D. Ruzhitskaya[1], K.E. Lakhmanskiy[1,2], O.V. Borovkova[1,3]

1- Russian Quantum Center,121205, Moscow, Skolkovo, Innovation Center territory
2- Moscow Institute of Physics and Technology, Dolgoprudny, Russia
3- Faculty of Physics, Lomonosov Moscow State University, 119991 Moscow, Russia

* k.minkov@rqc.ru

This study introduces a method for reinforcing tapered fibers to ensure stable coupling with whispering gallery mode (WGM) microresonators. It has been found that a slight curvature in the tapered fiber enhances its fixation, thereby preventing adhesion between the fiber and the microresonator. Experimental evidence demonstrates the successful excitation of WGMs using a reinforced curved tapered fiber with a curvature radius of approximately 15 mm.

Optical microresonators have diverse applications in optoelectronics and quantum computing, including their use in optical comb generators, narrowband laser sources, and visible-range LIDAR systems [1]. Practical implementations require that both the microresonators and their associated coupling elements, which are essential for exciting the microresonator, maintain stable properties and fixed configurations.

Various coupling methods exist for optical microresonators [2]. The most effective techniques involve the tunneling of an evanescent field from either a prism coupler or a tapered fiber to the whispering gallery mode of an optical microresonator [3]. Tapered fibers are advantageous because they can operate in a single-mode regime, facilitating the achievement of critical coupling. However, there are challenges in adjusting and operating tapered fibers. Tightly stretched tapered fibers are prone to vibrations and can even adhere to the microresonator, disrupting the conditions necessary for the excitation of whispering gallery modes.

In this study, we present a method for securing tapered fibers that prevents undesirable vibrations and adhesion to the microresonator's lateral surface. The tapered fiber is produced using a fully automated version of the technique described in [4], allowing the creation of subwavelength tapered fibers with adiabatic properties along their length. This method enabled the fabrication of a quartz tapered fiber with a waist diameter of 400 nm and a length of up to 100 mm. The automated process ensures a transmission loss of 0.4 dB at a wavelength of 1550 nm.

Initially, the fabricated tapered fiber was fixed on a stand to form an arc, and then it was securely anchored. The curvature radius of the fabricated fiber is approximately 15 mm. Notably, this slightly bent waveguide does not exhibit vibrations or adhere to the microresonator. The quartz fiber's high stiffness helps maintain its curved shape. Experimental results demonstrate the excitation of WGMs at telecom wavelengths using the reinforced curved tapered fiber.

In summary, we propose a microresonator coupling element that utilizes a curved tapered fiber approaching the microresonator. We have developed a fabrication and fixation technique for this fiber on a stand. Our experimental results demonstrate the excitation of whispering gallery modes (WGMs) at telecom wavelengths using the reinforced curved tapered fiber, which has a curvature radius of approximately 15 mm.

[1] K.J. Vahala, Optical microcavities, Nature, Vol. 424, pp. 839-846, (2003).
[2] P. Solano, et al, Optical Nanofibers: A New Platform for Quantum Optics, Adv. At. Mol. Opt. Phys., 66, 439–505, (2017).
[3] M.L. Gorodetsky, Optical Microresonators with Giant Quality- Factor, Fizmatlit, (2011).
[4] A.D. Ivanov, K.N. Min'kov, A.A. Samoilenko, Method of producing tapered optical fiber, Journal of Optical Technology, Vol. 84, Issue 7, pp. 500-503, (2017).

The emission and laser properties of Nd^{3+} doped silica glass and fiber around 900 nm

L. Hu

Shanghai Institute of Optics and Fine Mechanics, Chinese Academy of Sciences, China

hulili@siom.ac.cn

900 nm laser has potential applications in biomedical imaging, deep sea measurement and material processing. In this talk, firstly, the effect of halogen ion co-doping and temperature on the emission properties at 900 nm and 1060 nm of Nd^{3+} ions in silica glass will be given. Then, the laser properties of around 900 nm both in CW and ML in Nd^{3+} doped silica fibers will be discussed.

Monolithic growth of GaAs templates on silicon

I. Ilkiv[1*], V. Lendyashova[1,2], D. Kirilenko[3], G. Cirlin[1,2,4]

1- St. Petersburg State University, St. Petersburg 199034, Russia
2- Alferov University, St. Petersburg 194021, Russia
3- Ioffe Institute, St. Petersburg 194021, Russia
4- Institute for Analytical Instrumentation RAS, St. Petersburg 198095, Russia

* fiskerr@ymail.com

The integration of direct-bandgap III–V material components on Si platforms have been considered as promising solutions to achieve practical on-chip light-emitting sources on Si and the implementation of Si photonic integrated circuits. The most common approach relies on the bonding of Si and III–V wafers. Although the effectiveness of the method was repeatedly demonstrated and commercial devices have been already presented, the bonding process remains complex and expensive. Therefore, utmost attention is paid toward the monolithic integration of III–V materials on Si substrates by direct epitaxial growth, which is more cost-effective and scalable. Unfortunately, due to high lattice mismatch and differences in expansion coefficients, the direct growth of III-V materials on Si substrates generally faces the challenges concerning the formation of anti-phase domains, threading dislocations, and micro-cracks. To obtain a high quality of material, great attention has been given to develop special tricks, including the growth of the thick buffer with several filter layers, different variations of selective area growth, utilizing of misoriented Si(100) substrates, confined epitaxial lateral overgrowth, as well as migration-enhanced epitaxy growth. Meanwhile, one-dimensional quantum dots (QDs) are known to be relatively tolerant of defects and dislocations due to the effective strain relaxation. In this regard, the use of QDs opens up the possibilities for reducing total thicknesses of GaAs buffers on Si and achieving an efficient light source.

In this study, we report on the growth of relatively thin GaAs layers of on silicon substrates by molecular beam epitaxy. Various GaAs buffer layers were grown on Si(100) and 2-4° off-axis Si(100) substrates. The impact of the growth of Si buffer layer as well as of its high-temperature annealing on the propagation of inversion boundaries in subsequently grown GaAs layers is extensively studied by atomic-force and transmission electron microscopy.
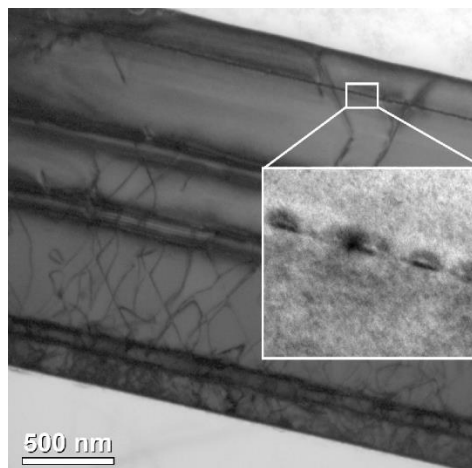
Fig.1. Cross-sectional transmission electron microscope image of QDs layer grown on GaAs/Si(100) template.

Using this GaAs buffer layers as a virtual substrates InAs/InGaAs QD in well heterostructures were fabricated (see Fig.1). Photoluminescence studies of the samples grown revealed efficient emission from InAs QDs at a wavelength of 1.25 μm at room temperature. These results can be a major step towards monolithic integration of III–V based light-emitters on Si.

The correlation of SHG responses with the (M) cation in TbM$_3$(BO$_3$)$_4$ (M = Al, Sc, Ga) orthoborates

A.Y. Jamous[1,2*], **A.B. Kuznetsov**[2], **V.A. Svetlichnyi**[1], **A.E. Kokh**[2]

1- Tomsk State University, Tomsk 634050, Russia
2- Sobolev Institute of Geology and Mineralogy SB RAS, Novosibirsk 630090, Russia

* ammarjamous2@gmail.com

The widespread use of laser devices in various industries, medicine, communication systems, etc., up to small household appliances, requires the improvement and optimization of the physical parameters and structural qualities of known optical materials that have already proven themselves in practice, with further control of their properties. Borate-based crystals due to their unique properties, such as a wide range of transparency, high threshold of laser destruction, physical and chemical stability, high thermal conductivity, etc., are widely used for nonlinear optic and laser technology [1]. Moreover, borates are characterized by an extremely wide variety of chemical composition and crystal structure, which provides a wide opportunity to search for and create new nonlinear optical crystals based on them. Among them one can highlight the complex rare-earth orthoborates with the general formula LnM$_3$(BO$_3$)$_4$ (Ln = La–Lu, Y; M = Al, Ga, Sc, Cr, Fe), which for some Ln and M belong to the huntite family (huntite CaMg$_3$(CO$_3$)$_4$, space group R32). Pure and activated LnM$_3$(BO$_3$)$_4$ compounds as well as their-based solid solutions are promising materials for lasers, nonlinear optics, spintronics, and photonics, which are characterized by multifunctional properties depending on a composition and crystal structure [2].

In this work, the second harmonic generation (SHG) response in new terbium orthoborates TbM$_3$(BO$_3$)$_4$ (M = Al, Ga, Sc) crystals are investigated. In particular the influence of the nature of the M cation on SHG efficiency. Both TbAl$_3$(BO$_3$)$_4$ and TbGa$_3$(BO$_3$)$_4$ are uniaxial trigonal crystals related to R32 space group. Since the ionic radius of scandium (r_{Sc} = 0.74 Å) is large comparing with the ionic radii of aluminum (r_{Al} = 0.53 Å) and gallium (r_{Ga} = 0.62 Å), and is close to the ionic radius of terbium (r_{Tb} = 0.92 Å) there is no R32 modification for TbSc$_3$(BO$_3$)$_4$ [3]. However, the R32 modification can be obtained by lanthanum doping in TbSc$_3$(BO$_3$)$_4$ matrix (r_{Al} = 1.02 Å) [4], thus the La:TbSc$_3$(BO$_3$)$_4$ crystal was used. The SHG response was investigated using Kurtz-Perry powder test [5]. Crystals were crushed and then sieved and distributed using calibrated sieves into successive particle size ranges (fractions) from 20 to 200 μm. To illuminate the powdered samples Q-switched YAG:Nd laser radiation (1064 nm, 7 ns) was used. Test was carried out under various pump power densities (I$_{pump}$) up to 70 MW/cm^2 for each powder fraction.

The Kurtz-Perry powder test showed the typical quadratic dependence of the SHG response on the pump power density for all powder fraction of the TbAl$_3$(BO$_3$)$_4$, La:TbSc$_3$(BO$_3$)$_4$ and TbGa$_3$(BO$_3$)$_4$ crystals. However, for I$_{pump}$ > 60 MW/cm^2 there is a deviation of the SHG intensity value from the quadratic function for TbGa$_3$(BO$_3$)$_4$ powders, that is due to laser-induced damage. Thus, the 50 MW/cm^2 power density was chosen from the SHG fitted curves to determine the dependence of SHG on particle size and calculate the effective nonlinearity coefficient (d_{eff}). For all studied crystals, the increase in the size of powder fractions leads to higher SHG signal, that is characteristic of crystals with phase matching. The results also show that there is a direct correlation between the atomic mass of the cation (M) and the SHG efficiency, and therefore the effective nonlinearity coefficient: d_{eff}(TbGa$_3$(BO$_3$)$_4$) = 1.19xd_{eff}(La:TbSc$_3$(BO$_3$)$_4$) = 1.33xd_{eff}(TbAl$_3$(BO$_3$)$_4$).

[1] R. Arun Kumar, Borate crystals for nonlinear optical and laser applications: a review, Journal of Chemistry, 2019, 154865, (2013).
[2] G.M. Kuz'micheva, I.A. Kaurova, V.B. Rybakov, et al, Crystallochemical Design of Huntite-Family Compounds, Crystals, 9(2), 100, (2019).
[3] G.M. Kuz'micheva, I.A. Kaurova, V.B. Rybakov, et al, Structural Instability in Single-Crystal Rare-Earth Scandium Borates RESc$_3$(BO$_3$)$_4$, Cryst. Growth Des., 18, 1571−1580, (2018).
[4] A. Kuznetsov, K. Kokh, N. Kononova, et al, New scandium borates R$_x$La$_y$Sc$_z$(BO$_3$)$_4$ (x+y+z=4, R=Sm, Tb): Synthesis, growth, structure and optical properties, Mater. Res. Bull., 126, 110850, (2020).
[5] S.K. Kurtz and T.T. Perry, A Powder Technique for the Evaluation of Nonlinear Optical Materials, J. Appl. Phys., 39, 3798–3813, (1968).

Simultaneous generation at three wavelengths in an optically pumped He-Ar-Kr active medium

A.V. Juriev, Yu.A. Adamenkov, M.A. Gorbunov, E.V. Kabak, A.A. Kalacheva, V.A. Shaidulina

FSUE "RFNC-VNIIEF", Mira str, 37, Sarov, Russia 607190

oefimova@otd13.vniief.ru

The optically pumped rare gas laser (OPRGL) is a new type of optically pumped gas laser with high quantum efficiency, which can convert the high output power of a diode laser into the output power of a gas laser with good beam quality. In [1], the first generation on inert gases was demonstrated.

A mixture of argon (1.5%), krypton (0.5%) and helium (98%) is used as the OPRGL active medium. The main purpose of using helium is to increase the collisional relaxation from the pumping level to the upper laser level in order to create the largest population inversion [2,3].

In this paper laser generation was obtained simultaneously at three wavelengths (912.3 nm, 893.1 nm and 877.7 nm). The dependence of generation power and ratio of intensities of separate lines in general generation on flow rate of gas mixture, pressure in cuvette and frequency of repetition of discharge pulses is experimentally investigated. The maximum laser emission power value (in total at all wavelengths) was about 8 mW.
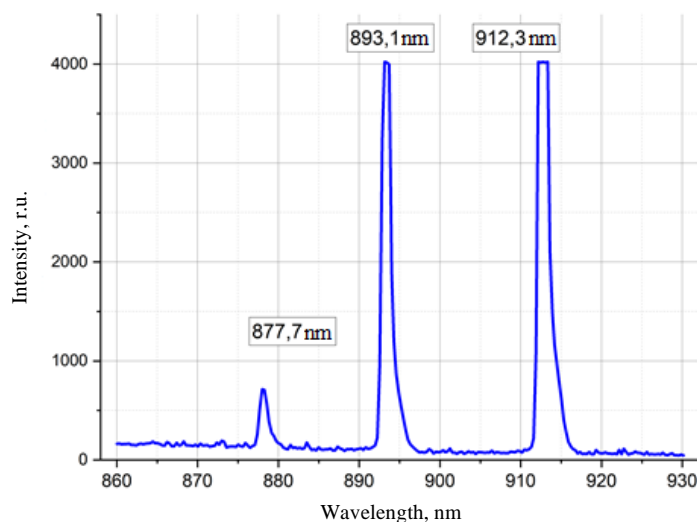
Fig.1. Spectrum of generation from dichroic mirror.

[1] J. Han and M.C. Heaven, Gain and lasing of optically pumped metastable rare gas atoms, Optics Letters. – 2012. – Vol. 37, No. 11, pp. 2157-2159.

[2] D. J. Emmons and D. E. Weeks. Kinetics of high pressure argon-helium pulsed gas discharge, Journal of Applied Physics. – 2017. – Vol. 121, No. 20.

[3] J. Han, L. Glebov, G. Venus, M.C. Heaven, Demonstration of diode-pumped metastable Ar laser, Optics Letters. – 2013. – Vol. 38, No. 24, pp. 5458-5461.

SRS-assisted pulse frequency conversion in mode-locked fiber lasers and its application in a deep tissues multiphoton microscopy

D.S. Kharenko[1,2*], E.E. Evmenova[1], V.M. Volosi[1,2], V.D. Efremov[1], A.A. Antropov[1], S.A. Babin[1,2]

1- IA&E SB RAS, 1 ac. Koptyug ave., Novosibirsk 630090, Russia
2- Novosibirsk State University, 1 Pirogova str., Novosibirsk 630090, Russia

* kharenko@iae.nsk.su

Fiber lasers differ from other types by a large number of nonlinear effects that affect the mode of generation. Such effects are often the limiting factor for achieving, for example, high peak power or short pulse duration. But they also open the door for large variability in output parameters such as repetition frequency or carrier wavelength. The last one has great importance for biological applications like multiphoton microscopy (MPM) [1]. To maximize the penetration depth into a sample and image contrast, it is preferable to use laser radiation with a wavelength near 1.3 or 1.7 microns. To date, many approaches to obtaining pulses in these spectral regions have been demonstrated, both by direct generation methods using novel doped active fibers [2] and by nonlinear effects, in particular stimulated Raman scattering (SRS) [3,4]. However, the best results can be obtained by combining both approaches.

I this work, we present the latest results in the generation of ultrashort pulses by the stimulated Raman scattering effect as well as its amplification in all fiber schemes for further application in MPM. Both wavelength ranges may be covered by changing the pump wavelength from 1.09 to 1.55 µm. The latter has the advantage of being easy to control the net dispersion of the external cavity, so dispersion-managed solitons can be generated. Such solitons often have a shorter duration and do not require an external grating compressor, which can be important in some applications. We have also demonstrated that the highly chirped pulses can be effectively amplified by continuous wave radiation due to the SRS effect. But the best results in terms of pulse energy and efficiency were obtained in a hybrid amplification scheme based on a combination of Raman and Bi-doped fiber stages. In this case, the peak power of the pulse compressed down to 650 fs exceeds 12 kW which should be suitable for deep tissue multiphoton microscopy.

In conclusion, we demonstrated that the SRS effect provides an effective way for pulse carrier frequency conversion in an all-fiber scheme. As a result, a robust and relatively low cost laser system can be built to operate with a multiphoton scanning microscope.

[1] S. Fan, S. Wang, C. Yang, F. Wise, L. Kong, Advances of Mode-Locking Fiber Lasers in Neural Imaging, Advanced Optical Materials, vol. 11, p. 2202945 (2023).
[2] A. Khegai, et al, NALM-based bismuth-doped fiber laser at 1.7µm, Optics letters, vol. 43, p. 1127 (2018).
[3] E.A. Evmenova, A.A. Antropov, D.S. Kharenko, All-fiber amplification of highly chirped dissipative solitons around a 1.3 micron using stimulated Raman scattering, Optics letters 48, 6444 (2023).
[4] I. Zhdanov, et al, Raman dissipative soliton source of ultrashort pulses in NIR-III spectral window, Optics Express, vol. 31, p. 35156 (2023).

Artificial intelligence for fiber lasers and sensors

A. Kokhanovskiy[1]

1- School of Physics and Engineering, ITMO University, St. Petersburg 197101, Russia

In recent years, fiber lasers and optical sensors have become an integral part of numerous high-tech applications, ranging from industrial monitoring and medical diagnostics to telecommunications [1]. These photonics devices offer unique advantages, such as high precision, a wide measurement range, and the ability to operate in extreme conditions. However, as demands for measurement accuracy, speed, and reliability increase, along with the growing volumes of data that need to be processed, there arises a need for new methods of data analysis and processing.

Artificial intelligence (AI) algorithms, particularly machine learning (ML), open up new horizons for improving the performance of optical sensors. With their ability to analyze large volumes of data and uncover hidden patterns, AI can significantly enhance the sensitivity, accuracy, and reliability of these devices. The application of ML allows for the automation of sensor calibration, prediction of sensor failures, and improvement of real-time signal processing.

This article explores the application of artificial intelligence algorithms in both fiber lases and fiber sensors. Special attention will be given to analyzing current achievements and development prospects in this rapidly evolving area. Also, the recent progress of our group will be demonstrated. We demonstrate that the Reinforcement learning algorithm utilizes sophisticated strategies to ensure a guaranteed harmonic mode-locked regime of the highest order by efficiently managing the laser system's pumping power and the nonlinear transmission of a nanotube absorber. Also, Using the example of a fiber sensor based on a multicore optical fiber with densely written fiber Bragg gratings, the possibility of increasing spatial resolution by a factor of five is demonstrated through the interpretation of complex reflection spectra by deep learning algorithms.

[1] G. Genty, et al, Machine learning and applications in ultrafast photonics, Nature Photonics 15(2), 91-101 (2021).
[2] A. Kokhanovskiy, et al, Highly dense FBG temperature sensor assisted with deep learning algorithms, Sensors 21(18) 6188 (2021).
[3] A. Kokhanovskiy, et al, Multistability manipulation by reinforcement learning algorithm inside mode-locked fiber laser, Nanophotonics (2024).

Lasers for mid IR range on the base of rare earth ions doped chalcogenide glasses

**V.V. Koltashev[1]*, V.G. Plotnichenko[1], B.I. Denker[2], B.I. Galagan[2], S.E. Sverchkov[2],
M.V. Sukhanov[3], A.P. Velmuzhov[3], M.P. Frolov[4]**

1- Prokhorov General Physics Institute of the RAS, Dianov Fiber Optics Research Center, Moscow, Russia
2- Prokhorov General Physics Institute of the RAS, Moscow, Russia
3- Devyatykh Institute of Chemistry of HighPurity Substances of the RAS, Nizhny Novgorod, Russia
4- Lebedev Physical Institute of the RAS Moscow, Russia

* kvv@fo.gpi.ru

Chalcogenide glasses with rare earth doping have long been considered as promising laser materials for mid-infrared spectral range. But only recently bulk and fiber lasers with practically significant efficiency became reality: laser action covering the spectral range of 4.6-6.1 μm was demonstrated in selenide glasses activated by a number of rare earth ions: Ce^{3+}, Pr^{3+}, Nd^{3+} and Tb^{3+} (Fig. 1) [1].
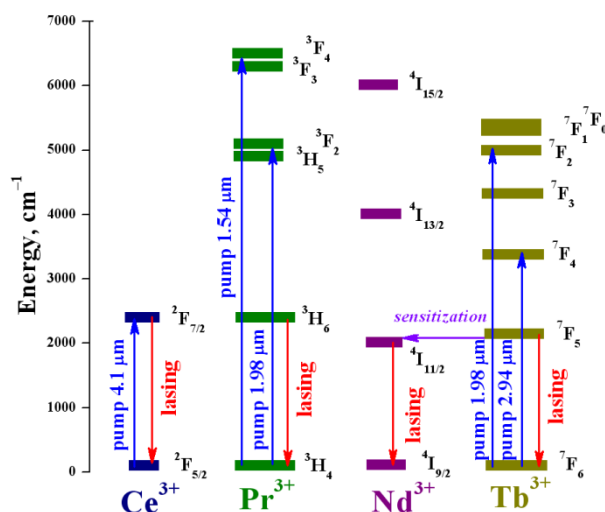

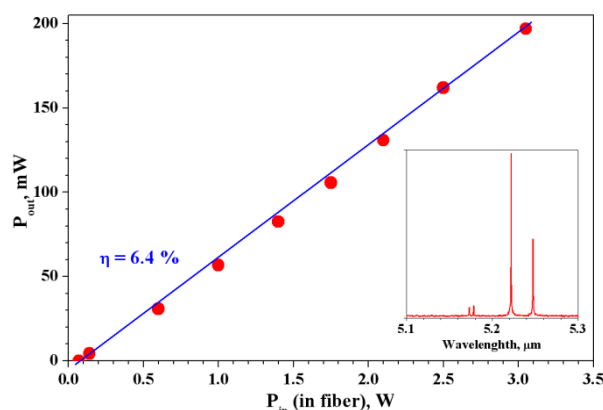Fig. 1. Rare earth ions energy level schemes in selenide laser glasses.

Fig. 2. Output power of Tb^{3+} fiber laser versus incident pump power. In the inset: output spectrum.

The directions of our efforts were to maximise the power and efficiency of chalcogenide glass lasers as well as to widen their possible tuning range. To achieve these goals, the unique features of definite laser active ions were successfully used. Tb^{3+} ions are attractive due to pumping convenience (by ~ 2 μm Tm^{3+} or ~ 3 μm Er^{3+} pump lasers). Ce^{3+} ions have the advantage of maximum gain cross section. Nd^{3+} ions exhibit long-wavelength emission reaching 6 μm combined with high enough quantum yield. However, the traditionally used optical pumping of neodymium ions at wavelengths of 0.8 or 0.9 microns is not applicable for selenide glasses, since it does not fall into the transparency region of these glasses. Therefore, we proposed an alternative pumping method − a sensitization scheme using Tb^{3+} ions. In coactivated Tb and Nd glass, Tb^{3+} ions can absorb radiation from ~2.9 microns of YAG:Er^{3+} pump lasers followed by nonradiative transmission to neodymium ions. The results of the laser experiments are summarised in [1].

For Tb^{3+}-doped optical fibers (doping level 1×10^{19} cm^{-3}) the laser output power up to 200 mW was obtained under 1.908 μm pumping, slope efficiency was 6.4% (Fig. 2).

For Ce^{3+}-doped optical fibers (doping level 5.5×10^{18} cm^{-3}) the output power up to 7 mW was obtained under 4.14 μm pumping, the lasing threshold was as low as 10 mW and the slope efficiency reached 17%.

The tuning range of Nd^{3+}-doped selenide glass laser complements the lasing wavelengths of Ce^{3+} and Tb^{3+} lasers (4.5-5.6 μm) and extends from 5.56 to 6.01 μm. This wavelength band includes the longest emission wavelengths of any rare-earth doped glass lasers obtained so far.

[1] B. Denker, P. Fjodorow, M. Frolov, B. Galagan, V. Koltashev, V. Plotnichenko, M. Sukhanov, S. Sverchkov, A. Velmuzhov, Rare-Earth-Doped Selenide Glasses as Laser Materials for the 5-6 μm Spectral Range, *Photonics*, *vol.* 10, 1323 (2023).

Stimulated Raman scattering of broadband chirped Ti:sapphire laser pulse in calcium carbonate with Stokes seeded by narrowband nanosecond Nd:YAG laser pulse

V.I. Kovalev[*], **I.O. Kinyaevskiy, A.V. Koribut, Ya.V. Grudtsyn**

P.N. Lebedev Physical Institute of the Russian Academy of Sciences, 53 Leninskiy Pr., 119991 Moscow, Russia

* kovalevvi@lebedev.ru

Stimulated Raman scattering (SRS) pumped by a broadband, compared to a bandwidth of material excitation, chirped 50-picosecond pulse with Stokes seeding by a 20-nanosecond narrowband pulse is experimentally and theoretically investigated. In experiment pulses generated by a femtosecond 0.95 μm Ti:sapphire laser system and a Q-switched 1.064 μm Nd:YAG laser were used for pumping and seeding SRS. An SRS-active $CaCO_3$ crystal was used because of its Raman resonance frequency (~1089 cm^{-1} [1]) is nearest to the frequency difference of pump and seed radiation sources. It is shown that, despite a narrowband seed, the generated a Stokes pulse spectrum mimics the pump pulse spectral width promising a possibility for its recompression back to femtoseconds [2]. Achieved SRS conversion efficiency saturates at of 40% with a weak dependence on seeding pulse energy and on detuning of pump-seed frequency difference from the Raman resonance. Theoretical modeling confirms the observed effects and allows one to predict the characteristics of the investigated system on variation its parameters.

The demonstrated dual-frequency laser source will be used for mid-IR pulse generation at ~9.3 μm wavelength by means of difference frequency generation in a nonlinear crystal, like in [3].

[1] P. Černý, H. Jelínková, P.G. Zverev, T.T. Basiev, Solid state lasers with Raman frequency conversion, Progr. in Quantum Electron., 28, 113-143 (2004).

[2] F.B. Grigsby, P. Dong, M.C. Downer, Chirped-pulse Raman amplification for two-color, high-intensity laser experiments, JOSA B, 25, 346-350 (2008).

[3] I.O. Kinyaevskiy, A.V. Koribut, L.V. Seleznev, Y.M. Klimachev, E.E. Dunaeva, A.A. Ionin, Frequency conversion of a chirped Ti:sapphire laser pulse to 11.4 μm wavelength with $SrMoO_4$ Raman shifter and $LiGaS_2$ DFG crystal, Opt. Laser Technol., 169, 110035 (2024).

The effect of post-growth annealing on $CaMoO_4$ optical properties and elemental composition

N.S. Kozlova[1*], **E.V. Zabelina**[1], **V.M. Kasimova**[1], **E.A. Scryleva**[1], **O.A. Buzanov**[2]

1- National University of Science and Technology "MISIS", 119049, Russia, Moscow, Leninsky pr., 4, b. 1
2- FOMOS-MATERIALS, 107023, Russia, Moscow, Buzheninova st., 16

* kozlova_nina@mail.ru

Synthesized calcium molybdate (povellite) $CaMoO_4$ is a well-known material. The first works on $CaMoO_4$ crystals growth date back to the 40s of the 20th century. $CaMoO_4$ calcium molybdate single crystals are characterized by a scheelite-type structure, belong to tetragonal symmetry, the space symmetry group is I41/a, the point symmetry group is 4/m. The unit cell is tetragonal, volume-centered, and contains 4 formula units. Initially, $CaMoO_4$ single crystals were used as a material for tunable acousto-optical filters, and later was considered as a material for Raman lasers. In recent years, this material was investigated due to the possibility of using isotope-enriched calcium molybdate $^{40}Ca^{100}MoO_4$ as a cryogenic phonon-scintillation detector with a metallic magnetic calorimeter (MMC) and Superconducting Quantum Interference Device (SQUID) in experiments searching for double neutrinoless beta decay. The crystals used for the manufacture of such detectors must have a large sensitive mass and exceptionally high optical quality, in particular, they must be optically homogeneous, characterized by the absence of color and structural defects, the attenuation index μ at the maximum emission at a wavelength of 520 nm must be no more than 0.01 cm^{-1}. The specified characteristics must be maintained throughout the entire period (years) of operation of the detector. The practical use of $CaMoO_4$ crystals for optical purposes is complicated by the presence of defect centers in them, such as color centers, which appear as yellow, blue or bright blue color. This color of the crystals is usually associated with the presence of oxygen vacancies. The reasons of those vacancies is a evaporation of volatile molybdenum oxide MoO_3 from the melt during the growth process. Isothermal annealing in an atmosphere with a controlled oxygen content leads to bleaching of such crystals. This is associated with the filling of oxygen vacancies with oxygen ions, while the electrical neutrality of the crystal is achieved, presumably, due to the recharging of molybdenum.

The purpose of this work was to study the effect of post-growth isothermal annealing in air on the optical properties and elemental composition of calcium molybdate crystals.

$CaMoO_4$ crystals were grown at Fomos-Materials using the Czochralski method from a charge of stoichiometric composition with the addition of an excess amount of MoO_3, from platinum crucibles in Kristall-3M set-up using a high-frequency heating method. The samples were studied in the initial state and after high-temperature annealing in air for 6 and 100 hours at a temperature of 1000°C, and in vacuum for 7 hours at a temperature of 1250°C.

The optical properties of the sample were investigated in the accredited tested laboratory of semiconductor materials and dielectrics "Single Crystals and Stock on their base" of National University of Science and Technology "MISIS". The spectral dependences of the transmittance $T(\lambda)$ were measured taking into account optical anisotropy and dichroism on a Cary-5000 spectrophotometer (Agilent Technologies) with a universal measurement accessory (UMA).

The elemental composition of $CaMoO_4$ crystals in the initial state and after isothermal annealing in air for 100 hours (colorless) was studied by X-ray photoelectron spectroscopy (XPS).

Annealing of $CaMoO_4$ crystals leads to a change in the concentrations of the main elements, however, all elements remain in charge states typical for the compound; we also did not detect a change in the charge state of molybdenum. Apparently, the generally accepted model of defect formation in calcium molybdate crystals should be revised.

Tm^{3+}, Li$^+$ ZnWO$_4$: novel 2-μm laser crystal

<u>D. Lis</u>[1*], K. Subbotin[1,2], Yu. Zimina[1,2], Ya. Didenko[2],
S. Pavlov[2], A. Titov[2], E. Zharikov[1]

1- Prokhorov General Physics Institute, Russian Academy of Sciences, 38 Vavilova St., 119991 Moscow, Russia
2- Mendeleev University of Chemical Technology of Russia, 9 Miusskaya Sq., 125047 Moscow, Russia

* lisdenis@mail.ru

We report on the crystal growth, spectroscopic investigation, and laser performance of Tm^{3+}-doped monoclinic zinc tungstate (Tm:ZnWO$_4$). Tm^{3+}-doped ZnWO$_4$ crystals containing charge compensator (Li$^+$ ions) were grown using the Czochralski (Cz) method in air using a Pt crucible. The actual Tm^{3+} doping level for this second crystal was 1.59 at.% and the segregation coefficient is almost 0.4 owing to the positive effect of Li$^+$ codoping. Meanwhile, the actual Li$^+$ content in the crystal was measured to be 1.65 at.%, and the segregation coefficient is only ~ 0.2.

ZnWO$_4$ belongs to the monoclinic class adopting the C_{2h}^4 - P2/c space group and the 2/m point group, with a general multiplicity Z of 2. The lattice constants are a = 4.692Å, b = 5.721Å, c = 4.928Å, and the monoclinic angle β = a ^ c = 90.632°. ZnWO$_4$ optical properties are described within the optical indicatrix frame, featuring three mutually orthogonal principal axes denoted as N_p, N_m, and N_g. One of them (N_p) is parallel to the crystallographic **b**-axis, aligned with the 2-fold symmetry axis. The other two axes of the optical indicatrix, N_m and N_g, lie in the **a-c** plane.

The polarized absorption spectra reveal a strong polarization anisotropy of absorption properties. The maximum absorption cross-sections σ_{abs} is 1.09×10^{-20} cm^2 at 803.6 nm and the corresponding absorption bandwidth is 16 nm for light polarization **E** $\parallel N_g$. For the other two polarization states, σ_{abs} is smaller, amounting to 0.83×10^{-20} cm^2 at 807.7 nm (for **E** $\parallel N_p$), and 0.24×10^{-20} cm^2 at 802.7 nm (for **E** $\parallel N_m$).

A Judd-Ofelt analysis is conducted, the spontaneous emission probabilities, luminescence branching ratios and radiative lifetimes are determined. The crystal-field splitting of the $^3H_6$ and $^3F_4$ Tm^{3+} multiplets was achieved using low-temperature spectroscopy. The ZnWO$_4$ crystal exhibits a relatively large total Stark splitting of the Tm^{3+} ground state, $\Delta E(^3H_6)$ of 644 cm^{-1}, evidencing a relatively strong crystal-field for this material. This leads to the longest wavelength of a purely electronic transition $^3F_4 \rightarrow {}^3H_6$ of 2028 nm, i.e., above 2 μm, which is rarely observed for commonly used laser host crystals.

Polarized luminescence spectra and decay kinetic are obtained. Tm^{3+} ions in ZnWO$_4$ exhibit a significant polarization anisotropy of their emission properties that is favorable for achieving linearly polarized laser output. The maximum stimulated-emission (SE) cross-sections, σ_{SE} reaches 2.93×10^{-20} cm^2 at 1871 nm for light polarization **E** $\parallel N_p$. In the long-wave spectral region where laser action is expected to be supported by the reabsorption from the ground-state for quasi-three-level 2-μm Tm lasers, the peak SE cross-sections are 0.77×10^{-20} cm^2 at 2015 nm and 0.70×10^{-20} cm^2 at 1971 nm also for light polarized **E** $\parallel N_p$. Tm^{3+} ions exhibit smooth and broad emission spectral profiles extending beyond 2 μm, positioning Tm^{3+}-doped ZnWO$_4$ as a promising candidate for generation of femtosecond pulses in this spectral range which is well detuned from the structured absorption of water vapors in the air.

The decay of $^3F_4$ level is well described by the single-exponential law, yielding a luminescence lifetime τ_{lum} of 1.57 ms for the powdered sample, as compared to 2.08 ms for the bulk crystal.

The laser element was cut from the annealed crystal for light propagation along the N_g optical indicatrix axis (N_g-cut). The continuous-wave Tm^{3+}, Li$^+$: ZnWO$_4$ laser generated a maximum output power of 282 mW at 1964-1983 nm (exhibiting a broad laser spectrum) with a slope efficiency η of 14.7% with respect the absorbed power and a laser threshold of 188 mW. The combined attributes of large Stark splitting, polarized emission, spectral broadening, and prolonged luminescence lifetime position Tm-doped ZnWO$_4$ crystals as promising candidates for advanced laser systems.

The optimal dopants concentrations search of Yb,Li:ZnWO$_4$ laser crystals

O. Lis[1*], Yu. Zimina[1,2], P. Volkov[3], D. Lis[1], K. Subbotin[1,2], A. Titov[1], S. Pavlov[1,2]

1- Prokhorov General Physics Institute of the Russian Academy of Sciences, Moscow, Russia
2- Mendeleev University of Chemical Technology of Russia: Moscow, Russia
3- NRC "Kurchatov Institute" – IREA Shared Knowledge Center, Moscow, Russia

* ozaytceva@mail.ru

The results of our attempts to improve Yb segregation coefficient in ZnWO$_4$ crystal and the mechanical straights characteristics of Yb:ZnWO$_4$ laser crystals by the addition of Li$^+$ charge compensator are presented in the talk.

ZnWO$_4$, Yb:ZnWO$_4$ and Yb,Li:ZnWO$_4$ single crystals with various concentrations of Yb^{3+} and Li$^+$ ions were grown by the Czochralski technique using Pt crucibles. The seeds for the growth were cut from undoped ZnWO$_4$ crystal parallel to the (010) crystallographic plane. Preliminary studies have shown that unlike the case of the undoped crystals, doping of ZnWO$_4$ crystal by Yb^{3+} ions without the appropriate amount of charge compensator sharply deteriorates the mechanical characteristics of the samples. Yb-doped samples contain numerous cracks, predominantly, along the (010) crystallographic plane.

Atomic emission spectroscopy with inductively coupled plasma, as well as polarized optical absorption spectroscopy were used for the determination of actual dopants concentrations. The mutual influence Yb^{3+} and Li$^+$ ions onto their segregation coefficients in the crystal was revealed.

Yb,Li:ZnWO$_4$ crystals, grown from the melts, containing 5-5.5 at.% Yb^{3+} and 8-12 at.% Li$^+$, possess the best hardness and fracture toughness. Less Li$^+$ concentration results in too big difference between the actual Yb^{3+} and Li$^+$ contents in the crystal, and, hence, in too large amount of Zn vacancies. It substantially weaken the crystal lattice and lead to reduction of the crystal mechanical strength.

Fiber lasers with self-sweeping frequency effect: physics and applications for sensing tasks

N.R. Poddubrovskii[1], A.Yu. Tkachenko[1], S.I. Kablukov[1], I.A. Lobach[1*]

1- Institute of Automation and Electrometry SB RAS

* lobach@iae.nsk.su

Distributed fiber sensors (DFS) are one of the most powerful tools in the field of measurements of physical parameters such as temperature, strain, etc. Among all of the advantages of DFS one can note long sensing range (up to 100 km) and resistance to electromagnetic impact. DFS consist of a fiber-based sensor and an analyzer, with the latter generating probe optical radiation and analyzing the back-scattered signal returning from the sensor. Three main types of light scattering in fibers – Rayleigh, Brillouin, and Raman – are typically used in DFS. The resistance of results to optical losses and as result higher accuracy are achieved in DFS based on spectral analysis of the scattered signal (Rayleigh or Brillouin DFS) in contrast to amplitude one (Raman DFS). A key element of the spectral analyzer in DFS is a tunable laser. To realize such a tunable laser, rather expensive special spectral selectors such as tunable fiber Bragg gratings or diffraction gratings are typically used. An alternative to using such selectors are dynamic gratings (DGs) formed in doped fibers under influence of standing waves formed in a laser cavity [1]. Under certain conditions, a DG formed by the standing wave with one optical frequency can cause lasing at another adjacent optical frequency. When the process repeats multiple times in the same direction, the changes looks like frequency tuning which is known as self-sweeping effect. One of the main features of the self-sweeping lasers is high coherence (linewidth less than 1 MHz) of the laser radiation which is related to high selective property of DG due to its large length. As a result, the self-sweeping lasers are very competitive alternative compared to conventional single-frequency tunable ones in applications demanding tunable radiation, because of their simplicity, high coherence, broad sweeping range (up to several dozens of nm) at various spectral ranges (from 1 to 2.1 μm). To date, a number of practical applications have already been demonstrated (from sensor interrogation to gas analysis).

The report will review the latest advances in the field of DFS with spectral analysis based on self-sweeping fiber lasers: Rayleigh-based Coherent Optical Frequency Domain Reflectometry (COFDR) and Brillouin Optical Time Domain Analysis (BOTDA). Discreteness of frequency change determined by longitudinal mode structure in the single-frequency self-sweeping lasers is highly attractive for Fourier analysis in COFDR [2]. A series of papers demonstrates that COFDRs based on self-sweeping lasers can be used for various tasks including optical elements characterization, sensing, vibration measurements, and gas analysis at lengths of about ten meters with spatial resolution as high as 200 μm. At the same time the sensitivity as good as -120dB/mm makes it possible to analyze back-scattered Rayleigh signal. Recently the first demonstration of BOTDA without any microwave devices typically used in similar systems was presented in [3]. Distributed temperature measurements with sensing line length of 25 km, spatial resolution of 10 m, and sensitivity of 2°C was demonstrated in a BOTDA system based on a self-sweeping fiber laser.

[1] N.R. Poddubrovskii, R.V. Drobyshev, I.A. Lobach, S.I. Kablukov, Fiber Lasers Based on Dynamic Population Gratings in Rare-Earth-Doped Optical Fibers, Photonics, 9, p. 613 (2022).

[2] A.Yu. Tkachenko, I.A. Lobach, S.I. Kablukov, Coherent Optical Frequency Reflectometry Based on a Fiber Self-Scanning Laser: Current Status and Development Prospects (Review), Instrum Exp Tech 66, pp. 730–736, (2023).

[3] N.R. Poddubrovskii, I.A. Lobach, S.I. Kablukov, Microwave-free BOTDA based on a continuous-wave self-sweeping laser, Opt. Lett. 49, pp. 282-285, (2024).

Direct laser metallization from deep eutectic solvents on polymer substrates

L. Logunov[1*], E. Khairullina[1], A. Shishov[2], A. Komlev[3], D. Shestakov[3]

1- School of Physics and Engineering, ITMO University, Lomonosova, 9, Saint-Petersburg, 191002, Russia
2- Institute of Chemistry, Saint Petersburg State University, 7/9 Universitetskaya nab., St. Petersburg 199034, Russia
3- Department of Physical Electronics and Technology, Saint Petersburg Electrotechnical University "LETI", Saint St. Petersburg 197376, Russia

* levlogunov@gmail.com

Direct laser metallization is unique technic for one step metal deposition on almost any surface. Method based on chemical reaction which induced by ultra-fast heating under the focused laser irradiation. We have developed method for various metal deposition such as copper, nickel and others [1,2]. In previous works, we were unable to achieve deposition on polymer substrates due to overheating of the substrates. In this work, we developed new approach to reduce the required laser irradiation power density by using an additional photoactive layer above the deep eutectic solvent film. The DES composition used was the same as in previous work [2]. The properties of conductive copper structures on PDMS, PET and polyamide substrates were created and demonstrated. We achieved resistivity of copper substrates closed to pure copper, the resolution of method was min 60 µm width and 1 µm thickness of single structure.

The idea of new approach was focusing on decreasing the laser power density. That was caused by optical properties of DES. As we used 1064 nm picosecond laser, DES has weak extinction coefficient on that wavelength, that leads to use high power density of laser irradiation to heat the film up to necessary temperature, but after the first milliseconds of deposition nucleates of metal start to absorb the laser light dramatically. Extra heating transfer appears to the substrate and in case of polymer substrates excess heat causes damage to the substrate. We added a thin black color layer above DES film using simple by whiteboard marker. We achieved the effect of reducing the power density by 5-6 times, while the quality of the resulting structures greatly improved, since the excess laser radiation density did not lead to damage to the center of the resulting structures during a single scan.

Finally, we created prototypes of different electronic devises on flexible polymer substrates, such as RFID tag, microheaters, electrochemical sensors and circuit board. In this work we show their properties and application field. Direct laser metallization from deep eutectic solvents is a new ecological, simple and cheap method for device fabrication in small batches.

[1] E.M. Khairullina, I.I. Tumkin, D.D. Stupin, A.V. Smikhovskaia, A.S. Mereshchenko, A.I. Lihachev, A.V. Vasin, M.N. Ryazantsev, M.S. Panov, Laser-assisted surface modification of Ni microstructures with Au and Pt toward cell biocompatibility and high enzyme-free glucose sensing, ACS omega, 6(28), pp.18099-18109, (2021).

[2] D. Shestakov, E. Khairullina, A. Shishov, S. Khubezhov, S. Makarov, I. Tumkin, L. Logunov, Picosecond laser writing of highly conductive copper micro-contacts from deep eutectic solvents, Optics & Laser Technology, 167, p.109777, (2023).

Glass-forming tendency in fiber optics Ge-As-Se-S chalcogenide glass materials

R.I. Alekberov, S.I. Mekhtiyeva, <u>S.M. Mammadov</u>[*]

Republic of Azerbaijan Ministry of Science and Education Institute of Physics named after Academician Hasan Abdullayev, G. Javid ave 131, AZ1143 Baku

* smmemmedov@mail.ru

The results of scientific research show that chalcogenide glasses containing germanium (Ge) and arsenic (As) have a wide range of optical transparency, low optical loss, high stability and non-linear optical properties, which can be effectively used in solving numerous application problems arising mainly in the field of fiber optics [1]. It is necessary choosing a mode that excludes crystallization and liquefaction during the synthesis process, as well as being resistant to crystallization and humidity when preparing fiber optic transmitters, fiber lasers and amplifiers with high performance indicators from chalcogenide glass materials containing germanium (Ge) and arsenic (As) with high chemical and phase purity. The analysis of various scientific articles shows that the addition of a certain atomic percentage of Ge to Ge-As-Se-S system with complex components will increase their mechanical strength and the operating temperature range of fiber transmissions [2].

The aim of the article is to study the local structure, the glass forming ability, the thermal stability, the glass and crystallization regions of substances corresponding to different topological glass states (isostatic, rigid, elastic) depending on the atomic percentage of chalcogenous (Se, S) and non-chalcogenous (Ge, As) constituent elements in Ge-As-Se-S glassy systems according to the idea of layered structure and chemically ordered network models.

X-ray diffraction results shows that, the values of d and L increase proportionally with the increase in the atomic percentage of Ge (except for $Ge_{25}As_{10}S_{25}Se_{40}$ content). For the composition ($Ge_{25}As_{10}S_{25}Se_{40}$) according to the chemical regularity (R=1 and $<r>$=2.6) violates the above mentioned proportional dependence. That is, the ratio of the sum of (S+Se) with small atomic radius to the amount of As in the mentioned composition has a maximum value. As a result, it ensures that $Ge_{25}As_{10}S_{25}Se_{40}$ composition is formed only from pyramidal and tetrahedral structural elements. The obtained results prove that the composition of $Ge_{25}As_{10}S_{25}Se_{40}$, which corresponds to the state of chemical order (R=1) and is close to the topological order (f~0, N~3), is more resistant to crystallization (ΔT_{g-c} ~87 K), and also are characterized by relatively high the ability of glass formation and high values of thermal stability (H_r =0.469; H'=0.159). The glass formation ability (H_r), thermal stability parameters (H', S), decrease significantly in $Ge_{33}As_{17}S_{35}Se_{15}$ with high atomic percentage of Ge, S, and relatively low amount of Se.

[1] J.L. Adam and X. Zhang, Chalcogenide Glasses, Preparation, Properties and Applications, Cambridge: Woodhead Publishing Limited, p. 703, (2014).
[2] I. Inagawa, R. Iizuka, T. Yamagishi, R. Yokota, Optical and thermal properties of chalcogenide Ge-As-Se-Te glasses for IR fibers, J. Non-Crystal. Solids, 95, pp. 801–808, (1987).

Effective picosecond pulse amplification schemes based on Nd-doped crystals at saturation conditions

V.B. Morozov[1*], **A.N. Olenin**[1], **D.V. Yakovlev**[1]

1- Physics Faculty of M.V. Lomonosov Moscow State University, 119899 Leninskiye Gory, Moscow, Russia

* *morozov@phys.msu.ru*

Neodymium-doped crystalline laser media are widely used to generate and amplify picosecond pulses due to their suitable gain bandwidth, typically a few units of 1/cm. Effective amplification aimed to obtaining pulsed-periodic radiation of high peak and average power usually involves the use of regenerative and then linear amplifiers. The overall efficiency of a laser system is determined primarily by the linear amplification output stages, which ought to operate in saturation mode. Up to the energy level of single output pulses of several mJ and repetition rates of ~1 kHz, the most attractive way is the use of amplification schemes with longitudinal pulse pumping which provide both the best overlap of the laser beam with the pump profile in the active crystal and the ability to work at high repetition frequencies. A significant limitation of such schemes is associated with the aberrational nature of the thermal lens, leading to additional losses and degradation of beam quality at high pump power. Nevertheless, up to repetition rates of the order of and above 1 kHz, such schemes prove to be effective.

At a linear amplifier operating near the saturation condition, the optimal solution, from the point of view of pump conversion efficiency, is the use of two-pass amplifying schemes that provide uniform complete exhaustion of population inversion along the entire length of the pumped laser medium.

In the present work, we develop and analyze operation of a picosecond Nd:YAG laser/ amplifier system based on longitudinal pumping with use of pulsed fiber coupled diode laser arrays with the peak power of up to 60 W. The scheme with two stages of two-pass amplifiers provides pulses of 25 ps duration with an energy not less than 5 mJ at the fundamental wavelength of 1064 nm with a repetition rate of 1 kHz. Following the scaling conditions such a design allows further increase in output energy and average power.

Two-pass longitudinally pumped amplifiers operating close to or under saturated conditions are important structural parts of the scheme. In this regard, we compare the capabilities of amplifiers based on Nd:YAG and Nd:YLF. When implementing this approach, we pay attention to two significant points.

Firstly, the amplification of picosecond pulses with a duration of 10-100 ps is a significantly non-stationary process, which actually follows a three-level scheme, in contrast to the case of nanosecond pulses corresponding to classical four-level scheme. Therefore, it is important that the time delay between two successive passes of a two-pass amplifier exceeded the lifetime of the lower laser level. In contrast to the lifetimes of the upper laser levels in the Nd:YAG and Nd:YLF, whose values are well known, there are significant differences in understanding regarding the lower levels lifetimes. The most detailed study [1] provides values of 170-225 ps for Nd:YAG and more than 10 ns for Nd:YLF. In our recent study based on direct measurements of gain dynamics at saturation it was found that in Nd:YAG the lifetime of the lower laser level is even shorter, that is, less than 100 ps. Thus, the differences between these two popular laser media must be adequately taken into account when developing the optimal design.

The second important point is that in the case of picosecond pulses, the saturation fluence values turn out to be closely comparable with the laser crystal surface breakdown threshold, which is mainly determined by the dielectric coating. And the saturation energy densities in Nd:YAG and Nd:YLF differ approximately twice. When characterizing the optical breakdown threshold of laser dielectric coatings, there are usually indicated values related to nanosecond pulses. While there are practically no systematic data in relation to picosecond pulses. We fulfilled a series of measurements of the optical breakdown power density and energy fluence using high-power pulses with durations of 20 and 110 ps.

The results obtained are ought to be taken into account at designing effective picosecond pulse amplification schemes based on Nd:YAG and Nd:YLF.

[1] C. Bibeau, S.A. Payne, H.T. Powell, J. Opt. Soc. Am. B 12(10) 1981-1992 (1995).
[2] V.B. Morozov, A.N. Olenin, D.V. Yakovlev, ALT 2023, Samara, Book of Abstracts, LS-0-14 (2023).

The effect of ethyl alcohol on the mechanical parameters of optical fibers in an acrylate protective coating

M. Naparin[1,2*], N. Kasatkin[1,2], J. Lapteva[1]

1- Public Joint Stock Company "Perm Scientific-Industrial Instrument Engineering Company", Perm
2- Perm State University, Perm

* denegf@yandex.ru

In the absence of data concerning the adverse effects of ethyl alcohol on acrylate protective coating (PC), ethyl alcohol is employed during the processing of optical fibers (OF). It is used for cleaning the ends of OF from dirt and stripped PC, for degreasing purposes during cable laying or for installation of optical systems. The research project in question considers the impact of ethyl alcohol on the mechanical parameters of fibers.

The samples were placed in the desiccator (Fig. 1) and incubated for periods from one hour to five days in ethyl alcohol and its vapours. Following each soaking period, the following parameters were measured: the degree of polymerisation of the secondary PC and the ultimate strength, which was determined by the two-point bending method. The results of the optical microscope inspection revealed that direct contact of ethyl alcohol with acrylate PC leads to the formation of defects and complete peeling of PC after interaction for 12 hours (Fig. 2).
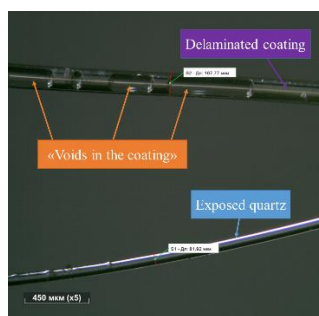

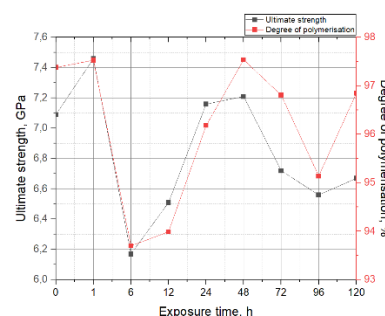Fig. 1. Desiccator.　　Fig. 2. Microscope examination results.　　Fig. 3. Results of ultimate strength and degree of polymerization.

The onset of the interaction between ethyl alcohol and acrylate coating is assumed to be due to the presence of microcracks on the coating surface during the operation or manufacturing of the OF, into which the ethyl alcohol enters.

In order to demonstrate the nature of the changes of parameters as a function of exposure time, an object with a slow reaction – OF in ethyl alcohol vapour – was considered. The graph (Fig. 3) shows the change in the degree of polymerisation and the ultimate strength from the time of exposure of the sample in alcohol vapour. From the results obtained, the ultimate strength and the degree of polymerisation are related. A decrease of polymerisation and ultimate strength indicates an increase in the local defect concentration on the PC. Presumably, polymer restructuring (breaking/crosslinking of polymer chains) takes place in the 6-12 and 96 hours exposure, which may be accompanied by the formation of new microcracks on the surface. In the case of that, there is a high probability of the formation of "voids in the coating", leading to coating peeling (Fig. 2). After 12 hours of exposure to ethyl alcohol, a large number of areas of completely delaminated PC are formed (Fig. 4).

Fig. 4. A fragment of an entangled section of the winding.

Reduction in mechanical parameters and peeling of the coating can potentially lead to malfunction of optical systems with this OF (drops of alcohol may remain on the OF sections when buffer coating is applied). Ethyl alcohol can act as an aggressive medium for the acrylic PC during prolonged interaction. During the study, hypothesis is proposed that exposure of OF with acrylate PC to ethyl alcohol or its vapours could be used as a technique to assess the quality of the acrylate PC promptly.

Microlenses at the ends of optical fibers that preserve radiation polarization

A.S. Pankov[1*], R.S. Ponomarev[1]

1- Perm State University, integrated photonics laboratory, Perm 614990, Russia

* lab.photon.psu@gmail.com

Abstract: The paper describes a method for creating microlenses based on Panda fibers, while maintaining the radiation polarization. It also presents methods for measuring the key characteristics of these lenses: focal length, mode field diameter (MFD), polarization attenuation coefficient.

Introduction

One of the main challenges in integrated optics is the issue of the inextricable connection between optical fibers (OF) and waveguides in a photonic integrated circuit (PIC), which has a characteristic diameter comparable to the wavelength of the guided light [1]. The use of OF with a core diameter of approximately 9 micrometers to dock with PIC with waveguide dimensions of approximately 1.5-2 micrometers results in an increase in optical signal loss. An effective solution to minimizing optical losses when connecting these optical elements is the use of lensed tapered fiber (LTF) with a focal spot size of approximately 2 micrometers. LTF – optical components, which are a fiber-optic guide, on the end of which a microlens is formed [2].

Materials and Methods

For the manufacture of microlenses at the ends of the OF, fiber was used while maintaining the polarization of radiation. The Fujikura FSM-100 welding machine was used to create microlenses. Microlensing occurs in several stages. At the first stage, by continuously exposing the OF to an electric arc, it is softened and stretched until the desired tightness with the required parameters is achieved. Then, in the absence of an electrical arc, the OF breaks in the narrowest area of the constriction. As a result of the breakage, two segments of OF with conical tips are obtained. Additionally, the resulting cones are melted using an electrical arc. The fused section of the optical fiber, under the influence of surface tension forces, forms a symmetrical, convex surface. As a result, a conical lens is created at the end of the fiber.

Polarization-preserving microlenses have the following characteristics: focal length, MFD and polarization attenuation coefficient. The focal length and MFD were measured using the Fabry-Perot method and far-field infrared camera methods, respectively. The polarization attenuation coefficient of a microlens is the numerical difference between the value of this coefficient at the entrance of the lensed fiber and its value at the exit of the lens [3].

Results and Discussion

This paper presents a method for manufacturing and measuring the key parameters of microlenses, with a focal spot size of 2 micrometers. The proposed method makes it possible to obtain lenses with radiation polarization at the output up to 40 dB and a polarization drop in the lens of no more than 3 dB.

[1] Y. Jung, G. Brambilla, D.J. Richardson, Polarization-maintaining optical microfiber, Opt. Lett., vol. 35(12), pp. 2034–2036, (2010).

[2] C.-H. Lin, S.-C. Lei, et al, Micro-hyperboloid lensed fibers for efficient coupling from laser chips, Optics Express, vol. 25(20) pp. 24480-24485, (2017).

[3] A.S. Pankov, L.O. Zhukov, R.S. Ponomarev, Measurement of key characteristics of a lensed optical fiber, A special issue of Photon Express Science, vol. 6, pp. 494-495, (2023).

GHz pulse repetition rate in waveguide lasers at 1-2 μm with graphene

**M. Ponarina[1], A. Okhrimchuk[1,2], E. Obraztsova[1], T. Dolmatov[1],
V. Bukin[1], P. Obraztsov[1,3]**

1- Prokhorov General Physics Institute of the Russian Academy of Sciences, Moscow, Russia
2- D. Mendeleyev University of Chemical Technology of Russia, Moscow, Russia
3- University of Eastern Finland, Joensuu, Finland

Pulsed laser sources with repetition rates over 1 GHz are important for applications in telecommunications, microprocessing of materials and radiophotonics. Here we present an approach to create compact single-mode waveguide lasers with gigahertz repetition rate using graphene saturable absorber mirror as the output coupler. In particular, due to very efficient coupling of pump light into the femtosecond laser inscribed waveguide and wavelength insensitive properties of graphene this approach demonstrates the possibility to achieve single- and dual-wavelength generation in Nd :YAG and Tm :YAP active media with over 8 GHz pulse repetition rate. The proposed approach is not limited to Nd :YAG and Tm :YAP crystals, but is also applicable to other active media operating in the near-IR region.

Faraday fiber-optic sensor for measuring ultrahigh currents

Y.V. Przhiyalkovskiy[1,2*], N.I. Starostin[1], S.K. Morshnev[1], A.I. Sazonov[1]

1- Kotelnikov Institute of Radio Engineering and Electronics (Fryazino Branch) of the Russian Academy of Sciences, Vvedensky Sq. 1, Fryazino, Moscow region, 141190 Russia
2- ERSO Transformer Solutions LLC, 21, Elektrozavodskaya Street, Moscow, 107023

* yankus.p@gmail.com

An optical method of electric current sensing employing the Faraday effect has become widely popular in the high energy industry due to its accuracy, safety, and ease of implementation. Contemporary optical current sensors are typically based on a fiber reflective interferometer that uses a spun highly birefringent optical fiber (spun fiber) as the sensing element [1]. The range of currents that can be measured by such a sensor is naturally constrained by the maximum value of the Faraday phase shift $\pi/2$, which corresponds to a current of $I_{max} \approx 500$ kA. However, in applications such as measuring the plasma current in thermonuclear reactors, the current can exceed this limit and reach a value of several mega-amperes [2]. To address this issue, the differential method of current measurement using a typical fiber-optic sensor scheme can be used [3]. The method is based on using two sequentially spliced spun fibers with different megneto-optical sensitivities and covering the current conductor in opposite directions (Fig. 1). The residual phase shift that light accumulates after passing through the fibers will be considerably less than the phase shift induced in a single-fiber sensing element. The integral sensitivity of the sensor is thus reduced, thereby resulting in an increase in the upper limit of the measured current.

The most practical way to obtain the appropriate spun fibers is to draw them with different birefringence or spin pitch. However, a change in the parameters at the fibers splice causes mode coupling. As a result, the secondary waves arising there contribute to the interference signal, thus making the sensor's output characteristic nonlinear [4]. In this study, we propose a new signal processing for the correct current value recovering, adapted for differential measuring method. The new approach compensates for this effect, making the response of a sensor with a differential sensing element linear.

In the experiment, we demonstrated the ability to measure currents up to 50 MA with high linearity. For this, spun fibers with a spin pitch of 3 mm and birefringence beatlengths of 7.1 mm and 10.7 mm at a wavelength of λ=1.55 μm were used.

The work was carried out within the framework of the state task of the Kotelnikov Institute of Radio Engineering and Electronics of the Russian Academy of Sciences.

Fig. 1. Optical circuit.

[1] K. Bohnert, et al, Optical fiber sensors for the electric power industry, Optics and Lasers in Engineering 43.3-5 (2005): 511-526.
[2] M. Wuilpart, et al, Polarimetric optical fibre sensing for plasma current measurement in thermonuclear fusion reactors, 2020 22nd International Conference on Transparent Optical Networks (ICTON). IEEE, 2020.
[3] Patent RF RU2792207C1 (PCT WO2023158334A1), Volokonno-opticheskij chuvstvutelnij element datchika elektricheskogo toka i magnitnogo polja [Fiber-optical sensing element of an electric current and magnetic field sensor], S.K. Morshnev, Y.V. Przhiyalkovskiy, N.I. Starostin, M.Y. Yanin, Declared 15.02.2022. Published 20.03.2023. (In Russian).
[4] Y.V. Przhiyalkovskiy, et al, Fiber-Optic Sensor for MA Current Measuring, Journal of Lightwave Technology, vol. 42, no. 9, pp. 3423-3429 (2024).

Double harmonic mode-locking in soliton fiber ring laser

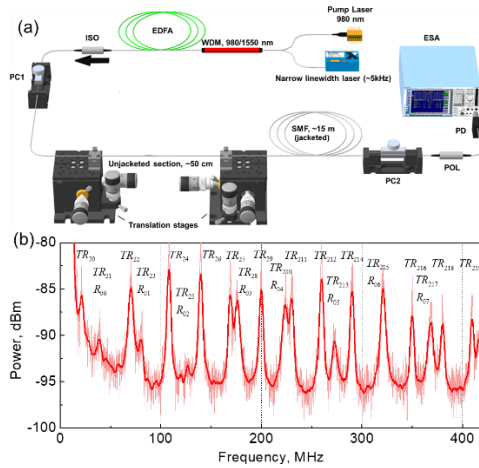**V.A. Ribenek**[1*], **P.A. Itrin**[1], **D.A. Korobko**[1], **A.A. Fotiadi**[1,2]

1- Ulyanovsk State University, 42 Leo Tolstoy Street, Ulyanovsk, 432970, Russian Federation
2- Electromagnetism and Telecommunication Department, University of Mons, Mons, B-7000, Belgium

* ribl98@mail.ru

Passive harmonic mode-locking (HML) of a soliton fiber laser locked to optoacoustic resonance (OAR) in the cavity fiber ensures high-frequency laser operation, high pulse stability, and low timing jitter [1]. However, the pulse repetition rate (PRR) of such lasers is limited to ~1 GHz for standard fibers due to the available acoustic modes [1-4]. Here, we address these limitations by demonstrating a soliton fiber laser built from standard fiber components and subjected to double harmonic mode-locking (DHML) [5].

In our experiment, the laser adjusted to operate at 15-th harmonic of its cavity matching the OAR ($TR_{2,9}$ GAWBS mode) at ~200 MHz (Fig.1) could be driven to operate at a high harmonic of this particular OAR frequency, thus reaching ~12 GHz (Fig.2, a). This breakthrough is made possible through controllable optoacoustic interactions in a short, 50 cm segment of unjacketed cavity fiber implemented through its stretching (Fig.1). We propose that the precise alignment of the laser cavity harmonic and fiber acoustic modes leads to a long-lived narrow-band acoustic vibration. This vibration sets the pace for pulses circulating in the cavity by suppressing modes that do not conform to the Vernier principle. The surviving modes, equally spaced by the OAR frequency, in cooperation with the gain depletion and recovery mechanism, facilitate the formation of stable high-frequency pulse sequences, enabling DHML. In this process, the OAR rather than the laser cavity defines the elementary step for laser PRR tuning (Fig.2, a). Throughout the entire PRR tuning range, the soliton fiber laser exhibits enhanced stability, demonstrating a better than ~40 dB supermode suppression levels (SSL), improved pulse timing jitter and relative intensity noise (RIN) (Fig.2, b-d).

Fig. 1. Experimental setup of the soliton NPE laser (a); Guided acoustic wave Brillouin scattering (GAWBS) spectra recorded with 1-km G.652.D fiber (Fujikura) (b).

Fig. 2. The PRR as a function of the increasing pump power (a) and the SSL (b), timing jitter (c) and RIN (d) as functions of the PRR measured in HML (blue) and DHML (red) regimes.

[1] A.N. Pilipetskii, E.A. Golovchenko, C.R. Menyuk, Acoustic effect in passively mode-locked fiber ring lasers, Optics Letters 20, 907-909 (1995).

[2] E.M. Dianov, A.V. Luchnikov, A.N. Pilipetskii, A.M. Prokhorov, Long-range interaction of picosecond solitons through excitation of acoustic waves in optical fibers, Applied Physics B 54, 175-180 (1992).

[3] W. He, M. Pang, D.H. Yeh, P.S.J. Russell, Optoacoustic mode-locking based on micro-core photonic crystal fibre, in 2021 26th Microoptics Conference (MOC), 1-2 (2021).

[4] V.A. Ribenek, P.A. Itrin, D.A. Korobko, A.A. Fotiadi, Double harmonic mode-locking in soliton fiber ring laser acquired through the resonant optoacoustic coupling, APL Photonics 9(5), 056105 (2024).

Russian development and production of lasers: hybrid, solid-state and fiber laser systems

D.V. Sachenko[1]

1- JSC "NordLase", Saint-Petersburg

NordLaser LLC is a leading company in the field of development, production and service of laser systems. This presentation highlights the company's competencies, emphasizing expertise in the development, production and service of lasers and laser technologies.

The presentation will present the results of the development of new laser sources, technological solutions and describe their applicability in such fields as medicine, scientific research, micro- and nano-processing.

Lasing on optically pumped Ar-Ne active medium at 912 nm

V.A. Shaidulina, **Yu.A. Adamenkov, M.A. Gorbunov, E.V. Kabak, A.A. Kalacheva, A.V. Juriev**

FSUE "RFNC-VNIIEF", Mira str, 37, Sarov, Russia, 607190

oefimova@otd13.vniief.ru

The optically pumped rare gas laser (OPRGL) is a new type of optically pumped gas laser with high quantum efficiency, which can convert the high output power of a diode laser into the output power of a gas laser with high beam quality. In [1], the first generation on inert gases was demonstrated. According to published open sources, there has been a serious step in the world in studying the properties of the active medium on the model of a laser source based on a mixture of rare gases with optical pumping. The discharge was optimized and became stable at atmospheric pressure [2,3].

Results of measurement of laser output power on mixture of inert gases with optical pumping (OPRGL) are presented. An experimental gas mixture consisting of 98% Ne (buffer gas) and 2% Ar was used as the active medium.

The main registered parameter of the experiments was the generation power, which was measured by an optical calorimeter. Variable parameters in experiments were: pressure and flow rate of the gas mixture in the discharge chamber, reflection of the output mirror of the (flat) optical resonator, repetition rate of discharge pulses. Laser generation at a wavelength of 912 nm was obtained and the generation power level was investigated depending on the experimental setup parameters. The maximum value of the obtained lasing power was 110 mW.

[1] J. Han and M.C. Heaven, Gain and lasing of optically pumped metastable rare gas atoms, Optics Letters. – 2012. – Vol. 37, No. 11, pp. 2157-2159.

[2] D.J. Emmons and D.E. Weeks, Kinetics of high pressure argon-helium pulsed gas discharge, Journal of Applied Physics. – 2017. – Vol. 121, No. 20.

[3] J. Han, L. Glebov, G. Venus, M.C. Heaven, Demonstration of diode-pumped metastable Ar laser, Optics Letters. – 2013. – Vol. 38, No. 24, pp. 5458-5461.

Lasing on optically pumped metastable krypton atoms at 893 nm

V.A. Shaidulina, Yu.A. Adamenkov, M.A. Gorbunov, E.V. Kabak, A.A. Kalacheva, A.V. Juriev

FSUE "RFNC-VNIIEF", Mira str, 37, Sarov, Russia, 607190

oefimova@otd13.vniief.ru

The optically pumped rare gas laser (OPRGL) is a new type of optically pumped gas laser with high quantum efficiency, which can convert the high output power of a diode laser into the output power of a gas laser with high beam quality. In [1], the first generation at a wavelength of 893.1 nm was demonstrated. According to published open sources, there has been a serious step in the world in studying the properties of the active medium on the model of a laser source based on a mixture of rare gases with optical pumping. The discharge was optimized and became stable at atmospheric pressure [2,3].

A mixture of krypton (3%) and helium (97%) is used as the LONIG active medium. The main purpose of using helium is to increase the collisional relaxation from the pump level to the upper laser level in order to create the largest population inversion.
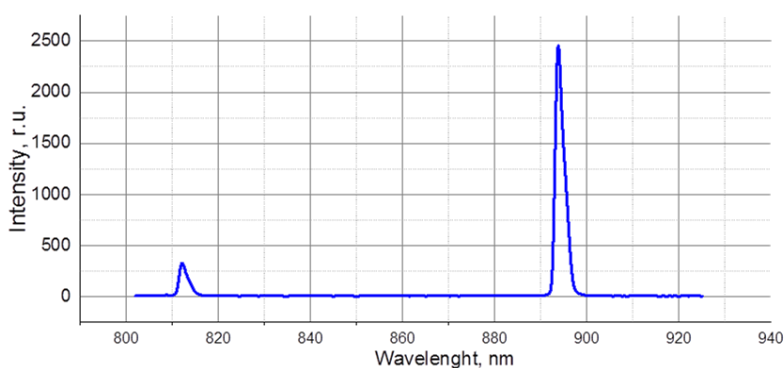
Fig.1. Pump laser at a wavelength of 811 nm and krypton generation at a wavelength of 893 nm.

The results of an experiment on laser generation using metastable krypton atoms with optical pumping 893 nm are presented. An electric discharge was used to obtain metastable krypton atoms at atmospheric pressure. Optical pumping was performed using diode laser radiation. Kinetic model of the Ar-He and Kr-He plasmas were created. Efficiency of metastable atom production in these plasmas was compared. The lasing power measured with an optical calorimeter was 30 mW.

[1] J. Han and M.C. Heaven, Gain and lasing of optically pumped metastable rare gas atoms, Optics Letters. – 2012. – Vol. 37, No. 11, pp. 2157-2159.
[2] D.J. Emmons and D.E. Weeks, Kinetics of high pressure argon-helium pulsed gas discharge, Journal of Applied Physics. – 2017. – Vol. 121, No. 20.
[3] J. Han, L. Glebov, G. Venus, M.C. Heaven, Demonstration of diode-pumped metastable Ar laser, Optics Letters. – 2013. – Vol. 38, No. 24, pp. 5458-5461.

Kinetic processes in argon-helium plasma

A.V. Juriev, Yu.A. Adamenkov, M.A. Gorbunov, E.V. Kabak, A.A. Kalacheva, V.A. Shaidulina

FSUE "RFNC-VNIIEF", Mira str, 37, Sarov, Russia 607190

oefimova@otd13.vniief.ru

The optically pumped rare gas laser (OPRGL) is a new type of optically pumped gas laser with high quantum efficiency, which can convert the high output power of a diode laser into the output power of a gas laser with good beam quality. In [1], the first generation on inert gases was demonstrated. The article presents a theoretical investigation of the kinetic processes occurring in the argon-helium plasma of a pulsed discharge.

Included in the kinetics of the argon-helium plasma model is the consideration of 11 energy states of argon and helium atoms: argon atoms Ar and helium He in the ground state, argon atoms Ar^* and helium He^* in the excited state, atomic ions of argon Ar^+ and helium He^+, homonuclear ions of argon Ar_2^+ and helium He_2^+, heteronuclear ion $HeAr^+$ and excimer molecules of argon Ar_2^* and helium He_2^*. The excitation and ionization energies of the argon-helium plasma particles are shown in Table 1.

Table 1 – Excitation and ionization energy of argon-helium plasma particles.

Particle	Ar^*	He^*	Ar^+	He^+	Ar_2^+	He_2^+	$HeAr^+$	Ar_2^*	He_2^*
Energy, eV	11.55	19.8	15.76	24.59	14.5	22.23	15.74	11.06	17.97

A model of argon-helium plasma was created and the main reactions of formation and quenching of plasma particles were studied. A general scheme of kinetic processes of the plasma of inert gases of a pulsed discharge has been formed.

As a result of the work, the following results were achieved: kinetic model of Ar-He plasma was compiled, taking into account the interaction of 11 energy states of argon and helium in 64 interaction reactions; plasma particle concentration was calculated and the rate of each interaction reaction was determined. For each argon and helium energy state, the mechanisms that have the greatest effect on particle concentration are indicated; scheme of key reactions occurring in argon-helium plasma has been determined.

[1] J. Han and M.C. Heaven, Gain and lasing of optically pumped metastable rare gas atoms, Optics Letters. – 2012. – Vol. 37, No. 11, pp. 2157-2159.

Competition between stimulated Raman scattering and nonlinear phase modulation in crystals under pumping by powerful subpicosecond laser

S.N. Smetanin[*], **D.P. Tereshchenko, Yu.A. Kochukov, A.G. Papashvili, K.A. Gubina,
V.V. Bulgakova, A.A. Ushakov, V.E. Shukshin, E.E. Dunaeva, I.S. Voronina, L.I. Ivleva**

Prokhorov General Physics Institute of the Russian Academy of Sciences, Vavilova 38, 119991, Moscow, Russia

* ssmetanin@bk.ru

Multiwavelength ultrafast laser sources with wavelengths in a range of 1000-1300 nm of the therapeutic transparency window of biological tissue are of high importance for optical multiresonance biomedical diagnostics [1]. Non-invasive exposure to biological tissue requires the use of ultrashort laser pulses with a duration of about 1 ps and shorter. Increasing the number of spectral components of ultrafast laser radiation in this range can be realized by transient stimulated Raman scattering (SRS) in scheelite-type crystals ($BaWO_4$, $SrWO_4$, $SrMoO_4$, and others) having dual Raman modes with comparable integral cross-sections of Raman scattering [2]. However, decreasing the laser pulse duration shorter than the Raman mode dephasing time of the order of 1 ps leads to competition between SRS and nonlinear phase modulation (self-phase modulation of the pump pulse and cross-phase modulation of the Stokes pulse) suppressing such highly transient SRS [3]. Recently, highly transient, multiwavelength, single-pass SRS generation on dual Raman modes (888 cm^{-1} and 327 cm^{-1}) has been obtained in a $SrMoO_4$ crystal under ultrafast single-pulse pumping by a powerful, subpicosecond, 1030-nm Yb fiber laser [4]. A controllable negative chirp of the input pump laser pulse compensating a positive chirp of the pump pulse self-phase modulation in the crystal allowed increasing SRS conversion efficiency into one of four (1066, 1134, 1177, and 1261 nm) radiation components with the combined Raman shifts in the desired range.

In this contribution, for the first time to our knowledge, competition between highly transient SRS on dual Raman modes and nonlinear phase modulation in crystals is investigated under conditions of not only chirping of input subpicosecond pump pulses, but also using a double-pulse pumping scheme [5]. In the double-pulse scheme, the second pump pulse, delayed relative to the first pump pulse for a delay of the order of a dephasing time of the Raman mode, is efficiently scattered on the vibration coherently driven by the first pump pulse. As a result, more efficient and simultaneous Raman generation on dual Raman modes in the desired range of 1000-1300 nm has been achieved in a wide range of the chirped pump pulse durations for the double-pulse than for the single-pulse pumping scheme.

[1] Ch. Stringari, L. Abdeladim, G. Malkinson, P. Mahou, X. Solinas, I. Lamarre, S. Brizion, J.-B. Galey, W. Supatto, R. Legouis, A.-M. Pena, E. Beaurepaire, Multicolor two-photon imaging of endogenous fluorophores in living tissues by wavelength mixing, Sci. Rep. 7, 3792 (2017).
[2] M. Frank, M. Jelínek, D. Vyhlídal, V.E. Shukshin, L.I. Ivleva, E.E. Dunaeva, I.S. Voronina, P.G. Zverev, V. Kubeček, Stimulated Raman scattering in alkali-earth tungstate and molybdate crystals at both stretching and bending Raman modes under synchronous picosecond pumping with multiple pulse shortening down to 1 ps, Crystals, 9, 167 (2019).
[3] L.L. Losev, J. Song, J.F. Xia, D. Strickland, V.V. Brukhanov, Multifrequency parametric infrared Raman generation in KGd(WO$_4$)$_2$ crystal with biharmonic ultrashort-pulse pumping, Opt. Lett. 27, 2100-2102 (2002).
[4] A.G. Papashvili, Yu.A. Kochukov, D.P. Tereshchenko, S.N. Smetanin, P.D. Kharitonova, V.E. Shukshin, E.E. Dunaeva, I.S. Voronina, L.I. Ivleva, Highly transient stimulated Raman scattering in SrMoO$_4$ under ultrafast laser pumping with a controllable chirp, Opt. Lett. 48, 4528-4531 (2023).
[5] A.V. Konyashchenko, L.L. Losev, V.S. Pazyuk, Femtosecond Raman frequency shifter-pulse compressor, Opt. Lett. 44, 1646-1649 (2019).

Laser speckle-vibrometer for detection of transverse and angular displacements

A.I. Trikshev[*], **V.A. Kamynin, V.B. Tsvetkov**

Prokhorov General Physics Institute of the Russian Academy of Sciences, Vavilov St., 38, 119991, Moscow, Russia

* trikshevgpi@gmail.com

Laser speckle vibrometry is a modern technology for remote measurement of mechanical vibrations of objects [1-4]. The main advantages of the measurement method include: remote and non-contact measurement of vibration; no influence on the resonance properties of objects; no preliminary preparation of the object surface is required. The main advantage of this method is that the speckle pattern is formed in the whole space around the scattering object. This pattern can be observed both at zero angle to the surface and at large deviations from the normal. Specificity of the measurement technique allows to carry out measurements both at short distances (less than a meter) and at long distances (tens of meters) due to the adjustment of the optical system.

The setup used a single-frequency semiconductor laser diode with a 976 nm wavelength. A monochrome camera with a lens with a focal length of 100 mm was used as an image receiver. Linear translation stage and mini rotation stage were used to realize the displacements. The screen was installed on a stage. The distance from the screen to the speckle vibrometer was more than 2.5 m. Figure 1 shows speckle patterns obtained when the screen was moved transversely by 0.1 mm. The short line indicates the original position of the line.

| a) | b) | c) | d) |
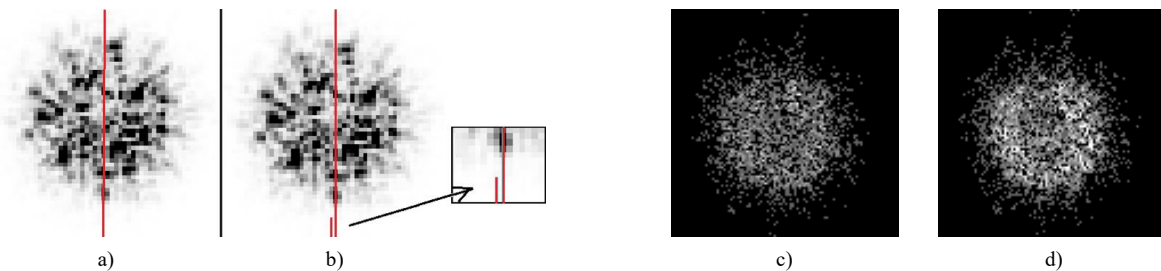
Fig. 1. Speckle patterns a) before and b) after transverse movement of the screen by 0.1 mm; c) difference pattern of two adjacent frames, d) difference pattern of frames before and after the displacement by 10 µm.

Difference patterns were used to register movement over a distance of 10 µm (Fig.1 c,d). This is because the image displacement on the matrix was less than 1 pixel. With optimization of the optical system and more careful mathematical processing of the data, a movement of 1 µm could be recorded. In Fig. 2. speckle patterns obtained at an angular screen offset of 0.001 rad are presented.
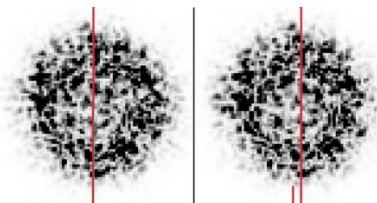
Fig. 2. Speckle patterns obtained when the screen was moved angularly by 0.001 rad.

As a result, transverse displacements up to 1 µm and angular displacements up to 0.001 rad at distances greater than 2.5 m were recorded. However, according to the data obtained for angular displacements it follows that with additional processing it is possible to determine angular displacements better than 10^{-4} rad.

[1] H. Hong, J. Liang, L. Deng, W. Guo, X. Wang, Optics Letters, vol. 48, p. 3837, 2023.
[2] M. Sheinin, et al, Proceedings of the IEEE/CVF Conference on Computer Vision and Pattern Recognition, p. 16324-16333, 2022.
[3] X. Huang, et al, Optics & Laser Technology, vol. 148, p. 107759, 2022.
[4] N. Wu, S. Haruyama, Sensors, vol. 21(9), p. 2938, 2021.

Specific features of measuring the electrophysical parameters in polar crystals

V. Umylin[1]*, N. Kozlova[1], E. Zabelina[1], V. Petrakov[1], A. Temirov[1]

1- University of Science and Technology MISIS; Leninsky avenue, 4, Moscow, Russia, 119049

* v.umylin@mail.ru

Currently, there is a high demand for devices that use polar cuts of crystals covered with current conductive coatings. Such devices are compact and highly reliable, but their service life is limited. In particular, due to the processes of degradation and aging of the surfaces of crystalline elements upon contact with conductive coatings.

Degradation is usually associated with external influences that lead to a significant negative change in the required properties. Aging is considered as a spontaneous change in electromechanical properties with time without the application of external stress and at a constant temperature. Therefore, aging and degradation lead to unreliability of the readings transmitted by devices and a reduction in their service life.

It is known that a conductive coating can greatly influence to the electrical and dielectric properties and even the phase stability of the material. This leads to degradation and aging of the surfaces of crystalline elements. Typically, consideration of the contribution of conductive coatings to the effects of fatigue and aging is usually limited to the processes of delamination of conductive coatings, as well as changes in their microstructure or geometric parameters. However, other phenomena are also observed.

The purpose of this work was to study the features of measuring electrophysical parameters in samples of polar cuts of α-LiIO$_3$ crystals with different conductive coatings materials and using various measurement schemes.

The samples of α-LiIO$_3$ polar cut (perpendicular to the 6th order inversion axis) without preliminary polarization and external influences with different conductive coating materials (In, Al, Ar, Cu, Cr) were used for research. Samples with symmetrical conductive coatings were studied $E_1|crystal|E_1$. Samples with different conductive coatings were also studied according to the following principle: $E_1|^+crystal^-|E_2$ then $E_2|^+crystal^-|E_1$. Investigation of samples with the above-mentioned conductive coatings were carried out in the temperature range 25-210°C. To set and maintain a certain temperature regime, a heating chamber, a temperature control system and a heater power supply were used. The furnace temperature was recorded using a chromel-alumel thermocouple.

The temperature dependences of the short-circuit currents of the samples were obtained. The influence of the material of conductive coatings and the side of application of the electrodes on the value of the short-circuit currents and the direction of their flow has been established.

Sub-nanosecond light pulse generator based on FDML-laser

X. Yang[1,2], R.V. Romashko[1], J. Zhang[2*]

1- Institute of Automation and Control Processes, Far Eastern Branch, Russian Academy of Science,
5 Radio Str., Vladivostok, Russia
2- Key Lab of In-Fiber Integrated Optics, Ministry Education of China, Harbin Engineering University,
Harbin 150001, China

* zhangjianzhong@hrbeu.edu.cn

Fourier-Domain Mode-Locked (FDML) laser represent a significant advancement in the fields of optical coherence tomography (OCT) and high-speed imaging applications [1]. Widely used in the detection of cancer, ophthalmology, and dermatological diseases [2-4]. FDML laser function as high-speed spectrometers in the time domain [5]. Ensuring the consistency between the cavity's fundamental frequency and the tunable filter's frequency across different wavelengths in the laser cavity is essential [6].

We address these challenges by using Fiber Bragg Gratings (FBG) for wavelength calibration to mitigate the inherent hysteresis and creep issues of the tunable filter, and dynamic PZT for dispersion compensation to counteract the dispersion caused by the kilometers-long fiber in the FDML system. These measures enable us to achieve a stable time-wavelength relationship and stable laser output. Additionally, we are developing an FDML laser-based bubble detection system and exploring its potential in marine resource development and medical isotope preparation.
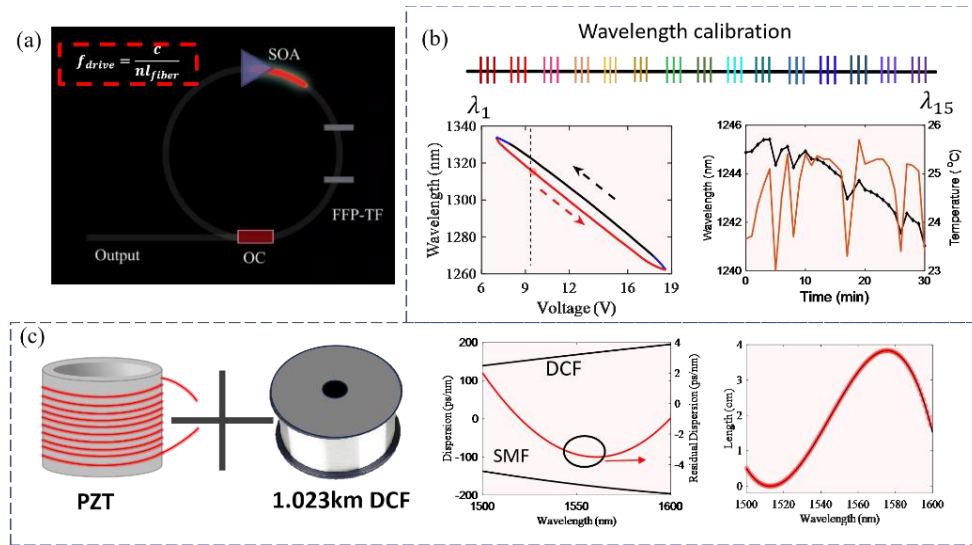
Fig. 1. (a) is the system installation diagram of FDML, and Fig. 1. (b) shows the wavelength calibration system of the FBG array, the hysteresis curve of the tunable filter, and the effect of temperature on the tunable filter. Fig. 1. (c) shows the solution of combining dynamic PZT and dispersion compensation fiber, the dispersion coefficient curves of 10.2km fiber and 1.023km dispersion compensation fiber, and the responsivity of PZT.

[1] R. Huber, M. Wojtkowski, J.G. Fujimoto, Fourier Domain Mode Locking (FDML): A new laser operating regime and applications for optical coherence tomography, Opt. Express 14(8), 3225–3237 (2006).
[2] R. Raghunathan, M. Singh, M.E. Dickinson, K.V. Larin, Optical coherence tomography for embryonic imaging: a review, J. Biomed. Opt. 21(05), 1 (2016).
[3] R.A. Leitgeb, En face optical coherence tomography: a technology review [Invited], Biomed. Opt. Express 10(5), 2177–2201 (2019).
[4] A. Zhang, Q. Zhang, C.-L. Chen, R.K. Wang, Methods and algorithms for optical coherence tomography-based angiography: a review and comparison, J. Biomed. Opt. 20(10), 100901 (2015).
[5] D. Huang, Y. Shi, F. Li, P.K.A. Wai, Fourier Domain Mode Locked Laser and Its Applications, Sensors 22(9), 3145 (2022).
[6] C. Jirauschek, B. Biedermann, R. Huber, A theoretical description of Fourier domain mode locked lasers, Opt. Express, 2009.

Optical properties of LiNb$_{1-x}$Ta$_x$O$_3$ solid solution crystals

E.V. Zabelina[1*], **A.A. Mololkin**[1,2,3], **N.S. Kozlova**[1], **V.M. Kasimova**[1],
R.R. Fakhrtdinov[3], **V.E. Umylin**[1], **A.V. Sosunov**[4]

1- National University of Science and Technology "MISIS", 119049, Russia, Moscow, Leninsky pr., 4, b. 1
2- FOMOS-MATERIALS, 107023, Russia, Moscow, Buzheninova st., 16
3- Institute of Microelectronics Technology and High Purity Materials, Russian Academy of Sciences,
142432, Russia, Moscow region, Chernogolovka, Academician Osipyan st., 2
4- Perm State University, 614990 Russia, Perm, Bukireva st., 15

* zabelina.ev@misis.ru

LiNbO$_3$ (LN) and LiTaO$_3$ (LT) are well-known ferroelectric crystals that are widely used in the field of optics and acoustics to create electro-optics products, nonlinear optics, surface acoustic wave devices, piezoelectric sensors, etc. LN and LT are isomorphs, have a pseudo-ilmenite structure in the ferroelectric phase, belong to the 3m point symmetry group, and are described within the sp. gr. R3c.

In the ternary quasi-binary Li$_2$O–Nb$_2$O$_5$–Ta$_2$O$_5$ system, a series of complex oxides may exist. The composition of these oxides vary, depending on the ratio of isomorphic cations. The lithium oxide concentration of 50% may result in the formation of a continuous series of LiNb$_{(1-x)}$Ta$_x$O$_3$ (LNT) solid solutions with different ratios of isomorphic cations (from LiNbO$_3$ to LiTaO$_3$). This makes it possible to obtain crystals of LNT solid solutions of intermediate compositions. Composition change makes it possible to significantly regulate the physical properties of the material and obtain crystals with different properties.

In this regard, the goal of this work was to obtain LNT crystals of intermediate compositions and study their optical properties.

LNT were grown at the Institute of Microelectronics Technology and High Purity Materials of the Russian Academy of Sciences by the Czochralski method in Pt crucibles using an upgraded NIKA-3M system [1].

The crystals were grown from a charge of two different compositions: LiNb$_{0.95}$Ta$_{0.05}$O$_3$ and LiNb$_{0.97}$Ta$_{0.03}$O$_3$. According to the phase diagram, crystals of the composition LiNb$_{0.88}$Ta$_{0.12}$O$_3$ are grown from the charge LiNb$_{0.95}$Ta$_{0.05}$O$_3$, and from the charge LiNb$_{0.97}$Ta$_{0.03}$O$_3$ – crystals with composition LiNb$_{0.93}$Ta$_{0.07}$O$_3$.

After the growth, the crystals were subjected to longterm annealings in the growth chamber at a temperature of 950–1100°C for 8–12 h.

From LiNb$_{0.88}$Ta$_{0.12}$O$_3$ and LiNb$_{0.93}$Ta$_{0.07}$O$_3$ crystals we prepared samples in the form of rectangular parallelepipeds with polished faces oriented along the crystallophysical axes in a standard setup. All samples were subjected to high-temperature electrodiffusion treatment (monodomenization) to bring the crystals to the single-domain state and eliminate the macro- and microdefect structure.

The optical properties of the sample were investigated in the accredited tested laboratory of semiconductor materials and dielectrics "Single Crystals and Stock on their base" of National University of Science and Technology "MISIS". The spectral dependences of the transmittance T(λ) were measured on a Cary-5000 spectrophotometer (Agilent Technologies) with a universal measurement accessory (UMA) in natural polarized visible light (300–700 nm).

[1] D. Roshchupkin, R. Fakhrtdinov, B. Redkin, et al, Growth of ferroelectric lithium niobate-tantalate LiNb$_{(1-x)}$Ta$_x$O$_3$ crystal, Journal of Crystal Growth, vol. 621. № 1, pp. 1-8, (2023).

Er-Yb all-fiber lasers with sub-GHz pulses repetition rates based on composite active fibers

A. Zverev[1]*, **V. Kamynin[1], V. Tsvetkov[1], B. Denker[1], S. Sverchkov[1], V. Velmiskin[1],**
Y. Gladush[2], D. Krasnikov[2], A. Nasibulin[2]

1- Prokhorov General Physics Institute of the Russian Academy of Sciences, Russia
2- Skolkovo Institute of Science and Technology, Moscow, Russia

* izverevad@gmail.com

The intensive development in the creation of ultrashort pulse (USP) sources with high repetition rates (sub-gigahertz level) operating in the 1.5-micron spectral range is driven by their wide application in fields such as analog-to-digital converters [1], frequency comb-based spectroscopy [2], and laser material processing [3]. One method of obtaining a stable sequence of ultrashort pulses with such high repetition rates is the implementation of mode-locking in a laser with a very short cavity, based on specially heavily doped composite active fibers (which lack the drawbacks of purely phosphate fibers) and hybrid optical components.
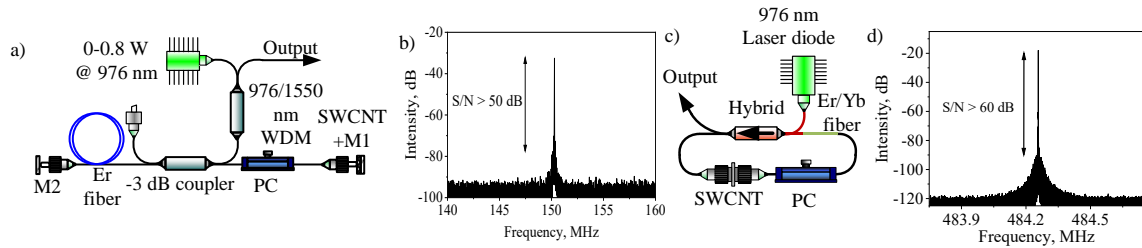
Fig.1. a) Initial scheme of an erbium fiber laser with a linear cavity. b) RF spectrum of initial signal.
c) A ring laser based on a hybrid element. d) The radio frequency spectrum of the ring laser signal.

Initially, to test the feasibility of using composite fiber (with an erbium ion concentration of about $N \approx 10^{20}$ cm^{-3}) as the active medium of USP sources with a high repetition rate, we tested a linear cavity (Figure 1(a)). The active fiber, only 12 cm long, was pumped by a laser diode at a wavelength of 976 nm through a multiplexer and an optical splitter. One polarization controller (PC) was used to tune the laser generation mode. Aluminum foil pressed against optical ferrules served as mirrors (SWCNT+M1 and M2) in the cavity. To achieve mode-locking, single-walled carbon nanotubes (SWCNTs) were applied to one of the ferrules. With the maximum possible reduction in the length of the resonator in this configuration, stable generation of USP with a repetition rate of 150 MHz (the radio-frequency spectrum of the output signal is shown in Figure 1(b)) at the central wavelength was obtained at a pump power of 740 mW. The pulse duration was 0.5 ps, and the average output power was 9.2 mW. Next, to increase the pulse repetition rate and reduce the required pump power, we decided to change the resonator scheme to a ring configuration (Figure 1(c)), using an 18 cm long composite fiber doped with an Er/Yb complex and a hybrid element (WIT) serving as a WDM, isolator, and optical splitter (the coupler split was 90/10 with a 10% yield). Mode-locking was also achieved with SWCNT placed between two optical connectors. In this configuration, a straightforwardly launched mode-locking regime with a fundamental pulse repetition rate of 484 MHz (the radio-frequency spectrum of the signal is shown in Figure 1(d)) was obtained at a central emission wavelength of 1542.8 nm (the spectral width at half maximum was 1.6 nm) at a pump power of 168 mW. The pulse duration and average output power were 1.6 ps and 1.5 mW, respectively.

Thus, we have carried out an optimization of the laser circuit, as a result, sources with a repetition rate of ultrashort pulses from 150 to 484 MHz have been obtained.

[1] G.C. Valley, Photonic analog-to-digital converters, Optics express, 15(5), 1955-1982, (2007).
[2] T. Fortier and E. Baumann, 20 years of developments in optical frequency comb technology and applications, Communications Physics, 2(1), 153, (2019).
[3] H. Kalaycıoğlu, P. Elahi, Ö. Akçaalan, F.Ö. Ilday, High-repetition-rate ultrafast fiber lasers for material processing, IEEE Journal of selected topics in quantum electronics, 24(3), 1-12, (2017).

LASER DIAGNOSTICS AND SPECTROSCOPY

On the possibility of using neural network in tasks of laser induced breakdown spectroscopy

A.V. Bulanov[1]

1- V.I. Il'ichev Pacific Oceanological Institute, FEB RAS, Vladivostok, Russia

a_bulanov@me.com

In the context of increasing human impact on ecosystems and the introduction of international carbon taxes, it becomes extremely important to study the flows, emissions and "burial" of carbon dioxide in various environments, as well as the creation of corresponding "carbon polygons". The use of optical spectroscopy methods allows for continuous monitoring of many environmental characteristics in real time, both directly on site and at a distance. To solve a number of fundamental and applied problems, regular measurements taken in the water column are necessary. The use of spark and laser-induced breakdown spectroscopy (LIBs) methods for elemental analysis of liquids in oceanological research is a relevant research, but is accompanied by certain difficulties.

To solve the problems of studying the World Ocean, an automated complex for studying the spectral optical characteristics and hydrophysical characteristics of the upper layer of the sea using the flow method was developed, which makes it possible to study the variability of the optical and hydrophysical structure of the marine environment along the vessel route crossing various water masses.

In order to record optical data, a specially developed spark complex was used. To analyze the obtained spectral data, a program was created in the Python programming language, designed for processing and visualizing statistical data of laser breakdown. The input data for the program was a set of *.csv data breakdown spectrum image files, generated using STM32 and transferred to a microcomputer via a serial port. The program indicated the wavelength of the monochromator when recording optical breakdown. Processing of files into folders with different values of exposure, delay, etc. was implemented. Preset analytical algorithms for optical image processing (averaging, finding peaks, etc.) were implemented. The result was a breakdown spectrum with highlighted spectral lines of chemical elements. As a result, the dependence of the intensity of the spectral lines of chemical elements, such as sodium and calcium, was obtained during optical breakdown in an aerosol cloud from sea water using ultrasound.

In addition to the above listed experimental methods for studying matter in order to improve the sensitivity of LIS spectroscopy, the problem of processing a large amount of data received in real time was solved. It should be noted that the rapid processing of numerous spectra obtained as a result of optical breakdown measurements is associated with detailed analysis and in a significant number of cases is a labor-intensive procedure. The rapid development of current trends related to the use of neural networks and machine learning algorithms could come to the rescue and allow more accurate classification, regression, clustering and other operations with samples to obtain information about the spectrum and study of matter. To further improve the sensitivity of the LIBs method, analysis of breakdown signals using artificial neural networks (ANN) was proposed, which was used to estimate the contribution of dissolved organic and inorganic carbon in a carbon test site.

The model was implemented in Python using TensorFlowTM, and the weights and biases of the model were optimized using a backpropagation algorithm.

To summarize, the obtained studies of laser breakdown made it possible to formulate the basic principles of creating a method of combined ultrasonic laser spark spectroscopy and to create a compact automated complex for studying the spectral optical and hydrophysical characteristics of the upper layer of the sea using the flow method. This complex was successfully tested under expeditionary conditions during voyage No. 81 of the R/V Professor Gagarinsky in the Sea of Japan in August 2022, as well as during the 52nd voyage of the R/V Akademik Boris Petrov in the Atlantic Ocean and in the plume of the Amazon River in October - December 2022. Using this complex, new data on the state of sea water with high spatial resolution were obtained.

Nanosensor based on carbon dots with anti-Stokes luminescence

S. Burikov[1*], K. Laptinskiy[1,2], T. Dolenko[1]

1- Department of Physics, Lomonosov Moscow State University, Leninskie Gory 1/2, 119991 Moscow, Russia
2- Skobeltsyn Institute of Nuclear Physics, Lomonosov Moscow State University, Leninskie Gory 1/2, 119991 Moscow, Russia

* sergey.burikov@gmail.com

Carbon dots (CD) are a class of nanomaterials characterized by intense and stable luminescence, good dispersibility in water and biocompatibility. Recently, the study of the optical properties of CD has been of great interest. In particular, it was found that CD interact with environmental molecules in suspensions and can act as pH sensors [1]. One of the problems that arise when using CD-based sensors for the diagnostics of biological media and natural waters is the need to solve the problem of separating the contribution of CD luminescence against the background signal of intrinsic luminescence of the medium (autoluminescence).

However, this problem can be eliminated if it is possible to realize excitation of anti-Stokes luminescence when excited by radiation in the red region of the spectrum. In this case, CD luminescence spectrum is shifted to the short-wavelength region with respect to the wavelength of the exciting radiation, while the autoluminescence signal is not excited.

In this study, it is shown that for CD synthesized by the hydrothermal method from citric acid and ethylenediamine, it is possible to implement an anti-Stokes luminescence excitation mode under excitation by nanosecond laser pulses. It is shown that the luminescent properties of such CD in aqueous suspensions can depend on the temperature and pH of the medium, on interaction with ions and molecules present in the medium. Nanosensors of metal ions have been developed on the basis of CD with anti-Stokes luminescence and the accuracy of determining their concentration in solutions has been evaluated.

[1] K.A. Laptinskiy, M.Yu. Khmeleva, S.A. Burikov, A.M. Vervald, T.A. Dolenko. Carbon dots with up-conversion luminescence as pH-sensor. Applied Sciences, 2022, N12, 12006.

Development of a multimodal optical carbon ion nanosensor using neural networks

G. Chugreeva[1*], K. Laptinskiy[1,2], O. Sarmanova[1], T. Dolenko[1]

1- Faculty of Physics, M.V. Lomonosov Moscow State University, Russia
2- D.V. Skobeltsyn Institute of Nuclear Physics, M.V. Lomonosov Moscow State University, Russia

* chugreeva.gn17@physics.msu.ru

Carbon dots (CD) are nanoparticles with stable intense photoluminescence (PL), depending on the conditions of nanoparticle synthesis and extremely sensitive to changes in environmental parameters [1]. This combination of CD properties opens up broad prospects for the use of nanoparticles as optical nanosensors of the medium [2,3]. In all known publications on the nanosensorics of carbon nanoparticles, CD were considered as nanosensors of 1-2 environmental parameters, while in most practical tasks it is necessary to control changes in several parameters simultaneously.

In this study it is shown that using 2D convolutional neural networks, it is possible to solve the inverse problem of luminescent spectroscopy to determine the type and concentration of several ions in a medium at once using the excitation-emission matrices of PL CD. The results of the development of a photoluminescent nanosensor based on CD, capable to determine the concentrations of heavy metal cations Cu^{2+}, Ni^{2+}, Co^{2+}, Pb^{2+}, Al^{3+}, Cr^{3+} and anion NO_3^- in aqueous solutions simultaneously with an average absolute error of 0.77 mM, 1.22 mM, 0.79 mM, 0.58 mM, 0.39 mM, 0.28 mM and 1.64 mM, respectively, are presented (Fig. 1). The accuracy of solving the inverse problem satisfies the needs of monitoring the composition of technological and industrial waters.
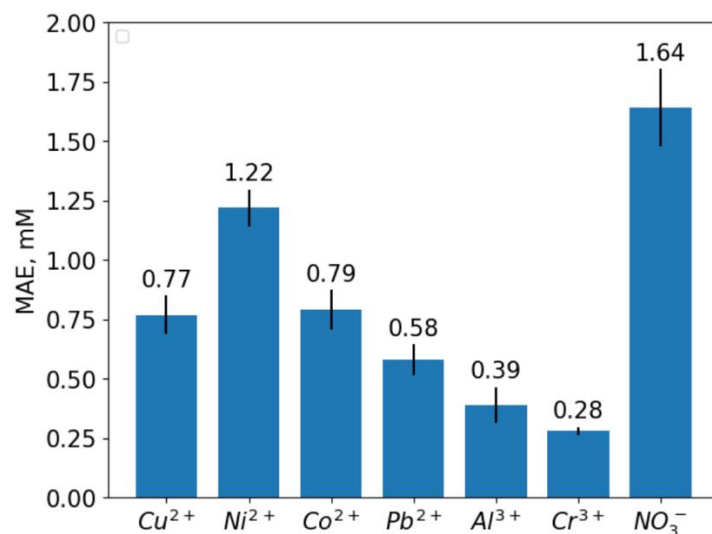
Fig. 1. Mean absolute errors (MAE) of ion concentration determination.

[1] A.M. Vervald, K.A. Laptinskiy, G.N. Chugreeva, S.A. Burikov, T.A. Dolenko, Quenching of Photoluminescence of Carbon Dots by Metal Cations in Water: Estimation of Contributions of Different Mechanisms, J. Phys. Chem. C, vol. 127, pp. 21617-21628, 2023.
[2] Y. Guo, Z. Wang, H. Shao, Hydrothermal synthesis of highly fluorescent carbon nanoparticles from sodium citrate and their use for the detection of mercury ions, Carbon, vol. 52, pp. 583–589, 2013.
[3] S. Liu, J. Tian, L. Wang, A general strategy for the production of photoluminescent carbon nitride dots from organic amines and their application as novel peroxidase-like catalysts for colorimetric detection of H_2O_2 and glucose, RSC Adv, vol. 2, pp. 411-413, 2012.

Determination of heavy metal ions in river water by spectroscopy and machine learning: use of transfer learning approach

A. Guskov[1,2], I. Isaev[1,3], S. Burikov[1,2], T. Dolenko[1,2], K. Laptinskiy[1], <u>S. Dolenko</u>[1*]

1- D.V. Skobeltsyn Institute of Nuclear Physics, M.V. Lomonosov Moscow State University, 1/2 Leninskie Gory, Moscow, 119991 Russian Federation
2- Faculty of Physics, M.V. Lomonosov Moscow State University, 1/2 Leninskie Gory, Moscow, 119991 Russian Federation
3- V.A. Kotelnikov Institute of Radio Engineering and Electronics, 11/7 Mokhovaya st., Moscow, 125009 Russian Federation

* dolenko@srd.sinp.msu.ru

Heavy metals ions are a class of substances that are often present not only in wastewater, but also in nature waters, and that are harmful for public health. That is why detection of such impurities and determination of their concentrations is a very topical task. Use of methods of chemical analysis provides high precision of measurement, but it requires special sample preparation, expensive reagents and high qualification of personnel. At the same time, spectroscopic methods are express and they can be used in remote mode.

However, to provide sufficient precision of spectroscopy-based measurements, one should use special data processing methods. In this study we use laser Raman spectroscopy, IR and optical absorption spectroscopy. While the shape of water spectra of all the three types is highly sensitive to presence of ions, simultaneous presence of several types of ions causes specific non-linear dependencies in spectra channel intensities on ion concentrations. Moreover, adequate modeling of spectra of such solutions is yet far beyond reasonable computational capabilities. By all these reasons, machine learning (ML) methods turn out to be a class of data processing methods that are very effective in solving such inverse problems.

At the same time, use of ML methods encounters its own specific difficulties. To provide an acceptable precision of concentration measurements, one needs a representative set of data to train the ML methods. As specified above, model spectra are unavailable, and obtaining a large enough database of experimental spectra is difficult and may be quite laborious and expensive.

If we speak of nature waters, there is one more problem complicating the spectra analysis. Nature waters always contain dissolved organic matter (DOM), which has intense and highly variable fluorescence partly overlapping the most interesting spectral regions. As DOM fluorescence depends on the origin of water, there is a need to introduce a special procedure that would make ML models resilient to variations in nature water spectra.

In this study, we consider two approaches that turn out to be efficient in this situation. One is integration of several spectroscopic methods – joint use of several types of spectra of the same sample. The other one is use of the so called transfer learning approach. Within this approach, one first trains an ML model on a large enough and representative dataset obtained in simple conditions (here we use spectra of about 3700 model solutions prepared in laboratory conditions in distilled water). After that, a much smaller amount of patterns (spectra) obtained for a specific situation (in this case, 200-400 samples prepared in river water) is used for fine tuning or the ML model, providing the sufficiently low error of determination of ion concentrations. We demonstrate [1] that both approaches are effective, and in some situations the most effective way is to use both method integration and transfer learning at once.

[1] A.A. Guskov, I.V. Isaev, S.A. Burikov, T.A. Dolenko, K.A. Laptinskiy, S.A. Dolenko. Transfer Learning for Neural Network Solution of an Inverse Problem in Optical Spectroscopy. Moscow University Physics Bulletin, V. 78, Suppl. 1, pp. S115–S121 (2023).

Mechanisms of interactions of carbon nanoparticles with metal ions and biomacromolecules

S. Burikov[1], A. Vervald[1], K. Laptinskiy[1,2], O. Sarmanova[1], G. Chugreeva[1], T. Dolenko[1*]

1- Department of Physics, Lomonosov Moscow State University, Leninskiye Gory 1/2, 119991 Moscow, Russia
2- Skobeltsyn Institute of Nuclear Physics, Lomonosov Moscow State University, Leninsky Gory 1/2, 119991 Moscow, Russia

* tdolenko@mail.ru

Currently, researches concerning photoluminescent carbon nanoparticles are actively developed due to their wide prospects for use in biomedicine, nanosensory, optoelectronics, etc. One of the such nanomaterials are carbon quantum dots (CQD), which have chemical stability, nontoxicity, biocompatibility, intense stable photoluminescence (PL), sensitive to surrounding molecules and environmental parameters. Namely sensitivity of the PL of CQD to the environment is basis for the widespread use of nanoparticles as nanosensors and medical nanoagents. It is obvious that the effective use of CQD in various applications is impossible without knowledge of the mechanisms of formation of their PL. Therefore, the study of the interactions of surface groups of CQD with metal ions and biomacromolecules and the effect of these interactions on the PL of nanoparticles is an urgent task.

In this study, CQD synthesized by hydrothermal method from citric acid and ethylenediamine were the objects of research. The results of studying the interactions of CQD with molecules of various solvents, ions of solutions of metal salts and proteins are presented.

Using Raman laser spectroscopy, a general tendency has been established for all studied CQD to weaken hydrogen bonds in proton solvents. Numerical estimates of the energy of hydrogen bonds in various solvents have been obtained.

It was found that photoluminescence of CQD with carboxyl and hydroxyl surface groups significantly depends on the pH of the medium. The mechanism of the pH effect on the PL of such nanoparticles is caused by the (de)protonation of the carboxyl and hydroxyl groups on the surface of CQD.

Quenching of PL of CQD by the ions Fe^{3+}, Cr^{3+}, Al^{3+}, Co^{2+}, Cu^{2+}, Pb^{2+}, Zn^{2+}, Ni^{2+}, Mg^{2+} present in the medium was detected. Using the Stern-Volmer theory and measured PL decay kinetics, it was found that Cu^{2+}, Zn^{2+}, Ni^{2+}, Mg^{2+} are characterized by a static type of quenching, while Fe^{3+}, Cr^{3+}, Al^{3+}, Co^{2+}, Pb^{2+} are characterized by a dynamic type of quenching. The molecular dynamics method was used to simulate the dynamics of molecular interactions in water with carboxyl, hydroxyl and amide groups and the specified metal ions. The analysis of the constructed functions of the radial distribution of ions of salts relative to the surface groups of CQD showed that metal cations and NO_3^- anions, when interacting with oppositely charged groups of CQD (deprotonated carboxyl group -COO– and superprotonated amide group $-NH_3^+$, respectively), are located at distances of 4.5, 7 and 9 Å from them. Thus, there are 1, 2 or 3 hydrate layers with a certain network of hydrogen bonds between the surface groups of nanoparticles and metal cations. A high correlation has been established between the theoretical and experimental series in terms of the degree of quenching PL of CQD.

The results were obtained using laser Raman spectroscopy, photoluminescent spectroscopy, laser time-resolved spectroscopy, laser correlation spectroscopy, and IR absorption spectroscopy. Quantum chemical calculations and the method of molecular dynamics were used.

Anomalous femtosecond dynamics in hybrid and all-metal magnetophotonic metasurfaces

T.V. Dolgova[1*], M.A. Kiryanov[1], I.A. Novikov[1], G.S. Ostanin[1], D.A. Safiullin[1], M. Inoue[2], A.A. Fedyanin[1]

1- Faculty of Physics, Lomonosov Moscow State University, Moscow, 119991 Russia
2- Department of Electrical and Electronic Information Engineering, Toyohashi University of Technology 1-1 Tempaku-cho, Toyohashi, Aichi, 441-8580 Japan

* dolgova@nanolab.phys.msu.ru

Resonant plasmonic systems can significantly increase both the degree of impact to an electromagnetic wave on the medium and the influence of the medium on the electromagnetic wave. On the other hand, powerful femtosecond laser pulses are widely used to study and control ultrafast processes in solid-state nanostructures. Therefore, it is possible to use non-steady-state ultrafast plasmonics to solve various fundamental problems. Laser heating with high peak power pulses has a nonlinear effect on the optical response of both homogeneous materials and metasurfaces. Such a pulse heats the electron gas in the metal, leading to a change in the dielectric constant. There is a theoretical model that describes the temperature of a metal when heated by a femtosecond pulse, also known as the two-temperature model [1]. The metal is considered as a two-temperature system consisting of an electron and a phonon subsystems. The model assumes that at the beginning the electron gas is heated under the influence of the incident pulse, remaining all the time in an equilibrium state. However, it turns out that such a description is not always sufficient. In resonant plasmonic and hybrid metal-dielectric systems, the dynamics of the optical response can deviate greatly from those predicted by the two-temperature model.

This work provides examples of resonant systems with the features: an all-nickel magnetoplasmonic crystal with surface modulation that implements the critical coupling condition, a hybrid metal-dielectric metasurface of gold nanospheres in yttrium-iron-garnet matrix. The results of experiments in a pump-probe scheme with features of the relaxation dynamics of the optical and magneto-optical response will be presented. Methods for describing such relaxation beyond the two-temperature model are discussed.

Besides, femtosecond laser pulses in a pump-probe design are also widely used to photogenerate charge carriers in a semiconductor to control terahertz radiation [2]. In terahertz semiconductor antennas, under the influence of a photon in the optical range, an electron-hole pair is created, which significantly changes the properties of the semiconductor in terms of the interaction of terahertz waves with it (transmission, absorption), and also allows the generation of terahertz radiation due to nonlinear interactions. If, using a femtosecond pulsed laser source, an image of a mask is projected onto a semiconductor crystal, for example, GaAs, an amplitude and phase mask corresponding to the image is formed on its surface [3]. The experimental results on propagating plasmon excitation in a tunable photoinduced gratings on GaAs surface are demonstrated above metallization fluence threshold.

[1] S.I. Anisimov and B.L. Kapeliovich, Electron emission from metal surfaces exposed to ultrashort laser pulses, J. Exp. Theor. Phys. 66, 375-377 (1974).

[2] I. Chatzakis, P. Tassin, L. Luo, N.-H. Shen, L. Zhang, J. Wang, T. Koschny, C.M. Soukoulis, One- and two-dimensional photo-imprinted diffraction gratings for manipulating terahertz waves, Appl. Phys. Lett. 103, 043101 (2013).

[3] G. Georgiou, H.K. Tyagi, P. Mulder, G.J. Bauhuis, J.J. Schermer, J. Gómez Rivas, Photo-generated THz antennas, Sci Rep 4, 3584 (2014).

Carrier-envelope phase control of single cycle pulse generation and pump-probe spectroscopy

I.V. Saitsky[1], A.A. Voronin[1,2], E.A. Stepanov[1,2], A.A. Lanin[1,2],
P.B. Glek[1], R.M. Aliev[1], <u>A.B. Fedotov</u>[1,2*]

1- Physics Department, M.V. Lomonosov Moscow State University, Moscow 119992, Russia
2- Russian Quantum Center, Skolkovo, Moscow Region, 143025 Russia

* a.b.fedotov@physics.msu.ru

The carrier-envelope phase (CEP) of near single cycle laser pulses plays an important role in physics of strong field interaction and attosecond optics [1-4]. Our approach of such pulses generation is based on exploring nonlinear optical transformation of the femtosecond laser pulses with the central wavelength near 2 μm in anti-resonant hollow-core fiber (AR HCF) filled with argon [5]. The supercontinuum generation is leaded by the soliton self-compression (SSC) scenario, with additional enhancement from the self-steepening effect and parametric generation of four-wave components in the blue wing of the soliton spectrum. In such condition it is possible to form very short pulses with the duration less than on cycle of the field with the noticeable influence of CEP.

In our investigation we explore the signatures of phase dependence in the visible part of the SC generated during SSC down to single-cycle pulsewidth in an anti-resonant hollow-core fiber (AR HCF) filled with argon. This phenomenon is observed within the small parameter range, when the pulse reaches its maximum compression ratio, but there is still no strong ionization, leading to pulse decay. Theoretical analysis by means of the numerical solution of the generalized nonlinear Schrödinger equation (GNSE) reveals that the phase dependence arises from the broadband third harmonic generation (THG) in the range from 250 nm to 800 nm at the moment of a sub-cycle pulse composition and its spectral interference with the visible part of the SC. The CEP control of this ultrabroadband f-3f interference provides a signature of the sub-cycle pulse synthesis during SSC in the fiber with duration of 0.4 optical cycles and peak power more than 2 GW on the fiber output [6].

By means of such CEP controlled pulses with a duration about one optical period and pump-probe scheme, we experimentally demonstrated the generation of spectral components sensitive to the phase of the carrier relative to the pump pulse envelope on plasma nonlinearity in a thin film of zinc selenide (ZnSe). The probing pulse is scattered by the plasma, generating new phase-sensitive spectral components at the edges of its spectrum. A theoretical analysis of the generation of these components on nonperturbative plasma nonlinearity is carried out.

[1] P.B. Corkum and F. Krausz, Attosecond science, Nat. Phys., vol. 3, pp. 381–387 (2007).
[2] G. Vampa, T.J. Hammond, N. Thiré, B.E. Schmidt, F. Légaré, C.R. McDonald, T. Brabec, P.B. Corkum, Linking high harmonics from gases and solids, Nature, vol. 522, pp. 462–464 (2015).
[3] O. Schubert, M. Hohenleutner, F. Langer, B. Urbanek, C. Lange, U. Huttner, D. Golde, T. Meier, M. Kira, S.W. Koch, R. Huber, Sub-cycle control of terahertz high-harmonic generation by dynamical Bloch oscillations, Nat. Photonics, vol. 8, pp. 119–123 (2014).
[4] A. Baltuška, T. Udem, M. Uiberacker, M. Hentschel, E. Goulielmakis, C. Gohle, R. Holzwarth, V.S. Yakovlev, A. Scrinzi, T.W. Hänsch, Attosecond control of electronic processes by intense light fields, Nature, vol.421, 611 (2003).
[5] I.V. Savitsky, E.A. Stepanov, A.A. Lanin, A.B. Fedotov, A.M. Zheltikov, Single-Cycle, Multigigawatt Carrier–Envelope-Phase-Tailored Near-to-Mid-Infrared Driver for Strong-Field Nonlinear Optics, ACS Photonics, vol. 9, pp. 1679–1690 (2022).
[6] I.V. Savitsky, A.A. Voronin, E.A. Stepanov, A.A. Lanin, A.B. Fedotov. Sub-cycle pulse revealed with carrier-envelope phase control of soliton self-compression in anti-resonant hollow-core fiber, Optics Letters, 48(17):4468 (2023).

Optical properties of silicon nanowires for sensor applications

K.A. Gonchar[1]

1- Lomonosov Moscow State University, Physics Department, Leninskie Gory 1, 119991 Moscow, Russia

k.a.gonchar@gmail.com

Silicon nanowires (SiNWs) fabricated by metal-assisted chemical etching exhibit properties such as photoluminescence in the visible and infrared spectral ranges, low reflectance in the visible spectral range, and enhanced Raman scattering compared to the original crystalline silicon substrate [1]. These properties can be used to create various optical sensors based on them. Also when SiNWs are coated with noble metal nanoparticles, these structures can be used as a signal-amplifying substrate in giant Raman scattering.

It has been shown that porous SiNWs can be used as a sensitive element of an optical oxygen sensor [2]. The nonspecific binding of viruses to the surface of nanostructures made from SiNW arrays was demonstrated for the first time, and the possibility of using this effect to produce a nonspecific optical [3] and impedance sensor [4] for diagnosing viruses was shown. Using the surface-enhanced Raman spectroscopy bilirubin was successfully detected on SiNWs decorated with gold nanoparticles [5], internalin B, a protein associated with the pathogenic bacteria Listeria monocytogenes, was successfully detected on SiNWs decorated with silver nanoparticles [6] and Listeria innocua was successfully detected on SiNWs decorated with silver and gold nanoparticles [7].

[1] L.A. Osminkina, K.A. Gonchar, V.S. Marshov, K.V. Bunkov, D.V. Petrov, L.A. Golovan, F. Talkenberg, V.A. Sivakov, V.Yu. Timoshenko, Optical properties of silicon nanowire arrays formed by metal-assisted chemical etching: evidences for light localization effect, Nanoscale Research Letters, 7, 524 (2012).

[2] V.A. Georgobiani, K.A. Gonchar, E.A. Zvereva, L.A. Osminkina, Porous silicon nanowire arrays for reversible optical gas sensing, Phys. Stat. Sol. A, 215(1), 1700565 (2018).

[3] K.A. Gonchar, S.N. Agafilushkina, D.V. Moiseev, I.V. Bozhev, A.A. Manykin, E.A. Kropotkina, A.S. Gambaryan, L.A. Osminkina, H1N1 influenza virus interaction with a porous layer of silicon nanowires, Mater. Res. Express, 7, p. 035002 (2020).

[4] M.B. Gongalsky, U.A. Tsurikova, J.V. Samsonova, G.Z. Gvindzhiliiia, K.A. Gonchar, N.Yu. Saushkin, A.A. Kudryavtseva, E.A. Kropotkina, A.S. Gambaryan, L.A. Osminkina, Double etched porous silicon nanowire arrays for impedance sensing of influenza viruses, Results in Materials, 6, p. 100084 (2020).

[5] A.D. Kartashova, K.A. Gonchar, D.A. Chermoshentsev, E.A. Alekseeva, M.B. Gongalsky, I.V. Bozhev, A.A. Eliseev, S.A. Dyakov, J.V. Samsonova, L.A. Osminkina, Surface-enhanced Raman scattering-active gold-decorated silicon nanowire substrates for label-free detection of bilirubin, ACS Biomater. Sci. Eng., 8(10), 4175-4184 (2022).

[6] K.A. Gonchar, E.A. Alekseeva, O.D. Gyuppenen, I.V. Bozhev, E.V. Kalinin, S.A. Ermolaeva, L.A. Osminkina, Optical express monitoring of Internalin B, a protein of the pathogenic bacterium Listeria monocytogenes, using SERS-active silver-decorated silicon nanowires, Optics and Spectroscopy, 130(11), 1482-1486 (2022).

[7] D.A. Nazarovskaia, P.A. Domnin, O.D. Gyuppenen, I.I. Tsynyaykin, S.A. Ermolaeva, K.A. Gonchar, L.A. Osminkina, Advanced bacterial detection with SERS-active gold- and silver-coated porous silicon nanowires, Bulletin of the Russian Academy of Sciences: Physics, 87(Suppl.1), S41–S46 (2023).

Localization of dye molecules in zero mode waveguides

A. Gritchenko[*], **M. Markov, A. Kalmykov, V. Balykin, P. Melentiev**

Institute of Spectroscopy RAS, 108840, Fizicheskaya st. 5, Troitsk, Moscow, Russia

* gritchenkoant@gmail.com

Detection, sensing and spectroscopy at the single-molecule level is a rapidly developing field of science at the interface of nanophotonics, chemistry and biochemistry. One of the fundamental problems in this field is the localization and long-term tracking of single molecules in space with nanometer precision. To date, there are several approaches to the localization of single molecules: embedding molecules in a polymer matrix [1], optical tweezers [2], immobilization of molecules by chemical and biochemical reactions on surfaces [3], electrophoretic methods [4].

Recently, approaches have been developed in the field of single-molecule detection and spectroscopy that involve the use of zero-mode waveguides (ZMWs). ZMWs are nanoholes with diameter of 50-200 nm in an approximately 100 nm thick metal film on the glass surface. The use of ZMWs provides many advantages: an increase in the signal-to-noise ratio during detection, the ability to work with physiological analyte concentrations, the possibility of parallel detection and spectroscopy with ZMW arrays. Detection and spectroscopy methods with ZMWs are actively used in single-molecule sequencing of DNA molecules [5].

In our work, we propose an approach to localize single fluorescent molecules in ZMW by using hydrogen bonds that can be effectively formed between the molecules and the quartz bottom of the ZMW (Figure 1a). We demonstrate, through measurements, the possibility to localize dye molecules in ZMWs on a time scale ranging from 10 ms to 10 seconds. This process can be finely controlled by the local density of free charges in the buffer solution used. By using different salts at appropriate concentrations, we can deterministically switch the localization process on and off (see Figure 1b). We discuss the use of the single molecule localization approach in ZMW in various applications: (i) detection and study of single molecules by fluorescence; (ii) sensing at the single molecule level; (iii) sequencing of single DNA molecules. The study was supported by a grant Russian Science Foundation No. 23-42-00049, https://rscf.ru/project/23-42-00049/.
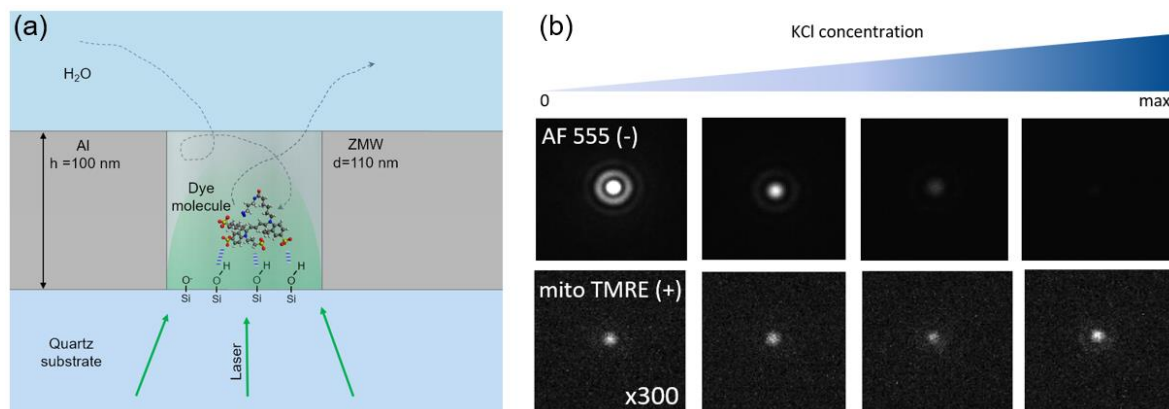
Figure 1. Localization of a dye molecule in ZMW: (a) schematic representation of the trajectory of the AF555 dye molecule in ZMW, (b) fluorescence image of a single ZMW with localized AF555 molecule (the molecule is negatively charged, four upper images in a row) and mito-TMRE molecule (the molecule is positively charged, four lower images in a row, note that the images are amplified by a factor of 300 compared to the upper images) at different KCl concentrations in the buffer solution used (the concentration level is shown schematically above).

[1] W.E. Moerner and M. Orrit, Illuminating single molecules in condensed matter, Science (1979). American Association for the Advancement of Science, 1999. Vol. 283, № 5408, P. 1670–1676.

[2] G. Sirinakis, et al, Combined versatile high-resolution optical tweezers and single-molecule fluorescence microscopy, Review of Scientific Instruments, AIP Publishing, 2012. Vol. 83, № 9.

[3] J.L. Zimmermann, et al, Thiol-based, site-specific and covalent immobilization of biomolecules for single-molecule experiments, Nature Protocols, 2010 5:6. Nature Publishing Group, 2010. Vol. 5, № 6, P. 975–985.

[4] A.E. Cohen and W.E. Moemer, Method for trapping and manipulating nanoscale objects in solution, Appl Phys Lett. AIP Publishing, 2005. Vol. 86, № 9, P. 1–3.

[5] J. Eid, et al, Real-time DNA sequencing from single polymerase molecules, Science (1979), American Association for the Advancement of Science, 2009. Vol. 323, № 5910, P. 133–138.

SERS substrates for glucose determination: a study on the use of polymer substrate functionalized with metal nanoparticles

O. Gusliakova[1*], V. Bakal[1], J. Cvjetinovic[2], E. Prikhozhdenko[1]

1- Saratov State University, 83, Astrakhanskaya st., Saratov, 410012, Russian Federation
2- Center for Photonic Science and Engineering, Skolkovo Institute of Science and Technology, Bolshoy Boulevard 30, bld. 1, 121205 Moscow, Russia

* olga.gusliakova17@gmail.com

Optical approaches for glucose detection have received much attention in recent years due to their relatively low cost, portability, and low or noninvasive nature. Raman spectroscopy in combination with SERS substrates provides extremely high sensitivity due to signal amplification and specificity due to the unique vibrational coupling spectra of molecules of interest. However, direct detection of glucose using SERS substrates is difficult due to the poor adsorption of glucose onto clean metal surfaces and the low scattering cross section of glucose [1].

The results of screening a SERS platform based on polymer substrates for the quantitative determination of glucose in the concentration range specific to biological fluids are presented. In particular, configurations of glucose sensors based on PDMS and biocompatible polymer (PLGA, PCL) films modified with metal nanoparticles (gold nanorods and silver nanoparticles) were considered. PDMS substrates had an ordered array of depressions (of a given geometry). The possibility of using the wells themselves with a pre-modified surface with nanoparticles as microreservoirs has been considered, since in modern literature there is data on the amplification of the signal from glucose molecules upon repeated reflection of a laser beam, achieved by propagation in a cavity whose walls are covered with gold nanoparticles [2]. The technology of forming arrays of aggregates (of a given geometry) of metal nanoparticles by means of filling holes in a PDMS substrate and subsequent imprinting on a smooth surface, imitating the technique of obtaining microchambers [3], is also considered.

[1] X. Sun, Glucose detection through surface-enhanced Raman spectroscopy: A review, Analytica Chimica Acta, 1206, 339226, (2022).
[2] C.M. Jin, J.B. Joo, I. Choi, Facile amplification of solution-state surface-enhanced Raman scattering of small molecules using spontaneously formed 3D nanoplasmonic wells, Analytical chemistry, 90(8), 5023-5031, (2018).
[3] O.A. Sindeeva, O.I. Gusliakova, O.A. Inozemtseva, A.S. Abdurashitov, E.P. Brodovskaya, M. Gai, ... & G.B. Sukhorukov, Effect of a controlled release of epinephrine hydrochloride from PLGA microchamber array: in vivo studies, ACS applied materials & interfaces, 10(44), 37855-37864, (2018).

Raman spectroscopy and photoluminescence of semiconductor nanostructures with nanometer spatial resolution

A.G. Milekhin[1*], **I.A. Milekhin**[1,2], **N.N. Kurus**[1], **L.S. Basalaeva**[1],
R.B. Vasiliev[3], **A.V. Latyshev**[1,2], **D.R.T. Zahn**[4]

1- A.V. Rzhanov Institute of Semiconductor Physics, 630090, Novosibirsk, Lavrentjev av. 13, Russia
2- Novosibirsk State University, Novosibirsk, 630090, Pirogov str., 1
3- Department of Material Science, Moscow State University, Moscow, Russia
4- Russia Semiconductor Physics, Chemnitz University of Technology, D-09107 Chemnitz, Germany

* milekhin@isp.nsc.ru

Tip-enhanced Raman scattering and photoluminescence (TERS and TEPL, respectively) taking advantages of conventional micro-Raman and -PL spectroscopies and atomic-force microscopy allow to study the phonon and electron spectra of semiconductor nanostructures with the nanometer spatial resolution and to derive information of their local properties such as built-in mechanical strain or structural defects.

Here, the results of TERS and TEPL study of GaAs nanocrystals (NCs) and nanocolumns, as well as graphene flakes and monolayers of metal chalcogenides (MoS_2 and WS_2) are presented.

AFM images, TERS, TEPL, and conventional micro-Raman as well as micro-PL spectra were obtained using an AFM AIST-NT coupled with a Raman spectrometer (Xplora, Horiba). All PL and Raman spectra were recorded using an objective (100×, 0.7 NA) at normal light incidence under laser excitation with a wavelength of 638 and 532 nm at room temperature. TERS probes metallized with Au or Ag were used in the experiments.

TEPL imaging of single GaAs NCs and nanocolumns with a spatial resolution of about 10 nm that is much below the diffraction limit is performed. It is shown that localized surface plasmon resonance originated at metallized TERS tip can be effectively used for imaging of single GaAs nanostructures. TERS by vibrational modes from arsenic nanoclusters allows their spatial distribution over the GaAs NC surface to be established.

On the base of the analysis of TERS and TEPL spectra for atomically thin MoS_2 and WS_2 islands, the size, shape of the nanostructures as well as their structural defects and built-in mechanical strain are established. For further enhancement of the optical response, graphene and MoS_2 monolayers were transferred on the plasmonic substrate consisting of Au nanodisk array for which the gap-mode plasmon TERS is realized [1]. It is shown that the local built-in mechanical strain in the MoS_2 monolayer deposited on an Au nanocluster can be locally changed on the scale of about 2 nm reaching a value of ~2%.

Acknowledgements

[1] N.N. Kurus, V. Kalinin, N.A. Nebogatikova, et al, Resonant Raman Scattering on Graphene: SERS and gap-mode TERS, RCS Advances, vol. 14, pp. 3667-3674, (2024).

Polarization-dependent TERS analysis of a single AlN nanowire with nanoscale spatial resolution

I. Milekhin[1,2*], **V. Mansurov[2]**, **T. Malin[2]**, **K. Zhuravlev[2]**, **A. Milekhin[2]**, **A. Latyshev[1,2]**

1- Novosibirsk State University, Pirogov, 1, 630090 Novosibirsk, Russia
2- A.V. Rzhanov Institute of Semiconductor Physics, pr. Lavrentieva, 13, 630090, Novosibirsk, Russia

* i.milekhin@g.nsu.ru

Tip-enhanced Raman scattering (TERS) is a relatively new and rapidly developing method, which combines the advantages of conventional Raman spectroscopy for chemical analysis, a high sensitivity of surface-enhanced Raman spectroscopy, and the nanoscale spatial resolution provided by atomic force microscopy (AFM). The emerging region of the enhanced electromagnetic field between the metalized AFM tip and the sample surface ("hot spot") makes it possible to overcome the diffraction limit and significantly enhance the phonon response. TERS is based on the ability to control the location of the hot spot between the tip and the sample surface, and simultaneously perform TERS mapping.
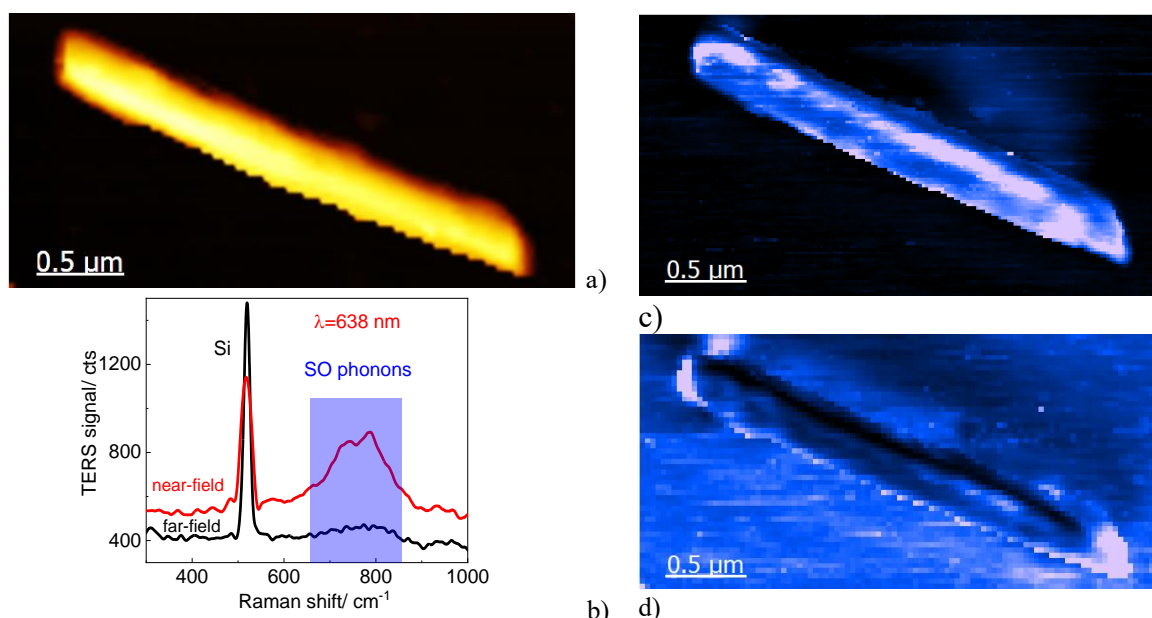
Fig. 1. A) AFM image of a single AlN nanowire mechanically transferred onto Au/Si substrate. B) Comparison of TERS spectra of the nanowire recorded in the near- and far-fields. C),d) TERS maps (taken in the spectral range shown by rectangular in (b)) of the AlN nanowire presented in (a). The laser light is polarised along (c) and perpendicular (d) to the TERS probe axis.

In this work, we present the results of a TERS experiment with a single AlN nanowire grown by molecular beam epitaxy and subsequently transferred to a gold surface (Fig. 1a). The TERS method allows one to remarkably enhance its optical response and investigate both bulk-like and surface optical (SO) modes of a single AlN nanowire located in the gap between a gold substrate and the tip of a metalized (Ag) AFM probe (Fig. 1b). The TERS tip provides a high sensitivity to AlN SO phonons and allows to achieve 10 nm spatial resolution under ambient conditions. The laser with an excitation energy of 1.94 (638 nm) was used in the TERS experiment for a single AlN nanowire. TERS mapping (Fig. 1c, d) at different light polarizations makes it possible to determine the spatial localization of surface optical phonons in the nanostructure. Our results open up the possibility for TERS diagnostics of single AlN nanostructures to identify the MBE growth features and visualize edge effects.

Acknowledgements

Nonlinear optical microscopy of epitaxial garnet films

A.I. Maydykovskiy[1], T. Murzina[1*]

1- Lomonosov Moscow State University, Department of Physics, Leninskie Gory 1, 119991, Moscow, Russia

* murzina@mail.ru

The composition and properties of the domain structure of various specimen are of high interest, as they are the main building blocks for such important media as ferroelectrics and magnetics. A proper place here belongs to magnetic domains, which reveal a wide variety of types and shapes depending on the constituent materials, e.g. metals or dielectrics, as well as on the structural parameters [1]. It is also well recognized that the domain structure in the bulk of a material and at its interfacial layers can also be quite different. Thus the search and development of efficient non-destructive diagnostics methods is very much desired. Commonly magnetic domain composition in the volume of the transparent dielectrics is revealed by optical polarization and magneto-optical microscopy, while the surface layers can be studied in much detail by magnetic force microscopy (MFM) and the Lorentz microscopy [2,3].

It has been shown recently that nonlinear optical microscopy based on second harmonic generation (SHG) can provide additional information about the organization of magnetic domains in crystalline iron-garnet films [3]. The functional potential of the SHG probe is based on unique sensitivity of the second-order nonlinear optical response to any kind of symmetry breaking in a medium, including the surface and nanostructure effects in the case of centrosymmetric materials, as well as the electric- or magnetic field-induced subjection. Importantly that the characteristic values of the magnetization induced effects in the SHG response (the nonlinear optical analogues of the magneto-optical Faraday and Kerr effects) are one-two orders of magnitude larger than in the linear optics. This allows for a high contrast in the SHG images of the magnetic domain structures. In combination with the confocal microscopy scheme and the use of a common femtosecond titanium-sapphire laser operating in the near IR wavelength range, the SHG probe provides a submicron in-plane spatial resolution, while along the direction normal to the surface it is about 1-2 microns. Symmetry analysis of the SHG response induced by the nonlinear susceptibility tensor allows to estimate the orientation of the magnetic moment of a medium not only along the normal to the surface as in the case of the MFM, while in the other directions as well. Consequently, noninvasive and relatively simple SHG microscopy technique can be applied for the studies of a 3D microstructure of magnetic domains in epitaxial garnet films of several micrometers in thickness both in the bulk of the film and at their surface layers, as is shown in our experiments.

We estimated the mutual orientation of the magnetization in the surface and bulk stripe domains, and showed that the thickness of the surface ones is about 1-1.5 μm in the studied garnet film. The SHG microscopy also showed the changes in the magnetization processes of a free garnet layer and of that decorated by regular arrays of ferromagnetic particles. Further extension of the nonlinear optical microscopy in application to the garnet films is the use of the third harmonic generation (THG) as the probe; in these experiments we demonstrate even higher resolution of this method for the studies of magnetic domains [4].

[1] A. Hubert, R. Schafer, Magnetic Domains: The Analysis of Magnetic Microstructures (Springer, 1998).

[2] X. Yu, J.P. DeGrave, Y. Hara, T. Hara, S. Jin, Y. Tokura, Observation of the magnetic skyrmion lattice in a MnSi nanowire by Lorentz TEM, Nano Lett. 14, 3755-3759 (2013).

[3] M.P. Temiryazeva, E.A. Mamonov, A.I. Maydykovskiy, A.G. Temiryazev, T.V. Murzina, Magnetic Domain Structure of $Lu_{2.1}Bi_{0.9}Fe_5O_{12}$ Epitaxial Films Studied by Magnetic Force Microscopy and Optical Second Harmonic Generation, Magnetochemistry 8(12), 180(10) (2022).

[4] A.I. Maydykovskiy, N.S. Popov, T.V. Murzina, Third harmonic generation microscopy of magnetic domains in garnet films, Las. Phys. Letters 21, 025401 (6pp) (2024).

SERS detection of anticancer drugs using a composite nanostructure based on porous silicon and gold nanoparticles

D. Nazarovskaia[1*], M. Vasilieva[1], P.A. Tyurin-Kuzmin[2], J. Samsonova[3], L.A. Osminkina[1]

1- Lomonosov Moscow State University, Faculty of Physics, Leninskie gory 1, 119991, Moscow, Russia
2- Lomonosov Moscow State University, Faculty of Medicine, Leninskie gory 1, 119991, Moscow, Russia
3- Lomonosov Moscow State University, Faculty of Chemistry, Leninskie gory 1, 119991, Moscow, Russia

* nazarovskaia.da22@physics.msu.ru

Over the recent years, Raman spectroscopy (RS) methods have been largely employed in biomedical analysis. Generally, it is based on the detection of molecular vibrations which are activated by laser radiation and subsequent inelastic light scattering. Resulting spectra constitutes a distinctive "fingerprint" that contains detailed molecular information. Cells, microorganisms, metabolites, small molecules and etc can be detected through RS. Furthermore, the combination of RS and confocal microscopy leads to both spectroscopic monitoring and imaging which is beneficial in the research of nanocontainers for drug delivery. Although Raman scattering is initially weak, its intensity can be enhanced up to 15 orders of magnitude by exciting surface plasmon resonances on the nanorough surfaces of noble metals. This effect, surface-enhanced Raman scattering (SERS), has opened novel opportunities for biomedical analytics, and different metal nanostructures may serve as SERS substrate.

Porous silicon nanoparticles (pSiNPs) are promising nanocontainers for drug delivery due to their high drug-loading capacity, biocompatibility and degradation into non-toxic silicic acid in the living body environment [1]. Notably, it is well known that crystalline silicon has a specific Raman band at 520.5 cm^{-1} that allows monitoring of the uptake, intracellular localisation, and dissolution of pSiNPs in cells. For the first time, Raman studies of the biodegradation of doxorubicin-loaded pSiNPs and drug release kinetics inside cancer cells were successfully demonstrated in [2]. Also, the cellular uptake and biodistribution of pSiNPs loaded with sunitinib, another anticancer drug, were studied by RS in [3]. However, the modification of pSiNPs surface with Au nanoparticles (AuNPs) is expected to achieve the considerable enhancement of the Raman signal of the loaded drug due to SERS effect.

In this work, a method of the fabrication of a new composite nanomaterial Au-pSi NPs was developed. Au-pSi NPs were characterized using RS, infrared (IR) spectroscopy, dynamic light scattering (DLS), transmission electron microscopy (TEM), scanning electron microscopy (SEM). Doxorubicin and sunitinib were loaded into Au-pSi NPs and the drugs releases were measured using spectrophotometry and SERS.
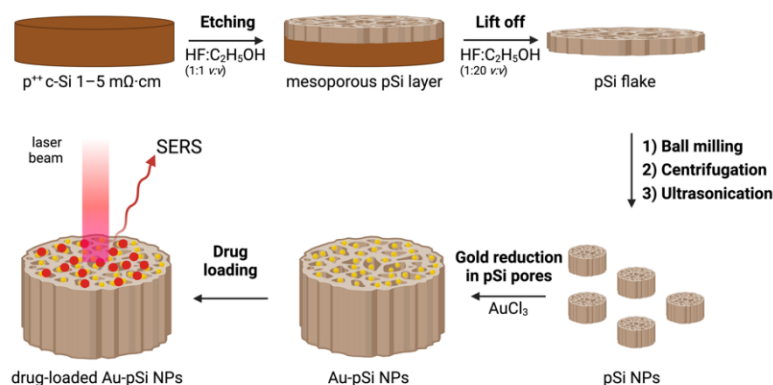
Figure 1. – Schematic illustration of Au-pSi NPs nanocontainers fabrication.

The obtained results emphasise future applications of composite nanostructures based on porous silicon and gold nanoparticles for controlling drug release from nanocontainers using SERS.

[1] J.-H. Park, et al, Biodegradable luminescent porous silicon nanoparticles for in vivo applications, Nat. Mater., vol. 8, pp. 331–336, (2009).
[2] P.V. Maximchik, et al, Biodegradable Porous Silicon Nanocontainers as an Effective Drug Carrier for Regulation of the Tumor Cell Death Pathways, ACS Biomater., Sci. Eng., vol. 5 (11), pp. 6063-6071, (2019).
[3] E. Tolstik, et al, Raman and fluorescence micro-spectroscopy applied for the monitoring of sunitinib-loaded porous silicon nanocontainers in cardiac cells, Front. pharmacol., vol. 13, pp. 962763, (2022).

Raman evaluation of structure of poly(L-lactide-co-ε-caprolactone) and poly(L-lactide)/poly(ε-caprolactone) blends

S.O. Liubimovskii[1], V.S. Novikov[1,2]*, S.M. Kuznetsov[1,2], E.V. Anokhin[3],
V.A. Demina[3,4], N.G. Sedush[3,4], S.N. Chvalun[3,4], E.A. Sagitova[1],
G.Yu. Nikolaeva[1], M.N. Moskovskiy[2], S.V. Gudkov[1,2]

1- Prokhorov General Physics Institute of the Russian Academy of Sciences, Vavilov Str. 38, 119991 Moscow, Russian Federation
2- Federal Scientific Agronomic and Engineering Center VIM, 1st Institutsky proezd 5, 109428 Moscow, Russian Federation
3- Enikolopov Institute of Synthetic Polymeric Materials of the Russian Academy of Sciences, Profsoyuznaya St. 70, 117393 Moscow, Russian Federation
4- National Research Centre "Kurchatov Institute", Akademika Kurchatova Pl. 1, 123182 Moscow, Russian Federation

* vs.novikov@kapella.gpi.ru

Biodegradable and biocompatible poly(L-lactide-co-ε-caprolactone) and poly(L-lactide)/poly(ε-caprolactone) blends have great potential for applications in various fields, including tissue engineering, drug delivery systems and packaging materials. The physical and chemical properties of these copolymers and blends can be varied in a flexible way by changing by the conditions of the synthesis and treatment. In particular, the properties can be effectively adjusted by varying the relative contents of the co-monomers or blend components.
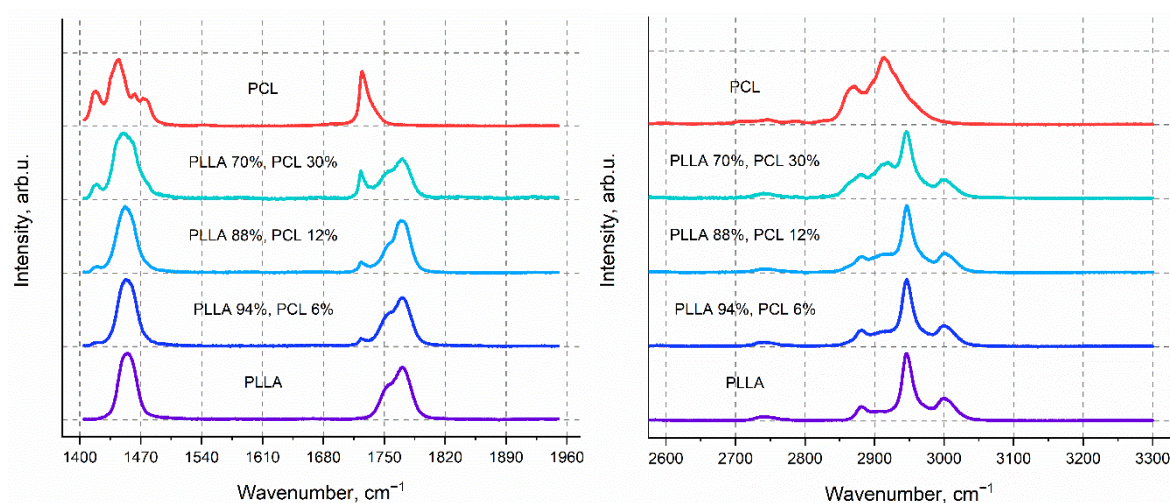
Fig. 1. Raman spectra of poly(L-lactide)/poly(ε-caprolactone) blends. The spectra are recorded at the 785 nm excitation.

Raman spectroscopy is a powerful tool to study the structure of molecular substances in terms of the chemical composition, configurational, conformation and phase order. The aim of this work is the development of Raman methods for structural analysis of poly(L-lactide-co-ε-caprolactone) and poly(L-lactide)/poly(ε-caprolactone) blends.

As an example, Fig. 1 demonstrates two regions of Raman spectra of poly(L-lactide)/poly(ε-caprolactone) blends with different contents of the blend components. We showed that analysis of the Raman spectra in the region at around 3000 cm^{-1} allows to evaluate the chemical composition of the copolymers and blends, while analysis of the poly(L-lactide) band at around 410 cm^{-1} makes it possible to evaluate the crystallinity degree of poly(L-lactide) areas in these materials. To confirm the conclusions, based on Raman data, we also applied two traditional methods: X-ray diffraction analysis and differential scanning calorimetry.

Au/Ag-functionalized silicon nanostructures: a comprehensive study of SERS efficiency for rapid detection and analysis of chemicals, biomolecules and bio-objects

L.A. Osminkina[1*]

1- Lomonosov Moscow State University, Faculty of Physics, Leninskie gory 1, 119991, Moscow, Russia

* osminkina@physics.msu.ru

Development of highly sensitive nano-biosensors for rapid detection and analysis of chemicals, biomolecules, and bio-objects is a crucial task in laser technology. A serious breakthrough in the field of biosensorics is now expected from the application of the optical non-invasive method of Surface-Enhanced Raman Scattering (SERS) for these purposes, as it is characterized by high sensitivity, specificity and rapid response. The SERS method consists in amplifying the intensity (in billions of times) of the optical Raman signal from the molecules of the analyzed substance using special SERS-active substrates containing noble metal particles (usually gold, silver, copper) to register the signal. The sensitivity of the method directly depends on the morphological features of the substrates used: not only the shape and size of metal particles, but also their location in the solid-state matrix – the base of the sensor layer – is of great importance.

Our investigation delves into the intricate details of Au/Ag-functionalized silicon nanostructures, considering factors such as morphology, composition, and arrangement. These factors play a crucial role in enhancing the SERS efficiency of the nanostructures. Through a comprehensive study, we seek to optimize their performance for a wide range of applications, including label-free determination of biomolecules [1], metabolites [2], virus and bacteria [3] diagnostics (Fig.1), and rapid bacteria antibiotic sensitivity analysis.
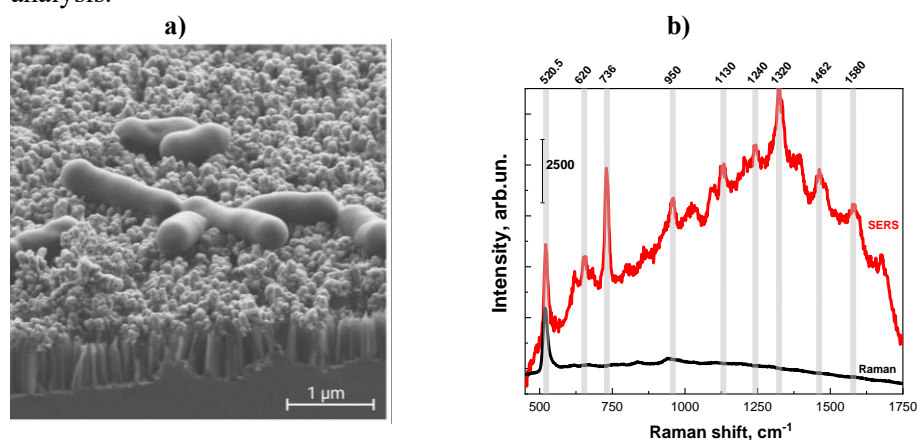
Figure 1. (**a**) SEM microphotograph of AuAg@pSiNWs after incubation with *L. innocua*. (**b**) Raman and SERS spectra of *L. innocua* absorbed on pSiNW and AuAg@pSiNW substrates, respectively. [3]

Ultimately, our work highlights the promising applications of Au/Ag-functionalized silicon-based nanostructures in the development of laser technologies for biomedical diagnostics. By combining the advantages of using nanotechnology and advanced laser technologies for biosensing, we aim to contribute to the development of innovative solutions for the rapid and accurate detection of pathogens and biomolecules, which will ultimately benefit public health.

[1] A.D. Kartashova, et al, Surface-enhanced Raman scattering-active gold-decorated silicon nanowire substrates for label-free detection of bilirubin, ACS Biomaterials Science & Engineering, 2021. vol. 8. №. 10. pp. 4175-4184.

[2] O. Žukovskaja, et al, Rapid detection of the bacterial biomarker pyocyanin in artificial sputum using a SERS-active silicon nanowire matrix covered by bimetallic noble metal nanoparticles, Talanta, 2019. vol. 202. pp. 171-177.

[3] D.A. Nazarovskaia, et al, Advanced Bacterial Detection with SERS-Active Gold-and Silver-Coated Porous Silicon Nanowires, Bulletin of the Russian Academy of Sciences: Physics, 2023. vol. 87. №. Suppl 1. pp. S41-S46.

Raman study of phase transitions in thin films of hafnium oxide

M. Martyshov[1], D. Zhigunov[2], A. Pavlikov[1*]

1- Faculty of Physics, M.V. Lomonosov Moscow State University, Moscow, Russia
2- Skolkovo Institute of Science and Technology, Moscow, Russia

* pavlikovav@my.msu.ru

Hafnium dioxide (HfO_2) is a good dielectric with a wide bandgap and a high dielectric constant. It is used as a replacement for silicon dioxide as an insulating layer in thin film capacitors and in the gates of field effect transistors. Transistor-based memories no longer meet modern needs due to problems with their scalability and power consumption. One of the main candidates that can replace it is resistive random access memory (RRAM) [1]. It is a non-volatile type of memory that stands out due to its simple two-pin design, high potential scalability and speed of operation.

In this work, thin films of hafnium oxide were obtained, which were subsequently annealed in a furnace in an air atmosphere. To study the optical properties of the films, Raman spectra were measured, which provide information about the crystal structure of the samples under investigation. The spectra were measured using a Horiba HR-800 micro-Raman spectrometer. A helium-neon laser with a wavelength of 633 nm was used for excitation. 10x, 50x and 100x objectives were applied to focus the laser beam.

Comparing our experimental data on Raman scattering with the literature, we can conclude that the pristine sample does not have pronounced peaks and is initially in the amorphous phase. At a temperature of 400°C, lines characteristic of the crystalline monoclinic phase begin to appear in the sample, the shape of which reaches sharpness already at 500°C and does not change significantly with the next increase in the annealing temperature. The spectra contain a photoluminescent background, and the width of the lines that appeared at temperatures of 500°C and 600°C indicates the nanosize of the crystallites. Based on these data, it can be assumed that nanocrystals with a monoclinic structure are formed in the sample already at a temperature of about 500°C.

[1] E. Linn, Resistive Switching (John Wiley & Sons), Chapter 2, (2016).

Growth, thermal and spectroscopic properties of Tm:MgMoO$_4$ crystal

S.K. Pavlov[1,2], **K.A. Subbotin**[1,2], **A.I. Titov**[1,2], **Y.I. Zimina**[1,2], **D.A. Lis**[2], **Y.S. Didenko**[1,2]

1- Prokhorov General Physics Institute, Russian Academy of Sciences, Moscow
2- Mendeleev University of Chemical Technology of Russia, Moscow

In the recent years, the crystal family of divalent metal monotungstates MWO$_4$ (where M = Mg, Zn, Mn, Cd, etc.), has attracted much attention as laser host media for doping with trivalent rare-earth ions. Recently, highly efficient, low-threshold and wavelength-tunable lasing [1,2] have been demonstrated using Tm:MgWO$_4$ crystals. Furthermore, in 2017, the first generation of sub-100 fs pulses from a bulk solid-state laser at ~2 µm was demonstrated using a Tm:MgWO$_4$ crystal [3]. However, these MgWO$_4$ crystals are grown by the Top-Seeded Solution Growth method.

The MgMoO$_4$ crystal, also known as the molybdate counterpart of MgWO$_4$, melts congruently and can be easily grown by the Czochralski (Cz) method. However, there is no report in the literature on the growth or study of Tm^{3+}-doped MgMoO$_4$ crystals. In the present work, we report on the successful Czochralski growth, as well as the structural, thermal and spectroscopic investigations of both undoped and Tm^{3+}-doped MgMoO$_4$ single crystals.

The single crystals of MgMoO$_4$ and Tm:MgMoO$_4$ were grown by the Cz method. Both crystals exhibited a bright saffron-yellow colour, most likely caused by the hole centers at the molybdenum vacancies. The actual Tm^{3+} concentration in the MgMoO$_4$ crystal was measured by inductively coupled plasma atomic emission spectroscopy and was 0.1 at.%. Differential thermal analysis was carried out in the temperature range of 20-1400°C with only one sharp thermal effect at 1322°C corresponding to congruent melting/crystallization. Linear thermal expansion coefficients were calculated from high-temperature X-ray powder diffraction analysis. The thermal conductivity of undoped MgMoO$_4$ was measured by the method of stationary longitudinal heat flow in the temperature range of 50 – 300 K along the c-axis. It monotonously decreases with temperature, from 19.51 to 2.64 Wm^{-1}K^{-1}.

The polarized Raman spectra of a b-cut Tm:MgMoO$_4$ crystal contain intense peaks within two distinct ranges, 122 – 424 cm^{-1} and 754 – 969 cm^{-1}. For the $^3H_6 \rightarrow {}^3H_4$ Tm^{3+} transition peak absorption cross-section σ_{abs} is 1.60×10^{-20} cm^2 at 794.2 nm corresponding to an absorption full width at half maximum of 6.6 nm. Tm^{3+} ions in MgMoO$_4$ exhibit a broad and strongly polarized emission band from 1.6 up to 2.15 µm. The measured luminescence lifetime of the $^3F_4$ excited state was 1.972 ms.

[1] P. Loiko, J.M. Serres, X. Mateos, M. Aguiló, F. Díaz, L.Z. Zhang, Z.B. Lin, H.F. Lin, G. Zhang, K. Yumashev, V. Petrov, U. Griebner, Y.C. Wang, S.Y. Choi, F. Rotermund, W.D. Chen, Monoclinic Tm3+:MgWO4: Novel crystal for continuous-wave and passively Q-switched lasers at ~2 µm, Opt. Lett. 42(6) (2017), 1177-1180.

[2] P. Loiko, L. Zhang, J.M. Serres, Y. Wang, M. Aguiló, F. Díaz, Z. Lin, H. Lin, G. Zhang, E. Vilejshikova, E. Dunina, A. Kornienko, L. Fomicheva, V. Petrov, U. Griebner, W. Chen, and X. Mateos, Monoclinic Tm:MgWO4 crystal: Crystal-field analysis, tunable and vibronic laser demonstration, J. Alloy Compd 763 (2018), 581-591.

[3] Y. Wang, W. Chen, M. Mero, L. Zhang, H. Lin, Z. Lin, G. Zhang, F. Rotermund, Y.J. Cho, P. Loiko, X. Mateos, U. Griebner, V. Petrov, Sub‐100 fs Tm:MgWO4 laser at 2017 nm mode‐locked by a graphene saturable absorber, Opt. Lett. 42(16) (2017), 3076-3079.

Magneto-optical harmonics generation spectroscopy of semiconductors and dielectrics

V.V. Pavlov

Ioffe Institute, 194021, St. Petersburg, Russia

pavlov@mail.ioffe.ru

Nonlinear spectroscopy based on optical harmonics generation enables a possibility for giving new information as compared with linear optical phenomena. This is due to the fundamental difference between selection rules for single-photon and multi-photon processes [1]. The nonlinear optical phenomenon such as optical second harmonic generation (SHG) results from the space-inversion symmetry operation breaking. SHG plays particular role in the fundamental studies of noncentrosymmetric bulk materials, as well as surface and interface states of centrosymmetric media. Moreover, it can be used as an important tool for studying electronic, crystallographic and spin structures of magnetically ordered materials, including antiferromagnets [2,3]. However, SHG studies of magnetically ordered materials at energetically narrow excitonic states are rather scarce.

New nonlinear magneto-optical phenomena in different types of semiconductors and magnetic dielectrics will be discussed. Various aspects of nonlinear optical spectroscopy will be analysed such as polarization, temperature and field dependencies. Excitonic phenomena associated with optical harmonics in antiferromagnetically ordered materials will be considered. The possibility of visualization of antiferromagnetic domains indistinguishable by linear optics methods will be demonstrated. Excitonic nonlinear magneto-optical phenomena in semiconductors will be discussed. The possibilities of optical harmonics generation technique for revealing new mechanisms for nonlinear optical interaction on exciton states will be shown [4].

[1] Y.R. Shen, The principles of nonlinear optics, (Wiley, New York, 1984).
[2] M. Fiebig, V.V. Pavlov, R.V. Pisarev, Second-harmonic generation as a tool for studying electronic and magnetic structures of crystals: review, J. Opt. Soc. Am. B 22, 96 (2005).
[3] F. Manfred, Nonlinear optics on ferroic materials, (Blackwell Verlag GmbH, 2023).
[4] V.V. Pavlov, Magnetic field effects in optical harmonics generation by excitons, Phys. Solid State 62, 1624 (2020).

The effect of concentrated deposition of nanoparticles during the evaporation of bicomponent droplets and its application in optical sensors

G. Pavliuk[1*], A. Zhizhchenko[2], O. Vitrik[2]

1- Far Eastern Federal University, Ajax Bay, 10, Russky Island, Vladivostok, Russia, 690922
2- Institute of Automation and Control Processes (IACP) FEB RAS, Vladivostok, Russia, 690041

* georgii.23542@gmail.com

The deposition of nanoparticles from liquid solutions onto a local surface area of minimal area is required in various applications related to the self-structuring of nanomaterials, surface enhanced Raman spectroscopy (SERS), matrix-assisted laser desorption and ionization spectrometry (MALDI), as well as in many other areas [1-3]. This work presents an express method for localizing nanoparticles and molecules from their liquid solutions using the features of the evaporation of bicomponent droplets. It has been established that strong toroidal Marangoni flows arising inside an evaporating droplet consisting of a mixture of isopropyl and water are capable of localizing suspended nanoparticles in the center of the droplet. In this case, at the end of the evaporation process, nanoparticles precipitate in the form of a single cluster. As it was shown, with a certain ratio of components and when selecting optimal evaporation conditions, it is possible to achieve a high degree of nanoparticles localization in the cluster without complex sample preparation and the presence of specially manufactured substrates reduce. Moreover, the cluster area is reduced by three orders of magnitude compared to the area of the initial contact of the drop. It was also be shown that the efficiency of the nanoparticle localization process can be significantly improved by additional heating of the substrate. It allows to achieve the deposit cluster with a diameter 160 μm. To demonstrate the applicability of the described approach for sensory tasks, the organic dye Rhodamine 6G (R6G), characterized by good chemical affinity with gold, as well as intense photoluminescence signals, was added to a suspension of gold nanoparticles. After evaporation, a cluster of gold nanoparticles and rhodamine molecules was formed. The presence of rhodamine was detected in the cluster by SERS method even in case of trace initial concentrations of R6G (10^{-10} M) in aqueous isopropyl solution.

The developed technique can be used in a detailed study of nanoparticles synthesized in liquid media (especially at their small initial concentrations), as well as in biochemical studies and sensor applications related to the optical detection of molecular analytes contained in liquid media in ultra-low concentrations.

[1] O. Kudina, B. Eral, F. Mugele, e-MALDI: an electrowetting-enhanced drop drying method for MALDI mass spectrometry, Analytical chemistry, 88(9), 4669-4675 (2016).
[2] Y.-H. Lai, Y.-H. Cai, H. Lee, et al, Reducing spatial heterogeneity of MALDI samples with Marangoni flows during sample preparation, Journal of The American Society for Mass Spectrometry, 27(8), 1314-1321 (2016).
[3] W. Zhou, A. Hu, S. Bai, et al, Surface-enhanced Raman spectra of medicines with large-scale self-assembled silver nanoparticle films based on the modified coffee ring effect, Nanoscale research letters, 9, 1-9 (2014).

Quantitative ultrafast carrier imaging in perovskite microlaser with optical coherence microscopy

A. Popkova[1*], **M. Sirotin**[1], **I. Soboleva**[1], **A. Pushkarev**[2], **S, Makarov**[2,3],
V. Bessonov[1], **A. Fedyanin**[1]

1- Lomonosov Moscow State University, Russian Federation
2- ITMO University, Russian Federation
3- Harbin Engineering University, China

* popkova@nanolab.phys.msu.ru

Lead halide perovskites are the promising materials for integrated photonics due to their low lasing threshold and broadband spectral tunability, as well as simple fabrication of small lasers by various cost-efficient approaches [1,2]. The perovskites have a high refractive index, which significantly changes under the action of free carrier generation [3]. At the same time, the spatiotemporal dynamics of carriers significantly affects the efficiency of laser generation and the quantum yield of fluorescence. Registration of ultrafast refractive index modulation (Δn) is an indispensable tool for studying light-matter interaction on fundamental and applied levels. With the development of nanophotonic devices new methods for ultrafast refractive index modulation visualization with high spatial and temporal resolution became of particular relevance.

In this work, we succeeded in implementing the pump-probe scheme with a probe in the form of an optical coherence microscopy (OCM) [4], which makes it possible to register changes in the refractive index with a resolution of 1 ps in time, 0.5 µm in space, and Δn sensitivity of down to 10^{-3} RIU. The possibilities of the method are demonstrated on perovskite microcrystals, in which laser generation can be caused by a femtosecond pump pulse either illuminating the entire sample or acting locally, that makes it possible to study the spatial dynamics of a locally generated plasma cloud. With the help of the developed method, direct quantitative spatiotemporal visualization of the dynamics of carriers in a perovskite crystal during lasing is carried out, and the relaxation and diffusion constants are determined.

[1] G. Xing, N. Mathews, S.S. Lim, N. Yantara, X. Liu, D. Sabba, M. Grätzel, S. Mhaisalkar, T.C. Sum, Nat. Mater. 13, 476 (2014).
[2] A.P. Pushkarev, V.I. Korolev, D.I. Markina, F.E. Komissarenko, A. Naujokaitis, A. Drabavicius, V. Pakstas, M. Franckevicius, S.A. Khubezhov, D.A. Sannikov, S. Makarov, ACS Appl. Mater. Interfaces 11, 1040 (2019).
[3] M.V. Kovalenko, L. Protesescu, M.I. Bodnarchuk, Science 358, 745–750 (2017).
[4] M.A. Sirotin, M.N. Romodina, E.V. Lyubin, I.V. Soboleva, A.A. Fedyanin, Biomed. Opt. Express 13, 14–25 (2022).

Machine learning techniques in the analysis of Raman data

O.A. Mayorova[1], M.S. Saveleva[1], Yu.I. Svenskaya[1], D.N. Bratashov[2], E.S. Prikhozhdenko[2*]

1- Science Medical Center, Saratov State University, Saratov, Russia
2- Department of Innovations, Physics Institute, Saratov State University, Saratov, Russia

* prikhozhdenkoes@gmail.com

Raman spectroscopy is a versatile and powerful technique for determining the chemical composition of samples [1]. However, challenges arise when analyzing macromolecules of similar nature (e.g., proteins and fatty acids [2]) or when one component of a mixture is present in low concentrations [3]. Machine learning algorithms can enhance the analysis and provide more accurate results in such cases. Dimensionality reduction techniques, such as principal component analysis (PCA) and t-distributed stochastic neighbor embedding (t-SNE), can be used to identify patterns in the data [4] and improve the signal-to-noise ratio without significantly reducing the Raman intensity [3]. Complex tasks may require the training of regression or classification models. Ensemble models, such as those based on gradient boosting, not only provide high accuracy in distinguishing between samples with small differences, but also identify the most significant Raman wavenumbers for the analysis. Thus, Gradient Boosting Classifiers were trained on datasets containing Raman spectra of whey protein isolate (WPI) and WPI with different amounts of hyaluronic acid (HA): 0.1%, 0.25% and 0.5%. (Fig. 1). The accuracy of the models was calculated based on the number of samples in each class. Although the model, which was trained on a dataset of 200 spectra (50 spectra per class), has an accuracy of 0.7 (Fig. 1A), it is still able to differentiate between the spectra of WPI and WPI+0.1% HA with an 83.3% success rate.
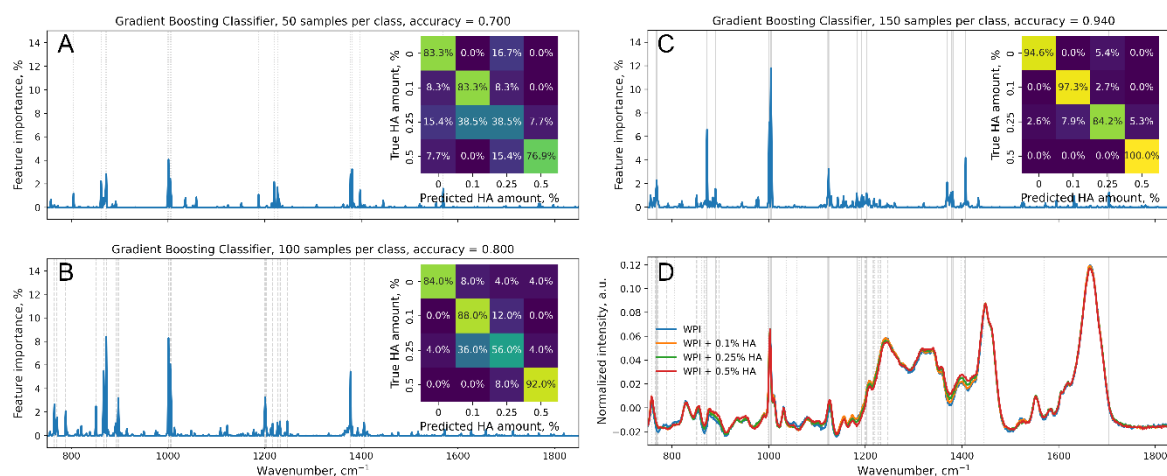
Figure 1. Efficiency of classification models based on gradient boosting depending on the number of spectra per class. (A-C) Feature importances calculated for models trained on 50 (A), 100 (B), 150 (C) samples per class. (A-C, insets) Confusion matrices of models calculated on test portion of dataset (20% of all dataset). (D) Average Raman spectra of each class. Light gray vertical lines indicate wavenumbers with importance > 1%.

Evaluation of model performance based on the number of samples analyzed is of great significance. Although the general assumption is that more data is better, a relatively small number of collected spectra can still yield valuable results.

[1] A. Orlando, F. Franceschini, C. Muscas, S. Pidkova, M. Bartoli, M. Rovere, A. Tagliaferro, A comprehensive review on Raman spectroscopy applications, Chemosensors, 9 (9), 262, (2021).
[2] I.Yu. Yanina, Yu.I. Svenskaya, E.S. Prikhozhdenko, D.N. Bratashov, M.V. Lomova, D.A. Gorin, G.B. Sukhorukov, V.V. Tuchin, Optical monitoring of adipose tissue destruction under encapsulated lipase action, Journal of biophotonics, 11(11), e201800058, (2018).
[3] O.A. Mayorova, M.S. Saveleva, D.N. Bratashov, E.S. Prikhozhdenko, Combination of Machine Learning and Raman Spectroscopy for Determination of the Complex of Whey Protein Isolate with Hyaluronic Acid, Polymers, 16(5), 666, (2024).
[4] Y.J. Liu, M. Kyne, C. Wang, X.Y. Yu, Data mining in Raman imaging in a cellular biological system, Computational and Structural Biotechnology Journal, 18, pp.2920-2930, (2020).

The results of lidar studies of long-range aerosol transport from the Gobi and Taklamakan deserts

<u>V. Lisitsa</u>[1], K. Shmirko[1*], A. Pavlov[1], O. Konstantinov[2]

1- Institute for automation and control processs FEB RAS, 690041, 5 Radio str, Vladivostok, Russia
2- V.I. Il'ichev Pacific Oceanological Institute FEB RAS690041, 43 Baltiyskaya str, Vladivostok, Russia

* kshmirko@vk.com

The results of lidar measurements of the vertical distribution of optical characteristics of dust aerosol from the Gobi and Taklamakan deserts in the troposphere of Vladivostok are presented. A Mi-Raman lidar with a crosspolarization channel was used as a tool, which allows to obtain vertical profiles of a set $(3\beta+2\varepsilon+\delta)$-3 backscattering coefficients (355.532.1064 nm), 2 extinction coefficients and one depolarization coefficient at a wavelength of 532 nm. For the Gobi desert, the value of the depolarization coefficient is $\delta=0.13\div0.15$, typical for dust aerosol particles of submicron size, noted in the altitude range 3.00 – 4.25 km. Low values of the Angstrom coefficient corresponded to this height range ($\alpha355/532=0.5$) and high single scattering albedo values $SSA=0.98\div0.99$. At the same time, the complex refractive index inside the dust layer has the values $m_r=1.48\div1.56$, $m_i=0.001$ characteristic of dust particles. The effective radius varies between $0.2 – 0.4$ microns with a maximum value at an altitude of 3.8 km. The volume distribution function inside the dust layer represents a well-defined two-modal structure with a slight excess of the coarse-dispersed mode over the fine-dispersed one. The modal radii of the modes had values $R_{fine}=0.18$ µm and $R_{coarce}=0.8$ µm, respectively, for fine and coarse modes. For the Taklamakan desert, the value of the depolarization coefficient has the value $\delta=0.14$, which is typical for dust aerosol particles of submicron size. These particles are located mainly in the height range of $5 – 10$ km. The two-layer structure of the dust aerosol was clearly observed in the behavior of the optical characteristics. The area of low lidar ratio values in the altitude range of $8 – 10$ km was compared with the area of cirrus cloud formation, the presence of which was indicated by satellite images of the MODIS radiometer on the day of measurements. The results of the inversion showed a more than twofold increase in the effective radius of dust particles during the transition from the subclacial layer to the cirrus cloud layer. At the same time, the complex refractive index did not experience visible variability over the entire height range, and its value was in good agreement with the values typical for a dust aerosol.

Femtosecond laser-structured chalcogenide vitreous semiconductor films: hierarchical surface relief and optical anisotropy

D. Shuleiko[1*], D. Pepelyaev[2], E. Kuzmin[1], P. Pakholchuk[1], S.V. Zabotnov[1], P.K. Kashkarov[1]

1- Faculty of Physics, Lomonosov Moscow State University, 1/2 Leninskie Gory, Moscow, Russia
2- Institute of Advanced Materials and Technologies, National Research University of Electronic Technology,
1 Shokina Sq., Zelenograd, Russia

* shuleyko.dmitriy@physics.msu.ru

Chalcogenide vitreous semiconductors (ChVS) possess high transparency in the near-infrared (IR) range, providing their applicability in infrared photonics. An important feature of these materials is possibility to form optically anisotropic controllable femtosecond laser-induced periodic surface structures (LIPSS) [1] which are of interest for polarization optics and optical data storage with multi-level coding [2,3]. In our work we produce various LIPSS types on arsenic selenide vitreous films (As_2Se_3, $As_{50}Se_{50}$) and analyze their structural and optical properties.

To form LIPSS on thin (850 ± 5 nm) ChVS films on chromium or quartz glass substrates, femtosecond laser pulses were used (Satsuma Amplitude Systems, 515 nm, 300 fs), with different fluence $E = 34 - 270$ mJ/cm^2 and the number of applied pulses $N = 10 - 1600$.

Scanning electron microscopy revealed that as a result of irradiation, various types of LIPSS with both subwavelength (~170 nm) and wavelength (~500 nm) periods are formed on the surface of ChVS films. The ridges of the structures are parallel or perpendicular to the laser polarization, respectively, and their height, according to atomic force microscopy measurements, reaches up to 100 nm. As N increases from 50 to 1600 while the value of E is constant (34 mJ/cm^2), the subwavelength LIPSS transform into wavelength ones. At intermediate values of N, simultaneous formation of both structure types in the form of a hierarchical surface relief is observed. Optical transmission analysis of the of irradiated ChVS films in polarized light (633 nm) revealed optical retardance of up to 30 nm (Fig. 1), caused by the presence of one-dimensional surface relief.
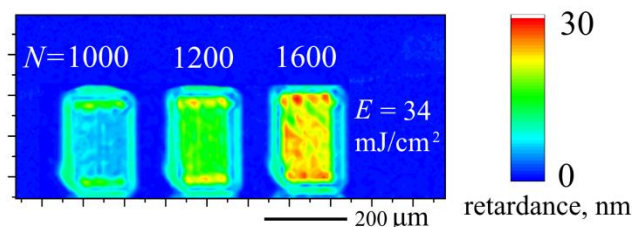
Fig. 1. Optical retardance at 633 nm wavelength in As50Se50 film at different laser irradiation parameters.

The possibility to control retardance in the irradiated film by varying the number of applied pulses N is shown. The difference in the refractive indices of ordinary and extraordinary waves in the IR range was up to 0.1, determined from the position of interference maxima in the IR spectra.

Thus, the possibility of creating an optically anisotropic surface relief on ChVS films using femtosecond laser pulses has been demonstrated, opening perspectives of such structures as the basis for polarization-sensitive IR optics and optical memory devices.

[1] S. Zabotnov, A. Kolchin, D. Shuleiko, et al, Periodic relief fabrication and reversible phase transitions in amorphous $Ge_2Sb_2Te_5$ thin films upon multi-pulse femtosecond irradiation, Micro, vol. 2, pp. 88–99 (2022).
[2] K. Makino, Y. Saito, P. Fons, et al, Anisotropic lattice response induced by a linearly-polarized femtosecond optical pulse excitation in interfacial phase change memory material, Scientific Reports, vol. 6, 19758 (2016).
[3] H. Wang, Y. Lei, L. Wang, et al, 100-Layer Error-Free 5D Optical Data Storage by Ultrafast Laser Nanostructuring in Glass, Laser Photonics Rev., vol 16, art. 2100563 (2022).

Silicon nanowires uniformly decorated with Au nanoparticles for SERS detection of viruses

I. Sobina[1*], **A. Erokhina**[1], **I. Tsiniaikin**[1], **K. Gonchar**[1], **E. Boravleva**[2],
J. Samsonova[3], **L. Osminkina**[1]

1- Lomonosov Moscow State University, Department of Physics, 119991 Moscow, Russia
2- FSASI "Chumakov Federal Scientific Center for Research and Development of Immune-and-Biological Products of Russian Academy of Science" (Institute of Poliomyelitis), 108819, Moscow, Russia
3- Lomonosov Moscow State University, Department of Chemistry, 119991 Moscow, Russia

* igo.sobina@yandex.ru

Rapid detection and identification of pathogenic viruses is one of the key tasks of modern biomedicine. PCR and ELISA methods widely used in medical practice today allow effective virus identification, but they have their own disadvantages: expensive equipment is required for such tests, and the time to obtain a result takes from several hours. Therefore, it is necessary to develop new fast and inexpensive methods of virus detection. Raman spectroscopy is one of the promising methods for the study of bioobjects [1], but this method has poor sensitivity, so for its effective application it is necessary to create structures that enhance this effect.

Silicon is a biocompatible material, it is safe and has no toxic effects on bioobjects. In the presence of noble metal nanoparticles (Au, Ag) due to the emergence of localized plasmon resonances, a significant increase in the intensity of the optical signal of Raman scattering (10^4-10^6 times) is observed – the effect of surface-enhanced Raman scattering (SERS) [2]. Thus, silicon structures decorated with noble metal nanoparticles will provide highly sensitive, fast and specific registration of the optical signal from surrounding molecules, including biomolecules [3].

In this work, arrays of silicon nanowires decorated with gold nanoparticles along their entire length (Au@SiNWs) were prepared (Fig. 1). The SiNWs were prepared by metal-assisted chemical etching (MACE) of silicon wafers (12 Ohm*cm). For uniform coating of the SiNWs along the entire length, the samples were immersed in $HAuCl_4 \cdot 3H_2O$ (0.005 M) aqueous solution for 30 min. Then, the nanowires were immersed for 10 seconds in HF (5 M) solution and finally were washed in MQ. This uniform coating of the Au@SiNWs provides higher SERS activity for virus detection.
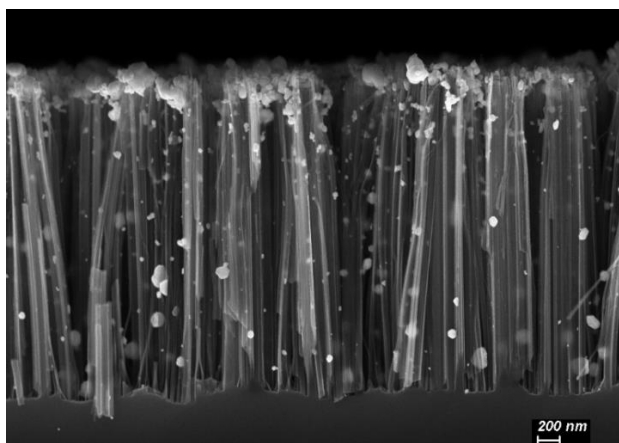
Fig. 1. Scanning electron microscopy micrograph of Au@SiNWs.

[1] J.-Y. Lim, J.-S. Nam, S.-E. Yang, H. Shin, Y.-H. Jang, G.-U. Bae, T. Kang, K.-I. Lim, Y. Choi, Identification of Newly Emerging Influenza Viruses by Surface-Enhanced Raman Spectroscopy, Analytical Chemistry, Vol. 87, pp. 11652–11659, (2015).
[2] B. Sharma, R.R. Frontiera, A.I. Henry, E. Ringe, R.P. Van Duyne, SERS: Materials, applications, and the future, Materials Today, Vol. 15, pp. 16-25, (2012).
[3] Z. Movasaghi, S. Rehma, I. Rehman, Raman Spectroscopy of Biological Tissues, Applied Spectroscopy Reviews, Vol. 42, pp. 493-541, (2007).

Raman-fluorescence tags for bioimaging by plasmon-enhanced spectroscopy

<u>E. Solovyeva</u>[*]**, V. Svinko, A. Smirnov, A. Demenshin, A. Shevchuk, A. Smirnov**

Institute of Chemistry, Saint-Petersburg State University, Saint Petersburg, Russian Federation

* solovyeva.elena.v@gmail.com, e.solovieva@spbu.ru

The development of bioimaging tools for cells, tissues and organs is important to improve the quality and completeness of medical diagnosis and treatment. The potential of gold nanoparticles as optical amplifiers and photothermal agents has been demonstrated repeatedly in many studies [1,2]. Hybrid structures based on gold nanoparticles combined with chromophores not only consolidate the beneficial properties of the two components, but can also demonstrate synergistic effects, such as enhanced Raman scattering, luminescence and etc. However, the development of hybrid bioimaging tags requires thorough optimization of their composition and structure. In this work, we present a wide range of core-shell tags (Fig. 1), differing in the morphology of gold nanoparticle, shell material, chromophore used, its position and method of immobilization in the shell (electrostatic adsorption or covalent conjugation).
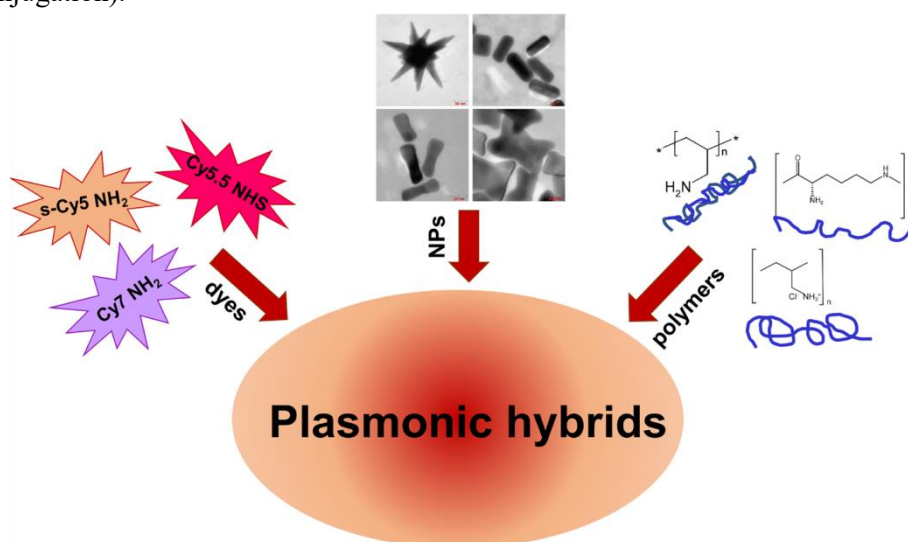
Fig. 1. General representation of hybrids composition developed for bioimaging by plasmon-enhanced spectroscopy.

The optical studies of the tags were performed by surface-enhanced Raman scattering (SERS) and fluorescence spectroscopy for both colloidal suspensions and incubated cell samples. The optimized parameters were found at which the tags are able to operate in a bimodal regime. The refusal of covalent conjugation of the chromophore and its location at a distance of 2-3 nm from the plasmonic core are the key factors in achieving the bimodality.

Biological tests revealed that obtained hybrid structures undergo endocytosis, regardless of the morphology of gold core and coating material, and are localized in the cell cytoplasm. Cytotoxicity tests showed that the tags are non-toxic in the concentration range of 5-15 μg/mL.

[1] A.N. Smirnov, A.I. Shevchuk, A.V. Volkova, V.D. Kalganov, E.V. Solovyeva, Gold-silica plasmonic nanobones with tunable size and optical bimodality for bioimaging, Colloids Surf. A, vol. 684, 133115, 2024.
[2] V.O. Svinko, A.N. Smirnov, A.I. Shevchuk, A.I. Demenshin, A.A. Smirnov, E.V. Solovyeva, Comparative study of fluorescence core-shell nanotags with different morphology of gold core, Colloids Surf. B, vol. 226, 113306, 2023.

Resonant phenomena in luminescence response of low-dimensional silicon photonic structures

M. Stepikhova[1*], **A. Peretokin**[1], **S. Dyakov**[2], **M. Petrov**[3], **V. Verbus**[1], **Zh. Smagina**[4],
V. Zinoviev[4], **D. Yurasov**[1], **D. Shengurov**[1], **E. Rodyakina**[4], **A. Novikov**[1]

1- Institute for Physics of Microstructures Russian Academy of Sciences, Nizhny Novgorod, 603950, Russia
2- Skolkovo Institute of Science and Technology, Moscow, 143025, Russia
3- Department of Physics and Engineering, ITMO University, St. Petersburg, 197101, Russia
4- Rzhanov Institute of Semiconductor Physics, Siberian Branch of Russian Academy of Sciences, Novosibirsk, 630090, Russia

* mst@ipmras.ru

The development of modern technologies opens up new possibilities for creating photonic structures with sizes comparable to and less than the wavelength of radiation, identifying new optical phenomena and possibilities for controlling the radiating properties of the active medium. In this paper, we will consider the possibilities of controlling the radiating properties of the active medium due to the effects of its interaction with resonant modes of low-dimensional photonic structures, in particular: two-dimensional photonic crystals (PhC), low-dimensional disk resonators and their arrays. Silicon structures with Ge(Si) nanoislands were used as the active medium. These structures seem promising for creating radiation sources integrated into silicon nanophotonics circuits. The paper discusses such peculiar phenomena as bound states in the continuum (BIC) characterized by the appearance of high-Q, resonant lines in the photoluminescence (PL) spectra. Symmetry protected and accidental BICs have been found in 2D photonic crystals with a hexagonal lattice of holes [1,2]. The features of the manifestations of these modes are the presence of a discontinuity in the band diagram of the photonic crystals emissivity and the characteristic vortex polarization. The vortex behavior of luminescence polarization related with BICs will be shown for the first time. The possibilities for realignment, selection and control of the dispersion characteristics of BIC modes in 2D photonic crystals by changing their parameters will also be discussed [3,4]. Another possibility of observing BICs is related with low-dimensional disk resonators. In this case, quasi-BICs were observed in the micro-PL spectra of disk resonators, which are the result of destructive interference of Mie and Fabry-Perot modes. The observed quasi-BICs are characterized by a specific radiation pattern oriented along the disk axis. Additionally, using the example of structures with arrays of low-dimensional disk resonators, the manifestations of collective phenomena, such as collective Mie modes, interaction phenomena of plasmonic and photonic modes in square lattices of metallic disks, and others will be considered [5,6]. In all cases, the observed resonant phenomena allow us to significantly modify the radiating properties of the active medium, increasing its radiative efficiency up to two orders of magnitude.

[1] S. Dyakov, M. Stepikhova, A. Bogdanov, et al, Photonic bound states in the continuum in Si structures with the self-assembled Ge nanoislands, Laser & Photonics Reviews, vol. 15, pp. 2000242, (2021).
[2] M.V. Stepikhova, S.A. Dyakov, A.V. Peretokin, et al, Interaction of Ge(Si) Self-Assembled Nanoislands with Different Modes of Two-Dimensional Photonic Crystal, Nanomaterials, vol. 12, pp. 2687, (2022).
[3] A.V. Peretokin, D.V. Yurasov, M.V. Stepikhova, et al, Tuning the Luminescence Response of an Air-Hole Photonic Crystal Slab Using Etching Depth Variation, Nanomaterials, vol. 13, pp. 1678, (2023).
[4] D.V. Yurasov, S.A. Dyakov, I.A. Smagin, et al, Symmetry breaking of bound states in continuum in luminescence response of photonic crystal slabs with embedded Ge nanoislands, Appl. Phys. Lett., (2024) – submitted.
[5] V.A. Zinovyev, Z.V. Smagina, A.F. Zinovieva, et al, Emission Enhancement of Ge/Si Quantum Dots in Hybrid Structures with Subwavelength Lattice of Al Nanodisks, Nanomaterials, vol. 13, p. 2422 (2023).
[6] V.A. Zinovyev, Z.V. Smagina, A.F. Zinovieva, et al, Collective Modes in the Luminescent Response of Si Nanodisk Chains with Embedded GeSi Quantum Dots, Photonics, vol. 10, p. 1248 (2023).

Chiral atomically thin AIIBVI nanostructures: colloidal growth and chiroptical properties of 2D excitons

D.A. Kurtina, A.I. Lebedev, <u>R.B. Vasiliev</u>[*]

Lomonosov Moscow State University, Leninskie Gory119991, Moscow, Russia

* romvas@inorg.chem.msu.ru

Chirality refers to a geometrical property of mirror asymmetry when an object cannot be superimposed onto its mirror image. Chiral semiconductor nanostructures have attracted tremendous interest due to a variety of intriguing properties [1]. Due to the chiral shapes of the nanostructures and/or the chirality of the molecular orbitals forming excited states in semiconductor nanostructures, excitons in such nanostructures acquire mirror asymmetry, which leads to different interaction with left- and right-handed circularly polarized photons. Such nanostructures with chiral excitation are promising candidates for biosensing, stereoselective reactions, and enantioselective separation. In this repot, we present a study of chiroptical properties of 2D atomically thin organic-inorganic nanostructures of cadmium and zinc chalcogenides hybridized with enantiomeric L-/D-cysteine derivative ligands and showed a distinctive circular dichroism (CD) of 2D excitons.

We used a colloidal method for the growth of atomically thin nanostructures (nanosheets) of cadmium and zinc chalcogenides with a thickness of less than 1 nanometer (only 2 or 3 monolayers in thickness) and lateral sizes up to 1 micron (anisotropy factor up to 1000). A system of cadmium (zinc) acetate/octadecene/oleic acid/oleylamine was used for the nanostructure growth in the temperature range of 110–250°C [2-4] and we achieved the formation of nanostructures with a precise (with an accuracy of 1 monolayer) thickness in the range of 0.6–0.9 nm. Ligand exchange protocols were developed for the exchange of native oleic acid ligand for enantiomers of L-/D-cysteine derivative: L-/D-cysteine, N-acetyl-L-/D-cysteine and N-oleoyl-L-/D-cysteine. A detailed study using TEM, HAADF-STEM, SAED and XRD methods showed the composition of nanostructures followed the ratio $[M_{n+1}E_nL_2]$ (M – zinc or cadmium, E – chalcogen, L – organic ligand, n – number of atomic planes) with n = 2 and 3.

The optical and chiroptical properties of nanostructures were studied by optical absorption and luminescence spectroscopy, CD spectroscopy, magnetic CD spectroscopy, and polarimetry. CD spectra of nanostructures showed distinct, sign-alternating bands related to 2D excitons with high g-factor of dissymmetry up to 0.03. The combination of chiroptical measurements in dependence on type of ligand and DFT calculations of ligand coordination showed that high dissymmetry factor arises from helicoidal distortion of crystal structure and high rotational strength of 2D excitons. To prove the pseudomagnetic nature of the splitting of circular dichroism bands, measurements of the magnetic circular dichroism of samples of nanostructures were carried out when a magnetic field was applied. Based on the dependence of the value of the circular dichroism of the HH transition on the field strength, the value of the internal pseudomagnetic field was found to be on the order of 2 T. Specific optical rotation for the thinnest nanostructures was $[\alpha] = + 805 \pm 76$ grad, which is more than 40 times higher than the specific rotation of the individual ligand. We believe that our work opens up new possibilities for creating artificial chiral nanostructures and will be useful for polarization-enabled applications in photonics.

[1] N.H. Cho, A. Guerrero-Martínez, J. Ma, et al, Bioinspired chiral inorganic nanomaterials. Nat Rev Bioeng 1, 88–106 (2023).

[2] D.A. Kurtina, et al, Atomically Thin Population of Colloidal CdSe Nanoplatelets: Growth of Rolled-up Nanosheets and Strong Circular Dichroism Induced by Ligand Exchange, Chem. Mater., 31, 9652–9663, (2019).

[3] D.A. Kurtina, et al, Induction of Chirality in Atomically Thin ZnSe and CdSe Nanoplatelets: Strengthening of Circular Dichroism via Different Coordination of Cysteine-Based Ligands on an Ultimate Thin Semiconductor Core, Materials, 16, 1073 (2023).

[4] D.A. Kurtina, et al, Chirality in Atomically Thin CdSe Nanoplatelets Capped with Thiol-Free Amino Acid Ligands: Circular Dichroism vs. Carboxylate Group Coordination, Materials 17, 237 (2024),

Dynamic speckle diagnostics of irreversible processes in biological and technical objects

A. Vladimirov[1,2,3*]

1- E.S. Gorkunov Institute of Engineering Science of the Ural Branch of the Russian Academy of Sciences, 34 Komsomolskaya str., Yekaterinburg, 620219, Russia
2- Ural Federal University named after B.N. Yeltsin, 19 Mira str., Yekaterinburg, 620002, Russia
3- FSRIVI "Virome" Rospotrebnadzor, 23 Letnaya str., Yekaterinburg, 620039, Russia

* vap52@bk.ru

The purpose of the report is to review the research conducted by the author over the past 5 years on the application of a new optical method. The method makes it possible to determine dynamic deformations caused by changes in the shape and volume of gas, liquid and solid bodies with a spatial resolution of Δl of the order of 1 μm. The subjects of our research are intracellular processes in cultured cells, high-cycle fatigue of materials and turbulent flows. The relevance of these studies is related to the absence of methods that allow real-time monitoring of intracellular processes, assessing the accumulation of fatigue damage, and determining the parameters of turbulent flows. The results obtained earlier can be found in the chapters of the books [1,2]. In these publications, the theoretical, experimental and metrological justification of the time-averaged speckle image method was given. It was shown that the parameter characterizing the intensity of metabolic processes, as well as the accumulation of fatigue damage to materials, is the standard deviation σ of the difference in the optical paths Δu of pairs of waves propagating at a characteristic distance of Δl. In the articles [3,4], the theory of the method was further developed. The problem of speckle dynamics in the image plane of a transparent and reflective object, respectively, was solved under the assumption that the random variable Δu is the sum of independent quantities Δu_m, $m=1,2,...M$. These values correspond to processes occurring simultaneously in different layers of transparent or at different scale levels of reflective objects. A tomographic method for determining the mean values, variances σ^2 and correlation (relaxation) time τ_m of Δu_m, as well as two simple methods for determining $\sigma_m(\tau_m)$ dependencies, was substantiated. These dependences characterize the relative contribution of processes occurring at different speeds to cellular metabolism, fatigue degradation of materials and to the turbulent flow of liquids and gases. An excellent coincidence of theory and experiment was obtained (Fig.1).

The method has been successfully used to identify the nature of high-cycle fatigue of materials. It is shown that the key point of low-, high- and giga-cycle fatigue is the localization of irreversible processes in small zones and the appearance of areas that are constantly in a tensile state as a result. In these areas, cyclic creep first occurs, followed by deformation softening of the material, leading to the formation of a macro-fracture. To assess the life of the parts, the creation of devices and methods of non-destructive testing of a new generation based on the use of matrix-type sensors with cell sizes of the order of 10 microns is justified. Dependences $\sigma_m(\tau_m)$ are given for cultured cells in normal conditions and with the introduction of toxic substances, as well as for the turbulent flow of heated air.
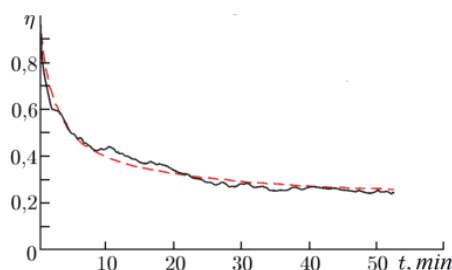

Fig.1. The normalized ACF of radiation intensity fluctuations in the image plane of a group of cells [3]. Theory and experiment.

[1] A. Vladimirov and A. Bakharev, Dynamic speckle interferometry of thin biological objects: theory, experiments, and practical perspectives, In book: Optical Interferometry (Intech), Chapter 6 (2017).
[2] A. Vladimirov, Dynamic speckle interferometry of technical and biological objects, In book: Interferometry (Intech), Chapter, (2018).
[3] A. Vladimirov, Speckle tomography of the living-cell functions, Radiophysics and Quantum Electronics, Vol. 63 (8), pp. 592-604, (2021).
[4] A. Vladimirov, N. Drukarenko Yu. Mikhailenko, Speckle diagnosis of irreversible processes occurring in some living and technical objects, In book: Optical Flow Research Methods (Pero Publishing House), pp. 51-62, in Russian, (2021).

Structural and optical properties of PbSe(S) thin films

S.N. Yasinova[1*], S.I. Mekhtiyeva[2], M.H. Huseynaliyev[1], R.I. Alekberov[2]

1- The Ministry of Science and Education of Azerbaijan, Institute of Natural Resources, H.Aliyev ave. 76, AZ7000, Nakhchivan
2- The Ministry of Science and Education of Azerbaijan, Institute of Physics named after Academician Hasan Abdullayev, G. Javid ave 131, AZ1143 Baku

* sara.novruzova@yahoo.com

The purpose of this work is to analyze the changes in the structural properties of lead chalcogenides (PbSe and PbS) thin films obtained by chemical bath deposition and the mechanisms of their influence on Raman scattering. Studies show that transverse and surface phonon modes are usually not observed due to symmetry constraints [1]. The main reason for the mentioned uncertainty is the observation of rapid photooxidation processes in thin layers of PbS and PbSe under the influence of laser radiation applied to observe Raman scattering [2]. In particular, while weak Raman scattering is expected to be observed in the region of relatively low wave numbers (154, 205 and 454 cm^{-1}) in PbS, photooxidation processes occurring on the surface of thin films under the influence of a laser beam artificially enhance the Raman scattering signal [2]. It was determined that as a result of semi-substitution of selenium with sulfur, along with the increase in the size of the nanoparticles, the bond within the nanoparticles is strengthened due to the chemical activity and high bond energy of the sulfur atoms. As the elastic force constant (k) increases as a result of the increase in bond connectivity, the frequency of the Raman active oscillation modes expressed below, based on the molecular structure model, increases. The crystallite sizes of nanoparticles belonging to PbSe, PbS and $PbS_{0.5}Se_{0.5}$ were calculated by applying the Debye-Scherrer formula (1) given below to the results X-ray.

$$d = \frac{0.9\lambda}{\beta\cos\theta} \tag{1}$$

In formula (1), **d** is the crystallite size of nanoparticles, **λ** is the wavelength of the X-ray beam (λ=1.54 Å), β is the half-width of the sharp maxima described in the X-ray diffraction scattering curves of the samples and **θ** is the Bragg reflection angle. The results of X-ray diffraction scattering show that the crystallite sizes found in thin layers of $PbS_{0.5}Se_{0.5}$ are larger and vary in the range of 17.9÷30.8 nm.

[1] S. Hoomi, R. Yousefi, F. Jamali-Sheini, A. Saaedi, M. Cheraghizade, W.J. Basirun, N.M. Huang, Large-scale and facile fabrication of PbSe nanostructures by selenization of a Pb sheet Functional Materials Letters, Vol. 8, No. 6, 1550063 (2015).
[2] M.J. Bierman, Y.K. Albert Lau, S. Jin, Hyperbranched PbS and PbSe Nanowires and the Effect of Hydrogen Gas on Their Synthesis, Nano Letters, Vol. 7, No. 9, pp. 2907-2912 (2007).

NONLINEAR AND TERAHERTZ PHOTONICS

Joint generation of THz radiation and electron flow in gas-cluster media under laser excitation

A.V. Balakin[1*], **N.A. Kuzechkin**[2], **P.M. Solyankin**[2], **A.P. Shkurinov**[1]

1- Faculty of Physics, Lomonosov Moscow State University, Moscow, Russia
2- National Research Centre "Kurchatov Institute", Moscow, Russia

* *a.v.balakin@physics.msu.ru*

Complex study of interaction of high intense femtosecond laser pulses with gas-cluster targets is of a great interest to reveal fundamental features of the process and to next implementation of the results in plenty of applications, such as efficient generation of radiation in an extremely wide spectral range from X-ray through deep-UV to THz, as well as generation and acceleration of flow of fast charged particles [1-6]. Usually, an adiabatic expansion of gas into vacuum through a special supersonic nozzle is applied to form gas-cluster nanoscale targets. The resulted gas-cluster jet inherits a unique feature as high local and relatively low average density of matter, and effectively interacts with high-intensity femtosecond laser pulses.

Here we present and discuss our recent results on study the processes of generation of THz radiation and electron flow occurring jointly in gas-cluster jet under laser excitation. Ti:Sapphire laser system produced pulses at 1 kHz repetition rate with 35 fs duration and energy of up to 6 mJ per pulse was used as an excitation source in our experiments. A variety of gases and gas mixtures were examined to form gas-cluster target, and SF_6:Ar gas mixture (molar ratio 1:8) was selected finally, as it demonstrated the better electrons yield. We have investigated properties and measured base characteristics of generated electron beam and THz radiation under various conditions of the gas-cluster target excitation and parameters of the laser radiation. In particularly, it was found that optimal position of laser focus in the gas-cluster jet differs significantly for the effective generation of electron flow and THz radiation. Another remarkable result is that varying of polarization state of laser radiation from linear to circular results in decrease of electrons yielding whereas the THz yielding increases under the same change.

[1] T. Nagashima, H. Hirayama, K. Shibuya, M. Hangyo, M. Hashida, S. Tokita, S. Sakabe, Terahertz pulse radiation from argon clusters irradiated with intense femtosecond laser pulses, Opt. Exp., vol 17, p. 8907, 2009.

[2] V.M. Gordienko, M.S. Dzhidzhoev, I.A. Zhvaniya, V.P. Petukhov, V.T. Platonenko, D.N. Trubnikovc, A.S. Khomenko, Effective generation of characteristic K-rays from large laser-excited SF6 clusters in the presence of an Ar carrier gas, JETP Letters, vol. 91, pp. 355-362, 2010.

[3] L.M. Chen, J.J. Park, K.-H. Hong, J.L. Kim, J. Zhang, C.H. Nam, Emission of a hot electron jet from intense femtosecond-laser–cluster interactions, Physical Review E., vol 66, p. 025402, 2002.

[4] A. Mondal, R. Sabui, S. Tata, R.M.G.M. Trines, S.V. Rahul, F. Li, S. Sarkar, W. Trickey , R.Y. Kumar, D. Rajak, J. Pasley, Z. Sheng, J. Jha, M. Anand, R. Gopal, A.P.L. Robinson, M. Krishnamurthy, Laser structured micro-targets generate MeV electron temperature at 4×10^{16} W/cm^2, arXiv preprint arXiv:2107.03866, 2021.

[5] I.A. Zhvaniya, K.A. Ivanov, T.A. Semenov, M.S. Dzhidzhoev, R.V. Volkov, I.N. Tsymbalov, A.B. Savel'ev, V.M. Gordienko, Electron acceleration up to MeV level under nonlinear interaction of subterawatt femtosecond laser chirped pulses with Kr clusters, Laser Phys. Lett., vol. 16, p. 115401, 2019.

[6] F. Salehi, A.J. Goers, G.A. Hine, L. Feder, D. Kuk, B. Miao, D. Woodbury, K.Y. Kim, H.M. Milchberg, MeV electron acceleration at 1 kHz with < 10 mJ laser pulses, Optics letters, vol 42, pp. 215-218, 2017.

Nonlinear effects in the interaction between semiconductor lasers and high-Q microresonators

D.M. Sokol[1], A.E. Shitikov[1], N.Yu. Dmitriev[1], D.A. Chermoshentsev[1], V.E. Lobanov[1], I.A. Bilenko[1,2*]

1- Russian Quantum Center 121205, Moscow
2- M.V. Lomonosov Moscow State University, 119991, Moscow

* igorbilenko@gmail.com

The report presents new results of theoretical analysis and experimental studies of the nonlinear dynamics of high-Q optical microcavities. It is shown that in a microcavity-laser system, stable multi-frequency lasing modes with a difference frequency in the microwave range are possible. Self-injection locking (SIL) of several lasers on the same resonator could provide powerful microwave signal at the detector. New four wave mixing rejime was discovered in the states close to the SIL.

For the first time, a high ($Q > 10^8$) quality factor in microcavities with "whispering gallery" modes was demonstrated in quartz microspheres [1].

Currently, microring and microdisk optical resonators are widely used in physical measurements and technical applications. The record quality factor $Q = 10^{11}$ was demonstrated in crystalline CaF_2 resonators [2]. The long lifetime of photons in the cavity material determines the low threshold for the manifestation of nonlinear effects [3]. The emergence of technology for manufacturing integrated circuits (chips) with microcavities on the Si_3N_4 platform with a quality factor $Q > 10^7$ using CMOS compatible technology [4] has led to their rapid spread both as devices for fundamental research and elements of applied development. In particular, in such resonators the generation of optical frequency combs and the formation of solitons is possible.

In our recent studies, we have shown that double (bichromatic) pumping allows for threshold-free four-wave mixing and generation of combs in both resonators with anomalous and normal group velocity dispersion. Degenerate mixing leads to parametric generation at the central frequency, the special properties of which (two possible phase values, compression along one of the quadrature components) are of great interest for the implementation of quantum measurements and quantum computing. It was discovered that the interaction of forward and backward waves in a laser medium leads to the emergence of new effects – multi-frequency self-injection locking and four-wave mixing, as a result of which it is possible to obtain a narrow linewidth microwave signals at the output of the photodetector.

[1] V.B. Braginsky, M.L. Gorodetsky, V.S. Ilchenko, Physics Letters A. 137, 393, (1989).
[2] A.A. Savchenkov, A.B. Matsko, V.S. Ilchenko, et al, Optics express, 15(11), 6768-6773, (2007).
[3] D.V. Strekalov, C. Marquardt, A.B. Matsko, et al, Journal of Optics 18(12), 123002, (2016).
[4] C. Xiang, J. Liu, J. Guo, L. Chang, R.N. Wang, W. Weng, ... & J.E. Bowers, Laser soliton microcombs heterogeneously integrated on silicon. Science, 373(6550), 99-103, (2021).
[5] N.M. Kondratiev, V.E. Lobanov, A.E. Shitikov, et al, Frontiers of Physics 18(2), 21305, (2023).

Nonlinear control of coherent tunnelling by adiabatic passage in hybrid integrated waveguides

O. Borovkova[1*], **I. Bilenko**[1,2], **D. Chermoshentsev**[1,3,4]

1- Russian Quantum Center, Skolkovo Innovation Center, Bolshoy boulevard, 30, bld. 1, 121205, Moscow, Russia
2- Faculty of Physics, Lomonosov Moscow State University, Leninskie Gory, Moscow 119991, Russia
3- Moscow Institute of Physics and Technology, 141701, Dolgoprudny, Russia
4- Skolkovo Institute of Science and Technology, Moscow 143025, Russia

* o.borovkova@rqc.ru

Integrated photonics is a perspective platform for various applications from biosensors to compact light sources, from quantum technologies to neural networks and information processing, etc. Optical waveguides and directional couplers made by CMOS-compatible technology are basic elements for integrated photonics; and advances of light routing and control in them attracts an interest of researchers. In our work we analyze the possibilities of the light routing and transfer provided by the integrated planar waveguide structure on the silicon dioxide chip based on the coherent tunnelling by adiabatic passage (CTAP) [1-3]. The CTAP is an optical analogue of the stimulated Raman adiabatic passage (a laser-based method of efficient and selective transfer of population between quantum states) well-known for atomic and molecular physics [4]. In optical CTAP scheme the waveguides adiabatically couple with each other and enable light evolution via the dark state of the three-state system (composed of two weakly-curved waveguides and one straight waveguide between them). The most interesting is the so-called counter-intuitive scheme, when coupling between idle waveguides (one of lateral waveguides and the central one) appears before the excited waveguide becomes coupled with one of them. As a result, the central waveguide is not excited via coupling, but just serves for light transfer. An advantage of such scheme is that light transfer can be effectively controlled via parameters and optical properties of the central waveguide, but there is no light transfer in it.

We consider the hybrid integrated waveguide scheme, where the lateral bent waveguides are made of silicon nitride and the central waveguide can be made of different material, e.g., from the lithium niobate, that is well-known due to its large second-order nonlinear susceptibility and greater refractive index than silicon nitride. We show that the light transfer in such waveguide scheme can be controlled by external field applied to the central waveguide. It is demonstrated that the efficiency of the light transfer in the hybrid CTAP scheme is higher than in pure silicon nitride one, and the intermediate waveguide in this case doesn't carry any signal at all. Also, we address the robustness of the CTAP scheme to the polarization state of the transferred light and revealed that both polarizations (TE and TM) possess close transmittance coefficients due to the adiabatic character of the light transfer. This aspect is especially important for practical applications. Moreover, we performed the optimization of the parameters of the considered setup to achieve the maximum transmittance of the setting.

[1] S. Longhi, G. Della Valle, M. Ornigotti, P. Laporta, Coherent tunneling by adiabatic passage in an optical waveguide system, Phys. Rev. B, vol. 76, pp. 201101, (2007).
[2] S. Longhi, Quantum-optical analogies using photonic structures, Laser and Photon. Rev., vol. 3, pp. 243-261, (2009).
[3] K. Bergmann, et al, Roadmap on STIRAP applications, J. Phys. B: At. Mol. Opt. Phys., vol. 52, pp. 202001, (2019).
[4] U. Gaubatz, P. Rudecki, S. Schiemann, K. Bergmann, Population transfer between molecular vibrational levels by stimulated Raman scattering with partially overlapping laser fields. A new concept and experimental results, J. Chem. Phys., vol. 92, pp. 5363-5376, (1990).

Efficient strong-field THz generation from organic crystal BNA pumped by 1030 nm Yb-laser

<u>K. Brekhov</u>[1,2*], S. Kolar[3], E. Chiglintsev[2,3], A. Chernov[2,3]

1- MIREA - Russian Technological University, Vernadsky Avenue 78, Moscow, 119454, Russia
2- Russian Quantum Center, Skolkovo Innovation City, Moscow, 121205, Russia
3- Moscow Institute of Physics and Technology, Institutskiy Pereulok 9, Dolgoprudny, Moscow Oblast, 141701, Russia

* brekhov_ka@mail.ru

With successive development, terahertz (THz) radiation can be achieved in various materials, such as solid, gas, liquid, and plasma, pumped by ultrafast laser pulses. THz radiation is used both for THz spectroscopy and for studying the dynamics of various processes that arise in a medium under the influence of THz pulses.

To date, the common methods of THz generation are based on photoconductive antennas, spintronic emitters and nonlinear crystals. To study THz-induced dynamics in various materials, sources of high THz fields are needed. Currently, for this are used, for example, semiconductors such as gallium phosphide and zinc telluride and ferroelectric crystal such as lithium niobate. However, they have low conversion of optical to THz radiation. The greatest efficiency of such conversion is demonstrated by organic crystals such as OH1, DSTMS, DAST and BNA. Since compared to inorganic crystals, organic crystals have a much higher second-order nonlinear optical susceptibility, which benefits THz generation via optical rectification (OR).

However, to fulfill the phase matching condition for THz generation, most organic crystals need to be excited by infrared laser centered at 1300–1700 nm, provided by optical parametric amplifiers (OPA). This is unfortunate because present high energy near infrared pump lasers operate below 1.3 μm, such as Cr:forsterite (1.24 μm), Yb-lasers (1.05 μm) and Ti:Sap-lasers (0.8 μm) [1]. Infrared OPA sources have been employed to pump DSTMS and DAST crystals and Cr:forsterite lasers have been employed to pump OH1 crystal for strong-field THz generation. But such systems are normally high-cost and complex to operate. Ti:Sap lasers have also been used to pump BNA organic crystals for THz generation, but with relatively low energy conversion efficiency.

Therefore, an economical, miniaturized, high-power ytterbium Yb-doped laser has attracted the researcher's attention. It is typically sub-picosecond in pulse duration and up to several millijoules in pulse energy with a high level of technological maturity and has been commercially available in scientific research and industry. Nevertheless, there is still a lack of reports on strong-field THz generation based on Yb-laser. There are two reasons for this. One is that the picosecond pulse duration of the Yb-laser is too long for effective OR process; and the second is that the thermal properties were believed to be a limiting factor for high average power excitation.

Here we present BNA organic crystal as a candidate for efficient THz generation from near infrared laser systems. We report collinear strong-field THz generation from the BNA organic crystal on a sapphire substrate for heat dissipation, driven by an industrial-grade Yb-laser operating at 1030 nm. The laser pulse duration was compressed up to 20-100 fs by using Compulse – Hollow Fiber Pulse Compressor and chirped mirrors. The dependence of the emission spectrum on the pump pulse duration was estimated. The output THz energy reaches 0.45 μJ, with a conversion efficiency of 0.37%. The peak electric field was about 440 kV/cm. So, we demonstrate that a 1030 nm Yb-laser is used to pump BNA organic crystal for efficient THz generation in a simple collinear geometry, which provides a promising THz source based on an industrial-grade ultrafast laser.

[1] K. Wang, Z. Zheng, H. Li, et al, Efficient strong-field THz generation from DSTMS crystal pumped by 1030nm Yb-laser, Appl. Phys. Lett. 124, 121102 (2024).
[2] H. Zhao, Y. Tan, T. Wu, et al, Efficient broadband terahertz generation from organic crystal BNA using near infrared pump, Appl. Phys. Lett. 114, 241101 (2019).

Biomedical application of terahertz radiations in the coming years

O. Cherkasova[1,2]

1- Institute of Automation and Electrometry, Siberian Branch of the Russian Academy of Sciences,
1 Academician Koptyug Ave., 630090 Novosibirsk, Russia
2- National Research Centre "Kurchatov Institute", 123182 Moscow, Russia

o.p.cherkasova@gmail.com

More than a century has passed since the discovery of terahertz (THz) radiation and the first experience in biology and medicine [1]. However, biomedical application of THz radiation is still an actively developing field of knowledge. Terahertz spectroscopy has shown great potential in biomedical research due to its unique features, such as the non-invasive and label-free identification of biological samples and medical imaging [2]. The report will provide a review of the known data and our own studies on THz spectroscopy of blood for diabetes [3], thyroid [4] and liver cancer [5] diagnosis. We will discuss applications of machine learning techniques to THz spectroscopy data, which will help to advance the method into clinical practice [6-8]. We will demonstrate the unique capabilities of THz radiation in the diagnosis of benign and malignant neoplasms of different nosology and localization [2,9], diabetic foot [10] and in ophthalmology [11]. We also highlight the biological effects of THz radiation and establishment of safe doses [12]. Further development of biomedical application of THz radiation is impossible without creation convenient and cheaper THz devices, super-resolution THz optical systems, THz waveguide. In conclusion, the most promising directions of further biomedical application of THz radiation are formulated.

[1] R. Singh, J. C. Bose and the German scientific community: scientific and political context, Current Science, vol. 96 (3), 419-422 (2009).
[2] O.A. Smolyanskaya, N.V. Chernomyrdin, A.A. Konovko, et al, Terahertz biophotonics as a tool for studies of dielectric and spectral properties of biological tissues and liquids, Progress in Quantum Electronics, vol. 62, 1-77 (2018).
[3] O.P. Cherkasova, M.M. Nazarov, A.A. Angeluts, A.P. Shkurinov, Analysis of blood plasma at terahertz frequencies, Optics and Spectroscopy, vol. 120 (1), 50-57 (2016).
[4] M.R. Konnikova, O.P. Cherkasova, et al, Malignant and benign thyroid nodule differentiation through the analysis of blood plasma with terahertz spectroscopy, Biomedical Optics Express, vol. 12 (2), 1020-1035 (2021).
[5] M.M. Nazarov, O.P. Cherkasova, et al, A Complex Study of the Peculiarities of Blood Serum Absorption of Rats with Experimental Liver Cancer, Optics and Spectroscopy, vol. 126 (6), 721-729 (2019).
[6] D. Vrazhnov, A. Knyazkova, et al, Analysis of Mouse Blood Serum in the Dynamics of U87 Glioblastoma by Terahertz Spectroscopy and Machine Learning, Appl. Sci., vol. 12, 10533 (2022).
[7] D. Vrazhnov, D.A. Ovchinnikova, et al, Terahertz Time-Domain Spectroscopy of Blood Serum for Differentiation of Glioblastoma and Traumatic Brain Injury, Appl. Sci., vol. 14, 2872 (2024).
[8] O. Cherkasova, D. Vrazhnov, et al, Terahertz Time-Domain Spectroscopy of Glioma Patient Blood Plasma: Diagnosis and Treatment, Appl. Sci., vol. 13, 5434 (2023).
[9] N.V. Chernomyrdin, G.R. Musina, et al, Terahertz technology in intraoperative neurodiagnostics: A review, Opto-Electronic Advances, vol. 6, 220071 (2023).
[10] G.G. Hernandez-Cardoso, S.C. Rojas-Landeros, M. Alfaro-Gomez, et al, Terahertz imaging for early screening of diabetic foot syndrome: A proof of concept, Sci. Rep. vol. 7, 42124 (2017).
[11] I. Ozheredov, M. Prokopchuk, M. Mischenko, et al, In vivo THz sensing of eye cornea, Laser Phys. Lett., 15 (5), 055601 (2018).
[12] O.P. Cherkasova, D.S. Serdyukov, E.F. Nemova, et al, Cellular effects of terahertz waves, Journal of Biomedical Optics, 26 (9), 090902 (2021).

Super-resolution THz microscopy and endoscopy of biological tissues

N.V. Chernomyrdin[1*], V.A. Zhelnov[1], D.R. Il'enkova[1], D.D. Rybnikov[1], A.A. Gavdush[1], A.S. Kucheryavenko[2], G.M. Katyba[2], V.N. Kurlov[2], I.E. Spektor[1], K.I. Zaytsev[1]

1- Prokhorov General Physics Institute of the Russian Academy of Sciences, Moscow, Russia
2- Institute of Solid State Physics of the Russian Academy of Sciences, Chernogolovka, Russia

* chernik-a@yandex.ru

Terahertz (THz) technologies are finding numerous applications in biophotonics and medical diagnosis [1-3]. However, some problems are still inherent to THz optical systems, among them: low spatial resolution [4] and lack of efficient endoscopes [5]. In our work we develop methods of super-resolution THz microscopy based on solid immersion (SI) effect. This approach allows to overcome Abbe diffraction limit by focusing electromagnetic beam at a small distance behind SI lens made of high-index material [4]. SI optical system can reach resolution up to 0.15λ (where λ is a free-space wavelength) using high-resistivity silicon SI lens [6,7], and even up to 0.06λ using rutile SI lens [8]. Developed THz SI microscope was applied for studying dielectric media and different types of healthy and pathological biological tissues *ex vivo* [6,7,9]. THz SI microscope coupled with linear polarizer and analyzer was applied to study optical anisotropy of rat brain tissues *ex vivo* [10]. In our works we also introduce THz waveguides and endoscopes based on sapphire shaped crystals, which provide low dispersion and low radiation loss [5,11]. Sapphire waveguides based on photonic crystal or antiresonant mechanisms of radiation transfer were manufactured using edge-defined film-fed growth (EFG) technique without any polishing or drilling [12]. We have developed THz endoscope based on antiresonant hollow-core sapphire waveguide coupled with a sapphire SI lens and experimentally demonstrated 0.2λ focal spot diameter of this endoscope [13]. We have also proposed an approach for THz refractometry of hard to access objects based on a hollow-core antiresonant waveguide, formed by a polytetrafloroethylene (PTFE)-coated sapphire tube with the outer end closed by a monolithic sapphire window [14].

[1] O.A. Smolyanskaya, et al, Terahertz biophotonics as a tool for studies of dielectric and spectral properties of biological tissues and liquids, Progress in Quantum Electronics, Vol. 62, P. 1–77 (2018).
[2] K.I. Zaytsev, et al, The progress and perspectives of terahertz technology for diagnosis of neoplasms: a review, Journal of Optics, Vol. 22, P. 013001 (2020).
[3] N.V. Chernomyrdin, et al, Terahertz technology in intraoperative neurodiagnostics: A review, Opto-Electronic Advances, Vol. 6, № 4. P. 220071 (2023).
[4] N.V. Chernomyrdin, et al, Terahertz solid immersion microscopy: Recent achievements and challenges, Applied Physics Letters, Vol. 120, № 11, P. 110501 (2022).
[5] G.M. Katyba, et al, Sapphire waveguides and fibers for terahertz applications, Progress in Crystal Growth and Characterization of Materials, Vol. 67, № 3, P. 100523 (2021).
[6] N.V. Chernomyrdin, et al, Reflection-mode continuous-wave 0.15λ-resolution terahertz solid immersion microscopy of soft biological tissues, Applied Physics Letters, Vol. 113, № 11, P. 111102 (2018).
[7] N.V. Chernomyrdin, et al, Quantitative super-resolution solid immersion microscopy via refractive index profile reconstruction, Optica, Vol. 8, № 11, P. 1471–1480 (2021).
[8] V.A. Zhelnov, et al, Hemispherical Rutile Solid Immersion Lens for Terahertz Microscopy with Superior 0.06–0.11λ Resolution, Advanced Optical Materials, Vol. 12, № 1, P. 2300927 (2024).
[9] A.S. Kucheryavenko, et al, Terahertz dielectric spectroscopy and solid immersion microscopy of ex vivo glioma model 101.8: brain tissue heterogeneity, Biomedical Optics Express, Vol. 12, № 8, P. 5272–5289 (2021).
[10] N.V. Chernomyrdin, et al, Quantitative polarization-sensitive super-resolution solid immersion microscopy reveals biological tissues' birefringence in the terahertz range, Scientific Reports, Vol. 13, № 1, P. 16596 (2023).
[11] K.I. Zaytsev, et al, Terahertz photonic crystal waveguides based on sapphire shaped crystals, IEEE Transactions on Terahertz Science and Technology, Vol. 6, № 4, P. 576–582 (2016).
[12] G.M. Katyba, et al, Sapphire shaped crystals for waveguiding, sensing and exposure applications, Progress in Crystal Growth and Characterization of Materials, Vol. 64, № 4, P. 133–151 (2018).
[13] A.S. Kucheryavenko, et al, Super-resolution THz endoscope based on a hollow-core sapphire waveguide and a solid immersion lens, Optics Express, Vol. 31, № 8, P. 13366 (2023).
[14] G.M. Katyba, et al, Terahertz refractometry of hard-to-access objects using the sapphire endoscope suitable for harsh environments, Applied Physics Letters, (Accepted in 2024).

Organic kainate single crystals as a broadband THz source for spectroscopy

E.O. Chiglintsev[1,2*], K.A. Brekhov[2,3], A.I. Chernov[1,2], P. Ginzburg[4]

1- Center for Photonics and 2D Materials, Moscow Institute of Physics and Technology (MIPT), Dolgoprudny, Russia
2- Russian Quantum Center, Skolkovo, Moscow region, Russia
3- Department of Nanoelectronics, MIREA - Russian Technological University, Moscow, Russia
4- Department of Physical Electronics, Tel Aviv University, Ramat Aviv, Tel Aviv69978, Israel

* chiglintsev.eo@phystech.edu

Organic crystals have recently attracted attention of researchers for their ability of efficient nonlinear frequency generation. This work focuses on investigation of organic kainate single crystals [1] for time-domain terahertz (TD-THz) spectroscopy. We have obtained a broadband THz signal from kainate crystals, with a bandwidth of approximately up to 8 THz. To pump the crystal, we used an Yb laser with the wavelength of 1030 nm in a THz time-domain spectrometer setup. The generated THz spectrum of the kainate crystal was compared to that of another well-known organic crystal, BNA [2] (Fig.1). These results could be applied to explore optical properties of materials in the THz range.
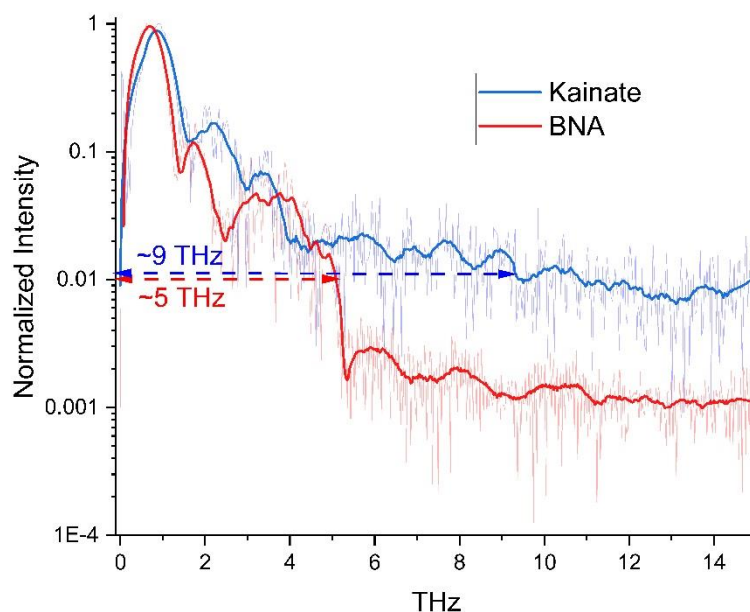
Fig.1. THz spectra of kainate and BNA organic crystals.

[1] H. Barhum, C. McDonnell, T. Alon, R. Hammad, M. Attrash, T. Ellenbogen, P. Ginzburg, Organic Kainate Single Crystals for Second-Harmonic and Broadband THz Generation, ACS Applied Materials & Interfaces 2023 15 (6), 8590-8600 (2023).
[2] M. Jazbinsek, U. Puc, A. Abina, A. Zidansek, Organic Crystals for THz Photonics., Appl. Sci. 2019, 9, 882 (2019).

Towards closing "terahertz gap" of quantum cascade lasers

A.A. Dubinov[1*], D.V. Ushakov[2], A.A. Afonenko[2], R.A. Khabibullin[3]

1- Institute for Physics of Microstructures RAS, GSP-105, 603950, Nizhny Novgorod, Russia
2- Belarusian State University, 4 Nezavisimosti Av., 220030, Minsk, Belarus
3- V.G. Mokerov Institute of Ultra-High Frequency Semiconductor Electronics RAS, 7/5 Nagornyy Pr., 117105 Moscow, Russia

* sanya@ipmras.ru

Over the two decades of their existence, quantum cascade lasers in the terahertz frequency range (THz QCLs) have come a long way from cryogenic devices with relatively low output powers to powerful THz sources with thermoelectric cooling based on Peltier elements [1]. However, there is a frequency range of the "terahertz gap" (6–10.5 THz), where QCLs do not work due to strong phonon absorption in the arsenide-based heterostructures (AlInGaAs) from which they are made.

Heterostructures with GaInP/AlGaInP quantum wells (QWs) are a promising active medium for solving the problem of creating QCLs with an operating frequency range of 6–7 THz, due to their higher optical phonon energies compared to arsenides. For the first time, the temperature dependences of gain and absorption at frequencies of 6.3–6.9 THz were calculated for a QCL based on GaInP/AlGaInP with 2 QWs in a cascade and a double metal waveguide. It has been shown that the maximum operating temperature of such a QCL can reach 108 K [2].

In addition, we have shown that the capabilities of GaAs/AlGaAs QW heterostructures are wider than previously thought. The possibility of creating such a GaAs/AlGaAs QCL design (with suppression of non-radiative recombination) with a double metal waveguide, which provides lasing with a frequency greater than 6 THz at temperatures above 77 K, was investigated. For this purpose, a band QCL design with a lasing frequency of 5.7–6.3 THz and active region based on 4 GaAs/$Al_{0.14}Ga_{0.86}As$ QWs [3].

Also we propose to use HgCdTe as an alternative material for THz QCLs thanks to a lower phonon energy than in arsenide-based semiconductors. HgCdTe-based QCLs operating with a target frequency of 8.3 THz have been theoretically investigated using the balance equation method. We have analyzed the temperature dependence of the peak gain and predicted the maximum operating temperatures of 170 K and 225 K for three- and two-well designs, respectively [4,5].

The results of these studies open the way to the creation of QCLs for operation in the GaAs phonon absorption band, which is inaccessible to existing arsenide-based QCLs.

[1] A. Khalatpour, A.K. Paulsen, C. Deimert, Z.R. Wasilewski, Q. Hu, High-power portable terahertz laser systems, Nat. Photonics, 15, 16-20 (2021).

[2] D.V. Ushakov, A.A. Afonenko, R.A. Khabibullin, M.A. Fadeev, A.A. Dubinov, Phosphides-based terahertz quantum-cascade laser. Phys. Stat. Solidi RRL, 18, 2300392 (2024).

[3] D.V. Ushakov, A.A. Afonenko, An.A. Afonenko, R.A. Khabibullin, M.A. Fadeev, V.I. Gavrilenko, A.A. Dubinov, Feasibility of GaAs/AlGaAs quantum cascade laser operating above 6 THz. J. Appl. Phys., 135, 133108 (2024).

[4] D. Ushakov, A. Afonenko, R. Khabibullin, D. Ponomarev, V. Aleshkin, S. Morozov, A. Dubinov, HgCdTe-based quantum cascade lasers operating in the GaAs phonon Reststrahlen band predicted by the balance equation method. Opt. Exp., 28, 25371-25382 (2020).

[5] A.A. Dubinov, D.V. Ushakov, A.A. Afonenko, R.A. Khabibullin, M.A. Fadeev, S.V. Morozov, Thin active region HgCdTe-based quantum cascade laser with quasi-relativistic dispersion law. Opt. Lett., 47, 5048-5051 (2022).

Second harmonic generation due to the spatial structure of radiation beam

M.V. Durnev[*], **A.A. Gunyaga, S.A. Tarasenko**

Ioffe Institute, 194021, St. Petersburg, Polytechnicheskaya 26

* durnev@mail.ioffe.ru

Nonlinear transport and optical effects in two-dimensional (2D) electronic systems are at the focus of modern research in the condensed-matter physics. Among them, the second harmonic generation (SHG) is of particular interest, both fundamentally and in terms of applications. This effect emerges in structures with broken space inversion symmetry and, therefore, has been established as a sensitive tool to probe structural inhomogeneity, crystalline symmetry, the staking and twist of 2D crystal flakes, etc. [1].

The main SHG mechanisms, which are studied at the moment, are related to the absence of inversion center in 2D crystals, photon wave vector at oblique incidence of radiation or the sample geometry, for example, the presence of an edge [2,3]. In our work, we show that the second harmonic generation is also possible in an isotropic 2D medium, provided that the radiation itself is spatially inhomogeneous. From the symmetry point of view, this effect is analogous to the effect of generation of a direct electric current by an inhomogeneous field of structured radiation [4].

We have studied the SHG induced by the spatial structure of incident radiation in a 2D electron gas (2DEG). We have shown that structured radiation with intensity, polarization, or phase, which vary in the 2DEG plane, leads to the generation of local electric currents oscillating at double frequency. These currents, in turn, emit secondary waves at double frequency, see Fig. 1. We have developed a kinetic theory of this effect for the incident field of the terahertz spectral range with an arbitrary spatial profile and have derived a general analytical expression for the current density. As an example, we have considered the SHG by a beam of twisted photons carrying an orbital angular momentum. It is shown that the secondary radiation is also twisted and characterized by a double angular momentum.
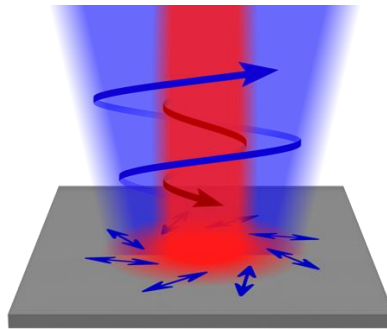
Fig. 1. Second harmonic generation due to the spatial structure of radiation beam. Nonuniform electromagnetic field of the twisted radiation beam generates electric currents oscillating at double frequency. These currents, in turn, emit twisted electromagnetic wave at double frequency.

[1] L. Zhou, et al, Nonlinear optical characterization of 2D materials, Nanomaterials, 10, 2263 (2020).
[2] M.M. Glazov and S.D. Ganichev, High frequency electric field induced nonlinear effects in graphene, Physics Reports, 535, 101 (2014).
[3] M.V. Durnev and S.A. Tarasenko, Second harmonic generation at the edge of a two-dimensional electron gas, Phys. Rev. B, 106, 125426 (2022).
[4] A.A. Gunyaga, M.V. Durnev, S.A. Tarasenko, Photocurrents induced by structured light, Phys. Rev. B, 108, 115402 (2023).

THz-IR spectroscopy of astrophysical ices: recent achievements and challenges

A.A. Gavdush[1*], F. Kruczkiewicz[2,3], B.M. Giuliano[2], B. Müller[2], G.A. Komandin[1], K.I. Zaytsev[1], A.V. Ivlev[2], P. Caselli[2]

1- Prokhorov General Physics Institute of the Russian Academy of Sciences, Russia, 119991 Moscow, Russia
2- Max-Planck-Institut für Extraterrestrische Physik, Gießenbachstraße 1, Garching 85748, Germany
3- Aix-Marseille Univ, CNRS, CNES, LAM, Marseille, France

* arsenii.a.gavdush@gmail.com

Solutions of relevant astrophysical problems [1-4] require the knowledge of the physical properties of interstellar and circumstellar ices. Among them are large-scale issues such as the evolution of molecular clouds and the genesis of stellar systems as well as local problems related to the formation of new molecular compounds in space and their prevalence. Most of the interstellar matter in the Universe is represented by ice of various molecular composition, including many organic compounds. Ices form mantles on the surface of dust particles; they can be found on the surface of satellites and asteroids, as a part of comets. Without the knowledge of the broadband dielectric properties of ices, it is impossible to determine molecular composition during the analyzes of astronomical observational data. Scattering in ices must also be taken into account when modeling radiative transfer in dense and cold University regions.

The observations of the interstellar medium are preferred to be taken in the far infrared (IR) and terahertz (THz) ranges in last decades. This approach allows to increase the number of possible objects under study due to their emission in the considered frequency ranges. Despite the importance of THz-IR dielectric properties of ices, there are still no data on the absolute values of the complex dielectric permittivity of astrophysical ice analogues in a wide spectral range, as well as their scattering properties. In the first works [5,6] in a series of publications we have focused on the developing of new approaches to reconstruct the complex dielectric response of astrophysical ice analogues in THz-IR ranges. We have shown the possibility of direct reconstruction of the ices complex dielectric permittivity in the broad spectral range, taking into account the existing amplitude and phase information for THz pulsed spectroscopy (TPS) measurements, merging of the TPS and Fourier-transform IR spectroscopy (FTIR) data and estimating phase information for FTIR data based on the Kramers-Kronig relations and TPS phase. Complex dielectric properties of several ices (CO, CO_2, N_2) are studied in the THz-IR range. The obtained results are parameterized using classical models of complex dielectric permittivity. First estimates for the scattering in ices are proposed which based on the assumptions of the porous structure of ices under study. The developed approach to study scattering in ices makes it possible to approximately obtain the properties of bulk ice, taking into account the use of the effective medium theory.

[1] A.C.A. Boogert, P.A. Gerakines, D.C.B. Whittet, Observations of the Icy Universe, Annual Review of Astronomy and Astrophysics, vol. 53(1), pp. 541–581 (2015).
[2] S.L. Widicus Weaver, Millimeterwave and Submillimeterwave Laboratory Spectroscopy in Support of Observational Astronomy, Annual Review of Astronomy and Astrophysics, vol. 57(1), pp. 79–112 (2019).
[3] D.V. Mifsud, et al, The Role of Terahertz and Far-IR Spectroscopy in Understanding the Formation and Evolution of Interstellar Prebiotic Molecules, Frontiers in Astronomy and Space Sciences, vol. 8 (2021).
[4] D.V. Mifsud, et al, Sulfur Ice Astrochemistry: A Review of Laboratory Studies, Space Science Reviews, vol. 217(1), pp. 14 (2021).
[5] B.M. Giuliano, et al, Broadband spectroscopy of astrophysical ice analogues: I. Direct measurement of the complex refractive index of CO ice using terahertz time-domain spectroscopy, Astronomy & Astrophysics, vol. 629, pp. A112 (2019).
[6] A.A. Gavdush, et al, Broadband spectroscopy of astrophysical ice analogues: II. Optical constants of CO and CO$_2$ ices in the terahertz and infrared ranges, Astronomy & Astrophysics, vol. 667, pp. A49 (2022).

Detectors of terahertz radiation based on 2D materials

K.V. Shein[1,2], E. Zharkov[3], A. Lyubchak[1,2], P. Bondareva[1,2], R. Izmaylov[2], E. Baeva[1,2], A. Kolbatova[1,2], G.N. Goltsman[1,2], I. Charaev[4], D.A. Bandurin[5], I. Gayduchenko[1,2*]

1- National Research University Higher School of Economics, Moscow, Russia, 101000
2- Moscow Pedagogical State University, Moscow, Russia, 119435
3- Programmable Functional Materials Lab, Brain and Consciousness Research Center, Moscow, Russia, 121205
4- University of Zürich, Zürich, Switzerland, 8057
5- Department of Materials Science and Engineering, National University of Singapore, Singapore, 117575

* igaiduchenko@hse.ru

Recently terahertz range (THz) of EM spectrum has been of great interest due to a wide spectrum of potential applications: medical diagnostics, non-destructive testing, security systems, and observational astronomy. Hot-electron bolometers (HEBs) play a crucial role in a variety of such applications. The operation principle of such thermal detectors is based on the sensitivity of their resistance to the radiation-induced change in electronic temperature. One of the parameters limiting the sensitivity of such detectors is electronic heat capacity. While conventional superconducting HEBs are typically produced from sputtered Nb or NbN films, their thickness and quality are limited by the magnetron sputtering system, making it exceedingly difficult to achieve thicknesses in the nanometer range to reduce the electronic heat capacity.

In this work, we study alternative platform for this research based on layered van der Waals materials (vdW) owing to the simplicity of achieving few-layer thicknesses and low electronic heat capacity. First, we report the fabrication of superconducting HEBs out of few-layer $NbSe_2$ microwires [1]. By improving the interface between $NbSe_2$ and metal leads connected to a broadband antenna, we overcome the impedance mismatch between this vdW superconductor and the radio frequency (RF) readout circuitry that allowed us to achieve large responsivity THz detection over the range from 0.13 to 2.5 THz with minimum noise equivalent power of 7 pW/Hz$^{0.5}$.

Next, we explore a novel approach to inventing graphene-based THz bolometers using noise thermometry. The heating of electrons caused by the absorption of THz radiation is detected by measuring noise spectral density in graphene devices. The potential advantages of this approach include high sensitivity, as well as the ability to easily multiplex detector signals, which allows the creation of detector arrays.

[1] K. Shein, et al, Fundamental Limits of Few-Layer $NbSe_2$ Microbolometers at Terahertz Frequencies, Nano Letters, 24 (7), 2282-2288, (2024).

Characteristics of THz surface waves propagating through metal and composite graphene nanofilms

V.V. Gerasimov[1,2,*], **A.K. Nikitin**[3], **V.D. Kukotenko**[1], **V.S. Vanda**[1,2],
A.G. Lemzyakov[1,4], **A.I. Ivanov**[5], **I.V. Antonova**[5], **I.A. Azarov**[2,5]

1- Budker Institute of Nuclear Physics of SB RAS, 11, Lavrentiev prospect, 630090, Novosibirsk, Russia
2- Department of Physics, Novosibirsk State University, 630090 Novosibirsk, Russia
3- Scientific and Technological Centre of Unique Instrum. of RAS, 15, Butlerova str., 117342, Moscow, Russia
4- Synchrotron Radiation Facility SKIF, 1, pr. Nikolsky, 630559 Kol'tsovo, Russia
5- Rzhanov Institute of Semiconductor Physics SB RAS, 13 Lavrentiev Aven., Novosibirsk 630090, Russia

* v.v.gerasimov@inp.nsk.su

With the general trend towards miniaturization and integration of devices, THz range technologies occupy a unique position for combining electronic and photonic components within a single integrated circuit [1]. In recent years, promising results have been demonstrated in this field [2], and with the advancement of wireless communication technologies, the THz range has become a key one in solving the spectrum shortage problem and meeting the increasing demands for data volume and transmission speed in 6G systems and beyond [3]. THz technologies promise significant improvements in the energy efficiency of data transmission compared to the existing 5G systems [4]. Of particular interest in this context is the research on plasmonic materials, which enable creation of compact antennas with high element density due to the subwavelength localization of surface plasmons [5].

Surface plasmon polaritons (SPPs), or simply "surface plasmons", are a complex of coupled oscillations of a surface electromagnetic wave and a wave of charges propagating along the interface between a conductor and a dielectric [6]. The field of the surface electromagnetic wave exponentially decays on both sides of the interface, and its penetration depth into the dielectric (most often air) can be of the order of or even less than the wavelength of the bulk radiation to generate SPPs, which allows one to overcome the diffraction limit.

Metals, semiconductors, graphene, and other materials can be used as a conductor for propagation of SPPs. The choice of a particular material for plasmonics is determined by its efficiency in the generation of SPPs, the distance of SPP propagation along the conductor, availability and ease of fabrication, and the possibility of control of its optical properties with external influences (temperature and electric or magnetic fields).

The talk will review results, including recent ones, on the characteristics of SPPs propagating over metal-dielectric and composite graphene surfaces using THz radiation from the Novosibirsk free electron laser in the range 0.8-6 THz. The results include an analysis of the influence of roughness, conductivity, and manufacturing technology of conductive materials on energy losses and field localization of SPPs at the conductor surface.

[1] K. Sengupta, T. Nagatsuma, D.M. Mittleman, Terahertz integrated electronic and hybrid electronic–photonic systems, Nat Electron, vol. 1, no. 12, pp. 622–635 (2018).
[2] J. Xie, et al, A Review on Terahertz Technologies Accelerated by Silicon Photonics, Nanomaterials, vol. 11, no. 7, p. 1646 (2021).
[3] I.F. Akyildiz, C. Han, Z. Hu, S. Nie, J.M. Jornet, Terahertz Band Communication: An Old Problem Revisited and Research Directions for the Next Decade, IEEE Trans. Commun., vol. 70, no. 6, pp. 4250–4285 (2022).
[4] H. Sarieddeen, N. Saeed, T.Y. Al-Naffouri, M.-S. Alouini, Next Generation Terahertz Communications: A Rendezvous of Sensing, Imaging, and Localization, IEEE Commun. Mag., vol. 58, no. 5, pp. 69–75 (2020).
[5] V.J. Sorger, R.F. Oulton, R.-M. Ma, X. Zhang, Toward integrated plasmonic circuits, MRS Bull., vol. 37, no. 8, pp. 728–738 (2012).
[6] S.A. Maier, Plasmonics: Fundamentals and Applications. New York, NY: Springer US (2007).

Gyrotrons: towards to the design of powerful THz radiation source

G.G. Denisov[1], E.M. Tai[1,2], A.N. Kuftin[1], Y.K. Kalynov[1], S.V. Samsonov[1], A.V. Savilov[1], E.A. Soluyanova[1,2], A.P. Fokin[1,2], M.Yu. Glyavin[1*]

1- Institute of Applied Physics RAS, 46 Ul'yanov str., Nizhny Novgorod, Russia
2- GYCOM Ltd., 46 Ul'yanov str., Nizhny Novgorod, Russia

* glyavin@ipfran.ru

Gyrodevices, in particular gyrotrons, currently are the most popular sources of powerful radiation in the sub-THz and THz frequency band [1,2]. The main area of gyrotron applicating associated with electron cyclotron resonance heating (ECH) and current drive in controlled thermonuclear fusion (NF) facilities. For the ITER project, GYCOM/IAP RAS implemented a CW (pulse duration of about 1000 sec) gyrotron with a MW power level at a frequency of 170 GHz [2,3]. Currently, in connection with an increase of ECH power from 24 MW (24 tubes) to 48 MW and, in the future, up to 80 MW, the possibility of 1.2 - 1.5 MW gyrotrons is being discussed. The solution connected to utilization of higher operating modes and using an external signal for frequency locking and suppression of parasitic oscillations [4]. For the next generation of NF installations this purpose, a powerful gyrotron with an operating frequency of 230 GHz has been developed [5]. The mastering of the terahertz frequency range by gyro-devices continues, and the main attention is paid not even to achieving record values of power and efficiency, but to controlling of the spectral characteristics [6] and searching for possibilities for smooth frequency tuning, which is due to the prospects of spectroscopy applications. Through the use of original methods of electronic and electrodynamic selection, stable single-mode generation at cyclotron harmonics was achieved at frequencies up to 1.2 THz [7-9]. Work is underway to create HTSC magnetic systems, which makes it possible to expect operating frequencies of gyrodevices up to 2 THz. The possibility of frequency multiplication has been demonstrated [10], which makes it possible to obtain tens of Watts in continuous mode at frequencies up to 1.5 THz. Using an original electrodynamic system based on quasi-optical elements, tuning of the generation frequency in a band of about one octave was demonstrated [11].

[1] G.S. Nusinovich, M.K.A. Thumm, M.I. Petelin, The Gyrotron at 50: Historical Overview, J Infrared Milli Terahertz Waves, 35, 325–381, (2014).

[2] M.K.A. Thumm, G.G. Denisov, K. Sakamoto, M.Q. Tran, High-power gyrotrons for electron cyclotron heating and current drive, Nuclear Fusion, 59, 7, 073001.

[3] A.G. Litvak, G.G. Denisov, M.Y. Glyavin, Russian Gyrotrons: Achievements and Trends, IEEE Journal of Microwaves, 1, 1, 260-268, (2021).

[4] A.N. Kuftin, G.G. Denisov, A.V. Chirkov, et al, First Demonstration of Frequency-Locked Operation of a 170 GHz/1 MW Gyrotron, IEEE Electron Device Letters, 44, 9, 1563-1566, (2023).

[5] M.Y. Glyavin, G.G. Denisov, E.M. Tai, A.G. Litvak, Russian gyrotrons: overview and challenge, 24th International Vacuum Electronics Conference (IVEC), Chengdu, China, (2023).

[6] G.G. Denisov, M.Y. Glyavin, A.E. Fedotov, et al, Theoretical and Experimental Investigations of Terahertz-Range Gyrotrons with Frequency and Spectrum Control, J Infrared Milli Terahertz Waves, 41, 1131–1143, (2020).

[7] I.V. Bandurkin, A.P. Fokin, M.Y. Glyavin, et al, Demonstration of a Selective Oversized Cavity in a Terahertz Second-Harmonic Gyrotron, IEEE Electron Device Letters, 41, 9, 1412-1415, (2020).

[8] I. Bandurkin, A. Fedotov, M. Glyavin, et al, Development of Third-Harmonic 1.2-THz Gyrotron with Intentionally Increased Velocity Spread of Electrons, IEEE Transactions on Electron Devices, 67, 10, 4432-4436, (2020).

[9] Y.K. Kalynov, I.V. Bandurkin, I.V. Osharin, A.V. Savilov, Third-Harmonic 1 THz Large-Orbit Gyrotron with an Improved Quasi-Regular Cavity, IEEE Electron Device Letters, 44, 10, 1740-1743, (2023).

[10] G.G. Denisov, I.V. Zotova, A.M. Malkin, et al, Boosted excitation of an ultra-high cyclotron harmonic based on frequency multiplication by a weakly relativistic beam of gyrating electrons, Phys. Rev. E 106, L023203, (2022).

[11] S.V. Samsonov, G.G. Denisov, A.A. Bogdashov, et al, Quasi-Optical Gyro-BWO With Zigzag Transmission Line As One-Octave Bandwith Sub-THz Source, 24th International Vacuum Electronics Conference (IVEC), Chengdu, China, 2023.

On the possibility of measuring the number of THz photons using a superconducting HEB bolometer

T. Novikova[1], K. Kuznetsov[1], I. Korolev[1], P. Prudkovskii[1], <u>G. Kitaeva</u>[1*]

1- Lomonosov Moscow State University, Leninskie Gory 1-2, Moscow 119991 Russia

* gkitaeva@physics.msu.ru

We study statistical distributions of output signals of a superconducting HEB detector [1] exposed to weak photon pulses of 1 THz frequency. The pulses with variable photon numbers were generated under strongly non-degenerate parametric down-conversion (PDC) in Mg: LiNbO$_3$ crystal cooled down to 4.8 K [2]. The experiments were carried out in two different PDC pumping modes, with the laser pulse durations of 28 ps and 10 ns.

It is shown that statistical distributions of signals obtained under irradiation by nanosecond pulses contain information about the mean number of discrete photon-counting events [3]. The nanosecond-mode histograms were successfully modeled as sums of discrete contributions with Gaussian statistics and taking into account Poisson statistics for the numbers of these events. Dependence of the approximation parameters on the PDC pump power totally corresponds to theoretical predictions concerning the numbers of incident THz photons.

At the same time, switching to the picosecond irradiation mode totally changes the main features of the statistical distributions of signals from the same HEB detector. The discrete structure disappears when the irradiation time intervals become less than the detector temporal resolution ~50 ps. The average output signals remain still proportional to the number of incident photons. But the histogram shapes and the signal dispersions do not change when the number of incident photons increases starting from the zero (dark noise) level.

Various scenarios of processes occurring when a superconducting HEB detector is irradiated by several THz photons are discussed, as well as the parameters of photon pulses capable of detecting individual photons.

[1] S. Seliverstov, S. Maslennikov, S. Ryabchun, M. Finkel, T. M. Klapwijk, N. Kaurova, Yu. Vachtomin, K. Smirnov, B. Voronov, G. Goltsman, Fast and sensitive terahertz direct detector based on superconducting antenna-coupled hot electron bolometer, IEEE Trans. Appl. Supercond., vol. 25, No. 2300304 (2015).

[2] A. Leontyev, K. Kuznetsov, P. Prudkovskii, D. Safronenkov, G. Kitaeva, Direct measurement of the correlation function of optical–terahertz biphotons, JETP Letters, vol.114, pp. 565-571 (2021).

[3] P. Prudkovskii, A. Leontyev, K. Kuznetsov, G. Kitaeva, Towards measuring terahertz photon statistics by a superconducting bolometer Sensors, vol. 21, p. 4964 (2021).

Eclipse z-scan for sensitivity increasing of cubic nonlinearity measurements in THz frequency range

S.A. Kozlov[1*], A.O. Ismagilov[1], A.O. Nabilkova[1], D.V. Gushchin[1], M.S. Guselnikov[1], M.V. Melnik[1], A.N. Tsypkin[1]

1- ITMO University, Saint Petersburg, Russia

* kozlov@mail.ifmo.ru

The development of radiation sources has enabled the observation of nonlinear optical effects when working with different matter. The study of nonlinear optical properties of matter is of interest due to the potential applications. The emergence of powerful radiation sources in the terahertz radiation range has made it possible to study nonlinear properties in this range as well.

This work is novelty usage the eclipse z-scan method to measure the optical nonlinearity in the THz range. The eclipse z-scan method employed in this study represents a modification of the traditional z-scan method, which is used to analyse the third-order optical nonlinearity of a variety of materials, including liquids and crystals [1]. This method enhances the sensitivity of the system by an order of magnitude by blocking the central region of the beam and observing only its outer edges using a disk aperture. Despite the advantages of this method, our group is one of the first to use it to measure the nonlinear refractive index in the terahertz (THz) range. The terahertz radiation source, TERA-AX (Avesta Pr.), was used. The generation of terahertz radiation in this system is based on the optical rectification of femtosecond pulses in a lithium niobate crystal. The output pulse energy of the THz radiation was 400 nJ with a pulse duration of 1 ps and a centre wavelength of 0.6 mm (0.5 THz). As previously stated, this radiation source exhibits a wide, asymmetric spectrum, and its characteristics have been examined and illustrated in Fig. 1(a) [2].

The spatial dimension of the radiation at the generator output was 17.5 mm. In order to enhance the intensity of the terahertz beam, a short-focus parabolic mirror with a focal length of 12.7 mm and a large numerical aperture was used. The peak intensity of the radiation in the terahertz beam caustic was equal to 0.5×10^8 W/cm^2 [3]. Subsequently, the radiation is directed towards a disk that attenuates 80% of the radiation and focuses it on a detection system in the form of a bolometer (Gentec-EO). In this study, a negative uniaxial congruent lithium niobate (cLN) crystal cut along the plane (001) with a thickness of L = 0.52 mm was used as a measurement sample. The refractive index (n_0) of this crystal has been determined to be 6.5 within the frequency range of 0.25–1.25 THz. The THz eclipse z-scan curve of this sample is illustrated in Fig. 1(b) [4].
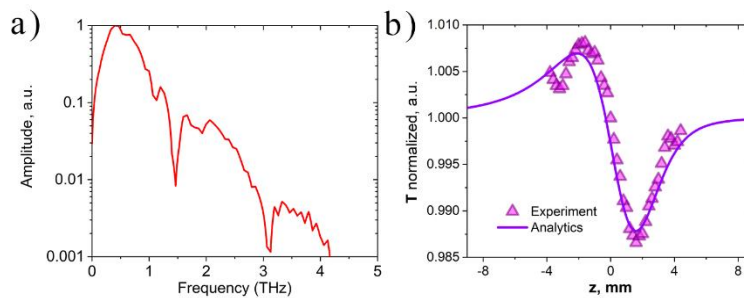

Fig. 1. a) Spectrum of THz radiation source, b) THz eclipse z-scan curve of cLN.

The demonstrated increased sensitivity of the eclipse z-scan allows us to conclude that it is possible to evaluate the properties of materials exhibiting lower nonlinear refractive indices, thereby expanding the applicability of the method to characterize a variety of nonlinear optical materials. This work was supported by the Ministry of Science and Education of the Russian Federation (Passport No. 2019-0903).

[1] T. Xia, et al, Eclipsing Z-scan measurement of $\lambda/10^4$ wave-front distortion, Optics letters, 19.5, pp. 317-319, (1994).

[2] I. Artser, et al, Radiation shift from triple to quadruple frequency caused by the interaction of terahertz pulses with a nonlinear Kerr medium, Scientific Reports, 12.1, p. 9019, (2022).

[3] A. Tcypkin, et al, Giant third-order nonlinear response of liquids at terahertz frequencies, Phys. Rev. Appl., 15.5, p. 054009, (2021).

[4] A. Nabilkova, et al, Sensitivity enhancement of cubic nonlinearity measurement in THz frequency range, IEEE Transactions on Terahertz Science and Technology, ACCEPTED, (2024).

Photo- and electroluminescence in mid-infrared range from HgCdTe based waveguide structures

S. Morozov[1*], V. Rumyantsev[1], A. Okomelkov[1], V. Utochkin[1], M. Fadeev[1], K. Mazhukina[1], A. Razova[1], A. Yantser[1], N. Mikhailov[2], S. Dvoretskii[2], V. Varavin[2], S. Kraev[1], E. Arkhipova[1], V. Gavrilenko[1]

1- Institute of Microstructure Physics RAS, Nizhny Novgorod, 603087, Russia
2- Institute of Semiconductor Physics RAS, Novosibirsk, 630090, Russia

* more@ipmras.ru

Currently, the development of semiconductor emitters in the mid-infrared range (IR) is one of the priority tasks in applied physics. Heterostructures with HgCdTe/CdHgTe quantum wells (QWs) offer a number of unique properties for interband lasers in the mid-IR and THz ranges. In particular, "threshold" Auger recombination can be significantly reduced for a given energy of interband transitions. Stimulated emission under optical pumping of HgCdTe heterostructures (MCT) at wavelengths from 2.5 to 31 μm was reported in [1]. However, current pumping is preferred for a semiconductor emitter, while it is difficult to obtain *p*-type MCT materials. Group I elements diffuse very easily outside the doping region during growth and Group V elements require additional annealing for dopants to be incorporated in Te sites rather than that of Cd or Hg. This work investigates an alternative method of current pumping: impact ionization in a strong electric field. Nonequilibrium degenerate distribution of charge carriers is expected to provide amplification via interband transitions without forming a *p-n* junction.

Structure under study were grown by molecular beam epitaxy on semi-insulating GaAs (013) substrates with ZnTe and CdTe buffers. The active region contained a number of QW or a bulk HgCdTe with a cadmium content of ~21% (Table 1). To carry out current pumping, two rectangular multilayer Ti/Mo/Au contacts with corresponding thicknesses of 20/30/100 nm were deposited onto the surface of the sample. The gap between the lateral stripe contacts was either 200 or 500 μm. Copper or silver wire was soldered to the contacts through indium solder.
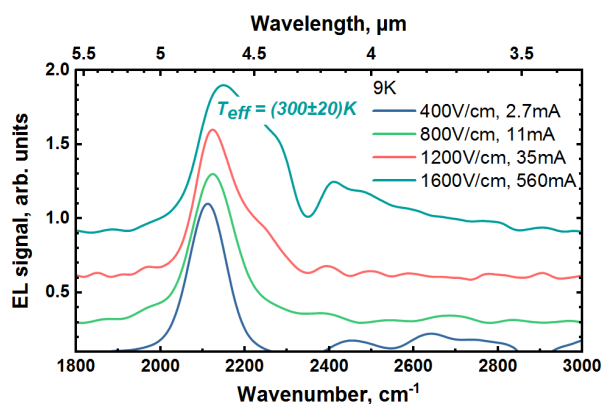
Fig. 1. Electroluminescence spectra of sample Q14 at different electric fields.

Table 1. Parameters and characteristics of structures.

x_{Cd} is the fraction of Cd in the active layer, d is the thickness of the QW, N – number of QWs, D_{clad} is the thickness of the upper cladding waveguide layer, E_{br} is the electric field strength of the breakdown, E_{dm} is the electric field at which irreversible degradation of the structure occurs, W is the energy in the current pulse during electric E_{dm} field.

#	x_{Cd}	d×N, nm	D_{clad}, nm	E_{br}, V/cm	E_{dm}, kV/cm	W, μJ
B1	0.21	5000	100	300	1	3000
Q14	0.33	95	500	1200	2	50
Q15	0.02	3.2×5	750	1200	1.5	220
Q21	0.06	2.8×15	300	6000	10	120

All four samples provided both photo- and electroluminescence accompanied by a superlinear current-voltage characteristic. However, only spontaneous emission was observed. Comparison with theoretical estimations [2] indicate that lasing requires higher electric field, which entails contact area degradation. The ways to refine the contact for stable operation at high electric fields are discussed.

[1] S.V. Morozov, et al, ACS Photonics, Vol. 8, No. 12, 3526–3535, (2021).
[2] A.A. Dubinov, Journal of Luminescence 263, 120066, (2023).

Stimulated emission in HgCdTe-based quantum wells: toward continuous wave lasing in THz range

S.V. Morozov

Institute for Physics of Microstructures of RAS, Nizhny Novgorod, Russia, 603950

more@ipmras.ru

Hg(Cd)Te/CdHgTe heterostructures with quantum wells (QW) are an attractive a material for mid infrared (IR) lasers. Due to importance of HgCdTe-based heterostructures for the industry of IR detectors their quality is reaching the quality of A3B5 heterostructures. Hg(Cd)Te/CdHgTe QWs also provide a unique opportunity to change the bandgap from 0 to over 1200 meV, while maintaining the ability to tailor the energy spectrum of the carriers by changing the content of solid solution of the barriers and the QW. In the long-wavelength part of mid Hg(Cd)Te/CdHgTe QWs offer the quasi-relativistic dispersion law of the carriers which suppresses Auger recombination, enabling stimulated emission (SE) up to 31 μm, and laser generation up to 24 μm in the temperature range from 10 to 80 K [1,2]. The wavelength of emission, which is demonstrated in our experiments, is six times larger than the previous results for HgCdTe lasers [3,4]. The record wavelength of 31 μm (inaccessible for existing cascade lasers) was achieved by a peculiar design of the structure utilizing the reflection of the waveguide mode from the substrate near the Reststrahlen band of GaAs. Quasi-relativistic dispersion law of the carriers in HgTe/CdHgTe QWs is useful at even longer wavelengths, in terahertz range, where we have recently managed to experimentally demonstrate "Landau emission" (optical transitions between non-equidistant Landau levels formed when quasi-relativistic electron system is placed in magnetic field) between 1 and 3 THz with the frequency adjustable by magnetic field and carrier concentration [5]. These results open up an avenue for a new type of terahertz Landau lasers controlled by magnetic field and gate voltage.

In this work, by carefully optimizing the waveguides and mitigating carrier heating, we achieve stimulated emission at 14–24 μm in HgCdTe QWs under optical pumping in quasi-continuous wave regime (pulse duration 20–500 μs). The intensity is as low as 1.5–2 W/cm^2 [6]. The impact of AR happening right after the excitation on the carrier temperature is investigated both theoretically (using the balance equations and calculated AR rates) and experimentally (via PL spectrum analysis). When such 'hot' AR is eliminated due to long-wavelength pumping carrier lifetimes are shown to be only slightly limited by Shockley-Read-Hall recombination. Its contribution is also directly investigated via time resolved measurements of the photoconductivity decay and PL spectroscopy of trap states in the bandgap. Finally, we estimate that implementing microdisc cavities would allow continuous-wave operation of HgCdTe lasers in the very long-wavelength infrared range (14–30 μm) and beyond when pumped by last generation quantum cascade lasers.

Considering the short-wavelength pat of the IR spectrum, we focus our attention to the atmospheric transparency window of 3–5 μm. In this range the competition between different types of lasers is very stacked because of its importance for chemical analysis. In this range the advantage of Hg(Cd)Te/CdHgTe QWs is that in addition to the suppression of threshold Auger process, we are able to mitigate QW-specific non-threshold processes associated with non-radiative transitions into barriers. Our results show that by optimizing the parameters of the QE and barriers and increasing the band offset in the valence band it is possible to reach the maximum temperature of SE up to 270 K and optically pumped laser action utilizing whispering gallery modes up to 230 K in the wavelength range of 3–4 μm [7].

[1] S.V. Morozov, et al, ACS Photonics, Vol. 8, No. 12, 3526–3535 (2021).
[2] V.V. Rumyantsev, et al, Appl. Phys. Lett., Vol. 121, No. 18, 182103 (2022).
[3] J.M. Arias, et al, Semicond. Sci. Technol., Vol. 8, S255–S260 (1993).
[4] E. Hadji, et al, Appl. Phys. Lett., Vol. 67, 2591 (1995).
[5] S. Gebert, et al, Nat. Photon., Vol. 17, 244–249 (2023).
[6] V.V. Rumyantsev, et al, Appl. Phys. Lett. 124, 161111 (2024).
[7] A.A. Razova, et al, Appl. Phys. Lett. 123, 161105 (2023).

Terahertz photonics of nonlinear crystals

N. Nikolaev

Institute of Automation and Electrometry SB RAS, Novosibirsk, Russia

nazar@iae.nsk.su

One of the current issues that needs to be resolved in order to create powerful compact THz sources appropriate for a variety of real-world applications is the search for nonlinear optical crystals (NOCs) that can efficiently convert the frequencies of intense lasers into terahertz radiation. Here we provide an overview of NOCs, divided into four hypothetical classes: dielectric, ferroelectric, semiconductor, and molecular. Single-stage conversions are commonly employed in NOCs and can be described by the formalism of optical rectification of ultrashort laser pulses or by difference frequency generation. However, their efficiency is proportional to the square of the product of the frequency and the effective nonlinear coefficient $\eta \sim (\omega \cdot d_{\text{eff}})^2$ [1], and therefore tends to small values when converting frequencies of the visible and near-IR ranges into the THz region, which is from 2 to 3 orders of magnitude lower in frequency.

The solution may be a cascaded (multistage) conversion. It is based on the generation of infrared radiation in the NOC's local transparency windows, which are close to strong optical phonons, and the subsequent downconversion of that radiation into the THz range. In this instance, the phonon contribution may lead to a considerable increase in the quadratic susceptibility (d_{eff}), which will produce a more effective frequency conversion than a single-stage procedure. Efficient narrow-band radiation generation near or between phonon frequencies has been reported in BBO at a frequency close to 10.6 THz [2], in KTP at 5.6 THz [3] and in GUHP crystal at 1.5 THz [4]. The development of the proposed approach requires the next step, which is a thorough study of the optical properties of NOCs in the phonon region, and finding the conditions for further frequency downconversion. In conclusion, we discuss the prospects of the proposed approach and the nonlinear crystal optics of the terahertz range in general.

[1] Y.R. Shen, The Principles of Nonlinear Optics (Wiley), (2002).
[2] D.A. Valverde-Chávez, D.G. Cooke, Multi-cycle terahertz emission from β-barium borate, Journal of Infrared, Millimeter, and Terahertz Waves, vol. 38, pp. 96-103, (2017).
[3] M.H. Wu, W.C. Tsai, Y.C. Chiu, Y.C. Huang, Generation of ~100 kW narrow-line far-infrared radiation from a KTP off-axis THz parametric oscillator, Optica, vol. 6(6), pp. 723-730, (2019).
[4] A. Sinko, P. Solyankin, A. Kargovsky, V. Manomenova, E. Rudneva, N. Kozlova, A. Shkurinov, A monoclinic semiorganic molecular crystal GUHP for terahertz photonics and optoelectronics, Scientific reports, vol. 11(1), p. 23433, (2021).

Generation of terahertz multimode vortex surface plasmon polariton

N. Osintseva[1*], V. Gerasimov[1,2], V. Pavelyev[3,4], Yu. Choporova[1], K. Tukmakov[3], B. Knyazev**

1- Budker Institute of Nuclear Physics SB RAS, 11 Ac. Lavrentieva Ave., Novosibirsk 630090, Russia
2- Novosibirsk State University, 1 Pirogova St., Novosibirsk 630090, Russia
3- Samara National Research University, 34 Moskovskoye Shosse, Samara 443086, Russia
4- Image Processing Systems Institute, NRC "Kurchatov Institute", 151 Molodogvardeyskaya St.,
Samara 443001, Russia

* natalyaosintseva@gmail.com ** v.gerasimov@nsu.ru

In today's world, the terahertz range is attracting increasing interest from researchers, especially with the active shift towards the sub-terahertz frequency range (120–350 GHz) in wireless networks, such as 6G data transmission. The use of terahertz vortex Bessel beams (VBBs) with multiplexing capabilities can greatly enhance data capacity. VBBs also have applications in wired data transmission.

The waveguide approach for data transmission in miniature integrated optical devices in the terahertz region is currently under development. However, there is an alternative solution that involves excitation of surface waves (surface plasmon polaritons, SPPs) on the surface of an axisymmetric conductor by perfect vortex Bessel beams through an end-fire coupling technique. Previous research [1] has demonstrated the generation of vortex SPPs on a cylindrical line, their transmission along the line, and diffraction into a vortex free-wave with the same topological charge.

In this study, we present experimental results on the generation of multimode vortex surface plasmon polaritons on a metallic cylinder coated with a 1-µm thick zinc sulfide layer, using a 130 µm radiation of the Novosibirsk Free Electron Laser. Two VBBs with the topological charges 3 and 9 were generated in the arms of a tilted Mach-Zehnder interferometer (60° to the optical axis of the input beam) using spiral phase binary axicons. A combined beam at the interferometer output formed in the back focal plane of a lens a two-mode perfect vortex beam, which was used for the excitation of vortex plasmons with the same topological charges. Recording the output radiation with the optical system shown in Fig. 1, we investigated the possibility to identify multiplex signals passing the system and use it in data transmission applications. The experiments were carried out at the Novosibirsk free electron laser, which is a part of the Shared Research Facility "Siberian Synchrotron and Terahertz Radiation Center".
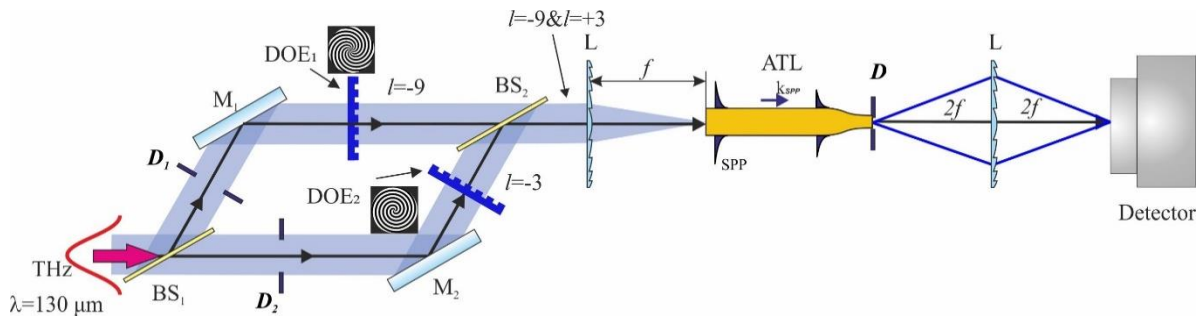
Fig. 1. Experimental scheme for vortex multimode SPP generation in Mach-Zehnder interferometer: BS – beamsplitter, D – iris diaphragm, M – flat mirror, DOE – spiral binary axicons, L – kinoform lens with *f*=80 mm with λ=130 µm, ATL – axisymmetric transmission line, Detector – microbolometer array.

[1] V. Gerasimov, et al, Vortex surface plasmon polaritons on a cylindrical waveguide: Generation, propagation, and diffraction, Journal of Optics, vol. 23, pp. 10LT01, (2021).

Terahertz imaging and spectroscopy of molecular condensed matter

A.A. Plekhanov[1]*, A.E. Akmalov[1], G.E. Kotkovskii[1], Yu.A. Kuzishchin[1], I.L. Martynov[1], E.V. Osipov[1], A.A. Chistyakov[1]

1- National Research Nuclear University "MEPhI", 31, Kashirskoe Highway, Moscow, 115409 Russia

* AAPlekhanov@mephi.ru

The work provides an overview of the current state of research and development in the terahertz (THz) photonics. In particular, various THz sources and detectors are considered. Current results in the field of studying of molecular condensed matter using THz imaging and spectroscopy are discussed. In this case, special attention is paid to the study of nitro compounds, as well as the features of their detection and identification in the THz range.

The prospects for using terahertz video cameras for visualization (radiovision) with spectral resolution are considered. Their application is demonstrated with broadband and narrowband THz sources. The possibility of using microbolometer terahertz video cameras with photoconductive antennas to study the spatial distribution of radiation intensity for THz beams in separate frequency bands has been demonstrated. This is also shown for studying the scattering process during the interaction of THz radiation with molecular condensed matter using the example of powders and films of organic substances [1]. At the same time, the results of real-time detection of trace amounts of nitro compounds in the form of single microcrystals are presented (both in the optical scheme for transmission and in the optical scheme for reflection) [2].

The current state of the art in the development of THz inspection devices is discussed. The prospects for using modern THz sources based on impact ionization avalanche transit time (IMPATT) diodes as part of compact (portable) terahertz imaging systems with spectral resolution are considered.

[1] A.A. Plekhanov, A.E. Akmalov, G.E. Kotkovskii, K.I. Kozlovskii, Yu.A. Kuzishchin, I.L. Martynov, E.M. Maksimov, E.V. Osipov, A.A. Chistyakov, Study of terahertz reflection spectra of optically thin RDX samples by terahertz imaging with spectral resolution, Optical Engineering, vol. 62(3), pp. 034109-034109, (2023).

[2] A.A. Plekhanov, A.E. Akmalov, G.E. Kotkovskii, Yu.A. Kuzishchin, I.L. Martynov, E.V. Osipov, A.A. Chistyakov, THz visualization of particles of organic substances, XV International Conference on Physics and Technology of Nanoheterostructure Microwave Electronics, May 22–23, 2024, Conference Proceedings, pp. 87-88 (2024).

Broadband THz emitters: from single chips to large-area devices

D. Lavrukhin[1], A. Yachmenev[1], N. Zenchenko[1], R. Khabibullin[1]
Yu. Goncharov[2], I. Spektor[2], K. Zaytsev[2], <u>D. Ponomarev</u>[1*]

1- Institute of Ultra High Frequency Semiconductor Electronics of the Russian Academy of Sciences, Moscow, Russia
2- Prokhorov General Physics Institute of the Russian Academy of Sciences, Moscow, Russia

* ponomarev_dmitr@mail.ru

Modern THz spectroscopic and imaging setups require high-power THz generation, and, hence, an improvement of the THz-beam power becomes more and more challenging. The THz power enhancement in a broadband photoconductive antenna (PCA)-emitter is limited by a few factors [1,2]. On the one hand, both bias voltage and laser pump power should be increased. On the other hand, an increased electric field might cause an electrical breakdown of a semiconductor, while an intense laser pump might cause screening effects, thermal breakdown of a semiconductor, also affecting the carrier mobility, and thus decreasing the THz bandwidth. The very promising approach for the THz power boost is to resort from a single small-area emitter to a large-area PCA-emitter (LAPE), with the electrodes in form of a strip line array [3,4]. In this case, an increase in pump power is possible without any overheating or breakdown of the emitter. Unfortunately, LAPE usually requires a layer of masking metal to prevent destructive interference of THz waves from adjacent strips or the specific couplers of laser pump, such as an array of plano-convex microlenses, cylindrical micro-lenses, or diffractive optical elements, that severely complicates fabrication of LAPEs and reduces their cost efficiency.

We demonstrate both numerically and experimentally how the LAPE performance can be improved using an array of cylindrical near-field lenses made of sapphire fibers [5]. A judicious design of such high-refractive-index sapphire lenses allows strong confinement of a laser pump near the semiconductor surface, yielding an 8.5-fold THz power boost and + 9.3 dB in single-to-noise ratio [6].

[1] D. Ponomarev, A. Yachmenev, D. Lavrukhin, et al, Optical-to-terahertz switches: state of the art and new opportunities for multispectral imaging, Phys. Usp., 67, 3–21 (2024).
[2] A. Yachmenev, R. Khabibullin, D. Ponomarev, Recent advances in THz detectors based on semiconductor structures with quantum confinement: a review, J. Phys. D: Appl. Phys., 55(19), 193001 (2022).
[3] A. Dreyhaupt, S. Winnerl, T. Dekorsy, et al, High-intensity terahertz radiation from a microstructured large-area photoconductor, Appl. Phys. Lett., 86, 121114 (2005).
[4] M. Mittendorff, M. Xu, R. Dietz, et al, Large area photoconductive terahertz emitter for 1.55 μm excitation based on an InGaAs heterostructure, Nanotech.24, 214007 (2013).
[5] D. Ponomarev, D. Lavrukhin, N. Zenchenko, et al, Boosting THz photoconductive antenna-emitter using optical light confinement behind a high refractive sapphire fiber-lens, Opt. Lett., 47(7), 1899 (2022).
[6] N. Zenchenko, D. Lavrukhin, R. Galiev, et al, Enhanced terahertz emission in a large-area photoconductive antenna through an array of tightly-packed sapphire fibers, Appl. Phys. Lett., 124(12), 121107 (2024).

Frequency-angular properties of terahertz emission during single-color filamentation

L. Seleznev[1,2*], G. Rizaev[1,2], D. Pushkarev[1,2]

1- P.N.Lebedev Physical institute of RAS, Russia 119991 Moscow Leninskii pr. 53
2- Faculty of Physics, Lomonosov Moscow State University, Leninskie Gory, Moscow 119991, Russia

* *seleznev@lebedev.ru*

Propagation of a femtosecond laser pulse with overcritical power through transparent medium results in self-focusing and plasma channels formation (process of filamentation [1]). Plasma formed during filamentation of laser pulses is one of terahertz radiation sources [2]. The simplest scheme for terahertz generation is single-color filamentation in air. However the mechanisms and properties of the terahertz emission from single-color filament have been poorly studied due to relatively low efficiency.

In our experiments we used laser pulses with 740 nm wavelength, 90 fs duration and energy up to 5 mJ. To create filament plasma focusing elements with different numerical apertures were used. We detected terahertz emission with a bolometer sensitive in the range of 0.1–12 THz. To distinguish various frequencies we set narrowband terahertz filters in front of the bolometer input window. By moving the bolometer around the plasma channel, we measured two-dimensional angular distributions of terahertz radiation.
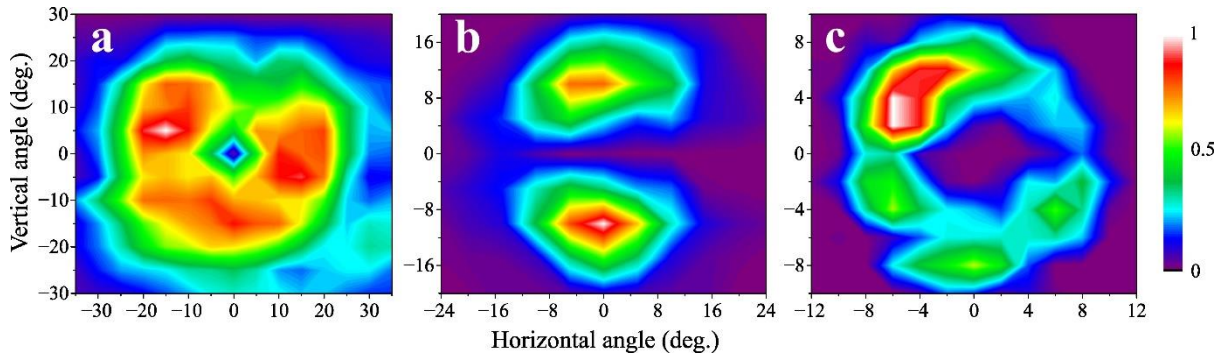
Fig. 1. Normalized two-dimensional angular distributions of terahertz radiation at frequency of 0.3 THz (a), 1 THz (b) and 10 THz (c). The pulse energy is 3 mJ, the numerical aperture is 0.02.

For example, Fig. 1 shows normalized two-dimensional angular distributions of terahertz radiation at different frequencies. At a frequency of 0.3 THz (Fig. 1a), terahertz radiation propagates into a cone with a minimum on the axis. At a frequency of 1 THz (Fig. 1b), the pattern structure takes the form of two maxima located on the axis perpendicular to laser polarization. At higher frequencies the cone-shaped structure is restored again. Figure 1c shows the distribution at 10 THz.

It should be noted that the propagation angles of terahertz radiation at different frequencies differ significantly and for low frequencies can reach more than 30 degrees. In addition to information about the propagation structure, energy characteristics of terahertz radiation can be obtained from two-dimensional patterns by integrating signals over the distribution. This approach allows to take into account terahertz radiation propagating at wide angles. Thus, we investigated terahertz patterns, spectral and energy characteristics of terahertz emission under various laser parameters such as wavelength, pulse duration, numerical aperture and energy.

[1] A. Couairon, A. Myzyrowicz, Phys. Reports 441, 47 (2007).
[2] W. Sun, X. Wang, Y. Zhang, Opto-Electronic Science 1, 220003 (2022).

The NovoFEL facility – source of high-power, narrow-band, tunable in wide range terahertz radiation

__O.A. Shevchenko__[*], N.A. Vinokurov, V.S. Arbuzov, K.N. Chernov, O.I. Deichuly, E.N. Dementyev,
B.A. Dovzhenko, Ya.V. Getmanov, Ya.I. Gorbachev, D.A. Kolomeec, A.A. Kondakov,
V.R. Kozak, E.V. Kozyrev, S.A. Krutikhin, V.V. Kubarev, G.N. Kulipanov, E.A. Kuper,
I.V. Kuptsov, G.Ya. Kurkin, L.E. Medvedev, S.V. Motygin, V.K. Ovchar, V.N. Osipov,
V.M. Petrov, A.M. Pilan, V.M. Popik, V.V. Repkov, T.V. Salikova, M.A. Scheglov, I.K. Sedlyarov,
S.S. Serednyakov, A.N. Skrinsky, S.V. Tararyshkin, A.G. Tribendis, V.G. Tcheskidov,
M.G. Vlasenko, V.N. Volkov

Budker Institute of Nuclear Physics, 11, Acad. Lavrentieva Pr., Novosibirsk, 630090, Russia

* O.A.Shevchenko@inp.nsk.su

The Novosibirsk free electron laser (FEL) facility includes three FELs operating in terahertz, far- and mid-infrared spectral ranges. The FELs undulators are installed on different tracks of the multi-turn energy recovery linac. The first FEL of this facility has been operating for users of terahertz radiation since 2004. Its initial wavelength range had been 90 – 240 μm but recently it was increased up to 400 μm. This FEL still remains the world's most powerful source of coherent narrow-band radiation in its wavelength range.

The second FEL was commissioned in 2009. The wavelength range of this FEL had been 35 – 80 μm until its old electromagnetic undulator was replaced by a new undulator with variable period in 2021. After this undulator replacement we obtained lasing in the wavelength range 15 – 120 μm and in a couple of years we increased this range up to 156 μm. Recently we also demonstrated high macropulse averaged radiation power (more than 800 W) at the wavelength of 70 μm.

The third FEL was commissioned in 2015 to cover the wavelength range of 5 – 20 μm. Its undulator comprises three separate sections. Such lattice suits very well to demonstrate the new off-mirror way of radiation outcoupling in FEL oscillator (so-called electron outcoupling) which we also plan to do in near future.

In this talk we present overview of the facility and discuss our recent achievements and future plans.

Periodically poled ferroelectric crystals and thin films for light frequency conversion

**<u>V. Shur</u>[1*], A. Akhmatkhanov[1], M. Chuvakova[1], B. Slautin[1],
B. Lisjikh[1], M. Kosobokov[1], A. Boyko[2,3]**

1- School of Natural Sciences and Mathematics, Ural Federal University, Ekaterinburg, Russia
2- Institute of Laser Physics SB RAS, 630090 Novosibirsk, Russia
3- Novosibirsk State University, Novosibirsk, Russia

* vladimir.shur@urfu.ru

We present the achievements and recent progress in fabrication of effective nonlinear frequency converters based on quasi-phase matching realized by creation of the stable periodic domain structure with nanoscale period reproducibility. Application of the domain engineering methods allowed to achieve the submicron domain periods in lithium niobate thin films. The all-optical domain switching in the crystal bulk by applications of near-IR femtosecond laser irradiation was used successfully for creation of the periodical domain structures and three-dimensional nonlinear photonic crystals [1-3].

The obtained achievements are based on complex study of the domain structure evolution with high spatial and temporal resolution in uniaxial ferroelectrics of lithium niobate, lithium tantalate (LT) and potassium titanyl phosphate (KTP) families. The realized methods of domain engineering are based on application of the electric field using: (1) periodical stripe electrodes [4], (2) biased tip of scanning probe microscope [5,6], (3) focused electron and ion beams [7] and via pulse heating by IR laser irradiation [1,3]. The created tailored domain structures allowed to realize the out-of-cavity second harmonics generation with record efficiency and highly effective optical parametric oscillation (OPO).

The periodical poling has been carried out in thin single-crystalline ion sliced submicron LN films on SiO_2 isolation layer (LNOI) by conductive tip of the scanning probe microscope. The stable domain structures with period less than 200 nm have been produced [5,6].

The creation of tunable mid-infrared pulsed optical parametric amplifier (OPA) based on periodically poled LN with fan-out domain structure pumped by 1053 nm laser has been demonstrated [8]. It was shown that the fan-out periodical domain structures allowed to obtain super-wide OPA tuning range from 2.5 to 4.5 µm in one element [9].

The creation of the three-dimensional nonlinear photonic crystals and periodical domain structures in the bulk was demonstrated in the plates of single-domain MgO doped LN as a result of irradiation by femtosecond laser emitting pulses at the 1030 nm wavelength [1,10].

[1] B. Lisjikh, M. Kosobokov, A. Turygin, A. Efimov, V. Shur, Creation of a periodic domain structure in MgOLN by femtosecond laser irradiation, Photonics, vol.10, p.1211 (2023).
[2] B.I. Lisjikh, M.S. Kosobokov, A.V. Efimov, D.K. Kuznetsov, V.Ya. Shur, Thermally assisted growth of bulk domains created by femtosecond laser in magnesium doped lithium niobate, Ferroelectrics, vol.604, pp.47-52 (2023).
[3] V.Ya. Shur, M.S. Kosobokov, A.V. Makaev, D.K. Kuznetsov, M.S. Nebogatikov, D.S. Chezganov, E.A. Mingaliev, Dimensionality increase of ferroelectric domain shape by pulse laser irradiation, Acta Materialia, vol.219, p.117270 (2021).
[4] V.Ya. Shur, A.R. Akhmatkhanov, and I.S. Baturin, Micro- and nano-domain engineering in lithium niobate, Appl. Phys. Rev., vol.2, p.040604 (2015).
[5] B.N. Slautin, A.P. Turygin, E.D. Greshnyakov, A.R. Akhmatkhanov, H. Zhu, V.Ya. Shur, Domain structure formation by local switching in the ion sliced lithium niobate thin films, Appl. Phys. Lett., vol.116, p.152904 (2020).
[6] B.N. Slautin, H. Zhu, V.Ya. Shur, Submicron periodical poling by local switching in the ion sliced lithium niobate thin films with dielectric layer, Ceramics International, vol.47, pp.32900-32904 (2021).
[7] D.S. Chezganov, E.O. Vlasov, E.A. Pashnina, M.A. Chuvakova, A.A. Esin, E.D. Greshnyakov, V.Ya. Shur, Domain structure formation by 6electron beam irradiation in lithium niobate crystals at elevated temperatures, Appl. Phys. Lett., vol.115, p.092903 (2019).
[8] E. Erushin, B. Nyushkov, A. Ivanenko, A. Akhmathanov, V. Shur, A. Boyko, N. Kostyukova, D. Kolker, Tunable injection-seeded fan-out-PPLN optical parametric oscillator for high-sensitivity gas detection, Laser Phys. Lett. vol.18, p.116201 (2021).
[9] O.L. Antipov, D.B. Kolker, A.A. Dobrynin, Yu.A. Getmanovskiy, V.V. Sharkov, M.A. Chuvakova, A.R. Akhmathanov, V.Ya. Shur, I.A. Shestakova, S.V. Larin, Mid-infrared optical parametric oscillation and second harmonic generation of repetitively-pulsed radiation of a fiber-laser pumped Tm^{3+}:YAP laser in a fan-out periodically poled $MgO:LiNbO_3$ crystal, Quantum Electronics, vol.52, pp.254-261 (2022).
[10] S. Kudryashov, A. Rupasov, M. Kosobokov, A. Akhmatkhanov, G. Krasin, P. Danilov, B. Lisjikh, A. Turygin, E. Greshnyakov, M. Kovalev, A. Efimov, V. Shur, Ferroelectric nanodomain engineering in bulk lithium niobate crystals in ultrashort-pulse laser nanopatterning regime, Nanomaterials, vol.12, p.4147 (2022).

Narrowband terahertz sources based on the molecular crystals and metasurface terahertz filters

A. Sinko[1,2,3*], **N. Kozlova**[1], **V. Manomenova**[1], **M. Konnikova**[1,2,3], **A. Shkurinov**[1,2,3]

1- NRC Kurchatov Institute, Moscow, Russia
2- Faculty of Physics, Lomonosov Moscow State University, Moscow, Russia
3- Laboratory of Laser Molecular Imaging and Machine Learning, Tomsk State University, Tomsk, Russia

* as.sinjko@physics.msu.ru

Previously in [1,2] we demonstrated the possibility of creating a coherent high-quality source of narrowband terahertz radiation on the basis of GUHP molecular crystal, for which NIR single ultrashort laser radiation pulses act as pumping. This phenomenon is set up by the second-order nonlinear optical processes, Raman and IR activity of phonon oscillations of the molecular crystal lattice.

Narrowband terahertz radiation generation was achieved for the first time in molecular crystals of phthalic acid salts ($C_6H_4COOH \cdot COOM$, M=Na,K,Rb) NaAP, KAP, RbAP and in a sucrose crystal ($C_{12}H_{22}O_{11}$). At cryogenic temperatures, the femtosecond laser pumped molecular crystals act as effective narrowband terahertz sources due to the good localization of molecular vibrations. The obtained terahertz radiation spectra for KAP crystal are presented in Fig. 1.
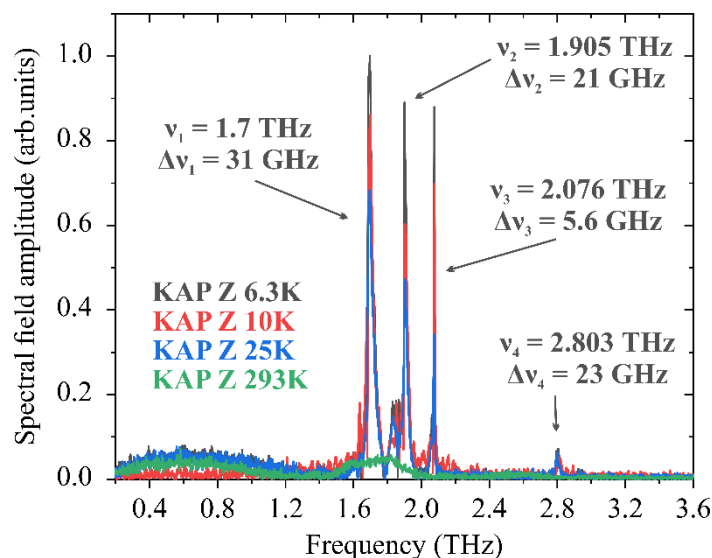
Fig. 1: Spectra of generated in KAP terahertz radiation.

Since the obtained series of narrowband sources have several generation lines in the range of 0.2-3 THz, the use of metasurfaces as terahertz radiation filters [3] was proposed to isolate individual narrow spectral emission lines. This approach is also promising due to the possibility of controlling the transmission of such filters by changing their parameters with external excitation [4].

[1] A. Sinko, et al, A monoclinic semiorganic molecular crystal GUHP for terahertz photonics and optoelectronics, Scientific reports 11.1 (2021): 23433.
[2] A.S. Sinko, et al, Polarization sensitive Raman scattering and Stimulated terahertz emission from GUHP molecular crystal, IEEE Transactions on Terahertz Science and Technology 13.5 (2023): 526-538.
[3] L. Wang, et al, A review of THz modulators with dynamic tunable metasurfaces, Nanomaterials 9.7 (2019): 965.
[4] M.R. Konnikova, et al, GeTe₂ phase change material for terahertz devices with reconfigurable functionalities using optical activation, ACS Applied Materials & Interfaces 15.7 (2023): 9638-9648.

Emission of energetic electrons from a nanotip under combined exposure to intense terahertz and femtosecond laser fields

S.B. Bodrov, A.A. Murzanev, A.V. Romashkin, <u>A.N. Stepanov</u>[*], A.E. Fedotov

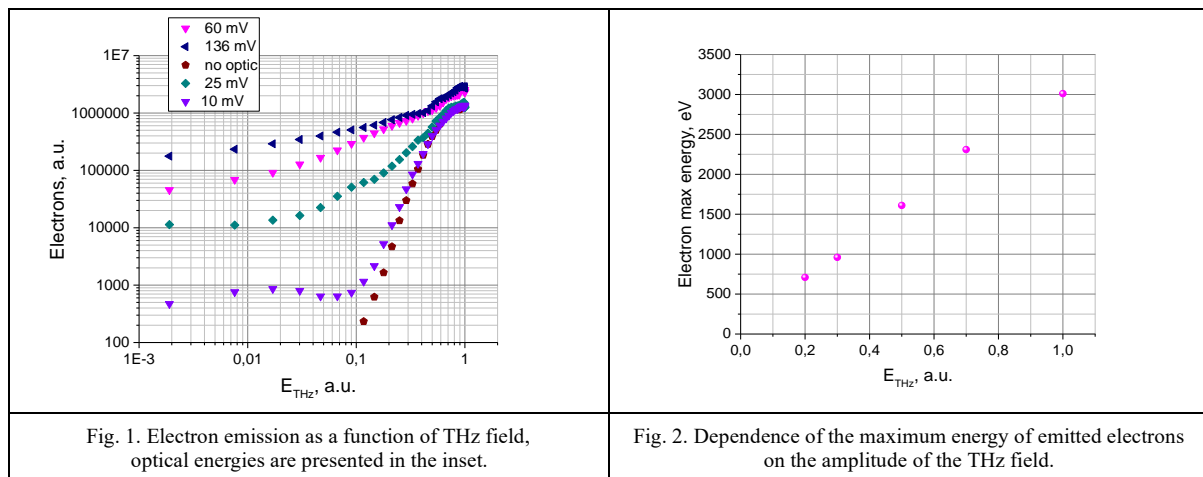*Institute of Applied Physics, Russian Academy of Sciences, Nizhny Novgorod 603950, Russia*

* step1an@ipfran.ru

The creation of short-pulse point sources of electrons with an energy of several keV is of interest for a wide range of problems: from the creation of bunches of seed electrons for free electron lasers to projection electron microscopes with high time resolution. In this work, to solve this problem, we used an approach based on irradiation of a submicron metal tip with a combination of femtosecond laser and picosecond terahertz radiation.

A polycrystalline tungsten needle with a radius of curvature of the tip r_{tip} = 170 nm was placed on a three-coordinate motorized stage in a vacuum chamber (p ≈ 5·10^{-5} Torr) and irradiated with focused femtosecond laser (τ = 100 fs, F = 10 Hz, intensity up to 3×10^{12} W/cm^2) and terahertz (τ_{THz} ~1 ps, E_{max} ≈ 300 kV/cm) pulses with field polarization directed along the needle axis. Electrons emitted from the needle were recorded using a microchannel plate.

Figure 1 presents experimentally obtained results on the efficiency of electron emission at different laser radiation intensities depending on terahertz fields. The results presented show that adding optical radiation to the THz field significantly increases the emission efficiency especially in low THz field region. Note that the maximum emitted charge of the electron bunch was several picocoulombs, similar to work [1]. By placing the grid in front of the MCP and applying an adjustable negative voltage to it, measurements were taken of the energy distribution function of electrons emitted from the needle. It was shown that the maximum electron energy increases linearly with increasing terahertz field (Fig. 2), reaching 3 keV at the maximum THz fields used.

Thus, the experimental studies performed indicate that a submicron metal needle irradiated with femtosecond optical and THz pulses can be a point source of short electron bunches with a charge of the pico-coulomb level and an electron energy of several kiloelectronvolts.

Fig. 1. Electron emission as a function of THz field, optical energies are presented in the inset.

Fig. 2. Dependence of the maximum energy of emitted electrons on the amplitude of the THz field.

[1] N.A. Abramovsky, S.B. Bodrov, A.M. Kiselev, A.A. Murzanev, A.V. Romashkin, A.N. Stepanov, *Generation of electron bunches of the picoculomb level from a metal needle under the influence of femtosecond radiation from a titanium-sapphire laser*, High Temperature, 58, 938–941, (2020).

Quasi-phase matching of elliptically polarized high-order harmonic generation by atomic systems in two-color laser fields

S. Stremoukhov[1,2]

1- Faculty of Physics, M.V. Lomonosov Moscow State University, Leninskie Gory, 1/2, 119991 Moscow, Russia
2- National Research Centre "Kurchatov Institute", Akademika Kurchatova sq. 1, 123182 Moscow, Russia

sustrem@gmail.com

High-order harmonic generation (HHG) in media exposed to intense laser field is one of the most actively studied non-linear optical phenomenon. To date, a significant number of methods have been developed to control the intensity, ellipticity and width of the spectrum of generated radiation. At the same time, the search for new ways to increase the efficiency of harmonic generation and control of their polarization properties continues [1]. The development of methods for generating intense harmonics with controlled polarization characteristics in a wide spectral range will make it possible not only to create a compact arbitrary polarized multispectral source of coherent radiation, but also to use the generated radiation as a seed to improve both the energy and coherent properties of radiation generated by free electron lasers [2], as well as create pulses of attosecond duration [3].

The development of methods for controlling the HHG characteristics is carried out both at the microscopic (atomic) [4] and at the macroscopic level of description of the problem [5]. At the same time, various methods of phase and quasi-phase matching during the propagation of laser radiation in a medium are considered [6]. Within the current study, a unified theoretical approach is used to describe the HHG phenomenon, which takes into account the dynamics of changes in the atomic discrete and continuous spectra levels populations of atoms distributed in the medium during their interaction with intense laser fields, the parameters of which depend on the position of atoms in the medium due to the effects of laser propagation radiation. The single atom response description of the laser fields action is realized by using a unique non-perturbative theoretical approach [7]. The response of an extended medium is simulated within the framework of the interference model [8]. Using the non-perturbative theory and interference model, a series of numerical studies of the effects associated with the generation of coherent radiation when exposed to intense laser radiation on media representing both a single gas jet (to study the effects of phase matching) and a set of gas jets separated by vacuum intervals (to study the features of quasi-phase matching) have been carried out. We recently presented a study of the influence of interaction parameters (medium parameters and laser radiation wavelength) on the HHG efficiency [9]. In the present studies, the emphasis was placed on studying the polarization characteristics of the generated harmonics when varying the interaction parameters. The main results of the studies are presented and discussed. In particular, we have shown that varying the initial time delay between pulses allows one to effectively control the amount of ellipticity of harmonics generated under quasi-phase matching conditions.

The conducted series of studies opens up broad prospects for using the HHG effect in creating compact multispectral sources of coherent arbitrarily polarized radiation.

[1] E. Appi, R. Weissenbilder, et al, Two phase-matching regimes in high-order harmonic generation, Opt. Express, 31, 31687-31697 (2023).
[2] G. Lambert, T. Hara, D. Garzella, et al, Injection of harmonics generated in gas in a free-electron laser providing intense and coherent extreme-ultraviolet light, Nat. Phys, 4, 296–300 (2008).
[3] P. Corkum and F. Krausz, Attosecond science, Nat. Phys, 3, 381 (2007).
[4] S. Yu. Stremoukhov, Non-Perturbative Theory of Atomic Systems Interaction with Intense Laser Fields, Bull. Rus. Acad. Sc.: Phys., 88, 38–43 (2024).
[5] R. Weissenbilder, S. Carlström, et al, How to optimize high-order harmonic generation in gases, Nat. Rev. Phys., 4, 713–722 (2022).
[6] L. Hareli, G. Shoulga, A. Bahabad, Phase matching and quasi-phase matching of high-order harmonic generation-a tutorial, J.Phys.B: At.Mol.Opt.Phys, 53, 233001 (2020).
[7] A.V. Andreev, S.Yu. Stremoukhov, O.A. Shoutova, Light-induced anisotropy of atomic response: prospects for emission spectrum control. Eur. Phys. J. D. 66.16 (2012).
[8] S.Yu. Stremoukhov and A.V. Andreev, Quantum-mechanical elaboration for the description of low- and high-order harmonics generated by extended gas media: prospects to the efficiency enhancement in spatially modulated media, Las. Phys. 28, 035403 (2018).
[9] S.Stremoukhov, Role of gas pressure in quasi-phase matching in high harmonics driven by two-color laser field, Atoms, 11, 103 (2023).

Gapped bilayer graphene for terahertz and infrared photodetection

**E. Titova[1,2*], M. Kashchenko[1,2], D. Mylnikov[1], V. Semkin[1],
I. Domaratskiy[1], D. Bandurin[3], D. Svintsov[1]**

1- Center for Photonics and 2D Materials, Moscow Institute of Physics and Technology, Dolgoprudny 141700, Russia
2- Programmable Functional Materials Lab, Center for Neurophysics and Neuromorphic Technologies, Moscow 127495, Russia
3- Department of Materials Science and Engineering, National University of Singapore, Singapore 117575, Singapore

* titova.elenet@gmail.com

Terahertz (THz) and infrared (IR) detectors are used in many areas of science and technology – from wireless communication systems and medical scanning to the study of astronomical objects. However, in this range of electromagnetic radiation there is a dip in the sensitivity of photodetectors compared to detectors in the neighboring optical and radio ranges. Graphene has a number of unique properties that make it possible to use this material for effective terahertz detection [1]. For example, graphene exhibits low heat capacity and high phonon energy, which leads to rapid heating of photoinduced electrons and slow cooling of them on the crystal lattice. Due to the effect of "hot electrons" in graphene, the photo-thermoelectric effect is large, which can be used for photodetection in structures with a lateral p-n junction [2]. The use of bilayer graphene makes it possible to increase the temperature sensitivity of the material due to the possibility of electrostatically inducing a band gap in bilayer graphene, potentially resulting in a stronger photo-thermoelectric response.

In this work, we investigated graphene photodetectors, which are transistor structures based on bilayer graphene with lateral p-n junctions. We have shown that inducing a bandgap in bilayer graphene improves the terahertz responsivity and noise equivalent power (NEP) of the detector several times (see Fig. 1). The maximum responsivity at cryogenic temperature in our detectors reached 50.5 kV/W for voltage and 22.8 A/W for current, while the NEP dropped to 36.4 fW/Hz$^{1/2}$ with band gap induction up to 25 meV [3]. The dominant rectification mechanism at cryogenic temperatures is photo-thermoelectric, against which there are features of an additional mechanism – presumably, rectification at tunnel junctions. We demonstrated the presence of tunnel transport in our structures based on photoresistivity analysis [4].
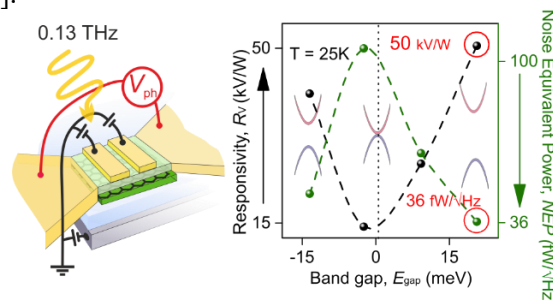

Figure 1. Schematic representation of the transistor structure based on bilayer graphene, as well as the dependence of THz responsivity and NEP on the band gap in the structure.

We also studied low-resistance edge states in the graphene channel, which manifest themselves in the saturation of the channel resistance as a function of the band gap in graphene. We have shown that using structures with a natural graphene edge, as opposed to a chemically etched edge, eliminates such edge states. We have shown that ON/OFF current ratios can exceed 10^5 in natural edge graphene transistors [5].

In addition, we studied similar graphene phototransistors at room temperature. We have shown that such transistors can serve as photodetectors in both the terahertz and infrared ranges.

[1] F. Bonaccorso, et al, Nature Photonics, Vol. 4, 2010.
[2] N.M. Gabor, et al, Science, Vol. 334, Issue 6056, 2011.
[3] E. Titova, et al, ACS Nano, 17, 9, 8223–8232, 2023.
[4] D. Mylnikov, et al, Nano Letters, 23, 1, 220–226, 2023.
[5] I.K. Domaratskiy, et al, Russian Microelectronics, Vol. 52, 2023.

THz high resolution spectroscopy for medical diagnostics of cancer diseases of urinary tract

V.L. Vaks[1,2*], **V.A. Atduev**[3,4], **A.V. Maslennikova**[2,4]

1- Institute for Physics of Microstructures of Russian Academy of Sciences, Nizhny Novgorod 603087, Russia
2- Lobachevsky State University, Nizhny Novgorod 603022, Russia
3- Privolzhsky District Medical Center of the Federal Medical and Biological Agency of Russia, Nizhny Novgorod 603001, Russia
4- Privolzhsky Research Medical University, Nizhny Novgorod 603005, Russia

* vax@ipmras.ru, elena@ipmras.ru

Nowadays the approach to diagnostics based on identifying and changing the metabolic human profile specified for disease as well as a therapy monitoring is a modern trend in medicine. Biological liquids (in particularly, urine) respond fast to changes in a person's organism at disease. Therefore they are used for clinical tests (the primary tests for making a diagnosis and therapy monitoring are general urine and blood tests). There are congenital and acquired diseases of the urinary system. Congenital diseases include pathologies of the structure and development of organs. Acquired diseases are the result of an inflammatory process or injury. Prostate cancer (PC) is one of the most common male diseases of the urinary system worldwide. The prostate specific antigen (PSA) is the most commonly used serum marker of prostate cancer. In addition to PSA tests in urine, other urine metabolites were studied to identify PC markers that allow detecting the disease at earlier stages.

In the metabolic approach biological liquids are the most promising objects for identifying biomarkers. The methods of spectroscopy operating in the frequency ranges from microwave to ultra-violet are used for biological and medical applications. The THz spectroscopy technique based on the effect of freely decaying polarization involves periodic induction and decay of macroscopic polarization in a sample of a gas mixture. The THz spectroscopy is the promising method for analysis of multicomponent gas mixtures of various origins. The aim of the work is application of nonstationary high-resolution THz spectroscopy for studying the characteristic set of metabolites of thermal decomposition products of urine of conditionally healthy volunteers and cancer patients to identify markers typical of PC.

The advantage of terahertz gas spectroscopy is high resolution because the absorption lines at working pressure are narrow and overlapped rarely. The line of rotational spectrum is fingerprint of specific substance because such absorption line parameters as central frequency and line strength are determined by molecular structure. Some substances of urine sample are volatile and appeared in gas mixture over the sample without heating. The heating of samples in liquid or solid states allows obtaining the gas state of sample. Some of large biological molecules as proteins, sugars, fats are decomposed at heating, but there are specific features in content of resulting gas mixture of products of thermal decomposition characterizing the patient state.

Differences in the composition and content of substances in urine samples of cancer patients and of conditionally healthy volunteers have been identified, which enables preliminary conclusions about substances that are promising for use as markers of prostate cancer in urine. The appearance of nitriles (acetonitrile, butyronitrile, pentannitrile, pentanedienenitrile, benzonitrile, aminopropionitrile) in the urine of prostate cancer patients can be caused by thermal decomposition of amino acids including ones in PCA. The presented approach is novel for urine analysis and is promising for developing a method for noninvasive study of the composition of biological liquids, which makes it possible to identify metabolite markers of various pathologies and diseases.

Microwave-range soliton combs formed based on nonlinear electron-wave interaction

N. Ginzburg, G. Denisov, S. Samsonov, A. Sergeev, V. Vilkov, L. Yurovskiy, <u>I. Zotova</u>[*]

A.V. Gaponov-Grekhov Institute of Applied Physics of the Russian Academy of Sciences, Russia

* zotova@ipfran.ru

Solitons are well-studied objects of optics and appear in many laser systems. Of particular interest is the possibility of periodic formation of so-called dissipative solitons [1,2], which is used, for example, to implement sources of ultrashort light pulses in mode-locked lasers with saturable absorbers [3] or to form ultra-wide frequency combs in Kerr-type microcavities pumped by coherent laser radiation [4,5]. Recently, it was theoretically shown that periodic trains of solitons (hereinafter referred to as soliton combs) can occur in microwave electronics, where they arise due to the nonlinearity of electron-wave interaction. In some cases, the mechanisms of formation of such soliton combs are similar to those known in laser physics. This is due to the fact that, depending on the interaction conditions, the electron beam can act as an active (inverted, emitting), passive (non-inverted, absorbing) or reactive nonlinear medium. At the same time, there are certain specifics associated with the movement of the electron beam, the dispersion of waveguide systems, etc.

The report will present the results of research aimed at the formation of microwave soliton combs. Two main mechanisms are considered. The first type is the modulation of a counterpropagating monochromatic wave and the emergence of solitons of self-induced transparency during cyclotron resonant interaction with magnetized initially rectilinear (passive) electron beams. Of fundamental importance here is the relativistic dependence of the gyrofrequency on the particle energy. The second type is dissipative solitons, similar to those produced in mode-locked lasers and Kerr microcavities. Passive mode locking is implemented in two-section microwave generators consisting of a coupled electron amplifier and a saturable absorber based on cyclotron resonant absorption. The possibility of observing Kerr-like dissipative solitons based on the interaction of monochromatic microwave radiation with a reactive electron beam in a high-Q resonator is also discussed.

Along with the results of theoretical analysis, the results of conducted and planned experiments are presented. We have currently implemented implementing a Ka-band generator of 100 kW/0.4 ns pulses based on a helical-waveguide gyro-TWT mode-locked by a cyclotron-resonance absorber driven by an electron beam [7]. Currently, the same absorber powered by a Ka-band gyro-BWO is planned to be used to observe solitons of self-induced transparency. The feasibility of this mechanism is confirmed on the basis of direct PIC (particle-in-cell) simulations.

[1] E.V. Vanin, A.I. Korytin, A.M. Sergeev, D. Anderson, M. Lisak, L. Vázquez, Dissipative optical solitons, Phys. Rev. A, vol. 49, 2806-2811 (1994).
[2] T.J. Kippenberg, A.L. Gaeta, M. Lipson, M.L. Gorodetsky, Dissipative Kerr solitons in optical microresonators, Science, vol. 361, 567-578 (2018).
[3] H.A. Haus, Mode-locking of lasers, IEEE J. Sel. Top. Quantum Electron., vol.6, 1173-1185 (2000).
[4] P. Del'Haye, A. Schliesser, O. Arcizet, T. Wilken, R. Holzwarth, T.J. Kippenberg, Optical frequency comb generation from a monolithic microresonator, Nature, vol.450, 1214-1217 (2007).
[5] S. Coen and M. Erkintalo, Universal scaling laws of Kerr frequency combs, Optics Letters, vol. 38, 1790-1792 (2013).

PHOTONICS IN QUANTUM TECHNOLOGIES

Wigner crystal state in two-dimensional semiconductor

A. Abramov[1,2*], E. Chiglintsev[2,3], A. Chernov[2,3], V. Kravtsov[1,2]

1- School of Physics and Engineering, ITMO University, Saint-Petersburg, Russia
2- Russian Quantum Center, Skolkovo, Moscow, Russia
3- Moscow Institute of Physics and Technology (National Research University), Dolgoprudny, Russia

* artem.abramov@metalab.ifmo.ru

Two-dimensional materials are of great interest as a platform for the development of new optoelectronic devices. This is achieved by making the optical and transport properties of two-dimensional materials easily tunable by external influences such as material deformation, application of an external electromagnetic field, or doping. Therefore, the study of strongly correlated electronic states is important for understanding the processes occurring in two-dimensional materials. Electrons break the symmetry of continuous translation and form a periodic lattice (Wigner crystal) when Coulomb repulsion begins to dominate over their kinetic energy [1]. However, the creation of the necessary conditions for the formation of such a state has so far remained a difficult task. The main method of research was the measurement of the conductivity of electrons in semiconductors at one Landau level under the action of a strong magnetic field. Another way to observe a Wigner crystal is to create a Moiré potential [2]. The use of transition metal dichalcogenide monolayers for Wigner crystal observation is possible due to a high electron effective mass and reduced dielectric screening, which allows the observation of charge order even at zero magnetic field [3].

In this work, we demonstrate the Wigner crystal by measuring the optical reflectance spectra of a doped WSe_2 monolayer at a temperature of 8 K. For this purpose, we assembled a structure consisting of a top and bottom graphene gate and a WSe_2 monolayer separated by layers of dielectric hexagonal boron nitride. Monolayers of two-dimensional materials were obtained by mechanical exfoliation and then the structure was assembled by polycarbonate transfer on sapphire substrate. Then, the gold contacts were brought to the structure using high-resolution electronic lithography. The obtained sample was investigated by reflectance spectroscopy in a closed-loop helium cryostat. Illumination by the lamp light and collection of the reflected signal were performed using a 50x objective mounted on three-axis piezotranslator. The doping of the WSe_2 monolayer was carried out by setting the voltage between the monolayer and one of the gates, while the other gate was grounded. The blue shift of the main exciton resonance X with energy of 1.72 eV and the appearance of trions with energies of 1.69-1.70 eV due to the increase in carrier density can be observed on the dependence of the reflection spectrum of the WSe_2 monolayer. However, when carefully examining the region with low charge densities, we also observe another high-energy resonance, which, due to the low power of the oscillator, is visible only on the energydifferentiated reflection map. We associate this feature with high-energy excitonic umklapp resonances, which indicates the appearance of a Wigner crystal at a low electron density value [4].

The results of our research work are important for studying strong electron correlated states in structures based on two-dimensional materials.

[1] E. Wigner, On the interaction of electrons in metals, Phys. Rev. 46, 1002–1011 (1934).
[2] T. Smoleński, et al, Signatures of Wigner crystal of electrons in a monolayer semiconductor, Nature, 595, 53-57 (2021).
[3] E.C. Regan, et al, Mott and generalized Wigner crystal states in WSe_2/WS_2 moiré superlattices, Nature, 579, 359-363 (2021).
[4] Y. Shimazaki, et al, Optical signatures of periodic charge distribution in a Mott-like correlated insulator state. Physical Review X. 11, 021027 (2021).

Photodetectors based on 2D superconducting NbSe₂ films integrated on silicon nitride waveguide

K.V. Shein[1,2], E. Zharkov[3], A. Lyubchak[1,2], G.N. Goltsman[1,2], I. Charaev[4], D.A. Bandurin[5], I. Gayduchenko[1,2*]

1- National Research University Higher School of Economics, Moscow, Russia, 101000
2- Moscow Pedagogical State University, Moscow, Russia, 119435
3- Programmable Functional Materials Lab, Brain and Consciousness Research Center, Moscow, Russia, 121205
4- University of Zürich, Zürich, Switzerland, 8057
5- Department of Materials Science and Engineering, National University of Singapore, Singapore, 117575

* igaiduchenko@hse.ru

Photonic integrated circuits (PICs) represent a promising platform for quantum technologies such as quantum computing and cryptography. One of the key components of such systems is a detector based on thin superconducting films. Despite the successful demonstration of superconducting detectors in planar geometry, their integration on waveguides in the form of thin superconducting films of the same quality remains technologically challenging. As an alternative approach, in this work we present the concept of an on-chip superconducting detector based on a two-dimensional mechanically exfoliated superconductor. The advantages of this approach are the ease of integration of the device on the waveguide, as well as the possibility of a single-layer detector thickness.

Niobium diselenide (NbSe₂) is a promising material for creating superconducting waveguide detectors due to its superconducting properties up to the monolayer limit. Moreover, NbSe₂ has already demonstrated sensitivity as a detector in the terahertz [1] and near-IR [2] ranges. In this work, we demonstrate an hBN/NbSe₂/hBN photodetector integrated on silicon waveguide. We first simulate the absorption of electromagnetic radiation by hBN/NbSe₂/hBN flakes on silicon waveguide to optimize the photodetector geometry. Based on the simulation results, it is proposed to integrate photodetector on silicon microring resonator to enhance the absorption of electromagnetic radiation. Next, we develop technological route for manufacturing the device, including the transfer of 2D superconductor on the waveguide, the formation of low-resistance contacts and the patterning of NbSe₂ films. Finally, we demonstrate the strong bolometric response of the fabricated device in the visible and near-infrared regions. The results provide the basis for prototyping fully integrated quantum photonic integrated circuits.

[1] Y. Meng, et al, Photonic van der Waals integration from 2D materials to 3D nanomembranes, Nat Rev Mater, 8, 498–517 (2023).
[2] K. Shein, et al, Fundamental Limits of Few-Layer NbSe₂ Microbolometers at Terahertz Frequencies, Nano Letters, 24 (7), 2282-2288 (2024).

Luminescence properties of single-photon sources in hexagonal boron nitride flakes

A. Gritsienko[1,2*], M. Pugachev[1,2], A. Vitukhnovsky[1,2], A. Kuntsevich[1]

1- P.N. Lebedev Physical Institute of the Russian Academy of Sciences, 53 Leninskiy Pr., 119991 Moscow, Russia
2- Moscow Institute of Physics and Technology, National Research University, 9 Institutskií Per., 141700 Dolgoprudnyí, Russia

* grits_alex@rambler.ru

The appearance of emitters in hexagonal boron nitride (hBN) and their use as single photon sources has recently been actively discussed in the literature [1]. A hallmark of these emitters is their stable ultrahigh brightness at room temperature as well as their high internal and external quantum yields [2,3]. It has been found that these emitters have different spectral compositions, brightnesses, and photostabilities [4]. To date, there has been no understanding of the atomic structures of most of the emitters observed in hBN.

We report on the fabrication and optical characterization of emitters in hBN flakes, with a sub-nanosecond decay time. We find that bright emitters meet most of the criteria for quantum applications, including high purity and a rate of >1 GHz at the zero-phonon line. These emitters exhibit unusual photodynamics, switching between dark and bright states and possibly deactivating completely. The dynamics suggest the presence of an excited state close to the conduction band, indicating that possible electron escape to defects may be the main mechanism for deactivation.

We also studied homostructures consisting of two separate layers of hBN, in which microbubbles form spontaneously. Heat treatment of the obtained homostructures in an oxygen-rich medium led to the formation of single-photon emitters directly at the locations where bubbles formed. These emitters had high luminescence intensities, which did not degrade during optical measurements. The spectral response varied from emitter to emitter, with individual emitters having luminescence maxima in the range of 550–750 nm. Our results demonstrate that the formation of these emitters is linked to the presence of carbon compounds and local stresses in boron nitride.

[1] J. Caldwell, I. Aharonovich, G. Cassabois, J. Edgar, B. Gil, D. Basov, Photonics with hexagonal boron nitride, Nature Reviews Materials, vol. 4, pp. 552-567, (2019).
[2] G. Grosso, H. Moon, B. Lienhard, S. Ali, D. Efetov, M. Furchi, P. Jarillo-Herrero, M. Ford, I. Aharonovich, D. Englund, Tunable and high-purity room temperature single-photon emission from atomic defects in hexagonal boron nitride, Nature Communications, vol. 8, p. 705, (2017).
[3] N. Nikolay, N. Mendelson, E. Özelci, B. Sontheimer, F. Böhm, G. Kewes, O. Benson, Direct measurement of quantum efficiency of single-photon emitters in hexagonal boron nitride. Optica, vol. 6, pp. 1084-1088, (2019).
[4] I. Aharonovich, J. Tetienne, M. Toth, Quantum emitters in hexagonal boron nitride, Nano Letters, vol. 22, pp. 9227-9235, (2022).

Towards quantum repeaters

R.A. Akhmedzhanov[1], L.A. Gushchin[1], <u>A.A. Kalachev</u>[2*], I.Z. Latypov[2], N.A. Nizov[1], V.A. Nizov[1], A.V. Shkalikov[2], D.A. Sobgaida[1], D.A. Turaykhanov[2], I.V. Zelensky[1]

1- A.V. Gaponov-Grekhov Institute of Applied Physics of the Russian Academy of Sciences, 46 Ul'yanov Street, Nizhny Novgorod, 603950, Russia
2- Kazan Scientific Center of Russian Academy of Sciences, 2/31 Lobachevsky str., Kazan, 420111, Russia

* a.a.kalachev@mail.ru

One of the most important tasks in the development of quantum technologies is the scaling of quantum networks in order to distribute quantum information over long distances [1]. Solving this problem will make it possible to create a quantum Internet, which is expected to significantly expand the capabilities of quantum communications, quantum computing and quantum measurements.

In this presentation, we discuss the principles of operation of a quantum repeater, a device designed to distribute the entangled states of quantum systems over long distances, which is necessary for operation of future quantum networks. In particular, an overview of the progress in the field of experimental implementation of its simplest version – a first-generation quantum repeater, is presented [1], and our recent experimental results [2-4] devoted to developing a system of compatible narrowband two-photon sources and quantum memories are discussed.

[1] A. Kalachev, Quantum Repeaters: Current Developments and Prospects, Quantum Electronics (in Russian), 53, pp. 609-621, (2023).
[2] R.A. Akhmedzhanov, L.A. Gushchin, A.A. Kalachev, N.A. Nizov, V.A. Nizov, D.A. Sobgayda, I.V. Zelensky, Memory for polarization state of light based on atomic frequency comb in a ^{153}Eu:Y_2SiO_5 crystal, Laser Physics Letters, 20, 015204, (2023).
[3] D.A. Turaykhanov, I.Z. Latypov, A.V. Shkalikov, A.A. Kalachev, Narrowband entangled photon pair source for a quantum repeater based on solid-state quantum memory, Radiophysics and Quantum Electronics, 67, No 1, (2024).
[4] R.A. Akhmedzhanov, L.A. Gushchin, A.A. Kalachev, N.A. Nizov, V.A. Nizov, D.A. Sobgaida, I.V. Zelensky, Quantum memory in a Eu:YSO crystal for polarization and time-bin qubit states, Radiophysics and Quantum Electronics, 67, No 1, (2024).

Photonic elements with nonclassical sources of light fabricated by two-photon lithography

D.A. Kolymagin[1*], **A.V. Gritsienko**[1,2], **N.S. Kurochkin**[1,2], **A.I. Prokhodtsov**[1,3], **A.G. Vitukhnovsky**[1,2]

1- Moscow Institute of Physics and Technology (national research university), Institutsky lane, 9, 141700, Dolgoprudny, Russia
2- Lebedev Physical Institute RAS, Leninsky Prospekt 53, 119991, Moscow, Russia
3- National University of Science and Technology "MISiS", 119049, Moscow, Russia

* kolymagin@phystech.edu

Among of advanced additive 3D printing techniques variety, two-photon lithography (TPL) uniquely offers a significant advantage of submicron resolution [1]. This advantage allows to fabricate elements and devices on a micro scale for various applications. Such resolution of TPL in all 3 dimensions is possible due to the nonlinear two photon absorption (TPA) effect. Because of TPA photopolymerization occurs only in near the focal spot (Figure 1). The 3D-microstructure is obtained through femtosecond focused laser beam scanning of the substrate and subsequent development process. The 3D printed structures can also act as mold to pattern other materials into structures with high resolution, as many categories of materials are not suitable to be directly fabricated with TPL.
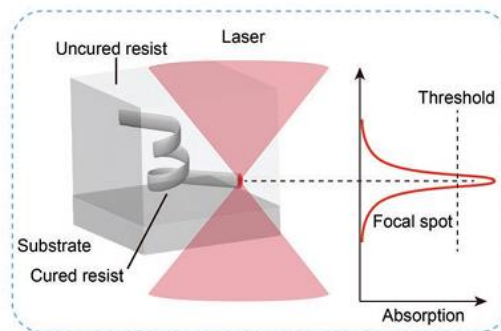
Fig.1: Schematic illustration of TPL process.

Photonics and quantum photonics are fast-growing fields, that were evolving from laser development and miniaturization of all optical components. However, one of the problems is connection of photonic elements and integration quantum elements in devices. Photonic wire bonding (PWB) is an exact example of a 3D laser polymerization technology transfer to solve on-a-chip integration challenges for micro-lasers couple to waveguides and optical circuits. Moreover, nonclassical light sources could be integrated into PWB structures [2]. Such approach could to provide high effective method of fabrication quantum photonics integral circuits.

In this work we reported the fabrication of PWB elements on silicon photonic chips and optical fibers for chip-to-fiber and chip-to-chip coupling. The total loss for these elements less than 5 dB. Also the integration of microdiamonds with NV centers was shown. Such integration improves the signal to noise ratio for NV center luminescence at 632 nm.

[1] A. Camposeo, L. Persano, M. Farsari, D. Pisignano, Additive manufacturing: applications and directions in photonics and optoelectronics, Advanced optical materials, vol. 7, №1, 1800419, (2019).
[2] A.W. Schell, et al, Three-dimensional quantum photonic elements based on single nitrogen vacancy-centres in laser-written microstructures, Scientific reports, vol. 3, 1477, (2013).

Towards a fully integrated quantum optical chip

<u>V. Kovalyuk</u>[1,2*], I. Venediktov[2,1], K. Sedykh[2,1], D. Kobtsev[2,1], A. Golikov[3,4], A. Prokhodtsov[1,4],
A. Kuzin[1,5], I. Florya[1,3], V. Galanova[1,5], R. Kasimov[1,3], S. Hydyrova[1,6], T. Krivenkov[1],
E. Sheveleva[3,7], G. Goltsman[2,7]

1- Laboratory of Photonic Gas Sensors, University of Science and Technology MISIS, 119049 Moscow, Russia
2- National Research University Higher School of Economics, 109028 Moscow, Russia
3- Moscow State Pedagogical University, 119991 Moscow, Russia
4- National Research University MIET, 124498 Zelenograd, Russia
5- Center for Photonics and Engineering, Skolkovo Institute of Science and Technology, 121205 Moscow, Russia
6- Bauman Moscow State Technical University, 105005 Moscow, Russia
7- Russian Quantum Center, 121205 Moscow, Russia

* kovaliuk.vv@misis.ru

Over the past few decades, quantum technologies have opened up new possibilities for the world, including quantum key distribution [1] that allows secure communications, quantum metrology [2] that allows more accurate measurements than the classical ones, and quantum lithography [3] that allows the fabrication of devices with dimensions much smaller than the wavelength of light. However, the most anticipated quantum technology is a quantum computer, which promises exponentially faster computations for a certain class of problems [4]. Currently, the most common platforms for the physical implementation of quantum bits (qubits) are those based on superconductors, neutral atoms, ions, and photons. Due to their unique characteristics: a large number of degrees of freedom for encoding information (phase, frequency, polarization, angular momentum, etc.), as well as the ability to move over long distances in optically transparent media, photons are considered the most promising basis for a quantum computer. The first demonstrations of photon-based quantum data processing were made on an optical table, but further scaling is impossible without transferring the elements to a chip. The creation of such a chip (or quantum photonic circuit) requires the combination of three main functional blocks: a photon source block, a logic block, and a single-photon detector block. Currently, the most advanced technology of these three blocks is the hybrid integration of superconducting detectors [5] with optical waveguides. The report considers several levels of integration of such detectors in the way of creating scalable devices. The first level is the integration of the detector with various photonic materials. Since the first demonstration in 2011 [6], to date, several research groups have demonstrated superconducting single-photon detectors on waveguides made of silicon, silicon nitride, polycrystalline diamond, lithium niobate on an insulator, etc. The second level of integration includes the combination of detectors with more complex devices: AWG demultiplexers, photonic crystal waveguides, and planar echelettes. At this level, the devices can be used not only as components of quantum optical devices but also as separate devices, namely single-photon spectrometers that record spectral and temporal information about the objects under study. The third level of integration is associated with devices that combine single-photon sources, logical elements, and detectors. Several schemes and approaches based on the use of quantum dots, nanotubes or nonlinear four-wave mixing have been demonstrated so far, but all suffer from low system efficiency or difficult scalability [7]. Work in this direction can be of a breakthrough nature; therefore, it is actively carried out throughout the world, but requires high-tech nanofabrication and access to clean rooms.

[1] N. Gisin, G. Ribordy, W. Tittel, H. Zbinden, Quantum cryptography, Reviews of modern physics, 74(1), 145, (2002).
[2] V. Giovannetti, S. Lloyd, L. Maccone, Quantum-enhanced measurements: beating the standard quantum limit, Science, 306(5700), 1330-1336, (2004).
[3] A.N. Boto, P. Kok, D.S. Abrams, S.L. Braunstein, C.P. Williams, J.P. Dowling, Quantum interferometric optical lithography: exploiting entanglement to beat the diffraction limit, Physical Review Letters, 85(13), 2733, (2000).
[4] J.L. O'Brien, Optical quantum computing, Science, 318(5856), 1567-1570, (2007).
[5] G.N. Gol'tsman, O. Okunev, G. Chulkova, A. Lipatov, A. Semenov, K. Smirnov, ... & R. Sobolewski, Picosecond superconducting single-photon optical detector, Applied physics letters, 79(6), 705-707, (2001).
[6] W.H. Pernice, C. Schuck, O. Minaeva, M. Li, G.N. Goltsman, A.V. Sergienko, H.X. Tang, High-speed and high-efficiency travelling wave single-photon detectors embedded in nanophotonic circuits, Nature communications, 3(1), 1325, (2012).
[7] S. Khasminskaya, F. Pyatkov, K. Słowik, S. Ferrari, O. Kahl, V. Kovalyuk, ... & W.H. Pernice, Fully integrated quantum photonic circuit with an electrically driven light source, Nature Photonics, 10(11), 727-732, (2016).

The influence of the hydrogen-containing surface of nanodiamonds on the luminescence intensity of "silicon-vacancy" centers

O. Kudryavtsev[1*], R. Bagramov[2], V. Korepanov[3], T. Rudneva[3], V. Filonenko[2], I. Vlasov[1]

1- Prokhorov General Physics Institute of the Russian Academy of Sciences, Russia
2- Vereshchagin Institute of High-Pressure Physics of the Russian Academy of Sciences, Troitsk, Russia
3- Institute of microelectronics technology and high purity materials of the Russian Academy of Sciences, Chernogolovka Russia

* leolegk@mail.ru

Nanodiamonds (NA) with negatively charged silicon vacancy color centers (SiV) are successfully used by us as sensors of ultralocal "temperature" fields [1,2]. One of the most promising methods for producing such products is their synthesis from hydrocarbons at high temperature and high pressure (NRNT synthesis). The surface of such layers is terminated by hydrogen, which induces a near-surface conductive layer of the acceptor type. The presence of a large number of acceptors can affect the charge state of the SiV centers in the NA, transferring them to an optically inactive neutral state. It has a negative impact on SiV centers. This work is devoted to the study of the effect of the hydrogen-terminated surface of HPNT nanodiamonds with a size of 100-300 nm on the luminescence intensity of silicon vacancy centers. To do this, hydrogen was removed from the surface of nanodiamonds by annealing in air at various temperatures in the range of 400-600 degrees. The efficiency of hydrogen removal from the surface of nanodiamonds was controlled by IR absorption spectroscopy. It was found that during annealing of nanodiamonds at a temperature of 600 degrees, the lines of C-H valence vibrations completely disappear in the IR spectrum, which indicates the effective removal of hydrogen from the surface of nanodiamonds at this temperature. Analysis of the spatial distribution of the intensity of SiV luminescence before and after annealing for a large ensemble of NA dispersed on the surface of a silicon substrate showed that the average intensity level increases by about 50% after removal of hydrogen from the surface of NA. The greatest luminescence amplification is observed for particles of about 100 nm in size, and practically no amplification occurs for 300 nm particles.

[1] A. Romshin, V. Zeeb, A. Martyanov, O. Kudryavtsev, D. Pasternak, V. Sedov, V. Ralchenko, A. Sinogeykin, I. Vlasov, A new approach to precise mapping of local temperature fields in submicrometer aqueous volumes, Sci. Rep., vol.11, pp.14228, (2021).
[2] A. Romshin, V. Zeeb, E. Glushkov, A. Radenovic, A. Sinogeikin, I. Vlasov, Nanoscale thermal control of a single living cell enabled by diamond heater-thermometer, Sci. Rep., vol.13, pp.8546, (2023).

Optical characterization of individual single-walled carbon nanotubes

F. Maksimov[1,2*], **A. Goldt**[3], **S. Dozmorov**[3], **Yu. Gladush**[3], **A. Nasibulin**[3], **A. Chernov**[1,2]

1- Russian Quantum Center, 30, Bolshoy Bulvar, Building 1, Skolkovo Innovative Center, Moscow, Russian Federation
2- Center for Photonics and 2D Materials, Moscow Institute of Physics and Technology (MIPT), Dolgoprudny, Russian Federation
3- Skolkovo Institute of Science and Technology, Bolshoy Boulevard 30, bd. 1, Moscow, 121205, Russian Federation

* maksimov.fm@phystech.edu

Single-walled carbon nanotubes (SWCNTs) are promising low-dimensional material with many applications in quantum technologies. One of the applications that stems from the optical properties of SWCNTs [1,2] is using them as a basis for a single photon source. The main advantages of such emitters are the possibility of obtaining single photons at room temperature, as well as the possibility of choosing the wavelength of emission in the near infrared range by selecting the chirality of the nanotube, which allows, for example, to tune the emitters to the wavelength of telecommunication networks 1550 nm [3]. Such sources are necessary for quantum computing on photons and also for quantum communication. Here we investigate created by aerosol method [4] low-concentration nanotubes deposited on sapphire substrates using resonant Raman spectroscopy and detect the photoluminescence response in the near-IR range. The measurements were performed with a tunable CW laser with a microscope objective (Mitutoyo x100 NIR) and a spot size of about 1 µm. The nanostage (MadCityLabs Nano T-225) was used for mapping and the signal was collected with a spectrometer (Horiba iHR 320 with Synapse plus/Symphony II detector). As a result, a map of G-band Raman peak signal of a sample was obtained. Further the photoluminescence mapping of functionalized nanotubes was performed. Functionalization of SWCNTs with aryl groups allows the creation of localized sp^3 defects on the surface of the nanotube and increases the quantum efficiency of the photoluminescence, which is necessary for the subsequent creation of a single-photon source [5]. Mapping of a single functionalized nanotube allows to determine the position of the defect and finally to integrate them into resonant nanostructures that provide further increase of the photoluminescence efficiency. Unambiguous detection, characterization and further measurement of optical properties allow to reveal the possibility of implementation of individual SWCNTs as a single-photon source.

[1] V.A. Eremina, et al, Separation and optical identification of semiconducting and metallic single-walled carbon nanotubes, Physica status solidi (b), 254.5, (2017).
[2] A.I. Chernov, E.D. Obraztsova, Metallic single-wall carbon nanotubes separated by density gradient ultracentrifugation, Physica status solidi (b), 246.11-12, (2009).
[3] X. He, et al, Tunable room-temperature single-photon emission at telecom wavelengths from sp^3 defects in carbon nanotubes, Nature Photonics, 11.9, (2017).
[4] D.A. Ilatovskii, et al, Photophoretic deposition and separation of aerosol-synthesized single-walled carbon nanotubes, Carbon, (2023).
[5] J. Zaumseil, Luminescent Defects in Single-Walled Carbon Nanotubes for Applications, Advanced Optical Materials, 10.2, (2022).

Single quantum dots spectromicroscopy:
state of art under the Nobel prize 2023 spotlight

A.V. Naumov[1-3*], **A.I. Arzhanov**[1,2], **I.Yu. Eremchev**[1-3], **M.G. Gladush**[1-3], **P.A. Frantsuzov**[4], **K.R. Karimullin**[1-3], **M.A. Knyazeva**[1,2], **K.A. Magaryan**[1-3], **A.O. Tarasevich**[1-3], **E.A. Podshivaylov**[4], **N.V. Surovtsev**[5]

1- P.N. Lebedev Physical Institute of the Russian Academy of Sciences, Troitsk Branch, Moscow, Troitsk, Russia
2- Moscow Pedagogical State University (MPGU), Moscow, Russia
3- Institute of Spectroscopy RAS, Moscow, Troitsk, Russia
4- Voevodsky Institute of Chemical Kinetics and Combustion SB RAS, Novosibirsk, Russia
5- Institute of Automation and Electrometry SB RAS, Novosibirsk, Russia

* a_v_naumov@mail.ru; www.single-molecule.ru

The 2023 Nobel Prize in Chemistry has brought significant attention to the already booming field of physics and chemistry of semiconductor nanocrystals – quantum dots (QD) [1]. In fact one of the critical point in this field development was achievement to measure photoluminescence (PL) of single QDs. In this lecture we overview the works devoted to the synthesis, study of photophysical and spectral properties of QDs. The fundamental laws connecting the morphology of quantum dots with its optical-spectral characteristics are discussed, as well as some theoretical models that allow describing various effects and processes: the quantum-dimensional effect, local field effects [2], electron-phonon interaction [3], photoluminescence blinking [3,4] of single quantum dots. The results of original experimental and theoretical studies of the temperature dependences of the spectra of single colloidal quantum dots with a CdSe emitting core are presented, which made it possible to clarify the nature of the formation of the optical spectra (absorption, luminescence and Raman) of single quantum dots and their ensembles [5,6]. Some possible applications in quantum technologies will be also discussed [7].

[1] A.A. Rempel, et al, Quantum dots: modern methods of synthesis and optical properties, Russian Chemical Reviews 93 (2024) Rcr5114.
[2] M.G. Gladush, et al, Dispersion of Lifetimes of Excited States of Single Molecules in Organic Matrices at Ultralow Temperatures, Journal of Experimental and Theoretical Physics, 2019, 128, 655-663.
[3] E.A. Podshivaylov, et al, A quantitative model of multi-scale single quantum dot blinking, J. Mater. Chem. C, 2023,11, 8570-8576.
[4] I.Yu. Eremchev, et al, Detection of Single Charge Trapping Defects in Semiconductor Particles by Evaluating Photon Antibunching in Delayed Photoluminescence, Nano Lett. 2023, 23, 2087–2093.
[5] K.R. Karimullin, et al, Combined photon-echo, luminescence and Raman spectroscopies of layered ensembles of colloidal quantum dots, Laser Phys. 2019, 29, 124009.
[6] A.I. Arzhanov, et al, Photonics of Semiconductor Quantum Dots: Basic Aspects, PHOTONICS Russia 15, 622-641 (2021).
[7] A.I. Arzhanov, et al, Photonics of Semiconductor Quantum Dots: Applied Aspects, PHOTONICS Russia 16, 96-112 (2022).

New type of fluorescence in hydrogen-terminated nanodiamond

D. Pasternak[1*], A. Romshin[1], R. Bagramov[2], A. Galimov[3], A. Toropov[3], D. Kalashnikov[4], V. Leong[4], A. Satanin[5], O. Kudryavtsev[1], A. Gritsienko[6], A. Chernev[7], V. Filonenko[2], I. Vlasov[1]

1- Prokhorov General Physics Institute of the Russian Academy of Sciences, 38 Vavilov str, Moscow 119991, Russia

2- Vereshchagin Institute of High-Pressure Physics of the Russian Academy of Sciences, 14 Kaluzhskoe shosse, Moscow, Troitsk 108840, Russia

3- Ioffe Institute, 26 Politekhnicheskaya str, 194021, St. Petersburg, Russia

4- Institute of Materials Research and Engineering (IMRE), Agency for Science Technology and Research (A*STAR), 2 Fusionopolis Way, Innovis #08-03, Singapore 138634, Republic of Singapore

5- National Research University Higher School of Economics, 20 Myasnitskaya str, Moscow 101000, Russia

6- P.N. Lebedev Physical Institute of the Russian Academy of Sciences, 53 Leninskiy pr., Moscow 119991, Russia

7- Laboratory of Nanoscale Biology, Institute of Bioengineering, Ecole Polytechnique Federale de Lausanne, 1015, Lausanne, Switzerland

* dg.pasternak@physics.msu.ru
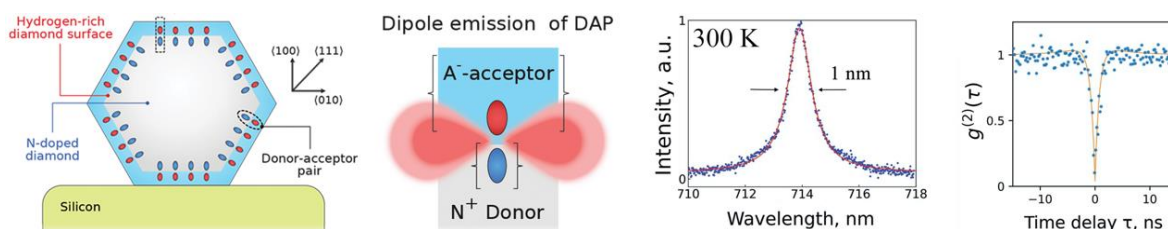
Fluorescence spectra of nanodiamonds synthesized at high pressure and high temperature (HPHT synthesis) from adamantane and other organic compounds show narrow lines of unknown origin in a spectroscopic range from 500 to 800 nm (2.48-1.55 eV).

We have identified a connection of the narrow fluorescent lines (NFLs) with single substitutional nitrogen and a 2D layer of surface acceptors formed in the H-terminated nanodiamonds. This allowed us to conclude that the new lines originate due to the radiative recombination of donor-acceptor pairs (DAPs) consisting of nitrogen donors and surface acceptors. The next main characteristics of the single DAP fluorescence were determined at room temperature: spectral width 0.5-2 nm; fluorescence lifetime ~1 ns; highest recorded photon emission rate 1.2 million counts/s. Various spectral characteristics of the NFLs were studied within the wide temperature range 10-300 K. The new type of fluorescence found in hydrogen-terminated is promising for use both as a source of single photons and as temperature sensors.

Inhomogeneous broadening in the luminescence spectra of single SnV and GeV centers in CVD diamonds at cryogenic temperatures

**M. Pavlenko[1,2*], A. Neliubov[3], I. Eremchev[1,4], V. Sedov[5],
A. Martyanov[5], V. Ralchenko[5], A. Naumov[1,4]**

1- Moscow Pedagogical State University, Malaya Pirogovskaya str. 1/1, Moscow, 119435, Russia
2- National Research University Higher School of Economics, Staraya Basmannaya str. 21/4, 109028, Moscow, Russia
3- Center for Engineering Physics, Skolkovo Institute Science and Technology, Nobel str. 1, Moscow 121205, Russia
4- Institute of Spectroscopy RAS, Troitsk, Fizicheskaya str. 5, Moscow 108840, Russia
5- Prokhorov General Physics Institute of the Russian Academy of Sciences, Vavilov str. 38, Moscow 119991, Russia

* mipavlenko@edu.hse.ru

This paper presents a low temperature study of the spectral properties of tin-vacancy (SnV) and germanium-vacancy (GeV) color centers in diamonds synthesized by plasma chemical deposition from the gas phase (CVD). In experiments with SnV centers at T = 7 K, a large spread of narrow zero-phonon lines (ZPL) in the range of 615-630 nm was observed, while the full width at half maximum (FWHM) was about 0.05 nm (Fig. 1(a)) [1]. In the obtained photoluminescence spectra of the sample with GeV centers at T = 8 K narrow lines were observed, the FWHM of which was limited by the resolution of the spectrometer (~ 0.028 nm). The line spread of the ensemble was in the range of 600-608 nm (Fig. 1(b)). The observed shifts of the ZPL are explained by the stresses of the crystal lattice formed during the growth of the diamond. The variation in spectral positions can be attributed to the difference in individual microcrystal stresses. The effect of diamond crystal lattice stresses on the spectral position of the ZPL of impurity center has already been observed for GeV and SiV centers. The detected lines at cryogenic temperatures correspond to the luminescence of small ensembles (up to single emitters) of color centers, which is confirmed by the observation of spectral diffusion, blinking and linear polarization of the radiation of individual ZPL.
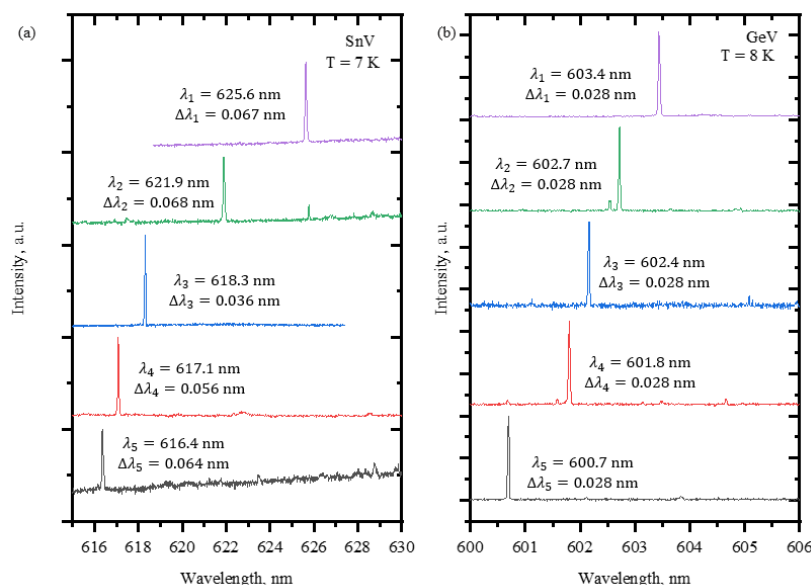

Fig. 1. (a) Spectra of PL SnV centers; (b) Spectra of PL GeV centers.

[1] V. Sedov, A. Martyanov, et al, Narrowband Photoluminescence of Tin-Vacancy Colour Centres in Sn-Doped Chemical Vapour Deposition Diamond Microcrystals, Phil. Trans. R. Soc. A 382: 20230167 (2023).

MBE growth and properties of III-V quantum dots in nanowires for single photon sources

R. Reznik[1]*, D. Barettin[2], R. Radhakrishnan[3], N. Akopian[3], G. Cirlin[4]

1- St. Petersburg State University, Universitetskaya Embankment 7-9, 199034 St. Petersburg, Russia
2- Università degli Studi Niccolò Cusano - Telematica, via don Carlo Gnocchi 3, 00166 Rome, Italy
3- Technical University of Denmark, DK 2800 Lyngby, Denmark
4- Alferov University, Khlopina 8/3, 194021 St. Petersburg, Russia

* r.reznik@spbu.ru

A combination of nanowires (NWs) with quantum dots (QDs), are promising building blocks for future optoelectronic devices, in particular, single-photon emitters [1]. The most studied epitaxially grown QDs are self-assembled, i.e., grown by island nucleation in the Stranski-Krastanov growth mode. In common case, the size, shape, and density of self-assembled QDs can be changed by growth parameters, but it is a strain induced process and controlling the properties of the array independently is a challenging task [2]. QDs in nanowires have in contrast shown great potential as a highly controllable system. The diameter, height, and density of the QDs are defined by the NW diameter, the growth time, and the NW density, respectively, and can be chosen more predictable. Moreover, the unique morphology of NWs makes it possible to integrate such direct-gap hybrid nanostructures with a silicon platform [3].
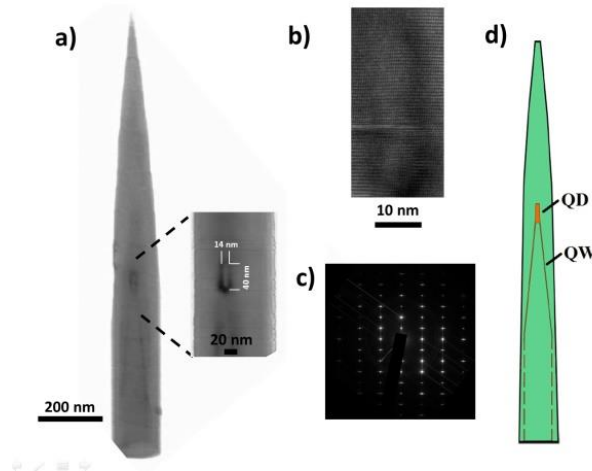
Fig. 1. (a) Typical TEM image of single AlGaAs NW with InGaAs QD grown at 510°C. (b) Typical HRTEM image of InGaAs QD in single AlGaAs NW grown at 510°C. (c) Typical diffraction pattern obtained in QD location. (d) Schematic representation of AlGaAs NWs with InGaAs QDs structure.

In this work we present for the first time MBE growth of QDs in NWs based on (In)GaAs/AlGaAs materials system on silicon surface also studied their physical properties. The example of AlGaAs NW with InGaAs QD typical transmission electron microscopy (TEM) images, diffraction pattern and schematic representation of the structure are shown in the Fig. 1 (a-d). Studies results have shown that grown hybrid nanostructures are efficient single photons sources and by changing the size and composition of QDs we can strictly control the emission energy from the QD in a wide range. It is important to note that the direction of emission from QDs in the body of NWs was studied experimentally and theoretically. Our work opens new prospects for integration of direct band-gap semiconductors and single-photon sources on silicon platform for various applications in the fields of silicon photonics and quantum information technology.

[1] R. Singh and G. Bester, Nanowire quantum dots as an ideal source of entangled photon pairs, Physical review letters, 103, 063601, (2009).
[2] V.G. Dubrovskii, G.E. Cirlin, V.M. Ustinov, Kinetics of the initial stage of coherent island formation in heteroepitaxial systems, Physical Review B, 68, 075409, (2003).
[3] T. Mårtensson, C.P.T. Svensson, B.A. Wacaser, M.W. Larsson, W. Seifert, K. Deppert, A. Gustafsson, L.R. Wallenberg, L. Samuelson, Epitaxial III−V nanowires on silicon, Nano letters, 4, 1987-1990, (2004).

Timescale of thermal transport in "diamond-water" nanointerface

A. Romshin[*], **D. Pasternak, I. Tiazhelov, A. Martyanov, V. Sedov, I. Vlasov**

Prokhorov General Physics Institute of the Russian Academy of Sciences, Moscow, Russia

* alex_31r@mail.ru

Recent advancements in thermal nanoprobing techniques, which enable the mapping of temperature distribution and precise heat perturbation in physical and living systems [1], underscore the need for a deep understanding of nanoscale thermal transport. Conventional theory of heat transfer is insufficient to accurately describe the phenomena observed at such scales, where the interface conductance between solid particles and liquids becomes a critical factor [2]. In recent years, heat transfer mechanisms at solid-liquid interfaces have been studied in either nanostructured bulk crystals wetted with liquid [3] or colloidal suspensions of metallic nanoparticles [4]. However, these methods often yielded averaged thermal properties and can result in inaccurate estimations of interfacial thermal conductance.

In this work thermal transport across the diamond-water nanointerface is investigated. Utilizing single diamond micro- and nanoparticles, which combine thermometric and heating capabilities, we precisely determine the rise and relaxation times of stepwise heating with submicrosecond resolution for a wide range of crystal sizes from 250 nm to 1.5 μm. For the 1.5 μm diamond, it was found that the time required to heat the local volume of water by 10°C and reach thermodynamic equilibrium is approximately 5.2 μs, while the relaxation to environmental conditions takes longer, around 116 μs. Subsequently, the rate of thermal transport significantly increases with decreasing particle size. For the smallest nanodiamond, the rise and relaxation times were determined to be 90 ns and 1.6 μs, respectively. An order of magnitude superiority of rising rate over relaxation one might be connected with fast heating of nanocrystal separately from water due to higher thermal conductivity of diamond compared to water. Our results allow for an accurate assessment of the thermal properties at the interface, providing insights that are critical for advancing nanotechnology and improving the thermal management of nanoscale systems.

[1] A. Romshin, V. Zeeb, E. Glushkov, A. Radenovic, A. Sinogeikin, I. Vlasov, Nanoscale thermal control of a single living cell enabled by diamond heater-thermometer, Scientific Reports, vol. 13, pp. 8546, (2023).
[2] G. Baffou, H. Rigneault. Femtosecond-pulsed optical heating of gold nanoparticles. Physical Review B, 84(3), 035415, (2011).
[3] J. Tomko, D. Olson, A. Giri, J. Gaskins, B. Donovan, S. O'Malley, P. Hopkins, Nanoscale wetting and energy transmission at solid/liquid interfaces, Langmuir, 35(6), 2106-2114, (2019).
[4] O. Wilson, X. Hu, D. Cahill, P. Braun. Colloidal metal particles as probes of nanoscale thermal transport in fluids. Physical Review B, 66(22), 224301, (2002).

Quantum memristors as a new stage on the way from quantum to neuromorphic computing

S. Stremoukhov[1,2,3*], **P. Forsh**[1,2], **K. Khabarova**[1,4], **N. Kolachevsky**[1,4]

1- P.N. Lebedev Physical Institute of the Russian Academy of Science, Leninskiy pr., 53, 119991 Moscow, Russia
2- Faculty of Physics, M.V. Lomonosov Moscow State University, Leninskie Gory, 1/2, 119991 Moscow, Russia
3- National Research Centre "Kurchatov Institute", Akademika Kurchatova sq. 1, 123182 Moscow, Russia
4- Russian Quantum Center, Bolshoy Bulvar, 30 Bld. 1, 121205 Moscow, Russia

* sustrem@gmail.com

Quantum computing is currently one of the fastest growing topics. To date, the main basic computing tools have been created on four platforms – optical, superconducting, atomic and ionic [1-4]. Scalable quantum computers hold the promise to solve hard computational problems, such as prime factorization, combinatorial optimization, simulation of many-body physics, quantum chemistry as well as simulating the physics of open systems [5]. On the other hand, it has been shown that neuromorphic computing also has a number of advantages due, first of all, to a significant reduction in energy consumption during calculations through the use of one device – a classical memristor – both directly for calculations and information storage [6]. Combining neuromorphic and quantum computing through the use of a quantum memristor as a device that consolidates the ability to store quantum information, as well as quantum parallelism and entanglement, will enable quantum neuromorphic computing. In addition, a classic memristor is close in its properties to a synapse, which ensures contact between neurons in the brain. At the same time, many scientists, in particular Nobel laureate R. Penrose [7], are inclined to believe that the work of the brain is determined by the laws of quantum physics. If this is true, then the quantum memristor and computing systems based on it can more accurately imitate the functioning of the brain.

Quantum memristor concepts have been proposed on superconducting [8], photonic [9], and ionic [10,11] platforms. This paper discusses the features of ionic quantum memristors based on ultracold Yb^+ ions. It is shown that at certain values of the parameters of laser pulses, which ensure the movement of the population of selected levels of the ion, a "memristive dependence" of the output signal on the input signal occurs (which is the population of one of the levels at different times, correlated with the action of two laser fields). Two options for creating a quantum memristor have been proposed: on a single ultracold ion and on a chain of ultracold ions connected by a low-frequency vibrational mode of the center of mass. This makes such coupled quantum memristors to be the best candidate for use in neuromorphic computing.

[1] A.A. Houck, H.E. Türeci, J. Koch, On-chip quantum simulation with superconducting circuits, Nat. Phys. 8, 292 (2012).
[2] R. Blatt and C.F. Roos, Quantum simulations with trapped ions, Nat. Phys. 8, 277 (2012).
[3] C. Gross and I. Bloch, Quantum simulations with ultracold atoms in optical lattices, Science 357, 995 (2017).
[4] A. Aspuru-Guzik and P. Walther, Photonic quantum simulators, Nat. Phys. 8, 285 (2012).
[5] A.S. Kazmina I.V. Zalivako, A.S. Borisenko, N.A. Nemkov, A.S. Nikolaeva, I.A. Simakov, A.V. Kuznetsova, E.Yu. Egorova, K.P. Galstyan, N.V. Semenin, A.E. Korolkov, I.N. Moskalenko, N.N. Abramov, I.S. Besedin, D.A. Kalacheva, V.B. Lubsanov, A.N. Bolgar, E.O. Kiktenko, K.Yu. Khabarova, A. Galda, I.A. Semerikov, N.N. Kolachevsky, N. Maleeva, A.K. Fedorov, Demonstration of a parity-time-symmetry-breaking phase transition using superconducting and trapped-ion qutrits, Phys. Rev. A 109, 032619 (2024).
[6] D.B. Strukov, G.S. Snider, D.R. Stewart, R.S. Williams, The missing memristor found. Nature 453, 80–83 (2008).
[7] R. Penrose, The Emperor's New Mind (Oxford University Press) (1989).
[8] P. Pfeifer, I.L. Egusquiza, M. Di Ventra, M. Sanz, E. Solano, Quantum memristors. Scientific Reports, 6, 29507 (2016).
[9] M. Sanz, L. Lamata, E. Solano, Invited Article: Quantum memristors in quantum photonics, APL Photonics, 3.8, 080801 (2018).
[10] S. Stremoukhov, P. Forsh, K. Khabarova, N. Kolachevsky, Proposal for trapped-ion quantum memristor, Entropy, 25, 1134 (2023).
[11] S.Yu. Stremoukhov, P.A. Forsh, K.Yu. Khabarova, N.N. Kolachevsky, Model of Coupled Quantum Memristors Based on a Single Trapped $^{171}Yb^+$ Ion, JETP Letters, Vol. 119, No. 5, pp. 352-356 (2024).

Recent advances in quantum frequency standards and other quantum sensors

S.N. Bagayev[1,2], D.V. Brazhnikov[1,2], S.V. Chepurov[1], A.N. Goncharov[1-3], O.N. Prudnikov[1], M.N. Skvortsov[1], <u>A.V. Taichenachev</u>[1,2*], V.I. Yudin[1-3]

1- Institute of Laser Physics SB RAS, Novosibirsk 630090, Russia
2- Novosibirsk State University, Novosibirsk 630090, Russia
3- Novosibirsk State Technical University, Novosibirsk 630073, Russia

* taichenachev@mail.ru

In this talk we give a brief overview of our recent works on quantum sensors based on two different platforms: i) ultracold atoms and ions, including optical frequency standards [1,2] and atomic interferometers for inertial force sensing (gravimetry and gyroscopy) [3,4]; ii) alkali-metal vapors at room temperature, including atomic clocks based on coherent population trapping resonances [5], optical frequency standards based on saturation absorption resonances [6], and optically pumped magnetometers for ultra-weak magnetic field sensing [7]. Several new spectroscopic methods [8-10], including generalized Ramsey spectroscopy [11], are discussed as well as new methods of laser cooling and trapping of neutral atoms and ions [12-14], specially tailored for needs of quantum sensors.

[1] A.N. Goncharov, et al, Quantum Electronics, 48, 410-414 (2018).
[2] S.V. Chepurov, et al, Quantum Electronics, 51, 473-478 (2021).
[3] A.V. Taichenachev, et al, Journal of Physics: Conference Series, 1508, 012002 (2020).
[4] D.N. Kapusta, et al, Source of ultracold rubidium atoms for atomic interferometer-gravimeter, JETP, accepted (2024).
[5] M.N. Skvortsov, et al, Quantum electronics, 50, 576 (2020).
[6] D. Brazhnikov, et al, In European Frequency and Time Forum (2020, April).
[7] D. Brazhnikov, et al, Optics Letters, 45, 3309-3312 (2020).
[8] D.V. Brazhnikov, et al, Quantum Electronics, 50, 1015 (2020).
[9] D.V. Kovalenko, et al, Quantum Electronics, 51, 495-501 (2021).
[10] V.I. Yudin, et al, New Journal of Physics, 23, 023032 (2021).
[11] A.V. Taichenachev, V.I. Yudin, Generalized Ramsey Methods in Precision Laser Spectroscopy: from Atomic Clocks to Interferometers, Journal of Physics: Conference series, accepted (2024).
[12] O.N. Prudnikov, et al, Phys. Rev. A, 108, 043107 (2023).
[13] D.S. Krysenko, et al, Phys. Rev A, 108, 043114 (2023).
[14] O.N. Prudnikov, et al, Laser cooling of ytterbium-171 ion without the use of magnetic field, JETP, accepted (2024).

Promising applications of fluorescent nanodiamonds

I.I. Vlasov

Prokhorov General Physics Institute of the Russian Academy of Sciences, Moscow, Russia

vlasov@nsc.gpi.ru

Nanosized diamonds containing single fluorescent centers are promising material platform for the development of single-photon sources (SPS). Their main advantages over bulk diamond structures are the possibility of (1) high spatial localization of a single emitter, which is determined by the size of the diamond nanoparticle, (2) coupling with various types of micro- and nano-resonators in order to increase the photon emission rate, (3) scaling of single-photon emitters. To date, we have developed SPS based on silicon-vacancy (SiV) centers in 200-nm HPHT nanodiamonds with an emission rate of more than 1 million photons per second. The developed SPS are proposed to be used in quantum communication and computing technologies.

In recent years, we have been actively developing an all-optical method for measuring ultra-local temperature fields based on detecting the shift and broadening of the spectral line of luminescent silicon-vacancy centers in nanodiamonds when they are heated [1]. We have also developed a new approach to controlled local heating using luminescent nanodiamonds. The approach is based on combining the properties of a heater and a thermometer in one material – a polycrystalline nanodiamond particle, and using one such particle, which can be positioned with high spatial accuracy (up to several nanometers) at any given point in the studied medium [2]. The first results of the successful application of a diamond thermometer-heater in biological research are presented.

[1] A.M. Romshin, V. Zeeb, A.K. Martyanov, O.S. Kudryavtsev, D.G. Pasternak, V.S. Sedov, V.G. Ralchenko, A.G. Sinogeykin, I.I. Vlasov, A new approach to precise mapping of local temperature fields in submicrometer aqueous volumes, Sci. Rep., 11, 14228 (2021).
[2] A.M. Romshin, V. Zeeb, E. Glushkov, A. Radenovic, A.G. Sinogeikin, I.I. Vlasov, Nanoscale thermal control of a single living cell enabled by diamond heater-thermometer, Sci. Rep., 13, 8546 (2023).

Generation, detection and characterization of ultralow energy light

<u>V.I. Kovalev</u>[1,2*]

1- P.N. Lebedev Physical Institute of the Russian Academy of Sciences, Leninsky pr. 53, Moscow, 119991, Russia
2- Heriot-Watt University, Edinburgh, EH14 4AS, UK

* kovalevvi@lebedev.ru

These days generation, detection and characterization of an ultralow energy light is a topic of wide interest in optical physics. Vast majority of correspondent studies presume "single photon" level of light energy. Such studies, however, look a tricky because the thing, which conventionally called "photon", is not defined. For example, A. Einstein pointed out in 1951 (letter to M. Besso): "*These days, every lump thinks that he knows what a photon is, but he is wrong*", W. Lamb noted in [1] that "*there is no such thing as a photon. Only a comedy of errors and historical accidents led to its popularity among physicists and optical scientists.*" J. Eberly with colleagues [2] concluded that most of traditionally meant to be quantum phenomena can be seen, studied, accounted and exploited in frames of classical optics. In [3] V. Kovalev proposed a classical model for a sub-single photon detector operation. In this work a performance of the system made up of a "single-photon emitter", an optical pathway to a detector and a "single-photon detector" will be considered in frames of classical optics.

[1] W.E. Lamb Jr., Anti-photon, Appl. Phys. B, Lasers and Optics, 60, 77-84 (1985).
[2] X.-E. Qian, A.N. Vamivakas, J.H. Eberly, Emerging connections classical and quantum optics, OPN, 28, 34-41 (2017).
[3] V.I. Kovalev, Nature of Photoelectric Effect in a Ge-on-Si SPAD at Ultralow Energy in Incident Pulsed Laser Radiation, Optics, 2, 45-53 (2021).

ADVANCED OPTICAL MATERIALS & METAMATERIALS

The influence of copper ions on eumelanin hydration examined by mid-infrared spectroscopy

P.A. Abramov[1*], A.B. Mostert[2], K.A. Motovilov[1]

1- Moscow Institute of Physics and Technology, Dolgoprudny, Moscow Region, 141700 Russia
2- Swansea University, Department of Chemistry, Singleton Park, Wales, UK

* pbrmv@phystech.edu

Melanins are promising natural materials for applications in bioelectronic devices such as organic electrochemical transistors [1], memristors [2], supercapacitors [3], and pH sensors [4]. Similar to bioorganics the properties of melanins are highly influenced by water and naturally occurring d-elements. Being a critical part of tyrosinase synthesis machinery, copper ions are widely presented in biologically derived melanins. In the current study we examine water and Cu^{2+} ions effects on eumelanin by infrared spectroscopy for the first time. Our findings reveal that copper ions significantly alter the properties of both melanin and hydration layers. Notably, with an increase of copper content, the fraction of 4-hydrogen bonded water molecules also increases, rendering general water behavior more ice-like. Copper ions shift the comproportionation reaction between quinone and hydroquinone moieties towards the formation of semiquinone radicals even in the dry system. Also, we demonstrate that these ions tend to decrease the contribution of some signatures of aqueous proton cations. The general picture explains the mechanisms of conductivity inhibition induced in melanin by copper ions via both trapping electron density of semiquinone radicals in corresponding complexes and by decreasing the proton diffusion efficiency via the transformation of water into a more ice-like structure.

[1] M. Sheliakina, A.B. Mostert, P. Meredith, An all-solid-state biocompatible ion-to-electron transducer for bioelectronics, Mater. Horiz., vol. 5, no. 2, pp. 256–263, Mar. 2018.
[2] M. Ambrico, et al, Memory-like behavior as a feature of electrical signal transmission in melanin-like bio-polymers, Appl. Phys. Lett., vol. 100, no. 25, p. 253702, Jun. 2012.
[3] P. Kumar, et al, Melanin-based flexible supercapacitors, J. Mater. Chem. C, vol. 4, no. 40, pp. 9516–9525, Oct. 2016.
[4] A. Gouda, F. Soavi, C. Santato, Eumelanin electrodes in buffered aqueous media at different pH values, Electrochimica Acta, vol. 347, p. 136250, Jul. 2020.

The influence of hyperdoping gold film thickness on the photoresponse of laser hyperdoped silicon

__A. Akhmatkhanov__[1*], R. Saifetdinov[1], V. Pryakhina[1], A. Sherstobitov[1],
M. Kovalev[1,2], S. Kudryashov[1,2]

1- Ural Federal University, Ekaterinburg, Russia
2- Lebedev Physical Institute, Moscow, Russia

* andrey.akhmatkhanov@urfu.ru

The working range of conventional Si-based photodetectors is limited by 1.1 μm bandgap-related value thus excluding most of the telecommunication bands in the near-infrared region (NIR). This spectral range can be covered by alternative technologies, including InGaAs, HgCdTe and Ge-based detectors, however their integration with existing Si platform for efficient signal processing can be complicated and expensive. Alternative approach to this problem is related to the developing of hyperdoped Si NIR detectors, which implies doping of deep level impurities (such as gold) at concentrations above the equilibrium solubility level. An intermediate impurity band formed in this case enables efficient sub-bandgap light adsorption. Nanosecond laser hyperdoping through laser melting and dopant diffusion is one of the most widely used technique within this approach.

In this work we study the influence of hyperdoping gold film thickness on the photoresponse of Au-hyperdoped Si detectors.

Commercial 200-μm-thick nominally pure Si (100) wafers (resistivity > 1000 Ohm cm) were used. The 3×10 mm^2 Si samples were covered by Au films with thickness from 20 to 100 nm by magnetron sputtering. The sample surface was single-pass scanned in the ambient atmosphere by 100-ns laser pulses at 1064-nm wavelength (repetition rate 80 kHz, scan speed 80 mm/s, filling 100 lines/mm, fluence 8 J/cm^2, laser beam diameter 50 μm) using a MiniMarker-2 M20 marking system (LTC, Russia). Residual metal film was removed after laser hyperdoping by chemical etching in HNO$_3$:HCl 1:3 mixture and HF aqueous solution. Ohmic indium contacts were soldered on obtained samples for further two- and four-probe resistivity and photoresponse measurements.

We have measured the change of sample's resistivity as a result of laser light irradiation at 1550 nm wavelength. The experimental setup was based on the continuous ELM-1550-5-LP fiber laser (IPG Photonics, IRE-Polus, Russia) and microscope stage THMS600 (Linkam Scientific Instruments, UK) with temperature control. Sample resistivity was measured using Keithley 6430 sub-femtoamp Remote SourceMeter (Keithley, USA). The measurements were carried out in the temperature range from -175°C to room temperature. Additional precautions were made to take into account the influence of sample heating during laser light irradiation on resistivity change. Preliminary measurements of temperature dependence of samples resistivity have revealed the appearance of dopant levels with depth about 0.15-0.2 eV.

We have revealed that laser light irradiation leads to up to 17% decrease of sample resistivity at room temperature. It should be noted that the highest resistivity change was observed for the samples hyperdoped using 20-nm-thick Au films. The decrease of sample temperature leads to strong increase of the photoresponse resulting in 20-fold decrease of sample resistivity for temperature -175°C.

The possible mechanisms of hyperdoping film thickness influence on the Au-hyperdoped Si are discussed. Obtained results pave the way towards reproducible creation of reliable and cost-effective Au-hyperdoped Si detectors for the near infrared range.

Multilayer polymer microoptical elements in solid porous silicon dioxide made by two-photon lithography

T. Baluian[1,2*], D. Pechkurova[1], A. Fedyanin[1]

1- Lomonosov Moscow State University, Department of Physics. 119991, Russia, Moscow, GSP-1, Leninskie gory 1
2- MSU-BIT University Shenzhen, Department of Materials Science, Shenzhen 517182, P.R.C.

* baluyan@nanolab.phys.msu.ru

Modern microoptical devices, especially designed for endoscopic applications and integrated photonics, require high manufacturing accuracy and demand precise alignment. Both of these problems are hard to solve due to small feature size of the optical elements. First problem may be overpassed by applying modern manufacturing techniques, such as two-photon lithography. Two-photon lithography is a precise direct writing method that provides enough accuracy to produce well-shaped microlenses and diffraction elements, for example the microlens was printed directly on the endoscopic fiber in [1]. However, it is still challenging to produce multilayer optics like objectives or multilayer constructions for diffraction neural networks [2] in free space due to structure damage during development. One of the ways to overcome this difficulty is based on using the solid matrix to print elements in. In this work we printed various microoptical elements in the solid matrix of porous silicon dioxide.

Porous silicon dioxide is well-suited for visible light applications due to opacity and low refractive index: it may vary from 1.1 to 1.47 dependent on the pore average size and distribution. We used porous silicon dioxide with average pore size of 40 nm and 80% porosity. The resulting refractive index was 1.14. Pores were filled with OrmoComp photoresist with approximate refractive index 1.51 using the vacuum chamber. After photoresist deposition, we used self-assembled two-photon lithography setup with 780 nm wavelength laser to print various optical elements in the porous silicon dioxide matrix. We also modernised the resist developing technique in order to completely remove non-polymerised photoresist and developer from the nanoscale pores to preserve matrix opacity.

As a result we demonstrate various optical elements printed in the porous silicon dioxide including diffraction grating, set of micro lenses and multilayer masks for visible range diffraction neural networks. It proves that porous silicon dioxide combined with two-photon lithography provides an opportunity to create easy to use compound optical elements that might be integrated with different optical systems.

[1] T. Gissibl, S. Thiele, A. Herkommer, H. Giessen, Nat. Photon. 2016, 10, 554.
[2] B. Bai, et al, To image, or not to image: class-specific diffractive cameras with all-optical erasure of undesired objects, eLight. – 2022. – Vol. 2. – №. 1. – P. 14.

Novel approaches to chiral meta-mirrors, asymmetric cavities, and polaritons

D.G. Baranov[1]

1- Center for Photonics and 2D Materials, Moscow Institute of Physics and Technology,
Dolgoprudny 141700, Russia

Geometrical chirality is a universal phenomenon that surrounds us on many different length scales ranging from geometrical shapes of various living organisms to DNA and drug molecules. The majority of molecules involved in biological processes are chiral. Acting on a biological receptor, opposite enantiomers of the same molecule cause different response, perceived as different odor or taste. In pharmaceutics, the opposite enantiomer of a drug molecule can be useless at best, but often it is toxic for the chiral human body. In this regard, there is a great demand from the pharmaceutical industry to develop effective methods of separating chiral enantiomers.

Interaction of chiral matter with circularly polarized electromagnetic fields leads to the effect of circular dichroism, which underlies numerous methods for distinguishing molecular enantiomers. However, those interactions are usually weak and can be well understood without the need to consider a correlated motion between light and matter. If and how strong light-matter interaction can aid those challenging tasks remained largely unclear thus far.

In this talk, I will overview the fundamentals of chirality of light and matter, present optical designs required for realization of chiral polaritonic states, discuss recently developed theoretical models, and speculate on the exciting phenomena that can be enabled by strong coupling between chiral light and matter [1,2]. Recent theoretical efforts indicate that chiral polaritonic systems may feature non-trivial optical phenomena, where the interplay of light and matter chirality plays the key role in determining the eigenfunctions of the system, as well as its response to external electromagnetic fields [3,4]. Finally, I will present how van der Waals technology can be utilized to assemble helical homostructures with chiral properties without the necessity for sophisticated nanofabrication techniques [5]. The proposed strategy is based on the formation of twisted helical van der Waals homostructures with chiral arrangement of biaxial films.

[1] D.G. Baranov, B. Munkhbat, N.O. Länk, R. Verre, M. Käll, T. Shegai, Nanophotonics 9, 283 (2020).
[2] K. Voronin, A.S. Taradin, M.V. Gorkunov, D.G. Baranov, ACS Photonics 9, 2652 (2022).
[3] C. Schäfer and D.G. Baranov, J. Phys. Chem. Lett. 14, 3777 (2023).
[4] D.G. Baranov, C. Schäfer, M.V. Gorkunov, ACS Photonics 10, 2440 (2023).
[5] K.V. Voronin, A.N. Toksumakov, G.A. Ermolaev, A.S. Slavich, M.K. Tatmyshevskiy, S.M. Novikov, A.A. Vyshnevyy, A.V. Arsenin, K.S. Novoselov, D.A. Ghazaryan, and others, Laser & Photonics Reviews, 2301113 (2024).

Semiconductor nanowires for integrated and nonlinear photonics

A. Bolshakov[1]

1- Centre for Photonics and Two-Dimensional Materials, Moscow Institute of Physics and Technology,
141701 Dolgoprudny, Russia

bolshakov@live.com

Here we utilize and explore epitaxial gallium phosphide (GaP) nanowires (NWs) as a platform for integrated nanophotonics. We highlight the unique properties of GaP NWs, such as high crystallinity, mechanical strength, low optical losses, and a high refractive index, which make them ideal candidates for developing photonic devices.

First, the presented research investigates the waveguiding capabilities of GaP NWs, both theoretically and experimentally, demonstrating their ability to support waveguiding modes throughout the visible and near-IR ranges. The study explores the limitations of waveguiding in GaP NWs, particularly focusing on the lateral dimensions of waveguides for a given wavelength range.

Additionally, the manuscript delves into the practical applications of GaP NWs in developing advanced photonic elements, such as optical couplers, and discusses the potential pathways for their integration into integrated optical circuits and logic elements. We provide insights into the design and fabrication processes utilizing GaP NWs and highlight their potential for future computing applications.

The optomechanical manipulation and optical characterization was performed with single GaP NWs as promising platform for future nanophotonic circuitry. The study investigates the nonlinear generation efficiency of optically trapped GaP NWs, considering their geometry and SH response. Experimental and theoretical analyses provide insights into phase-matching conditions and optimization strategies for NW geometries in optoelectronic applications. Various optical signals are utilized for comprehensive characterization, including a wideband supercontinuum white laser for linear spectroscopy and a femtosecond infrared source for trapping and second harmonic generation. This research sheds light on the potential of GaP NWs for integrated photonics devices and demonstrates the impact of geometry on nonlinear optical properties, paving the way for advanced nanophotonic applications.

Overall, this manuscript contributes to the growing field of integrated nanophotonics by showcasing the unique capabilities of GaP NWs and opening up new possibilities for the development of photonic devices and circuits.

Fizeau fringes in resonant photonic structures with spatially varying parameters

D.A. Bykov[1,2*], **E.A. Bezus**[1,2], **L.L. Doskolovich**[1,2]

1- Samara National Research University, 34 Moskovskoye shosse, Samara, 443086, Russia
2- Image Processing Systems Institute, NRC "Kurchatov Institute", 151 Molodogvardeyskaya st., Samara, 443001, Russia

* bykovd@gmail.com

Fizeau interferometer is a Fabry-Pérot interferometer with a wedged central layer (Fig. 1a). Resonant transmission in such structures occurs at different spatial positions depending on the wavelength of the incident light. This allows one to divide the incident radiation into a large number of spectral channels. In this regard, nowadays, such structures are usually referred to as linear variable filters (LVFs) and are used in spectrometers and refractive index sensors [1]. When both the wedge angle and the reflection coefficients of the interfaces are quite large, the spatial profile of the resonant peak has a characteristic non-symmetric shape containing the main peak and several secondary peaks. Resonant peaks with such shape are sometimes referred to as Fizeau fringes. Taking this effect into account is important when designing compact optical filters [1].
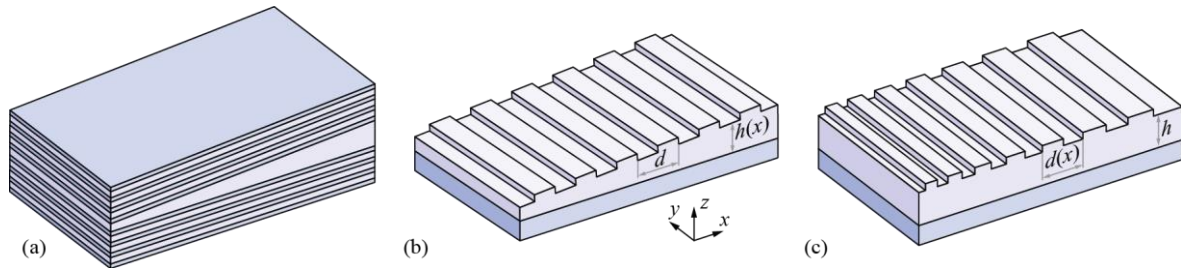
Fig. 1. LVF based on Fizeau interferometer (a) and considered GMRGs with varying thickness (b) and period (c).

In this work, we show that similar effects arise in guided-mode resonant gratings (GMRGs) with varying period (Fig. 1c) as well as in GMRGs with varying thickness of the waveguide layer (Fig. 1b). Such structures can also be used as filters in spectrometric optical systems [2]. To describe the appearance of the Fizeau fringes in GMRGs, we developed a spatiotemporal coupled-mode theory (CMT). Such theory is written as two coupled nonuniform unidirectional wave equations [3]. Importantly, all parameters of the proposed CMT – the coupling coefficients – can be obtained by analyzing a strictly periodic GMRG with constant parameters. We show that the CMT predictions are in perfect agreement with the results of rigorous solution of Maxwell's equations using the superperiod approach incorporated into the Fourier modal method. By solving the plane wave diffraction problem, we calculated the reflected and transmitted field distributions exhibiting pronounced Fizeau-like fringes with the main peak accompanied by several secondary peaks. In contrast to the conventional Fizeau interferometer, in which secondary peaks appear on one side of the main peak, in GMRGs the secondary peaks may appear on both sides.

Interestingly, a similar CMT can also be developed for a conventional Fizeau interferometer, e.g., for a wedge with Bragg claddings shown in Fig. 1a. In this case, the coupled-mode theory is written as a second-order partial differential equation. The obtained results can be used to design linear variable filters based on GMRGs as well as for the design of optical resonators, in which the parameters of the structure vary in space in a nonlinear fashion.

[1] R.R. McLeod, T. Honda, Improving the spectral resolution of wedged etalons and linear variable filters with incidence angle, Opt. Lett., vol. 30, pp. 2647–2649 (2005).
[2] H.-Y. Hsu, Y.-H. Lan, C.-S. Huang, A gradient grating period guided-mode resonance spectrometer, IEEE Photon. J., vol. 10, p. 4500109 (2018).
[3] D.A. Bykov, E.A. Bezus, A.A. Morozov, V.V. Podlipnov, L.L. Doskolovich, Optical properties of guided-mode resonant gratings with linearly varying period, Phys. Rev. A, vol. 106, p. 053524 (2022).

2D materials for quantum applications

E. Chiglintsev[1,2], E. Barulina[1], A. Shupletsov[1], <u>A. Chernov</u>[1,2*]

1- Russian Quantum Center, Skolkovo Innovation City, Moscow 121205, Russia
2- Center for Photonics and 2D Materials, Moscow Institute of Physics and Technology
(National Research University), Dolgoprudny 141700, Russia

* ach@rqc.ru

Two-dimensional materials have attracted much attention due to various opportunities for applications. In example, optical properties of transition metal dichalcogenides monolayers can be controlled by several approaches, including via induced interface interaction with magnetic materials [1]. Moreover, the approach of constructing of layered monolayers one on another opened the new routes for advanced devices.

Enhanced infrared photodetection in graphene-based heterostructures due to tunneling barriers has been recently demonstrated [2]. Small-angle twisted bilayer graphene (tBLG) has also attracted much attention due to appearance of low-energy flat bands of the emerging moiré superlattice [3]. Strong electron-electron interactions within the bands lead to correlation-driven phenomena, realization of correlated phases, and result in new devices. We have performed the photoresponse measurements at $5 - 10$ μm in the tBLG, where the mis-orientation angle is close to the magic one. We detect the enhanced photoresponse compared to the previous works and reveal the polarization dependence.

Finally, twisted heterostructures are important for creation of quantum simulator to study the Hubbard model physics.

[1] V. Kravtsov, T. Ivanova, A.N. Abramov, P.V. Shilina, P.O. Kapralov, D.N. Krizhanovskii, V.N. Berzhansky, V.I. Belotelov, I.A. Shelykh, A.I. Chernov, I.V. Iorsh, Valley polarization of trions in monolayer $MoSe_2$ interfaced with bismuth iron garnet, 2D Materials, 9(1), p.015019, (2021).
[2] D.A. Mylnikov, M.A. Kashchenko, K.N. Kapralov, D.A. Ghazaryan, E.E. Vdovin, S.V. Morozov, K.S. Novoselov, D.A. Bandurin, A.I. Chernov, D.A. Svintsov, Infrared photodetection in graphene-based heterostructures: bolometric and thermoelectric effects at the tunneling barrier, npj 2D Materials and Applications, 8(1), p.34, (2024).
[3] S. Bhowmik, A. Ghosh, U. Chandni, Emergent phases in graphene flat bands, arXiv preprint arXiv:2309.08938, (2023).

Highly regular nanogratings on metal and amorphous semiconductor thin films: diversity of formation mechanisms, properties and applications

K. Bronnikov[1,2], V. Terentiev[2], V. Simonov[2], V. Fedyaj[2,3], S. Babin[2,3], A. Zhizhchenko[4], A. Kuchmizhak[4,5], A. Dostovalov[2]*

1- School of Physics and Engineering, ITMO University, 191002 St. Petersburg, Russia
2- Institute of Automation and Electrometry of the SB RAS, 1 Acad. Koptyug Ave., 630090 Novosibirsk, Russia
3- Novosibirsk State University, 630090 Novosibirsk, Russia
4- Institute of Automation and Control Processes of the FEB RAS, 5 Radio St., 690041 Vladivostok, Russia
5- Far Eastern Federal University, 690041 Vladivostok, Russia

* dostovalov@iae.nsk.su

During the last decades, the phenomenon of laser-induced periodic surface structures (LIPSS) formation under the impact of laser radiation with high intensity has been extensively studied in case of nearly all types of materials [1]. Due to a vacuum-free, single step and low-cost approach with a possibility to control structures morphology and optical properties, surface nanostructuring based on LIPSS has already found the applications in photonics, biomedicine, tribology and sensing. Recently, a new type of LIPSS called "thermochemical LIPSS" (TLIPSS) was discovered as a result of laser-driven chemical reaction of oxidation on the surface of titanium thin films [2]. The outstanding regularity of the structures obtained in the ablation-free process on a large scale stimulated the further research in this area.

In this work we review our recent results on TLIPSS formation in the case of femtosecond laser radiation impact on thin metal films of Ti, Hf, Al and Cr, as well as amorphous thin films of semiconductors (Si and Ge). In particular, sub-wavelength ($\lambda/1.5$) periodic surface structures were obtained on the mentioned above metal thin films in a broad range of experimental parameters (pulse energy, processing speed) possessing high regularity of the structures (deviation of angle orientation DLOA<2°) with a throughput up to 0.2 mm^2/s [3]. The influence of ambient atmosphere on a chemical reaction of oxidation and hence the morphology of obtained structures was also investigated [4]. In the case of amorphous semiconductors thin films, the new regimes of TLIPSS formation accompanied by laser-induced crystallization process in the case of Si [5] and oxide sublimation in the case of Ge thin films were revealed [6].

Moreover, the results of creation of structures with 2D periodicity in the different strategies of surface processing are shown. More specifically, regular square and hexagonal 2D structures depending on processing parameters were produced on Ti thin films providing the way for diffractive optical elements inscription based on this approach.

[1] J. Bonse, et al, Handbook of Laser Micro- and Nano-Engineering (Springer International Publishing), Laser-Induced Periodic Surface Structures (LIPSS), (2020).

[2] B. Öktem, et al, Nonlinear laser lithography for indefinitely large-area nanostructuring with femtosecond pulses, Nature Photonics, 7, 897–901 (2013).

[3] D. A. Belousov, et al, Thermochemical Laser-Induced Periodic Surface Structures Formation by Femtosecond Laser on Hf Thin Films in Air and Vacuum, Materials, 14, 6714 (2021).

[4] K. Bronnikov, et al, Regulating Morphology and Composition of Laser-Induced Periodic Structures on Titanium Films with Femtosecond Laser Wavelength and Ambient Environment, Nanomaterials 12, 306 (2022).

[5] A. Dostovalov, et al, Hierarchical anti-reflective laser-induced periodic surface structures (LIPSSs) on amorphous Si films for sensing applications, Nanoscale 12, 13431–13441 (2020).

[6] K. Bronnikov, et al, Highly regular nanogratings on amorphous Ge films via laser-induced periodic surface sublimation, Optics & Laser Technology 169, 110049 (2024).

Study on dynamic photo-thermal regulation of vanadium dioxide

S. Dou[1*], H. Wei[1], F. Ren[2], J. Gu[2], Y. Li[1,2]

1- Center for Composite Materials and Structure, Harbin Institute of Technology, Harbin 150001
2- Suzhou Laboratory, Suzhou 215123, China

* dousl@hit.edu.cn

VO_2 has received much attention because of its unique metal-insulator phase transition. Based on VO_2 thermotropic phase change materials, this paper introduces the dynamic electromagnetic regulation of VO_2 in the vision-microwave band. By constructing different optical devices, the ultra-wide spectrum electromagnetic wave of visible, near infrared, middle infrared and even terahertz microwave can be dynamically regulated. Combined with solar radiation and blackbody radiation energy distribution, the regulation of solar radiation and infrared radiation energy is realized, and its application prospects in intelligent window, intelligent thermal control and infrared adaptive camouflage are introduced. VO_2 has received much attention because of its unique metal-insulator phase transition. Based on VO_2 thermotropic phase change materials, this paper introduces the dynamic electromagnetic regulation of VO_2 in the vision-microwave band. By constructing different optical devices, the ultra-wide spectrum electromagnetic wave of visible, near infrared, middle infrared and even terahertz microwave can be dynamically regulated. Combined with solar radiation and blackbody radiation energy distribution, the regulation of solar radiation and infrared radiation energy is realized, and its application prospects in intelligent window, intelligent thermal control and infrared adaptive camouflage are introduced.

[1] H. Wei, S. Dou, Y. Li, et al, Light: Science & Applications (2024) 13:54.
[2] J. Gu, S. Dou, Y. Li, ACS Appl. Mater. Interfaces 2024, 16, 10352−10360.

Laser-based preparation of simple and complex oxide nanoparticles for photocatalytic applications

E. Fakhrutdinova[*], **A. Golubovskaya, A. Volokitina, O. Reutova, V. Svetlichnyi**

National Research Tomsk State University, 634050 Tomsk, Russia

* fakhrutdinovaed@gmail.com

Photocatalytic technologies for the safe purification and disinfection of water, the production of environmentally friendly fuel and the conversion of biomass into useful products are among the most in demand today [1]. Therefore, the development of safe, simple and effective methods for the synthesis of photocatalytic systems with controlled characteristics is an urgent task. Along with traditional chemical approaches, methods based on high-energy exposure hold great promise in photocatalysis. The use of pulsed laser ablation (PLA) of chemically active targets in a liquid with combination additional laser treatment of colloids of focused laser radiation with the formation of plasma makes it possible to create conditions for the formation of new phases and complex defect structures that are inaccessible to chemical synthesis methods. Freshly prepared PLA colloids have high activity, which also makes it easy to obtain new highly dispersed composite materials.

In the work, PLA targets (Ti, Zn, Bi, Si) using a Nd:YAG laser ($\lambda = 1064$ nm, $\tau = 7$ ns, $E_{imp} = 150$ mJ, $f = 20$ Hz) were obtained as simple (TiO_2, ZnO), and complex oxides ($Bi_{12}SiO_{20}$), which have high photocatalytic activity.

Dark TiO_2 obtained by PLA, due to the presence of a large number of defects (oxygen vacancies/Ti^{3+} ions), absorbs in the visible region of the spectrum [2] and exhibits high activity in the process of photocatalytic hydrogen evolution from a water-glycerol mixture. Additional modification of dark TiO_2 with metals (Pt, Cu) increases the apparent quantum yield (AQY) to 0.78 for Pt and 0.32 for Cu, respectively.

PLA ZnO also has a highly defective structure and exhibits good antibacterial activity, which increases upon irradiation due to the photogeneration of reactive oxygen species (ROS). It was found that with a minimum loading of ZnO NPs – 0.05 g/l, there is a decrease in the active growth of *S. aureus* bacteria in the nutrient medium and 100% death of *S. aureus* in the buffer medium under the soft UV (375 nm) irradiation. Under visible light (410 nm) irradiation, we achieved 100% death of bacteria within 2 hours of irradiation, and additional modification of zinc oxide with Ag NPs significantly accelerates the death of *S. aureus* even with a decrease in irradiation power.

The combination of PLA with laser irradiation of a mixture of colloids in plasma mode was used to obtain a complex oxide with the composition $Bi_{12}SiO_{20}$. The material contains a small amount of $Bi_2(CO_3)O_2$ impurity, which is also a photocatalytically active phase. These systems are effective in the photodegradation of persistent model pollutants – Rhodamine B dye and phenol. Under LED 375 nm irradiation, in both cases, complete decomposition of the aromatic rings occurs. The resulting materials also demonstrate high stability in cyclic tests [3].

[1] R.C. Forsythe, C.P. Cox, et al, Pulsed Laser in Liquids Made Nanomaterials for Catalysis Chem. Rev. 121, 7568−7637 (2021).
[2] E.D. Fakhrutdinova, A.V. Shabalina, et al, Highly defective dark nano titanium dioxide: preparation via pulsed laser ablation and application, Materials, 13, 1–17 (2020).
[3] A.G. Golubovskaya, D.A. Goncharova, et al, Photocatalytic activity of colloidal Bi–Si-based nanoparticles prepared by laser synthesis in liquid Mater Chem and Phys. 314, 128800 (2024).

Goos-Hänchen shift spatially resolves magneto-optical Kerr effect enhancement in magnetoplasmonic crystals

A.Yu. Frolov[1*], A.V. Makarova[1], A.A. Nerovnaya[1], D.N. Gulkin[1], V.V. Popov[1], A.A. Fedyanin[1]

1- Faculty of Physics, Lomonosov Moscow State University, Moscow 199991, Russia

* frolovay@my.msu.ru

Active control of the optical properties offers significant opportunities for applying optical devices in optical communications and computing. The magnetic field provides a versatile way to control light properties through well-known magneto-optical effects such as the Kerr and Faraday effects. They present a change in the intensity, polarization, and phase of light under an external magnetic field. However, the use of magneto-optical effects in light modulators is only possible with large-scale magnetooptical elements, due to the inherent small values of these effects.

The excitation of the surface plasmons (SPs), which are coupled oscillations of free electrons and light, can significantly enhance the magnitudes of magneto-optical effects and shrink the size of the magneto-optical elements to the nanoscale [2]. This is made possible by magnetoplasmonic crystals (MPCs), which are one- or two-dimensional, periodically structured surfaces or arrays of plasmonic nanoantennas, containing magnetic materials. However, in most studies on the resonant enhancement of magneto-optical effects, the spatial distribution of the reflected light intensity is not taken into account. In turn, reflected light can possess the Goos-Hänchen (GH) effect, which manifests itself as a lateral displacement of the reflected beam compared to the position determined by geometrical optics.

In this work, we have demonstrated that the application of a magnetic field in a transverse geometry results in a modulation of the spatial distribution of the light intensity of reflected beams in one-dimensional nickel magnetoplasmonic crystals (Figure 1) [3]. When the surface plasmon of the -1st order is excited, the Goos-Hänchen effect occurs, resulting in two reflected light beams that are separated by a distance d. It reaches d=15.3 μm (18λ). The application of a transverse magnetic field resulted in the modulation of the spatial distribution of reflected light intensity, as shown by the red and yellow curves. The observed change in the spatial distribution of light intensity under an external transverse magnetic field is referred to as the spatially resolved transverse magneto-optical Kerr effect [TMOKE(x)], which is defined as:

$$\text{TMOKE}(x) = 2\frac{I(x,+H) - I(x,-H)}{I(x,+H) + I(x,-H)} \times 100\% \, ,$$

where I(x,+H) and I(x,-H) are the spatial distributions of the reflected light intensity in the presence of an external transverse magnetic field in the opposite directions, respectively. We show that the observed lateral variation in intensity [TMOKE(x)] is several times greater (2.6 times) than in the case of conventional TMOKE measurements, which reveal the total change in reflected beam intensity under a magnetic field.
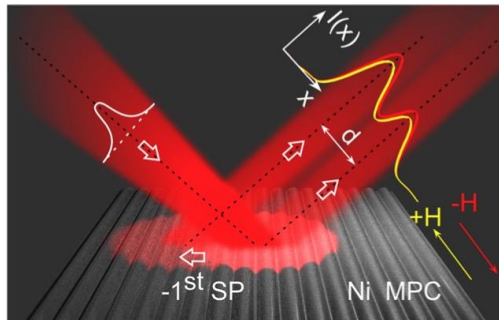

Fig. 1. The idea of the observation of the spatially resolved transverse magneto-optical Kerr effect [TMOKE(x)] under the Goos-Hänchen shift in a one-dimensional nickel magnetoplasmonic crystal.

[1] A.K. Zvezdin and V.A. Kotov, Modern Magnetooptics and Magnetooptical Materials (CRC Press) (1997).
[2] J. Qin, et al, Nanophotonic devices based on magneto-optical materials: recent developments and applications, Nanophotonics, vol. 11, pp. 2639−2659 (2022).
[3] A.V. Makarova, et al, Goos-Hänchen shift spatially resolves magneto-optical Kerr effect enhancement in magnetoplasmonic crystals, vol. 11, pp. 1619-1626 (2024).

Dielectric nanostructures for efficiency improvement of perovskite solar cells

A. Furasova[1*], S. Makarov[1,2]

1- The School of Physics and Engineering, ITMO University, Saint-Petersburg, Russia
2- Qingdao Innovation and Development Center, Harbin Engineering University, Qingdao 266000, Shandong, China

* *aleksandra.furasova@metalab.ifmo.ru*

Dielectric nanostructures are widely used to protect perovskite solar cells (PSCs) from ion migration between functional layers, improve charge transport properties through band alignment engineering or are aimed to increase a light harvesting inside thin-film devices [1-3]. Today many researchers have made many attempts to combine these approaches to increase J-V parameters for PSCs and make their novel developments more universal for various photoactive semiconductors of solar cells. Moreover, different methodologies are proposed to create nanofabrication, nanotexturing and nanostructuring in a large scale via laser-assisted techniques [4].

Dielectric Mie-resonant nanoparticles (NPs) is a powerful technology for light control at the nano- and microscale, which have been experimentally employed for a plenty of applications as high-speed and low-power consumption electro-optic modulators [5], modern nanolenses, where the size and shape of dielectric nanoarray plays a crucial role in the device performance. Moreover, we have recently shown that Silicon NPs are successfully used for the improvement of PSCs via light harvesting effect in a perovskite [6]. To synthesize these resonant NPs a femtosecond laser ablation is considered as a perfect method to prepare well-crystalline spherical samples with low impurities in a large-scale production with size distribution of 70-270 nm [6]. These particles can resonantly scatter the incident light in a broad-spectrum range. However, for PSCs with 1.4-1.8 eV of a band gap this wide size distribution is not useful and it is better to harvest the light where the own perovskite light absorption is low.

In our research we apply monodisperse silicon NPs which have been separated by a density gradient method after a laser ablation synthesis [7] to investigate optical effects responsible for the efficiency improvement of PSCs. The experimental analysis shows that the most optimal sizes of Si NPs for the mixed perovskite $FAMAPbICl_3$ (bandgap is 1.53 eV) are in the range 140–160 nm. In this case the optimization of absorption in the perovskite layer is around 500–800 nm range, where the Mie resonances in NPs are not completely damped but contribute to additional light trapping and scattering. By several theoretical approaches we have designed a cell with optimized light energy harvesting, leading to improvement of both short circuit current $J_{SC} \approx 1.2$ mA/cm^2 and open circuit voltage $V_{OC} \approx 0.02$ V. The highest achieved efficiency was 20.5% when solar cells included Si NPs with size of 150–170 nm. The fill factor (FF) was 79.4%, $J_{SC} = 23.77$ mA/cm^2 and $V_{OC} = 1.107$ V. A standard solar cell had a maximum 18.99% of efficiency with J_{SC} of 22.62 mA/cm^2 and V_{OC} of 1.089 V, at the same time, whereas FF value is almost unchanged (79.8%).

Our results can be useful not only for further optimization of perovskite solar cells, but also pave the way for improvement of a broader range of photovoltaic devices with integrated Mie-resonant NPs.

[1] Z. Huang, et al, Suppressed ion migration in reduced-dimensional perovskites improves operating stability, ACS Energy Letters 4.7 (2019): 1521-1527.
[2] A. Yakusheva, et al, Photo Stabilization of p-i-n Perovskite Solar Cells with Bathocuproine: MXene, Small 18.37 (2022): 2201730.
[3] A. Furasova, et al, Nanophotonics for perovskite solar cells, Advanced Photonics Research 3.9 (2022): 2100326.
[4] P.A. Dmitriev, et al, Laser fabrication of crystalline silicon nanoresonators from an amorphous film for low-loss all-dielectric nanophotonics, Nanoscale 8.9 (2016): 5043-5048.
[5] L. Ding, et al, Silicon Nanoantennas for Ultra-Compact, High-Speed and Low-Power Consumption Electro-Optic Modulators, Laser & Photonics Reviews (2024): 2301068.
[6] A. Furasova, et al, Resonant silicon nanoparticles for enhanced light harvesting in halide perovskite solar cells, Advanced Optical Materials 6.21 (2018): 1800576.
[7] A. Furasova, et al, Photovoltaic parameters improvement via size control of monodisperse Mie-resonant nanoparticles in perovskite solar cells, Chemical Engineering Journal (2024): 152771.

InGaN nanowires: MBE growth, physical properties and application

V.O. Gridchin[1-3*], **R.R. Reznik**[1-3], **G.E. Cirlin**[1-3]

1- Alferov University, Saint Petersburg, Russia
2- Saint Petersburg State University, Saint Petersburg, Russia
3- Institute for Analytical Instrumentation, Saint Petersburg, Russia

* gridchin@spbau.ru

Nowadays, significant research attention is focused on semiconductor nanowires (NWs). The rapid development of this field is supported by the fact that semiconductor materials in the NW structure can be synthesized with a crystalline quality that is an order of magnitude higher than the quality of the corresponding epitaxial layers and on the lattice-mismatched substrates with respect to the growing material, in particular, silicon. In this way, InGaN ternary compounds are being actively studied direct bandgap semiconductor materials, the band gap of which can be varied in the range from 0.7 to 3.4 eV by changing the indium mole fraction. Today, InGaN finds its application in advanced optoelectronic devices of visible spectral range, such as RGB micro- and nano- light emitting diodes. However, due to the significant mismatch of lattice constants between InN and GaN, InGaN towards to phase decomposition over almost the entire chemical range. In the case of epitaxial layers, this difficulty often leads to the uncontrolled formation of areas with high and low indium content and poor crystal and optical quality. But in the case of the NW growth, it is possible to fabricate novel nanoheterostructures, such as NWs with a spontaneously formed core-shell structure with a high In content in the cores [1], the study of the properties of which is of scientific and practical interest.

This work is devoted to an experimental study of the growth of InGaN NWs using plasma-assisted molecular beam epitaxy, the fabrication of nano- light emitting diodes based on the obtained NWs, and the study of the physical properties of the grown nanostructures. It has been established that InGaN NWs with a spontaneously formed core-shell structure and a high In content are formed at relatively high growth temperatures, exceeding the decomposition temperatures of InN in vacuum [2]. In this case, the In content inside NWs can be varied in the range of 30-45% by unsufficient reducing the growth temperature, which is explained by a decrease in In desorption from the growth surface. The influence of the III/V flux ratio on the formation of NWs has been studied and it has been shown that for their formation in the core-shell structure it is necessary to maintain the III/V flux ratio near 1, taking into account the desorption of In from the growth surface. A relationship was revealed between the In content, growth conditions, and optical properties of NWs. The possibility of creating nano- light emitting diode structures with a blue-green emission spectrum based on p-i-n structures consisting of GaN/InGaN NWs with bulk InGaN inserts has been demonstrated.

The results obtained can be used in the development of RGB diodes on silicon and in studying the growth processes of spontaneously formed nanoheterostructures in NWs based on ternary compounds.

[1] V.O. Gridchin, K.P. Kotlyar, R.R. Reznik, A.S. Dragunova, N.V. Kryzhanovskaya, V.V. Lendyashova, D.A. Kirilenko, I.P. Soshnikov, D.S. Shevchuk, G.E. Cirlin, Multi-colour light emission from InGaN nanowires monolithically grown on Si substrate by MBE, Nanotechnology, vol. 32, pp. 335604, (2021).
[2] G. Koblmüller, C. S. Gallinat, J. S. Speck, Surface kinetics and thermal instability of N-face InN grown by plasma-assisted molecular beam epitaxy, Journal of Applied Physics, vol. 101, pp. 083516, (2007).

Multi-level phase transitions in GST225 thin film coated on a fiber end face

D. Guryev[1*], I. Zhluktova[1], V. Kamynin[1], P. Lazarenko[2], D. Terekhov[2], S. Kozyukhin[3], V. Tsvetkov[1]

1- Prokhorov General Physics Institute of the Russian Academy of Sciences, Moscow, Russia
2- National Research University of Electronic Technology, Moscow, Russia
3- Kurnakov Institute of General and Inorganic Chemistry of the Russian Academy of Sciences, Moscow, Russia

* guryevden@gmail.com

Phase-change materials (PCMs) are ideal candidates for nonvolatile memories, in particular, the $Ge_2Sb_2Te_5$ (GST225) has the best performance in terms of speed and stability. Also, GST225 have large contrast in electrical/optical properties between the crystalline state and the amorphous state, furthermore, it has been shown that GST225 has opportunity to procced partial phase transitions (multi-level transitions) [1]. This is a good opportunity for producing all-optical devices for logic computing [2].

In this work, we have demonstrated an all-fiber system for performing and observing phase transitions in a GST225. The endface of a SMF28 fiber (core diameter 9 μm) was coated with GST225 film by magnetron sputtering of $Ge_2Sb_2Te_5$ polycrystalline target. According to the results of atomic force microscopy the film thickness was 458 nm.

An all-fiber system was assembled to perform phase transitions in the GST225 film and to observe the change in the optical properties of GST (fig. 1(a)). A pulsed amplified fiber laser [3] operating at a wavelength of 1070 nm was used as the writing laser. The repetition rate of the writing pulses was 1 MHz, the pulse energy could be varied from 1 to 14 nJ, and the pulse duration was ≈ 50 ps. A single pulse from a pulse train, or several pulses with a repetition rate of 1 MHz (fig. 1(c)), could be extracted with the acousto-optic modulator (AOM). Continuous-wave laser diode with a wavelength of 1550 nm and emission power < 4 mW was used as the probe laser.
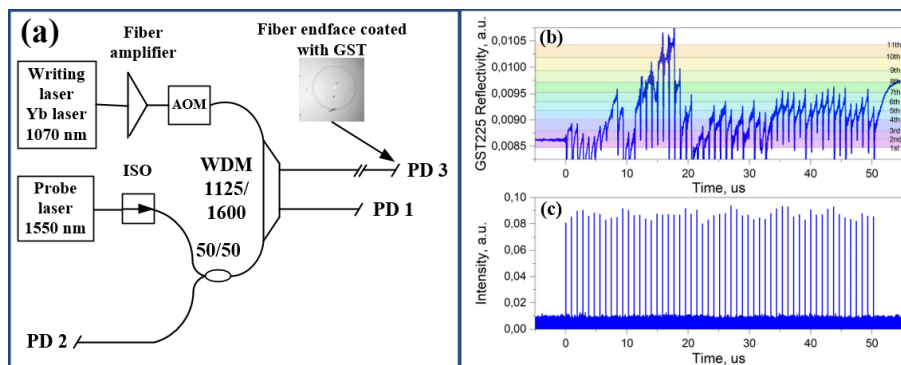

Figure 1. (a) – Scheme of the experimental setup: ISO – optical isolator, AOM – acousto-optic modulator, WDM – wave division multiplexer, PD 1-3 – photodetectors connected with fiber endfaces; PD 1 – registering of writing pulses; PD 2 – registering of the probe laser radiation reflected from the GST sample; PD 3 – registering of the probe radiation passed through the GST225 film; (b) – oscilloscope trace of the reflected radiation of the probe laser; (c) – oscilloscope trace of a series of writing pulses.

We were able to observe partial phase transitions (partial crystallization or partial amorphization) due to changes in film reflectance (increased reflectance-crystallization, decreased reflectance-amorphization). The possibility of multi-level phase transition (> 10 reflection levels) was also demonstrated due to the effect on the film of several consecutive writing pulses (fig. 1(b)).

This research may be useful for the development of optical modulators compatible with fiber systems and integrated circuits. In particular, this research may be useful for the development of all-fiber circuits for all-photonic computing, information storage and logic elements.

[1] G.P. Lazarenko, et al, Low power reconfigurable multilevel nanophotonic devices based on Sn-doped $Ge_2Sb_2Te_5$ thin films, Acta Materialia, vol. 234, pp. 117994, (2022).
[2] Z. Liu, et al, Intelligent all-fiber device: storage and logic computing, Photon. Res., vol. 10 (1), pp.357-363, (2022).
[3] I. Zhluktova, S. Filatova, A. Trikshev, V. Kamynin, V. Tsvetkov, All-Fiber 1125 Nm Spectrally Selected Subnanosecond Source, Appl. Opt., 59, pp. 9081, (2020).

In-situ laser-assisted turning of particle-reinforced aluminum matrix composites technology

W. Hu[1*], J. Zhang[1]

1- Center for Precision Engineering, Harbin Institute of Technology, Harbin, 150001, China

* hwj1995matt@gmail.com

While particle-reinforced aluminum matrix composites (PRAMCs) hold great promise for thermal management in electronic devices and the lightweighting of advanced structural components, achieving high-quality surfaces of PRAMCs is challenging due to the significant differences in physical and mechanical properties between the ductile matrix and the brittle particles, which leads to substantial surface damage and tool wear during machining. In this study, we propose a processing strategy of *in-situ* laser-assisted turning (In-LAT) that couples laser irradiation with diamond cutting to regulate the machining deformation behavior of PRAMCs. First, an optical analysis of the laser beam propagation within the diamond tool is conducted to determine optimal laser incidence parameters. Furthermore, a thermal model of SiCp/Al composites under turning conditions is developed to predict the impact of the laser beam on the composite's temperature field during In-LAT. Based on the optical-thermal analysis, an In-LAT device is setup and then cutting experiment of In-LAT of SiCp/Al composites is performed. The experimental results demonstrated a 60% reduction in surface roughness (Sa) of the SiCp/Al composites by In-LAT compared to ordinary turning. Current work provides a feasible method for achieving low-damage, high-quality surface in the machining of PRAMCs.

Tunable metasurface for ultrafast Fourier filtering

V.V. Yuskov[1*], P.D. Kiryanov[1], V.A. Sitnyanski[1], A.S. Shorokhov[1], A.A. Fedyanin[1]

1- Faculty of Physics, Lomonosov Moscow State University, Moscow 119991, Russian Federation

* iushkov@physics.msu.ru

Due to the limitations of the electronic devices for information processing, approaches allowing analog processing in optics are being investigated [1-3]. The most traditional approaches are the Green's function method, the Fourier approach and the use of diffraction neural networks. Each of these approaches has its own advantages and disadvantages. The Green's function method allows to simplify the optical scheme in comparison with the Fourier method. However, it can be very difficult to realize the desired but arbitrary complex transmission function by this method. A rapidly developing new optical processing method using diffraction networks looks promising, but it seems to be more suitable for classification tasks. In addition, the method is currently limited due to the challenges of creating an optical analog of the nonlinear activation function.

The above approaches use amplitude-phase filters to transform the light beams. Metasurfaces are promising candidates for such devices due to their compactness and lack of power consumption. Their application simplifies the optical scheme compared to the use of, for example, spatial light modulators, but the main limitation in their use is static response.

In our study, a gallium arsenide metasurface has been modeled for analog optical image processing using a Fourier approach with all-optical tuning. The choice of material can be explained by the large refractive index variation at a wavelength of 850 nm due to bandgap effects under photoinduced carrier generation. The complex transmittance of the metasurface is chosen so that the metasurface switches between different image processing modes when femtosecond optical pumping is used. Following this approach, the second derivative of the analyzed image without pumping and the first derivative under optical pumping have been numerically demonstrated.

[1] W. Fu, D. Zhao, Z. Li, S. Liu, C. Tian, K. Huang, Ultracompact meta-imagers for arbitrary all-optical convolution. Light Sci. Appl., 11, 62 (2022).

[2] M. Cotrufo, S. Singh, A. Arora, A. Majewski, A. Alù, Polarization imaging and edge detection with image-processing metasurfaces, Optica, 10, 1331-1338 (2023).

[3] T. Badloe, S. Lee, J. Rho, Computation at the speed of light: metamaterials for all-optical calculations and neural networks, Adv. Photon, 4, 064002 (2022).

Gradient optical metasurfaces for analog image processing

P.D. Kiryanov[1*], V.V. Iushkov[1], A.S. Shorokhov[1], A.A. Fedyanin[1]

1- Lomonosov Moscow State University, Moscow, Russia

* kirianov.fd20@physics.msu.ru

Optical computing based on the metasurfaces is currently an actively developing area of research. Metasurfaces are flat arrays of resonant nanoparticles of various geometries, arranged in the required way. Metasurfaces allow unprecedented control over the wavefront spatial distribution with subwavelength resolution [1]. It allows the implementation of various optical signal processing functions, including differentiation, integration, etc. One of the fundamental approaches for the simplest analog optical calculations is a method using the spatial Fourier transform which is carried out by two lenses in the 4f-correlator configuration [2]. One of the disadvantages of previously used for this purpose metasurfaces is the pixel architecture. Gradient metasurfaces have already been demonstrated [3,4] to significantly improve the optical response and lead to smoothly varying transmission and shift phases.

Here we expect to smooth out the discreteness of the metasurface, obtaining gradient transmission, and phase shift profiles by using several control parameters. The metasurface consists of square tori made of gallium arsenide immersed into glass surrounding medium and located at the same distance from each other, forming a 2D lattice. Thus, the main control parameters are the outer and inner diameter of the tori. By varying these two parameters, it is possible to smoothly control the wave front.

Numerical modeling of a gradient metasurface realizing the first and second differentiation over a two-dimensional image is performed. A comparison is made with a similar pixelized metasurface and an improvement in the quality of the processed image is shown.

[1] N. Yu, F. Capasso, Flat optics with designer metasurfaces, Nature Materials, vol.13, pp. 139-150, (2014).

[2] N.M. Estakhri, A. Alù, Recent progress in gradient metasurfaces, JOSA B, vol.33, pp. A21-A30, (2016).

[3] Z. Li, M.H. Kim, C. Wang, et al, Controlling propagation and coupling of waveguide modes using phase-gradient metasurfaces, Nature nanotechnology, vol.12, pp. 675-683, (2017).

[4] S. Abdollahramezani, O. Hemmatyar, A. Adibi, Meta-optics for spatial optical analog computing, Nanophotonics, vol.9, pp. 4075-4095, (2020).

BBO crystals for nonlinear- and electro-optics applications

A. Kokh[*], **D. Kokh, E. Simonova, O. Safonova**

Sobolev Institute of geology and mineralogy, 630090, Novosibirsk, Koptyug ave., 3

* a.e.kokh@gmail.com

Over a period of approximately three decades, the technology of beta barium borate (β-BaB$_2$O$_4$ or BBO) has been developed at the Institute of Geology and Mineralogy SB RAS [1-3]. The melt-solution method, also known as TSSG, is employed to facilitate the growth of noncentrosymmetric low-temperature β-phase. The use of oxides and fluorides of alkali metals as solvents represents a pivotal aspect of this process. The crucible containing the melt solution is surrounded by a thermal field with a third-order symmetry axis. This configuration gives rise to the formation of three convection cells within the melt solution, which enhances the mixing speed and yield coefficient. The improved flow in the vicinity of the crystallisation front postpones the effect of concentrational supercooling, thereby enhancing the optical quality. The photographs illustrate the BBO crystal, with a weight of 422 grams, that was grown in a 100 mm diameter crucible. The crystal can be used to produce non-linear optical elements with various orientations up to 10×15×18 mm and electro-optical modulators up to 8×8×20 mm with 1:1000 contrast.
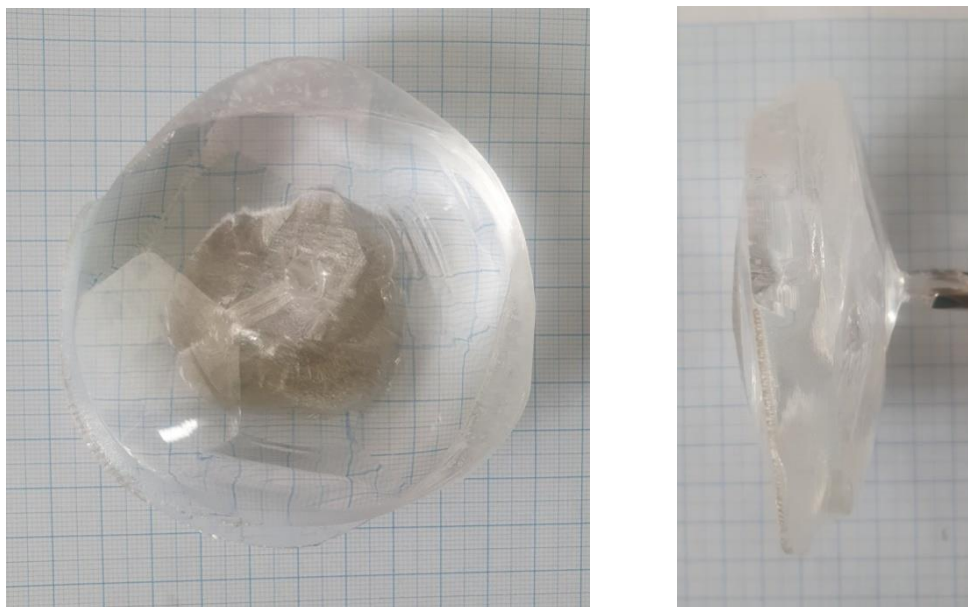
Fig. 1. BBO crystal weighted 422g, top and side views.

[1] A.E. Kokh, T.B. Bekker, V.A. Vlezko, K.A. Kokh, Development of the technique of β-BaB$_2$O$_4$ crystal growth in the heat field of three-fold axis symmetry, J. Crystal Growth, vol. 318, No. 1, pp. 602-605, (2011).
[2] L. Deyra, A. Maillard, R. Maillard, D. Sangla, F. Salin, F. Balembois, A.E. Kokh, P. Georges, Impact of BaB$_2$O$_4$ growth method on frequency conversion to the deep ultra-violet, Solid State Sciences, vol. 50, pp. 97-100, (2015).
[3] E. Simonova, A. Kokh, V. Shevchenko, A. Kuznetsov, A. Kragzhda, P. Fedorov, Growth of β-BaB$_2$O$_4$ Crystals from Solution in LiF–NaF Melt and Study of Phase Equilibria, Crystal Research & Technology, vol. 54, 1800267 (8 pgs), (2019).

Telluride-based PCMs for controlling active THz devices

M. Konnikova[1,2*], **A. Tretiakov**[3], **A. Shevchenko**[4], **A. Mumlyakov**[4], **M. Krasil'nikov**[4], **A. Anikanov**[4], **Yu, Kistenev**[3], **I. Ozheredov**[1,2], **A. Shkurinov**[1]

1- Faculty of Physics, Lomonosov Moscow State University, 119991, Moscow, Russia
2- National Research Centre "Kurchatov Institute" (NRC "Kurchatov Institute")
3- Laboratory of Laser Molecular Imaging and Machine Learning, Tomsk State University, Tomsk, Russia
4- Institute of Nanotechnology of Microelectronics of the Russian Academy of Sciences, Moscow, Russia

* konnikovamaria@gmail.com

Control of spectral and polarization characteristics of THz radiation is a key feature of next-generation wireless communication, sensing, and imaging devices in the THz band [1,2]. Phase change materials (PCMs) make a non-volatile phase transition from amorphous (insulating) to crystalline (conducting) state in nanosecond time intervals, changing their electrical and optical properties under thermal, electrical or optical influence. Since both states are characterized by strong differences in optical and electrical properties, these materials can be used for reconfigurable devices such as filters, amplitude, frequency, and polarization modulators [2]. The accurate retrieval of PCM film optical properties, such as its complex dielectric permittivity and conductivity, is key to creating reconfigurable devices for optical, infrared, and THz applications.

Here we propose a new approach to the study of PCM thin films, including simultaneous THz reflectance and transmittance measurements, which will minimize the uncertainty of the measured optical constants. Based on the calculated complex dielectric constant and conductivity of the films, we have designed and fabricated several tunable THz planar devices with a layer of tellurium compounds [2]. Laser irradiation parameters for optically induced phase transition of telluride-based PCMs films have been determined. The devices exhibit amplitude and frequency modulation of THz spectral characteristics at the phase transition of GeTe and GeTe$_2$ films show in Fig. 1.
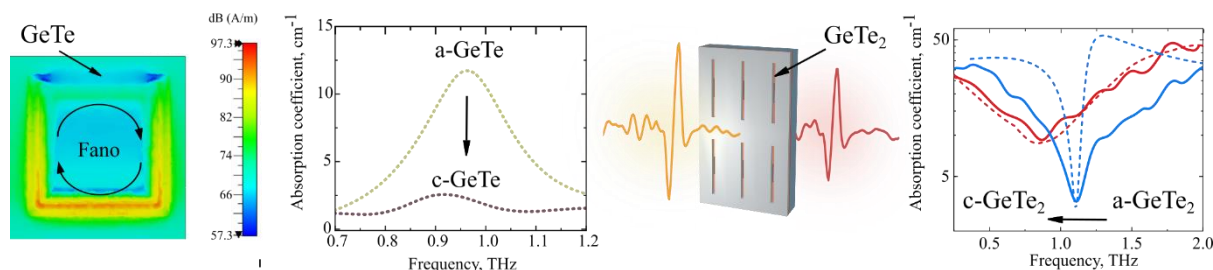

Fig. 1. The structures of tunable THz photonic devices based on GeTe and GeTe$_2$ and their measured absorption spectra.

Thus, based on our measurements, we have designed unique THz active planar metastructures that change the frequency, amplitude and polarization characteristics of the THz field ultrafastly.

[1] A. Manda, Y. Cui, L. McRae, B. Gholipour, Reconfigurable chalcogenide phase change metamaterials: a material, device, and fabrication perspective, J. Phys. Photonics, vol. 3(2), 2021.
[2] M. Konnikova, M. Khomenko, et al, GeTe$_2$ Phase Change Material for Terahertz Devices with Reconfigurable Functionalities Using Optical Activation ACS Appl. Mater. Interfaces, vol. 15(7), 2023.

High-Q IR plasmonic platforms produced by direct femtosecond laser printing

D. Pavlov[1], A. Kuchmizhak[1,2*]

1- Institute of Automation and Control Processes, Far Eastern Branch of RAS, Vladivostok, 690041 Russia
2- Far Eastern Federal University, 690090 Vladivostok, Russia

* alex.iacp.dvo@mail.ru

Proper arrangement of the plasmonic nanostructures into well-ordered arrays opens up pathways for excitation of collective resonance characterized by high Q-factors and strong light localization that is important for diverse applications including light-matter interaction, nonlinear optics and sensing. Excitation of so-called quasi-bound states in the continuum (q-BIC) in plasmonic nanostructures has recently gained substantial research interest, yet fabrication of such sophisticated nanostructure arrangement still relies on the expensive and time-consuming lithography-based approaches. In this presentation, the possibility of using direct femtosecond laser printing of specific nanostructure arrays supporting q-BICs will be discussed. The developed approach is based on rather unique thermo-mechanical behaviour of the gold film subjected to the exposure of nJ-energy laser pulse resulting in its ultrafast melting, local relaxation from the supporting substrate and recrystallization in the form of hollow-shape nano-cavities referred to as nanobumps or nanojets [1]. The process is highly controllable reflecting the ablation-free character of the laser patterning process (Figure 1). We showed that nanobumps and nanojets arranged into a square and hexagonal lattice supports the high-Q plasmonic modes resulting from coupling and destructive interference of the plasmonic waves. Existence of such modes were confirmed using Fourier spectroscopy and third-harmonic generation methods [2,3]. We also discussed applications of the developed laser-printed plasmonic platforms for optical nano-sensing and enhancing/shaping the spontaneous emission of the coupled HgTe quantum dots with photoluminescence yield at near-IR wavelengths matching the qBIC mode spectral position [4].
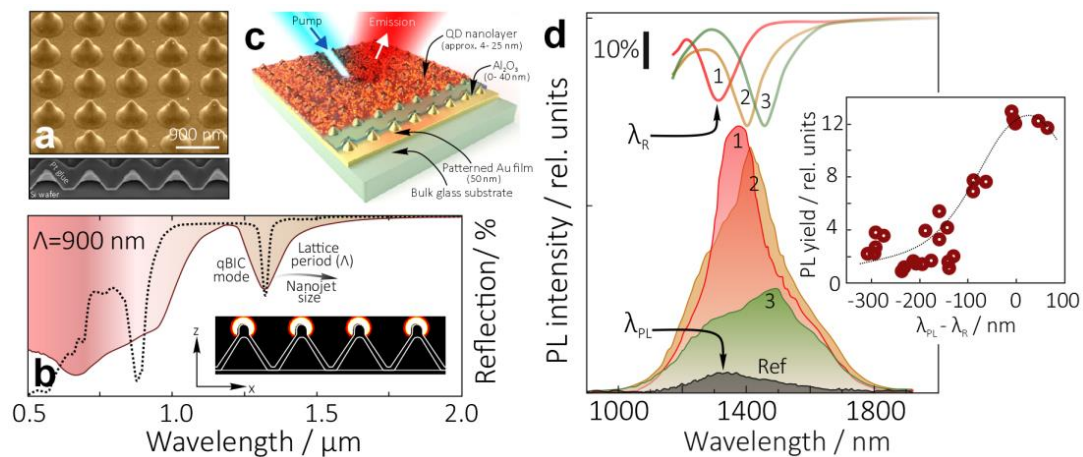

Figure 1. (a) SEM image of the nanobump arrays (bottom inset: cross-section cut revealing hollow structure of the bumps). (b) Measured and calculated reflectance spectra of the nanobump array. (c) Schematic illustration of the device of tailoring PL properties of the HgTe QDs as well as (d) PL spectra of the QDs monolayers depending on the spectral position of the qBIC mode supported by the device.

[1] A. Sergeev, et al, Tailoring spontaneous infrared emission of HgTe quantum dots with laser-printed plasmonic arrays. Light: Science & Applications 9 (1), 16 (2020).
[2] D. Pavlov, et al, Tuning collective plasmon resonances of femtosecond laser-printed metasurface. Materials 15 (5), 1834 (2022).
[3] A.B. Cherepakhin, et al, Laser-printed hollow nanostructures for nonlinear plasmonics, Applied Physics Letters 117 (4) (2020).
[4] K. Sergeeva, et al, Laser-Printed Plasmonic Metasurface Supporting Bound States in the Continuum Enhances and Shapes Infrared Spontaneous Emission of Coupled HgTe Quantum Dots, Advanced Functional Materials 33 (44), 2307660 (2023).

Ultrafast diamond nanophotonics in quantum technologies and gemology

S. Kudryashov[*]**, P. Danilov, D. Pomazkin, N. Smirnov, P. Pakholchuk, V. Vins,
M. Skorikov, A. Gorevoy, E. Kuzmin, G. Krasin, Yu. Gulina**

Lebedev Physical Institute, 119991 Moscow, Russia

* kudryashovsi@lebedev.ru

Even though ultrafast non-linear photonics were broadly harnessed in application to diverse dielectric materials over the last decades, it was scarsely utilized in diamond research, being limited by self-focusing, high-harmonics and multi-photon luminescence generation. However, recent single-photon atomistic source, lasing and laser nanoscale encoding studies in diamonds have brought up the issues of ultrasensitive and selective concentration measurements for the most important basic nitrogen-based embedded quantum emitters (optical centers A, B, C, N3, H3, NV etc.) at (sub)ppb level and nano/microscale spatial resolution (mapping), for their smart and robust functional harnessing. In our room-temperature broadband spectroscopic studies with a tunable optical parametric femtosecond-laser source, resonant and non-resonant ultrafast non-linear self-transmittance and photoluminescence were explored in order to measure saturated anti-Stokes absorption and Stokes emission cross-sections of nitrogen-based quantum emitters, while non-linear two-photon self-transmittance measurements were employed to calibrate, measure and map their local concentrations at ppb-ppm level [1,2]. These methods provide for the first time facile and sensitive room-temperature concentration measurements/spatial mapping of the most important nitrogen-based quantum emitters as key-enabling elements for advance and perspective (nano)photonic applications.

These preceding non-invasive ultrafast spectroscopic studies provided us an unique toolkit for predetermined resonant and non-resonant high-intensity femtosecond-laser atomistic structural modifications in diamonds for their commercial photoluminescent microencoding [3], (dis)coloration [4] and catastrophic disordering [5].

[1] S. Kudryashov, P. Danilov, N. Smirnov, P. Pakholchuk, M. Skorikov, Photo-physical characteristics of color N3-center in diamond studied via UV femtosecond-laser pumped luminescence, Optics Letters, 49 (1), 137-140, (2024).
[2] S. Kudryashov, P. Danilov, V. Vins, D. Pomazkin, P. Pakholchuk, One-photon femtosecond laser excitation of photoluminescence from H3 and H4 centers in natural diamond: A method to determine their concentration, JETP Letters, 119 (3), 173-178, (2024).
[3] youtu.be/X3Z_jcWowks
[4] S.I. Kudryashov, V.G. Vins, P.A. Danilov, E.V. Kuzmin, A.V. Muratov, G.Y. Kriulina, Permanent optical bleaching in HPHT-diamond via aggregation of C-and NV-centers excited by visible-range femtosecond laser pulses, Carbon, 201, 399-407, (2023).
[5] S. Kudryashov, P. Danilov, V. Vins, E. Kuzmin, A. Muratov, Intrapulse in situ Raman probing of electron, phonon and structural dynamics in synthetic diamond excited by ultrashort laser pulses: Insights into atomistic structural damage, Carbon, 217, 118606 (2024).

The impact of cationic isomorphism on the optical properties of a solid solution based on TbAl$_3$(BO$_3$)$_4$

A. Kuznetsov[1*], A. Jamous[1,2], M. Rachmanova[3], A. Kokh[1]

1- Sobolev Institute of Geology and Mineralogy SB RAS, Novosibirsk 630090, Russia
2- Tomsk State University, Tomsk 634050, Russia
3- Nikolaev Institute of Inorganic Chemistry SB RAS, Novosibirsk 630090, Russia

* *ku.artemy@igm.nsc.ru*

RM$_3$(BO$_3$)$_4$ (R=Y, La-Lu, M=Al, Ga, Cr, Fe), orthoborates are excellent compounds for optical applications. These compounds, known as huntites, are isotypical to the mineral CaMg$_3$(CO$_3$)$_4$, which crystallizes in the R32 space group [1]. Among the huntites, the compounds with aluminum can be promising materials for nonlinear optical, phosphor, and laser applications [2]. These materials have a low of concentration quenching of luminescence compared to RBO$_3$. In addition, they have chemical stability, mechanical strength, and unique thermal conductivity. The structural and optical properties of TbAl$_3$(BO$_3$)$_4$ single crystal have been studied in [3] where this crystal was explored as a new magneto-optic borate crystal. Faraday rotations and Verdet constants of TbAl$_3$(BO$_3$)$_4$ crystal were measured at wavelengths of 532, 633, and 1064 nm. The article [4] shows that the maximum intensity of luminescence is observed in YAl$_3$(BO$_3$)$_4$:5% Tb.

Despite the large number of experimental and theoretical studies, there is a lack of data on substitution between Al^{3+} and Tb^{3+} in TbAl$_3$(BO$_3$)$_4$. However, there is evidence of isomorphism in other systems, such as RAl$_3$(BO$_3$)$_4$ and RSc$_3$(BO$_3$)$_4$, which suggests that isovalent substitutions are possible for TbAl$_3$(BO$_3$)$_4$. Additionally, it is important to note that all huntite borates exhibit incongruent melting behaviors and cannot be grown directly from the melt [5]. Since the first syntheses by Blasse and Bril in 1967 [6], numerous growth methods have been proposed until the present day. However, melt-solution growth remains the most widely used method.

This work is devoted to the refinement of solid solution area for TbAl$_3$(BO$_3$)$_4$ in TbBO$_3$-(Al$_2$O$_3$:B$_2$O$_3$) systems by diffusion experiments, solid-state synthesis and combustion methods. In addition, crystals of TbAl$_3$(BO$_3$)$_4$ are grown from K$_2$Mo$_3$O$_{10}$-B$_2$O$_3$-Al$_2$O$_3$ flux. To compare emission and excitation spectra, QY and luminescence lifetimes, samples with different composition and synthesis conditions have been obtained. As a result, typical spectroscopic feature of Tb^{3+} is observed. There are four main bands in a wide wavelength range of 470–700 nm. These are due to transitions from the excitation state ^{5}D$_4$ to the ground states ^{7}F$_J$ (J = 6, 5, 4, 3) of the trivalent Tb ion in the host lattice. The strongest emission peak of the TbAl$_3$(BO$_3$)$_4$ is centered at a wavelength of 541 nm, indicating the emission of green light. According to the data obtained by Kurtz-Perry powder test on the second harmonic generation of the TbAl$_3$(BO$_3$)$_4$ compound, the intensity of the 50-100 μm fraction is higher than that of KDP.

[1] A.D. Mills, Crystallographic Data for New Rare Earth Borate Compounds, RX$_3$(BO$_3$)$_4$, Inorg Chem, vol. 1, pp. 960–961, (1962).
[2] N.I. Leonyuk, V.V. Maltsev, E.A. Volkova, O.V. Pilipenko, E.V. Koporulina, V.E. Kisel, N.A. Tolstik, S.V. Kurilchik, N.V. Kuleshov, Crystal growth and laser properties of new RAl$_3$(BO$_3$)$_4$ (R = Yb, Er) crystals, Opt Mater (Amst), vol. 30, pp. 161–163, (2007).
[3] Y. Saeed, N. Singh, U. Schwingenschlgl, First principles results on TbAl$_3$(BO$_3$)$_4$: A promising magneto-optical material, J Appl Phys, vol. 110, (2011).
[4] J. Li, J. Wang, X. Cheng, X. Hu, X. Wang, S. Zhao, Growth, optical properties and defects of Tb:YAl$_3$(BO$_3$)$_4$ crystal, Mater Lett vol. 58, pp. 1096–1099, (2004).
[5] N.I. Leonyuk, L.I. Leonyuk, Growth and characterization of RM$_3$(BO$_3$)$_4$ crystals, Progress in Crystal Growth and Characterization of Materials, vol. 31, pp. 179–278, (1995).
[6] G. Blasse and A. Bril, Energy transfer from Ce^{3+} to Tb^{3+} in scandium borate, J Lumin, vol. 3, pp. 18–20, (1970).

The fabrication of micro-structures on the fiber end by femtosecond laser two-photon polymerization technique

C.P. Lang[1*], H.R. Meng[1], D.H. Gao[1], M. Luo[1], X. Liu[1], Z.Y. Ma[1]**

1- Changchun Institute of Optics, Fine Mechanics and Physics, Chinese Academy of Sciences

* langchangpeng@ciomp.ac.cn, ** menghaoran@ciomp.ac.cn

Microstructures fabricated by two-photon polymerization (TPP) technique are widely applied in metasurface [1], micro mechanical [2], and micro-optical fields [3], owing to their advantages of high resolution, high precision and biological compatibility. In recent years, the microstructures on the optical fiber end-faces fabricated by using TPP technique have been reported to modulate the output light field. These structures are widely applied in integrated devices as the complex photoelectric conversion system is effectively avoided. Optical fiber sensors also have important applications in the integrated micro-device owing to their small sizes, light weights and anti-electromagnetic interference.

We fabricated different micro-structures on the fiber end by femtosecond laser two-photon polymerization technology, as shown in Fig. 1. The light signal emitted from optical fibers not only can be modulated by the micro-structures, but also can control the micro-structures composed of different responsive materials. The three-dimensional micro-structures fiber functional devices with good stability and high resolution can be used for sensing, imaging and integrated photonic chip applications [4]. Femtosecond laser induced two-photon polymerization has the advantages of ultrahigh processing accuracy which breaks through the optical diffraction limit and true three-dimensional processing ability of direct writing without mask. It has unique advantages in the processing of micro/nano-structure, and provides a new idea and possibility for the integration of micro/nano-structure and optical fiber.
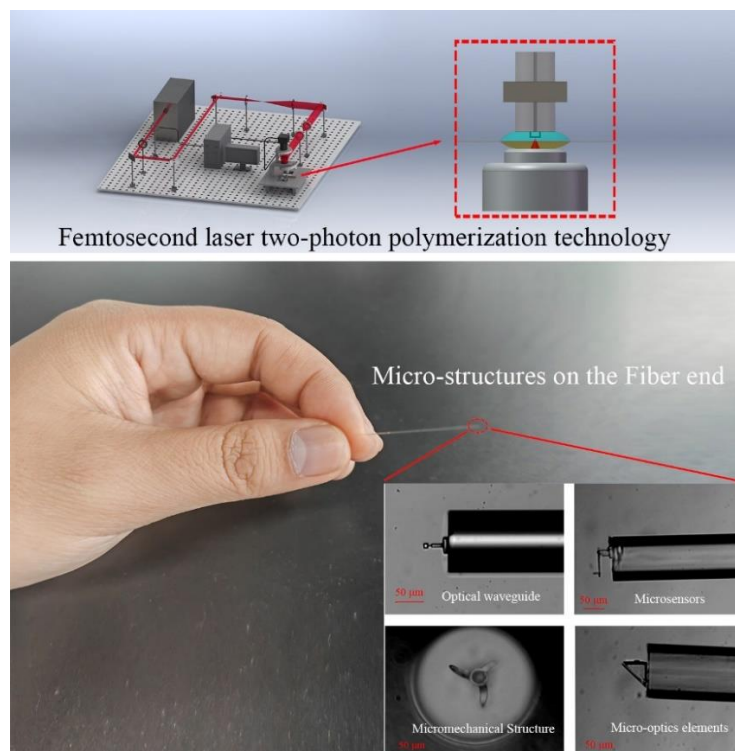

Fig. 1. The Fabrication of Micro-structures on the Fiber end by Femtosecond laser two-photon polymerization technology.

[1] F. Balli, M. Sultan, S.K. Lami, J.T. Hastings, A Hybrid Achromatic Metalens, Nature Communications, vol. 11, pp. 3892, (2020).

[2] M. Power, A.J. Thompson, S. Anastasova, G.Z. Yang, A monolithic force-sensitive 3d microgripper fabricated on the tip of an optical fiber using 2-photon polymerization, Small, vol. 14, pp. 1703964, (2018).

[3] T. Gissibl, S. Thiele, A. Herkommer, H. Giessen, Sub-micrometre Accurate Free-form Optics by Three-dimensional Printing on Single-mode Fibres, Nature Communications, vol. 7, pp. 11763, (2016).

[4] M.N. Liu, M.T. Li, H.B. Sun, 3D femtosecond laser nanoprinting, Laser & Optoelectronics Progress, vol. 55, pp. 011410, (2018).

Femtosecond laser-printed gold nanoantennas for electrically driven nanoscale light sources

D. Lebedev[1,2*], **N. Solomonov**[1], **A. Mozharov**[1], **D. Pavlov**[3], **A. Kuchmizhak**[3,4], **I. Mukhin**[1,5]

1- Saint Petersburg Academic University, St. Petersburg, 194021 Russia
2- Institute for analytical instrumentation RAS, St. Petersburg, 190103 Russia
3- Institute for Automation and Control Processes, FEB RAS, Vladivostok, 690041, Russia
4- Pacific Quantum Center, Far Eastern Federal University, Vladivostok, 690922, Russia
5- Peter the Great Saint Petersburg Polytechnic University, St. Petersburg 195251, Russia

* denis.v.lebedev@gmail.com

Recent advances in nanofabrication and plasmonic have led to renewed interest in the study of tunneling processes in sub-nanometer insulator gap in metal-insulator-metal (MIM) structures, specifically the light emission resulting from inelastic electron tunneling (LEIT). Visible and near-infrared (NIR) light sources based on the LEIT principle possess exceptional characteristics, such as sub-nanometer dimensions, radiation wavelength electrically tuned by gap bias voltage, and ultrafast response times of several femtoseconds limited only by the RC constant of the supply circuit. However, practical implementation of nanosized LEIT photon sources had long been hampered by insufficient quantum efficiency traditionally shown by such devices. This drawback primarily originated from relatively low local density of optical states (LDOS) in a flat tunnel gap, which led to the predominance of the elastic channel in the electron tunneling process providing no contribution to optical excitation. The incorporation of nanoantennas in the contact region had greatly enhanced the capabilities of LEIT devices [1].

Femtosecond (fs) laser pulses are known to drive local ultrafast liquid-to-solid phase transitions in the irradiated matter providing a simple and inexpensive way for fabrication of various plasmonic nanostructures that can be used in various applications, for example, for surface functionalization, SERS, microfluidic sensing, etc. [2].

The presented work justify facile and scalable direct fs-laser printing as a promising method for fabrication of nanoscale electrically driven light sources utilizing the effect of LEIT [3]. An important advantage of the direct laser printing method is its potential compatibility with modern photolithographic techniques employed in the manufacture of integrated circuits. Using this method, we formed on the surface of Au film an array of hemispherical nanobumps with a diameter of 520 nm, possessing the properties of optical nanoantennas. The performed study demonstrated that the nanobumps increase the LDOS in the visible (550 and 850 nm) spectral range. Therefore, such a nanobump can really act as a single nanoscale source of LEIT radiation. Moreover, the fabricated arrays of nanobumps showed collective resonances in the NIR spectral region (1.65 and 1.87 μm), due to the coupling and destructive interference of the propagating surface plasmons. The possibility of excitation of such collective oscillatory mode driven by inelastic electron tunneling was investigated for the first time. It confirmed that this opens the way to use the LEIT phenomenon in STMs not only for LDOS studies, but for investigation of collective modes associated with nanostructures at optical and IR frequencies.

Thus, the arrays of nanobumps studied in this work possess optical resonances in a broad spectral range (visible and NIR), which allows them to be employed in nanoscale electrically driven and bias-tuned sources of optical radiation with tunable wavelength.

[1] D. Lebedev, V. Shkoldin, A. Mozharov, et al, Scanning Tunneling Microscopy-Induced Light Emission and I/V (dI/dV) Study of Optical Near-Field Properties of Single Plasmonic Nanoantennas. The Journal of Physical Chemistry Letters, 12, pp.501–507, (2021).

[2] D. Pavlov, S. Syubaev, A. Kuchmizhak, et al, Direct laser printing of tunable IR resonant nanoantenna arrays. Applied Surface Science, 469, pp.514–520, (2019).

[3] D. Lebedev, N. Solomonov, L. Dvoretckaia, et al, Femtosecond Laser-Printed Gold Nanoantennas for Electrically Driven and Bias-Tuned Nanoscale Light Sources Operating in Visible and Infrared Spectral Ranges, The Journal of Physical Chemistry Letters, 14(22), pp. 5134-5140, (2023).

Promoted performance of curved surface laser texturing by 7-axis opto-mechanical synchronization

W. Ma[*], **J. Zhang**

Center for Precision Engineering, Harbin Institute of Technology, Harbin, 150001, China

* mawenqi_hrb@163.com

Laser Surface Texturing (LST) is a potent technique for surface enhancement. However, achieving both precision and efficiency in LST of complex curved surfaces remains a challenge due to varying laser-matter interactions. This study introduces an innovative 7-axis on-the-fly LST system for such surfaces, integrating a 5-axis linkage motion platform with a 2-axis galvanometer. We develop an algorithm to decompose the spatial texture trajectory into low and high frequency components, enabling the derivation of a synchronized kinematic model for the 7-axis system. The experimental setup includes mechanical stages, optical paths, numerical control units, and processing software. A case study on freeform aluminum surfaces demonstrates the superior processing efficiency and accuracy of the 7-axis system over conventional 5-axis LST. Analyses reveal that reduced following errors significantly enhance curved surface texturing performance. This research offers a viable approach for high-performance LST of intricate curved surfaces.

Optical conductivity and plasma frequency of ZnIn$_2$Se$_4$ crystals

I.A. Mamedova[1*], Z.A. Jahangirli[1,2], E.G. Alizade[1], T.G. Mammadov[3], N.A. Abdullayev[1,2]

1- Institute of Physics Ministry of science and education. Azerbaijan, Baku, Azerbaijan
2- Baku State University, Baku, Azerbaijan

* irada_mamedova@yahoo.com

ZnIn$_2$Se$_4$ crystals have special properties, such as optical anisotropy, birefringence, significant nonlinear susceptibility coefficients, high photosensitivity, and bright luminescence, which makes them promising materials for optoelectronics and nonlinear optics. Using the spectral ellipsometry method, we experimentally determined the spectral dependences of the real and imaginary parts of the dielectric function and optical conductivity, refractive indices, extinction and other optical parameters of ZnIn$_2$Se$_4$ crystals. A comparative analysis of the obtained experimental data with theoretical calculations from the first principles was carried out. Ab initio calculations of electronic and optical properties were performed based on DFT using the full-potential linearized augmented plane waves (FP-LAPW) method implemented in the Wien2k code.

Figure 1 shows the experimentally determined optical conductivity data $\sigma=\sigma_1+i\sigma_2$ (Fig. 1a), where $\sigma_1=\omega\varepsilon_0\varepsilon_2=2nk\omega\varepsilon_0$ is the real part, and $\sigma_2=\omega\varepsilon_0(n^2-k^2)$ – is the imaginary part of the optical conductivity, as well as the theoretically calculated from first principles (Fig. 1b) real σ_1 and imaginary part σ_2 of the optical conductivity for ZnIn$_2$Se$_4$ crystals. From the spectral dependence of the real parts of optical conductivity σ_1, the band gap of ZnIn$_2$Se$_4$ crystals is estimated.
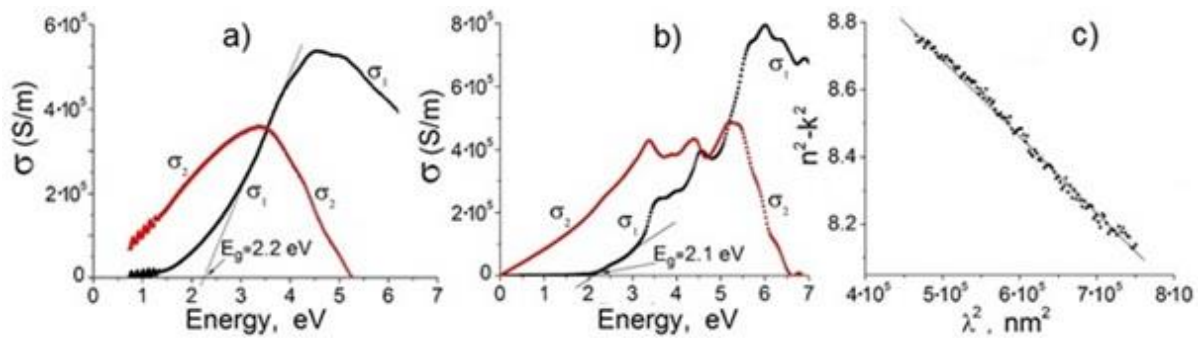

Figure 1. (a) and (b) Spectral dependences of the real σ_1 and imaginary σ_2 parts of the optical conductivity of ZnIn$_2$Se$_4$ crystals, calculated from experimental data and from first principles, respectively. (c) – Dependency (n^2-k^2) vs. λ^2 to determine the plasma frequency.

It is known that in the long-wave limit $n^2>>k^2$ the real part of the dielectric function $\varepsilon_1=n^2-k^2$ is described by the relation [1]:

$$\varepsilon_1 = \varepsilon_\infty - \frac{\omega_p^2}{\omega^2} = \varepsilon_\infty - \frac{\omega_p^2\cdot\lambda^2}{4\pi^2c^2} = \varepsilon_\infty - a\lambda^2, \text{ where plasma frequency } \omega^2{}_p=e^2N/\varepsilon_0m_e* \qquad (1)$$

Here, e is the elementary charge, ε_0 is the dielectric constant, N is the charge carrier density, m_e* is the effective mass. From the dependence in Fig. 1c with linear approximation, $\varepsilon_\infty=9.9$, plasma frequency $\omega_p=3\cdot10^{15}$ rad/s and $N/m_e*=3.1\cdot10^{57}$ m^{-3}kg^{-1} are determined.

[1] S. Belgacem and R. Bennaceur, Propriétés optiques des couches minces de SnO$_2$ et CuInS$_2$ airless spray, Rev. Phys. Appl. (Paris) 25, 1245-1258 (1990).

Laser-synthesized orthorhombic carbon flakes intercalated with Au-Ag nanoparticles as advanced optical material

A. Manshina

Institute of chemistry, St. Petersburg State University, 26 Universitetskii prospect,
Petergof, St. Petersburg, 198504, Russia

a.manshina@spbu.ru

The hybrid nanomaterials possess a wide spectrum of important properties that may be gained by controllably varying such parameters as their composition, structure and morphology. In addition, combining of different components in the same structure and their mutual influence enables obtaining materials that exhibit not only additive properties of the components but also new ones caused by synergetic effects.

Here we present the hybrid nanomaterial never realized before – combination of crystalline 2D carbon and incorporated bimetal Au-Ag nanoclusters [1-3]. Our experiments on laser-induced synthesis demonstrate the possibility of the direct creation of 2D hybrid metal/carbon flakes in just one step. The deposited flakes were found to be atomically smooth, regularly shaped flat structures of 1-2 μm × 4-7 μm with thickness of 10 – 100 nm, which consist of bimetal Au-Ag nanoclusters c.a. 3 nm in diameter stochastically distributed in crystalline carbonaceous matrix (Figure 1a). The carbonaceous matrix itself differs from known allotropes of carbon, and was found to be hydrogenated carbon with pure sp^2 hybridization and orthorhombic crystal cell.
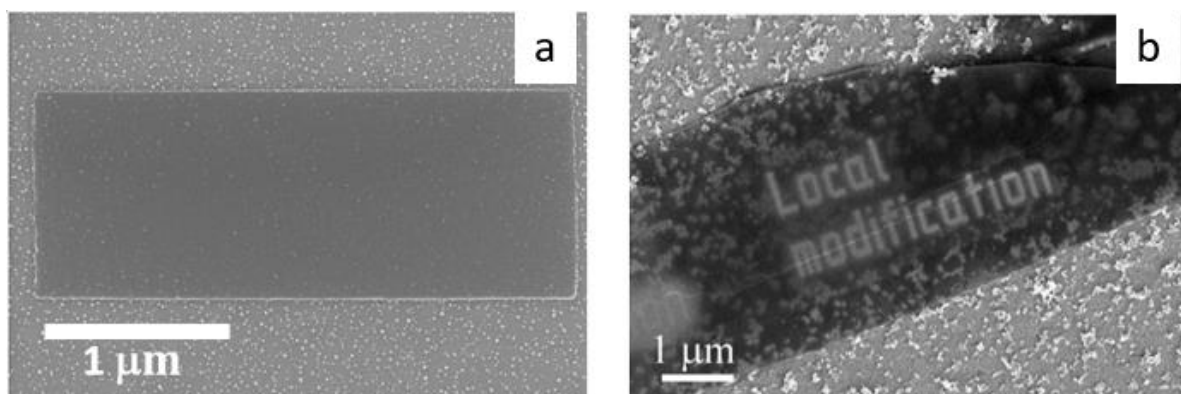

Figure 1. a) SEM image of the single hybrid flake, b) local modification of a nanoflake with focused helium-ion beam.

We found that the hybrid flakes can be cut or/and modified by means of irradiation with a focused helium ion beam (FIB) – Fig. 1b. Au-Ag@C flakes are very promising hybrid material with extraordinary potential in terms of its optical properties thanks to enhanced characteristics resulting from synergetic effects of their components – pronounced SERS effect, high birefringence, luminescence.

[1] A. Povolotckaia, et al, Plasmonic carbon nanohybrids from laser-induced deposition: controlled synthesis and SERS properties, J Mater Sci 54:8177–8186, (2019).
[2] M. Butt, et al, Investigating the Optical Properties of a Laser Induced 3D Self-Assembled Carbon–Metal Hybrid Structure, Small, 15, 1900512, (2019).
[3] M. Butt, et al, Hybrid orthorhombic carbon flakes intercalated with bimetallic Au-Ag nanoclusters: influence of synthesis parameters on optical properties, Nanomaterials 10 (7), 1376 (2020).

Laser synthesis of hybrid nanoparticles for optical nanosensing and light-to-heat conversion

E. Mitsai[1*], A. Kuchmizhak[1,2]

1- Institute of Automation and Control Processes of the FEB RAS, 5 Radio St., 690041 Vladivostok, Russia
2- Saint Petersburg State University, 26 Universitetskii Prospect, 198504 Saint-Petersburg, Russia

* mitsai@dvo.ru

We demonstrate the possibility of a one-step synthesis of silicon-germanium ($Si_{1-x}Ge_x$) alloyed nanoparticles (NPs) of controlled composition by nanosecond laser ablation of SiGe targets in isopropanol (Fig. 1.a). The synthesized product retains the stoichiometry of the targets, and the method of suspension centrifugation enables isolation of a product fraction with an average diameter of about 200 nm (Fig. 1.b). Nano-thermometry using registration and analysis of the Raman signal from these NPs demonstrated 3 times greater heating efficiency than similar-sized pure Si NPs under the influence of continuous laser radiation with a wavelength of 785 nm, located in the center of the "transparency window" of biological tissues (Fig. 1.c).
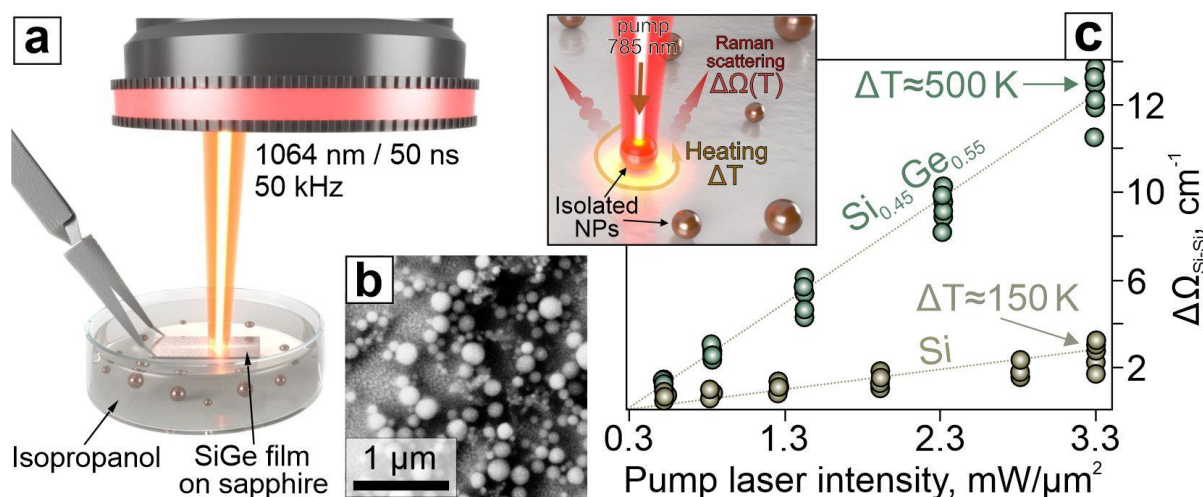

Fig. 1. (a) Schematic representation of the process of obtaining SiGe NPs by ablation of alloyed films on a sapphire substrate. (b) SEM image of NPs obtained after centrifugation of the resulting suspension. (c) Thermal-induced Raman peak shift ($\Delta\Omega_{Si-Si}$) of single Si and $Si_{0.45}Ge_{0.55}$ NPs with diameter ≈ 200 nm from the pumping intensity of laser radiation ($\lambda=785$ nm). The inset shows a schematic representation of the process of measuring the efficiency of laser-induced heating of isolated NPs.

An important feature of the synthesized NPs is their phase and structural transformation under the influence of continuous IR radiation-induced heating. The diffusion of Si atoms to the surface (when heated above 650 K) and their oxidation leads to the gradual transformation of alloyed SiGe NPs into Ge clusters encapsulated in a silicon oxide shell, which is important for the creation of tunable photonic elements. Also, since it is known that both the SiGe alloy and its decomposition products in biological fluids and tissues do not have a significant toxicological effect [1], the encapsulation of NPs' material into an oxide shell during heating potentially increases their biocompatibility and demonstrates high potential for the development of tumor photohyperthermia methods.

[1] S.K. Kang, G. Park, K. Kim, S.W. Hwang, H.Y. Cheng, J.H. Shin, S.J. Chung, M. Kim, L. Yin, J.C. Lee, K.M. Lee, J.A. Rogers, ACS Applied Materials & Interfaces, 7(17), pp. 9297-9305, (2015).

Enigmatic color centers in diamonds with bright, stable, and narrow-band fluorescence

A. Neliubov[1,2*], I. Eremchev[3], V. Drachev[1], S. Kosolobov[1], E. Ekimov[4], A. Naumov[2,3]

1- Skolkovo Institute of Science and Technology, Moscow, 121205, Russian Federation, Moscow, Russia
2- Lebedev Physical Institute of the Russian Academy of Sciences, Troitsk Branch, Moscow, Troitsk 108840, Russia
3- Institute for Spectroscopy of the Russian Academy of Sciences, Moscow, Troitsk 108840, Russia
4- Institute for High Pressure Physics, Russian Academy of Sciences, Moscow, Troitsk 108840, Russia

* arthur.neliubov@skoltech.ru

Color centers in diamonds attract great scientific attention due to their properties promising for sensing, biomarking, quantum information and quantum optics. The most studied and well-known color center in diamond to date is the Nitrogen-Vacancy (NV) center, which soon after its discovery showed great potential for various applications. However, a set of drawbacks accompanying NV centers has prompted researchers to introduce other elements of the Periodic table into the diamond lattice and, thus, to create new impurity centers with improved optical properties. Currently, the list of known color centers in diamond includes over a hundred of different examples and continues to grow [1].

In this work, we report the discovery and comprehensive characterization of new, as yet unidentified impurity centers in microdiamonds using combined scanning electron microscopy (SEM) and fluorescence spectroscopy (Fig. 1.a) [2]. The microdiamonds of study were synthesized by the high temperature-high pressure method. Most of the fluorescence signal of the detected emitters is concentrated in a narrow (up to 390 GHz at room temperature) and bright Zero-Phonon Line (ZPL). A typical photoluminescence spectrum of a single center is shown in Fig. 1.b. The photoluminescence excitation spectrum is also narrowband. In addition, we demonstrate the temperature sensitivity, spectral stability, and polarization dependence of ZPL. These results indicate that the discovered emitters have superior optical properties comparing to the known color centers and, thus, have great potential for applications.
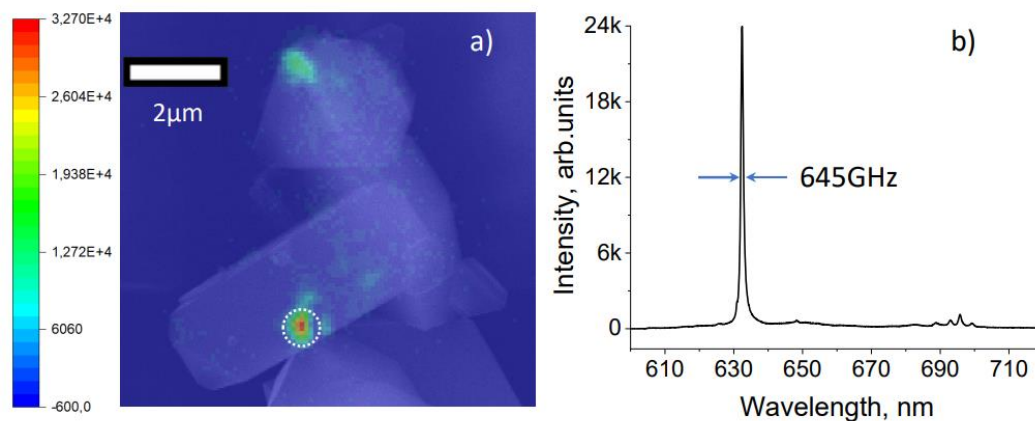

Fig. 1. (a) Combined SEM image and fluorescence map of a microdiamond cluster with two spatially resolved emission sources. (b) Photoluminescence spectrum of the bottom emitter in (a).

[1] K. Liu, S. Zhang, V. Ralchenko, et al, Advanced Materials 33 (6): p. 2000891 (2021).
[2] A. Neliubov, I. Eremchev, V. Drachev, et al, Physical Review B 107, L081406 (2023).

Magnetic-field-induced modulation of Goos-Hänchen effect in magnetophotonic crystals

A.A. Nerovnaya[1*], **M.S. Gavrushina**[1], **A.I. Musorin**[1], **I.V. Soboleva**[1], **A.Yu. Frolov**[1], **A.A. Fedyanin**[1]

1- Lomonosov Moscow State University, 119991, Leninskie gory 1, Moscow, Russia

* nerovnaia.aa19@physics.msu.ru

Nowadays, one of the main topics in modern nanophotonics is the study of optical effects in nanostructures that allow light to be controlled by external influences. These include the Goos-Hänchen (GH) effect [1]. Under the GH effect the reflected light beam experiences a lateral shift along the interface in comparison with the position predicted by the geometric optics. The GH effect can be enhanced by surface electromagnetic waves, for example, Bloch surface waves (BSWs), which propagates on the interface of photonic crystals. It is worth mentioning that magnetic field is also a powerful tool for tunability of the GH shift in magnetooptical structures, which can be used in magnetooptical sensors [2].

In this work, we observed the modulation of the spatial distribution of the reflected light intensity in the presence of the Goos-Hänchen effect in magnetophotonic crystals (MPC). MPC consists of 14 periodic layers of SiO_2 and Ta_2O_5 with thickness of 132 nm and 93 nm, refractive indexes 1.46 and 2.1, respectively. The layer of Bi:YIG with thickness of 1059 nm lies on the top of the MPC. Simulation and experimental measurements of the angular dependence of the GH effect was obtained. Excitation of the TE Bloch surface wave in the MPC leads to the GH effect up to 33 µm. A magnetic field applied to the sample in the polar geometry induces TM light components in the magnetic layer, leading to a change in the spatial distribution of the reflected light intensity. The magnetic-field-induced modulation of the spatial distribution of the reflected beam intensity has been defined by following equation:

$$\Delta(x) = \frac{I(x,H) - I(x,0)}{I(x,0)} \times 100\%, \qquad (1)$$

where I(x,H) and I(x,0) is the intensity spatial distribution of the reflected light measured with and without external magnetic field, respectively. Figure 1 shows that the maximum observed modulation of the spatial distribution of the reflected light intensity (black curve) was 7%, which is 7 times higher than the intensity modulation calculated integrally over the whole reflected beam for the given MPC. This effect can be extended to other magnetophotonic nanodevices for additional enhancement of magneto-optical effects, sensing and light modulation.
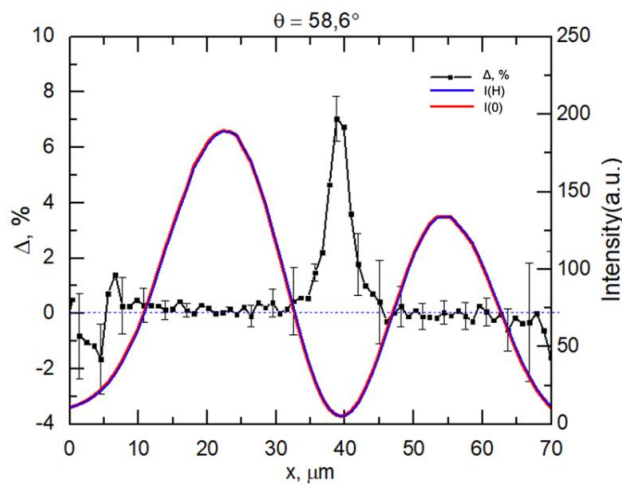

Fig. 1. Spatial distribution of the reflected beam intensity in the absence (red curve) and presence of the polar magnetic field (blue curve). The black curve shows the modulation of the spatial distribution of the reflected light intensity (Δ) caused by magnetic field.

[1] F. Goos and H. Hänchen, A new and fundamental experiment on total reflection, Ann. Phys (Leipzig), vol.1, 7–8, 333–346 (1947).
[2] T. Tang, et al, Weak measurement of magneto-optical Goos-Hänchen effect, Opt. Express, vol.27, 13, 17638–17647 (2019).

Highly reflective materials for radiative cooling and laser protection

L. Pan[1], **S. Li**[1], **X. Li**[1], **H. Xu**[1], **J. Zhao**[1], **Y. Li**[2]

1- School of Chemistry and Chemical Engineering, Harbin Institute of Technology, Harbin 150001, China
2- Center for Composite Materials and Structure, Harbin Institute of Technology, Harbin 150001, China

Highly reflective materials find broad applications across various fields. Material reflectivity is influenced by intrinsic optical properties as well as microstructure. In this study, a series of materials with high reflectivity has been prepared through microstructure adjustments to fulfill the requirements for applications in radiation cooling and laser protection.

We obtain flexible thermoplastic polyurethane (TPU) nanofiber membranes via electrospinning [1], realizing reversible *in-situ* solvent-free switching between radiative cooling and solar heating through changes in its optical reflectivity by stretching. In its radiative cooling state (0% strain), the nanofiber membrane shows a high and angular-independent reflectance of 95.6% in the 0.25–2.5 μm wavelength range and an infrared emissivity of 93.3% in the atmospheric transparency window (8–13 μm), reaching a temperature drop of 10°C at midday, with a corresponding cooling power of 118.25 W/m^2. The excellent mechanical properties of the nano membrane allows the continuous adjustment of reflectivity by reversibly stretching it, reaching a reflectivity of 61.1% ($\Delta R = 34.5\%$) under an elongation strain of 80%, leading to a net temperature increase of 9.5°C above ambient of an absorbing substrate and an equivalent power of 220.34 W m^{-2} in this solar heating mode.

To increase UV durability, a core of strontium barium titanate nanorods (BST NRs) is coaxially electrospun into the TPU nanofiber. Capitalizing on the UV absorption and free radical adsorption properties of BST NRs, the UV stability of the TPU membrane is significantly increased. Additionally, the inclusion of high refractive index BST NRs compensates for the decrease in total reflectivity caused by their UV absorption. After 216 h of continuous 0.7 kW m^{-2} UV irradiation, the BST@TPU membrane, which initially exhibits a reflectance of 97.2%, demonstrated a modest decline to 92.1%. Its net radiative cooling power maintains 85.78 W m^{-2} from the initial of 125.21 W m^{-2}, extending the useful lifetime of the TPU membrane threefold.

In addition to flexible fiber membranes, we achieving high reflectivity coatings by optimizing the ratio of low refractive index alumina particles to sodium methylsilicate adhesive. The coating exhibits a remarkable solar reflectance exceeding 0.95 and a high mid-infrared emissivity of 0.91, thus attaining a maximum theoretical cooling power of 109.01 W/m². After exposing the coating to UV irradiation at 0.7 kW/m² for 72 hours, we noted a mere 0.2% decrease in solar reflectance compared to the non-aged coatings. This high reflective inorganic coating can be used in laser protection too.

[1] X. Li, Z. Ding, G.E. Lio, et al, Strain-adjustable reflectivity of polyurethane nanofiber membrane for thermal management applications, Chemical Engineering Journal, 461, 142095-142104, (2023).
[2] X. Li, L. Pattelli, Z. Ding, et al, A Novel BST@TPU Membrane with Superior UV Durability for Highly Efficient Daytime Radiative Cooling, Advanced Functional Materials, 2315315-2315325, (2024).

From concept to reality: pioneering flexible electronics with laser engineering

R.D. Rodriguez[*], **M. Fatkullin, A. Lipovka, E. Dogadina,**
E. Abyzova, I. Petrov, A. Garcia, E. Sheremet

* raul@tpu.ru, www.ters-team.com

Laser processing is becoming more prominent in flexible electronics fabrication thanks to its scalability, sustainability, and versatility [1]. TERS-Team is a research group at Tomsk Polytechnic University that studies nanomaterials and their applications, exploiting laser processing to modify their properties. At the core of our research is the understanding that nanomaterials exhibit unique and tunable properties that can be harnessed for various applications, including electronics, energy storage, catalysis, and biomedicine. An exciting discovery has become the laser-induced formation of composites when irradiating nanomaterials on different substrates. This laser processing approach allows us to tune the material properties and obtain mechanically robust conductive patterns, preserve nanomaterial surface properties, and enhance gas response. We will discuss how this strategy can be applied to functionalized graphene, metallic nanoparticles, and different substrates – allowing the creation of a wide range of devices from piezoresistive and electrochemical sensors to GHz flexible antennas [2]. The mechanism of the nanomaterials and substrate modification, and the potential of these structures for applications in biomedicine, sensing, and heating, will be discussed.
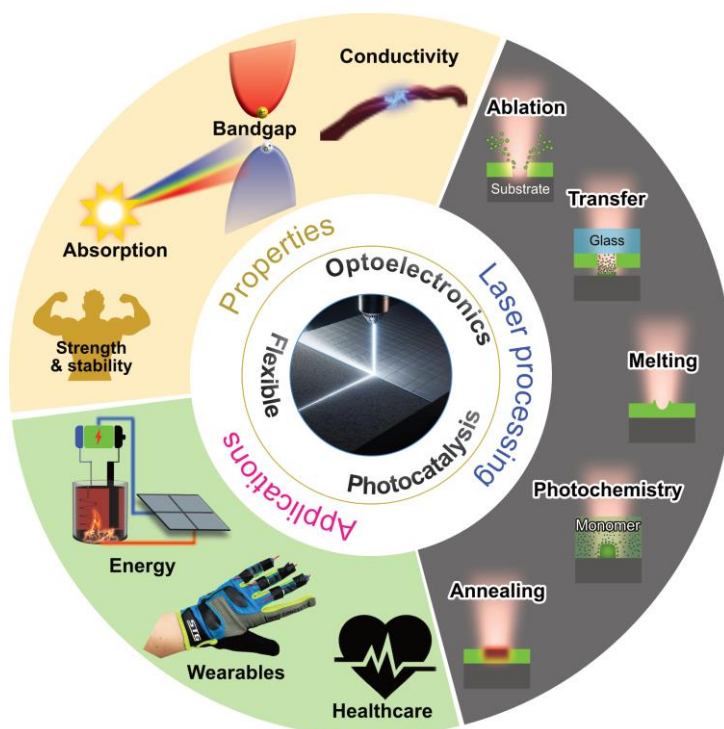
[1] A. Lipovka, et al, Laser Processing of Emerging Nanomaterials for Optoelectronics and Photocatalysis, Advanced Optical Materials, (2024).
[2] M. Fatkullin, et al, Nanomaterials/polymer-Integrated Flexible Sensors: A Full-Laser-Processing Approach for Real-Time Analyte Monitoring, IEEE Sens, J. (2024).

Superconducting niobium diselenide NbSe₂: a promising material for broadband frequency detection applications

K.V. Shein[1,2*], **E. Zharkov**[3], **A. Lyubchak**[1,2], **G.N. Goltsman**[1,2],
I. Charaev[4], **I. Gayduchenko**[1], **D.A. Bandurin**[3,5]

1- National Research University Higher School of Economics, Moscow, Russia 101000
2- Physics Department, Moscow Pedagogical State University, Russian Federation, 119435
3- Programmable Functional Materials Lab, Brain and Consciousness Research Center, Moscow, Russian Federation, 121205
4- University of Zürich, Zürich, Switzerland, 8057
5- Department of Materials Science and Engineering, National University of Singapore, Singapore, 117575

* sheinkv97@gmail.com

Two-dimensional (2D) materials represent a promising platform for the next generation of electronics and optoelectronics due to their distinctive properties. These properties include the capability to fabricate unique heterostructures and ultra-thin devices with exceptionally low heat capacities. Of particular interest are two-dimensional superconducting devices, which exhibit superconductivity down to the monolayer limit. These devices offer numerous technological advantages, such as the elimination of the need for costly magnetron sputtering processes and the facilitation of easy integration with other 2D structures. One notable material in this domain is niobium diselenide (NbSe₂). This material not only demonstrates intriguing transport characteristics, such as the superconducting diode effect [1] and charged density waves [2], but it has also shown considerable promise in optoelectronic applications [3-5]. In prior work [3], we demonstrated that superconducting NbSe₂ exhibits a substantial optical response at frequencies of 0.13 THz and 2.5 THz, with optical responsivity of 3 kV/W and a response time on the order of tens of nanoseconds. It is hypothesized that by reducing the NbSe₂ flake thickness to 2-3 atomic layers and optimizing the substrate selection, the sensitivity and performance of such a bolometer could be enhanced by more than an order of magnitude. Furthermore, NbSe₂ has proven to be a highly sensitive photodetector at near infrared wavelength range, exhibiting at 5 K noise equivalent power (NEP) characteristic 32 fW/Hz$^{0.5}$ at the wavelength λ = 1550 nm [4] and high sensitivity reaches 42.3 A/W at 3.8 K under λ = 72 nm [5]. These findings indicate that superconducting NbSe₂ holds significant potential as the foundation for a new generation of quantum detectors spanning a wide frequency range, with prospects for the development of superconducting single-photon detectors and integration into photonic circuits.

[1] L. Bauriedl, C. Bäuml, L. Fuchs, C. Baumgartner, N. Paulik, J.M. Bauer, K.-Q. Lin, J.M. Lupton, T. Taniguchi, K. Watanabe, C. Strunk, N. Paradiso, Supercurrent diode effect and magnetochiral anisotropy in few-layer NbSe₂, Nature Communications, 13, 4266, (2022).
[2] X. Xi, L. Zhao, Z. Wang, H. Berger, L. Forró, J. Shan, K.F. Mak, Strongly enhanced charge-density-wave order in monolayer NbSe₂, Nature Nanotechnology, 10, 765–769, (2015).
[3] K. Shein, E. Zharkova, M. Kashchenko, A. Kolbatova, A. Lyubchak, L. Elesin, E. Nguyen, A. Semenov, I. Charaev, A. Schilling, G. Goltsman, K.S. Novoselov, I. Gayduchenko, D.A. Bandurin, Fundamental Limits of Few-Layer NbSe₂ Microbolometers at Terahertz Frequencies, Nano Lett, (2024).
[4] G.J. Orchin, D. De Fazio, A. Di Bernardo, M. Hamer, D. Yoon, A.R. Cadore, I. Goykhman, K. Watanabe, T. Taniguchi, J.W.A. Robinson, R.V. Gorbachev, A.C. Ferrari, R.H. Hadfield, Niobium diselenide superconducting photodetectors, Appl. Phys. Lett., 114 (25), (2019).
[5] Y. Jin, Z. Ji, F. Gu, B. Xie, R. Zhang, J. Wu, X. Cai, Multiple mechanisms of the low temperature photoresponse in niobium diselenide, Appl. Phys. Lett., 119 (22): 221104, (2021).

Laser processing of the trivial semimetals towards advanced transparent conductors

D. Pavlov[1], V. Il'yaschenko[1], A. Bozhok[1,2], D. Banniy[1,2], A. Kuchmizhak[1,2], A. Shevlyagin[1,3]*

1- Institute of Automation and Control Processes, FEB RAS, Vladivostok, Russia
2- Far Eastern Federal University, Vladivostok, Russia
3- Institute of Chemistry, Saint Petersburg State University, Saint Petersburg, Russia

* shevlyagin@iacp.dvo.ru

We report a highly transparent in the wide band optical range of (0.4-7) µm mesh electrodes fabricated on thin semimetal films of calcium disilicide ($CaSi_2$) and digermanide ($CaGe_2$) by flat top beam shaped laser ablation (Fig. 1a). Compared with continuous films, mesh electrodes demonstrate an increase in the figure of merit as transparent conducting materials up to 0.9 Ω^{-1} (Figs. 1b,c). Of importance, both materials retain low sheet resistance not exceeding 20 Ω/sq after laser processing. Obtained material parameters allowed testing $CaGe_2$ and $CaSi_2$ mesh electrodes under actual conditions. In particular, a vertical Ge photodetector (PD), where the $CaGe_2$/Ge interface acts as a Schottky barrier was fabricated (Fig. 1d), which outperformed commercially available Ge device in terms of both photoresponse and operated spectral range (Fig. 1e). Meanwhile, perforated $CaSi_2$ film has been approved as an efficient (Fig. 1g) and stable under cyclic operation (Fig. 1h) heater with the modality of high optical transparency. For instance, a low power consumption was demonstrated by water droplets evaporation test under applied DC current (Fig. 1f).
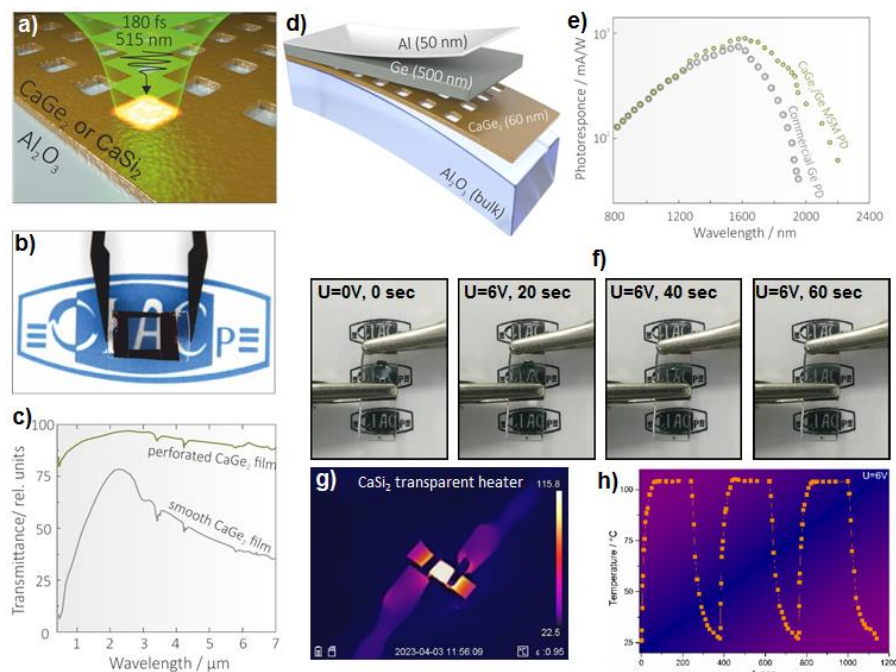

Fig. 1. a) Schematic view of fs-laser projection lithography for patterning $CaGe_2$ and $CaSi_2$ films. b) Photograph of the $CaGe_2$ film with a 4×4 mm^2 laser-patterned area. c) Relative transmittance of the $CaGe_2$/Al_2O_3 sample before (smooth film) and after laser patterning. d) A schematic view of the vertical Schottky-type Ge PD with a perforated $CaGe_2$ electrode. e) Room-temperature photoresponse spectra of $CaGe_2$/Ge PD and commercial one. f) Water evaporation performance of the $CaSi_2$ transparent heater under lower power consumption regime. g) Thermal infrared image of the $CaSi_2$ transparent heater under 6V applied. h) Switching cycles of the perforated $CaSi_2$ film between 0 and 6V.

Thus, laser perforation is suggested as an efficient tool toward advancing semimetal thin films for optoelectronic applications and transparent heaters development.

Laser treatment of materials to obtain superhydrophilicity for controlling heat exchange

S.V. Starinskiy[1,2*], **M.M. Vasiliev**[1,2], **Y.G. Shukhov**[1], **A.A. Rodionov**[1], **V.S. Sulyaeva**[3]

1- S.S. Kutateladze Institute of Thermophysics SB RAS, Lavrentyev Ave. 1, 630090 Novosibirsk, Russia
2- Novosibirsk State University, Pirogova Str. 2, 630090 Novosibirsk, Russia
3- A.V. Nikolaev Institute of Inorganic Chemistry SB RAS, Lavrentyev Ave. 3, 630090 Novosibirsk, Russia

* starikhbz@mail.ru

This study examines the influence of the surrounding environment on the properties of copper, nickel, and tin during nanosecond laser processing [1]. By comparing the results of processes conducted in vacuum and air, we conclude that changes in wetting properties cannot be solely attributed to development of surface microstructure. To elucidate this phenomenon, we conducted model experiments using a tin target. Laser processing parameters for the tin target were established, involving deep cavity melting without ablation, resulting in highly evolved material morphology. Under these conditions, laser processing in air did not lead to metal hydrophilization. Therefore, our study demonstrates that the primary cause of changes in material wetting properties during nanosecond laser processing is the re-deposition of ablation products onto the material surface. These products form a nanoporous layer that enhances wicking capabilities and subsequently serves as a sorbent for various impurities, gradually leading to the hydrophobization of most commonly used materials. The proposed mechanism opens the possibility for the development of new methods to create materials with biphilic and anisotropic wetting properties. The key insight lies in the control of the thickness of the nanoporous layer, as it emerges as a pivotal factor dictating wettability properties and wicking capability.

Based on the obtained data, we prepared samples with different wetting properties. The materials were used to analyze the micro and nanostructure at the Leidenfrost point and the dynamics of water droplet boiling on overheated surfaces. Optimization issues are discussed in terms of enhancing the heat dissipation characteristics of the materials. The obtained materials are considered as a basis for creating devices characterized by high-intensity heat exchange during the phase transition of liquid to vapor under conditions of liquid contact with a surface possessing hierarchical micro-/nanotexture. Special attention will be given to the possibility of using unique wetting properties to control heat exchange processes.

[1] M.M. Vasiliev, Y.G. Shukhov, A.A. Rodionov, V.S. Sulyaeva, D.M. Markovich, S.V Starinskiy, Why do metals become superhydrophilic during nanosecond laser processing? Design of superhydrophilic, anisotropic and biphilic surfaces, Appl. Surf. Sci. 653 (2024) 159392.

Femtosecond laser-induced periodic surface structuring of BaGa₄Se₇ crystal for near-infrared anti-reflection enhancement

A. Kuchmizhak[1], A. Dostovalov[2], S. Syubaev[1*]

1- Institute of Automation and Control Processes of the FEB RAS, 5 Radio str., Vladivostok, Russia
2- Institute of Automation and Electrometry of the SB RAS, 1 Acad. Koptyug Ave., Novosibirsk, Russia

* trilar@bk.ru

BaGa₄Se₇ (BGSe) crystal is a novel promising non-linear optical material for frequency conversion in the near- and mid-infrared ranges, characterizing by high nonlinear parameters, broadband transmission window and high laser damage thresholds [1]. Nevertheless, large Fresnel reflection losses, originating from refractive index difference between air and crystal media, limit the practical efficiency of BGSe. Thereby, the implementation of anti-reflective structures (ARs) is advantageous in reducing Fresnel optical loss from interface reflection, which in its turn make inexpensive and high-performing ARs fabrication techniques of high researcher's interest.

Femtosecond (fs) laser pulse processing has been justified as a powerful tool for nanostructures fabrication [2]. Being the one of the most common laser-induced nanomorphology, LIPSS (laser-induced periodic surface structures) were fabricated on almost all types of solid materials to modify surface properties, including colorization, super-hydrophobicity and anti-reflection.
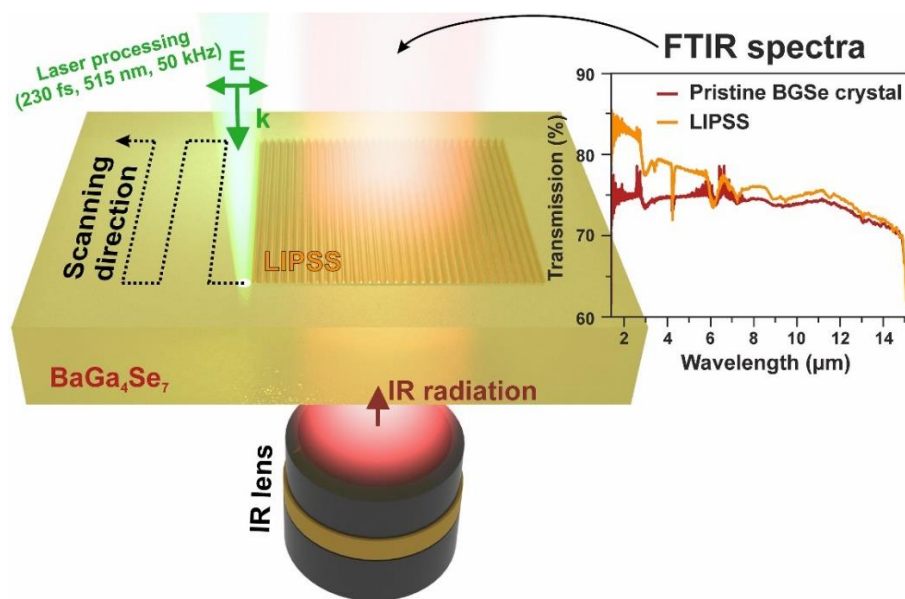

Figure 1. Schematic illustration of LIPSS formation under femtosecond laser treatment of BGSe surface in the snake-like trajectory. Inset demonstrates Fourier-transform Infra-Red transmission spectra of unprocessed BGSe and LIPSS, fabricated on the one side of crystal.

Here, we demonstrate simple, high-performing and single-step fs-laser multi-pulse processing of BaGa₄Se₇ crystal surface. The resulting morphology represent subwavelength-periodic (~360 nm) LIPSS with nanotrench orientation, perpendicular to the irradiating laser beam polarization. The variation of experimental parameters (scanning speed, laser pulse fluence, pulse overlapping) was demonstrated to slightly effect on the LIPSS periodicity. Fourier-transform Infra-Red (FTIR) spectroscopy revealed the increased NIR transmittance of LIPSS-textured BGSe surface, compared to the untreated crystal.

[1] A. Yelisseyev, S. Lobanov, P. Krinitsin, L. Isaenko, The optical properties of the nonlinear crystal BaGa₄Se₇, Optical Materials, 99, 109564 (2020).
[2] G. Stephan, Formation of laser-induced periodic surface structures on different materials: Fundamentals, properties and applications, Advanced Optical Technologies, 11-39 (2020).

Solar steam generation for high-performance desalination

A.V. Syuy[1*], **I.V. Martynov**[1], **D.I. Tselikov**[2], **G.I. Tselikov**[3], **M.S. Gurin**[1],
V.G. Efremenko[4], **D.V. Dyubo**[1], **A.V. Arsenin**[1], **V.S. Volkov**[3]

1- Moscow Institute of Physics and Technology (National Research University), Dolgoprudny, 141701, Russia
*2- Laboratory "Bionanophotonics", Institute of Engineering Physics for Biomedicine (PhysBio), MEPhI,
Moscow 115409, Russia*
*3- Emerging Technologies Research Center, XPANCEO, Internet City, Emmay Tower, Dubai, United Arab
Emirates*
4- Far Eastern State Transport University, Khabarovsk, 680021, Russia

* siui.av@mipt.ru

Photon heating opens up new opportunities for science and technology, offering innovative solutions for medicine and materials science. For example, photon heating using MXene nanoparticles to generate solar steam is a pioneering area of research that opens up new possibilities in the field of alternative energy. This process uses light to heat MXene nanoparticles in water, resulting in the generation of steam. MXene nanoparticles, known for their unique electronic and optical properties, can be optimized to enhance the photocatalytic process [1]. This allows accelerating the photocatalysis process and enhancing the photoresponse. The application of this method can be particularly useful in the field of solar energy, where efficient conversion of sunlight into energy is key. In addition, this process can be used to produce valuable chemicals or purify water [2]. This makes it potentially revolutionary in the field of alternative energy and sustainable development. This work demonstrates a simple and effective strategy to develop a composite membrane for efficient photothermal desalination based on MAX phase Ti_2AlC:Y (Y 0.2 wt.%) nanoparticles (fig.1). The solar energy-to-water vapor conversion efficiency of Ti_2AlC:Y (Y 0.2 wt.%) nanoparticles of MAX phase Ti_2AlC:Y is significantly superior to that for MXene $Ti_3C_2T_x$ nanoflakes and any other MXene nanoflakes.
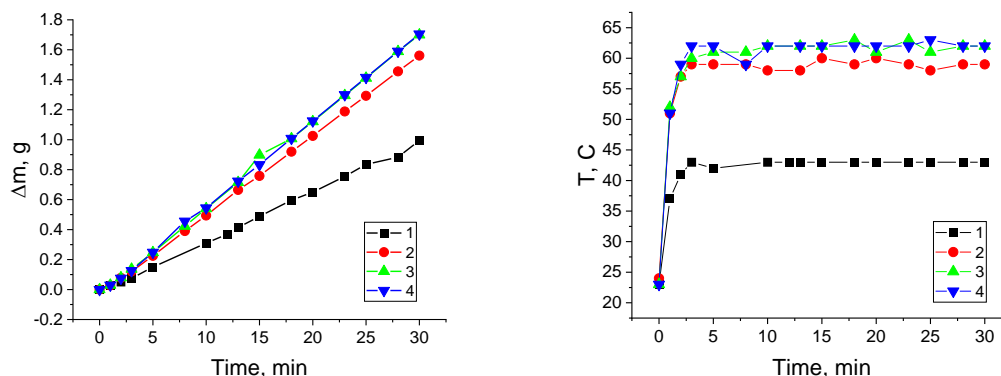

Fig.1. Time dependence of vaporization and heating rate of Ti_2AlC:Y (0.2 wt.%) samples.
1 – empty filter, 2 – sample with 3.6 g/m^2, 3 – sample with 4.9 g/m^2, 4 – sample with 10.8 g/m^2.

[1] L. Yuan, B.B. Bourgeois, C.C. Carlin, F.H. da Jornada, J.A. Dionne, Sustainable chemistry with plasmonic photocatalysts, Nanophotonics, 2023. Vol. 12(14). P. 2745–2762.
[2] B. Zhang, Q. Gu, C. Wang, Q. Gao, J. Guo, P.W. Wong, C.T. Liu, A.K. An, Self-Assembled Hydrophobic/Hydrophilic Porphyrin-$Ti_3C_2T_x$ MXene Janus Membrane for Dual-Functional Enabled Photothermal Desalination, ACS Applied Materials & Interfaces, 2021. Vol. 13 (3), P. 3762-3770.

Creation and study of thin-film heavy metal/ferro-(ferri)magnet nanostructures promising for spintronics

A. Telegin[1*], V. Bessonova[1], V. Teplov[1], V. Bessonov[1], S. Batalov[1], I. Lobov[1],
M.E. Stebliy[2], A. Ognev[2,3], Y. Kim[4], A. Samardak[2,3]

1- M.N. Mikheev Institute of Metal Physics, UB of RAS,620108, Yekaterinburg, S. Kovalevskaya str., 18
2- Far Eastern Federal University, 690922, Vladivostok, Ajax Bay, Russky Island
3- Sakhalin State University, 694420, Yuzhno-Sakhalinsk, Lenina str., 290
4- Korea University, Seoul, 02841, Republic of Korea

* telegin@imp.uran.ru

Being topologically protected skyrmions are regarded as the promising candidates for the role of information carriers in a new generation of energy efficient information processing technologies [1]. The presence of strong interfacial Dzyaloshinskii-Moriya interaction (iDMI) in ferromagnet/heavy metal (HM/FM) thin-film multilayers has significantly expanded the range of materials in which skyrmions can be created [2]. Throughout several comprehensive studies we theoretically and experimentally explored the evolution of iDMI and dynamics of skyrmions in two types of material systems: FM and ferrimagnetic (FiM) multilayers.

Samples of nanostructures with high perpendicular magnetic anisotropy were fabricated using magnetron sputtering techniques, and current-carrying structures with locally enhanced current density were also formed using ion-plasma etching and photolithography. Using vibration magnetometry, Kerr spectroscopy and electric-probe-measurements, the magnetic, magnetooptical and magnetotransport properties of thin-film nanostructures were studied. It was shown that all samples exhibit a magnetic response to current flow due to the Hall spin effect. The specific current-induced field parameters and the efficiency of current-induced switching were determined for the obtained nanostructures, as well as their dependence on the parameters of HM and FM layers. The maximum efficiency of current-induced processes was obtained in FiM alloys [3]. The Kerr microscopy demonstrates the presence of the domain structure and the magnetic skyrmions in the obtained samples. An estimation of the magnitude of the DMI was made based on the features of the domain structure behavior (e.g. asymmetric movement of chiral domain walls).

The laser spectroscopy experimental technique based on the Mandelstam-Brillouin light scattering (contactless spin-wave method) was employed to study the spin dynamics as well as estimation of iDMI in the samples. It was directly demonstrated that the magnitude of the shift, frequency and half-width of resonance lines in the spectra of spin waves of nanostructures closely correlate with the parameters of layers, type of the interface, and even the type of non-magnetic layer. A pronounced non-linear temperature dependence of the iDMI in FM/oxide nanostructures was observed for the first time.

Using micromagnetic modeling methods, the processes of magnetization reversal of nanostructures and the movement of skyrmions under the influence of electric and spin current in FM and FiM structures were studied. The influence of the DMI, damping, magnetic anisotropy, and magnetic fields on the speed of movement of skyrmions under the influence of AC/DC was also considered [4]. It was shown, the current-induced effects can be effectively used to control skyrmions in FiM metallic nanostructures.

Finally, the results showed that multi-sublattice ferrimagnetic films are a promising materials system, paving a path forward for the field of spintronics.

[1] A. Fert and F.N. Van Dau, Spintronics, from giant magnetoresistance to magnetic skyrmions and topological insulators, Comptes Rendus Physique, vol.20, pp. 817-831, (2019).
[2] J. Park, et al, Compositional gradient induced enhancement of Dzyaloshinskii–Moriya interaction in Pt/Co/Ta heterostructures modulated by Pt–Co alloy intralayers, Acta Materialia, vol.241, p. 118383, (2022).
[3] A. Telegin, V. Bessonov, I. Lobov, et al, Efficient current-induced magnetization reversal in metallic nanostructures, Physics of the Solid State, vol.12, p. 2158, (2023).
[4] A. Telegin, M. Stebliy, A. Ognev, et al, Dynamics of skyrmion textures in thin ferrimagnetic films, Indian J. Phys., (2024).

Development of high performance photodetectors based on porous Si-2D materials heterostructures

N. Tripathi

Samara National Research University, 34, Moskovskoye Shosse, Samara, 443086, Russia

tripati.n@ssau.ru, nishant.tripathi.11@gmail.com

The present study explores two contemporary topics: the creation of high-performance self-powered photodetectors, and the synthesis of heterostructures between transition metal chalcogenides (TMCs) and other promising materials like porous silicon (P-Si) or silicon nanowires for the aforementioned photodetectors. The fundamental mechanisms for photodetection and photocatalysis are largely similar, indicating that the proposed heterostructures will be beneficial not only for the photodetectors discussed but also for future photocatalysis reactions and other light energy harvesting applications.

Currently, the development of highly sensitive and self-powered photodetectors is both relevant and innovative [1,2]. Self-powered photodetectors, which operate without an external power supply, represent a new class of photodetectors [3]. The key to achieving self-powered functionality in a photodetector is the photovoltaic effect, typically occurring in photodiodes with a heterostructure [4]. For instance, in a p-n junction, the gradient in charge carrier concentration leads to the movement of holes and electrons, forming a built-in electric field. When this junction is exposed to light, electron-hole pairs are separated by the built-in electric field at the junction interface, moving to the external circuit connected to this heterostructure [4]. Notably, self-powered photodetectors exhibit minimal dark current, significantly enhancing photodetection efficiency [5].

To develop highly sensitive self-powered photodetectors, researchers are combining various materials to achieve optimal photodetection performance. Porous silicon (P-Si) has garnered considerable attention for use in optoelectronic devices, especially following the discovery of its effective visible photoluminescence and electroluminescence [6,7]. P-Si boasts a broad modulated direct energy band gap, a single-crystal structure compatible with bulk silicon [8], high resistivity, diverse structures (micro-, meso-, and macro-structures) with a large surface area to volume ratio [9,10], a cost-effective and simple fabrication process, and compatibility with modern silicon microelectronic manufacturing processes [11]. These advantages make P-Si an excellent candidate for photodetectors [12].

[1] D. Wu, J. Guo, J. Du, C. Xia, L. Zeng, Y. Tian, Z. Shi, Y. Tian, X.J. Li, Y.H. Tsang, J. Jieet, Highly polarization-sensitive, broadband, self-powered photodetector based on graphene/PdSe$_2$/germanium heterojunction, ACS nano 13 (9) (2019) 9907-9917.
[2] Y. Xin, X. Wang, Z. Chen, D. Weller, Y. Wang, L. Shi, X. Ma, C. Ding, W. Li, S. Guo, R. Liu, Polarization-sensitive self-powered type-II GeSe/MoS$_2$ van der Waals heterojunction photodetector, ACS Applied Materials & Interfaces 12 (13) (2020) 15406-15413.
[3] H. Qiao, Z. Huang, X. Ren, S. Liu, Y. Zhang, X. Qi, H. Zhang, Self-powered photodetectors based on 2D materials, Adv. Optical Mater. (2019) 1900765.
[4] J. Jiang, Y. Wen, H. Wang, L. Yin, R. Cheng, C. Liu, L. Feng, J. He, Recent Advances in 2D Materials for Photodetectors, Adv. Electron. Mater. 7 (2021) 2001125.
[5] S. Kim, M. Kim, H. Kim, Self-powered photodetectors based on two-dimensional van der Waals semiconductors, Nano Energy 127 (2024) 109725.
[6] L. Canham, Silicon quantum wire array fabrication by electrochemical and chemical dissolution of wafers, Appl Phys Lett 57 (1990)1046–1048.
[7] N. Koshida, H. Koyama, Visible electroluminescence from porous silicon, Appl Phys Lett 60 (1992) 347–349.
[8] M.-K. Lee, C.-H. Chu, Y.-H. Wang, S. Sze, 1.55-μm and infrared-band photoresponsivity of a Schottky barrier porous silicon photodetector, Opt. Lett. 26 (2001) 160–162.
[9] P. Fauchet, J. Von Behren, K. Hirschman, L. Tsybeskov, S. Duttagupta, Porous silicon physics and device applications: a status report, Phys Status Solidi (A) 165 (1998) 3–13.
[10] R. Herino, G. Bomchil, K. Barla, C. Bertrand, J. Ginoux, Porosity and pore size distributions of porous silicon layers, J Electrochem Soc 134 (1987) 1994–2000.
[11] H.A. Lopez, Porous silicon nanocomposites for optoelectronic and telecommunication applications in University of Rochester (2001).
[12] H. Hadi, R. Ismail, N. Habubi, Optoelectronic properties of porous silicon heterojunction photodetector, Indian J. Phys. 88 (2014) 59–63.

Laser-driven nanoparticle synthesis with tunable size, shape and composition from 2D materials

<u>G. Tselikov</u>[1*], G. Ermolaev[1], A. Minnekhanov[1], A. Arsenin[1], V. Volkov

1- Emerging Technologies Research Center, XPANCEO, Dubai, 00000, United Arab Emirates

* celikov@xpanceo.com

Two-dimensional (2D) layered transition metal dichalcogenides (TMDCs) have attracted tremendous research interests due to their unique properties for developing new-generation electronic and optoelectronic devices [1]. Nanostructures made from transition metal dichalcogenides represent unique platform for nanophotonics due to its high dielectric constants and nontrivial excitonic physics. The important feature of TMDCs nanoparticles (NPs) that distinguishes them from pure all-dielectric silicon NPs is the possibility of realization of Mie-exciton coupling regime that boosts light-matter interaction at the nanoscale manifesting itself in resonant enhancement of second harmonics generation [2], light scattering [3] and photothermal response [4]. However, it is worth noting that despite the recent significant progress in the field of dichalcogenide nanophotonics, the problem of nanostructuring of TMDCs remains open. On the one hand, it can be solved using standard technological approaches (such as lithography, ion beam etching). However, these methods have several limitations. For instance, they do not facilitate the production of spherical TMDCs nanoparticles. Meanwhile, various theranostic approaches rely on resonant spherical nanoparticles (NPs). These NPs enable both the visualization of nanoparticles within biological tissues and the treatment of malignancies through nanoparticle-enhanced phototherapy.

In this work, we demonstrate a simple method for synthesizing such well-defined nanoparticles of various shapes using femtosecond laser ablation. We establish that any of the TMDCs, MXenes, and perovskites we studied can be synthesized in the form of such particles from two-dimensional precursor materials. We experimentally prove the composition of the obtained nanoparticles and discuss the extensive potential of their applications. Their development and integration into devices and systems have the potential to drive innovations and improve performance in energy, catalysis, medicine, neuromorphic electronics, and environmental remediation. The results obtained will be useful in ongoing research to fully exploit the potential of such nanoparticles.

[1] B. Munkhbat, B. Küçüköz, D.G. Baranov, T.J. Antosiewicz, T.O. Shegai, Nanostructured Transition Metal Dichalcogenide Multilayers for Advanced Nanophotonics, Laser Photonics Rev, 17, 2200057 (2022).

[2] A.A. Popkova, I.M. Antropov, G.I. Tselikov, G.A. Ermolaev, I. Ozerov, R.V. Kirtaev, S.M. Novikov, A.B. Evlyukhin, A.V. Arsenin, V.O. Bessonov, V.S. Volkov, A.A. Fedyanin, Nonlinear Exciton-Mie Coupling in Transition Metal Dichalcogenide Nanoresonators, Laser & Photonics Reviews, 16(6) 2100604 (2022).

[3] G.I. Tselikov, G.A. Ermolaev, A.A. Popov, G.V. Tikhonowski, A.S. Taradin, A.A. Vyshnevyy, K. Novoselov, V.S. Volkov, Transition metal dichalcogenide nanospheres for high-refractive-index nanophotonics and biomedical theranostics, PNAS 119(39) e2208830119 (2022).

[4] A.S. Chernikov, G.I. Tselikov, M.Yu. Gubin, A.V. Shesterikov, K.S. Khorkov, A.V. Syuy, G. Ermolaev, I.S. Kazantsev, R.I. Romanov, A. Markeev, A.A. Popov, G.V. Tikhonowski, O.O. Kapitanova, D.A. Kochuev, A.Yu. Leksin, D.I. Tselikov, A.V Arsenin, A.V. Kabashin, V.S. Volkov, A.V. Prokhorov, Tunable optical properties of transition metal dichalcogenide nanoparticles synthesized by femtosecond laser ablation and fragmentation, J. Mater. Chem., 11, 3493-3503 (2023).

Excitation of surface plasmon polaritons by inhomogeneities of the surface of a plasmonic material

A. Dyshlyuk[1], A. Proskurin[2], A. Bogdanov[2,3], O. Vitrik[1*]

1- Institute of Automation and Control Processes (IACP) FEB RAS, Far Eastern Federal University (FEFU) and Vladivostok State University (VSU), 690041 Vladivostok, Russia
2- School of Physics and Engineering, ITMO University, 197101 St. Petersburg, Russia
3- Qingdao Innovation and Development Base of Harbin Engineering University, Sansha road 1777, 266000, Qingdao, China

* oleg_vitrik@mail.ru

Illumination of metal surfaces with regular and irregular microscopic inhomogeneities of relief leads not only to excitation of local plasmon resonances in such inhomogeneities, but also to interaction of these structures by means of surface plasmon-polariton (SPP) waves [1]. This interaction can lead to the formation of new modes with other spectral and spatial properties and, of course, to significant changes in the optical properties of surfaces. However, prediction and analysis of these properties are hampered by the complexity of analytical solution of the problem of SPP excitation by surface objects of arbitrary configuration. This problem can be solved analytically in the dipole approximation for small plasmonic nanoparticles on a metallic substrate illuminated by a plane wave using the formalism of the dyadic Green's function [2,3]. This method gives good agreement with full-wave numerical simulations, but it is rather cumbersome and requires the calculation of Sommerfeld integrals.

We present an alternative approach using the Lorentz reciprocity theorem and orthogonality of modes, similar to the method used in waveguide theory [4]. The problem is solved analytically for "point" nanoantennas in both 2D and 3D geometries, when SPPs are excited by an infinitely long cylindrical wire or a plasmonic sphere, and in the simplest case of a nanostructured surface with a sinusoidally perturbed boundary. In all cases, the obtained analytical solutions are compared with the results of numerical simulations. The results of such comparison demonstrate almost perfect agreement of analytical and numerical solutions for "point" nanoantennas with radius of curvature less than $\lambda/10$. In the case of a sinusoidally perturbed boundary, the analytical solution correctly predicts the optimal corrugation height (x_{opt}), which provides the maximum SPP excitation efficiency. At the same time, analytical and numerical values of the SPP amplitude agree when the corrugation height x turns out to be $x \ll x_{opt}$ or $x \gg x_{opt}$; at $x = x_{opt}$ their mismatch does not exceed 25%. The limitations of the analytical model leading to such mismatches are discussed. We believe that the presented approach can be useful for modeling various phenomena related to SPP excitation.

[1] L. Novotny and B. Hecht, Principles of Nano-Optics. Publisher: Cambridge University Press, 537 p., 2006.
[2] B. Evlyukhin and S.I. Bozhevolnyi, Point-dipole approximation for surface plasmon polariton scattering: Implications and limitations, Phys. Rev. B, 71, no. 13, p. 134304, Apr. 2005.
[3] T. Søndergaard and S.I. Bozhevolnyi, Surface plasmon polariton scattering by a small particle placed near a metal surface: An analytical study, Phys. Rev. B - Condens. Matter Mater. Phys. 69, no. 4, pp. 1-10, 2004.
[4] A.W. Snyder and J.D. Love, Optical Waveguide Theory. Publisher: Chapman and Hall, 734 p., 1983.

The effect of HIP on the microstructure and luminescent properties of SPS Al$_2$O$_3$−Ce:YAG composites

A.A. Vornovskikh[1*], O.O. Shichalin[1], A.P. Zavjalov[1], S.S. Balabanov[2], D.Yu. Kosyanov[1]

1- Far Eastern Federal University, 10 Ajax Bay, Russky Island, Vladivostok 690922, Russia
2- G.G. Devyatykh Institute of Chemistry of High-Purity Substances of the RAS, 49 Tropinin str.,
Nizhny Novgorod 603137, Russia

* vornovskikh_aa@dvfu.ru

The use of laser diodes (LDs) as excitation sources makes it possible to obtain white light with a high lumen density. Al$_2$O$_3$–Ce:YAG composite ceramic phosphors are considered as promising components of white LDs. At the same time, fine-grained composites show better applicability when combined with LDs in the reflection mode, where the proper scattering ability of the phosphor plays a key role.

Spark plasma sintering (SPS), as one of the high-speed consolidation techniques under pressure, is considered a proven one-step method for producing opto-functional ceramics with fine microstructure and some inherent residual porosity. An additional hot isostatic pressing (HIP) step is being considered as a way to improve the optical properties of such ceramic materials.

A series of Al$_2$O$_3$−Ce:YAG (0.05-0.3 at% Ce^{3+}) composite ceramics were obtained using the individual SPS technique and its combination with HIP post treatment. The HIP stage contributed to some homogenization of the secondary phase grains in the garnet matrix, while reducing their dispersion. The average grain sizes of the constituent phases YAG and Al$_2$O$_3$ were ~4 μm and ~2 μm, respectively.

The SR luminescence spectra and luminescence kinetics were studied at the wavelength 535 nm of Ce:YAG. The maximum intensity was achieved at 0.2 at% Ce^{3+}, the effect of HIP on the position of the Ce:YAG line is insignificant – a monotonic increase of ~527–534 nm is observed at 0.05–0.3 at% Ce^{3+}. The luminescence kinetics was characterized by two decay modes. An increase in the decay time of ~0.7–3.0 ns and a monotonic decrease in its fraction from ~22–35 to ~14% were observed with increasing Ce^{3+} content for the fast mode, while increasing the time from ~20–30 to ~47–57 ns for the slow mode.

The luminous properties of phosphors were attestated as a function of the input 454 nm LD power density in reflection mode. Laser-induced luminescence saturation was not observed up to 14 W/mm^2. LF (LE) and CCT (CRI) values of 3300–3260 lm (212–210 lm/W) and 7352–5700 K (58–52), respectively, were obtained for 1 mm-thick Al$_2$O$_3$–Ce:YAG (0.1-0.3 at% Ce^{3+}) SPS+HIP−composites.

Biomimetic microstructures for radiative cooling

H. Xu

Harbin Institute of Technology, China

Recently, biomimetic photonic structural materials have significantly improved their radiative cooling performance. However, most research has focused on understanding cooling mechanisms, with limited exploration of sensitive parameter variations. Traditional numerical methods are costly and time-consuming and often struggle to identify optimal solutions, limiting the scope of high-performance microstructure design. To address these challenges, we integrated machine learning into the design of Batocera LineolataHope bionic photonic structures, using SiO_2 as the substrate. Deep learning models provided insights into the complex relationship between bionic metamaterials and their spectral response, enabling us to identify the optimal performance parameter range for truncated cone arrays (height-to-diameter ratio (H/D bottom) from 0.8 to 2.4), achieving a high average emissivity of 0.985. Experimentally, the noon temperature of fabricated samples decreased by about 8.3°C. This data-driven approach accelerates the design and optimization of robust biomimetic radiative cooling metamaterials, promising significant advancements in standardized passive radiative cooling applications.

Optical and electrophysical anisotropy in amorphous silicon films irradiated with femtosecond laser pulses

S. Zabotnov[1*], **D. Shuleiko**[1], **M. Martyshov**[1], **E. Kuzmin**[1,2], **P. Pakholchuk**[1,2], **L. Volkovoynova**[3], **A. Serdobintsev**[3], **P. Kashkarov**[1]

1- Lomonosov Moscow State University, Faculty of Physics, 1/2 Leninskie Gory, Moscow, 119991, Russia
2- P.N. Lebedev Physical Institute of RAS, 53 Leninsky Ave., Moscow, 119991, Russia
3- Saratov State University, 83 Astrakhanskaya St., Saratov, 410012, Russia

* zabotnov@physics.msu.ru

Advanced technologies of photonics and microelectronics allow designing compact planar elements for integrated optics and integrated photonic circuits based on silicon. Femtosecond laser pulses irradiation of thin silicon films might change their phase states (amorphous or crystalline) and provide surface texturing via fabrication of laser-induced periodic surface structures (LIPSSs) with micron and even submicron periods [1,2]. Such structures can be considered as metasurfaces with artificial anisotropy.

In our work, we fabricated large area LIPSSs (up to 5×5 mm^2) in the amorphous silicon thin films and studied reflectance spectra in the infrared range at various incident light polarizations for the irradiated films as well as carried out conductivity measurements in plane of the samples along and orthogonally LIPSSs.

Three types of samples were irradiated and examined: an amorphous silicon layer only, an amorphous silicon layer with a flexible polyimide underlayer, and an amorphous silicon layer with a 10 nm aluminum coating. The amorphous silicon layers have thickness of 600–1000 nm.

The samples were irradiated in the raster mode with femtosecond laser pulses generated by Satsuma Amplitude Systems (300 fs, 515 or 1030 nm) and Avesta (125 fs, 1250 nm) lasers. LIPSSs were fabricated in all samples. The periods of the surface gratings obtained are close to the wavelengths used.

The appearance of the LIPSSs is caused by photoinduced surface plasmon-polaritons generation and is confirmed by calculations with the Sipe-Drude theory [3].

Reflectance spectra for all samples were measured in the range of 1.5–18 μm at an incident angle of 13° and s- and p-polarizations. The measured spectra indicate the presence of dichroism in the irradiated samples. Its value reaches the maximum value of 0.12 μm^{-1} in the samples without the aluminum coating. All the spectra are characterized by thin film interference. Analysis of interference maxima positions made it possible to find the refractive indices for the ordinary and extraordinary waves. The maximum birefringence value is 0.2 in the range of 1.9–2.7 μm for the sample with the aluminum coating. The results obtained are in a good agreement with calculations in the framework of the generalized Bruggeman model [4] for alternating components from amorphous and crystalline silicon.

Raman spectroscopy data show partial nanocrystallization of the surface (up to 70%). The silicon nanocrystal presence leads to growth of the specific conductivity up to 3 orders for the irradiated samples in comparison with non-irradiated ones. Additionally, the in-plane conductivity anisotropy was revealed. This result is in a good agreement with the Bruggeman model too and absorption spectra for the surface possessing artificial anisotropy.

Thus, the silicon films with LIPSSs can be considered as a promising base to design planar devices which are sensitive to the incident light polarization and the applied current direction.

[1] D. Shuleiko, M. Martyshov, D. Amasev, et al, Fabricating femtosecond laser-induced periodic surface structures with electrophysical anisotropy on amorphous silicon, Nanomaterials, 11, 42, (2021).
[2] D. Shuleiko, S. Zabotnov, M. Martyshov, et al, Femtosecond laser fabrication of anisotropic structures in phosphorus- and boron-doped amorphous silicon films, Materials, 15, 7612, (2022).
[3] J. Bonse, S. Höhm, S.V. Kirner, et al, Laser-induced periodic surface structures – a scientific evergreen, IEEE J. Sel. Top. Quantum Electron., 23, 9000615, (2017).
[4] V.I. Ponomarenko and I.M. Lagunov, Generalized formula for effective dielectric permeability of the medium with ellipsoidal inclusions, J. Commun. Technol. El., 66, 403-407, (2021).

Continuously fabricating macro/micro textures on freeform surface by optical-mechanical coupled on-the-fly five-axis laser micromachining

J. Zhang[1]

1- Center for Precision Engineering, Harbin Institute of Technology, Harbin, 150001, China

zhjj505@gmail.com

While laser surface texturing is greatly needed for promoting functionalities of components and parts, how to achieve high uniformity and high precision on large area curved surface by laser surface texturing based on galvanometer is challenging, mainly due to the variant beam incidence angle with coordination evolution of laser beam. In the present work, we propose a strategy of simultaneously coupling both the galvanometer and the five-axis mechanical motion platform for laser surface texturing of large area freeform surface, which enables the constant coincidence of laser beam with ablated curved surface normal. In particular, the projection and transformation of pre-determined planar pattern on spherical surface are investigated, which are then used to derive the precise path of laser-surface interaction point. Meanwhile, a virtual prototype of the multi-axis laser milling with embedded interpolation algorithm is established. Finally, complex macro/micro patterns are continuously structured on large area freeform surface by employing the proposed multi-axis laser milling method, and subsequent characterization demonstrates both long range uniformity and local high accuracy of the fabricated patterns. Current work provides a feasible method for the continuously laser surface texturing of large area curved surfaces.

Hybrid metal-dielectric nanostructures: fundamentals, applications and perspectives

D. Zuev[1]

1- ITMO University, Kronverksky Pr. 49, bldg. A, St. Petersburg, 197101, Russia

d.zuev@metalab.ifmo.ru

Resonant hybrid metal-dielectric nanostructures bridging the gap between plasmonics and high refractive index (dielectric) nanoparticles has become a fast-developing field of nanophotonics. Indeed, manipulation of optical resonances of metal and/or dielectric components of united hybrid nanosystem pave the way to enhance optical effects as well as demonstrate new ones, and as a result, realize wide range of applications.

In this talk we start from a description of the optical properties which can be implemented in different metal-dielectric nanostructures. Then the fabrication techniques making possible to create a large platelet of hybrid nanostructures geometries (e.g. hybrid nanosponges, asymmetrical nanoantennas, etc.) are discussed. The particular emphasis is placed to optical properties in such systems originating from both material properties and resonant behavior of the nanostructure components, e.g. optical generation of static electric field, white light luminescence spectra control by the microstructure reconfiguration, second harmonic generation tuning through unification of plasmonic, semiconductor and polymer materials in a single system, etc. The application potential of metal-dielectric nanostructures for nanoscale light sources, unclonable security labels, reconfigurable devices, biosensors bi-functional sensor-catalytic systems is also described. Finally, perspectives of hybrid nanophotonics development are also highlighted.

AGRICULTURAL AND BIOPHYSICAL PHOTONICS

Simulation modeling of multiple scattering media to optimize the geometry of nephelometric sensors in agriculture

M.E. Astashev[1,2*], **D.N. Ignatenko**[1], **A.V. Shkirin**[1], **S.V. Gudkov**[1]

1- Prokhorov General Physics Institute of the Russian Academy of Sciences, 38 Vavilova St., 119991 Moscow, Russia
2- Institute of Cellular Biophysics, FRC PSCBR, Russian Academy of Sciences, 3 Institutskaya St., 142290 Pushchino, Russia

* astashev@yandex.ru

The use of nephelometric sensors for quantitative analysis of the composition of milk, its derivatives and other livestock products allows us to solve the problem of on-line monitoring of technological processes at all stages of the production [1]. Nephelometric sensors are relatively simple, cheap, reliable, and allow various designs and geometry that meet the requirements of compatibility of construction materials to food products. The problem is the lack of a mathematical description of the interaction of the optical range electromagnetic radiation with a multiply scattering medium, which makes it possible to predict with sufficient accuracy the result of this interaction in a system with an arbitrary cell geometry, location of radiation sources and receivers. We have proposed and studied a simple simulation model for the distribution of light power of a point source of radiation in a cell of arbitrary shape. At its core, the model represents a cellular automaton with simple rules for the interaction of neighboring cells, simulating the process of radiation redistribution during a single act of interaction of radiation with scattering particles, which makes it possible to use the results of scatterometric measurements of highly dilute suspensions, with the formation of the Muller matrix, to set parameters when modeling a highly scattering medium. We have obtained a satisfactory agreement between the simulation results and the results of measuring the scattering process in a nephelometric sensor with cylindrical geometry we had constructed before [2]; so we have obtained light scattering indicatrices similar to the real sensor. Scattering assessments were also carried out in systems with linear geometry of receivers and transmitters. These studies are of interest in the future of developing sensors for transport systems for milk and its derivatives with pipelines of complex geometry.

[1] S.V. Gudkov, R.M. Sarimov, M.E. Astashev, R.Y. Pishchalnikov, D.V. Yanykin, A.V. Simakin, A.V. Shkirin, D.A. Serov, E.M. Konchekov, o. Gusein-zade Namik Guseynaga, V.N. Lednev, M.Y. Grishin, P.A. Sdvizhenskii, S.M. Pershin, A.F. Bunkin, M.K. Ashurov, A.G. Aksenov, N.O. Chilingaryan, I.G. Smirnov, D.Y. Pavkin, D.O. Hort, M.N. Moskovskii, A.V. Sibirev, Y.P. Lobachevsky, A.S. Dorokhov, A.Y. Izmailov, Modern physical methods and technologies in agriculture, Physics-Uspekhi 67(02) 194-210, (2023).
[2] A.V. Shkirin, M.E. Astashev, D.N. Ignatenko, N.V. Suyazov, S.N. Chirikov, V.V. Kirsanov, D.Y. Pavkin, Y.P. Lobachevsky, S.V. Gudkov, A Monoblock Light-Scattering Milk Fat Percentage and Somatic Cell Count Sensor for Use in Milking Systems, Sensors 23(20) (2023).

Laser methods and technologies in agriculture

S.V. Gudkov

Prokhorov General Physics Institute of the Russian Academy of Sciences, Moscow 119991, Russia

s_makariy@rambler.ru

The report at the conference will present both new theoretical and practical results of the use of modern laser, optical, and other methods and technologies in agriculture [1]. Technologies and materials for passive control of the solar spectrum in greenhouses will be considered [2]. A review of the instrumental base used for laser remote sensing of agro- and biosystems, modern laser express technologies used for rapid analysis of the chemical composition of a substance will be carried out [3,4]. Optical methods used in biological and agricultural diagnostics will be described [5,6], including methods based on Müller matrix polarimetry [7]. A separate part of the report will be devoted to the production and use of nano-sized objects in agriculture and the food industry [8,9]. The application of numerous plasma technologies in agriculture will also be discussed [10].

[1] S.V. Gudkov, R.M. Sarimov, M.E. Astashev, R.Yu. Pishchalnikov, D.V. Yanykin, A.V. Simakin, A.V. Shkirin, D.A. Serov, E.M. Konchekov, N.G. Gusein-zade, V.N. Lednev, M.Ya. Grishin, P.A. Sdvizhenskii, S.M. Pershin, A.F. Bunkin, M.Kh. Ashurov, A.G. Aksenov, N.O. Chilingaryan, I.G. Smirnov, D.Yu. Pavkin, D.O. Hort, M.N. Moskovskii, A.V. Sibirev, Ya.P. Lobachevsky, A.S. Dorokhov, A.Yu. Izmailov, Modern physical methods and technologies in agriculture, Physics-Uspekhi, vol. 67(2), pp. 194-210, (2024).
[2] M.O. Paskhin, D.V. Yanykin, S.V. Gudkov, Current Approaches to Light Conversion for Controlled Environment Agricultural Applications: A Review, Horticulturae, vol. 8, pp. 885, (2022).
[3] V.N. Lednev, P.A. Sdvizhenskii, A.S. Dorohov, S.V. Gudkov, S.M. Pershin, Improving LIBS analysis of non-flat heterogeneous samples by signals mapping, Applied Optics, vol. 62(8), pp. 2030-2038, (2023).
[4] V.N. Lednev, M.Y. Grishin, P.A. Sdvizhenskii, R.K. Kurbanov, M.A. Litvinov, S.V. Gudkov, S.M. Pershin, Fluorescence Mapping of Agricultural Fields Utilizing Drone-Based LIDAR, Photonics, vol. 9, pp. 963, (2022).
[5] D.E. Burmistrov, D.Y. Pavkin, A.R. Khakimov, D.N. Ignatenko, E.A. Nikitin, V.N. Lednev, Y.P. Lobachevsky, S.V. Gudkov, A.V. Zvyagin, Application of Optical Quality Control Technologies in the Dairy Industry: An Overview, Photonics, vol. 8, pp. 551, (2021).
[6] S.V. Gudkov, T.A. Matveeva, R.M. Sarimov, A.V. Simakin, E.V. Stepanova, M.N. Moskovskiy, A.S. Dorokhov, A.Y. Izmailov, Optical Methods for the Detection of Plant Pathogens and Diseases (Review), AgriEngineering, vol. 5, pp. 1789-1812 (2023).
[7] D.N. Ignatenko, A.V. Shkirin, Y.P. Lobachevsky, S.V. Gudkov Applications of Mueller Matrix Polarimetry to Biological and Agricultural Diagnostics: A Review, Appl. Sci., vol. 12, pp. 5258, (2022).
[8] D.A. Serov, V.V. Khabatova, V. Vodeneev, R. Li, S.V. Gudkov, A Review of the Antibacterial, Fungicidal and Antiviral Properties of Selenium Nanoparticles, Materials, vol. 16, pp. 5363, (2023).
[9] S.V. Gudkov, D.E. Burmistrov, V.V. Smirnova, A.A. Semenova, A.B. Lisitsyn, A Mini Review of Antibacterial Properties of Al_2O_3 Nanoparticles, Nanomaterials, vol. 12(15), pp. 2635, (2022).
[10] E.M. Konchekov, N. Gusein-zade, D.E. Burmistrov, L.V. Kolik, A.S. Dorokhov, A.Y. Izmailov, B. Shokri, S.V. Gudkov, Advancements in Plasma Agriculture: A Review of Recent Studies, Int. J. Mol. Sci., vol. 24, pp. 15093, (2023).

Analysis of the dispersion composition of highly scattering polydisperse media using laser diagnostics

D.N. Ignatenko[1*], **A.V. Shkirin**[1], **M.E. Astashev**[1], **S.V. Gudkov**[1]

1- Prokhorov General Physics Institute of the Russian Academy of Sciences, Moscow, Russia

* dmitriyek13104@yandex.ru

Dispersed systems are ubiquitous in various fields of science and technology: medicine, ecology, food industry, oil refining industry, metallurgy, and so on [1-5]. Determining the characteristics of particles is an important component of research and development, production, and quality control of dispersed materials, as well as a significant tool in advanced scientific fields such as biotechnology or nanoparticle production.

Currently, optical methods are most commonly used to determine the content, size, shape, and structure of particles. Spectrophotometry, fluorimetry, optical coherence tomography, electron microscopy, ellipsometry, and scatterometry are among the most frequently used methods for studying highly dispersed colloidal systems [6]. The latter group of methods is interesting in that they allow for determining the dispersion analysis based on the form of light scattering indicatrix [7].

On the other hand, milk is a typical case of highly scattering dispersed media, as it represents a complex bioorganic system consisting of many groups of components: fats, proteins, lactose, amino acids, as well as microbiological impurities. The operational quantitative assessment of the composition of milk is usually carried out using optical spectrophotometry devices [8]. Like milk spectroscopic analyzers, light-scattering milk composition sensors are very promising as they can be made compact, fast, and inexpensive while providing sufficient accuracy in measuring the percentage content of fat and protein. Although there are several research studies proposing some schemes for using light scattering to determine the percentage content of components in milk [9-12], commercial offerings of light-scattering milk composition sensors are currently lacking.

In this work, promising methods for diagnosing turbid media based on light scattering were considered, and their capabilities were evaluated. Several new approaches to light-scattering diagnostics of turbid media, using milk as an example, were also proposed.

[1] O.B. Kudryashova, Dispersed Systems: Physics, Optics, Invariants, Symmetry, 14, p. 1602, 2022.
[2] J.M. Sullivan, M.S. Twardowski, Angular shape of the oceanic particulate volume scattering function in the backward direction, Applied Optics, 48, 6811-6819, 2009.
[3] D. Koestner, D. Stramski, R.A. Reynolds, Polarized light scattering measurements as a means to characterize particle size and composition of natural assemblages of marine particles, Applied optics, 59, pp. 8314-8334, 2020.
[4] T. Palberg, M. Ballauff, F. Kremer, G. Lagaly, Optical methods and physics of colloidal dispersions, Springer, 1997.
[5] K. Sobczyk, R. Chmielewski, L. Kruszka, R. Rekucki, Analysis of the Influence of Silty Sands Moisture Content and Impact Velocity in SHPB Testing on Their Compactability and Change in Granulometric Composition, Applied Sciences, 13, p. 4707, 2023.
[6] D.N. Ignatenko, A.V. Shkirin, Y.P. Lobachevsky, S.V. Gudkov, Applications of Mueller matrix polarimetry to biological and agricultural diagnostics: a review, Applied Sciences, 12, p. 5258, 2022.
[7] S.V. Gudkov, R.M. Sarimov, M.E. Astashev, R.Yu. Pishchalnikov, D.V. Yanykin, A.V. Simakin, A.V. Shkirin, D.A. Serov, E.M. Konchekov, N.G. Gusein-zade, V.N. Lednev, M.Ya. Grishin, P.A. Sdvizhenskii, S.M. Pershin, A.F. Bunkin, M.Kh. Ashurov, A.G. Aksenov, N.O. Chilingaryan, I.G. Smirnov, D.Yu. Pavkin, D.O. Hort, M.N. Moskovskii, A.V. Sibirev, Ya.P. Lobachevsky, A.S. Dorokhov, A.Yu. Izmailov, Modern physical methods and technologies in agriculture, Physics-Uspekhi, 67, pp. 194-210, 2024.
[8] D.E. Burmistrov, D.Y. Pavkin, A.R. Khakimov, D.N. Ignatenko, E.A. Nikitin, V.N. Lednev, Y.P. Lobachevsky, S.V. Gudkov, A.V. Zvyagin, Application of optical quality control technologies in the dairy industry: An overview, Photonics, 8, p. 551, 2021.
[9] P. Jain, S.E. Sarma, Light scattering and transmission measurement using digital imaging for online analysis of constituents in milk. Proceedings of the Optical Measurement Systems for Industrial Inspection IX, pp. 951-959, 2015.
[10] T. Katsumata, H. Aizawa, S. Komuro, S. Ito, T. Matsumoto, Quantitative analysis of fat and protein concentrations of milk based on fibre-optic evaluation of back scattering intensity, International Dairy Journal, 109, p. 104743, 2020.
[11] S. Ohtani, T. Wang, K. Nishimura, M. Irie, Milk fat analysis by fiber-optic spectroscopy, Asian-Australasian Journal of Animal Sciences, 18, pp. 580-583, 2005.
[12] F. Angrasari, A. Arifin, B. Abdullah, Fabrication of Milk Fat Sensor based on Plastic Optical Fiber, Proceedings of the Journal of Physics: Conference Series, p. 082038, 2019.

Raman spectroscopy method for evaluation of punicic acid content in pomegranate seed oil

S.M. Kuznetsov[1*], P.K. Laptinskaya[1], V.S. Novikov[1], M.N. Moskovskiy[2], S.V. Gudkov[1], G.Yu. Nikolaeva[1], E.A. Sagitova[1]

1- Prokhorov General Physics Institute of the Russian Academy of Sciences, 38 Vavilov St., 119991 Moscow, Russia
2- Federal Scientific Agro-Engineering Center VIM, 1st Institutskiy Proezd 5, 109428 Moscow, Russia

* kuznetsovsm@kapella.gpi.ru

Punicic acid ($C_{18}H_{30}O_2$, also called pomegranate acid or omega-5) is a polyunsaturated fatty acid. This acid is the main component of pomegranate seed oil (PSO) with the content of 65 – 85%. Punicic acid is extremely useful for human health due to its antioxidant, anti-inflammatory, antiparasitic, antiangiogenic and anticarcinogenic properties; it can also suppress cellular inflammation and tumor growth [1].

Traditionally, the content of fatty acids is studied using chromatographic methods. However, punicic acid and its isomers are chemically active due to the presence of three conjugated C=C bonds in their structure that can brake during the sample preparation. Therefore, their identification needs other techniques that do not require sample preparation, such as Raman spectroscopy. It is a fast and informative method for identifying and analyzing the quality of vegetable oils, including the detection of counterfeit products.

In this work, for the first time, we provided a Raman study of punicic acid contained in 13 mixtures of PSO and sunflower oil (SO) with various component ratios using two excitation wavelengths (λ_{exc}) of 532 and 785 nm. Figure 1 represents several Raman spectra (λ_{exc} = 532 nm) of pure SO and PSO, and their mixtures.
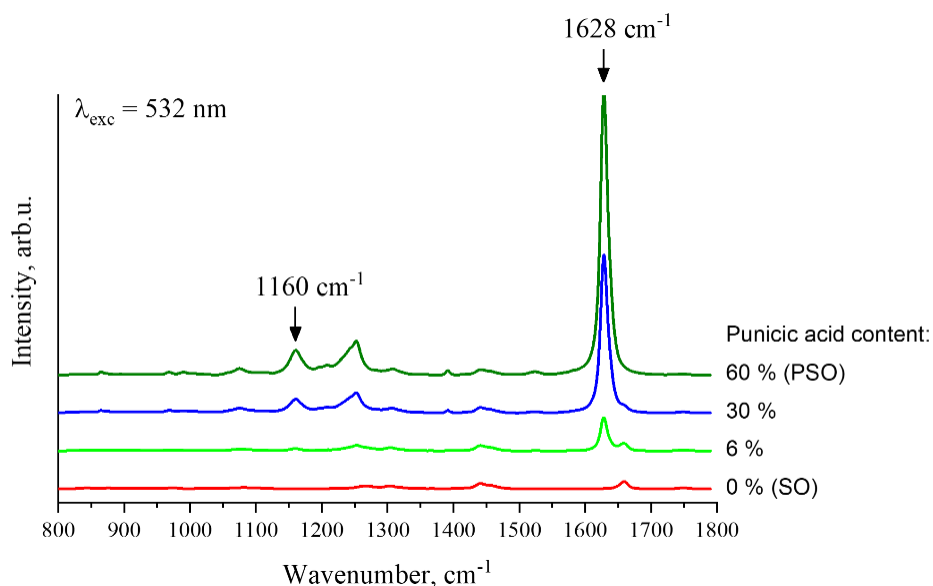

Figure 1. Raman spectra of mixtures of PSO and SO with various component ratios.
The percentage in the legend refers to the content of the punicic acid in the samples.

Our results show that Raman spectra contain bands at 1160 and 1628 cm^{-1} that are characteristic of punicic acid in PSO and are not observed in spectra of other vegetable oils. The band at 1628 cm^{-1} is observable in our work even in case of the mixture with a very low punicic acid content of 0.05 mass %.

[1] M.T. Boroushaki, H. Mollazadeh, A.R. Afshari, Pomegranate seed oil: a comprehensive review on its therapeutic effects, International Journal of Pharmaceutical Sciences and Research, vol. 7, pp. 430-442, (2016).

Laser spectroscopy for environment sensing and agriculture applications

V.N. Lednev[1*], M.Ya. Grishin[1], P.A. Sdvizhenskii[1], S.M. Pershin[1], A.F. Bunkin[1]

1- Prokhorov General Physics Institute, Russian Academy of Science, Moscow, Russia

* lednev@kapella.gpi.ru

The urbanization and rapid population growth resulted in negative impact for the environment as well as for the agriculture industry. The high quality and efficient farming require continuous monitoring of different samples types at any stage of food production chain (soil, fodder, plant materials and meat) in order to prevent any pollution by hazardous materials but sustaining the good state of the environment. Optical instruments can be used to remotely provide the online sensing for different purposes but laser spectroscopy techniques provided superior results due to unique properties of laser emission [1]. Here we reviewed the applications of laser spectroscopy techniques for environmental and agriculture sensing. Specifically, laser induced fluorescence, Raman spectroscopy and laser induced breakdown spectroscopy (LIBS) techniques have been discussed with the emphasis on its perspectives for online sensing. The examples of the developed compact instruments capable to provide express measurements including sensing from the drones (i.e., unmanned aircraft or ship vehicles) are presented. Simple and economy fluorescence imager can be very useful for online control of the cattle food preparation control. Furthermore, compact fluorescence LIDAR (LIght Detection And Ranging) was installed at the small drone for early detection and location of plants under stress in agricultural fields [2]. The developed Raman LIDAR demonstrated perspectives of space resolved sensing of freshwater reservoirs for water quality monitoring as well as ecology diagnostics.

Fig. 1. Compact fluorescence (a) and eye-safe (b) LIDAR systems developed at Prokhorov General Physics Institute of RAS. Compact LIDAR installed at a small drone (c). Raman LIDAR (d) developed for fresh and seawater monitoring (e).

[1] S.V. Gudkov, et al, Modern physical methods and technologies in agriculture, Uspekhi Fizicheskikh Nauk, Vol. 194, № 2, 208-226 (2024).
[2] M.Ya. Grishin, et al, Ultracompact Fluorescence Lidar Based on a Diode Laser (405 nm, 150 mW) for Remote Sensing of Waterbodies and the Underlying Surface from Unmanned Aerial Vehicles, Doklady Physics, Vol. 66, № 6, (2021).

Application of fluorescence spectroscopy for early detection of fungal infection of winter wheat grains

T. Matveeva[*], R. Sarimov, S. Gudkov

Prokhorov General Physics Institute of the Russian Academy of Sciences, Russia, 119991, Moscow, Vavilova st., 38

* matveevata@kapella.gpi.ru

Rapid, on-line and cheap monitoring of plant diseases on their early stages is an actual and important problem of food security and food safety. Different optical methods meet these requirements and they are already widely used in the agriculture sector [1,2]. Fluorescence-based techniques are broadly applied in the investigation of biological samples and in particular for the separation of infected crop samples [3].

This work focused on using fluorescence spectroscopy to characterize and compare healthy and fungal pathogen-infected wheat grains. The aim of the work is to determine the characteristic features, parameters, and wavelengths to distinguish between healthy and infected grains at an early stage of infection and different types of infection. The excitation-emission matrices of whole-wheat grains were measured using a Fluorescence Spectrometer Jasco FP-8300.

The samples included control healthy samples, both dry and wet, and manually infected grains with *Fusarium graminearum* and *Alternaria alternata* fungi. The five distinct spectral areas were identified by analyzing the location of the fluorescence peaks at each measurement. The area centered at λ_{em}=328/λ_{ex}=278 nm (emission/excitation of an amino acid peak) showed a twofold increase in intensity for grains infected with *A. alternata* after one day, whereas samples with *F. graminearum* showed a tenfold increase in fluorescence after seven days of infection. Another area with the center λ_{em}=480/λ_{ex}=400 nm is most interesting from the point of view of early diagnostics of pathogen development. A statistically significant increase of fluorescence maxima for samples with *F. graminearum* is observed on 1 day after infection, for *A. alternata* on day 2, and by day 7, the fluorescence of both groups decreases to the control level. Moreover, shifts in the emission peaks from 444 nm to 452 nm were recorded as early as 2–3 hours after infection. Since the area centered on λ_{em}=480/λ_{ex}=400 nm showed the greatest differences in the spectra of infected and uninfected samples, possible fluorophores for early detection were suggested from the literature, among which the most likely are metabolites (phenolics and quinones compounds) of fungi. The results highlight fluorescence spectroscopy as a promising technique for the early diagnosis of fungal diseases in cereal crops.

[1] S. Gudkov, T. Matveeva, R. Sarimov, A. Simakin, E. Stepanova, M. Moskovskiy, A. Dorokhov, A. Izmailov, Optical Methods for the Detection of Plant Pathogens and Diseases, Agriengineering, 5(4), pp. 1789-1812, (2023).
[2] S. Gudkov, R. Sarimov, M. Astashev, R. Pishchalnikov, D. Yanykin, A. Simakin, A. Shkirin, D. Serov, E. Konchekov, N. Gusein-zade, Modern physical methods and technologies in agriculture, Uspekhi Fizicheskikh Nauk, 194 (2), pp. 208-226, (2024).
[3] T. Matveyeva, R. Sarimov, A. Simakin, M. Astashev, D. Burmistrov, V. Lednev, P. Sdvizhenskii, M. Grishin, S. Pershin, N. Chilingaryan, N. Semenova, A. Dorokhov, S. Gudkov, Using Fluorescence Spectroscopy to Detect Rot in Fruit and Vegetable Crops, Applied Sciences, 12, pp. 3391, (2022).

Detection of mycotoxins using SERS-based aptamers

M. Moskovskiy[1*], R. Alieva[2], S. Kuznetsov[1], V. Novikov[1], A. Dorokhov[1], E. Zavyalova[2]

1- Federal Scientific Agro-Engineering Center VIM, 1st Institutskiy Proezd 5, 109428 Moscow, Russia
2- Chemistry Department of Lomonosov Moscow State University, Moscow, Russia

* maxmoskovsky74@yandex.ru

Mycotoxins are a group of compounds originating from the metabolism of filamentous fungi that causes many diseases. Fungi infect different plants contaminating food products with mycotoxins. More than 300 mycotoxins were found to induce toxicological effects in mammals. Among others, trichothecene type A (T-2 toxin) is one of the most dangerous mycotoxins because of the systemic toxicity can result from any route of exposure, i.e., dermal, oral, or respiratory [1].

In this work, we applied the surface-enhanced Raman spectroscopy (SERS), which is a highly sensitive and robust technique that provides a fingerprint of the analyte with a typical surface-assessed signal intensity increase by $10^6 - 10^8$ times [2].

In order to determine the presence of mycotoxins, the new aptamers were developed. They are artificially structured DNA or RNA oligonucleotides that can bind a chemical or biological target with high affinity and specificity. In this work, we estimated their affinity to mycotoxins, thermal stability, and thermal stability of a chosen aptamer in various salts that are significant for SERS intensity.

We obtained SERS spectra of T-2 and DON mycotoxins solutions with different mycotoxin content. Purified toxins (standards for chromatographic determination) were used in this experiment. Figure 1 shows the increase of the peak intensity of the band at about 1587 cm^{-1} with the content growth from 0 to 4 µg/mL. For T-2, this dependence is linear throughout this concentration range. In the case of DON, we can see a dramatic nonlinear increase of the band intensity starting with 3.5 µg/mL. We assume this is due to two sites of DON binding within the aptamer.
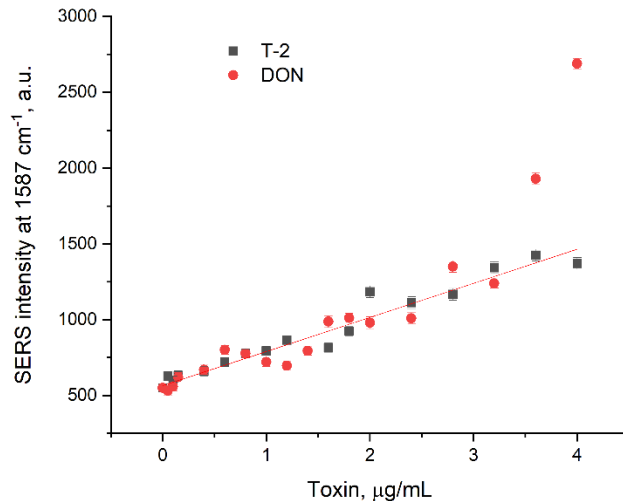

Figure 1. The dependence of SERS intensity of the peak at 1587 cm^{-1} on T-2 and DON concentration.

To sum up, the demonstrated SERS technique with the new developed aptamers can be used to determine the presence and concentration of mycotoxins in solutions. This test system is rapid (<20 min) and cheap consuming the simplest silver nanoparticles and the trace amounts of DNA aptamers.

[1] E. Janik, M. Niemcewicz, M. Podogrocki, et al, T-2 toxin – the most toxic trichothecene mycotoxin: metabolism, toxicity, and decontamination strategies, Molecules, vol. 26, art. № 6868, (2021).
[2] P.A. Mosier-Boss, Review of SERS substrates for chemical sensing, Nanomaterials, vol. 7, art. № 142, (2017).

The behavior of the protein-nanoparticle complex under laser-induced optical breakdown: an optical study

E. Nagaev[1*], A. Vedunova[2], T. Matveeva[1], A. Simakin[1], R. Sarimov[1]

1- Prokhorov General Physics Institute of the Russian Academy of Sciences, 119991 Moscow, Russia
2- Lobachevsky State University of Nizhny Novgorod, 603950 Nizhny Novgorod, Russia

* egorn97@mail.ru

Modern medicine operates state-of-the-art technologies. Among them laser surgery is on top. Surgical lasers made it possible to make minimal-invasive operations in comparison with traditional scalpels. Moreover, with surgical lasers it is possible to make operations, that could not be done before (for example, tissue welding). The results of the laser-tissue interaction depend on the parameters of the surgical lasers. Such lasers are divided by its operational wavelength (IR, visible, UV-region), working mode (continuous, pulsed) and beam power. Pulsed lasers are used in tissues welding, destruction of stones in kidneys, tattoo removal etc. It is well-known, that during laser-matter interaction non-linear effects can be occurred, when the pulse power is higher than the threshold. Among non-linear effects most studied are self-focusing, second and higher harmonic generation, laser-induced optical breakdown etc. It well-known, how laser-induced optical breakdown interacts with the tissues. But a little is known about such process in biological molecules solutions. Previously, we have shown how the typical surgical laser radiation interacts with BSA and HEWL solutions *in-vitro* [1,2]. It has been shown, that after 30 min of the experiment partial denaturation, aggregation and fragmentation of the protein molecules occurred. But the major volume of proteins remained as monomers. Modern nanotechnologies made it possible to use synthetic nanoparticles in bioimaging and therapy. This technological stack, when nanoparticles are used in the imaging and therapy, is called theranostics. Thus, there is a question: what would be happened, when the operation with the use of surgical laser would be in the presence of such nanoparticles?

In this work, we used laser-synthesized gold nanoparticles and the HEWL solutions with protein concentrations of 1 mg/ml and 8 mg/ml. Gold nanoparticles were added to protein solutions with the final concentration of nanoparticles of 10^{11} NPs/ml. The resulting solutions were irradiated with the Nd:YAG laser with second harmonic generation at 532 nm. The longest exposure time was 30 min. This time was chosen because some surgical operations are more than 30 min long. It is shown, that after adding gold nanoparticles to protein HEWL solutions, protein corona was formed. After exposure optical characteristics of the solutions were recorded. It shown, that the absorbance region, associated with nanoparticles surface plasmon resonance, changed over time – plasmon resonance peak decreased and longer-wavelength absorbance have been increased. Dynamic light scattering distributions shown, that the peak, associated with the protein monomers, has been disappeared after adding of NPs. After 30 min exposure this peak has been appeared, as in the control samples. Emission-excitation matrixes shown, that the amino acid peaks have been decreased (in the case of the protein concentration 8 mg/ml more than 50% decrease). Refraction indexes of both solutions have been increased, that can be associated with the partial denaturation of HEWL molecules. Activity of the protein solutions in the presence of the gold NPs, decreased. But the major volume of protein molecules stayed in the form of monomers.

[1] E.I. Nagaev, I.V. Baimler, A.S. Baryshev, M.E. Astashev, S.V. Gudkov, Effect of laser-induced optical breakdown on the structure of BSA molecules in aqueous solutions: An optical study, Molecules, 27(19), 6752, (2022).
[2] R.M. Sarimov, T.A. Matveyeva, V.A. Mozhaeva, A.I. Kuleshova, A.A. Ignatova, A.V. Simakin, Optical Study of Lysozyme Molecules in Aqueous Solutions after Exposure to Laser-Induced Breakdown, Biomolecules, 12(11), 1613, (2022).

SERS identification of Fusarium fungi

V. Novikov[1*], S. Kuznetsov[1], D. Serebryakov[2], A. Gulyaev[1], A. Dorokhov[1], M. Moskovsky[1]

1- Federal Scientific Agroengineering Center VIM, 1st Institutskiy Proezd 5, 109428 Moscow, Russia
2- Yaroslav the Wise Novgorod State University, 106k4 Bolshaya St. Petersburg Street, 173008 Veliky Novgorod

* vasiliy1992@gmail.com

Fusarium disease affects wheat, barley and rye – it is a disease of grain crops. Its causative agents are fungi of the genus *Fusarium*. This is explained by the fact that at different periods of their development they infect all parts of the plant: ear, leaves and roots. Mycelia and spores remain in the soil and on plant debris for a long time. *Fusarium* reduces the quality of grain, its nutritional value, as well as the germination capacity and germination weight of seed material [1]. In the early stages of fungal development, visual inspection of plants does not allow one to determine the presence of the disease. However, this is very important, as it will both save money spent on fungicide treatment and improve the ecological condition of plants and soil. The use of the SERS technique made it possible to determine the presence of fungi in very low concentrations. In our work, we made flushes from fungi of the genus *Fusarium*, adding a solution of nanoparticles and coagulum. Next, the Raman spectrum of the resulting solution was recorded.
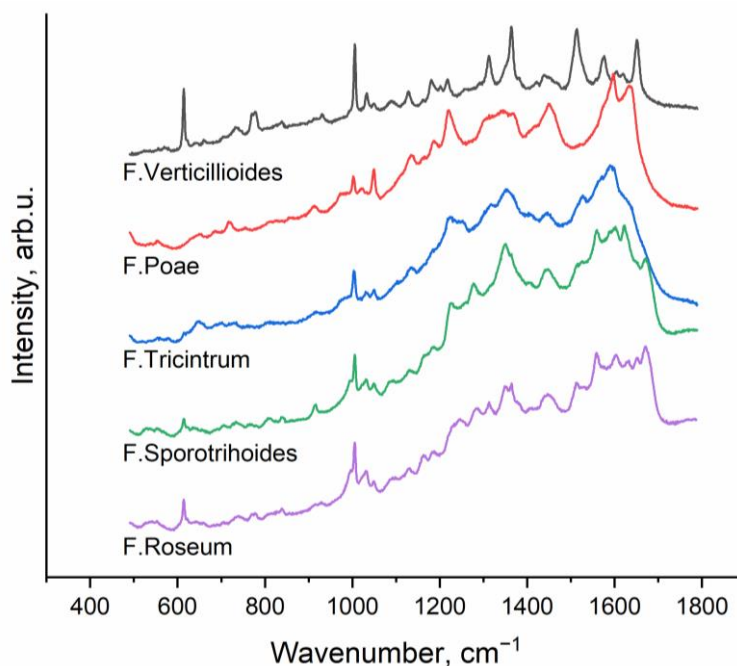

Fig. 1. SERS spectra of Fusarium fungi flush with nanoparticles of silver.

We recorded Raman spectra of 12 samples of fungi of the genus *Fusarium*. Fig. 1 shows spectra of five Fusarium fungi as an example. We found that the spectra of different fungi differ from each other, which makes it possible not only to detect the presence of fungi, but also to determine the type of fungus.

[1] M. Moskovskiy, A. Sibirev, A. Gulyaev, et al, Raman Spectroscopy Enables Non-Invasive Identification of Mycotoxins p. Fusarium of Winter Wheat Seeds, Photonics, vol. 8(12), 587 (2021).

Biophysical aspects of increasing plant productivity when grown under nanocomposite photoconversion materials

<u>M.O. Paskhin</u>[1*], D.V. Yanykin[1,2], S.V. Gudkov[1]

1- Prokhorov General Physics Institute, Russian Academy of Sciences, 38 Vavilova St., 119991 Moscow, Russia
2- Institute of Basic Biological Problems, FRC PSCBR, Russian Academy of Sciences, 2 Institutskaya St., 142290 Pushchino, Russia

* pashin.mark@mail.ru

Modern agriculture cannot be imagined without the introduction of smart and efficient technologies. These, undoubtedly, include technologies for directed regulation of the illumination of agricultural plants, because light is one of the crucial factors determining the growth and development of plants [1]. The quantity and quality of natural light determine the economics and feasibility of crop production in various regions of the world. To stimulate photosynthetic processes in plants, they are illuminated with light in the wavelength range from 400 nm to 700 nm, called photosynthetically active radiation. Depending on the climatic conditions of cultivation, farmers shade or additionally illuminate the plants, and they also change the spectrum of the light reaching the plants. One of the ways to change the spectral composition of light is through the use of photoconversion covers, which convert light little used by plants into photosynthetically active radiation [2,3].

We have developed several metal-containing and carbon-containing photoconversion coatings based on nanoparticles: $Sr_{0.955}Yb_{0.020}Er_{0.025}F_{2.045}$ and $Sr_{0.910}Yb_{0.075}Er_{0.015}F_{2.090}$ (1), Eu_2O_3 (2), Eu^{3+}:LaF_3 (3), graphene oxide (4), and ZnO (5). Nanoparticles were obtained by various methods: co-precipitation, laser fragmentation, and hydrothermal-microwave treatment. 1–4 nanoparticles were mixed with fluoroplastic varnish and applied by cold synthesis at room temperature; 5 nanoparticles were mixed with acrylic polymer and is applied using a magnetron. 1 cover absorb light in the near-infrared range and fluoresced in the green-red range. 2–5 covers absorb light in the ultraviolet range and fluoresced in the red (2), orange (3), blue and red (4), and blue (5) ranges.

The effectiveness of obtained photoconversion covers was studied when growing plants. As a result, these covers were shown to improve plant growth and development. Almost all covers improved the morphological parameters of plants, but each in a slightly different way. For example, covers-based $Sr_{0.955}Yb_{0.020}Er_{0.025}F_{2.045}$ and $Sr_{0.910}Yb_{0.075}Er_{0.015}F_{2.090}$ accelerated the adaptation of tomato plants to a new type of lighting. Cover based on Eu_2O_3 accelerated the adaptation of photosystems in tomato plants when the light was turned on, which allowed plants to use more solar energy for photosynthesis and less for repair processes. However, this cover did not affect cucumber plants in any way. Cover based on Eu^{3+}:LaF_3 did not affect the parameters of plant growth and development, while it contributed to the adaptation of plants to stressful abiotic conditions, in particular to high and positive low temperatures. This is due to the fact that additional orange light helps to increase the synthesis of antioxidant enzymes such as superoxide dismutase, peroxidase, and so on [4]. A photoconversion cover based on graphene oxide, due to its wide fluorescence spectrum in the range of photosynthetically active radiation, significantly increased the growth and development of tomato plants. A cover based on ZnO nanoparticles improved the morphological parameters of pepper and cucumber plants by 25–30%. In addition, this cover had bacteriostatic properties but was biocompatible with eukaryotic cells.

[1] S.W. Hogewoning, E. Wientjes, P. Douwstra, G. Trouwborst, W. van Ieperen, R. Croce, J. Harbinson, Photosynthetic Quantum Yield Dynamics: From Photosystems to Leaves, Plant Cell, 24, 1921–1935, (2012).
[2] M.O. Paskhin, D.V. Yanykin, S.V. Gudkov, Current Approaches to Light Conversion for Controlled Environment Agricultural Applications: A Review, Horticulturae, 8, 885, (2022).
[3] S.V. Gudkov, R.M. Sarimov, M.E. Astashev, R.Y. Pishchalnikov, D.V. Yanykin, A.V. Simakin, A.V. Shkirin, D.A. Serov, E.M. Konchekov, N.G. Gusein-zade, V.N. Lednev, M.Ya. Grishin, P.A. Sdvizhenskii, S.M. Pershin, A.F. Bunkin, M.Kh. Ashurov, A.G. Aksenov, N.O. Chilingaryan, I.G. Smirnov, D.Yu. Pavkin, D.O. Hort, M.N. Moskovskii, A.V. Sibirev, Ya.P. Lobachevsky, A.S. Dorokhov, A.Y. Izmailov, Modern physical methods and technologies in agriculture, Uspekhi Fizicheskikh Nauk, 194(2), 208-226, (2024).
[4] A. Brazaityte, P. Duchovskis, A. Urbonaviciute, G. Samuoliene, J. Jankauskiene, A. Kasiuleviciute-Bonakere, Z. Bliznikas, A. Novickovas, K. Breive, A. Zukauskas, The Effect of Light-Emitting Diodes Lighting on Cucumber Transplants and after-Effect on Yield, Zemdirb.-Agric, 96, 102–118, (2009).

Neural networks determining wine composition with IR spectroscopy: overcoming data scarcity issues

O. Sarmanova[1,2*], **L. Utegenova**[2], **A. Guskov**[1], **S. Burikov**[1,2], **I. Plastinin**[1], **T. Dolenko**[1,2], **S. Dolenko**[1]

1- Skobeltsyn Research Institute of Nuclear Physics, Lomonosov Moscow State University, 1/2 Leninskie Gory, Moscow, 119991, Russian Federation
2- Faculty of Physics, Lomonosov Moscow State University,1/2 Leninskie Gory, Moscow, 119991, Russian Federation

* oe.sarmanova@physics.msu.ru

Wine is a complex object containing various alcohols (ethanol, methanol, glycerol, aliphatic and aromatic alcohols), esters, acetals, waxes and oils, carbohydrates, organic acids, mineral and phenolic compounds, vitamin-like substances, etc. [1]. Concentration of these substances must be controlled during the wine production process via cheap, express and non-destructive analysis method.

In this work, the problem of determining the composition of wines by their IR absorption spectra using neural networks (NN) was solved. The IR spectrum of wine consists of a set of overlapping bands of different shapes and intensities characteristic of its constituent substances and it is deformed due to interactions between their molecules. Using IR spectra to train adaptive models requires obtaining a representative data set, what may be difficult to do experimentally.

In this study it is proposed to use IR absorption spectra of solutions modeling white and red wines to circumvent the problem of data scarcity and lack of models to analyze the IR absorption spectra of real wines. Therefore, the main components of model solutions were selected in such a way that the IR absorption spectra of the model solutions were similar to the IR spectra of both white and red wines. This approach allows experimentally obtaining a representative set of IR spectra with known concentrations of the main components of wines for NN training and using trained networks to determine the concentrations of these components in real wines.

Aqueous solutions containing ethanol, a mixture of glucose, fructose and sucrose, tartaric, malic and citric acids, glycerin and sulfur dioxide were used as models. The concentration ranges of these components in the model solutions were from 8 to 18 vol.% for ethanol, from 10 to 200 g/l for sugars (glucose, fructose and sucrose), from 3 to 12 g/l for acids (tartaric, malic and citric acid), from 5 to 25 g/l for glycerin, from 0.1 to 1 g/l for sulfur dioxide. A total of 1734 IR absorption spectra of model solutions were experimentally obtained.

Partial least squares (PLS), multilayer perceptron (MLP), convolutional neural network (CNN) were trained to predict wine components concentration in model solutions and real wines. Even though PLS and CNN demonstrated a similar level of mean absolute error (MAE) in determining the concentration of components in model solutions, PLS could not determine the concentration of the desired components in real wines. The MAE for determining the concentration of ethanol, sugar, acids, and glycerol with CNN in real wines (10 samples) was 0.8 vol.%, 5.1 g/L, 1.6 g/L, 1.9 g/L, respectively, which satisfies the needs of winemaking.

[1] M. Butnariu and A. Butu, Qualitative and Quantitative Chemical Composition of Wine, Quality Control in the Beverage Industry, 385–417, (2019).

Prototype of an optical system for identifying micro- and macrodamage to plant tissues

A.Yu. Izmailov[*], A.S. Dorokhov, <u>A.V. Sibirev</u>

1- FSBSI "Federal Scientific Agronomic and Engineering Center VIM", Russia, Moscow, 109428

* vim@yandex.ru

When storing fruit and vegetable products, one should note the circumstance caused by the natural loss of potato weight depending on the degree of damage to the tubers, which ranges from 11% to 22%, and waste in the form of rot is 7...25%, while for potatoes without mechanical damage, natural loss is 5%, and waste is 2...4% [1,2]. To meet these standards and ensure product quality, the development of non-invasive, high-throughput methods for recognizing and classifying fruits and vegetables, identifying their disease damage during sorting in real time is required. In order to automatically recognize infected and damaged vegetable crops, potatoes and apple fruits during post-harvest processing, together with Sapsan LLC (Voronezh), an optical system for identifying biological objects has been developed using laser and spectral technologies to obtain correlation-spectral patterns. The optical identification system is intended for express diagnostics of the functional state of vegetable crops, potatoes and apple fruits during post-harvest processing [3,4]. The optical identification system provides the required performance indicators for recognizing biological objects based on discriminant functions with multi-class recognition using the minimal risk method and determining the quantitative characteristics of the objects under study. The optical system for identifying micro- and macro-damage to fruits and vegetables is a set of modules for feeding, optical and sorting biological objects (fruits and vegetables). The module for feeding fruits and vegetables consists of a conveyor with a width of at least 300 mm, made of polymer/rubber material and made with a directed relief for uniform distribution of biological objects over the working surface with an adjustable feed speed from 0.5 to 3.0 m/s. The optical module is a system consisting of technical vision devices and a control unit with a system for illuminating biological objects, with the ability to move above the surface of the conveyor-sorting adapter. A technical vision system consists of at least 2 cameras with a resolution of at least 5400 pixels and operating modes in the RGB+RGB or NIR+RGB spectral range. The sorting module consists of a conveyor-sorting adapter with 64 pneumatic actuators installed on the working surface and an air supply pressure in the range of 0.2 - 0.8 MPa with a maximum air flow of at least 1000 l/min. The working surface of the fruit and vegetable feeding module must be made of polymer/rubber material. The novelty of the development lies in obtaining correlation-spectral patterns for recognizing contaminated vegetable crops, potatoes and apple fruits using optical technologies that determine the physiological state and topological parameters of biological objects based on elements of artificial intelligence and machine learning. The uniqueness of the system for identifying infected biological objects lies in the presence of adaptive disease recognition devices depending on the culture using specialized optical systems. The accuracy of recognition of qualified biological objects is more than 95% of those affected by diseases. This ensures the possibility of obtaining potato seeds, vegetable crops and apple fruits in the absence of foci of mechanical damage and disease on their surface after storing them. The economic efficiency of the optical system for identifying micro- and macro-damage during the sorting operation makes it possible to reduce the number of personnel involved in the post-harvest processing stage, while increasing productivity by 1.8 times, as well as the quality of sorting of marketable products as a result of disease recognition during remote optical monitoring and subsequent rejection of substandard products. The practical significance lies in improving the quality of sorting potatoes and fruits and vegetables while eliminating the influence of the human factor by introducing a machine with a digital system for identifying contaminated biological objects and developing recommendations for post-harvest work when breeding new varieties and hybrids [5].

[1] P. Azizi, N.S. Dehkordi, R. Farhadi, Design, construction and evaluation of potato digger with rotary blade, Cercet. Agron. Mold. 2014, 47, pp.5–13.

[2] Abd. El-Rahman and M. Magda, Development and performance evaluation of a simple grading machine suitable for onion sets, Soil. Sci. and Agric. Eng. Mansoura Univ. 2014, 2, 213–226. p.9768.

[3] N.V. Byshov, S.N. Borychev, N.N. Yakutin, D.V. Kalmykov, N.V. Simonova, On the interaction of the tuberous layer with the digger's working organs, Bull. Ryazan State Agrotechnological Univ. P.A. Kostycheva, 2018, 40, pp.161–167.

[4] N.V. Byshov, N.N. Yakutin, R.Y. Koveshnikov, V.V. Rodionov, N.V. Serzhantov, P.S. Smirnov, Modernization of the KST-1.4 digger, Bull. Ryazan State Agrotechnological Univ. P.A. Kostycheva 2016, 30, pp.75–78.

[5] S. Bachche, K. Oka, Design, Modeling and Performance Testing of End-Effector for Sweet Pepper Harvesting Robot Hand, J. Robot. Mechatron, 2013, 25, pp.705–717.

Artificial monochromatic red light induces the biosynthesis of chlorogenic acids in calli of *Cynara cardunculus*

O.A. Tikhonova[1], S.A. Silantieva[2], V.P. Grigorchuk[2], E.P. Subbotin[1], Y.N. Kulchin[1], G.N. Veremeichik[2*]

1- Institute of Automation and Control Processes, Far Eastern Branch of the Russian Academy of Sciences (IACP FEB RAS), 5 Radio str., Vladivostok, 690041, Russia
2- Federal Scientific Center of the East Asia Terrestrial Biodiversity of the Far East Branch of the Russian Academy of Sciences, Vladivostok, 690022, Russia

* gala-vera@mail.ru

The stability of cell cultures is an important open question. It is believed that with long-term cultivation, the ability of calli to produce high levels of secondary metabolites is reduced [1]. In the present work, we compared the growth and biosynthetic characteristics of *Cynara cardunculus* var. altilis DC (Asteraceae) callus cultures obtained in 2014 and the characteristics of the same culture after 10 years of cultivation. This callus culture produced caffeoylquinic acids, 1,5-dicaffeoylquinic acid, 3,4-dicaffeoylquinic acid [2]. Caffeoylquinic acids are one of the most power antioxidant and have a lot of pharmacological properties. In the present work, we found that after this period, the biosynthesis of caffeoylquinic acids decreased more than 10 times. The use of LED light is becoming a new way to grow plants and activate the biosynthesis of secondary metabolites [3]. In the present work, we investigated the effect of monochromatic red artificial light of low, moderate, and high intensity (100, 300, and 600 μmol m^{-2}s^{-1}) on the biosynthesis of caffeoylquinic acids in a long-term cultured cell line of *C. cardunculus*. It is important to note that in our case, we examined not only the activation of secondary metabolism but also the possibility of overcoming the blockage of secondary metabolism, which apparently occurs in calli during long-term cultivation. Normal (100 μmol m^{-2}s^{-1}), moderate (300 μmol m^{-2}s^{-1}) and high (600 μmol m^{-2}s^{-1}) intensities of red light had no negative effect on the growth of calli. Moreover, growth of calli under low red light was significantly better (**Fig.1**). Treatment with normal (100 μmol m^{-2}s^{-1}) intensities of red light strongly activated caffeoylquinic acid biosynthesis. Cultivation under moderate and high red light intensity have no any effect on biosynthesis.
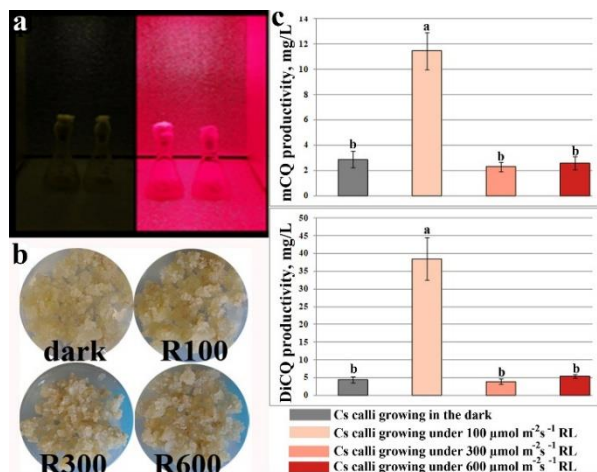

Fig.1. Growth chambers (**a**) and impact of artificial lighting on productivity (mg/L) of 30-day-old *C. cardunculus* calli: Production of caffeoylquinic acids in 12-year-old *C. cardunculus* callus cultures grown under red lighting conditions. Morphology (**b**) of a 10-year-old *C. cardunculus* callus culture grown under red light. Productivity (mg/l medium) of caffeoylquinic acids (**c**) in *M. maritima* callus cultures grown under red lighting conditions. The data obtained from three independent experiments with ten biological replicates are presented as the mean ± standard error of the mean, and asterisks above the error bars indicate statistically significant differences (ANOVA, $p < 0.05$).

[1] L. Liu, X. Fan, J. Zhang, M. Yan, M. Bao, Long-term cultured callus and the effect factor of high-frequency plantlet regeneration and somatic embryogenesis maintenance in Zoysia japonica, In Vitro Cell.Dev.Biol.-Plant 45 673–680 (2009).
[2] Y.V. Vereshchagina, V.P. Bulgakov, V.P. Grigorchuk, V.G. Rybin, G.N. Veremeichik, G.K. Tchernoded, T.Y. Gorpenchenko, O.G. Koren, N.H. Phan, N.T. Minh, L.T. Chau, Y.N. Zhuravlev, The rolC gene increases caffeoylquinic acid production in transformed artichoke cells, Appl Microbiol Biotechnol, 98(18):7773-80 (2014).
[3] G.N. Veremeichik, V.P. Grigorchuk, D.S. Makhazen, E.P. Subbotin, A.S. Kholin, N.I. Subbotina, D.V. Bulgakov, Y.N. Kulchin, V.P. Bulgakov, High production of flavonols and anthocyanins in Eruca sativa (Mill) Thell plants at high artificial LED light intensities, Food Chem. 408 (2023).

Study of pearl barley by THz high resolution spectroscopy

V. Vaks[1,2], V. Anfertev[1,2], E. Domracheva[1,2], M. Chernyaeva[1,2], A. Chernyaeva[1]

1- Institute for Physics of Microstructures RAS, 603950, Russia, Nizhny Novgorod, GSP-105
2- Lobachevsky University, 603022, Russia, Nizhny Novgorod, Gagarina av., 23

Nowadays spectroscopic analytical methods, operating in the frequency ranges from microwave to ultra-violet as well as other physic-chemical methods (mass-spectrometry, gas or liquid chromatography, microscopy etc.) are used for various applications (biology, medicine, agriculture etc.). One of the main problems of crop production and the food industry is fungal infections of grain. Diseases of grain crops lead to both plant death and loss of yield (for example, reduced germination of seeds, quality indicators of grain – loss of grain weight due to pathogenic damage, decreased nutritional and taste properties of grain, etc.). A number of metabolites produced by fungi are toxic to humans. Fungal diseases affect both plants as a whole and individual parts of plants (roots, stems, leaves, grains). Spread occurs both through the soil and through infected grain. The diagnostics of fungal infections of grain crops and the fight against them are current of importance for modern crop production and the food industry. The methods of high resolution terahertz (THz) gas spectroscopy are prospective for analysis of multicomponent gas mixtures and allow to reveal the metabolites of grain. The work is devoted to analyzing the metabolites composition of the barley grain by high-resolution THz spectroscopy.

A THz spectroscopy based on nonstationary effects such as inducing and decaying the free dumping polarization in a gas sample at the interaction of radiation and gas molecules can be considered as a high sensitive method of investigating the multicomponent gas mixtures. The devices can be realized in phase switching or fast sweeping modes of the probing radiation. The spectrometers with phase switching or with fast frequency sweeping developed by the authors, operating in the range of 118-178 GHz, were used. The sensitivity of the recorded absorption coefficient for these spectrometers at a cell length of 1 m is from 10^{-7} cm^{-1} to 5×10^{-8} cm^{-1}. The THz gas spectroscopy method allows to detect volatile compounds, in a multicomponent gas mixture (vapors and products of thermal decomposition), including ones of biological origin. Therefore, it is promising to study the volatile compounds (products of thermal decomposition of macromolecules) as secondary metabolites of starch, sugars etc., that appear when the sample is heated. The thermal decomposition products of pearl barley as refined barley was studied. Some of substances with high quantities of absorption lines in operating frequency range of spectrometer such as glycolaldehyde, acetaldehyde, propanediol (two isomers), phenylpropienitrile, urea, acetone, hydroxyacetone, acetic acid, vinyl cyanide, butyl cyanide, isopropyl cyanide, alanine appeared in products of thermal decomposition of samples. More than some hundred absorption lines of these substances were detected in frequency range of 118-175 GHz. The composition of metabolites of pearl barley can be used for comparing with the composition of unrefined grain of barley for revealing the parts of molecular content concerning with the common substances and rest specified for pathogens including fungus.

These results demonstrate the promise of THz spectroscopy based on nonstationary effects for applications in agriculture and food industry.

Effect of astrocyte's optogenetic stimulation on neural network activity in Alzheimer's disease modeling *in vitro*

E. Mitroshina[1], E. Kalinina[1], S. Gudkov[1,2], M. Vedunova[1*]

1- Institute of Biology and Biomedicine, Lobachevsky State University of Nizhny Novgorod, 23 Gagarin Avenue, 603022 Nizhny Novgorod, Russia
2- Prokhorov General Physics Institute of the Russian Academy of Sciences, 38 Vavilova St., 119991 Moscow, Russia

* mvedunova@yandex.ru

Alzheimer's disease (AD) is the most prevalent neurodegenerative disease, primarily affecting the elderly. AD impacts not only neurons but also glial cells, particularly astrocytes, leading to reactive astrogliosis and neuroinflammation. Astrocytes play a crucial role in regulating synaptic plasticity and neuronal excitability by releasing neuroactive substances known as gliotransmitters. Thus, examining the pathology of astroglial tissue is essential for understanding the etiology and pathogenesis of AD and developing treatment strategies. Optogenetics is a promising method for modulating cellular activity through the selective expression of opsins, which are exogenous light-sensitive protein-ion channels [1]. While traditionally used to control neuronal activity, recent studies have successfully applied optogenetics to astrocytes [2,3]. Therefore, exploring optogenetic therapy offers potential for advancing our understanding of AD mechanisms and discovering new treatments.

The aim of our study was to investigate the effect of optogenetic stimulation of astrocytes on the spontaneous bioelectrical activity of primary cultures of mouse hippocampal cells in a model of beta-amyloidosis. Fibrillar β-amyloid (3.5 μM) was applied at each medium change starting from day 10 of culture (DIV). Cultures were infected with the viral optogenetic construct AAV-hGFAP-ChR2-EYFP at 10 DIV. Bioelectrical activity was recorded daily from days 14 to 21 *in vitro* using the MEA2100-2x60-System-E (Multichannel Systems, Germany). Photostimulation of cultures transduced with the optogenetic construct was conducted daily using an optogenetic kit (Thorlabs Inc., USA) with 470 nm light at 50% diode power for 30 seconds. Electrophysiological data were processed with the MEAxtd software developed in Python.

It has been shown that modeling amyloidosis from 17 DIV leads to a decrease in the level of spontaneous bioelectrical activity in primary cultures of hippocampal cells. This includes a reduction in the number of small bursts of impulses and the number of spikes in a burst. In 50% of the studied cultures, burst activity was completely absent after the 17th day of cultivation. Chronic optogenetic stimulation of astrocytes supported the bioelectrical activity of hippocampal neuron-glial networks. In all studied cultures, burst activity remained, although there was a tendency toward a decrease in the number of bursts of impulses. The number of spikes in a burst on day 21 remained unchanged relative to day 14 of cultivation. Thus, optogenetic modulation of astrocytic activity may be a potential approach to correct neurodegenerative changes.

[1] M. White, M. Mackay, R.G. Whittaker, Taking Optogenetics into the Human Brain: Opportunities and Challenges in Clinical Trial Design, J Clin Trials, 12, 33–41, (2020).
[2] A.A. Borodinova, P.M. Balaban, I.B. Bezprozvanny, A.B. Salmina, O.L. Vlasova, Genetic Constructs for the Control of Astrocytes' Activity, Cells, 10, 1600, (2021).
[3] E. Mitroshina, E. Kalinina, M. Vedunova, Optogenetics in Alzheimer's Disease: Focus on Astrocytes, Antioxidants (Basel), 12, 1856, (2023).

ASIA-PACIFIC CONFERENCE ON FUNDAMENTAL PROBLEMS OF OPTO- AND MICROELECTRONICS

Numerical approach of spherical bubble oscillations in laser-induced microcavitations: effect of enthalpy

A.F. Abu-Bakr[1], A.K. Abu-Nab[1,2*], Z. AbuShaeer[3]

1- Department of Mathematics and Computer Science, Faculty of Science, Menoufia University, Shebin El-Koom, 32511, Egypt
2- Phystech School of Applied Mathematics and Informatics, Moscow Institute of Physics and Technology, Dolgoprudny, Moscow, 141700, Russia
3- Department of Basic Science, Higher Institute of Engineering and Technology, Kafrelsheikh, 33511, Egypt

* ahmed.abunab@yahoo.com

Over the past decades, interest has increased in studying different techniques to detect the importance of microbubbles in many industrial and medical applications such as mechanisms of hydraulic machinery cavitation erosion, histotripsy, and lithotripsy. The dynamics of laser-induced spherical microcavitation bubbles in water were by plasma photography, from initial nonlinear oscillations to late linear oscillations. Repetition of such delayed oscillations results in quantities of gas/vapour inside the spherical bubbles. In this work, we present a numerical investigation of the behavior of laser-induced microbubbles through a modified Gilmore model in biotissue system. The effect of enthalpy is considered into account. The proposed model is solved numerically using the numerical techniques as finite element method. In addition, the radius of the microbubbles is calculated as a function of time under the influence of the initial radius of these laser-induced microcavitations. Moreover, some physical properties and numerical calculations of the proposed mathematical model of laser-induced cavitation bubbles are deduced, analyzed and investigated.

Diffraction efficiency of a transmission hologram

M.A. Amanova[1*], V.N. Naunyka[2]

1- Institute of Telecommunications and informatics of Turkmenistan, Ashgabat, 744000 Turkmenistan
2- Mozyr State Pedagogical University named after I.P. Shamyakin, Mozyr, 247760 Republic of Belarus

* maral_amanova@mail.ru

Taking into account the piezoelectric effect the dependence diffraction efficiency of holograms formed in a photorefractive $Bi_{12}SiO_{20}$ crystal sample on the orientation angle, specific rotation and crystal thickness was studied.

Using a sample of a $Bi_{12}SiO_{20}$ crystal cut $(\bar{1}\bar{1}0)$ with a fixed thickness d=8 mm, the possibility of theoretically studying the dependence diffraction efficiency η of holograms on the orientation angle θ and the specific rotation ρ of the crystal is demonstrated. The appearance of two "humps" on the surface $\eta(\theta,\rho)$ at ρ=0.405 rad/mm cannot be explained without simultaneously taking into account the piezoelectric effect and optical activity.

It is shown that when the sign of the optical activity of a crystal changes, a shift in the maxima of the diffraction efficiency relative to the orientation angle equal to zero can occur mirror symmetrical for a plate 8 mm thick, asymmetrical for a plate 3.45 mm thick.

The dependence $\eta(\rho)$ is not hypothetical. The specific rotation of the polarization plane of different $Bi_{12}SiO_{20}$ crystal samples can indeed be different [1]. In particular, this is due to the fact that when doping crystals during the growth process, the addition of various dopants (Cu, Fe) can cause a significant change in the specific rotation of the crystal. Therefore, studying the simultaneous influence piezoelectric effect and specific rotation of the crystal may be useful and the results obtained will be used for the purpose of preliminary selection of parameters in the practical solution of the problem optimizing the output energy characteristics of holograms.

[1] V.V. Shepelevich, S.M. Shandarov, A.E. Mandel, Light diffraction by holographic gratings in optically active photorefractive piezocrystals, Ferroelectrics. – 1990. – Vol. 110. – P. 235–249.

Numerical simulation of the single silicon pillar scattering modes for second harmonic generation

M.A. Anikina[1,2*], **A. Kuznetsov**[1,2], **A.D. Bolshakov**[1,2]

1- Moscow Institute of Physics and Technology, Dolgoprudny, Russia
2- Alferov University, Saint Petersburg, Russia

* mari.a.nikina@yandex.ru

It is well-known that bulk single-crystal silicon does not exhibit second order nonlinear optical effects because of the presence of the inversion symmetry center. However, there are ways to break this symmetry, and as a result, the second harmonic generation (SHG) can be observed on silicon nanostructures [1,2]. Optical circuit engineering requires standardized design of components, and the initial step of such design is a numerical simulation of the individual structures.

This study reports numerical simulations of scattering spectra from a single silicon nanopillar. The calculations were provided by the finite-difference time-domain method (FDTD) according to Yee algorithm in Ansys Lumerical software. Single pillars were represented as cylinders of heights and radii standing on the Si substrate. The main goal is to match scattering peaks with pump and SHG wavelengths. The SHG at 550 nm is assumed for the considered structures. In Fig. 1 (a, b), the scattering spectra intensity maps in 500–1300 nm range are demonstrated for different diameters and heights of 0.45 and 1.8 μm.

In Fig. 1 (c), the change in mode composition of the spectrum at successive changes of the height and radius of the structure is presented, which allows us to precisely control the number of resonant modes and their spectral positions. Thus, a nanopillar with a radius of 112.5 nm and a height of 0.45 μm provides the perfect match of two scattered modes with pump and SHG spectral lines. The case of larger structures higher than 1 μm and thicker than 300 nm, which should be easier to fabricate, has also been considered. The numerical calculation of such structures shows that the scattering intensity increases significantly, but the number of modes visibly increases with the increase in pillar height. Additional longitudinal modes can affect the energy redistribution between them, which can lead to undesirable consequences such as a decrease the SHG response.
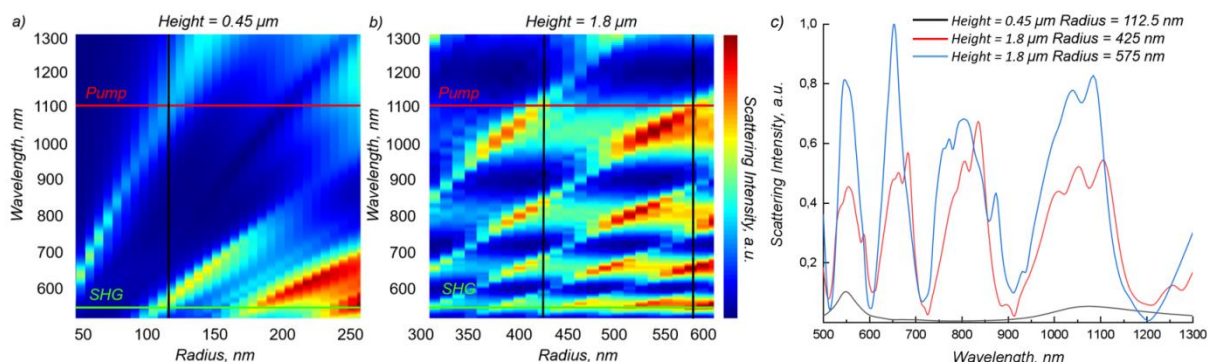
Fig. 1. Scattering spectra intensity maps of the single Si pillars of different radii a) 0.45 μm and b) 1.8 μm tall; c) scattering spectra of the single Si pillars with specific dimensions.

[1] S.V. Makarov, et al, Efficient second-harmonic generation in nanocrystalline silicon nanoparticles, Nano letters, 17(5), pp. 3047-3053, (2017).
[2] M. Cazzanelli, et al, Second-harmonic generation in silicon waveguides strained by silicon nitride, Nature materials, 11(2), pp. 148-154, (2012).

Effect of elastic stresses in FRP composite on the frequency characteristics of acoustic emission signals recorded by a fiber-optic sensor

O.V. Bashkov[1,2*], **R.V. Romashko**[2**], **I.O. Bashkov**[1], **M.N. Bezruk**[2], **T.A. Efimov**[2]

1- Komsomolsk-na-Amure State University, Komsomolsk-on-Amur, 681013 Russia
2- Institute of Automation and Control Processes of the Far Eastern Branch of the Russian Academy of Sciences, Vladivostok, 690041 Russia

* bashkov@knastu.ru, ** romashko@dvo.ru

The purpose of the work is to establish the influence of elastic stresses in fiberglass on the frequency characteristics of acoustic emission (AE) signals recorded by a piezoelectric and fiber-optic acoustic emission sensor. Samples of fibre reinforced plastic (FRP) composite were made in the form of plates using the vacuum infusion method. After that, samples were cut out from the plate for subsequent tensile testing on a tensile testing machine. The samples had the shape of a double blade. The fiber-optic sensor was made on the basis of an adaptive laser holographic interferometer. The sensitive element of the sensor is a multimode optical fiber, which was glued to the surface of the working part of the samples before testing. The piezoelectric transducer was installed on the non-working part of the sample. The sample was loaded with a tensile load in stages. At each loading stage, acoustic waves were excited in the middle part of the sample by a Su-Nielsen source. AE signals from propagating acoustic waves were recorded by both sensors. The analysis of changes in the AE signal spectra caused by elastic stresses in the FRP composite material is performed. At low-frequency harmonics of the Fourier spectrum, a shift in the spectrum to the high-frequency region is observed with an increase in the tensile load stress. However, at high frequencies up to 500 kHz, which are informative for recording AE, the effect of tensile stresses becomes nonlinear. The nature of the influence of external stresses on the signal spectrum as a whole is important in identifying the type of AE signal source caused by a certain type of destruction of the FRP composite.

Window functions applied in laser interferometry to investigate the spatial inhomogeneities and characteristics of waveguide elements optically induced in a lithium niobate crystal

A.D. Bezpaly[1*], **A.A. Novoselov**[1], **A.E. Mandel**[1], **V.I. Bykov**[1]

1- Tomsk State University of Control Systems and Radioelectronics, Tomsk, 634055 Russia

* aleksander.bezpalyi@tusur.ru

The laser radiation influence on various materials has been studied since the last century and has found application in such fields of science and technology as laser technologies, nonlinear and integrated optics, holography, optoelectronics, and photonics. Laser radiation may also be useful to create optical waveguide and diffraction elements or modify their characteristics in integrated photonic circuits and other compact quantum devices. The widely used material for such devices is lithium niobate crystal because of its unique set of optical, acousto-, and electrooptical properties. It is also known that the introduction of various impurities into the lithium niobate crystal can change its properties, including its sensitivity to optical radiation in a certain range. Using light influence on the lithium niobate, it is possible to induce different inhomogeneities both in the near-surface and bulk areas of the substrate. However, to create integrated optical devices based on waveguide and diffraction elements by inducing inhomogeneities, information about modulated refractive index in the local area is required. The value and spatial distribution of refractive index changes in the local area may be investigated by laser interferometry. This method is useful to study both large and small inhomogeneities with various topologies, but it has some difficulties when processing interferograms. To solve this problem, we propose in our work to use window functions when processing interferograms obtained in areas with optically induced refractive index changes. Our results show that using the window function makes interferogram processing simpler. It may also be useful for different areas of science and technology using the two-dimensional Fourier transform.

Adaptive holographic interferometer resistant to polarization fluctuations based on a gyrotropic photorefractive crystal

M.N. Bezruk[1*], **D.V. Storozhenko**[1], **T.A. Efimov**[1], **R.V. Romashko**[1]

1- Institute of automation and control processes FEB RAS, Radio 5 str, Vladivostok, Russia

* bezmisha@list.ru

We have introduced a new concept for a polarization-resistant (PR) adaptive interferometer utilizing the orthogonal geometry of vectorial two-wave mixing in a gyrotropic photorefractive crystal. We have developed a mathematical model to calculate the efficiency of two-wave mixing in gyrotropic crystal under orthogonal geometry. By applying this model, we have identified the conditions necessary for achieving a PR-mode in the adaptive interferometer. Our research demonstrates that the polarization independence mode is achievable due to the natural rotation of the polarization plane of light waves in the crystal caused by optical gyrotropy. A key advantage of this approach is the ability to achieve PR-mode using only a single reference wave, as opposed to other techniques that require two reference waves. This results in a significant simplification of the PR-adaptive interferometer setup. The research was funded by the Russian Science Foundation (Project. No. 24-22-00413).

Space-and-time current spectroscopy of high-resistive photoconductors: techniques and applications

M.A. Bryushinin[*], I.A. Sokolov

Ioffe Institute, St. Petersburg, Russia

* *mb@mail.ioffe.ru*

Space charge distributions define operation of the most photonic and electronic devices. Space-and-time current spectroscopy is one of the holography-related techniques for the investigation of space charge evolution in wide-bandgap semiconductors – functional materials for photonics and electronics. The technique is based on the so-called effect of non-steady-state photo-EMF, but not restricted by its classical realization. The effect manifests itself as an alternating electric current arising in a semiconductor illuminated by an oscillating interference pattern. The current is resulted from the interaction of the photoconductivity and space-charge field gratings (Fig. 1); and the signal amplitude is defined by the drift component of this current 0.
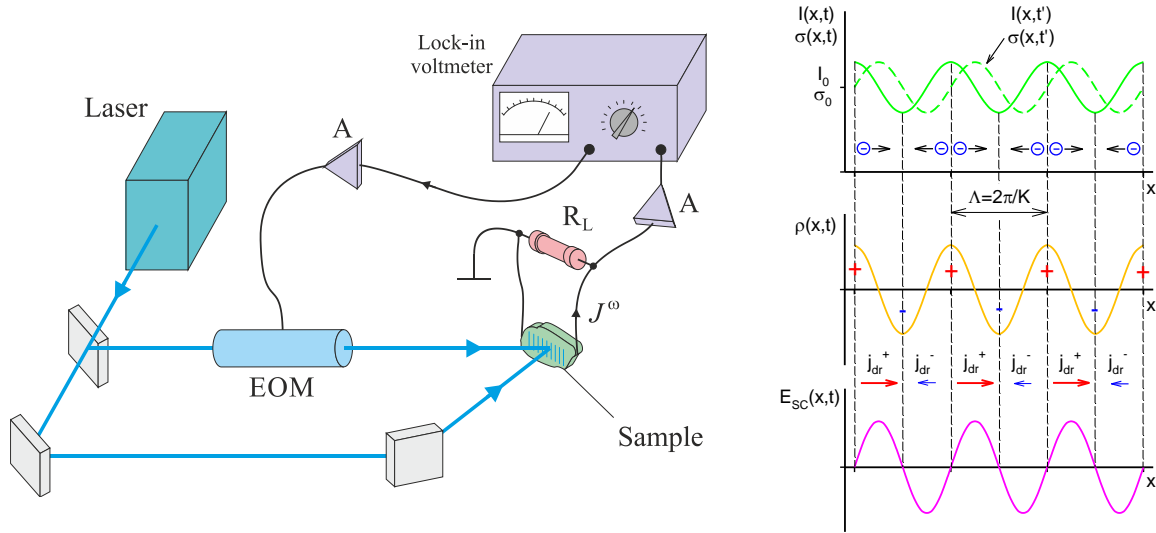

Fig. 1. Experimental setup for the investigation of non-stedy-state photo-EMF (on the left) and distributions of the light intensity, photoconductivity, space-charge density and electric field producing the electric current (on the right).

We present characterization of a wide group of photoconductive and photorefractive materials, such as $Bi_{12}SiO_{20}$, SnS_2, AlN, Ga_2O_3, etc. The main photoelectric parameters, such as the type and value of specific photoconductivity, its relaxation time, diffusion length of carriers are extracted from dependencies of the photo-EMF signal versus light intensity, spatial and temporal frequencies. Several advanced techniques related to the conventional non-steady-state photo-EMF, namely, the combined excitation of running space-charge and photoconductivity gratings, photo-EMF excitation by the frequency-modulated light are demonstrated as well. We briefly present applications of the non-steady-state photo-EMF and its variety for detection of phase- and frequency modulated optical signals, including laser-based adaptive vibrometry.

[1] S. Stepanov, in Handbook of Advanced Electronic and Photonic Materials and Devices, Vol. 2, edited by H.S. Nalwa (Academic Press) pp. 205–272, (2001).
[2] I.A. Sokolov and M.A. Bryushinin, Optically induced space-charge gratings in wide-bandgap semiconductors: techniques and applications (Nova Science Publishers, Inc., 2017).

Laser nanostructuring of thin films for magnetic biosensing application

I.O. Dzhun[1*], **D.V. Shuleiko**[2], **A.V. Nazarov**[1], **N.N. Perova**[2], **V.Yu. Nesterov**[2],
D.E. Presnov[2], **I.L. Romashkina**[1], **M.G. Kozin**[1], **N.G. Chechenin**[1,2], **S.V. Zabotnov**[2]

1- Skobeltsyn Institute of Nuclear Physics, Lomonosov Moscow State University, 1/2 Leninskie Gory, Moscow, 119991, Russia
2- Faculty of Physics, Lomonosov Moscow State University, 1/2 Leninskie Gory, Moscow, 119991, Russia

* irina.dzhun@gmail.com

Health monitoring and early diagnostics of diseases require portable point-of-care devices. For this purpose, lab-on-chips techniques that perform coin-size chips combining the functions of diagnostic laboratory are developed. Along with common optical methods magnetic biosensors that detect magnetically labeled cells and biomolecules are also of interest due to their high sensitivity, low energy consumption and low background noise. However, their detection limit and fabrication cost are still the subjects to improve.

Here we suggest the applying of laser nanostructuring technologies as a helpful tool in this area and perform the results of our pilot experiments. Laser technologies were applied in two paths: fabrication of magnetic nanoparticles via pulsed laser ablation in liquid (PLAL) and creation of sensors surface relief via femtosecond laser induced periodical surface structures (LIPSS) formation. At the first part MNPs colloids were produced by ablation of thin 250 nm magnetron sputtered on the glass substrate Fe films instead of commonly used bulk target. PLAL of such film in acetone leaded to creation of Fe@FeO core shell MNPs with mean size of 90 nm and thickness of oxide shell of about 20 nm as follows from our transmission and scanning electron microscopies. The presence of crystalline α-Fe core and FeO shell was indicated by Mössbauer spectroscopy and Raman scattering data. At the second part to form the surface relief of Si/Ta30nm/NiFe10nm/IrMn10nm/Ta15nm exchange biased layer stack the deposition of multilayer on the previously structured Si wafer was used to avoid undesirable thermal effects such as melting and layer intermixing. The magneto-optical Kerr effect microscopy investigation has shown the appearance of the out-of-plane magnetization of NiFe layer that is completely in plane in unstructured area and the remanence of exchange bias of about 150 Oe that makes the sensor more sensitive to MNPs stray fields. That is also confirmed by appearance of periodical contrast in magnetic force microscopy image with period equal to that of LIPSS. In final part the obtained MNPs colloid was dropped onto the multilayer structure. The scanning electron microscopy revealed the crowding of MNPs in relief area and inside the grooves. Thus obtained MNPs and relief-surface multilayer structures could be prospective elements for magnetic biosensors with improved detection limit.

Contact lens integrated stereogram for eye tracking sensor

I.M. Fradkin[1*], M.M. Chugunova[1], V.R. Solovey[1], A.V. Syuy[1], A.V. Arsenin[1], V.S. Volkov[1]

*1- Emerging Technologies Research Center, XPANCEO; UAE, Dubai, Internet City,
Emmay Tower, Floor G, Showroom 1&2*

* fradkinim@xpanceo.com

Tracking the user's gaze direction is crucial for augmented reality devices. While typically viewed as part of the user control interface, it is also essential for accurately projecting images in various systems and can be utilized to create peripheral vision effects and other applications. Current solutions primarily rely on computer vision techniques to analyze eye photos, with some advanced methods incorporating acoustic sensors or measuring the inductance of electrical loops integrated into contact lenses to enhance measurement precision.

In our study, to enhance eye tracking sensitivity, we have integrated a stereogram within the contact lens. This innovative approach leverages the dependence of the apparent position of a stereoscopic image on eye position, enabling reconstruction of the latter based on this effect. Our implementation of the stereogram utilizes the parallax barrier, which makes it passive, completely autonomous device. This novel approach not only paves the way for enhancement of eye tracking precision but also holds potential for other applications, such as serving as an identification mark for cybersecurity purposes.

Ultra-dense photonic integration of e-skid waveguides enabled by van der Waals materials

D.V. Grudinin[1*], G.A. Ermolaev[2], R.V. Kirtaev[2], A.S. Slavich[1], A.A. Vyshnevyy[1], K.V. Voronin[1], A.V. Arsenin[1], V.S. Volkov[2]

1- Center for Photonics and 2D Materials, Moscow Institute of Physics and Technology, 9 Institutskiy Lane, Dolgoprudny, 141701, Moscow Region, Russia
2- Emerging Technologies Research Center, XPANCEO, Dubai Investment Park First, Dubai, United Arab Emirates

* grudinin.dv@phystech.edu

Photonics represents the natural technological progression following the era of electronics. However, the diffraction limit of light and crosstalk present significant challenges for photonic elements, constraining their size and integration density. In this study, we demonstrate that layered semiconductors can overcome these challenges due to their pronounced optical anisotropy. Specifically, we explore silicon waveguides using hexagonal boron nitride (hBN), molybdenum disulfide (MoS$_2$), and tungsten disulfide (WS$_2$) as top and bottom claddings. These waveguides operate at a telecommunications wavelength of 1550 nm, just above the diffraction limit (by approximately 5%), and exhibit exceptional coupling between vertically stacked waveguides. This allows for the possibility of multiple layers of independent integrated components. We visualize these waveguides experimentally using near-field optical microscopy and provide extensive theoretical analysis of the effective mode area and coupling length of the waveguides. Our results pave the way for ultra-dense photonic integration based on layered materials.

Multimodal neural network analysis of Raman spectra and dermoscopic images of skin tumors

I. Matveeva[1]

1- Samara National Research University, Moskovskoye shosse 34, Samara, 443086, Russia

m-irene-a@yandex.ru

Accurate diagnosis of the cancer type and early diagnosis are key factors in the successful treatment of neoplasms [1]. Diagnosis of neoplasms by visual examination is difficult, since malignant and benign neoplasms may have similar external signs [2]. In addition to visual examination, there are instrumental methods of skin analysis such as dermatoscopy [3] and Raman spectroscopy [4,5]. However, the accuracy of these methods does not approach that of histological examination [6]. The aim of the research is to develop a method for identifying skin tumors based on multimodal joint analysis of Raman scattering data and dermatoscopic images.

An *in vivo* study of skin tumors was carried out at the Samara Regional Clinical Oncology Center. Experimental skin Raman spectra were recorded using a portable setup that includes a laser source with a central wavelength of 785 nm. The spectra were recorded with a spectral resolution of 0.2 nm in the range from 837 to 920 nm, which corresponds to 792-1874 cm^{-1}. Dermatoscopic images of skin neoplasms were obtained using a digital dermatoscope.

Machine learning methods, in particular, convolutional neural networks, were used to analyze the registered data. The classification model for malignant melanoma and pigmented nevus has shown an increase in classification accuracy compared to the analysis of Raman spectra or dermatoscopic images alone.

As a result, combined multimodal method for diagnosing skin cancer, which simultaneously takes into account both specific spectral features of tumors and spatial inhomogeneities in the distribution of optical density, has been proposed. The studied approaches to the analysis of optical biopsy data can be further used as part of the software for automated screening diagnostics of skin pathologies in order to detect tumors at an early stage of development.

[1] J. Ferlay, M. Colombet, I. Soerjomataram, D.M. Parkin, M. Piñeros, A. Znaor, F. Bray, Cancer statistics for the year 2020: An overview, International journal of cancer, vol. 149(4), pp. 778-789, 2021.

[2] H.A. Haenssle, C. Fink, R. Schneiderbauer, F. Toberer, T. Buhl, A. Blum, A. Kalloo, A.B.H. Hassen, L. Thomas, A. Enk, L. Uhlmann, Man against machine: diagnostic performance of a deep learning convolutional neural network for dermoscopic melanoma recognition in comparison to 58 dermatologists, Annals of oncology, vol. 29(8), pp. 1836-1842, 2018.

[3] I.A. Matveeva, A.I. Komlev, O.I. Kaganov, A.A. Moryatov, V.P. Zakharov, Multidimensional Analysis of Dermoscopic Images and Spectral Information for the Diagnosis of Skin Tumors, Journal of Biomedical Photonics & Engineering, vol. 10(1), pp. 010307, 2024.

[4] I.A. Bratchenko, L.A. Bratchenko, A.A. Moryatov, Y.A. Khristoforova, D.N. Artemyev, O.O. Myakinin, A.E. Orlov, S.V. Kozlov, V.P. Zakharov, In vivo diagnosis of skin cancer with a portable Raman spectroscopic device, Experimental Dermatology, vol. 30(5), pp. 652-663, 2021.

[5] I. Matveeva, I. Bratchenko, Y. Khristoforova, L. Bratchenko, A. Moryatov, S. Kozlov, O. Kaganov, V. Zakharov, Multivariate curve resolution alternating least squares analysis of in vivo skin Raman spectra, Sensors, vol. 22(24), p. 9588, 2022.

[6] G.V. Long, S.M. Swetter, A.M. Menzies, J.E. Gershenwald, R.A. Scolyer, Cutaneous melanoma, The Lancet, vol. 402(10400), pp. 485-502, 2023.

Stimulated emission sources based on ZnO nanostructures

S.A. Kadinskaya[1,2*], **V.M. Kondratev**[1,2], **A.V. Nikolaeva**[1], **D.S. Gets**[3], **I.Kh. Akopyan**[4], **A.Yu. Serov**[4],
M.E. Labzovskaya[4], **S.V. Mikushev**[4], **B.V. Novikov**[4], **I.V. Shtrom**[4,5], **A.D. Bolshakov**[1,2,4,6]

1- Center for Nanotechnologies, Alferov University, Khlopina 8/3, 194021 Saint Petersburg, Russia
2- Center for Photonics and 2D Materials, Moscow Institute of Physics and Technology, 9 Institutskiy Lane, 141701 Dolgoprudny, Russia
3- School of Physics and Engineering, ITMO University Lomonosov str 9, Saint Petersburg 191002, Russia
4- Faculty of Physics, St. Petersburg State University, Universitetskaya Embankment 13B, 199034 St. Petersburg, Russia
5- Institute for Analytical Instrumentation of the Russian Academy of Sciences, Rizhsky pr. 26, 190103 St. Petersburg, Russia
6- Laboratory of Advanced Functional Materials, Yerevan State University, Yerevan 0025, Armenia

* skadinskaya@bk.ru

Zinc oxide (ZnO) is one of the promising materials for development of UV emitters due to the band gap (3.37 eV at room temperature) and high exciton binding energy (60 meV) [1]. In addition, ZnO is inexpensive, relatively abundant, chemically stable, easily synthesized, and non-toxic. Although a wide variety of ZnO-based light-emitting devices (LEDs) have been developed so far, their performance, light-emitting ability, and production technology are still below expectations.

Hydrothermal synthesis is a method of growing various materials and compounds, based on the use of physical and chemical processes that take place in aqueous solutions at slightly elevated temperatures often used to obtain ZnO nanostructures [2].

In our work, Si (111) substrates are used for the hydrothermal synthesis of ZnO nanostructures since this material is known to be the most often used in nanoelectronics. Zinc acetate is used as a seed layer material. The growth solution consists of equimolar aqueous solutions of $Zn(NO_3)_2$ and hexamethylenetetramine (HMTA).

Two series of studies of the optical properties of zinc oxide were carried out using photoluminescence spectroscopy. The samples were placed in a closed-cycle helium cryostat (Janis Research Company, USA). The sample temperature was about 10 K. The PL was excited by a He-Cd laser ($\lambda = 325$ nm, excitation power W = 50 kW·cm^{-2}) and by an ultraviolet solid-state laser LCM-DTL-374QT ($\lambda = 355$ nm). The excitation power of this laser was varied in the range from 1 to 800 kW·cm^{-2}. The threshold generation value was 95 kW·cm^{-2}. Laser generation is observed at different points of the sample, which indicates the good quality of the synthesized structures.

The synthesized ZnO was transferred from the growth substrate to a glass substrate and coated with perovskite $CsPbBr_3$. Pumping was carried out at room temperature using a femtosecond laser (Light Conversion), pulse duration 150 fs, repetition rate 10 kHz, pump wavelength 480 nm. The threshold generation value was 70-120 µJ·cm^{-2}. Laser generation is observed on single ZnO structures.

The results show that a simple hydrothermal synthesis method is promising for fabricate efficient light-emitting devices based on ZnO.

[1] Ü. Özgür, Ya. I. Alivov, C. Liu, A. Teke, M.A. Reshchikov, S. Doğan, V. Avrutin, S-J Cho, H. Morkoç, A comprehensive review of ZnO materials and devices, Journal of Applied Physics, vol.98, pp. 041301, (2005).
[2] H.Y. Xu, H. Wang, Y.C. Zhang, W.L. He, M.K. Zhu, B. Wang, H. Yan, Hydrothermal synthesis of zinc oxide powders with controllable morphology, Ceramics International, vol.30(1), pp. 93-97, (2004).

Reducing the number of measuring lines in a fiber-optic tomographic measuring network

O. Kamenev[1,2*], A. Kamenev[1,2], Yu. Petrov[1]

1- Institute of Automation and Control Processes, Far Eastern Branch of Russian Academy of Sciences,
5 Radio str., 690041, Vladivostok, Russia
2- Far Eastern Federal University, Institute of High Technologies and Advanced Materials, 10 Ajax Bay, Russky
Island, 690922, Vladivostok, Russia

* okamenev@mail.ru

A fiber-optic tomographic measuring network is proposed, in which quasi-distributed measuring lines are laid along curved trajectories (Fig. 1).
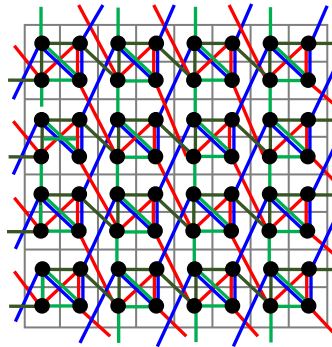

Fig. 1. Fiber-optic tomographic measuring network.

The measuring network presents a number of nonlinear measuring lines with fiber-optical amplitude sensing elements. The proposed topology of the measuring network makes it possible to significantly reduce the number of lines. The data processing is carried out by a neural network containing an inner layer of nonlinear neurons. The results of numerical experiments, as well as experiments with the layout of a measuring network of dimension 8×8, are presented (Fig. 2).
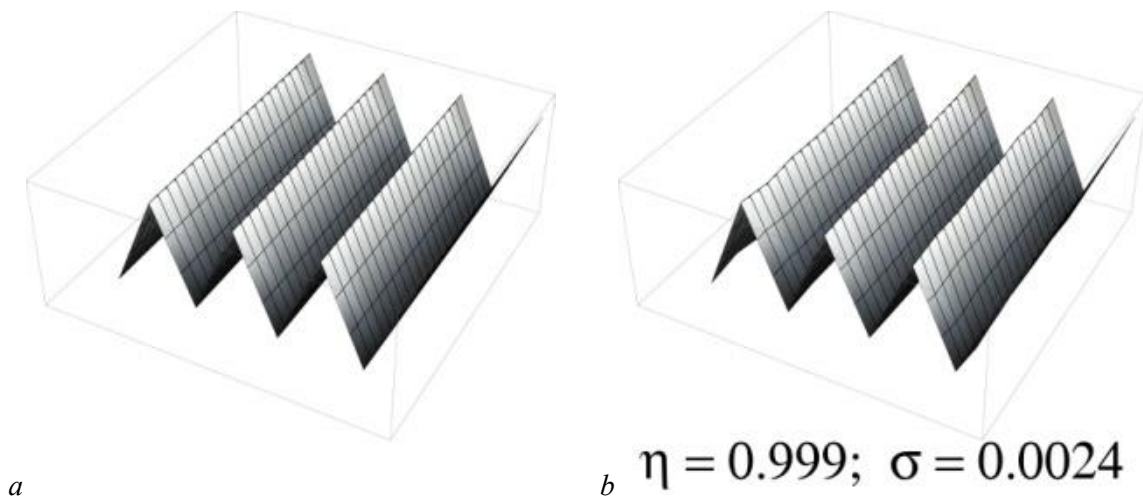

$$\eta = 0.999; \quad \sigma = 0.0024$$

Fig. 2. The results of numerical experiments: a – reconstructed physical field, b – result of reconstruction by neural network.

Non-contact monitoring of cortical perfusion by imaging photoplethysmography

A.A. Kamshilin[1,2*], A.V. Shcherbinin[2], V.V. Zaytsev[2], A.Yu. Sokolov[3,4]

1- Institute of Automation and Control Processes FEB RAS, Vladivostok, Russia
2- North-Western District Scientific and Clinical Center FMBA, St. Petersburg, Russia
3- Pavlov First Saint Petersburg State Medical University, St. Petersburg, Russia
4- Pavlov Institute of Physiology RAS, St. Petersburg, Russia

* alexei.kamshilin@yandex.ru

Intraoperative quantitative assessment of changes in tissue perfusion is extremely important as an objective quality control of surgical interventions, especially in brain surgery. The monitoring system should be easy to use, contactless and provide quantitative visualization of blood flow in real time. Various techniques have been proposed to solve this problem, but all of them have their drawbacks, leading to the fact that today neurosurgeons do not have a proper tool to assess cortical blood flow during surgery. In this presentation, we discuss a multimodal method of imaging photoplethysmography (IPPG) synchronized with an electrocardiogram (ECG), which we consider the most promising for assessing changes in cerebral blood flow parameters in the operating room. The results of both experiments on laboratory animals to assess changes in intracranial hemodynamics in response to various interventions and pilot studies on monitoring cortical perfusion during open-brain neurosurgery (44 different surgeries) will be presented.

Instrumental implementation of the IPPG system is very simple, since this requires only a video camera with proper illumination of the tissue under study. However, despite the fact that photoplethysmography has historically been the very first optical method for assessing blood flow *in vivo*, this technique has not yet found wide application in clinical practice. Most researchers believe that the main technical problem of IPPG is motion artifacts, which significantly exceed the light modulation at heart rate that bears useful information about perfusion. In our multimodal system, the efficiency of motion artifact compensation was significantly increased by using a special image stabilization algorithm, which includes correlation analysis of video frames with ECG. As a result, spatial distributions of cortical blood flow and their changes over time with a high signal-to-noise ratio were obtained in all neurosurgical operations and animal experiments without exception. It was our group that was the first to demonstrate the feasibility of cerebral perfusion assessment during open brain surgery using the multimodal IPPG system [1].

Nonetheless, despite the positive and reproducible results of these pilot studies, their interpretation is not always sufficiently justified due to ongoing discussions about the physico-physiological model of the origin of the IPPG signal. We are proponents of an alternative model of IPPG signal formation [2], which states that the key point is the elastic deformation of the microvascular bed by adjacent pulsatile arteries. According to this theory, the capillary bed serves as a distributed sensor-transducer for pulsations generated by deeper supplying arteries. Consequently, the amplitude of pulsatile component of the IPPG waveform is inversely proportional to the tone of blood vessels, and only arteries supplying the cortex are visualized in the perfusion maps evaluated in IPPG system [3]. In the presentation, we will show a number of experimental observations confirming the conclusions of the alternating theory of IPPG signal formation, which also underlines prospects of the multimodal IPPG system for important applications in clinical setting.

[1] O.V. Mamontov, A.V. Shcherbinin, R.V. Romashko, A.A. Kamshilin, Intraoperative imaging of cortical blood flow by camera-based photoplethysmography at green light, Applied Sciences., vol. 10, p. 6192, (2020).
[2] A.A. Kamshilin, E. Nippolainen, I.S. Sidorov, P.V. Vasilev, N.P. Erofeev, N.P. Podolian, R.V. Romashko, A new look at the essence of the imaging photoplethysmography, Scientific Reports, vol. 5, p. 10494, (2015).
[3] O.A. Lyubashina, O.V. Mamontov, M.A. Volynsky, V.V. Zaytsev, A.A. Kamshilin, Contactless assessment of cerebral autoregulation by photoplethysmographic imaging at green illumination, Frontiers in Neuroscience, vol. 13, p. 1235, (2019).

Enhancing public transportation: an IoT-based smart bus system for real-time fleet management and improved passenger experience

H.L. Prakruthi[1], P.B. Prathap[1], H.Y. Swathi[2], K. Saara[3*]

1- Department of Electronics and Communication Engineering, Malnad College of Engineering, Hassan- 573202
2- Department of Computer Science and Engineering (AI and ML), Malnad College of Engineering, Hassan- 573202
3- Department of Electronics and Communication Engineering, School of Engineering, Dayananda Sagar University, Bangalore-560114

* saarakhamar@gmail.com

The Bus Transportation System introduces an IoT-based Smart Transportation System designed to enhance the efficiency, accuracy, and passenger experience within public buses. Leveraging a network of sensors, including GPS, OBD-II, accelerometers, gyroscope, fuel level, and engine temperature sensors, the telemetry system continuously monitors and collects real-time data on various facets of bus performance. This data is wirelessly transmitted to a centralized system, empowering bus operators to track and optimize fleet performance. Moreover, an innovative module positioned near the bus entrance employs IR sensors to tally passengers boarding, updating real-time data accessible to waiting passengers via user-defined software. The web interface furnishes comprehensive information on bus availability, fares, current location, and passenger count, thereby enriching the commuting experience. Additionally, an RFID sensor-based tap-and-pay system is deployed outside the bus door, enabling passengers to enter upon tapping their unique ID cards preloaded with currency. The online platform further facilitates the management and replenishment of these cards, offering commuters a convenient and secure payment solution. This integration of telemetry, passenger counting, and tap-and-pay systems not only streamlines operations but also enhances the overall public transportation experience.

Si nanowire-based Schottky sensors for selective sensing of NH$_3$ and HCl via impedance spectroscopy

V. Kondratev[1*], **A. Bolshakov**[1]

1- Laboratory of Functional Nanomaterials, Center for Photonics and 2D Materials, Moscow Institute of Physics and Technology, 9 Institutskiy Lane, 141701 Dolgoprudny, Russia

* kondratev.vm@mipt.ru

This work is aimed at the development of a highly sensitive silicon (Si)-based sensor allowing for the selective detection and analysis of liquid solution compositions containing ammonia (NH$_3$) and hydrochloric acid (HCl) in an indirect manner using electrochemical impedance spectroscopy (EIS). The best sensitivity results were obtained with Si nanowires based Schottky Sensors, which provided a detection limit of 4 μmol·L^{-1} and resistive sensitivities of 0.8% per μmol·L^{-1} for HCl and 4 μmol·L^{-1}, −0.2% per μmol·L^{-1} for NH$_3$, respectively. Treatment with HF stimulated Si nanowires surface oxidation and increased the density of adsorption sites, making it promising for detecting analyte concentrations up to 1000 μmol·L^{-1}. Schematic of the Si nanowire-based schottky sensors operation is shown in Fig.1.
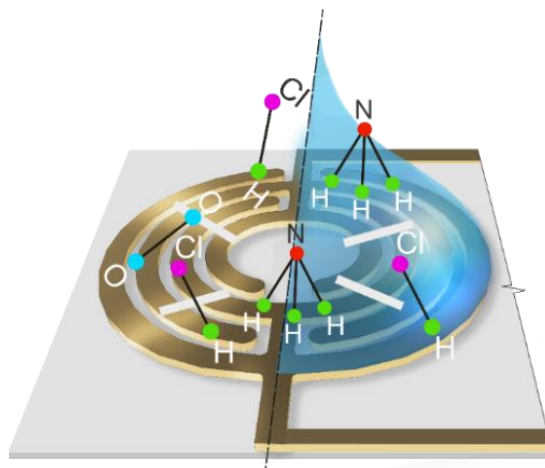

Figure 1 – Schematic of the Si nanowire-based Schottky sensors operation.

The experimental data were confirmed via density functional theory (DFT) modeling of the processes of adsorption and redox interaction between ammonia and hydrochloric acid molecules and the surface of silicon nanowires.

Finally, the sensor response was studied when exposed to NH$_3$ and HCl vapors simultaneously. Also, the approach for the EIS data analysis involving characterization of the sensor response with two parameters – resistance and EIS frequency corresponding to the change in the operation regime was developed. Due to the use of two parameters simultaneously, this approach is found as a pathway for qualitative and quantitative analysis of the gas mixture composition using only one sensor.

The results of the work shed light on the development of feasible highly sensitive sensors for health monitoring, allowing for selective mixed analytes detection [1].

[1] V.M. Kondratev, E.A. Vyacheslavova, T. Shugabaev, D.A. Kirilenko, A. Kuznetsov, S.A. Kadinskaya, Z.V. Shomakhov, A.I. Baranov, S.S. Nalimova, V.A. Moshnikov, A.S. Gudovskikh, A.D. Bolshakov, Si Nanowire-Based Schottky Sensors for Selective Sensing of NH$_3$ and HCl via Impedance Spectroscopy, ACS Applied Nanomaterials 2023 6 (13), 11513-11523.

The generation of vortex light fields using a sector spiral plate based on ferroelectric and ferrielectric liquid crystals

<u>S. Kotova</u>[1*], E. Pozhidaev[2], S. Samagin[1], T. Tkachenko[2]

1- Lebedev Physical Institute, Samara Branch, 221, Novo-Sadovaya, Samara, 443011, Russian Federation
2- Lebedev Physical Institute, 53, Leninskiy Prospekt, Moscow, 119991, Russian Federation

* kotova@fian.smr.ru

Increasing the conversion rate of spatial light field distributions is an important goal in modern photonics. The modulation frequency in modern phase space light modulators (SLM) based on nematic liquid crystals (LC) is in the range of several tens of hertz. This speed can be increased through orientation effects in liquid crystal ferroelectric materials (LCFs) and ferrielectrics with subwavelength spiral structures, particularly the Kerr effect [1-3]. The paper presents the results of research on the electro-optical properties of these materials for use in phase modulation applications, using the example of generating light fields with a sectorial spiral plate (SSP). A feature of the Kerr effect in these liquid crystals is the biaxial transformation of the ellipsoid of refractive indices and the rotation of its main optical axis when an electric field is applied. This prevents the implementation of pure phase modulation in cells with a planar orientation of the axis of the helix to the substrate.

We studied the modulation characteristics of several mixed LC ferroelectric materials synthesized at LPI [1], as well as the ferrielectric crystal FerriLCM-1 [3], whose spiral pitch is less than 100 nanometers. Using the experimental data obtained, we calculated the characteristics of vortex light fields that can be generated using a 12-segment spiral plate based on the studied ferroelectric liquid crystal mixture FLC-587-F-7 and FerriLCM-1 [4]. It was shown that the effect of amplitude modulation due to changes in the ellipticity state on the formation of vortex light fields using the SLM based on these materials is not significant.

An experimental sample of a 12-sector spiral plate was made using FLC-587-F-7 [5]. The SSP was controlled by an alternating supply voltage, with the signal frequency varying from 100 to 4000 Hz. The formation of ring-shaped light fields with topological charges ranging from 1 to 4, as well as a set of symmetric light spots, has been demonstrated. The value of the topological charge has been determined using the compensation method with a phase element created by a multi-pixel liquid crystal SLM.

Thus, ferroelectric and ferrielectric liquid crystals are compared as electro-optical media for phase modulation, using the example of the formation of vortex light fields. It has been shown that both types of LC provide comparable values for changes in the ellipticity of the modulated light field. The loss of light when cutting off the unwanted polarization component is less than 10%, which is more than sufficient for a number of practical applications. The control voltage required to achieve a 2π phase shift is 2.6 times lower in the case of ferrielectric LC than in ferroelectric LC, when considering the same LCD layer thickness.

[1] E.P. Pozhidaev, A.D. Kiselev, A.K. Schrivastava, et al, Orientational Kerr effect and phase modulation of light in deformed-helix ferroelectric liquid crystals with subwavelength pitch, Phys. Rev. E, vol. 87, 052502, (2013).
[2] S.P. Kotova, S.A. Samagin, E.P. Pozhidaev, A.D. Kiselev, Light modulation in planar aligned short-pitch deformed-helix ferroelectric liquid crystals, Phys. Rev. E, vol. 92, 062502, (2015).
[3] E.P. Pozhidaev, M.V. Minchenko, A.V. Kuznetsov, et al, Broad temperature range ferrielectric liquid crystal as a highly sensitive quadratic electro-optical material, Optics Letters. vol.47, pp. 1598-1601, (2022).
[4] E.P. Pozhidaev, S.P. Kotova, S.A. Samagin, Ferrielectric Liquid Crystal with a Subwavelength Helix Pitch As an Electro-Optic Medium for Phase Spatial Light Modulators, Bulletin of the Lebedev Physics Institute, vol. 50(Suppl 1), pp. S85-S95, (2023).
[5] S.P. Kotova, E.P. Pozhidaev, S.A. Samagin, et al, Ferroelectric liquid crystal with sub-wavelength helix pitch as an electro-optical medium for high-speed phase spatial light modulators, Optics & Laser Technology, vol.135, 106711, (2021).

Effect of linearly polarized light on the dynamics of maize plants development

Yu.N. Kulchin[1], S.O. Kozhanov[1*], A.S. Kholin[1], E.P. Subbotin[1], N.I. Subbotina[1]

1- Institute of Automation and Control Processes, Far Eastern Branch of the Russian Academy of Sciences (IACP FEB RAS), 5 Radio str., Vladivostok, 690041, Russia

* kozhanov_57@mail.ru

While there are many works in the literature that study the effect of such light parameters as wavelength, intensity, photoperiod on plants growth, very little attention is paid to parameter of light polarization. Nevertheless, this light characteristic, as shown in some studies [1-3], can have a significant effect on plant development. In most of these studies, the authors note the positive effect of light which is circularly polarized. In one of our previous studies [4], we showed that maize plants develop better under white linearly polarized light than under non-polarized.

In current work, we investigated the effect of linearly polarized light of white, red, green and blue ranges on the dynamics of maize plant development of the Rannyaya Lakomka and Kubansky Sakharny varieties during the week. The results (Fig.1) showed that the highest growth rates of maize plants of both varieties relative to non-polarized light treatment were demonstrated by plants grown under green and blue light. Under white light, this effect was less significant, and under red light it was not observed.
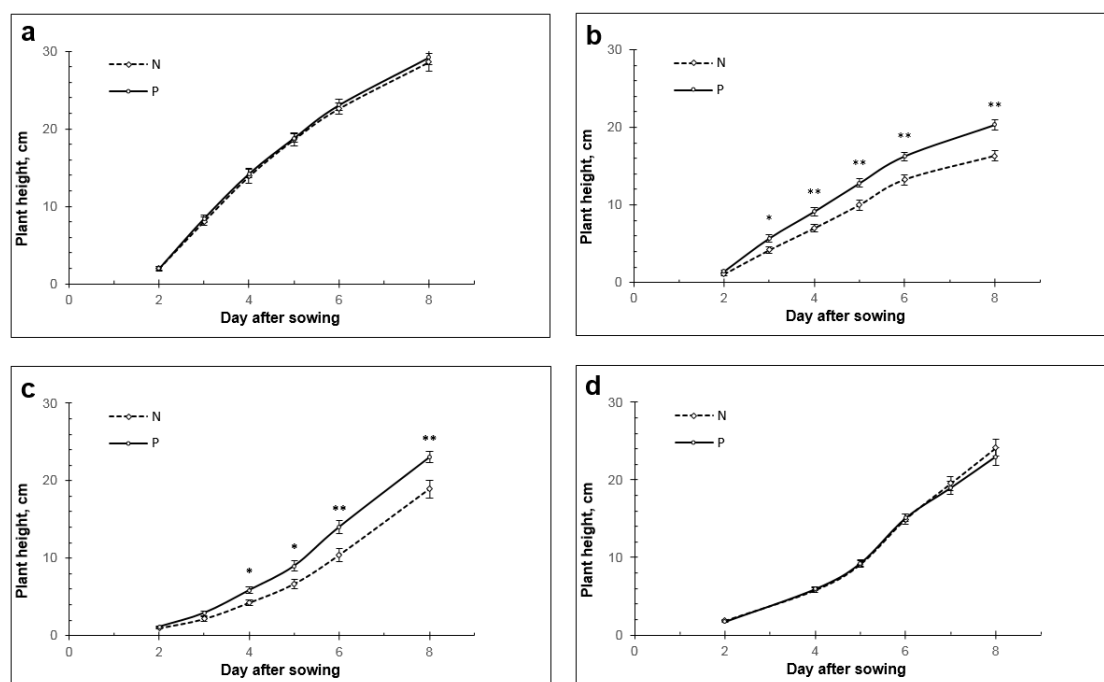

Fig.1 – Growth dynamics of maize plants (Kubansky Sakharny variety) under white (a), blue (b), green (c) and red (d) linearly polarized (P) and non-polarized (N) light. * $p<0.05$, ** $p<0.01$.

[1] P.P. Shibayev and R.G. Pergolizzi, The effect of circularly polarized light on the growth of plants, Int J Bot. 7, 113-117 (2011).

[2] E. Lkhamkhuu, K. Zikihara, H. Katsura, S. Tokutomi, T. Hosokawa, Y. Usami, K. Monde, Effect of circularly polarized light on germination, hypocotyl elongation and biomass production of arabidopsis and lettuce: Involvement of phytochrome B. Plant biotechnology, 37(1), 57-67 (2020).

[3] S. Gai, Y. Chen, Y. Long, X. Yi, Y. Luo, H. Zhang, Z. Zhou, Effects of Polarization/Vortex/Led Light on Growth and Photosynthetic Characteristics of Pepper (Capsicum Annuum L.) Seedlings.

[4] Y.N. Kulchin, S.O. Kozhanov, A.S. Kholin, E.P. Subbotin, K.V. Kovalevsky, N.I. Subbotina, A.S. Gomolsky, The Linearly Polarized Light Effect on Maize Development, Bulletin of the Russian Academy of Sciences: Physics, 87(3), S409-S415 (2023).

Photoelectric converter with aperture correction unit for power-over-fiber system

A.S. Pankov[1], A.A. Garkushin[2], R.S. Ponomarev[1], I.L. Volkhin[2], V.A. Maksimenko[2], <u>V.V. Krishtop</u>[1,2*]

1- Perm State National Research University, 15, Bukireva, Perm, 614068, Russia
2- Perm National Research Polytechnic University, 29, Komsomolsky prospect, Perm, 614990, Russia

* krishtop@list.ru

Power-over-fiber (PoF) systems are currently the subject of active research due to their potential for use in aggressive and explosive environments, where the use of metallic conductors may be unacceptable [1,2]. The key element of the PoF system, affecting the efficiency of the entire system, is the photoelectric converter module (PECM), which includes an optical fiber, a homogenizer case and a crystal [3].

This paper presents the developed aperture correction unit at the input of the PECM for a PoF system. The functional unit is implemented as a lens integrated with an optical fiber delivering laser radiation to the input of the photoelectric converter crystal. This unit allows to significantly increase the divergence angle of optical radiation and obtain its optimal value at the input of the PECM, which will reduce the homogenizer length and, as a result, reduce attenuation and weight and size of the entire PECM while maintaining the consistency of the radiation profile with the shape and size of the crystal and the required value of radiation uniformity on its surface. In the course of the study, the main characteristics influencing the efficiency of the aperture correction unit were studied: aperture value, focal length, radiation pattern and radiation profile. Estimated calculations of the optimal parameters of the unit for use in the photoelectric conversion module were performed. Based on the data of two-dimensional numerical modeling, the dependences of the aperture, focal length, directivity pattern and radiation profile on the radius of curvature of the lens and the geometry of the optical fiber core obtained under different lens manufacturing modes are obtained. Qualitative agreement between the experimental and simulation results and data is obtained.

[1] A.A. Garkushin, V.V. Krishtop, V.A. Maksimenko, M.A. Garipova, N.S. Milyukov, K.D. Trapeznikov, E.V. Nifontova, P.V. Zueva, Prospects for application of POWER-OVER-FIBER technology, Applied photonics, Vol. 9, no. 1, pp. 46-67 (2023).
[2] A.A. Garkushin, V.V. Krishtop, S.A. Storozhev, I.L. Volkhin, E.V. Nifontova, E.V. Urbanovich, D.A. Kustov, I.V. Kadochikov, Digital Twin of the Photoelectric Converter of the Power Transmission System over Optical Fiber, Journal of Physics: Conference Series. – IOP Publishing, vol. 2701, №. 1, pp. 012146, (2024).
[3] A.A. Garkushin, V.V. Krishtop, S.A. Storozhev, I.L. Volkhin, E.V. Nifontova, E.V. Urbanovich, D.A. Kustov, I.V. Kadochikov, Intelligent power supply system with power transmission via optical fiber, Bulletin of the Russian Academy of Sciences: Physics, vol. 88, No. 6, pp. 986–990, (2024).

Light guiding nanostructures based on non-van-der-Waals InGaS₃ thin layers

A. Kuznetsov[1,2*]**, E.S. Zavyalova**[2]**, P.A. Alexeev**[3]**, A.N. Toksumakov**[1]**, F.M. Maksimov**[1]**,
V.M. Kondratev**[1]**, M.A. Anikina**[1,2]**, A.D. Bolshakov**[1,2,4]

1- Moscow Institute of Physics and Technology, Institutskii per. 9, 141701, Dolgoprudny, Moscow region, Russia
2- Alferov University, Khlopina str., 8/3, 194021, St. Petersburg, Russia
3- Ioffe Institute, Polytekhnicheskaya st., 26, 194021, St. Petersburg, Russia
4- Yerevan State University, 1 Alex Manoogian, 0025, Yerevan, Republic of Armenia

* alkuznetsov1998@gmail.com

Today the search of novel optical materials for nanophotonics integrated circuits is under particular interest. One of the biggest problems in integrated photonics is the ways how to increase the surface packing density of the functional elements, which can be achieved using materials with high refractive index, operating in the range of shorter wavelengths than Si, for example in visible. InGaS₃ is a semiconductor with a large bandgap (2.73 eV) and high refractive index (< 2.5) [1]. It is a novel material with hexagonal crystal lattice and layered structure but the origin of interlayer bonds is not van-der-Waals but covalent. Its inhomogeneous distribution all over the layer and low density per unit area makes it quite easy to separate the thin layers from each other by a variety of methods [1].

In this work we've investigated the influence of strip and slot waveguides geometry on its optical properties. We've used numerical simulations in Ansys Lumerical software (FDFD and FDTD algorithms) to develop the design of square, rectangle and slot waveguides and evaluate the influence of its longitudinal and lateral size on eigenmodes field distribution, optical loss, transmittance spectra etc. For strip waveguides we've demonstrated the designs for square, rectangle TE and TM cross-section geometry behind the cut-off (~70-100 nm), in the single- (~120-170 nm) and multimode regime (>250 nm). Waveguiding cut-off assigned to field delocalization was identified by effective refractive index dependencies from the lateral size. Transmittance spectra demonstrated both cut-off and InGaS₃ intrinsic absorption (485-505 nm) ranges. Also several strip waveguides with cross-sections of 500×800 nm² were fabricated using atomic-force lithography which have demonstrated broadband waveguiding from 630 up to 500 nm.

For the slot waveguides the gap modes were calculated (for 505 nm wavelength) in the range of strips lateral sizes, for different gaps (10-50 nm) and different underlayer thickness in the gap region. Calculations were provided in accordance with the strip waveguides case. Transmittance spectra also demonstrated the delocalization spectral range shift for different gap size which allows us to develop the bandpass or longpass optical filters. The obtained results open the possibility for fabrication of novel photonic devices based on InGaS₃ thin layers.

[1] A.N. Toksumakov, et al, High-refractive index and mechanically cleavable non-van der Waals InGaS₃, npj 2D Materials and Applications, 6.1., pp. 85, (2022).

Laser beam steering via optical phased array antenna

N.S. Laskavyi[1,2*], A.A. Zhuravlev[1,3]

1- Public Joint Stock Company "Perm Scientific-Industrial Instrument Making Company" (PJSC "PNPPK"),
106, 25th October St., Perm, Russia, 614007
2- Perm National Research Polytechnic University, 29 Komsomolsky Ave., Perm, Russia, 614990
3- Perm State National Research University, 15 Bukireva St., Perm, Russia, 614068

* LaskavyiNS@gmail.com

Laser beam steering in power transmission and communication systems through free-space optical channel and light detection and ranging (LiDAR) has gained significant popularity in recent decades due to the advantages of photonics such as high-speed performance, wide bandwidth, electromagnetic immunity and security of communication channels.

Now, in most cases when it is necessary to change the direction of propagation of an optical beam, we use spatial optics or electromicromechanical systems. This study examines a different principle for steering a laser beam using an optical phased array (OPA). It consists of adding the radiation patterns of individual coherent optical emitting elements located in a one-dimensional or two-dimensional array and forming an interference pattern in the far field. The shape and direction of the total radiation pattern is controlled by adjusting the amplitude and phase of a separate radiating element. This method combines the theory and practice of developing radio frequency phased arrays (PA) and the advantages of photonics. Now, we distinguish fiber optic, microelectromechanical, liquid crystal, metastructural and solid-state (based on photonic integrated circuits) OPAs.

PIC OPA stand out as a promising solution for future dynamic beam steering systems, since this technology allows achieving high stability, beam steering speed and accuracy without mechanical movement of elements. This makes PIC OPA robust and unaffected by external factors such as acceleration.

PIC OPA generate narrow laser beams and have a wide scanning angle with tuning speeds in the range from MHz to GHz. The most common and developed PIC OPA now are silicon-based PIC, since this technology is compatible with the developed infrastructure of the complementary metal-oxide-semiconductor (CMOS) process [1-4]. However, the main disadvantage of this technology is the control of the phase of the optical signal due to the thermo-optical effect, which leads to increased inertia of laser beam control, the need to remove heat from the phase-shifting elements and relatively high power consumption.

One of the promising technologies is the use of lithium niobate $LiNbO_3$, the main advantage of this material can be considered the control of the phase of the optical signal due to the electro-optic effect. Such technologies for the formation of the topology of the PIC as proton exchange and titanium diffusion can be used in the production of PIC OPA. Nevertheless, due to the low contrast of the structures, these technologies do not allow the implementation of close waveguide channels necessary for the formation of a directional pattern with a small number of side maxima. Moreover, it is impossible to comply with the main requirement of the OPA: the distance between the radiating elements should not exceed half the wavelength of the electromagnetic radiation used ($\lambda/2$). For forming elements located relative to each other at a distance of $\lambda/2$ or less, it is possible to use a technology based on thin-film lithium niobate. Research in this area is already underway [5,6], in the author's opinion, this technology is the most promising in the development of OPA.

[1] Y. Guo, Y. Guo, C. Li, H. Zhang, X. Zhou, L. Zhang, Integrated Optical Phased Arrays for Beam Forming and Steering, Appl. Sci. 11(9), 4017 (2021).
[2] J. Sun, E. Timurdogan, A. Yaacobi, et al, Large-scale nanophotonic phased array, Nature 493, 195-199 (2013).
[3] C.V. Poulton, A. Yaacobi, D.B. Cole, M.J. Byrd, M. Raval, D. Vermeulen, M.R. Watts, Coherent solid-state LiDAR with silicon photonic optical phased arrays, Opt. Lett. 42, 4091–4094 (2017).
[4] X. Luo, Engineering Optics 2.0, a Revolution in Optical Theories, Materials, Devices and Systems, (Springer), 14 (2019).
[5] W. Li, X. Zhao, et al, High-speed 2D beam steering based on a thin-film lithium niobate optical phased array with a large field of view, Photon. Res. 11, 1912-1918 (2023).
[6] Z. Wang, X. Li, et al, Fast-speed and low-power-consumption optical phased array based on lithium niobate waveguides, Nanophotonics, vol. 13, n. 13, (2024).

Luminescent nanothermometry with quantum emitters

<u>A.V. Naumov</u>[1-3*], A.I. Arzhanov[1,2], E.A. Ekimov[4], I.Yu. Eremchev[1-3], K.R. Karimullin[1-3],
A.I. Neliubov[1,2], A.O. Savostianov[1,2], T.V. Plakhotnik[5], V.G. Ralchenko[6], V.S. Sedov[6]

1- P.N. Lebedev Physical Institute of the Russian Academy of Sciences, Troitsk Branch, Moscow, Troitsk, Russia
2- Moscow Pedagogical State University (MPGU), Moscow, Russia
3- Institute of Spectroscopy RAS, Moscow, Troitsk, Russia
4- L.F. Vereschegin Institute for High Pressure Physics RAS, Moscow Troitsk, Russia
5- Queensland University, Brisbane, Australia
6- A.M. Prokhorov General Physics Institute, Moscow, Russia

* a_v_naumov@mail.ru; www.single-molecule.ru

Luminescent thermometry is a rapidly growing scientific method based on the dependence of the luminescent and spectral characteristics of nano-sized quantum emitters, QE (organic molecules, semiconductor quantum dots, color centers in nano-/microcrystals, nanoparticles) on temperature [1]. There are different approaches to reconstruct temperature of QE local environment, namely, position and/or width of spectral peaks, ratio of amplitudes of different spectral peaks. The techniques of luminescent nanothermometry with QEs became to be much more powerful when use luminescence imaging – nanoscopy with reconstruction of spatial coordinates with extreme high accuracy (up to size of emitters, i.e. nanometers), thus realizing the idea of multiparameter optical nanoscopy [2]. Even all three spatial QEs coordinates can be reconstructed using adaptive optics techniques, for example double helix point spread function [3]. The accuracy of all methods depends significantly on the theoretical models used to describe the temperature behavior of the spectra. In this paper, we provide a brief overview of our recent results on single QEs spectroscopy and nanoscopy: single organic molecules [1,2,4], colloidal semiconductor quantum dots [5-7], color centers in CVD and HPHT diamonds [8-10].

We bring especial attention to new approaches to interpreting the temperature broadening of the spectral lines of single organic molecules in a polymer matrix as a result of electron-phonon interaction. We believe that the approach under consideration can be successfully applied to a variety of promising emitters used in luminescent thermometry.

[1] A.O. Savostianov, et al, Luminescence nanothermometry by single organic molecules: manifestation of electron-phonon interaction, PHOTONICS Russia 17, 508-515 (2023).
[2] A.V. Naumov, et al, Laser selective spectromicroscopy of myriad single molecules: Tool for far-field multicolour materials nanodiagnostics, The European Physical Journal D 68, 140414 (2014).
[3] I.Y. Eremchev, et al, Three-dimensional fluorescence nanoscopy of single quantum emitters based on the optics of spiral light beams, Physics-Uspekhi. 65, 617-626 (2022).
[4] A.O. Savostianov, et al, Key role of chromophore-modified vibrational modes on thermal broadening of single-molecule spectra in disordered solids, Physical Review B 110, 045430 (2024).
[5] K.R. Karimullin, et al, Combined photon-echo, luminescence and Raman spectroscopies of layered ensembles of colloidal quantum dots, Laser Phys. 2019, 29, 124009.
[6] A.I. Arzhanov, et al, Photonics of Semiconductor Quantum Dots: Basic Aspects, PHOTONICS Russia 15, 622-641 (2021).
[7] A.I. Arzhanov, et al, Photonics of Semiconductor Quantum Dots: Applied Aspects, PHOTONICS Russia 16, 96-112 (2022).
[8] A.Yu. Neliubov, et al, Enigmatic color centers in microdiamonds with bright, stable, and narrow-band fluorescence, Physical Review B 107, 081406 (2023).
[9] I.Yu. Eremchev, et al, Microscopic Insight into the Inhomogeneous Broadening of Zero-Phonon Lines of GeV-Color Centers in Chemical Vapor Deposition Diamond Films Synthesized from Gaseous Germane, J. Phys. Chem. C 125, 17774 (2021).
[10] A.Yu. Neliubov, Diamonds with Color Centers - A Novel Type of Functional Materials, Bulletin of the Russian Academy of Sciences: Physics 87, S421-S428 (2023).

Novel metal and hybrid nanomaterials for electronics and photonics applications synthesized by template synthesis in the pores of polymer track membranes

Yu.A. Filippova[1,2*], N.P. Kovalets[1], V.N. Gumerova[1], D.V. Panov[1], <u>A.V. Naumov</u>[1,3]

1- Moscow Pedagogical State University (MPGU), Moscow, Russia
2- M.V. Lomonosov Moscow State University, Moscow, Russia
3- P.N. Lebedev Physical Institute of the Russian Academy of Sciences, Troitsk Branch, Moscow, Troitsk, Russia

* yufi26@list.ru; www.mpgu.su

The Laboratory of Physics of Advanced Materials and Nanostructures and Educational and Scientific Center for Functional and Nanomaterials named after G.M. Bartenev at the Moscow Pedagogical State University (MPGU) are continuing work on the synthesis and technical application of nano-materials.

Promising method for obtaining rod-shaped nano-structures with variations in shape and size is template synthesis in etched polymer track membranes (TM). This field of science and technology have been initiated and developed by Prof. P.Yu. Apel at the Joint Institute for Nuclear Research (Dubna) and quickly growing last years [1]. The essence of the method for synthesis of secondary structures in the TM is to fill the pores in a matrix with a specific material. The simplicity of this technique and the possibility of electrochemical deposition allow for setting the desired parameters of structures, such as diameter, density, type of metal, shape, and length. In this work, TM acts as the matrix, and microscopic particles formed during this process – nanowires (NPs) – are formed in geometric shape by a precise replica of the corresponding pore, with varying lengths and radii. TM with already set parameters obtained at the Joint Institute for Nuclear Research (Dubna), using PET films with thickness up to dozen of μm and pore diameters from a few tens to a few hundreds of nm as initial matrices, are used.

Here we overview different types of nanomaterials synthesized in TM and their applications. On the basis of these nanowires, viscoelastic properties of magnetic liquids based on silicone oil or ferrogels based on hydroxypropylguar are synthesized and studied [2,3]. Grown Ag nanowires in polymers are used to prepare flexible film heaters with an active area that can be scaled, and a temperature range of 80-100°C [4]. Such composites (TM / metal) are used to study the mechanical properties under tension, including as model materials [5]. Deformation and destruction of composites depend significantly on the size and distribution of pores in the initial TM material. SERS-substrates obtained from TM (an array of nanowires and a system of microcracks on the metalized surface of the TM) are used to detect various substances [6-8]. Single ferromagnetic nanowire can be used in luminescent thermometry for anti-cancer treatment.

[1] P.Yu. Apel, Track etching technique in membrane technology, Radiation Measurements 34, 559-566 (2001).
[2] Y.A. Filippova, et al, Study of the geometry and physical characteristics of FeNi nanowires used in ferrofluids, Bull. Russ. Acad. Sci. Phys. 87, 1813-1818 (2023).
[3] Yu.A. Filippova, et al, FeNi Nanowires as a Promising Filler for Magnetic Sensitive Gel, Bull. Russ. Acad. Sci. Phys. 87, 1483–1487 (2023).
[4] E.P. Kozhina, et al, A thin-film polymer heating element with a continuous silver nanowires network embedded inside, Nanotechnology 35, 035601 (2024).
[5] V.N. Gumirova, et al, The Influence of Mechanical Stress Micro Fields around Pores on the Strength of Elongated Etched Membrane, Membranes 12, 1168 (2022).
[6] E. Kozhina, et al, Ag-Nanowire Bundles with Gap Hot Spots Synthesized in Track-Etched Membranes as Effective SERS-Substrates, Applied Sciences 11, 1375 (2021).
[7] N.P. Kovalets, et al, Towards single molecule surface-enhanced Raman scattering with novel type of metasurfaces synthesized by crack-stratching of metallized track membranes, J. Chem. Phys. 156, 034902 (2022).
[8] N.P. Kovalets, et al, Scratching of metallized polymer films by Vickers indenter as a method for controlled production of SERS-active metasurfaces, Journal of Luminescence 275, 120803 (2024).

Spectral properties of substituted arylpolyenes and cross-conjugate ketones perspective for photonics applications

N.L. Naumova[1*], I.A. Vasil'eva[1], S.N. Gladenkova[1], K.R. Karimullin[1,2], O.N. Korotaev[1], A.V. Naumov[1,2]

1- Moscow Pedagogical State University (MPGU), Moscow, Russia
2- P.N. Lebedev Physical Institute of the Russian Academy of Sciences, Troitsk Branch, Moscow, Troitsk, Russia

* n_l_naumova@mail.ru; www.mpgu.su

Important information about interaction of electronic and vibronic excitations in complex organic molecules can be obtained from optical spectroscopy of doped solids at low temperatures. Luminescence and absorption spectra of dye molecules in solid matrices consist of the vibronic bands which correspond to the transitions of molecules to different vibronic levels.

Here we investigate the optical spectra for two classes of molecules perspective for various photonics and optoelectronics applications: substituted arylpolyenes and cross-conjugate ketones.

The fluorescence and fluorescence excitation spectra of some substituted arylpolyenes in solid Shpol'skii matrices have been studied at a temperature of 4.2 K. The spectra exhibit a weakly pronounced vibrational structure. We have developed a method for determination of parameters responsible for the shape of spectra. The method is based on the modeling of the spectra by series of vibronic bands, each of which consists of a narrow zero-phonon line and a broad phonon sideband. This makes it possible to calculate the conjugated optical spectra with the weakly pronounced vibrational structure and compare them with the measured spectra. The deviations from the mirror symmetry between the measured fluorescence and fluorescence excitation conjugate spectra are explained by the combined effect of the Franck-Condon and Herzberg-Teller interactions.

The spectra of luminescence and absorption (fluorescence excitation) of some cross-conjugate ketones were studied at cryogenic temperatures. We found anomalies in the fluorescence and fluorescence-excitation spectra of some of the studied compounds: a pronounced upset of mirror symmetry of the spectra and a large Stokes shift. The experimental spectra and the spectra calculated theoretically using the theory of two-well adiabatic potentials were subjected to a comparative analysis.

A comparative analysis is performed of the parameters of the Franck-Condon and Herzberg-Teller interactions that determine the shape of the conjugated optical spectra of π-conjugated molecules having the same sets of structural molecular elements. The possibility of applying a fragmentary approach to analyzing the spectra of these molecules is demonstrated.

[1] N.L. Naumova, et al, Evaluation of parameters of intramolecular interaction from absorption and fluorescence spectra of substituted arylpolyene with poor resolved vibrational structure, Journal of Luminescence 111, 37-45 (2005).
[2] N.L. Naumova, et al, Study of vibronic interactions in impurity centers by conjugate fluorescence and absorption spectra with a poorly resolved vibrational structure, Optics and Spectroscopy 98, 535-542 (2005).
[3] N.L. Naumova, et al, Fluorescence Spectra of Some Cross-Conjugate Ketones: Experiment and Calculations Based on the Model of Two-Well Adiabatic Potentials, Optics and Spectroscopy, 92, 383-388 (2002).
[4] V.V. Kompaneets, K.R. Karimullin, I.A. Vasilieva, A.V. Naumov, Effect of Identical Sets of Structural Elements of π-Conjugated Molecules on the Parameters of Intra- and Intermolecular Interaction, Bulletin of the Russian Academy of Sciences: Physics 84, 272-280 (2020).

Use of circular polarization in imaging photoplethysmography

N.V. Nikitin, A.V. Belaventseva, N.P. Podolyan, R.V. Romashko, A.A. Kamshilin

Institute of Automation and Control Processes FEB RAS, Vladivostok, Russia

* nnikitin@dvo.ru

Imaging photoplethysmography (iPPG) is a very promising method for evaluating hemodynamic parameters *in vivo*, especially for visualizing and quantifying changes in organ perfusion during surgical operations [1,2]. An important element of the iPPG optical system is polarization filtering, usually implemented by means of two crossed linear polarizers. One of these polarizers is installed after the illuminator and serves to illuminate the organ under study with incoherent linearly polarized light. Another polarizer is attached to the camera lens. Its transmission axis is adjusted to be orthogonal with that of the first polarizer. Since red blood cells (RBC) are highly anisotropic, after interacting with them, the light acquires elliptical polarization. Such polarization filtration reduces the effect of both skin specular reflections and motion artefacts on the detected iPPG signal, thereby increasing the signal-to-noise ratio [3]. However, such a scheme has a practical disadvantage due to the need to adjust the polarization filter, which is not always feasible in an operating room.

Here we propose to implement polarization filtering using only one optical element, namely a circular polarizer combined with a linear one. Such type of polarizing filters is widely used in photography to reduce specular reflections and is known as a CPL-filter. In our iPPG module, eight or more light-emitting diodes (LED) are positioned around the camera lens to ensure proper illumination of the organ under study. The CPL filter covers both the lens and all LEDs in such a way that the light emitted by the LEDs first hits the side of the CPL filter with a linear polarizer. In such a configuration, the subject's skin is illuminated by circularly polarized light, the polarization of which remains circular after specular reflection from the skin, but with the opposite rotation, thereby preventing the reflected beam from passing through the CPL-filter and reaching the sensor of the camera. On the contrary, after interacting with RBCs, the light becomes elliptically polarized and passes through the CPL-filter. Therefore, CPL-filter provides filtering of specular reflections in a similar way, as a pair of crossed linear polarizers does. The advantages of using CPL filters in iPPG systems are: (i) no adjustment is needed, and (ii) easy integration into small-aperture optical systems, such as endoscopic and laparoscopic [4].

We have carried out a comparative study of polarization filtration provided by crossed linear polarizing filters and CPL filters when visualizing and quantifying perfusion distribution in subject's forearm. It was found that both schemes provide an increase in the signal-to-noise ratio of the iPPG signal compared to using nonpolarized light: by 36% and 44% for cross-polarized and CPL filtering, respectively.

In addition, the contrast factor (ratio of transmitted-to-suppressed light intensity) provided by CPL-filter is greater (1900 : 1) or at least not worse that contrast provided by the cross-polarized filtering (1550 : 1). Thus, the CPL-filter is not inferior to the cross-polarization filters in efficiency, its usage in iPPG systems is more advantageous, while parameters of CPL filter (thickness, light transmission, resistance to high temperature, supporting a coverage both light source and camera) open the possibility its application for polarization filtering of the photoplethysmographic signal in the iPPG laparoscopic systems [4].

[1] O.V. Mamontov, A.V. Shcherbinin, R.V. Romashko, A.A. Kamshilin, Intraoperative imaging of cortical blood flow by camera-based photoplethysmography at green light, Applied Sciences, vol. 10, p. 6192, (2020).
[2] A.A. Kamshilin, V.V. Zaytsev, A.A. Lodygin, V.A. Kashchenko, Imaging photoplethysmography as an easy-to-use tool for monitoring changes in tissue blood perfusion during abdominal surgery, Scientific Reports, vol. 12, p. 1143, (2022).
[3] I.S. Sidorov, M.A. Volynsky, A.A. Kamshilin, Influence of polarization filtration on the information readout from pulsating blood vessels, Biomedical Optics Express, vol. 7, pp. 2469–2474, (2016).
[4] V.A. Kashchenko, A.V. Lodygin, K.Y. Krasnoselsky, V.V. Zaytsev, A.A. Kamshilin, Intra-abdominal laparoscopic assessment of organs perfusion using imaging photoplethysmography, Surgical Endoscopy, vol. 37, pp. 8919–8929, (2023).

The temperature influence on the characteristics of the sensitive element of a resonator fiber-optic gyroscope

K.A. Ovchinnikov[1,2*], **D.G. Gilev**[1,2], **V.V. Krishtop**[1,2]

1- Perm Scientific-industrial Instrument Making Company, Perm, 614007 Russia
2- Perm National Research Polytechnic University, Perm, 614007 Russia

* OvchinnikovKA@pnppk.ru

Miniaturization is an important task in modern science and technology, which is also actively developing in the field of fiber-optic sensors. Reducing the size of the sensors allows you to expand the scope of applications and solve complex tasks that were previously unavailable. In the field of fiber-optic gyroscopy, fiber-optic resonators [1] are a promising candidate for solving the miniaturization problem, which make it possible to reduce the dimensions of the sensing element by repeatedly passing the optical path inside the closed cavity of the resonator.

Recently, more and more research has been devoted to a new scheme of resonator fiber-optic gyroscopes operating on broadband radiation, which reduces the influence of backscattered radiation noise and increases the stability of resonator gyroscopes [2,3].

An experimental study was conducted on the effect of ambient temperature in the range from -30°C to +50°C on the optical circuit of a resonator fiber-optic gyroscope with a resonant circuit length of 50 m and with a superluminescent diode with a central wavelength of 1550 nm as a radiation source. The study of the temperature effect on the optical circuit as a whole and on its individual components is an important step in the development of devices, since it helps to determine the critical parameters to ensure the temperature stability of the final device.

The analysis of experimental data shows that when developing such sensors to increase stability, it is necessary to take into account and compensate for the influence of such parameters as: changes in the total losses of the optical circuit, the central wavelength of the radiation source, the half-wave voltage of the phase modulator used and changes in the input power of the superluminescent diode at different temperatures.

[1] D.G. Gilev, K.A. Ovchinnikov, V.V. Krishtop, et al, Fiber Optic Resonators for Angular Rate Sensors, Bull. Russ. Acad. Sci. Phys. 86 (Suppl 1), S75–S80 (2022).
[2] S. Zhao, Q. Liu, Y. Liu, H. Ma, Z. He, Navigation-grade resonant fiber-optic gyroscope using ultra-simple white-light multibeam interferometry, Photon. Res. 10, 542-549 (2022).
[3] K.A. Ovchinnikov, D.G. Gilev, V.V. Krishtop, et al, A Prototype for a Passive Resonant Interferometric Fiber Optic Gyroscope with a 3×3 Directional Coupler, Sensors. 23(3):1319, (2023).

Broadband optical properties of anisotropic palladium diselenide

G. Ermolaev[1,2], A. Slavich[1], M. Tatmyshevskiy[1], G. Tselikov[1,2],
N. Pak[1*], D. Grudinin[1], I. Kruglov[1], A. Arsenin[1,2]

1- Center for Photonics and 2D Materials, Moscow Institute of Physics and Technology, Dolgoprudny, Russia
2- Emerging Technologies Research Center, XPANCEO, Dubai Investment Park First, Dubai, United Arab
Emirates

* pak.nv@phystech.edu

Noble metal dichalcogenides (NMDCs) are distinguished among other advanced materials because of their strong layer-dependence of optical properties and interlayer interaction [1,2]. A promising example of NMDCs is a high refractive index $PdSe_2$. This material has practical application due to impressive physical properties [2-4]. $PdSe_2$-based heterostructures can be applied to polarization resolved photodetectors, field effect transistors, infrared sensors [3,5]. To describe the optical phenomena, on which optoelectronic devices are based, one needs to know refractive index n and excitation coefficient k. Nevertheless, there are few works related to the experimental determination of fundamental optical constants of $PdSe_2$ [2,6], infrared region has not been not studied yet.

In this paper, we investigated broadband optical properties of bulk $PdSe_2$ over a wide range of wavelengths. We measured a refractive index and an extinction coefficient by imaging ellipsometry method. Then we extended optical constants dependency to the far-infrared region according to a theoretical model. To evaluate broadened results, we used experimental data obtained from micro-reflectance and scattering near-field optical microscopy and density functional theory computations. Optical constants obtained in our work are necessary in optics and optoelectronics.

[1] W. Nishiyama, T. Nishimura, K. Ueno, et al, Quantitative determination of contradictory bandgap values of bulk $PdSe_2$ from electrical transport properties, Adv. Funct. Mater., Vol. 32, No. 2108061 (2021).
[2] M.Y. Wei, Y. Zhang, C. Wang, et al, Layer-dependent optical and dielectric properties of centimeter-scale $PdSe_2$ films grown by chemical vapor deposition, npj 2D Mater. Appl., Vol. 6, No. 1 (2022).
[3] M. Long, Y. Wang, P. Wang, et al, Palladium diselenide long-wavelength infrared photodetector with high sensitivity and stability, ACS Nano, Vol. 13(2), pp. 2511-2519, (2019).
[4] Y. Gu, H. Kai, J. Dong, et al, Two-dimensional palladium diselenide with strong in-plane optical anisotropy and high mobility grown by chemical vapor deposition, Adv. Mater., Vol. 32(19) No. 1906238 (2020).
[5] Y. Wang, J. Pang, Q. Cheng, et al, Applications of 2D-layered palladium diselenide and its van der Waals heterostructures in electronics and optoelectronics, Nano-Micro Let., Vol. 13, No. 143 (2021).
[6] G. Ermolaev, K. Voronin, D.G. Baranov, et al, Topological phase singularities in atomically thin high-refractive-index materials, Nat. Commun., Vol. 13, No. 2049 (2022).

Periodically spallated Ag film as a high-performing SERS substrate for biogenic amines detection

A. Pilnik[1], E. Mitsai[1*], A. Kuchmizhak[1]

1- Institute of Automation and Control Processes of the FEB RAS, 5 Radio St., 690041 Vladivostok, Russia

* mitsai@dvo.ru

One of the important areas in modern society is quality control of food products. A common method of control is to determine the concentration of biogenic amines, which usually indicates the quality and freshness of the product. SERS spectroscopy methods are often used to detect biogenic amines, which require a large number of disposable substrates for every experiment. In this regard, there is a need for a method for fast, cheap, productive and chemically clean production of SERS substrates. The technology of metal films ablation with a pulsed fs-laser meets these criteria.

In this work, we used 500-nm Ag films deposited on glass by electron beam evaporation, that were modified by wide laser beam with a size of 12×0.6 μm. This method allows for fast modification of the surface on a mm^2-scale (Fig. 1a).
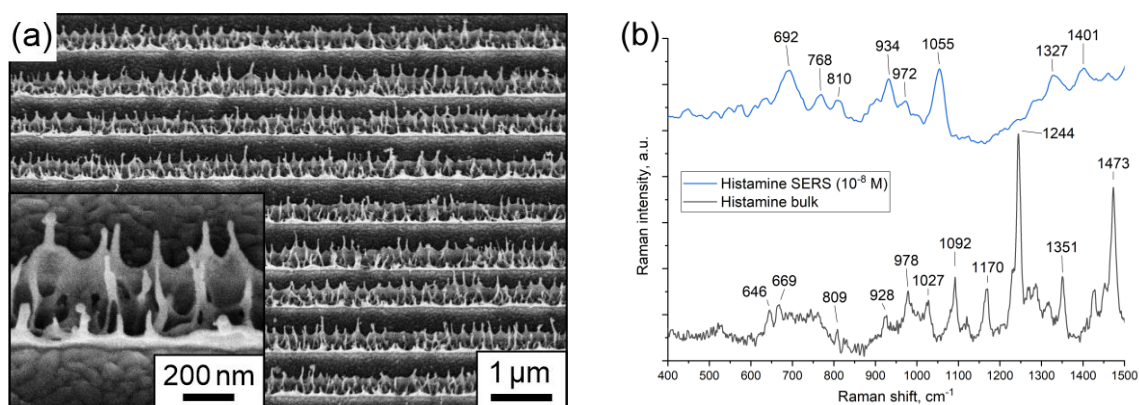

Fig. 1. (a) SEM image of periodically spallated Ag film. The inset shows close-up details of the morphology. (b) Raman spectrum of histamine (black line) and SERS spectra of histamine adsorbed on spallated Ag film (blue line). Both spectra have a signal accumulation time of 100 s.

The chemosensing performance of the spallated surfaces is demonstrated by SERS-detection of methanol solution of histamine at a concentration of 10^{-8} M. The substrate was immersed in a solution for an hour. Measurements were carried out after complete drying of the substrate with a CW laser ($\lambda=473$ nm) that was focused by dry microscope objective (NA=0.9, 100×) with a resulting intensity of 1.33 mW/μm^2.

Fig. 1b demonstrates typical SERS spectrum of histamine adsorbed on spallated Ag film with main peaks highlighted. Comparison of Raman and SERS spectra shows that molecular vibrational modes exhibit significant frequency shifts due to interaction with the Ag surface [1]. SERS bands associated with the characteristic vibrational modes of histamine observed at 692, 768, 810, 934, 1055, 1327 and 1401 cm^{-1} are attributed to C–C ring bending, ring A stretching coupled with bending $CH_2CH_2NH_2$ group, outer ring A stretching, C–H in-plane torsion bending, C–H in-plane torsion bending coupled with N–H in-plane stretching and C–H in-plane bending, respectively [2]. Therefore, this quickly produced SERS-substrate demonstrates the possibility of detecting biological analytes at low concentrations found in food products or in biofluids, that can be a promising tool for the diagnosis of biogenic amines-related diseases.

[1] W.C. Lin, T.R. Tsai, H.L. Huang, C.Y. Shiau, H.P. Chiang, SERS study of histamine by using silver film over nanosphere structure, Plasmonics, 7, 709-716, (2012).
[2] T. Zhang, G. Wang, J. Bao, C. Liu, W. Li, Z. Kong, X. Sun, J. Li, R. Lu, Fabrication of an Ag-based SERS nanotag for histamine quantitative detection, Talanta, 256, 124256, (2023).

Peculiarities of pulse arrival time revealed in human arms by imaging photoplethysmography

N.P. Podolyan[1*], I.A. Mizeva[2], R.V. Romashko[1], A.V. Sadoskiia[1,3], A.A. Kamshilin[1]

1- Institute of Automation and Control Processes FEB RAS, Vladivostok, Russia
2- Institute of Continuous Media Mechanics UrB RAS, Perm, Russia
3- Institute of Therapy and Instrumental Diagnostics, Pacific State Medical University, Vladivostok, Russia

* podolian@iacp.dvo.ru

The pulse arrival time (PAT), defined as the time difference between the R-peak of an electrocardiogram (ECG) and the onset of an increase in blood pressure at the periphery, is a useful tool for assessing the functional state of the cardiovascular system. PAT depends on many factors such as the structure of the vessels network, vessel diameter, wall stiffness, blood pressure, heart rate, etc. [1]. Either pressure or optical sensors are used for clinical assessment of PAT. In recent years, there has been a significant increase in interest to developing devices for cuffless estimation of blood pressure (BP) based on a photoplethysmography (PPG) and ECG techniques, which measure PAT to use it as a surrogate for BP [2]. The PPG signal in these systems is recorded directly from the patient's skin using a contact sensor affixed on distal part of the body (fingertip, forearm, earlobe, etc.), which can cause discomfort [3]. In addition, any contact-type sensor affects the blood flow in the contact area, which is often not evaluated and not taken into account, despite the well-known fact that any skin contact may affect cutaneous microcirculation. The aim of our work was to study how stable PAT is with changes in microvascular blood flow parameters, caused by the controlled local hyperemia.

The study was carried out using a multimodal system, which includes imaging photoplethysmography synchronized with ECG, and described in detail in our recent paper [4]. This technique allows us to measure PAT together with the perfusion index (PI). The skin of the subject's forearm with a transparent heater placed on it, was illuminated by green light-emitting diodes, and an image of the forearm was recorded by a video camera. The baseline lasted 5 minutes with the heater turned off, then the skin was heated up to ~40°C during 150 s and maintained at this temperature for 15 minutes, followed by 25-minute relaxation. Images of the forearm and the heater were recorded continuously and synchronously with ECG. The recorded signals were processed using a specially developed algorithm [4]. PAT in the area under study was calculated as the time between the R-peak of ECG and a minimum of the PPG waveform in every cardiac cycle.

A total of 52 volunteers, men, aged 48±10 years, were examined. The perfusion index and PAT values were assessed over a pair of time intervals: baseline (b) 10:140 s and heating (h) 520:650 s. It was found that in the baseline $PI_b = 0.25$ (0.1; 1.0) a.u. (here and further, the data is presented as median (quartile 1; quartile 3)), $PI_h = 1.50$ (0.6; 3.4) a.u., $P < 0.001$; $PAT_b = 200$ (136; 253) ms, $PAT_h = 142$ (74; 207) ms, $P < 0.001$. The median PAT difference between the baseline and heating stage was 58 ms or ~30%. Correlation analysis of the evolution of the parameters PI and PAT revealed their strong negative relationship ($r = -0.75$). At the same time, the heart rate of all the subjects remained unchanged throughout the experiment. In conclusion, we have shown for the first time that local changes in the microcirculatory perfusion significantly affect PAT against the background of unchanged heart rate.

[1] J.J. Oliver and D.J. Webb, Noninvasive Assessment of Arterial Stiffness and Risk of Atherosclerotic Events, Arteriosclerosis, thrombosis, and vascular biology, vol. 23, pp. 554-566, (2003).
[2] E. Finnegan, S. Davidson, M. Harford, J. Jorge, P. Watkinson, D. Young, L. Tarassenko, M. Villarroel, Pulse Arrival Time as a Surrogate of Blood Pressure, Scientific Reports, vol. 11, p. 22767, (2021).
[3] M. Sharma, K. Barbosa, V. Ho, D. Griggs, T. Ghirmai, S. Krishnan, T.K. Hsiai, J.-C. Chiao, H. Cao, Cuff-Less and Continuous Blood Pressure Monitoring: A Methodological Review, Technologies, vol. 5, p. 21, (2017).
[4] A.A. Kamshilin, V.V. Zaytsev, A.V. Belaventseva, N.P. Podolyan, M.A. Volynsky, A.V. Sakovskaia, R.V. Romashko, O.V. Mamontov, Novel Method to Assess Endothelial Function via Monitoring of Perfusion Response to Local Heating by Imaging Photoplethysmography, Sensors, vol. 22, p. 5727, (2022).

Fluorescence monitoring for early search harmful algae blooms

A. Popik[1*], S. Voznesenskiy[1], T. Dunkay[2], E. Gamayunov[1], T. Orlova[2], A. Leonov[1], A. Zinov[2]

1- Institute of Automation and Control Processes, Far Eastern Branch, Russian Academy of Sciences, 690041 Vladivostok, st. Radio 5, Russia
2- A.V. Zhirmunsky National Scientific Center of Marine Biology, Far Eastern Branch, Russian Academy of Sciences, 690041 Vladivostok, st. Palchevskogo 17, Russia

* popikay@yandex.ru

The harmful algae blooms (HABs) have a huge impact on the economies of countries that are most dependent on marine fisheries, farming and tourism [1]. Many countries in the Asia-Pacific region are facing this serious problem. Ocean warming trends are causing rapid and abrupt changes in Arctic marine ecosystems. In this regard, the economic risks associated with HABs are becoming relevant for the Russian coastal region as well [2].

The use of optical methods, such as probing water areas with submersible fluorescence sensors [3] or satellite probing of the color of the sea surface [4], allows us to determine the concentration of chlorophyll a. However, the absence of information on the species composition of marine algae introduces a large error in the data on the concentration of chlorophyll.

Measuring the fluorescence spectra of microalgae in a wide range of temperatures, with a given heating mode, allows us to study the characteristic changes in the photosynthetic apparatus of different groups of algae, which are reflected in their optical signals [5]. The temperature dependence of fluorescence spectra allows the creation of fluorescence temperature spectra, three-dimensional surfaces that can be used as fingerprints of microalgae. Figure 1 shows the fluorescence temperature spectra of three monocultures of microalgae that potentially cause HABs.
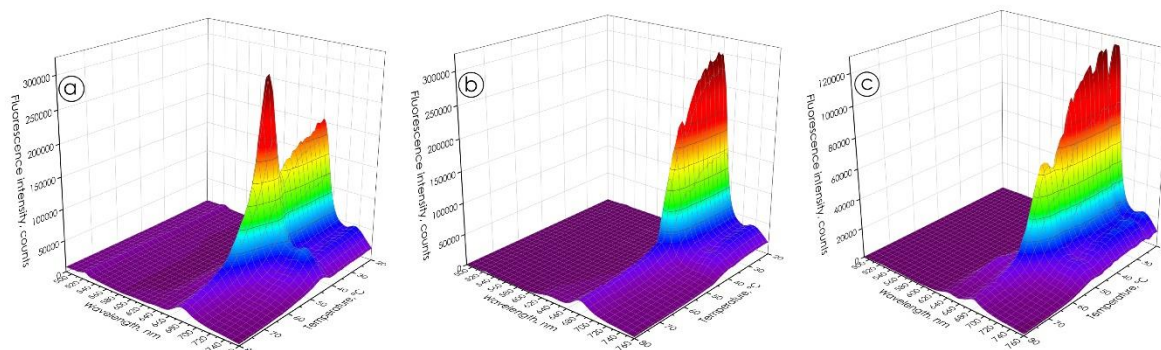
Figure 1. Fluorescence temperature spectra
a – *Alexandrium catenella*; b – *Pseudo-nitzschia multistriata*; c – *Heterosigma akashiwo.*

Development of a method for obtaining and analyzing temperature fluorescence spectra and the fluorescence characteristics of microalgae obtained with their help allows to identify monocultures of microalgae by their optical characteristics at the genus level and provides a potential opportunity to identify a blooming species when it dominates in natural waters.

[1] C.R.C. Kouakou, T.G. Poder, Economic impact of harmful algal blooms on human health: A systematic review, J. Water Health. 17 (2019) 499–516.
[2] T.Y. Orlova, T.V. Morozova, Dinoflagellate Cysts of the Genus Alexandrium Halim, 1960 (Dinophyceae: Gonyaulacales) in Recent Sediments from the Northwestern Pacific Ocean, Russ. J. Mar. Biol. 45 (2019) 397–407.
[3] S.S. Voznesenskiy, E.L. Gamayunov, A.Y. Popik, A.A. Korotenko, A fiber-optic fluorometer for measuring phytoplankton photosynthesis parameters, Instruments Exp. Tech. 57 (2014) 330–335.
[4] Y. Li, R.P. Stumpf, D.J. McGillicuddy, R. He, Dynamics of an intense Alexandrium catenella red tide in the Gulf of Maine: satellite observations and numerical modeling, Harmful Algae. 99 (2020) 101927.
[5] A.Y. Popik, E.L. Gamayunov, S.S. Voznesenskiy, Z.M. Markina, T.Y. Orlova, The study of fluorescence features of microalgae from the genus Pseudo-nitzschia and the possibility of their detection in water, Algal Res. 64 (2022) 102662.

Colloidal synthesis of halide perovskite microwires for photonics and optoelectronics

A. Pushkarev

Faculty of Physics, ITMO University, Kronverksky Pr. 49, 197101 St. Petersburg, Russia

anatoly.pushkarev@metalab.ifmo.ru

Over the last decade halide perovskite microwires have emerged as a platform for numerous photonic and optoelectronic applications including solar cells, lasers, optical gas sensors, photodetectors, electroluminescent photodetectors, integrated photonic devices, etc. [1-6] Colloidal synthesis of microwires have many advantages over frequently employed chemical vapor deposition (CVD) and substrate-assisted solution growth. Among them there are easy doping of perovskite crystal lattice by transition metal ions that results in bandgap tuning and change in conductivity, along with simplicity of microwires integration with various nanostructures and electrodes by using drop-casting to produce complex devices. However, there is the only report devoted to colloidal perovskite microwires so far [7]. In my talk, I will present a novel colloidal synthesis of all-inorganic perovskite microwires, laser action in them, as well as optoelectronic devices, in particular single-crystal-based gas sensor and memristor.

[1] J.-H. Im, J. Luo, M. Franckevičius, N. Pellet, P. Gao, T. Moehl, S. Zakeeruddin, M. Nazeeruddin, M. Grätzel, N.-G. Park, Nanowire Perovskite Solar Cell, Nano Lett., 15, 2120–2126, (2015).

[2] A. Zhizhchenko, A. Cherepakhin, M. Masharin, A. Pushkarev, S. Kulinich, A. Kuchmizhak, S. Makarov, Directional Lasing from Nanopatterned Halide Perovskite Nanowire, Nano Lett., 21, 10019–10025, (2021).

[3] D. Markina, S. Anoshkin, M. Masharin, S. Khubezhov, I. Tzibizov, D. Dolgintsev, I. Terterov, S. Makarov, A. Pushkarev, Perovskite Nanowire Laser for Hydrogen Chloride Gas Sensing, ACS Nano, 17, 1570–1582, (2023).

[4] Q. Ye, J. Zhang, P. Guo, H. Fan, D. Shchukin, B. Wei, H. Wang, Wet-Chemical Synthesis of Surface-Passivated Halide Perovskite Microwires for Improved Optoelectronic Performance and Stability, ACS Appl. Mater. Interfaces, 10, 43850–43856, (2018).

[5] A. Marunchenko, V. Kondratiev, A. Pushkarev, S. Khubezhov, M. Baranov, A. Nasibulin, S. Makarov, Mixed Ionic-Electronic Conduction Enables Halide Perovskite Electroluminescent Photodetector, Laser Photonics Rev., 17, 2300141, (2023).

[6] Q. Han, J. Wang, S. Tian, S. Hu, X. Wu, R. Bai, H. Zhao, D. Zhang, Q. Sun, L. Ji, Inorganic Perovskite-Based Active Multifunctional Integrated Photonic Devices, Nat. Commun., 15, 1536, (2024).

[7] W. Zhang, L. Peng, J. Liu, A. Tang, J.-S. Hu, J. Yao, Y. Zhao, Controlling the Cavity Structures of Two-Photon-Pumped Perovskite Microlasers, Adv. Mater., 28, 4040-4046, (2016).

Diffraction of light on multiplexed multilayer holographic diffraction structures with varying periods

D.S. Rastrygin[1*], V.O. Dolgirev[1], S.N. Sharangovich[1]

1- Tomsk State University of Control System and Radioelectronics, Lenin avenue 40,
634050 Tomsk, Russia

* gg9dragon9gg@gmail.ru

The application of diffraction optics in modern science and technology is relevant and significant. This branch of optics provides the opportunity to design and study optical elements that operate on the basis of diffraction phenomena, which has a wide range of potential applications [1,2].

This paper presents an analytical model of light diffraction by multiplexed multilayer period-varying holographic diffraction structures formed in photopolymer composite materials. As a result of numerical calculation, the influence of a varying period on the diffraction characteristics of such structures was demonstrated. The scheme of light diffraction on these structures is shown in Fig. 1. As a result, an increase in the angular selectivity width by several times is observed relative to the standard multiplexed multilayer structure. The numerical calculation results are presented in Fig. 2. This type of angular selectivity is set of local maxima and minima, number and the width of which depends on the stability parameters, including the number of diffraction layers and relation to their thickness. By such local maxi as stripes transmittance for specific wavelengths when deflected from Bragg diffraction regime, renders these structures suitable for application in optical devices designed for spectral filtering purposes [2].

The results obtained make it possible to use multiplexed multilayer holographic diffraction structures with varying periods as the main element for optical spectral filters for communication networks.
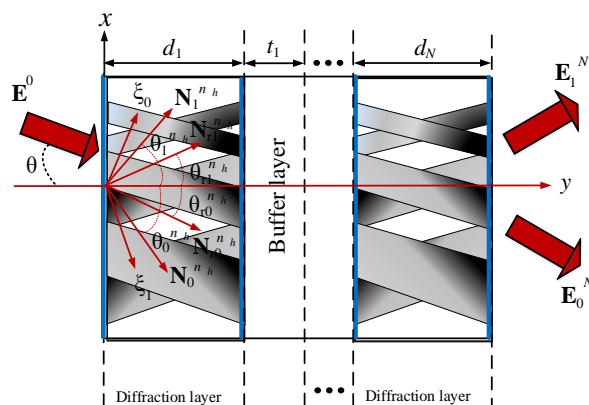

Fig. 1. Schematic of light diffraction on chirped multiplexed MIHDS with varying periods.
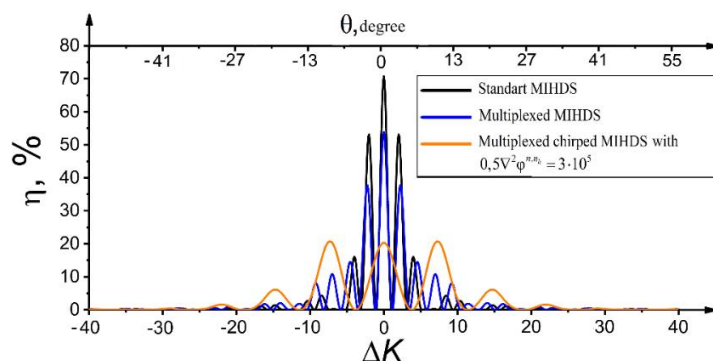
Fig. 2. Angular selectivity of standard and multiplexed chirped dual-layer HDS.

[1] R. Malallah, et al, Improving the uniformity of holographic recording using multilayer photopolymer. Part I. Theoretical analysis, J. Opt. Soc., vol. 36 (3), pp. 320-333, 2019.

[2] V.O. Dolgirev, S.N. Sharangovich, Study of light diffraction on electrically controlled multilayer inhomogeneous structures with smooth optical inhomogeneity based on photopolymerizing compositions with nematic liquid crystals, Bull. Russ. Acad. Sci. Phys., vol. 86(1), pp. S46-S49, 2022.

Casimir energy and Casimir torque in twisted stack of anisotropic gratings

N. Salakhova[1*], S. Dyakov[1], N. Gippius[1]

1- Skolkovo Institute of Science and Technology, Bolshoy Boulevard, 30, p.1, Moscow 121205, Russia

* Natalia.Salakhova@skoltech.ru

With the miniaturization of modern devices, new physical effects are becoming important. One such effect is the Casimir-Lifshitz force [1,2], which exists between any pair of bodies and increases significantly when the micro- and nanometer distance between them is reached. This force causes the problem of stiction or, on the contrary, can be used to detect small changes due to its sensitivity.

This paper investigates the Casimir force between two one-dimensional lattices of anisotropic material rotated relative to each other. The natural anisotropy of the material and the artificial anisotropy of the one-dimensional lattice lead to the dependence of the Casimir energy both on the rotation between the two lattices and on the angle between the anisotropy axis of the material and the direction of the lattice grooves. In our case, the Casimir energy reaches two local minima and two local maxima when the relative rotation angle changes from 0° to 180°. In comparison, a system consisting of general one-dimensional lattices [3] or plates made of anisotropic material [4] has only two local features: a minimum and a maximum at 0° or 90°. The dependence of the Casimir energy on the rotation angles gives rise to a rotational force called the Casimir torque.

We have shown that the Casimir energy and the Casimir moment depend on both the rotation angle and the lattice spacing, which allows us to establish a correspondence between these parameters. Moreover, this correspondence is determined by the angle with the anisotropy axis.

A twisted stack of one-dimensional gratings of anisotropic material may be relevant for measurement applications in micro- and nano-optomechanical devices.

[1] H.B. Casimir and D. Polder, The influence of retardation on the London-van der Waals forces, Physical Review, 73(4), 360, (1948).

[2] E.M. Lifshitz and M. Hamermesh, The theory of molecular attractive forces between solids, In Perspectives in theoretical physics (pp. 329-349). Pergamon, (1992).

[3] M. Antezza, H.B. Chan, B. Guizal, V.N. Marachevsky, R. Messina, M. Wang, Giant Casimir torque between rotated gratings and the θ= 0 anomaly, Physical review letters, 124(1), 013903, (2020).

[4] J.N. Munday, D. Iannuzzi, Y. Barash, F. Capasso, Torque on birefringent plates induced by quantum fluctuations, Physical Review A, 71(4), 042102, (2005).

The impact of Cd-doping on optical properties of all-inorganic halide perovskite microdisks

D. Tatarinov[1], E. Sapozhnikova[1*], A. Pushkarev[1]

1- ITMO University, Kronverksky pr. 49, bldg. A, 197101, St. Petersburg, Russia

* e.sapozhnikova@metalab.ifmo.ru

Substitution of Pb^{2+} by Cd^{2+} in all-inorganic lead halide perovskite crystal lattice has been established as a promising strategy to give control over photoluminescence (PL) spectrum, electric conductivity, and light- and electric field-induced ion segregation in alloyed compositions [1-3].

In our work, we employ pressure-assisted high temperature recrystallization to produce bulk $CsPb_{1-x}Cd_xBr_3$ perovskites for persistent lasing. Obtained microdisks enable to discover a reliable correlation between quantitative energy dispersive X-ray (EDX) spectroscopy data and PL. Time-resolved measurements reveal delayed radiative electron-hole recombination which could be explained by reversible electron $\Gamma \leftrightarrow R$-point transfer in the conduction band. Microdisks loaded with low Cd content show rapid deterioration of bright green PL under high fluence quasi-continuous-wave (Q-CW) laser excitation, whereas the high content results in persistent, however, low-intensity blue emission. We propose such a dramatic difference in temporal stability of lightly and heavily doped samples stems from reduced Auger recombination in the latter. Finally, the optimal Cd content of ca. 6% improves temporal stability of whispering gallery mode (WGM) lasing in microdisks by 3 times as compared to that of pure $CsPbBr_3$ counterparts.

[1] M. Imran, J. Ramade, F. Di Stasio, M. De Franco, J. Buha, S. Van Aert, L. Goldoni, S. Lauciello, M. Prato, I. Infante, S. Bals, L. Manna, Alloy $CsCd_xPb_{1-x}Br_3$ Perovskite Nanocrystals: The Role of Surface Passivation in Preserving Composition and Blue Emission, Chem. Mater., 32, 10641–10652 (2020).

[2] J. Guo, Y. Fu, M. Lu, X. Zhang, S.V. Kershaw, J. Zhang, S. Luo, Y. Li, W.W. Yu, A.L. Rogach, L. Zhang, X. Bai, Cd-Rich Alloyed $CsPb_{1-x}Cd_xBr_3$ Perovskite Nanorods with Tunable Blue Emission and Fermi Levels Fabricated through Crystal Phase Engineering, Adv. Sci., 7, 2000930 (2020).

[3] S.S. Anoshkin, E.V. Sapozhnikova, Y. Feng, Y. Ju, A. Pavlov, R.G. Polozkov, A. Yulin, H. Zhong, A.P. Pushkarev, Blue-Emitting $Cs(Pb,Cd)Br_3$ Nanocrystals Resistant to Electric Field-Induced Ion Segregation, ACS Appl. Mater. Interfaces, 16, 11656–11664 (2024).

Bioprinting of hierarchical auxetic coronary stents: from design to mechanical testing

E. Mazur[1], I. Shishkovsky[2*]

1- Skolkovo Institute of Science and Technology, 121205 Moscow, Russia
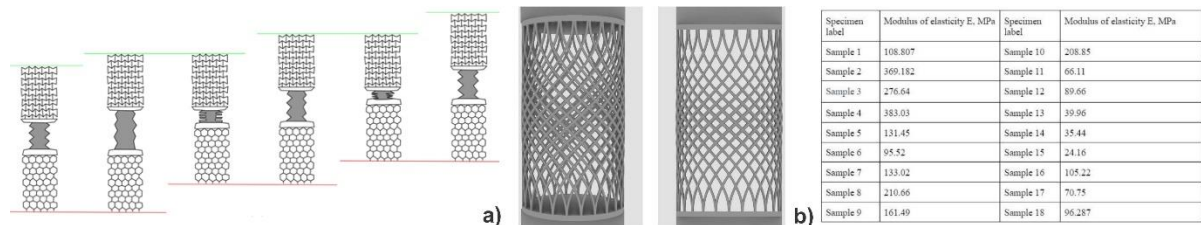*2- Lebedev Physical Institute of the RAS, 443011 Samara, Russia*

* shiv@fian.smr.ru

Samples of coronary stents, which are widely used in cardiac surgery and have an inner lattice structure, were fabricated (Fig. 1). Hierarchical auxetic materials based on rotating units are more versatile than similar non-hierarchical lattice materials, and thus they are a promising candidate not only for stent fabrication, but also for soft robotic applications. When reviewing soft robotics applications, it is important to consider the ability of auxetic structures to change shape when moving through narrow spaces. For example, a soft robot designed like an inchworm to crawl through blood vessels using mechanical metamaterials for synchronized movement of two passive clutches has been presented in [1]. Due to thermal or electrical activation, this design allows the robot to move through a confined passage using a single actuator, similar to the movement of an inchworm. The sequence of images in Fig. 1a shows three cycles of the bellows expanding and contracting. During expansion, the auxetic structure moves upward, while the normal structure remains stationary. During contraction, the auxetic structure remains fixed, while the normal structure slides upward.

The passive stent mechanism, based on complementary material properties, helps to reduce the number of actuators to one and avoid synchronization problems, as the smart synchronization is already built into the robot's material body. This type of robot can be used for navigation within soft capillaries, cylindrical blood channels with unknown cross-section, and other related applications.

Six different models were designed in Rhino 7 and Grasshopper, varying two key parameters: the number of fibers and fiber radius. Internal structure management and/or radius gradient creation can introduce auxetic properties into these scaffolds. The stents were manufactured using Anycubic 3D printing UV-sensitive resin material and a Zortax Inkspire 3D printer (digital light processing, DLP technology), and tested using an Instron 5269 machine.

Specimen label	Modulus of elasticity E, MPa	Specimen label	Modulus of elasticity E, MPa
Sample 1	108.807	Sample 10	208.85
Sample 2	369.182	Sample 11	66.11
Sample 3	276.64	Sample 12	89.66
Sample 4	383.03	Sample 13	39.96
Sample 5	131.45	Sample 14	35.44
Sample 6	95.52	Sample 15	24.16
Sample 7	133.02	Sample 16	105.22
Sample 8	210.66	Sample 17	70.75
Sample 9	161.49	Sample 18	96.287

Each set of samples included the following modifications: the radii of the wires inside the coronary were 0.25 and 0.30 m, and the number of wires used in the proposed design was 24, 29, and 34. During the design process, several issues need to be addressed. First, there is an overhang angle limitation due to the chosen printing technology. Secondly, there is a connection issue between the solid and lattice parts of the sample, which is a potential weak point of the model. To solve this problem, the lattice is embedded in the solid part, increasing the cross-sectional area of their contact.

Mechanical testing has shown that the lattice design parameters have a significant impact on the mechanical behavior of the samples. The sample with a wire radius of 0.25 mm and a wire number of 29 exhibited the highest Young's modulus of 383 MPa, compared to the minimum Young's modulus of 24.2 MPa determined in the experiment for the sample with a wire radius of 0.3 mm and a number of wires equal to 29. The design lies in the middle ground between the number of wires and the wire radius in this selected set of parameters, as adding more wires and/or increasing the wire radius tends to make the specimens less stiff. During mechanical testing, most of the samples broke in the middle region of the stent's lattice (see Table). To improve the mechanical properties, such as increasing the limit load of the samples, advanced design may be needed in the future. One possible solution is the use of a gradient lattice. Two options for implementation exist: additional wires could be added to the lattice, or the wire radius could be increased in the center of the sample (see Fig. 1b).

[1] A.G. Mark, S. Palagi, T. Qiu, P. Fischer, Auxetic metamaterial simplifies soft robot design, In Proceedings of the 2016 IEEE International Conference on Robotics and Automation (ICRA), Stockholm, Sweden, 16–21 May 2016; pp. 4951–4956.

Optical properties of biaxial van der Waals crystals for photonic applications

A. Slavich[1], **G. Ermolaev**[1], **I. Zavidovsky**[1], **D. Grudinin**[1], **M. Tatmyshevskiy**[1], **K. Kravtsov**[1],
A. Toksumakov[1], **O. Matveeva**[1], **A. Syuy**[1], **A. Vyshnevyy**[1], **I. Kruglov**[1], **D. Yakubovsky**[1],
S. Novikov[1], **D. Ghazaryan**[1], **A. Arsenin**[1], **V. Volkov**[2]

1- Center for Photonics and 2D Materials, Moscow Institute of Physics and Technology, Dolgoprudny, Russia
2- Emerging Technologies Research Center, XPANCEO, Dubai Investment Park First, Dubai, United Arab Emirates

Advancements in nanophotonic devices rely on materials with high refractive indices and optical anisotropy [1]. Van der Waals (vdW) crystals have garnered considerable interest due to their high refractive indices and intrinsic anisotropic properties arising from their complex layered structures [2-4]. In this study, we introduce a novel method for the identification and characterization of anisotropic materials. Using a combination of spectroscopic ellipsometry, polarized micro-transmittance, and Raman spectroscopy, we determine the optical constants of vdW microcrystals. Our experimental results reveal exceptional optical properties in the visible and near-ultraviolet ranges, characterized by strong optical anisotropy and high refractive indices. These findings suggest that such materials can significantly enhance the functionality of nanophotonic devices, enabling applications such as smart lenses, ultrathin wave plates and polarization-sensitive flexible photodetectors. This work also presents the theoretical and experimental data on the application of these results in next-generation optical devices.

[1] J.B. Khurgin, Expanding the Photonic Palette: Exploring High Index Materials, ACS Photonics, 9, pp. 743-751, (2022).
[2] G.A. Ermolaev, D.V. Grudinin, Y.V. Stebunov, K.V. Voronin, V.G. Kravets, J. Duan, A.B. Mazitov, G.I. Tselikov, A. Bylinkin, D.I. Yakubovsky, S.M. Novikov, D.G. Baranov, A.Y. Nikitin, I.A. Kruglov, T. Shegai, P. Alonso-González, A.N. Grigorenko, A.V. Arsenin, K.S. Novoselov, V.S. Volkov, Giant Optical Anisotropy in Transition Metal Dichalcogenides for Next-Generation Photonics, Nature Communications, 12, pp. 1–8, (2021).
[3] A.S. Slavich, G.A. Ermolaev, et al, Exploring van der Waals Materials with High Anisotropy: Geometrical and Optical Approaches, Light: Science & Applications, 13, p. 68, (2024).
[4] K.V. Voronin, A.N. Toksumakov, G.A. Ermolaev, et al, Chiral Photonic Super-Crystals Based on Helical van der Waals Homostructures, Laser Photonics Reviews, p. 2301113, (2024).

Efficient desalination of seawater under sunlight

A.V. Syuy[1*], I.V. Martynov[1], D.I. Tselikov[2], G.I. Tselikov[3],
D.V. Dyubo[1], A.V. Arsenin[1], V.S. Volkov[3]

1- Moscow Institute of Physics and Technology (National Research University), Dolgoprudny, 141701, Russia
2- Laboratory "Bionanophotonics", Institute of Engineering Physics for Biomedicine (PhysBio), MEPhI, Moscow 115409, Russia
3- Emerging Technologies Research Center, XPANCEO, Internet City, Emmay Tower, Dubai, United Arab Emirates

* siui.av@mipt.ru

Water scarcity is currently found to be a major issue in many parts of the planet Earth, and it is becoming worse every day as a result of environmental pollution, industrial expansion, changing climatic patterns, and a significant global population growth. The consumption of non-potable water carries health risks due to the presence of contaminants and pathogens, especially affecting vulnerable populations and contributing to the spread of diseases. Desalination processes are trustworthy methods that can handle the increasing need for clean water. Solar energy has long been seen as a pure, limitless source of energy, which has prompted studies on solar energy applications for the production of solar steam, and water desalination. However, balancing the solar energy produced with operational and manufacturing costs presents a hurdle for scientific and commercial applications. Interfacial solar steam generation (SSG) is emerging as a scalable and economically viable solution to the worldwide issues of water pollution and scarcity. Photothermal materials (PTMs) developments have also been the primary cause of the growing interest in SSG for water filtration in the past few years. The application of gold nanoparticles for the purpose of seawater desalination is investigated. The efficiency of gold nanoparticles under the action of solar radiation from the water surface, from the bottom and from the water volume is shown.

Quasi-two dimensional gold films for plasmonic and optoelectronic applications

D.I. Yakubovsky[1], **M.S. Mironov**[1], **A.S. Slavich**[1], **D.V. Grudinin**[1], **I.S. Kazantsev**[1], **G.A. Ermolaev**[2], **A.V. Arsenin**[1,2], **V.S. Volkov**[2]

1- Center for Photonics and 2D Materials, Moscow Institute of Physics and Technology, Russia
2- Emerging Technologies Research Center, XPANCEO, Dubai Investment Park First, Dubai, United Arab Emirates

Ultrathin metal films are a platform for a range of applications, from flexible transparent electrodes to plasmonic interconnects. Due to their small thickness (<10 nm) these films demonstrate high optical transmittance in visible spectrum and mechanical flexibility. Growth of high-quality ultrathin or quasi-two-dimensional (2D) plasmonic (Au, Ag, Cu) films requires the use of seed, adhesion layers and ultrasmooth surfaces [1]. However, to provide really continuous metal films growth the use of additional wetting 2D layers and methods of 2D materials growth can be applied. As example, addition of molybdenum disulfide (MoS_2) underlayers resulted in growth of continuous ultrathin gold films with high plasmonic and electric response [2]. Morphological homogeneity and smoothness of substrate surface affect the quality of ultrathin or quasi-2D metals, since they replicate morphology of the surface. The introduction of ultrathin metal films in different applications is restricted by the choice of wetting layers and substrates. Thus, the development of novel methods for production of ultrathin films are required.

Here, we demonstrate fabrication of ultrasmooth high-quality ultrathin gold films of thicknesses below 10 nm and performed their comprehensive study using atomic-force and scanning electron microscopy, ellipsometry, optical transmission and sheet resistance measurements, scanning near-field optical microscopy. We have confirmed surface plasmon polaritons propagation, as shown in Fig. 1a, and high local optical response [2]. In addition, we developed the method for the growth of quasi-2D gold films providing one of the best optoelectronic performance in terms of conductivity (10 Ω/sq) and transparency (80%) (see Fig. 1b). The obtained results are crucial for growth and characterization of ultrathin metals in their potential use in optoelectronics and photonics applications.
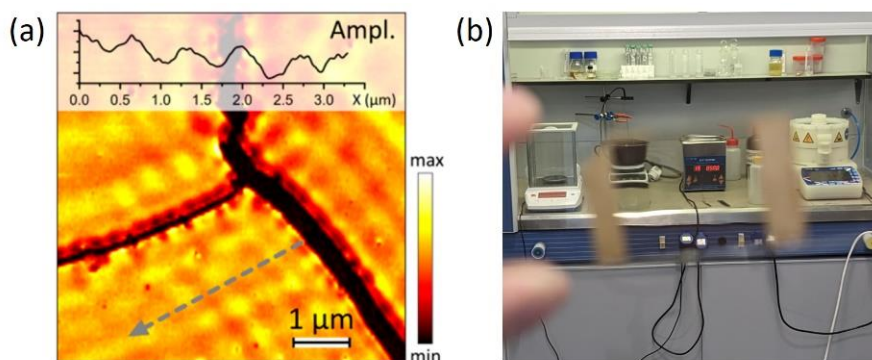

Figure 1. (a) Scanning near-field optical microscopy image of surface plasmon polariton propagation in ultrathin gold film. (b) Photo image of the produced sample with transparent conductive ultrathin film.

[1] R.A. Maniyara, D. Rodrigo, R. Yu, J. Canet-Ferrer, D.S. Ghosh, R. Yongsunthon, et al, Tunable plasmons in ultrathin metal films, Nature Photonics, 13, 328–333 (2019).
[2] D.I. Yakubovsky, D.V. Grudinin, G.A. Ermolaev, et al, Optical nanoimaging of surface plasmon polaritons supported by ultrathin metal films, Nano Letters, 23, 9461−9467 (2023).

SERS performance of plasmonic inks based on laser-ablated layered-material/gold hybrids

I. Zavidovskiy[1*], N. Beelozerova[1], M. Tatmyshevskiy[1], D.I. Tselikov[1,2], G.V. Tikhonowski[2], M.S. Savinov[2], I.V. Sozaev[2], A.A. Popov[2], S.M. Klimentov[2,3], A.V. Kabashin[4], A. Arsenin[1], S. Novikov[1]

1- Center for Photonics and 2D Materials, Moscow Institute of Physics and Technology (MIPT), 141700 Dolgoprudny, Russia
2- Laboratory "Bionanophotonics", Institute of Engineering Physics for Biomedicine (PhysBio), National Research Nuclear University MEPhI (Moscow Engineering Physics Institute), Moscow 115409, Russia
3- Department of Physics and Applied Mathematics, Vladimir State University named after A.G. and N.G. Stoletovs (VlSU), Vladimir 600000, Russia
4- CNRS, LP3, Aix-Marseille Université, Marseille 13288, France

* zavidovskii.ia@mipt.ru

Surface-enhanced Raman spectroscopy (SERS), a highly sensitive non-destructive analytical technique, has recently emerged as a probing tool in medical diagnostics, forensics, quality control, and food safety. The plasmonic ink approach is a well-known technique that enables the on-demand deposition of tailorable-morphology SERS-active coatings by extruding colloidal suspensions of SERS-active nanoparticles ("plasmonic inks") via micro-dispensers [1]. Currently, the study of plasmonic inks is focused on SERS-active noble-metal nanoparticles (NPs), such as silver [2], gold [3], gold-silver alloy NPs [4].

Hybrid SERS platforms comprised of noble-metal and layered-material phases, such as MXenes and transition metal dichalcogenides (TMDCs) have recently emerged as promising SERS-active media. For example, in recent study [5], it was demonstrated that $Au@MoS_2@Au$ core-shell NPs combine the electromagnetic field SERS enhancement from gold component and chemical SERS enhancement from TMDC.

In the current study, we investigate various plasmonic inks obtained by robust and tunable method of pulsed laser ablation in liquids. We demonstrate that structure of hybrid NPs, optical absorbance and SERS performance of resulting inks significantly depend on the ratio of layered and noble-metal components. The obtained results will pave the way to the development of highly reproducible analyte-selective plasmonic inks.

[1] L. Polavarapu, A.L. Porta, S.M. Novikov, M. Coronado-Puchau, L.M. Liz-Marzán, Pen-on-Paper Approach Toward the Design of Universal Surface Enhanced Raman Scattering Substrates, Small, vol. 10, pp. 3065–3071, (2014).
[2] L. Li, S. Yang, J. Duan, L. Huang, G. Xiao, Fabrication and SERS performance of silver nanoarrays by inkjet printing silver nanoparticles ink on the gratings of compact disc recordable, Spectrochimica Acta Part A: Molecular and Biomolecular Spectroscopy, vol. 225, p. 117598, (2020).
[3] N.V. Godoy, D. García-Lojo, F.A. Sigoli, J. Pérez-Juste, I. Pastoriza-Santos, I.O. Mazali, Ultrasensitive inkjet-printed based SERS sensor combining a high-performance gold nanosphere ink and hydrophobic paper, Sensors and Actuators B: Chemical, vol. 320, p. 128412, (2020).
[4] H. Tian, Y. Qin, H. Liu, T. Li, Y. Li, X. Fang, X. Zhang, Flexible Surface-enhanced Raman Scattering Strips Using Colloidal Ink of Gold-silver Alloyed Nanoparticles, Plasmonics, vol. 18, pp. 1553–1559, (2023).
[5] S. Guo, X. Ren, X. Li, Au@MoS2@Au Hierarchical Nanostructures for High-Sensitivity and Recyclable SERS Device, Plasmonics, vol. 15, pp. 591–598, (2020).

Features of thermal elastic deformation of polymer film caused by laser radiation of different powers

I. Zisser[1*], N. Rekunova[1], S. Piachin[1], Y. Zisser[1]

1- Far Eastern State Transport University, 680021, Russia, Khabarovsk, Serysheva st., 47

* irinazisser@gmail.com

When laser radiation acts on a polymer film, it heats up and the surface of this film warps due to elastic thermal deformation [1,2]. As a result of the change in the surface shape, the film becomes analogous to a spherical mirror with a variable focal length. The effects induced by laser radiation are one of the mechanisms of creating the relief of holograms [3]. A detailed study of this phenomenon is required for a controlled change in the relief of a polymer film exposed to laser radiation.

The kinetics of the change in the diameter of the light spot on the screen formed by the reflection of the laser beam from the deformed film were investigated. The higher the intensity of the laser radiation incident on the film, the greater the diameter of the reflected laser beam on the screen. The values of the laser spot diameter obtained from experiment were used to calculate the radius of curvature of the polymer film and the relative change in the film volume $\Delta V/V_0$ during its deformation:

$$\frac{\Delta V}{V_0} = \frac{2R^2}{h^2}\left(1 - \sqrt{1 - \frac{h^2}{R^2}}\right) - 1.$$

In the equation above, R is the radius of curvature of the deformed plate, h is the radius of the laser irradiation zone on the film. The ratio $\Delta V/V_0$ during film deformation in the laser beam spot grows within the first 10 seconds, and then remains practically unchanged.

The temperature of the film in the laser impact zone was measured. The coefficient of volumetric thermal expansion of the film material was calculated.

Table 1. Temperature, relative change in volume, coefficient of thermal expansion at different laser radiation intensities.

I_0, kW/m^2	1.6	3.2	4.9	6.5
ΔT, °C	21	32	44	58
$\Delta V/V_0 \cdot 10^5$	0.27	1.46	3.86	5.1
$\alpha_V \cdot 10^7$, 1/°C	1.24	4.54	8.68	8.72

Analysis of the obtained results is presented. At low intensities of incident laser radiation, the calculations yield a smaller value of the coefficient of volumetric expansion than at high radiation intensities.

[1] N.I. Koroteev, Физика мощного ядерного излучения (Physics of high-power laser radiation) (Moscow: Nauka), Chapter 2, (1991).

[2] V.I. Ivanov, K.N. Okishev, N.N. Rekunova, Деформация полимерной плёнки под действием лазерного излучения (Deformation of a polymer film under laser radiation), Bulletin of scientific reports, № 19, pp. 52-55, (2014).

[3] V.I. Ivanov, T.N. Livashvily, T.N. Bruhanova, N.N. Rekunova, Пространственно-временные характеристики механизма записи рельефных динамических голограмм (Spatio-temporal characteristics of the recording mechanism for relief dynamic holograms), Vestnik TOGU, № 1, pp. 065-068, (2011).